Electromechanical Motion Devices

IEEE Press
445 Hoes Lane
Piscataway, NJ 08855

Electromechanical Motion Devices

Second Edition

Paul Krause
Oleg Wasynczuk
Steven Pekarek

IEEE PRESS SERIES ON POWER ENGINEERING

IEEE

IEEE Press

WILEY

A JOHN WILEY & SONS, INC., PUBLICATION

Published by John Wiley & Sons, Inc., Hoboken, New Jersey.
Published simultaneously in Canada.

Library of Congress Cataloging-in-Publication Data:

Krause, Paul C.
Electromechanical motion devices. — 2nd ed. / Paul C. Krause, Oleg Wasynczuk, Steven Pekarek.
p. cm.
ISBN 978-1-118-29612-7 (hardback)
1. Electromechanical devices. 2. Magnetic circuits. I. Wasynczuk, Oleg. II. Pekarek, Steven. III. Title.
TK153.K73 2012
621.8—dc23 2011051670

Printed in the United States of America.

10 9 8 7 6 5 4 3 2

CONTENTS

PREFACE

Performance control of electric machines began in earnest with the advent of electronic switching devices in the mid 20th century and has since grown into a major industry. This growth has been accelerated in the last 25 years by the ever-increasing sophistication of switching devices and the emergence of electric drives, and now, the recent push to develop economically competitive hybrid and electric vehicles and a more efficient and cleaner power grid. These device improvements have enabled major breakthroughs in the performance control of ac machines. For example, the permanent-magnet ac machine and the induction machine can be controlled so that the resulting performance characteristics are unrecognizable from the traditional steady-state, torque-speed characteristics. However, it has been found that in the design of these controls, it is convenient if not necessary to incorporate a transformation for the ac variables so that the substitute variables resemble those of a dc machine and that this transformation must be embedded within the control. In addition, detailed computer simulations, which include the electric and mechanical transients, have become a design necessity. Reference-frame theory is the key player in all of this and it would be highly beneficial if it were at least introduced in undergraduate study of electric machines. The present-day academic maturity of the third-year electrical engineering student is more than sufficient to follow the concept of reference-frame theory if it is introduced in a straightforward and concise manner. This second edition is an attempt to accomplish this modernization goal.

The analysis of magnetically coupled windings, a direct approach to energy conversion that minimizes the traditional array of summations, distributed windings, and dc machines are covered in the first four chapters. Therein, the advantages and the performance features of the dc machine, which are the emulation goals of controlled ac machines, are established. Controlled converter switching for a dc drive is covered briefly; however, this is presented without the need for a background in automatic control or in semiconductor physics.

Reference-frame theory is introduced in Chapter 5. This is not a lengthy, involved three-phase dissertation; instead, it is a concise two-phase approach that, if studied carefully, makes the analysis of the electric machines covered in later chapters a straightforward and less-time consuming task. It has been the authors' experience that the concepts and advantages of reference-frame theory is often lost in the maze of the trigonometry involved in a three-phase analysis. Since most, if not all, of the concepts are contained in the two-phase approach, the student is able to focus on the basic principles and advantages of reference-frame theory with minimum trigonometric distraction. In fact, once familiar with the material in Chapter 5, the student is able to foresee the change of variables needed for the machines considered in the later chapters and the form of resulting transformed voltage equations without going through any additional derivation. Therefore, the instructor will find that the time spent on the material in Chapter 5 is paid back with handsome dividends in later chapters. Moreover, the analysis and the transient and steady-state performance characteristics of the two- and three-phase machines are essentially identical. The minor differences are addressed briefly at the end of the two-phase treatment of each machine, making the extension to the three-phase machine direct and easily presented.

Field-oriented control of induction machines, constant-torque and constant-power regions of permanent-magnet ac machines, brushless dc machines, and control of doubly fed induction machines for wind turbines are all applications that have become common in the last 25 years. Several of these applications are introduced in this text, not in extensive detail, but in detail sufficient to give the reader a clear first-look at these modern machine applications.

Topics from Chapters 1 through 5 form the basis for the subsequent chapters and the text is purposely written so that once these topics are covered, Chapters 6 through 9 can be covered in any order. Although topics from Chapter 6 should be covered before Chapter 10, the ordering of Chapters 6 through 9 is not based on requisites nor should the ordering in the text be taken as recommended. Although the ordering and depth of coverage are optional, there are perhaps two scenarios that bracket the possible classroom use of this text. To emphasize the electric-power area of study, parts of Chapter 3 could be omitted and topics from Chapters 6, 7, and 10 added. For the electric-drives area, topics from Chapters 6, 8, 9, and part of Chapter 10 could be added. Actually, this book can play various roles depending upon the background of the students and the goals of the instructor. Certainly, it is not intended for all of the material to be taught in one undergraduate course. The instructor can select the topics and depth of coverage so that the student is prepared for advanced study and to provide a modern background and a ready reference for the practicing engineer. Moreover, this text could be used in a two-course series in which the second course is at the senior or introductory graduate level. The text is purposely organized with material being repeated for convenient use as a reference. Once the instructor has become familiar with this feature, it will be found that topics can be covered thoroughly without presenting material previously covered.

Paul C. Krause

Oleg Wasynczuk

Steven D. Pekarek

Paul C. Krause retired from the Purdue University after serving for 39 years as Professor of Electrical and Computer Engineering. He also held teaching positions at the University of Kansas and the University of Wisconsin. He is a Life Fellow of IEEE and has authored or co-authored over 100 technical papers and three textbooks on electric machines. He was the 2010 recipient of the IEEE Nikola Tesla Award. He received B.S degrees in electrical and mechanical engineering, and an M.S. degree in electrical engineering from the University of Nebraska, and a Ph.D. from the University of Kansas. He is presently Chairman of the Board and CEO of PC Krause and Associates Inc. with offices in West Lafayette, IN. and Dayton, OH.

Oleg Wasynczuk is a Professor of Electrical and Computer Engineering at Purdue University. He has authored or co-authored over 100 technical papers and two textbooks on electric machines. He is a Fellow of IEEE and was the 2008 recipient of the IEEE Cyril Veinott Award. He received the B.S degree from Bradley University, and the M.S. and Ph.D. degrees from Purdue University, all in electrical engineering. He also serves as Chief Technical Officer of PC Krause and Associates Inc.

Steven D. Pekarek is a Professor of Electrical and Computer Engineering at Purdue University. He has authored or coauthored over 80 technical papers and is a Senior Member of IEEE. He served as the Secretary of the 2003 Future Energy Challenge, Chair of the 2005 Future Energy Challenge, Technical Co-Chair of the 2005 IEEE International Electric Machines and Drives Conference, and Chair of the 2008 IEEE Applied Power Electronics Conference. He is an Associate Editor for the IEEE Transactions on Power Electronics and the IEEE Transactions on Energy Conversion. He received his B.S. and Ph.D. degrees in electrical engineering from Purdue University.

Electromechanical Motion Devices, Second Edition
by Paul Krause, Oleg Wasynczuk and Steven Pekarek

Chapter 1

MAGNETIC AND MAGNETICALLY COUPLED CIRCUITS

1.1 INTRODUCTION

Before diving into the analysis of electromechanical motion devices, it is helpful to review briefly some of our previous work in physics and in basic electric circuit analysis. In particular, the analysis of magnetic circuits, the basic properties of magnetic materials, and the derivation of equivalent circuits of stationary, magnetically coupled devices are topics presented in this chapter. Much of this material will be a review for most, since it is covered either in a sophomore physics course for engineers or in introductory electrical engineering courses in circuit theory. Nevertheless, reviewing this material and establishing concepts and terms for later use sets the appropriate stage for our study of electromechanical motion devices.

Perhaps the most important new concept presented in this chapter is the fact that in all electromechanical devices, mechanical motion must occur, either translational or rotational, and this motion is reflected into the electric system either as a change of flux linkages in the case of an electromagnetic system or as a change of charge in the case of an electrostatic system. We will deal primarily with electromagnetic systems. If the magnetic system is linear, then the change in flux linkages results, owing to a change in the inductance. In other words, we will find that the inductances of the electric circuits associated with electromechanical motion devices are functions of the mechanical motion. In this chapter, we shall learn to express the self- and mutual inductances for simple translational and rotational electromechanical devices, and to handle these changing inductances in the voltage equations describing the electric circuits associated with the electromechanical system.

Throughout this text, we will give short problems (SPs) with answers following most sections. If we have done our job, each short problem should take less than ten minutes to solve. Also, it may be appropriate to skip or deemphasize some material in this chapter depending upon the background of the students. For example, those familiar with the concept of phasors may opt to skip all or most of the following section. At the close of each chapter, we shall take a moment to look back over some of the important aspects of the material that we have just covered and mention what is coming next and how we plan to fit things together as we go along.

1.2 PHASOR ANALYSIS

Phasors are used to analyze steady-state performance of ac circuits and devices. This concept can be readily established by expressing a steady-state sinusoidal variable as

$$F_a = F_p \cos \theta_{ef} \tag{1.2-1}$$

where capital letters are used to denote steady-state quantities and F_p is the peak value of the sinusoidal variation, which is generally voltage or current but could be any electrical or mechanical sinusoidal variable. For steady-state conditions, θ_{ef} may be written as

$$\theta_{ef} = \omega_e t + \theta_{ef}(0) \tag{1.2-2}$$

where ω_e is the electrical angular velocity and $\theta_{ef}(0)$ is the time-zero position of the electrical variable. Substituting (1.2-2) into (1.2-1) yields

$$F_a = F_p \cos[\omega_e t + \theta_{ef}(0)] \tag{1.2-3}$$

Since

$$e^{j\alpha} = \cos \alpha + j \sin \alpha \tag{1.2-4}$$

equation (1.2-3) may also be written as

$$F_a = Re\left\{F_p e^{j[\omega_e t + \theta_{ef}(0)]}\right\} \tag{1.2-5}$$

where *Re* is shorthand for the "real part of." Equations (1.2-3) and (1.2-5) are equivalent. Let us rewrite (1.2-5) as

$$F_a = Re\left\{F_p e^{j\theta_{ef}(0)} e^{j\omega_e t}\right\} \tag{1.2-6}$$

We need to take a moment to define what is referred to as the root-mean-square (rms) of a sinusoidal variation. In particular, the rms value is defined as

$$F = \left(\frac{1}{T}\int_0^T F_a^2(t)dt\right)^{\frac{1}{2}} \tag{1.2-7}$$

where F is the rms value of $F_a(t)$ and T is the period of the sinusoidal variation. It is left to the reader to show that the rms value of (1.2-3) is $F_p/\sqrt{2}$. Therefore, we can express (1.2-6) as

$$F_a = Re\left[\sqrt{2}\, F e^{j\theta_{ef}(0)} e^{j\omega_e t}\right] \tag{1.2-8}$$

By definition, the phasor representing F_a, which is denoted with a raised tilde, is

$$\tilde{F}_a = F e^{j\theta_{ef}(0)} \tag{1.2-9}$$

which is a complex number. The reason for using the rms value as the magnitude of the phasor will be addressed later in this section. Equation (1.2-6) may now be written as

$$F_a = Re\left[\sqrt{2}\tilde{F}_a e^{j\omega_e t}\right] \tag{1.2-10}$$

A shorthand notation for (1.2-9) is

$$\tilde{F}_a = F\underline{/\theta_{ef}(0)} \tag{1.2-11}$$

Equation (1.2-11) is commonly referred to as the *polar form* of the phasor. The *cartesian form* is

$$\tilde{F}_a = F\cos\theta_{ef}(0) + jF\sin\theta_{ef}(0) \tag{1.2-12}$$

When using phasors to calculate steady-state voltages and currents, we think of the phasors as being stationary at $t = 0$. On the other hand, a phasor is related to the instantaneous value of the sinusoidal quantity it represents. Let us take a moment to consider this aspect of the phasor and, thereby, give some physical meaning to it. From (1.2-4), we realize that $e^{j\omega_e t}$ is a constant-amplitude line of unity length rotating counterclockwise at an angular velocity of ω_e. Therefore,

$$\sqrt{2}\tilde{F}_a e^{j\omega_e t} = \sqrt{2}F\left\{\cos[\omega_e t + \theta_{ef}(0)] + j\,\sin\left[\omega_e t + \theta_{ef}(0)\right]\right\} \tag{1.2-13}$$

is a constant-amplitude line $\sqrt{2}F$ in length rotating counterclockwise at an angular velocity of ω_e with a time-zero displacement from the positive real axis of $\theta_{ef}(0)$. Since $\sqrt{2}F$ is the peak value of the sinusoidal variation, the instantaneous value of F_a is the real part of (1.2-13). In other words, the real projection of the phasor $\tilde{F}_a$ is the instantaneous value of $F_a/\sqrt{2}$ at time zero. As time progresses, $\tilde{F}_a e^{j\omega_e t}$ rotates at ω_e in the counterclockwise direction, and its real projection, in accordance with (1.2-10), is the instantaneous value of $F_a/\sqrt{2}$. Thus, for

$$F_a = \sqrt{2}F\,\cos\,\omega_e t \tag{1.2-14}$$

the phasor representing F_a is

$$\tilde{F}_a = Fe^{j0} = F\underline{/0^\circ} = F + j0 \tag{1.2-15}$$

For

$$F_a = \sqrt{2}F\,\sin\,\omega_e t \tag{1.2-16}$$

the phasor is

$$\tilde{F}_a = Fe^{-j\pi/2} = F\underline{/-90^\circ} = 0 - jF \tag{1.2-17}$$

Although there are several ways to arrive at (1.2-17) from (1.2-16), it is helpful to ask yourself where must the rotating phasor be positioned at time zero so that, when it rotates counterclockwise at ω_e, its real projection is $(1/\sqrt{2})F_p\,\sin\,\omega_e t$? Is it clear that a phasor of amplitude F positioned at $\frac{\pi}{2}$ represents $-\sqrt{2}F\,\sin\,\omega_e t$?

In order to show the facility of the phasor in the analysis of steady-state performance of ac circuits and devices, it is useful to consider a series circuit consisting of a resistance, an inductance, and a capacitance. Thus,

$$v_a = Ri_a + L\frac{di_a}{dt} + \frac{1}{C}\int i_a dt \tag{1.2-18}$$

For steady-state operation, let

$$V_a = \sqrt{2}\,V\,\cos\left[\omega_e t + \theta_{ev}(0)\right] \tag{1.2-19}$$

$$I_a = \sqrt{2}I\,\cos\left[\omega_e t + \theta_{ei}(0)\right] \tag{1.2-20}$$

where the subscript a is used to distinguish the instantaneous value from the rms value of the steady-state variable. The steady-state voltage equation may be obtained by substituting (1.2-19) and (1.2-20) into (1.2-18), whereupon we can write

$$\begin{aligned}\sqrt{2}V\cos[\omega_e t+\theta_{ev}(0)] = {} & R\sqrt{2}I\cos[\omega_e t+\theta_{ei}(0)] \\ & +\omega_e L\sqrt{2}I\cos[\omega_e t+\tfrac{1}{2}\pi+\theta_{ei}(0)] \\ & +\frac{1}{\omega_e C}\sqrt{2}I\cos[\omega_e t-\tfrac{1}{2}\pi+\theta_{ei}(0)]\end{aligned} \tag{1.2-21}$$

The second term in the right-hand side of (1.2-21), which is $L\frac{dI_a}{dt}$, can be written

$$\omega_e L\sqrt{2}I\ \cos\left[\omega_e t+\tfrac{1}{2}\pi+\theta_{ei}(0)\right] = \omega_e L Re[\sqrt{2}Ie^{j\frac{1}{2}\pi}e^{j\theta_{ei}(0)}e^{j\omega_e t}] \tag{1.2-22}$$

Since $\tilde{I}_a = Ie^{j\theta_{ei}(0)}$, we can write

$$L\widetilde{\frac{dI_a}{dt}} = \omega_e L e^{j\frac{1}{2}\pi}\tilde{I}_a \tag{1.2-23}$$

Since $e^{j\frac{1}{2}\pi}=j$, (1.2-23) may be written

$$L\widetilde{\frac{dI_a}{dt}} = j\omega_e L\tilde{I}_a \tag{1.2-24}$$

If we follow a similar procedure, we can show that

$$\frac{1}{C}\widetilde{\int I_a dt} = -j\frac{1}{\omega_e C}\tilde{I}_a \tag{1.2-25}$$

It is interesting that differentiation of a steady-state sinusoidal variable rotates the phasor counterclockwise by $\frac{1}{2}\pi$, whereas integration rotates the phasor clockwise by $\frac{1}{2}\pi$.

The steady-state voltage equation given by (1.2-21) can be written in phasor form as

$$\widetilde{V}_a = \left[R+j(\omega_e L-\frac{1}{\omega_e C})\right]\ \widetilde{I}_a \tag{1.2-26}$$

We can express (1.2-26) compactly as

$$\tilde{V}_a = Z\,\tilde{I}_a \tag{1.2-27}$$

where Z, the impedance, is a complex number; it is not a phasor. It is often expressed as

$$Z = R + j(X_L - X_C) \tag{1.2-28}$$

where $X_L = \omega_e L$ is the inductive reactance and $X_C = \dfrac{1}{\omega_e C}$ is the capacitive reactance.

The instantaneous power is

$$\begin{aligned} P &= V_a I_a \\ &= \sqrt{2}V \cos[\omega_e t + \theta_{ev}(0)]\sqrt{2}I \cos[\omega_e t + \theta_{ei}(0)] \end{aligned} \tag{1.2-29}$$

After some manipulation, we can write (1.2-29) as

$$P = VI \cos[\theta_{ev}(0) - \theta_{ei}(0)] + VI \cos[2\omega_e t + \theta_{ev}(0) + \theta_{ei}(0)] \tag{1.2-30}$$

Therefore, the average power P_{ave} may be written

$$P_{\text{ave}} = |\tilde{V}_a|\,|\tilde{I}_a| \cos[\theta_{ev}(0) - \theta_{ei}(0)] \tag{1.2-31}$$

where $|\tilde{V}|$ and $|\tilde{I}|$ are the magnitude of the phasors (rms value), $\theta_{ev}(0) - \theta_{ei}(0)$ is the power factor angle φ_{pf}, and $\cos[\theta_{ev}(0) - \theta_{ei}(0)]$ is referred to as the power factor. If current is positive in the direction of voltage drop then (1.2-31) is positive if power is consumed and negative if power is generated. It is interesting to point out that in going from (1.2-29) to (1.2-30), the coefficient of the two right-hand terms is $\frac{1}{2}(\sqrt{2}V\sqrt{2}I)$ or one-half the product of the peak values of the sinusoidal variables. Therefore, it was considered more convenient to use the rms values for the phasors, whereupon average power could be calculated by the product of the magnitude of the voltage and current phasors as given by (1.2-31).

We see from (1.2-30) that the instantaneous power of a single-phase ac circuit oscillates at $2\omega_e t$ about an average value. Let us take a moment to calculate the steady-state power of a two-phase ac system. Balanced, steady-state, two-phase variables (a and b phase) may be expressed as

$$V_a = \sqrt{2}V \cos[\omega_e t + \theta_{ev}(0)] \tag{1.2-32}$$

$$I_a = \sqrt{2}I \cos[\omega_e t + \theta_{ei}(0)] \tag{1.2-33}$$

$$V_b = \sqrt{2}V \cos[\omega_e t - \tfrac{1}{2}\pi + \theta_{ev}(0)] \tag{1.2-34}$$

$$I_b = \sqrt{2}I \cos[\omega_e t - \tfrac{1}{2}\pi + \theta_{ei}(0)] \tag{1.2-35}$$

The total instantaneous power is

$$P = V_a I_a + V_b I_b \tag{1.2-36}$$

Substituting (1.2-32) through (1.2-35) into (1.2-36) and after some trigonometric manipulation, the total power for a balanced two-phase system becomes

$$P = 2\,|\tilde{V}_a|\,|\tilde{I}_a|\,\cos\varphi_{\text{pf}} \tag{1.2-37}$$

It is important to note that the $2\omega_e t$ oscillation is not present. In other words, the total instantaneous steady-state power is constant. In the case of a three-phase balanced system, the phasors of the three voltages or currents are displaced 120° and the instantaneous steady-state power is also constant and three times the average power of one phase. In other words the 2 in (1.2-37) becomes 3 when considering a three-phase system.

Example 1A. It is often instructive to construct a phasor diagram. For example, let us consider a voltage equation of the form

$$\tilde{V} = Z\tilde{I} + \tilde{E} \tag{1A-1}$$

where Z is given by (1.2-28). Let us assume that $\tilde{V}$and $\tilde{I}$ are known and that we are to calculate $\tilde{E}$. The phasor diagram may be used as a rough check on these calculations. Let us construct this phasor diagram by assuming that $|X_L| > |X_C|$ and $\tilde{V}$and $\tilde{I}$ are known as shown in Fig. 1A-1. Solving (1A-1) for $\tilde{E}$ yields

$$\tilde{E} = \tilde{V} - [R + j(X_L - X_C)]\tilde{I} \tag{1A-2}$$

To perform this graphically, start at the origin in Fig. 1A-1 and walk to the terminus of $\tilde{V}$. Now, we want to subtract $R\tilde{I}$. To achieve the proper orientation to do this, stand at the terminus of $\tilde{V}$, turn, and look in the $\tilde{I}$ direction which is at the angle $\theta_{ei}(0)$. But we must subtract $R\tilde{I}$; hence, $-\tilde{I}$ is 180° from $\tilde{I}$, so do an about-face and now we are headed in the $-\tilde{I}$ direction, which is $\theta_{ei}(0) - 180°$. Start walking in the direction of $-\tilde{I}$ for the distance $R|\tilde{I}|$ and then stop. While still facing in the $-\tilde{I}$ direction, let us consider the next term. Now since we have assumed that $|X_L| > |X_C|$, we must subtract $j(X_L - X_C)\tilde{I}$, so let us face in the direction of $-j\tilde{I}$. We are still looking in the $-\tilde{I}$ direction, so we need only to j ourselves. Thus, we must rotate 90° in the counterclockwise direction, whereupon we are standing at the end of $\tilde{V} - R\tilde{I}$ looking in the direction of $\theta_{ei}(0) - 180° + 90°$. Start walking in this direction for the distance of $(X_L - X_C)|\tilde{I}|$, whereupon we are at

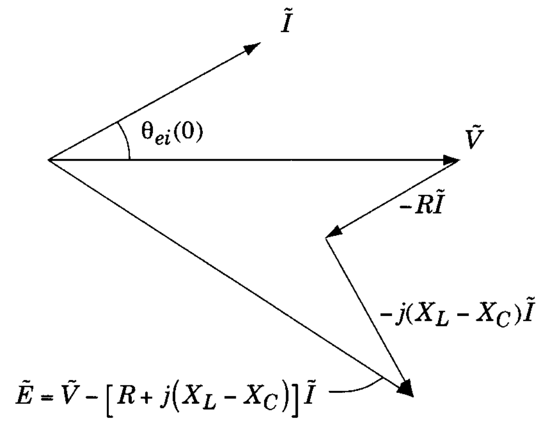

Figure 1A-1: Phasor diagram for (1A-2).

the terminus of $\tilde{V} - [R + j(X_L - X_C)]\tilde{I}$. According to (1A-2), $\tilde{E}$ is the phasor drawn from the origin of the phasor diagram to where we are.

The average steady-state power for a single-phase circuit may be calculated using (1.2-31). We will mention in passing that the reactive power is defined as

$$Q = |\tilde{V}||\tilde{I}|\sin[\theta_{ev}(0) - \theta_{ei}(0)] \tag{1A-3}$$

The units of Q are var (voltampere reactive). An inductance is said to absorb reactive power and thus, by definition, Q is positive for an inductor and negative for a capacitor. Actually, Q is a measure of the interchange of energy stored in the electric (capacitor) and magnetic (inductance) fields.

SP1.2-1 If $\tilde{V} = 1\underline{/0^\circ}$ and $\tilde{I} = 1\underline{/180^\circ}$ in the direction of the voltage drop, calculate Z and P_{ave}. Is power generated or consumed? [$(-1 + j0)$ ohms, 1 watt, generated]

SP1.2-2 For SP1.2-1, express instantaneous voltage, current, and power if the frequency is 60 Hz. [$V = \sqrt{2}\cos 377t$, $I = \sqrt{2}\cos(377t + \pi)$, $P = -1 + 1\cos(754t + \pi)$]

SP1.2-3 $A = \sqrt{2}\underline{/0^\circ}$, $B = \sqrt{2}\underline{/90^\circ}$. Calculate $A + B$ and $A \times B$. [$2\underline{/45^\circ}$, $2\underline{/90^\circ}$]

SP1.2-4 In Example 1A, $X_L > X_C$ and yet $\tilde{I}$ was given as leading $\tilde{V}$. How can this be? [$\tilde{E}$]

1.3 MAGNETIC CIRCUITS

An elementary magnetic circuit is shown in Fig. 1.3-1. This system consists of an electric conductor wound N times about the magnetic member, which is generally some type of ferromagnetic material. In this example system, the magnetic member contains an air gap of uniform length between points a and b. We will assume that the magnetic system (circuit) consists only of the magnetic member and the air gap. Recall that Ampere's law states that the line integral of the field intensity **H** about a closed path is equal to the net current enclosed within this closed path of integration. That is,

$$\oint \mathbf{H} \cdot d\mathbf{L} = i_n \tag{1.3-1}$$

where i_n is the net current enclosed. Let us apply Ampere's law to the closed path depicted as a dashed line in Fig. 1.3-1. In particular,

$$\int_a^b H_i dL + \int_b^a H_g dL = Ni \tag{1.3-2}$$

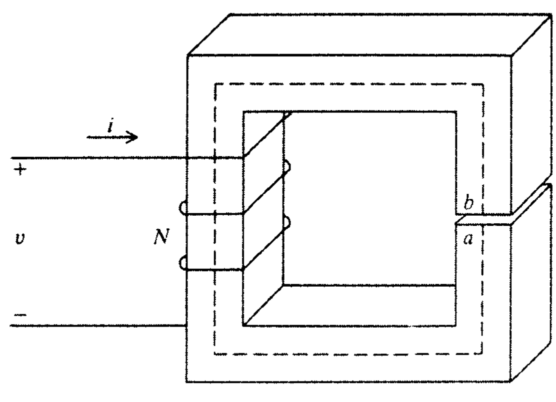

Figure 1.3-1: Elementary magnetic circuit.

where the path of integration is assumed to be in the clockwise direction. This equation requires some explanation. First, we are assuming that the field intensity exists only in the direction of the given path, hence we have dropped the vector notation. The subscript i denotes the field intensity (H_i) in the ferromagnetic material (iron or steel) and g denotes the field intensity (H_g) in the air gap. The path of integration is taken as the mean length about the magnetic member, for purposes we shall explain later. The right-hand side of (1.3-2) represents the net current enclosed. In particular, we have enclosed the current i, N times. This has the units of amperes but is commonly referred to as ampere-turns (At) or magnetomotive force (mmf). We will find that the mmf in magnetic circuits is analogous to the electromotive force (emf) in electric circuits. Note that the current enclosed is positive in (1.3-2) if the current i is positive. The sign of the right-hand side of (1.3-2) may be determined by the so-called "corkscrew" rule. That is, the current enclosed is positive if its assumed positive direction is in the same direction as the advance of a right-hand screw if it were turned in the direction of the path of integration, which in Fig. 1.3-1 is clockwise. Before continuing, it should be mentioned that we refer to **H** as the field intensity; however, some authors prefer to call **H** the field strength.

If we carry out the line integration, (1.3-2) can be written

$$H_i l_i + H_g l_g = Ni \tag{1.3-3}$$

where l_i is the mean length of the magnetic material and l_g is the length across the air gap. Now, we have some explaining to do. We have assumed that the magnetic circuit consists only of the ferromagnetic material and the air gap, and that the magnetic field intensity is always in the direction of the path of integration or, in other words, perpendicular to a cross section of the magnetic material taken in the same sense as the air gap is cut through the material. The assumed direction of the magnetic field intensity is valid except in the vicinity of the corners. The direction of the field intensity changes gradually rather than abruptly at the corners. Nevertheless, the "mean length approximation" is widely used as an adequate means of analyzing this type of magnetic circuit.

Let us now take a cross section of the magnetic material as shown in Fig. 1.3-2. From our study of physics, we know that for linear, isotropic magnetic materials the flux density **B** is related to the field intensity as

$$\mathbf{B} = \mu \mathbf{H} \tag{1.3-4}$$

Where μ is the permeability of the medium. Hence, we can write (1.3-3) in terms of flux density as

$$\frac{B_i}{\mu_i} l_i + \frac{B_g}{\mu_g} l_g = Ni \tag{1.3-5}$$

The surface integral of the flux density is equal to the flux Φ, thus

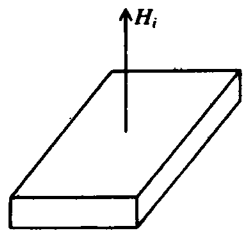

Figure 1.3-2: Cross section of magnetic material.

$$\Phi = \int_A \mathbf{B} \cdot d\mathbf{S} \tag{1.3-6}$$

If we assume that the flux density is uniform over the cross-sectional area, then

$$\Phi_i = B_i A_i \tag{1.3-7}$$

where Φ_i is the total flux in the magnetic material and A_i is the associated cross-sectional area. In the air gap,

$$\Phi_g = B_g A_g \tag{1.3-8}$$

where A_g is the cross-sectional area of the gap. From physics, it is known that the streamlines of flux density $\mathbf{B}$ are closed; hence, the flux in the air gap is equal to the flux in the core. That is, $\Phi_i = \Phi_g$, and, if the air gap is small, $A_i \cong A_g$, and, therefore, $B_i \cong B_g$. However, the effective area of the air gap is larger than that of the magnetic material, since the flux will tend to balloon or spread out (fringing effect), covering a maximum area midway across the air gap. Generally, this is taken into account by assuming that $A_g = kA_i$, where k, which is greater than unity, is determined primarily by the length of the air gap. Although we shall keep this in mind, it is sufficient for our purposes to assume $A_g = A_i$. If we let $\Phi_i = \Phi_g = \Phi$ and substitute (1.3-7) and (1.3-8) into (1.3-5), we obtain

$$\frac{l_i}{\mu_i A_i}\Phi + \frac{l_g}{\mu_g A_g}\Phi = Ni \tag{1.3-9}$$

The analogy to Ohm's law is at hand. Ni (mmf) is analogous to the voltage (emf), and the flux Φ is analogous to the current. We can complete this analogy if we recall that the resistance of a conductor is proportional to its length and inversely proportional to its conductivity and cross-sectional area. Similarly, $l_i/\mu_i A_i$ and $l_g/\mu_g A_g$ are the *reluctances* of the magnetic material and air gap, respectively. Generally, the permeability is expressed in terms of relative permeability as

$$\mu_i = \mu_{ri}\mu_0 \tag{1.3-10}$$

$$\mu_g = \mu_{rg}\mu_0 \tag{1.3-11}$$

where μ_0 is the permeability of free space ($4\pi \times 10^{-7}$ Wb/A·m or $4\pi \times 10^{-7}$ H/m, since Wb/A is a henry) and μ_{ri} and μ_{rg} are the relative permeability of the magnetic material and the air gap, respectively. For all practical purposes, $\mu_{rg} = 1$; however, μ_{ri} may be as large as 500 to 4000 depending upon the type of ferromagnetic material. We will use $\Re$ to denote reluctance so as to distinguish reluctance from resistance, which will be denoted by r or R. We can now write (1.3-9) as

$$(\Re_i + \Re_g)\Phi = Ni \tag{1.3-12}$$

where $\Re_i$ and $\Re_g$ are the reluctance of the iron and air gap, respectively.

Example 1B. A magnetic system is shown in Fig. 1B-1. The total number of turns is 100, the relative permeability of the iron is 1000, and the current is 10 A. Calculate the total flux in the center leg.

Let us draw the electric circuit analog of this magnetic system for which we will need to calculate the reluctance of the various paths:

$$\begin{aligned}\Re_{ab} &= \frac{l_{ab}}{\mu_{ri}\mu_0 A_i}\\ &= \frac{0.22}{1000(4\pi \times 10^{-7})(0.04)^2} = 109{,}419\ \text{H}^{-1}\end{aligned} \tag{1B-1}$$

Similarly,

$$\Re_{bcda} = \frac{0.25 + 0.22 + 0.25}{(1000)(4\pi \times 10^{-7})(0.04)^2} = 358{,}099\ \text{H}^{-1} \tag{1B-2}$$

Neglecting the air gap length,

$$\Re_{bef} = \Re_{gha} = \tfrac{1}{2}\Re_{bcda} = 179{,}049\ \text{H}^{-1} \tag{1B-3}$$

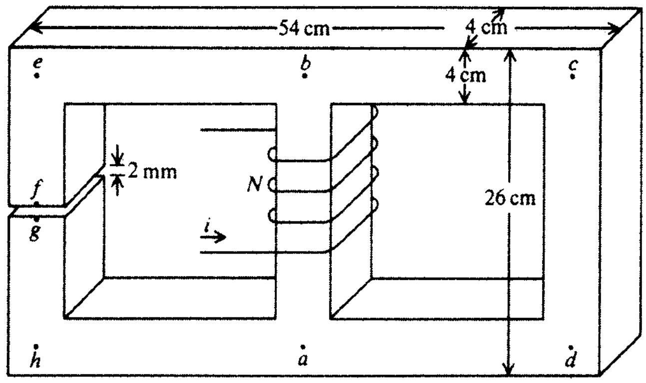

Figure 1B-1: Single-winding magnetic system.

The reluctance of the air gap is

$$\Re_{fg} = \frac{0.002}{(4\pi \times 10^{-7})(0.04)^2} = 994,718 \text{ H}^{-1} \tag{1B-4}$$

The electric circuit analog is given in Fig. 1B-2. The polarity of the mmf is determined by the right-hand rule. That is, if we grasp one of the turns of the winding with our right hand with the thumb pointed in the direction of positive current, then our fingers will point in the direction of positive flux which flows in the direction of an mmf rise. Or if we grasp the winding (center leg) with the fingers of our right hand in the direction of positive current, then our thumb will be in the direction of positive flux and in the direction of a rise in mmf.

We can now apply dc circuit theory to solve for the total flux, $\Phi_1 + \Phi_2$, flowing in the center leg. For example, we can use loop equations or, as we will do here, reduce the series-parallel circuit to an equivalent reluctance. The equivalent reluctance of the parallel combination is

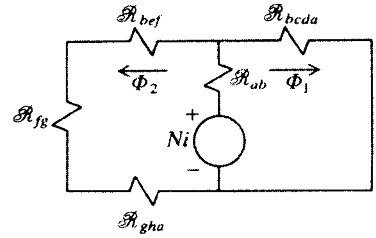

Figure 1B-2: Electric-circuit analog of Fig. 1B-1.

$$
\begin{aligned}
\Re_{eq} &= \frac{(\Re_{bcda})(\Re_{bef} + \Re_{fg} + \Re_{gha})}{\Re_{bcda} + \Re_{bef} + \Re_{fg} + \Re_{gha}} \\
&= \frac{(358,099)(179,049 + 994,718 + 179,049)}{358,099 + 179,049 + 994,718 + 179,049} \\
&= \frac{(358,099)(1,352,816)}{1,710,915} = 283,148 \text{ H}^{-1} \qquad \text{(1B-5)}
\end{aligned}
$$

$$
\begin{aligned}
\Phi_1 + \Phi_2 &= \frac{Ni}{\Re_{ab} + \Re_{eq}} \\
&= \frac{(100)(10)}{109,419 + 283,148} = 2.547 \times 10^{-3} \text{ Wb} \qquad \text{(1B-6)}
\end{aligned}
$$

Example 1C. Consider the magnetic system shown in Fig. 1C-1. The windings are supplied from ac sources and, in the steady state, $I_1 = \sqrt{2} \cos \omega_e t$ and $I_2 = \sqrt{2}\, 0.3 \cos(\omega_e t + 45^\circ)$, where capital letters are used to denote steady-state conditions. $N_1 = 150$ turns, $N_2 = 90$ turns, and $\mu_r = 3000$. Calculate the flux in the center leg.

The electric circuit analog is given in Fig. 1C-2. The reluctance $\Re_x$ is the reluctance of the center leg and $\Re_y$ is the reluctance of one of the two parallel paths from the top of the center leg through an outside leg to the bottom of the center leg. In particular,

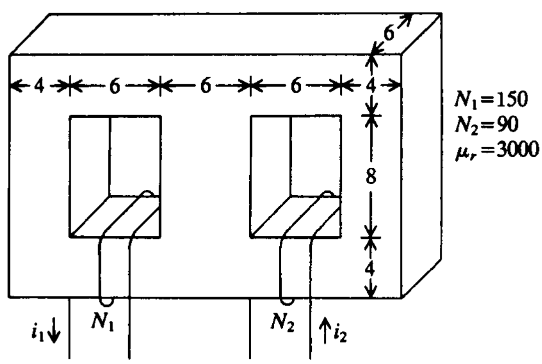

Figure 1C-1: A two-winding magnetic system with dimensions in centimeters.

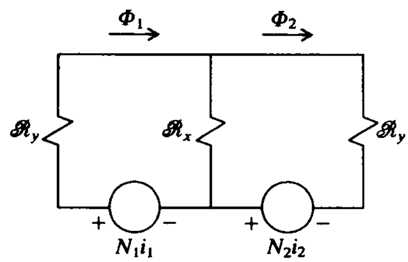

Figure 1C-2: Electric-circuit analog of Fig. 1C-1.

$$\Re_y = \frac{2(0.03 + 0.06 + 0.02) + 0.12}{3000(4\pi \times 10^{-7})(0.06)(0.04)} = 37,578 \text{ H}^{-1} \tag{1C-1}$$

$$\Re_x = \frac{0.12}{3000(4\pi \times 10^{-7})0.06^2} = 8,842 \text{ H}^{-1} \tag{1C-2}$$

Since the currents are sinusoidal, the mmf's will be sinusoidal. Thus, it is convenient to use phasors to solve for Φ_1 and Φ_2. The loop equations are

$$\tilde{\text{mmf}}_1 = \Re_y \tilde{\Phi}_1 + \Re_x(\tilde{\Phi}_1 - \tilde{\Phi}_2) \tag{1C-3}$$

$$\tilde{\text{mmf}}_2 = \Re_x(\tilde{\Phi}_2 - \tilde{\Phi}_1) + \Re_y \tilde{\Phi}_2 \tag{1C-4}$$

which may be written in matrix form as

$$\begin{bmatrix} \tilde{\text{mmf}}_1 \\ \tilde{\text{mmf}}_2 \end{bmatrix} = \begin{bmatrix} \Re_x + \Re_y & -\Re_x \\ -\Re_x & \Re_x + \Re_y \end{bmatrix} \begin{bmatrix} \tilde{\Phi}_1 \\ \tilde{\Phi}_2 \end{bmatrix} \tag{1C-5}$$

A review of matrix algebra is given in Appendix B. Now,

$$\tilde{\text{mmf}}_1 = N_1 \tilde{I}_1 = (150)(1\underline{/0^\circ}) = 150\underline{/0^\circ}\text{At} \tag{1C-6}$$

$$\tilde{\text{mmf}}_2 = N_2 \tilde{I}_2 = (90)(0.3\underline{/45^\circ}) = 27\underline{/45^\circ}\text{At} \tag{1C-7}$$

Solving (1C-5) yields

$$\tilde{\Phi}_1 = (3.434 + j0.081) \times 10^{-3} \text{ Wb} \tag{1C-8}$$

$$\tilde{\Phi}_2 = (1.065 + j0.427) \times 10^{-3} \text{ Wb} \tag{1C-9}$$

The flux flowing down through the center leg is

$$\tilde{\Phi}_1 - \tilde{\Phi}_2 = (2.369 - j0.346) \times 10^{-3}$$
$$= 2.39 \times 10^{-3}\underline{/ - 8.3^{\circ}} \text{ Wb} \qquad \text{(1C-10)}$$

SP1.3-1 Calculate Φ_1 in Example 1B. [$\Phi_1 = 2.014 \times 10^{-3}$ Wb]
SP1.3-2 Calculate $\tilde{\Phi}_1 + \tilde{\Phi}_2$ in Example 1B when $I = \sqrt{2}\,10\cos(\omega_e t - 30^{\circ})$. [$\tilde{\Phi}_1 + \tilde{\Phi}_2 = 2.547 \times 10^{-3}\ \underline{/ - 30^{\circ}}$ Wb, rms]
SP1.3-3 Remove the center leg of the magnetic system shown in Fig. 1C-1. Calculate the total flux when $I_1 = 9$ and $I_2 = -15$ A. [Zero]
SP1.3-4 Express the sinusoidal variation represented by $\tilde{\Phi}_2$ given by (1C-9). [$\sqrt{2}(1.147 \times 10^{-3})\cos(\omega_e t + 21.8^{\circ})$]

1.4 PROPERTIES OF MAGNETIC MATERIALS

We may be aware from our study of physics that, when ferromagnetic materials such as iron, nickel, cobalt, or alloys of these elements, such as various types of steels, are placed in a magnetic field, the flux produced is markedly larger (500 to 4000 times, for example) than that which would be produced when a nonmagnetic material is subjected to the same magnetic field. We must take some time to review briefly the basic properties of ferromagnetic materials and to establish terminology for later use.

Let us begin by considering the relationship between B and H shown in Fig. 1.4-1 which is typical of silicon steel used in transformers. We will assume that the ferromagnetic core is initially completely demagnetized (both B and H are zero). As we apply an external H field by increasing the current in a winding wound around the core, the flux density B also increases, but nonlinearly, as shown in Fig. 1.4-1. After H reaches a value of approximately 150 A/m, the flux density rises more slowly and the material begins to saturate when H is several hundred Ampere-turns per meter.

In ferromagnetic materials, the combination of the magnetic moments produced by the electrons orbiting the nucleus of an atom and the electron itself spinning on its axis produce a net magnetic moment of the atom that is not canceled by an opposing magnetic moment of a neighboring atom. Ferromagnetic materials have been found to be divided into magnetic domains wherein all magnetic moments (dipoles) are aligned. Although the

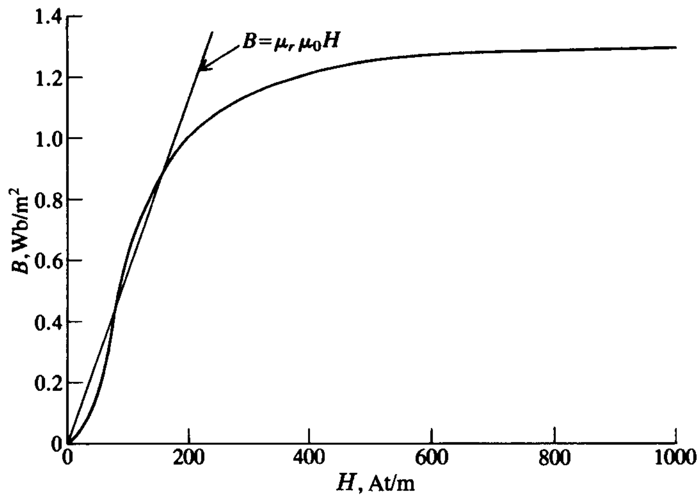

Figure 1.4-1: B-H curve for typical silicon steel used in transformers.

magnetic moments are all aligned within a magnetic domain, the direction of this alignment will differ from one domain to another.

When a ferromagnetic material is subjected to an external magnetic field, those domains, which originally tend to be aligned with the applied magnetic field, grow at the expense of those domains with magnetic moments that are less aligned. Thereby, the flux is increased from that which would occur with a nonmagnetic material. This is known as *domain-wall motion* [1]. As the strength of the magnetic field increases, the aligned domains continue to grow in nearly a linear fashion. Thus, a nearly linear B-H curve results ($B \cong \mu_r \mu_0 H$) until the ability of the aligned domains to take from the unaligned domains starts to slow. This gives rise to the knee of the B-H curve and the beginning of saturation. At this point, the displacements of the domain walls are complete. That is, there are no longer unaligned domains from which to take. However, the remaining domains may still not be in perfect alignment with the external H field. A further increase in H will cause a rotation of the atomic dipole moments within the remaining domains toward a more perfect alignment. However, the marginal increase in B due to rotation is less than the original increase in B due to domain-wall motion, resulting in a decrease in slope of the B-H curve. The magnetic material is said to be completely saturated when the remaining domains are perfectly aligned. In this case, the slope of the B-H curve becomes μ_0 [1]. If it is assumed that the magnetic flux is uniform through most of the magnetic material, then B is proportional to Φ and H is proportional to mmf. Hence, a plot of flux versus current is of the same shape as the B-H curve.

A transformer is generally designed so that some saturation occurs during normal operation. Electric machines are also designed similarly in that a machine generally operates slightly in the saturated region during normal, rated operating conditions. Since saturation causes the coefficients of the differential equations describing the behavior of an electromagnetic device to be functions of the winding currents, a transient analysis is difficult without the aid of a computer. However, it is not our purpose to set forth methods of analyzing nonlinear magnetic systems.

In the previous discussion, we have assumed that the ferromagnetic material is initially demagnetized and that the applied field intensity is gradually increased from zero. However, if a ferromagnetic material is subjected to an alternating field intensity, the resulting B-H curve exhibits hysteresis. For example, let us assume that a ferromagnetic material is subjected to an alternating field intensity (alternating current flowing in the winding) and initially the flux density and field intensity are both zero. As H increases from zero, B increases along the initial B-H curve, as shown in Fig. 1.4-2. However the field intensity varies sinusoidally and, when H decreases from a maximum, B does not follow back down the original B-H curve. After several cycles, the magnetic system will reach a steady-state condition and the plot of B versus H will form a hysteresis loop or a double-valued function, as shown in Fig. 1.4-2. What is happening is very complex. In simple terms, the growth of aligned domains for an incremental change in H in one direction is not equal to the growth of oppositely aligned domains if this change in H were suddenly reversed. We could become quite involved by discussing minor hysteresis loops which would occur if, during the sinusoidal variation of H, it were suddenly stopped at some nonzero value then reversed, stopped, and reversed again [1]. We shall only mention this phenomenon in passing.

A family of hysteresis loops is shown in Fig. 1.4-3. In each case, the applied H is sinusoidal; however, the amplitude of the H field is varied to give the family of loops shown in Fig. 1.4-3. A magnetization or B-H curve for a given material is obtained by connecting the tips of the hysteresis loops, as shown by the dashed line in Fig. 1.4-3. The locus of the tips of the hysteresis curves is about the same as the original B-H curve in Fig. 1.4-1, which corresponds to a gradual increase of H in an initially demagnetized material. If H were suddenly stopped at zero, the flux density remaining

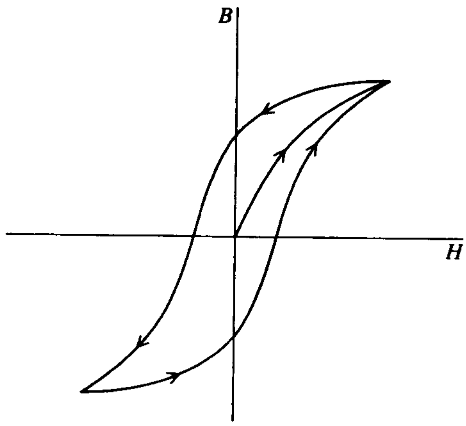

Figure 1.4-2: Hysteresis loop.

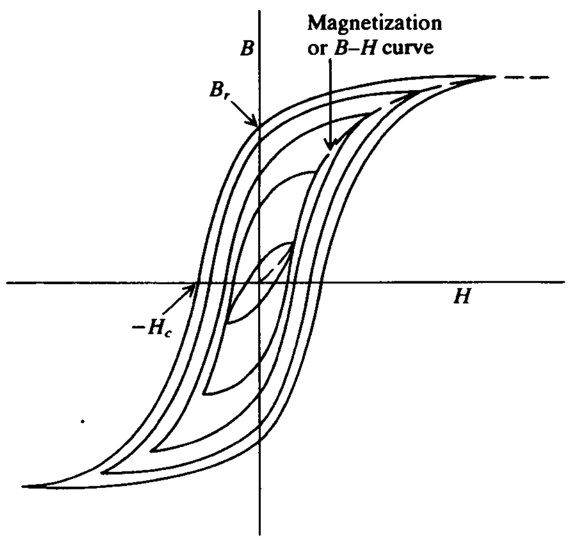

Figure 1.4-3: Family of steady-state hysteresis loops.

in the ferromagnetic material is called the *residual flux density* (B_r). The negative field intensity necessary to bring this residual flux density to zero is called the *coercive force* (H_c). These two quantities are indicated in Fig. 1.4-3 for the largest hysteresis loop shown.

Energy is required to increase the size of the magnetic domains of the ferromagnetic material. It can be shown that the energy necessary to align alternately the magnetic domains is equal to the area enclosed by the hysteresis loop. This energy causes a rise in the temperature of the magnetic material, and the power associated with this energy loss is called the *hysteresis loss.*

When a solid block of magnetic material such as that shown in Fig. 1.3-1 is subjected to an alternating field intensity, the resulting alternating flux induces current in the solid magnetic material, which will circulate in a loop perpendicular to the flux density ($\mathbf{B}$) inducing it. These so-called eddy currents have two undesirable effects. First, the mmf established by these circulating currents opposes the mmf produced by the winding, and this opposition is greatest at the center of the material because that tends to be also the center of the current loops. Thus, the flux would tend not to flow through the center of the solid magnetic member, thereby not utilizing the full benefits of the ferromagnetic material. Second, there is an i^2r loss associated with these eddy currents, called *eddy current loss,* which is dissipated as heat. These two adverse effects can be minimized in several ways, but the most common is to build the ferromagnetic core of laminations (thin strips) insulated from each other and oriented in the direction of the magnetic field ($\mathbf{B}$ or $\mathbf{H}$). These thin strips offer a much smaller area in which the eddy currents can flow; hence, smaller currents and smaller losses result.

The core losses associated with ferromagnetic materials are the combination of the hysteresis and eddy current losses. Electromagnetic devices are designed to minimize these losses; however, they are always present and are often taken into account in a linear system analysis by assuming that their effects on the electric system can be represented by a resistance.

SP1.4-1 The magnetic circuit of Fig. 1.3-1 is constructed by using silicon sheet steel. Its magnetization curve is given by Fig. 1.4-1. The gap length l_g is 1 mm, the mean core length l_i is 100 cm, $N = 500$, and $A_i = A_g = 25\,\text{cm}^2$. Determine the current needed to produce a flux Φ of $2.5 \times 10^{-3}\,\text{Wb}$. [*Hint:* First establish H_i, H_g, and use (1.3-3).] [$I = 1.99$ A]

1.5 STATIONARY MAGNETICALLY COUPLED CIRCUITS

Magnetically coupled electric circuits are central to the operation of transformers and electromechanical motion devices. In the case of transformers, stationary circuits are magnetically coupled for the purpose of changing the ac voltage and current levels. In the case of electromechanical devices, circuits in relative motion are magnetically coupled for the purpose of transferring energy between the mechanical and electric systems. Since magnetically coupled circuits play such an important role in energy conversion, it is important to establish the equations that describe their behavior and to express these equations in a form convenient for analysis. Many of these goals may be achieved by considering two stationary electric circuits that are magnetically coupled, as shown in Fig. 1.5-1. The two windings consist of turns N_1 and N_2, and they are wound on a common core, which is a ferromagnetic material with a permeability large relative to that of air. The magnetic core is not illustrated in three dimensions.

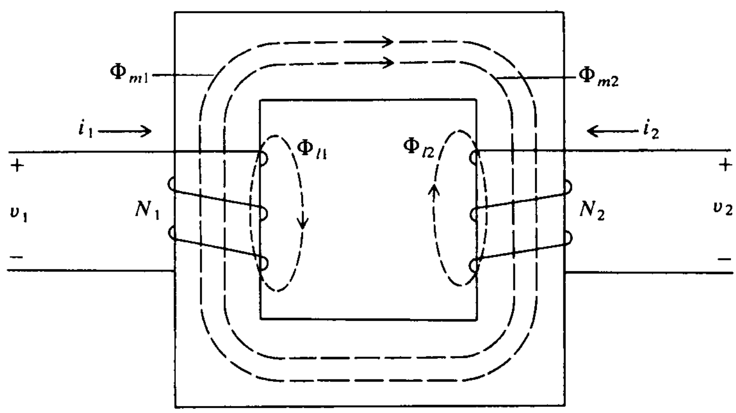

Figure 1.5-1: Magnetically coupled circuits.

Before proceeding, a comment or two is in order. Generally, the concept of an ideal transformer is introduced in a basic circuits course. In the ideal case, v_2 in Fig. 1.5-1 is $(N_2/N_1)v_1$ and i_2 is $-(N_1/N_2)i_1$. Only the turns-ratio of the transformer is considered. However, this treatment is often not sufficient for a detailed analysis of transformers, and it is seldom appropriate in the analysis of electromechanical motion devices, since an air gap is necessary for motion to occur; hence, the windings are not as tightly coupled as in the case of transformers and the leakage flux must be taken into account.

In general, the flux produced by each winding can be separated into two components: a leakage component denoted with the subscript l and a magnetizing component denoted by the subscript m. Each of these components is depicted by a single streamline with the positive direction determined by applying the right-hand rule to the directions of current flow in the winding. (The right-hand rule was reviewed in Example 1B.) The leakage flux associated with a given winding links only that winding, whereas the magnetizing flux, whether it is due to current in winding 1 or winding 2, links both windings. In some cases, i_2 is selected positive out of the top of winding 2 and a dot is placed at that terminal. Although the "dot notation" is convenient for transformers, it is seldom used in the case of electromechanical devices.

The flux linking each winding may be expressed as

$$\Phi_1 = \Phi_{l1} + \Phi_{m1} + \Phi_{m2} \tag{1.5-1}$$

$$\Phi_2 = \Phi_{l2} + \Phi_{m2} + \Phi_{m1} \tag{1.5-2}$$

The leakage flux Φ_{l1} is produced by current flowing in winding 1 and it links only the turns of winding 1. Likewise, the leakage flux Φ_{l2} is produced by current flowing in winding 2 and it links only the turns of winding 2. The flux Φ_{m1} is produced by current flowing in winding 1 and it links all turns of windings 1 and 2. Similarly, the magnetizing flux Φ_{m2} is produced by current flowing in winding 2 and it also links all turns of windings 1 and 2. Both Φ_{m1} and Φ_{m2} are called *magnetizing fluxes.* With the selected positive directions of current flow and the manner in which the windings are wound, magnetizing flux produced by positive current flowing in one winding adds to the magnetizing flux produced by positive current flowing in the other winding. For this case, we will find that the mutual inductance is positive.

It is appropriate to point out that this is an idealization of the actual magnetic system. It seems logical that all of the leakage flux will not link all the turns of the winding producing it; hence, Φ_{l1} and Φ_{l2} are "equivalent" leakage fluxes. Similarly, all of the magnetizing flux of one winding may not link all of the turns of the other winding. To acknowledge this practical aspect of the magnetic system, N_1 and N_2 are often considered to be the equivalent number of turns rather than the actual number.

The voltage equations may be expressed as

$$v_1 = r_1 i_1 + \frac{d\lambda_1}{dt} \tag{1.5-3}$$

$$v_2 = r_2 i_2 + \frac{d\lambda_2}{dt} \tag{1.5-4}$$

In matrix form,

$$\begin{bmatrix} v_1 \\ v_2 \end{bmatrix} = \begin{bmatrix} r_1 & 0 \\ 0 & r_2 \end{bmatrix} \begin{bmatrix} i_1 \\ i_2 \end{bmatrix} + \frac{d}{dt} \begin{bmatrix} \lambda_1 \\ \lambda_2 \end{bmatrix} \tag{1.5-5}$$

A review of matrix algebra is given in Appendix B. The resistances r_1 and r_2 and the flux linkages λ_1 and λ_2 are related to windings 1 and 2, respectively. Since it is assumed that Φ_1 links the equivalent turns of winding 1 (N_1) and Φ_2 links the equivalent turns of winding 2 (N_2), the flux linkages may be written as

$$\lambda_1 = N_1 \Phi_1 \tag{1.5-6}$$

$$\lambda_2 = N_2 \Phi_2 \tag{1.5-7}$$

where $\Phi_1$and Φ_2 are given by (1.5-1) and (1.5-2), respectively.

If we assume that the magnetic system is linear, we may apply Ohm's law for magnetic circuits to express the fluxes. Thus, the fluxes may be written as

$$\Phi_{l1} = \frac{N_1 i_1}{\Re_{l1}} \tag{1.5-8}$$

$$\Phi_{m1} = \frac{N_1 i_1}{\Re_m} \tag{1.5-9}$$

$$\Phi_{l2} = \frac{N_2 i_2}{\Re_{l2}} \tag{1.5-10}$$

$$\Phi_{m2} = \frac{N_2 i_2}{\Re_m} \tag{1.5-11}$$

where $\Re_{l1}$ and $\Re_{l2}$ are the reluctances of the leakage paths, and $\Re_m$ is the reluctance of the path of magnetizing fluxes. Typically, the reluctances associated with leakage paths are much larger than the reluctance of the magnetizing path. The reluctance associated with an individual leakage path is difficult to determine exactly, and it is usually approximated from test data or by using the computer to solve the field equations numerically. On the other hand, the reluctance of the magnetizing path of the core shown in Fig. 1.5-1 may be computed with sufficient accuracy as in Example 1B.

Substituting (1.5-8) through (1.5-11) into (1.5-1) and (1.5-2) yields

$$\Phi_1 = \frac{N_1 i_1}{\Re_{l1}} + \frac{N_1 i_1}{\Re_m} + \frac{N_2 i_2}{\Re_m} \tag{1.5-12}$$

$$\Phi_2 = \frac{N_2 i_2}{\Re_{l2}} + \frac{N_2 i_2}{\Re_m} + \frac{N_1 i_1}{\Re_m} \tag{1.5-13}$$

Substituting (1.5-12) and (1.5-13) into (1.5-6) and (1.5-7) yields

$$\lambda_1 = \frac{N_1^2}{\Re_{l1}} i_1 + \frac{N_1^2}{\Re_m} i_1 + \frac{N_1 N_2}{\Re_m} i_2 \tag{1.5-14}$$

$$\lambda_2 = \frac{N_2^2}{\Re_{l2}} i_2 + \frac{N_2^2}{\Re_m} i_2 + \frac{N_2 N_1}{\Re_m} i_1 \tag{1.5-15}$$

When the magnetic system is linear, the flux linkages are generally expressed in terms of inductances and the currents. We see that the coefficients of the first two terms on the right-hand side of (1.5-14) depend upon N_1 and the reluctance of the magnetic system, independent of the existence of winding 2. An analogous statement may be made regarding (1.5-15) with the roles of winding 1 and winding 2 reversed. Hence, the self-inductances are defined as

$$L_{11} = \frac{N_1^2}{\Re_{l1}} + \frac{N_1^2}{\Re_m} = L_{l1} + L_{m1} \tag{1.5-16}$$

$$L_{22} = \frac{N_2^2}{\Re_{l2}} + \frac{N_2^2}{\Re_m} = L_{l2} + L_{m2} \tag{1.5-17}$$

where L_{l1} and L_{l2} are the leakage inductances and L_{m1} and L_{m2} are the magnetizing inductances of windings 1 and 2, respectively. From (1.5-16) and (1.5-17), it follows that the magnetizing inductances may be related as

$$\frac{L_{m2}}{N_2^2} = \frac{L_{m1}}{N_1^2} \tag{1.5-18}$$

The mutual inductances are defined as the coefficient of the third term on the right-hand side of (1.5-14) and (1.5-15). In particular,

$$L_{12} = \frac{N_1 N_2}{\Re_m} \tag{1.5-19}$$

$$L_{21} = \frac{N_2 N_1}{\Re_m} \tag{1.5-20}$$

We see that $L_{12} = L_{21}$ and, with the assumed positive direction of current flow and the manner in which the windings are wound, the mutual inductances are positive. If, however, the assumed positive directions of current were such that Φ_{m1} opposed Φ_{m2}, then the mutual inductances would be negative.

The mutual inductances may be related to the magnetizing inductances. Comparing (1.5-16) and (1.5-17) with (1.5-19) and (1.5-20), we see that

$$L_{12} = \frac{N_2}{N_1} L_{m1} = \frac{N_1}{N_2} L_{m2} \tag{1.5-21}$$

The flux linkages may now be written as

$$\lambda_1 = L_{11} i_1 + L_{12} i_2 \tag{1.5-22}$$

$$\lambda_2 = L_{21} i_1 + L_{22} i_2 \tag{1.5-23}$$

where L_{11} and L_{22} are defined by (1.5-16) and (1.5-17), respectively, and L_{12} and L_{21}, by (1.5-21). The self-inductances L_{11} and L_{22} are always positive; however, the mutual inductances $L_{12}(L_{21})$ may be positive or negative, as previously mentioned.

Although the voltage equations given by (1.5-3) and (1.5-4) may be used for purposes of analysis, it is customary to perform a change of variables which yields the well-known equivalent T circuit of two windings coupled by a linear magnetic circuit. To set the stage for this derivation, let us express the flux linkages from (1.5-22) and (1.5-23) as

$$\lambda_1 = L_{l1} i_1 + L_{m1} \left(i_1 + \frac{N_2}{N_1} i_2 \right) \tag{1.5-24}$$

$$\lambda_2 = L_{l2} i_2 + L_{m2} \left(\frac{N_1}{N_2} i_1 + i_2 \right) \tag{1.5-25}$$

With λ_1 in terms of L_{m1} and λ_2 in terms of L_{m2}, we see two logical candidates for substitute variables, in particular, $(N_2/N_1)i_2$ or $(N_1/N_2)i_1$. If we let

$$i_2' = \frac{N_2}{N_1} i_2 \tag{1.5-26}$$

then we are using the substitute variable i_2', which, when flowing through winding 1, produces the same mmf as the actual i_2 flowing through winding 2; $N_1 i_2' = N_2 i_2$. This is said to be referring the current in winding 2 to winding 1 or to a winding with N_1 turns, whereupon winding 1 becomes the reference winding. On the other hand, if we let

$$i_1' = \frac{N_1}{N_2} i_1 \tag{1.5-27}$$

then i_1' is the substitute variable that produces the same mmf when flowing through winding 2 as i_1 does when flowing in winding 1; $N_2 i_1' = N_1 i_1$. This change of variables is said to refer the current of winding 1 to winding 2 or to a winding with N_2 turns, whereupon winding 2 becomes the reference winding.

We will demonstrate the derivation of the equivalent T circuit by referring the current of winding 2 to a winding with N_1 turns; thus i_2' is expressed by (1.5-26). We want the instantaneous power to be unchanged by this substitution of variables. Therefore,

$$v_2' i_2' = v_2 i_2 \tag{1.5-28}$$

Hence,

$$v_2' = \frac{N_1}{N_2} v_2 \tag{1.5-29}$$

Flux linkages, which have the units of V · s, are related to the substitute flux linkages in the same way as voltages. In particular,

$$\lambda_2' = \frac{N_1}{N_2} \lambda_2 \tag{1.5-30}$$

Now, replace $(N_2/N_1)i_2$ with i_2' in the expression for λ_1, given by (1.5-24). Next, solve (1.5-26) for i_2 and substitute it into λ_2 given by (1.5-25). Now, multiply this result by N_1/N_2 to obtain λ_2' and then substitute $(N_2/N_1)^2 L_{m1}$ for L_{m2} in λ_2'. If we do all this, we will obtain

$$\lambda_1 = L_{l1} i_1 + L_{m1}(i_1 + i_2') \tag{1.5-31}$$

$$\lambda_2' = L_{l2}' i_2' + L_{m1}(i_1 + i_2') \tag{1.5-32}$$

where

$$L'_{l2} = \left(\frac{N_1}{N_2}\right)^2 L_{l2} \tag{1.5-33}$$

The fiux linkage equations given by (1.5-31) and (1.5-32) may also be written as

$$\lambda_1 = L_{11}i_1 + L_{m1}i'_2 \tag{1.5-34}$$

$$\lambda'_2 = L_{m1}i_1 + L'_{22}i'_2 \tag{1.5-35}$$

where

$$L'_{22} = \left(\frac{N_1}{N_2}\right)^2 L_{22} = L'_{l2} + L_{m1} \tag{1.5-36}$$

and L_{22} is defined by (1.5-17).

If we multiply (1.5-4) by N_1/N_2 to obtain v'_2, the voltage equations become

$$\begin{bmatrix} v_1 \\ v'_2 \end{bmatrix} = \begin{bmatrix} r_1 & 0 \\ 0 & r'_2 \end{bmatrix} \begin{bmatrix} i_1 \\ i'_2 \end{bmatrix} + \frac{d}{dt} \begin{bmatrix} \lambda_1 \\ \lambda'_2 \end{bmatrix} \tag{1.5-37}$$

where

$$r'_2 = \left(\frac{N_1}{N_2}\right)^2 r_2 \tag{1.5-38}$$

The previous voltage equations, (1.5-37), together with the fiux linkage equations, (1.5-34) through (1.5-35), suggest the equivalent T circuit shown in Fig. 1.5-2. This method may be extended to include any number of windings wound on the same core.

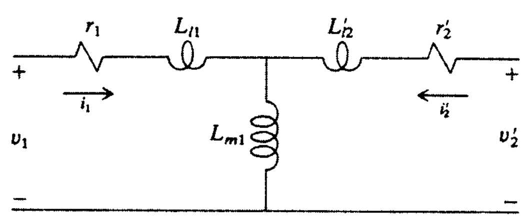

Figure 1.5-2: Equivalent T circuit with winding 1 selected as reference winding.

Earlier in this section, we mentioned that in the case of an ideal transformer only the turns ratio is considered, that is, $v_2 = (N_2/N_1)v_1$ and $i_2 = -(N_1/N_2)i_1$. We can now more fully appreciate the assumptions that are made in this type of analysis. In particular, the resistances r_1 and r_2 and the leakage inductances L_{l1} and L_{l2} are neglected, and it is assumed that the magnetizing inductance is large so that the magnetizing current $i_1 + i_2'$ is negligibly small.

The information presented in this section forms the basis of the equivalent circuits for many types of electric machines. Using a turns ratio to refer the voltages and currents of rotor circuits of electric machines to a winding with the same number of turns as the stator windings is common practice. In fact, the equivalent circuits for many ac machines are of the same form as shown in Fig. 1.5-2, with the addition of a voltage source referred to as a *speed voltage*. We shall talk much more about this speed voltage later—where it comes from and how it fits into the equivalent circuit.

Example 1D. It is instructive to illustrate the method of deriving an equivalent T circuit from open- and short-circuit measurements. When winding 2 of the two-winding transformer shown in Fig. 1.5-2 is open circuited and a voltage of 110 V (rms) at 60 Hz is applied to winding 1, the average power supplied to winding 1 is 6.66 W. The measured current in winding 1 is 1.05 A (rms). Next, with winding 2 short-circuited, the current flowing in winding 1 is 2 A when the applied voltage is 30 V at 60 Hz. The average input power is 44 W. If we assume $L_{l1} = L_{l2}'$, an approximate equivalent T circuit can be determined from these measurements with winding 1 selected as the reference winding.

The average power supplied to winding 1 may be expressed as

$$P_1 = |\tilde{V}_1|\,|\tilde{I}_1| \cos \varphi_{\text{pf}} \tag{1D-1}$$

where

$$\varphi_{\text{pf}} = \theta_{ev}(0) - \theta_{ei}(0) \tag{1D-2}$$

Here, $\tilde{V}_1$ and $\tilde{I}_1$ are phasors with the positive direction of $\tilde{I}_1$ taken in the direction of the voltage drop, and $\theta_{ev}(0)$ and $\theta_{ei}(0)$ are the phase angles of $\tilde{V}_1$ and $\tilde{I}_1$, respectively. Solving for φ_{pf} during the open-circuit test, we have

$$\varphi_{\text{pf}} = \cos^{-1}\frac{P_1}{|\tilde{V}_1||\tilde{I}_1|} = \cos^{-1}\frac{6.66}{(110)(1.05)} = 86.7^\circ \tag{1D-3}$$

Although $\varphi_{\text{pf}} = -86.7^\circ$ is also a legitimate solution of (1D-3), the positive solution is taken since $\tilde{V}_1$ leads $\tilde{I}_1$ in an inductive circuit. With winding 2 open-circuited, the input impedance of winding 1 is

$$Z = \frac{\tilde{V}_1}{\tilde{I}_1} = r_1 + j(X_{l1} + X_{m1}) \tag{1D-4}$$

With $\tilde{V}_1$ as the reference phasor, $\tilde{V}_1 = 110\underline{/0^\circ}$, $\tilde{I}_1 = 1.05\underline{/-86.7^\circ}$. Thus,

$$r_1 + j(X_{l1} + X_{m1}) = \frac{110\underline{/0^\circ}}{1.05\underline{/-86.7^\circ}} = 6 + j104.6\,\Omega \tag{1D-5}$$

If we neglect core losses, then, from (1D-5), $r_1 = 6\,\Omega$. We also see from (1D-5) that $X_{l1} + X_{m1} = 104.6\,\Omega$.

For the short-circuit test, we will assume that $\tilde{I}_1 = -\tilde{I}_2'$ since transformers are designed so that at rated frequency $X_{m1} >> |r_2' + jX_{l2}'|$. Hence, using (1D-1) again,

$$\varphi_{\text{pf}} = \cos^{-1}\frac{44}{(30)(2)} = 42.8^\circ \tag{1D-6}$$

In this case, the input impedance is $Z = (r_1 + r_2') + j(X_{l1} + X_{l2}')$. This may be determined as

$$Z = \frac{30\underline{/0^\circ}}{2\underline{/-42.8^\circ}} = 11 + j10.2\,\Omega \tag{1D-7}$$

Hence, $r_2' = 11 - r_1 = 5\,\Omega$ and, since it is assumed that $X_{l1} = X_{l2}'$, both are $10.2/2 = 5.1\,\Omega$. Therefore, $X_{m1} = 104.6 - 5.1 = 99.5\,\Omega$. In summary, $r_1 = 6\,\Omega$, $L_{l1} = 13.5\,\text{mH}$, $L_{m1} = 263.9\,\text{mH}$, $r_2' = 5\,\Omega$, $L_{l2}' = 13.5$ mH. Make sure we converted from X's to L's correctly.

SP1.5-1 Remove the center leg of the magnetic system shown in Fig. 1C-1. Calculate L_{11}, L_{22}, and L_{12}. Neglect the leakage inductances. [$L_{11} = 299.4\,\text{mH}$, $L_{22} = 107.8\,\text{mH}$, $L_{12} = 179.5\,\text{mH}$]

SP1.5-2 Consider the transformer and parameters calculated in Example 1D. Winding 2 is short-circuited and 12 V (dc) is applied to winding 1.

Calculate the steady-state values of i_1 and i_2. Repeat with winding 2 open-circuited. [$I_1 = 2$ A and $I_2 = 0$ in both cases]

SP1.5-3 Calculate the no-load (winding 2 open-circuited) current for the transformer given in Example 1D if $V_1 = \sqrt{2}\, 10 \cos 100t$. [$\tilde{I}_1 = 0.352\underline{/-77.8^\circ}$ A]

1.6 OPEN- AND SHORT-CIRCUIT CHARACTERISTICS OF STATIONARY MAGNETICALLY COUPLED CIRCUITS

It is instructive to observe the open- and short-circuit characteristics of a transformer with two windings. For this purpose, a transformer with the parameters given in Example 1D was simulated on a computer. The open-circuit characteristics are shown in Figs. 1.6-1 and 1.6-2. The variables plotted are λ, v_1, i_1, v_2', and i_2'. The variable λ is equal to $L_{m1}(i_1 + i_2')$, which is the last term on the right-hand side of (1.5-31) and (1.5-32). This is the flux linkage of winding 1 due to the flux in the transformer iron. It is often referred to as the *magnetizing flux linkage(s)* and denoted λ_m, λ_{mag}, or λ_φ, whereas $i_1 + i_2'$ is called the *magnetizing current.*

Initially, the windings are unexcited. At time zero ($t = 0$), the voltage applied to winding 1 with winding 2 open-circuited is $v_1 = \sqrt{2}\ 110 \cos 377t$ in Fig. 1.6-1 and $v_1 = \sqrt{2}\ 110 \sin 377t$ in Fig. 1.6-2. The waveforms of the steady-state current i_1 are identical in Figs. 1.6-1 and 1.6-2; however, since the inductive reactance is large, applying a sine wave voltage for v_1 at time zero results in a much larger transient offset in i_1 than when $v_1 = \sqrt{2}\ 110 \cos 377t$. (You are asked to show this in a problem at the end of the chapter.) Since $v_1 = \sqrt{2}\ 110 \sin 377t$ causes a larger transient offset, it makes it easier for us to identify the transient period. Therefore, we shall continue with v_1 as a sine wave. Although it is difficult to determine the time constant for the offset of the current i_1 (or λ) to decay to one-third of its original value, it is on the order of 50 ms. The calculated value of the no-load time constant is $\tau_{nl} = (L_{l1} + L_{m1})/r_1 = 46.2$ ms. Before leaving Figs. 1.6-1 and 1.6-2, note that, during steady-state conditions, I_1 lags V_1 by something close to 90° (86.7°, from Example 1D).

Let us now go to the short-circuit characteristics. The transient and steady-state response with $v_1 = \sqrt{2}\, 110 \sin 377t$ and with $v_2' = 0$ are shown

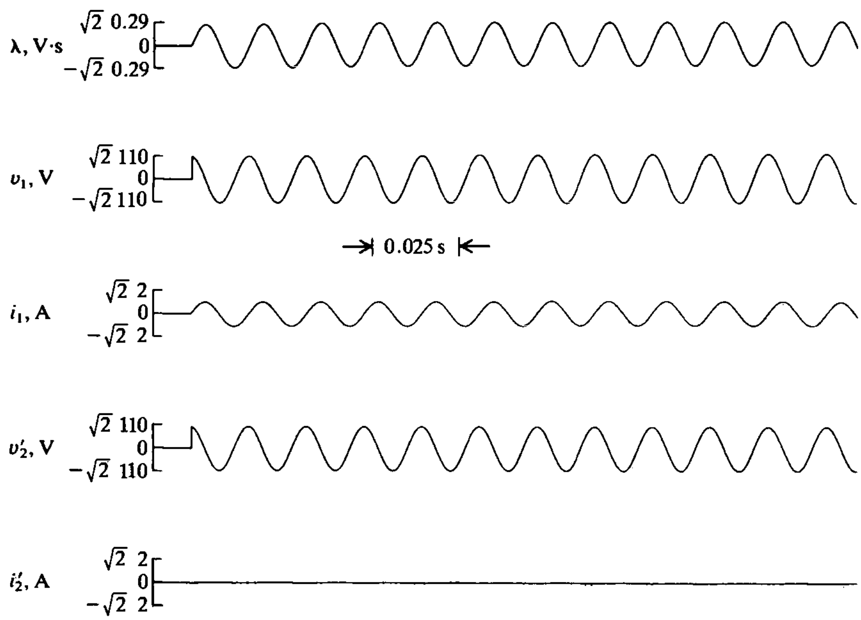

Figure 1.6-1: Open-circuit conditions of a two-winding transformer with $v_1 = \sqrt{2}\ 110 \cos 377t$.

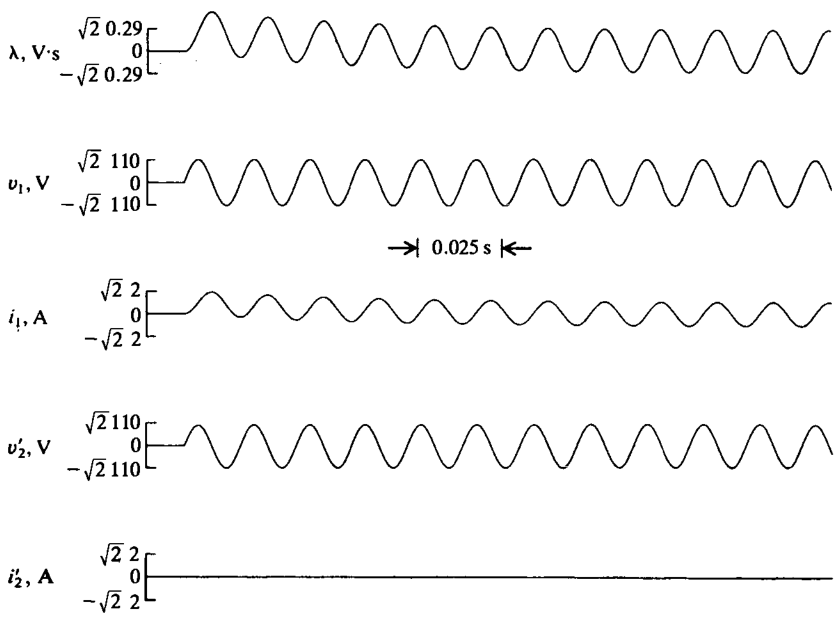

Figure 1.6-2: Open-circuit conditions of a two-winding transformer with $v_1 = \sqrt{2}\ 110 \sin 377t$.

in Fig. 1.6-3. There are several things to note. From Fig. 1.6-3, it appears that the time constant associated with the decay of i_1 is small, less than 5 ms. Now let us look at the magnetizing flux linkage λ. We see that it is smaller in amplitude than in the no-load case. We would expect this since during short-circuit conditions $i_1 \cong -i'_2$, whereby the mmf's of the two windings oppose, and the resulting flux in the transformer iron is less than for the no-load condition where $i'_2 = 0$. Looking at this in another way, we realize that i_1 and $-i'_2$ will be essentially equal during short-circuit conditions whenever the impedance of the magnetizing branch ($j\omega_e L_{m1}$) is much larger (say 8 to 10 times larger) than $r'_2 + j\omega_e L'_{l2}$. Here $\omega_e = 377\,\text{rad/s}$.

It is interesting to note that the decay of the magnetizing flux linkage λ is much slower than the apparent decay of the currents. As we mentioned, the time constant associated with i_1 is small; however, there is indeed a small difference between i_1 and $-i'_2$, and this small current (magnetizing current),

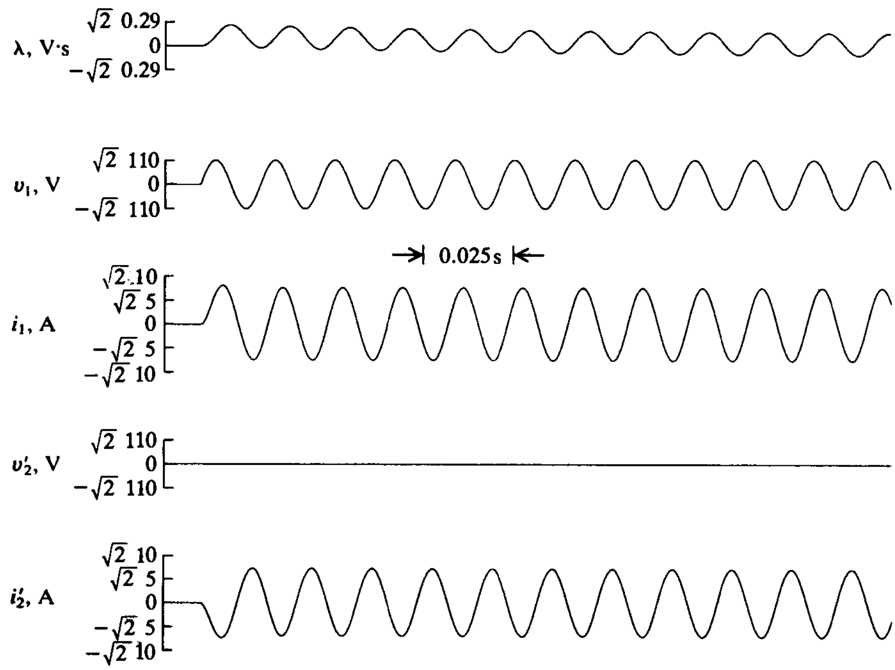

Figure 1.6-3: Short-circuit conditions of a two-winding transformer with $v_1 = \sqrt{2}\ 110 \sin 377t$.

which is actually a small part of i_1, must flow in the large inductance L_{m1}. Hence, the magnetizing current is associated with a longer time constant than the much larger component of the current i_1 which circulates through the series r_2' and L_{l2}'.

Let us take a brief look at the effects of saturation of the transformer iron. For this purpose we will assume that the λ versus $(i_1 + i_2')$ plot of the core of the transformer is that shown in Fig. 1.6-4. The slope of the straight-line part of this plot is L_{m1}. The saturation characteristics shown in Fig. 1.6-4 were implemented on the computer following the method outlined in [2]. Since λ is small during short-circuit conditions (Fig. 1.6-3), saturation does not occur. However, it is a different situation when we talk about the open-circuit conditions shown in Fig. 1.6-5, which is the same as Fig. 1.6-2 with saturation taken into account. Here, we see that during steady-state open-circuit conditions, the current i_1, which is the total magnetizing current since i_2' is zero, is rich in third harmonic. What is happening? Well, we realize that, if there were no r_1 and L_{l1}, then the time rate of change of λ must equal v_1, the applied voltage. In this case, the peak value of λ would be $\sqrt{2}\,110/377 = \sqrt{2}\ 0.29$ V·s. We see from Fig. 1.6-4 that saturation

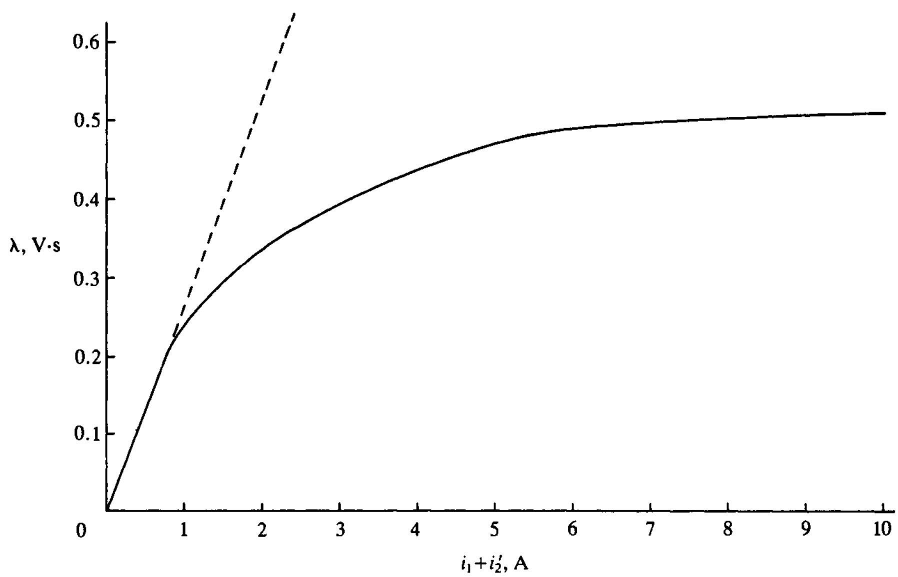

Figure 1.6-4: λ versus $i_1 + i_2'$.

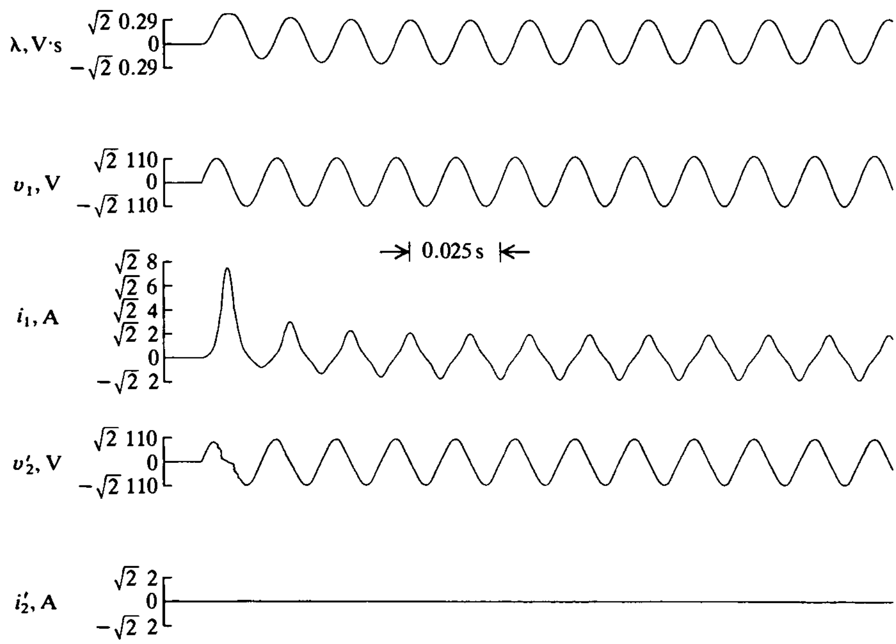

Figure 1.6-5: Same as Fig. 1.6-2 with saturation.

must occur in order for the core to produce this peak value of λ. In the saturated region, a much larger increase in current per unit increase in λ is required than when the transformer is not saturated. Hence, a peaking of the magnetizing current occurs. Now, in real life there is r_1 and L_{l1} and, hence, a voltage drop will occur across each of these components. Thus, the magnitude of $d\lambda/dt$ is somewhat less than that of v_1; nevertheless, saturation must occur to produce the required steady-state peak value of λ, which is approximately $\sqrt{2}\ 0.26$ V · s from Fig. 1.6-5.

There is one last item worthy of discussion. Recall that a relatively large transient offset in λ occurs when we apply a sine wave voltage for v_1. This large transient offset drives the core into saturation. Note λ during the first cycle in Fig. 1.6-5. Since the core is highly saturated, the magnetizing current necessary to produce the required λ is very large. In Fig. 1.6-5 we see that this current, which occurs upon "energizing" the transformer, is nearly three times the normal steady-state magnetizing current. In some transformers, this may be as high as 50 to 100 times the normal magnetizing current, and it may take several cycles before reaching steady-state conditions. For this reason, some transformers may "hum" loudly during energization as a result of forces created by the large inrush current. Also, note the waveform of v_2' during the first cycle of energization. The effects of saturation are reflected into the open-circuit voltage of winding 2. Since during saturation the change of the flux linkages is small, the open-circuit voltage will be small, as depicted in Fig. 1.6-5. However, these changes would probably not be as distinct in the open-circuit voltage of an actual transformer.

SP1.6-1 Use the plot of λ in Fig. 1.6-3 to approximate $|\tilde{I}_1 + \tilde{I}_2'|$. [$|\tilde{I}_1 + \tilde{I}_2'| \cong \frac{1}{2}$A]

SP1.6-2 Calculate, using reasonable approximations, the phase angle between the steady-state current $\tilde{I}_1$ and voltage $\tilde{V}_1$ for the conditions of Fig. 1.6-3. Check your answer from the plots. [$\tilde{V}_1$ leads $\tilde{I}_1$ by 42.8°]

SP1.6-3 Consider the transformer given in Example 1D. Assume $V_1 = \sqrt{2}\,110 \cos 1000t$, and a load is connected across winding 2. The impedance of this load referred to winding 1 is $21 + j5\,\Omega$. Calculate $\tilde{I}_2'$. Make valid approximations to reduce your work. [$\tilde{I}_2' \cong -2.4\underline{/-45°}$]

1.7 MAGNETIC SYSTEMS WITH MECHANICAL MOTION

In Chapter 2, relationships are derived for determining the electromagnetic force or torque established in electromechanical systems. Once this development is completed, three examples of elementary electromechanical systems are considered. It is convenient to introduce these three systems here for the purpose of establishing the voltage equations and expressions for the self- and mutual inductances, thereby setting the stage for the analysis to follow in Chapter 2. The first of these electromechanical systems is an elementary version of an electromagnet. It consists of a magnetic core, part of which is movable. The electric system exerts an electromagnetic force upon this movable member, thereby moving it relative to the stationary member. We shall analyze this device, and in Chapter 2 we shall observe its operating characteristics by computer traces. The second system is a rotational device commonly referred to as a reluctance machine. A large number of stepper motors operate on the reluctance-torque principle. The third device is also a rotational device that has two windings: one on the stationary member and one on the rotational member. This device, although somewhat impracticable, illustrates the concept of windings or magnetic systems in relative motion.

Elementary Electromagnet

An elementary electromagnet that we will consider is shown in Fig. 1.7-1. This system consists of a stationary core with a winding of N turns and a block of magnetic material that is free to slide relative to the stationary member. It is shown in more detail in Chapter 2, wherein a spring, a damper, and an external force are associated with the movable member. We do not need to consider that level of detail here; instead, we will assume that the movable member is at a distance x from the stationary member, which may be a function of time, that is $x = x(t)$.

The voltage equation that describes the electric system is

$$v = ri + \frac{d\lambda}{dt} \tag{1.7-1}$$

where the flux linkages are expressed as

$$\lambda = N\Phi \tag{1.7-2}$$

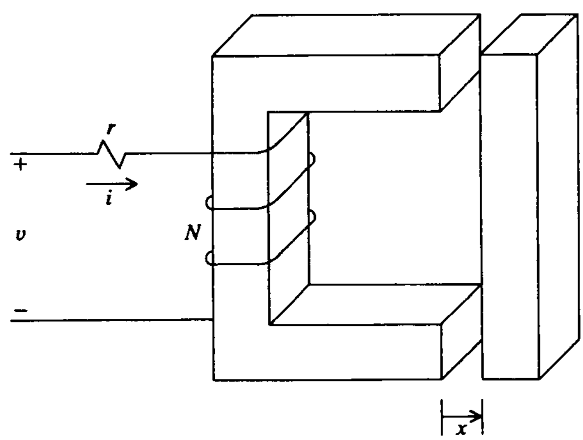

Figure 1.7-1: Elementary electromagnet.

The flux may be written as

$$\Phi = \Phi_l + \Phi_m \tag{1.7-3}$$

where Φ_l is the leakage flux and Φ_m is the magnetizing flux that is common to both the stationary and movable members. If the magnetic system is considered to be linear (saturation neglected), then, as in the case of the stationary coupled circuits, we can express the fluxes in terms of reluctances. That is,

$$\Phi_l = \frac{Ni}{\Re_l} \tag{1.7-4}$$

$$\Phi_m = \frac{Ni}{\Re_m} \tag{1.7-5}$$

where $\Re_l$ and $\Re_m$, are the reluctances of the leakage and magnetizing paths, respectively.

The flux linkages may now be written as

$$\lambda = \left(\frac{N^2}{\Re_l} + \frac{N^2}{\Re_m}\right) i \tag{1.7-6}$$

where the leakage inductance is

$$L_l = \frac{N^2}{\Re_l} \tag{1.7-7}$$

and the magnetizing inductance is

$$L_m = \frac{N^2}{\Re_m} \tag{1.7-8}$$

The reluctance of the magnetizing path is

$$\Re_m = \Re_i + 2\Re_g \tag{1.7-9}$$

where $\Re_i$ is the total reluctance of the magnetic material of the stationary and movable members and $\Re_g$ is the reluctance of one of the air gaps. If the cross-sectional area of the stationary and movable members is assumed to be equal and of the same material, the reluctances may be expressed as

$$\Re_i = \frac{l_i}{\mu_{ri}\mu_0 A_i} \tag{1.7-10}$$

$$\Re_g = \frac{x}{\mu_0 A_g} \tag{1.7-11}$$

We will assume that $A_g = A_i$. Even though, as we have mentioned previously, this may be somewhat of an oversimplification, it is sufficient for our purposes. Hence, $\Re_m$ may be written as

$$\Re_m = \frac{1}{\mu_0 A_i}\left(\frac{l_i}{\mu_{ri}} + 2x\right) \tag{1.7-12}$$

The magnetizing inductance now becomes

$$L_m = \frac{N^2}{(1/\mu_0 A_i)(l_i/\mu_{ri} + 2x)} \tag{1.7-13}$$

In this analysis, the leakage inductance is assumed to be constant. The magnetizing inductance is clearly a function of displacement. That is, $x = x(t)$ and $L_m = L_m(x)$. Heretofore, when dealing with linear magnetic circuits wherein mechanical motion is not present as in the case of a transformer, the change of flux linkages with respect to time was simply $L(di/dt)$. This is not the case here. When the inductance is a function of $x(t)$

$$\lambda(i, x) = L(x)i = [L_l + L_m(x)]i \tag{1.7-14}$$

and

$$\frac{d\lambda(i,x)}{dt} = \frac{\partial\lambda}{\partial i}\frac{di}{dt} + \frac{\partial\lambda}{\partial x}\frac{dx}{dt} \tag{1.7-15}$$

With (1.7-15) in mind, we see that the voltage equation (1.7-1) becomes

$$v = ri + [L_l + L_m(x)]\frac{di}{dt} + i\frac{dL_m(x)}{dx}\frac{dx}{dt} \tag{1.7-16}$$

Equation (1.7-16) is a nonlinear differential equation owing to the last two terms on the right-hand side.

Let us go back to the magnetizing inductance L_m as given by (1.7-13), for just a moment. In preparation for our work in Chapter 2, let us write (1.7-13) as

$$L_m(x) = \frac{k}{k_0 + x} \tag{1.7-17}$$

where

$$k = \frac{N^2 \mu_0 A_i}{2} \tag{1.7-18}$$

$$k_0 = \frac{l_i}{2\mu_{ri}} \tag{1.7-19}$$

When $x = 0$, $L_m(x)$ is determined by the reluctance of the magnetic material. That is, for $x = 0$,

$$L_m(0) = \frac{k}{k_0} = \frac{N^2 \mu_0 \mu_{ri} A_i}{l_i} \tag{1.7-20}$$

Depending upon the parameters of the magnetic material, $L_m(x)$ may be adequately predicted by

$$L_m(x) = \frac{k}{x} \quad \text{for } x > 0 \tag{1.7-21}$$

We will use this approximation in Chapter 2.

Elementary Reluctance Machine

An elementary reluctance machine is shown in Fig. 1.7-2. It consists of a stationary core with a winding of N turns and a movable member that rotates at an angular displacement and angular velocity of θ_r and ω_r, respectively. The displacement is defined as

$$\theta_r = \omega_r t + \theta_r(0) \tag{1.7-22}$$

The voltage equation is of the form given by (1.7-1). Similarly, the flux may be divided into a leakage and magnetizing flux, as given by (1.7-3). It is convenient to express the flux linkages as

$$\lambda = (L_l + L_m)i \tag{1.7-23}$$

where L_l is the leakage inductance and L_m is the magnetizing inductance. The leakage inductance is essentially constant, independent of θ_r; however, the magnetizing inductance is a periodic function of θ_r. That is, $L_m = L_m(\theta_r)$. In particular, with $\theta_r = 0$,

$$L_m(0) = \frac{N^2}{\Re_m(0)} \tag{1.7-24}$$

Here, the reluctance of the magnetizing path $\Re_m$ is maximum due to the large air gap when the rotor is in the vertical (unaligned) position. Hence, L_m is a minimum in this position. Note that this same situation occurs not only at $\theta_r = 0$ but also when $\theta_r = \pi, 2\pi$, and so on.

Now, with $\theta_r = \frac{1}{2}\pi$

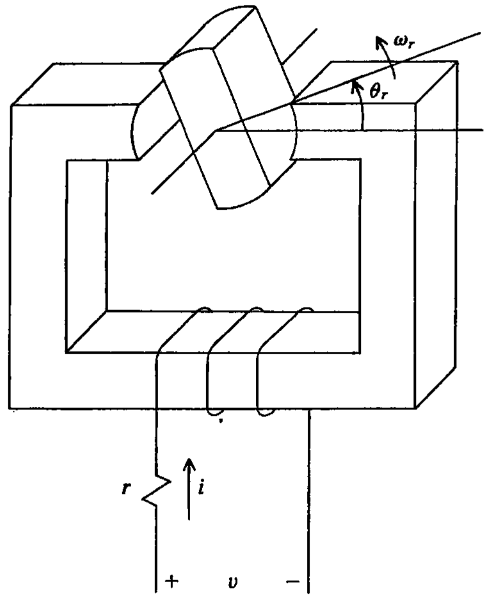

Figure 1.7-2: Elementary reluctance machine.

$$L_m(\tfrac{1}{2}\pi) = \frac{N^2}{\Re_m(\tfrac{1}{2}\pi)} \tag{1.7-25}$$

Here, $\Re_m$ is a minimum and, thus, L_m is a maximum. This same situation occurs at $\theta_r = \frac{3}{2}\pi$, $\frac{5}{2}\pi$, and so on. Hence, the magnetizing inductance varies between maximum and minimum positive values twice per revolution of the rotating member (rotor). Let us make it easy for ourselves and assume that this variation may be adequately approximated by a sinusoidal function. In particular, let $L_m(\theta_r)$ be expressed as

$$L_m(\theta_r) = L_A - L_B \cos 2\theta_r \tag{1.7-26}$$

whereupon

$$L_m(0) = L_A - L_B \tag{1.7-27}$$

$$L_m(\tfrac{1}{2}\pi) = L_A + L_B \tag{1.7-28}$$

and $L_A > L_B$. The average value is L_A is illustrated in Fig. 1.7-3. The self-inductance may now be expressed as

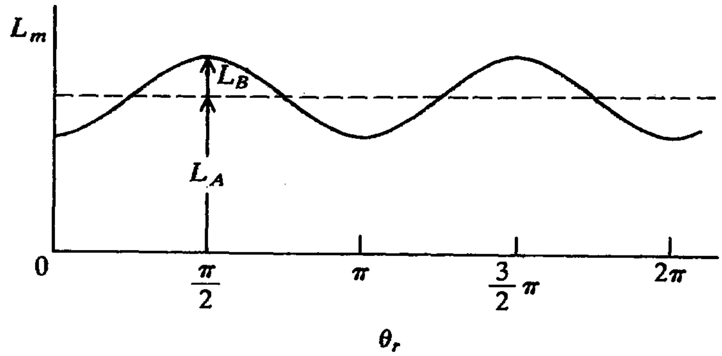

Figure 1.7-3: Approximation of magnetizing inductance of an elementary reluctance machine.

$$L(\theta_r) = L_l + L_m(\theta_r)$$
$$= L_l + L_A - L_B \cos 2\theta_r \tag{1.7-29}$$

The voltage equation is of the form given by (1.7-16) with x replaced by θ_r.

Windings in Relative Motion

The rotational device shown in Fig. 1.7-4 will be used to illustrate windings in relative motion. This device consists of two windings each containing several turns of a conductor. Winding 1 has N_1 turns and it is on the stationary member (stator); winding 2 has N_2 turns and it is on the rotating member (rotor). The $\otimes$ indicates that the assumed direction of positive current flow in the conductors is into the paper, whereas $\odot$ indicates positive current flow in the conductors is out of the paper. In a practical device, the turns of a winding are distributed over an arc (often 30 to 60°) of the stator and rotor. However, in this introductory consideration, it is sufficient to assume that the turns are concentrated in one position, as shown in Fig. 1.7-4. Also, the length of the air gap between the stator and rotor is shown exaggerated relative to the inside diameter of the stator.

The voltage equations may be written as

$$v_1 = r_1 i_1 + \frac{d\lambda_1}{dt} \tag{1.7-30}$$

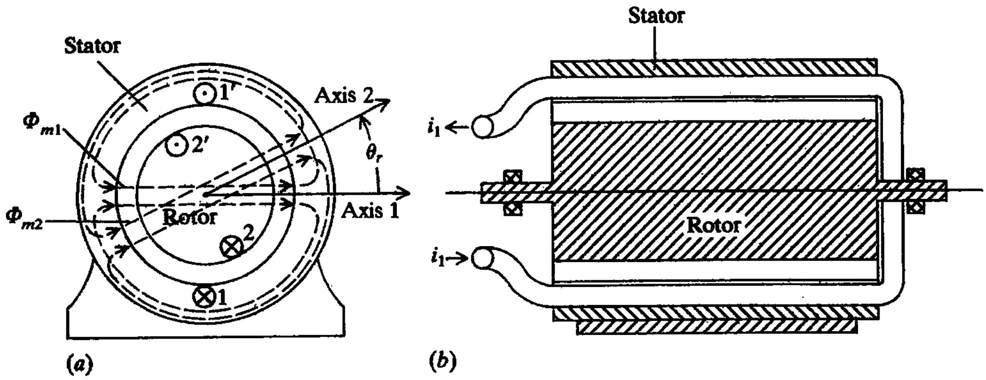

Figure 1.7-4: Elementary rotational electromechanical device. (a) end view; (b) cross-sectional view.

$$v_2 = r_2 i_2 + \frac{d\lambda_2}{dt} \tag{1.7-31}$$

where r_1 and r_2 are the resistances of winding 1 and winding 2, respectively. The magnetic system is assumed linear; therefore, the flux linkages may be expressed as

$$\lambda_1 = L_{11} i_1 + L_{12} i_2 \tag{1.7-32}$$

$$\lambda_2 = L_{21} i_1 + L_{22} i_2 \tag{1.7-33}$$

The self-inductances L_{11} and L_{22} are constants and may be expressed in terms of leakage and magnetizing inductances as

$$\begin{aligned} L_{11} &= L_{l1} + L_{m1} \\ &= \frac{N_1^2}{\Re_{l1}} + \frac{N_1^2}{\Re_m} \end{aligned} \tag{1.7-34}$$

$$\begin{aligned} L_{22} &= L_{l2} + L_{m2} \\ &= \frac{N_2^2}{\Re_{l2}} + \frac{N_2^2}{\Re_m} \end{aligned} \tag{1.7-35}$$

where $\Re_m$ is the reluctance of the complete magnetic path of Φ_{m1} and Φ_{m2}, which is through the rotor and stator iron and twice across the air gap. Clearly, it is the same for the magnetic system established by either winding 1 or winding 2.

Take a moment to note the designation of axis 1 and axis 2 in Fig. 1.7-4. These axes denote the positive direction of the respective magnetic systems with the assumed positive direction of current flow in the windings (right-hand rule). Now let us consider L_{12}. (Is it clear that $L_{12} = L_{21}$?) When θ_r, which is defined by (1.7-22), is zero, then the coupling between windings 1 and 2 is maximum. In particular, with $\theta_r = 0$ the magnetic system of winding 1 aids that of winding 2 with positive currents assumed. Hence, the mutual inductance is positive and

$$L_{12}(0) = \frac{N_1 N_2}{\Re_m} \tag{1.7-36}$$

When $\theta_r = \frac{1}{2}\pi$, the windings are orthogonal. The mutual coupling is zero. Hence,

$$L_{12}\left(\tfrac{1}{2}\pi\right) = 0 \tag{1.7-37}$$

Again let us make it as simple as possible by assuming that the mutual inductance may be adequately predicted by

$$L_{12}(\theta_r) = L_{sr} \cos \theta_r \tag{1.7-38}$$

where L_{sr} is the amplitude of the sinusoidal mutual inductance between the stator and rotor windings as given by (1.7-36).

In writing the voltage equations from (1.7-30) and (1.7-31) the total derivative of the flux linkages is required. This is accomplished by taking the partial derivative of both λ_1 and λ_2 with respect to i_1, i_2, and θ_r. Writing these voltage equations is a problem at the end of the chapter.

SP1.7-1 Let $L_m(x) = k/x$, $i = t$, and $x = t$. Express $d[L_m(x)i]/dt$. [Zero]

SP1.7-2 Express $L(\theta_r)$ of the elementary reluctance machine if minimum reluctance occurs at $\theta_r = 0$. [$L(\theta_r) = L_l + L_A + L_b \cos 2\theta_r$]

SP1.7-3 Express L_{11}, L_{22}, and L_{12} if positive i_2 is reversed from that shown in Fig. 1.7-4. [L_{11} and L_{22} are unchanged; $L_{12} = -L_{sr} \cos \theta_r$]

SP1.7-4 Consider Fig. 1.7-4. $I_1 = 1$ A, $L_{sr} = 0.1$ H, $\omega_r = 100$ rad/s, $\theta_r(0) = 0$, and winding 2 is open-circuited. Express V_2. [$V_2 = -10 \sin 100t$]

1.8 RECAPPING

We will analyze electromechanical motion devices from the coupled-circuits viewpoint. Although the coupled windings of many electromechanical devices are in relative motion, the equivalent circuit of stationary coupled windings (the transformer) is the beginning of the equivalent circuits that we will develop for these devices in later chapters. We will find the concept of referring variables from one winding to the other very useful as we proceed.

The first step in the analysis of electromechanical motion devices of the electromagnetic type is to express the voltage and flux linkage equations in terms of self- and mutual inductances. We will not consider saturation in our analysis; instead we will restrict our work to linear magnetic systems and leave the analytical treatment of saturation to a more advanced study of these devices. In this chapter, we learned that electromagnetic, electromechanical motion devices are characterized by self- or mutual inductances that vary with displacement of the movable member.

In the next chapter, we will first develop an analytical means of determining the electromagnetic force or torque in electromechanical motion devices. Once we have accomplished this, we will be able to express the electromagnetic force in the elementary electromagnet and the electromagnetic torque in the elementary rotational devices that we have just considered.

1.9 REFERENCES

[1] G. R. Slemon and A. Straughen, *Electric Machines,* Addison-Wesley Publishing Company, Reading, Mass., 1980.

[2] P. C. Krause, *Analysis of Electric Machinery,* McGraw-Hill Book Company, New York, 1986.

1.10 PROBLEMS

In all Problems sections, the more lengthy or involved problems are denoted by an asterisk.

1. Consider the magnetic system shown in Fig. 1.3-1. Let $\mu_r = 1500$, $N = 100$ turns, and $i = 2$ A. The cross section of the iron is square,

each side 4 cm in length. The air gap is 4 mm in length. The mean length of the iron is 200 times the air gap length. Neglect leakage flux and assume $A_i = A_g$. Calculate the flux.

2. Repeat Example 1B with a second air gap of 2 mm in length cut midway between c and d. Neglect leakage flux and assume $A_i = A_g$.

3. An iron-core transformer that has two windings is shown in Fig. 1.10-1. $N_1 = 50$ turns, $N_2 = 100$ turns, and $\mu_r = 4000$. Calculate L_{12}, L_{m1}, and L_{m2}.

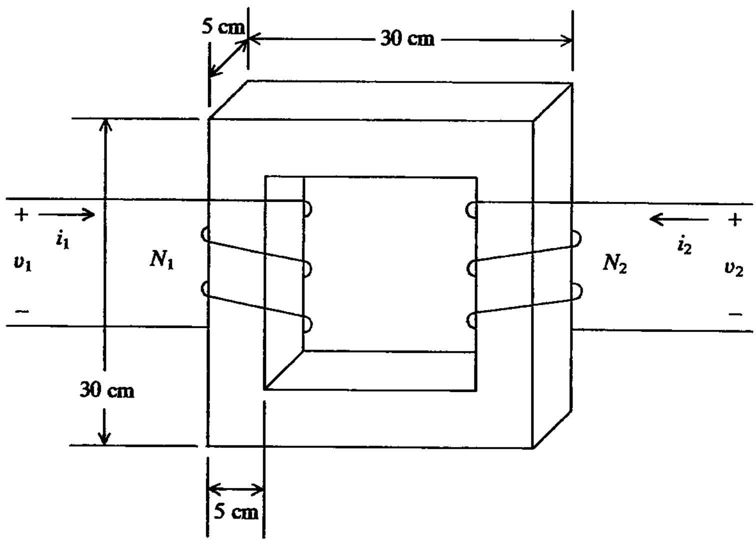

Figure 1.10-1: A two-winding iron-core transformer.

4. An iron "doughnut" (toroid) with two coils is shown in Fig. 1.10-2. $N_1 = 100$ turns and $N_2 = 200$ turns, $\mu_r = 10^4/4\pi$. Calculate L_{12}.

5. An air gap is cut through the left leg of the magnetic system shown in Fig. 1C-1 so that the associated reluctance is $10\,\Re_y$ rather than $\Re_y$. Express L_{12} and L_{21} in terms of N_1, N_2, $\Re_x$, and $\Re_y$.

6. Two coupled coils have the following parameters: $r_1 = 10\,\Omega$, $L_{l1} = 0.1\,L_{11}$, $r_2 = 2.5\,\Omega$, $L_{l2} = 0.1\,L_{22}$, $L_{11} = 100\,\text{mH}$, $N_1 = 100$ turns, $L_{22} = 25\,\text{mH}$, $N_2 = 50$ turns. Develop an equivalent T circuit with (a) winding 1 as the reference winding and (b) winding 2 as reference winding.

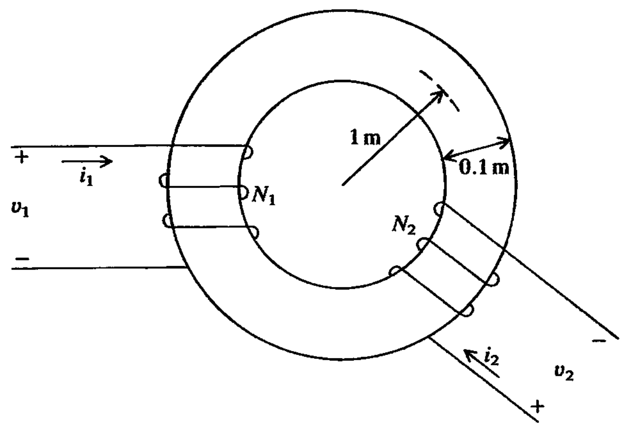

Figure 1.10-2: A two-winding iron-core toroid (not to scale).

7. Assume that the direction of positive current is reversed in winding 2 of Fig. 1.5-1. Express (a) L_{12} in terms of N_1, N_2, and $\Re_m$; (b) λ_1 and λ_2 in the form of (1.5-22) and (1.5-23); (c) λ_1 and λ_2' in the form of (1.5-31) and (1.5-32); and (d) v_1 and v_2' in the form of (1.5-37).

8. The parameters of a transformer are: $r_1 = r_2' = 10\,\Omega$, $L_{m1} = 300\,\text{mH}$, $L_{l1} = L_{l2}' = 30\,\text{mH}$. A 10-V peak-to-peak 30-Hz sinusoidal voltage is applied to winding 1. Winding 2 is short-circuited. Assume $i_1 = -i_2'$. Calculate the phasor $\tilde{I}_1$ with $\tilde{V}_1$ at zero degrees.

9. A transformer with two windings has the following parameters: $r_1 = r_2 = 1\,\Omega$, $L_{m1} = 1\,\text{H}$, $L_{l1} = L_{l2} = 0.01\,\text{H}$, $N_1 = N_2$. A 2-Ω load resistance R_L is connected across winding 2. $V_1 = 2 \cos 400t$. (a) Calculate $\tilde{I}_1$. (b) Express I_1.

10. A transformer with two windings has the following parameters: $r_1 = 1\,\Omega$, $L_{l1} = 0.01\,\text{H}$, $L_{m1} = 0.2\,\text{H}$, $N_2 = 2N_1$, $r_2 = 2\,\Omega$, $L_{l2} = 0.04\,\text{H}$, $L_{m2} = 0.08\,\text{H}$. A 4-Ω resistance R_L is connected across the terminals of winding 2 and a voltage $V_1 = \sqrt{2}\,2 \cos 400t$ is applied to winding 1. Calculate and draw the phasor diagram showing $\tilde{V}_1$, $\tilde{I}_1$, $\tilde{V}_2'$, and $\tilde{I}_2'$. Neglect the magnetizing current.

* 11. Consider the parameters of the transformer given in Example 1D. Calculate the input impedance measured from winding 1 with winding 2 short-circuited for (*a*) a dc source, (*b*) a 10-Hz source, and (*c*) a 400-Hz source. In each case, determine the input impedance first with the magnetizing current included and then with it neglected. The magnetizing current cannot be neglected as the frequency approaches zero. Why?

* 12. Analytically obtain the expression for i_1 in Figs. 1.6-1 and 1.6-2.

* 13. If, in Figs. 1.6-1 and 1.6-2, the resistance r_1 is zero, express i_1 for $t \geq 0$.

* 14. Determine the phase of v_1 in Fig. 1.6-3 in order to obtain the maximum offset i_1. Neglect the magnetizing current.

15. For the elementary electromagnet shown in Fig. 1.7-1, assume that the cross-sectional area of the stationary and movable member is the same and $A_i = A_g = 4\,\text{cm}^2$. Assume $l_i = 20$ cm, $N = 500$, and $\mu_{ri} = 1000$. Express $L_m(x)$ given by (1.7-17) and the approximation for $x > 0$ given by (1.7-21). Determine the minimum value of x when this approximate expression for $L_m(x)$ is less than 1.1 the value given by (1.7-17).

16. Express the voltage v of the elementary electromagnet given by (1.7-16) for $L_m(x)$ given by (1.7-17), $i = \sqrt{2}I_s \cos \omega_e t$ and $x = t$. Approximate v when t is large.

* 17. Express the voltage equation for the elementary reluctance machine shown in Fig. 1.7-2. Use (1.7-29) for $L(\theta_r)$.

18. Write the voltage equations for the coils in relative motion shown in Fig. 1.7-4. Use L_{11}, L_{22}, and L_{12} as expressed by (1.7-38).

Chapter 2

ELECTROMECHANICAL ENERGY CONVERSION

2.1 INTRODUCTION

The theory of electromechanical energy conversion is the cornerstone for the analysis of electrical motion devices. This theory allows us to express the electromagnetic force or torque in terms of device variables such as the currents and the displacement of the mechanical system. Since numerous types of electromechanical devices are used in motion systems, it is desirable to establish methods of analysis that may be applied to a variety of electromechanical devices rather than just to electric machines. Therefore, the theory of electromechanical energy conversion is set forth in considerable detail for the purpose of providing a background sufficient to analyze electromechanical systems other than just those treated in this text. The first part of this chapter is devoted to establishing analytically the relationships that can be used to express the electromagnetic force or torque. Although one may prefer to perform a separate derivation for each device because it is instructive to do so, a general set of formulas are given in tabular form that are applicable to a variety of electromechanical systems with a single mechanical input.

Once the theory of electromechanical energy conversion is established, a detailed analysis of the elementary electromagnet, which was introduced in Chapter 1, is performed with computer traces included to demonstrate its dynamic performance related to changes in the applied voltage and the external mechanical force. In the final sections, the expressions for the electromagnetic torque are developed for the elementary single-phase reluctance machine and for windings in relative motion. Brief discussions are given of several steady-state modes of operation of these devices, which help to illustrate, in an elementary form, the positioning of stepper motors and the operation of synchronous motors.

The material presented in this chapter is sufficient preparation to study dc machines covered in Chapter 3. However, Chapter 3 is not necessary for the analysis of electromechanical motion devices of the induction and synchronous types, which begins with Chapter 4.

2.2 ENERGY BALANCE RELATIONSHIPS

Electromechanical systems are comprised of an electric system, a mechanical system, and a means whereby the electric and mechanical systems can interact. Interctions can take place through any and all electromagnetic and electrostatic fields that are common to both systems, and energy is transferred from one system to the other as a result of this interaction. Both electrostatic and electromagnetic coupling fields may exist simultaneously and the electromechanical system may have any number of electric and mechanical subsystems. However, before considering an involved system, it is helpful to analyze the electromechanical system in a simplified form. An electromechanical system with one electric subsystem, one mechanical subsystem, and one coupling field is depicted in Fig. 2.2-1. Electromagnetic radiation is neglected, and it is assumed that the electric system operates at a frequency sufficiently low so that the electric system may be considered as a lumped-parameter system.

Figure 2.2-1: Block diagram of an elementary electromechanical system.

Heat loss will occur in the mechanical system due to friction, and the electric system will dissipate heat due to the resistance of the current-carrying conductors. Eddy current and hysteresis losses occur in the ferromagnetic materials, whereas dielectric losses occur in all electric fields. If W_E is the total energy supplied by the electric source and W_M the total energy supplied by the mechanical source, then the energy distribution could be expressed as

$$W_E = W_e + W_{eL} + W_{eS} \tag{2.2-1}$$

$$W_M = W_m + W_{mL} + W_{mS} \tag{2.2-2}$$

In (2.2-1), W_{eS} is the energy stored in the electric or magnetic fields, which are not coupled with the mechanical system. The energy W_{eL} is the heat loss associated with the electric system excluding the coupling field losses. This loss occurs due to the resistance of the current-carrying conductors as well as the energy dissipated in the form of heat owing to hysteresis, eddy currents, and dielectric losses external to the coupling field. The energy W_e is the energy transferred to the coupling field by the electric system. The energies common to the mechanical system may be defined in a similar manner. In (2.2-2), W_{mS} is the energy stored in the moving member and compliances of the mechanical system, W_{mL} is the energy loss of the mechanical system in the form of heat, and W_m is the energy transferred to the coupling field. It is important to note that, with the convention adopted, the energy transferred to the coupling field by either source is considered positive. Also, W_E (W_M) is negative when energy is supplied to the electric source (mechanical source).

If W_F is defined as the total energy transferred to the coupling field, then

$$W_F = W_f + W_{fL} \tag{2.2-3}$$

where W_f is energy stored in the coupling field and W_{fL} is the energy dissipated in the form of heat due to losses within the coupling field (eddy current, hysteresis, or dielectric losses). In order to comply with convention, we will use W_f to denote the energy stored in the coupling field rather than W_{fS}. The electromechanical system must obey the law of conservation of energy, thus,

$$W_f + W_{fL} = (W_E - W_{eL} - W_{eS}) + (W_M - W_{mL} - W_{mS}) \tag{2.2-4}$$

which may be written as

$$W_f + W_{fL} = W_e + W_m \tag{2.2-5}$$

This energy balance is shown schematically in Fig. 2.2-2.

The actual process of converting electric energy to mechanical energy (or vice versa) is independent of (1) the loss of energy in either the electric or the mechanical systems (W_{eL} and W_{mL}), (2) the energies stored in the electric

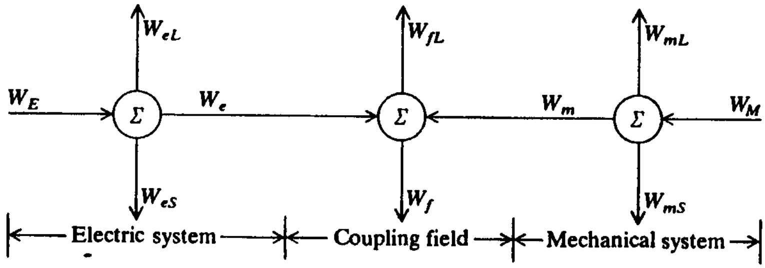

Figure 2.2-2: Energy balance.

or magnetic fields that are not common to both systems (W_{eS}), or (3) the energies stored in the mechanical system (W_{mS}). If the losses of the coupling field are neglected, then the field is conservative and (2.2-5) becomes

$$W_f = W_e + W_m \tag{2.2-6}$$

Examples of elementary electromechanical systems are shown in Figs. 2.2-3 and 2.2-4. The system shown in Fig. 2.2-3 has a magnetic coupling field, whereas the electromechanical system shown in Fig. 2.2-4 employs an electric field as a means of transferring energy between the electric and mechanical systems. In both systems, the space between the movable and stationary members is exaggerated for clarity. In these systems, v is the voltage of the electric source and f is an externally applied mechanical force. The electromagnetic or electrostatic force is denoted f_e. The resistance of the current-carrying conductor is denoted by r, with l denoting the inductance of a linear (conservative) electromagnetic system that does not couple the mechanical system. In the mechanical system, M is the mass of the movable member, and the linear compliance and damper are represented by a spring constant K and a damping coefficient D, respectively. The displacement x_0 is the zero force or equilibrium position of the mechanical system, which is the steady-state position of the mass with f_e and f equal to zero.

The voltage equation that describes the electric systems shown in Figs. 2.2-3 and 2.2-4, may be written as

$$v = ri + l\frac{di}{dt} + e_f \tag{2.2-7}$$

where e_f is the voltage drop due to the coupling field. The dynamic behavior of the translational mechanical systems may be expressed by employing

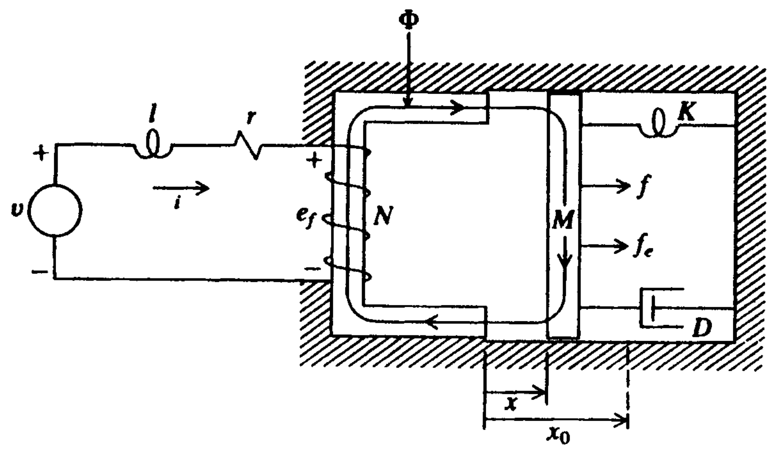

Figure 2.2-3: Electromechanical system with magnetic field.

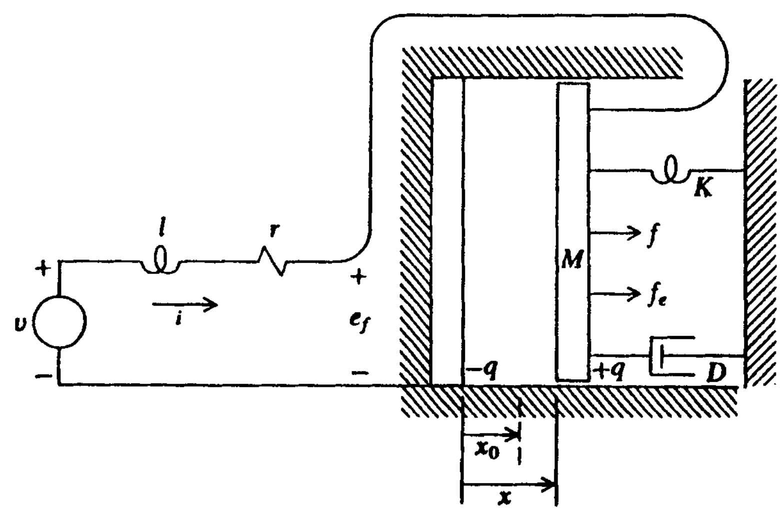

Figure 2.2-4: Electromechanical system with electric field.

Newton's law of motion. Thus,

$$f = M\frac{d^2x}{dt^2} + D\frac{dx}{dt} + K(x - x_0) - f_e \tag{2.2-8}$$

Since power is the time rate of energy transfer, the total energy supplied by the electric source is

$$W_E = \int vi dt \tag{2.2-9}$$

The total energy supplied by the mechanical source is

$$W_M = \int f dx \tag{2.2-10}$$

which may also be expressed as

$$W_M = \int f\frac{dx}{dt}dt \tag{2.2-11}$$

Substituting (2.2-7) into (2.2-9) yields

$$W_E = r\int i^2 dt + l\int i\frac{di}{dt}dt + \int e_f i dt \tag{2.2-12}$$

The first term on the right-hand side of (2.2-12) represents the energy loss due to the resistance of the conductors (W_{eL}). The second term represents the energy stored in the linear electromagnetic field external to the coupling field (W_{eS}). Therefore, the total energy transferred to the coupling field from the electric system is

$$W_e = \int e_f i dt \tag{2.2-13}$$

Similarly, for the mechanical system

$$W_M = M\int \frac{d^2x}{dt^2}dx + D\int (\frac{dx}{dt})^2 dt + K\int (x - x_0)dx - \int f_e dx \tag{2.2-14}$$

Here, the first and third terms on the right-hand side of (2.2-14) represent the kinetic energy stored in the mass and the potential energy stored in the spring, respectively. The sum of these two stored energies is W_{mS}. You should take a moment to look at the first term on the right-hand side of (2.2-14) and recognize that it can be written as $\frac{1}{2}M(dx/dt)^2$. The second term is the heat loss due to friction (W_{mL}). Thus, the total energy transferred to the coupling field from the mechanical system is

$$W_m = -\int f_e dx \tag{2.2-15}$$

It is important to note, from Figs. 2.2-3 and 2.2-4, that a positive force f_e is assumed to be in the same direction as a positive displacement dx. Substituting (2.2-13) and (2.2-15) into the energy balance relation, (2.2-6), yields

$$W_f = \int e_f i dt - \int f_e dx \tag{2.2-16}$$

The equations set forth may be readily extended to include an electromechanical system with any number of electric and mechanical inputs and any number of coupling fields. Considering the system shown in Fig. 2.2-5, the energy supplied to the coupling field may be expressed as

$$W_f = \sum_{j=1}^{J} W_{ej} + \sum_{k=1}^{K} W_{mk} \tag{2.2-17}$$

wherein J electric and K mechanical inputs exist. The total energy supplied to the coupling field from the electric inputs is

$$\sum_{j=1}^{J} W_{ej} = \int \sum_{j=1}^{J} e_{fj} i_j dt \tag{2.2-18}$$

The total energy supplied to the coupling field from the mechanical inputs is

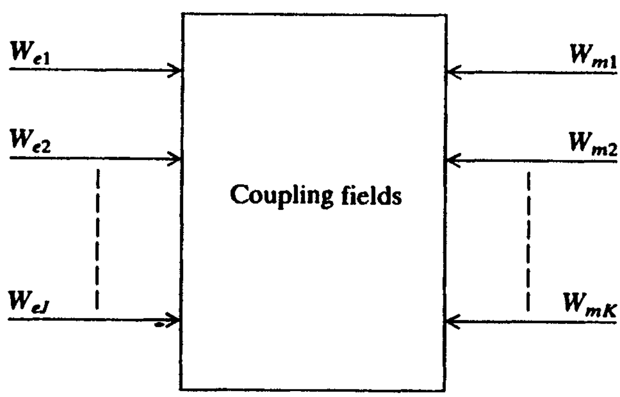

Figure 2.2-5: Multiple electric and mechanical inputs.

$$\sum_{k=1}^{K} W_{mk} = -\int \sum_{k=1}^{K} f_{ek} dx_k \tag{2.2-19}$$

In our analysis of electromechanical systems, we will consider devices with only one mechanical input, for example, the shaft of the electric machine or the moving arm of a magnetic relay. On the other hand, since ac and dc machines may have more than one electric terminal, it is necessary to consider systems with multiple electric inputs. In all cases, however, the multiple electric inputs have a common coupling field. Therefore, we need not become too ambitious in the following derivations. More specifically, hereafter we will restrict our analysis to electromechanical devices with only one mechanical input. Thus, the k subscript will be dropped from f_e, x, and W_m. This reduces our work considerably without restricting the practical application of our results. With one mechanical input, the energy balance equation becomes

$$W_f = \int \sum_{j=1}^{J} e_{fj} i_j dt - \int f_e dx \tag{2.2-20}$$

In differential form, which will be the form we will use extensively,

$$dW_f = \sum_{j=1}^{J} e_{fj} i_j dt - f_e dx \tag{2.2-21}$$

SP2.2-1 The current flowing in a 1-H inductor which is external to the coupling field is $i = kt + k_0$. Calculate W_{eS}, the energy stored in the inductor at $t = 1$ s. $[W_{eS} = \frac{1}{2}(k + k_0)^2]$

SP2.2-2 Express the undamped natural frequency of the mechanical system described by (2.2-8). $[\omega_n = (K/M)^{1/2}]$

SP2.2-3 Express the instantaneous power delivered to the inductor in SP2.2-1. $[P = k^2 t + k k_0]$

SP2.2-4 For two electric inputs, $e_{f1} = k_1 t$, $i_1 = k_0$, $e_{f2} = k_2 t^2$, and $i_2 = k_3 t$. Express the total energy supplied to the coupling field (W_e) in 2 s. $[W_e = 2k_0 k_1 + 4k_2 k_3]$

2.3 ENERGY IN COUPLING FIELD

Before using (2.2-21) to obtain an expression for the electromagnetic force f_e, it is necessary to derive an expression for the energy stored in the coupling field. Once we have an expression for W_f, we can take the total derivative to obtain dW_f, which can then be substituted into (2.2-21). When expressing the energy in the coupling field, it is convenient to neglect all losses associated with the electric or magnetic coupling field, whereupon the field is assumed to be conservative and the energy stored therein is a function of the state of the electrical and mechanical variables. Although the effects of the core losses of the coupling field may be functionally accounted for by appropriately introducing a resistance in the electric circuit, this refinement is generally not necessary since the ferromagnetic material is selected and arranged in laminations so as to minimize the hysteresis and eddy current losses. Moreover, most of the energy stored in the coupling field is stored in the air gap of the electromechanical device. Since air is a conservative medium, all of the energy stored therein can be returned to the electric or mechanical systems. Therefore, the assumption of a lossless coupling field is not as restrictive as it might first appear.

The energy stored in a conservative field is a function of the state of the system variables and not the manner in which the variables reached that state. It is convenient to take advantage of this feature when developing a mathematical expression for the field energy. In particular, it is convenient to fix mathematically the position of the mechanical system associated with the coupling field and then excite the electric system with the displacement of the mechanical system held fixed. During the excitation of the electric inputs, $dx = 0$, hence, W_m is zero even though electromagnetic or electrostatic forces may occur. Therefore, with the displacement held fixed, the energy stored in the coupling field during the excitation of the electric inputs is equal to the energy supplied to the coupling field by the electric inputs. Thus, with $dx = 0$, the energy supplied from the electric system may be expressed from (2.2-20) as

$$W_f = \int \sum_{j=1}^{J} e_{fj} i_j dt \quad \text{with } dx = 0 \tag{2.3-1}$$

Thus far in our discussion, we have considered both the electric and electromagnetic coupling fields. However, our primary interest is the electromagnetic system and, hereafter, we will direct our attention accordingly. Let us consider a singly excited electromagnetic system similar to that shown in Fig. 2.2-3. In this case, $e_f = d\lambda/dt$, whereupon (2.3-1) becomes

$$W_f = \int i d\lambda \quad \text{with } dx = 0 \tag{2.3-2}$$

Here $j = 1$; however, the subscript is omitted for the sake of brevity. The area to the left of the λi relationship, shown in Fig. 2.3-1 for a singly excited electromagnetic system, is the area described by (2.3-2). In Fig. 2.3-1, this area represents the energy stored in the field at the instant when $\lambda = \lambda_a$ and $i = i_a$. The λi relationship need not be linear; it need only be single-valued, a property that is characteristic of a conservative or lossless field. Moreover, since the coupling field is conservative, the energy stored in the field with $\lambda = \lambda_a$ and $i = i_a$ is independent of the excursion of the electrical and mechanical variables before reaching this state.

The area to the right of the λi curve is called the *coenergy* and can be

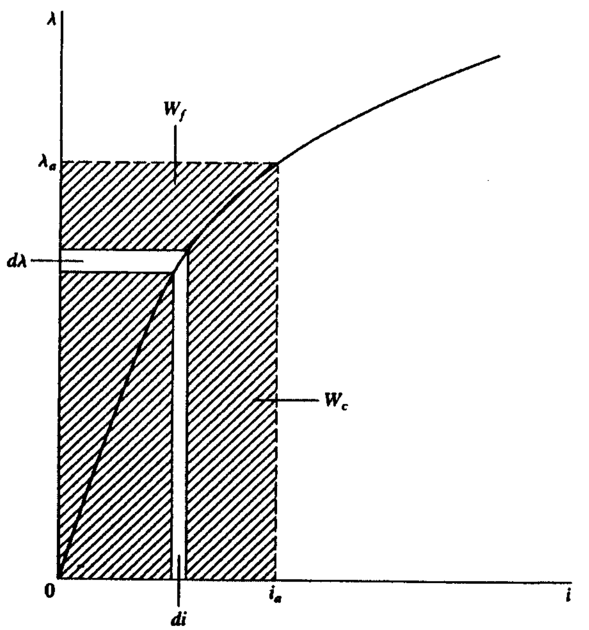

Figure 2.3-1: Stored energy and coenergy in a magnetic field of a singly excited electromagnetic device.

expressed as

$$W_c = \int \lambda di \quad \text{with } dx = 0 \tag{2.3-3}$$

Although the coenergy has little or no physical significance, we will find it a convenient quantity for expressing the electromagnetic force. From Fig. 2.3-1, we see that the sum of W_f and W_c is λ times i, that is,

$$\lambda i = W_c + W_f \tag{2.3-4}$$

which is also valid for multiple electric inputs, where λi in (2.3-4) is replaced by $\sum_{j=1}^{J} \lambda_j i_j$. It should be clear that, for a linear magnetic system where the λi plots are straight-line relationships, $W_f = W_c = \frac{1}{2}\lambda i$.

The displacement x defines completely the influence of the mechanical system upon the coupling field; however, since λ and i are related, only one is needed in addition to x in order to describe the state of the electromechanical system. Therefore, we can select either λ and x as independent variables or i and x. If i and x are selected as the independent variables, it is convenient to express the field energy and the flux linkages as

$$W_f = W_f(i,\ x) \tag{2.3-5}$$

$$\lambda = \lambda(i,\ x) \tag{2.3-6}$$

With i and x as independent variables, we must express $d\lambda$ in terms of di before substituting into (2.3-2). Thus, from (2.3-6),

$$d\lambda = \frac{\partial \lambda(i,x)}{\partial i} di + \frac{\partial \lambda(i,x)}{\partial x} dx \tag{2.3-7}$$

In the derivation of an expression for the energy stored in the field, dx is set equal to zero. Hence, in the evaluation of field energy where $dx = 0$, $d\lambda$ is equal to the first term on the right-hand side of (2.3-7). Substituting into (2.3-2) yields

$$\begin{aligned} W_f(i,\ x) &= \int i \frac{\partial \lambda(i,x)}{\partial i} di \\ &= \int_0^i \xi \frac{\partial \lambda(\xi,x)}{\partial \xi} d\xi \end{aligned} \tag{2.3-8}$$

where ξ is a dummy variable of integration. Evaluation of (2.3-8) gives the energy stored in the field of the singly excited system. The coenergy in terms of i and x may be evaluated from (2.3-3) as

$$\begin{aligned} W_c(i,\ x) &= \int \lambda(i,\ x)di \\ &= \int_0^i \lambda(\xi,\ x)d\xi \end{aligned} \tag{2.3-9}$$

With λ and x as independent variables

$$W_f = W_f(\lambda,\ x) \tag{2.3-10}$$

$$i = i(\lambda,\ x) \tag{2.3-11}$$

The field energy may be evaluated from (2.3-2) as

$$\begin{aligned} W_f(\lambda,\ x) &= \int i(\lambda,\ x)d\lambda \\ &= \int_0^\lambda i(\xi,\ x)d\xi \end{aligned} \tag{2.3-12}$$

To evaluate the coenergy with λ and x as independent variables, we need to express di in terms of $d\lambda$. Thus, from (2.3-11),

$$di = \frac{\partial i(\lambda, x)}{\partial \lambda} d\lambda + \frac{\partial i(\lambda, x)}{\partial x} dx \tag{2.3-13}$$

Since $dx = 0$ in this evaluation, (2.3-3) becomes

$$\begin{aligned} W_c(\lambda,\ x) &= \int \lambda \frac{\partial i(\lambda, x)}{d\lambda} d\lambda \\ &= \int_0^\lambda \xi \frac{\partial i(\xi, x)}{\partial \xi} d\xi \end{aligned} \tag{2.3-14}$$

For a linear electromagnetic system, the λi plots are straight-line relationships. Thus, for the singly excited magnetically linear system,

$$\lambda(i,\ x) = L(x)i \tag{2.3-15}$$

or

$$i(\lambda,\ x) = \frac{\lambda}{L(x)} \tag{2.3-16}$$

where $L(x)$ is the inductance. Let us evaluate $W_f(i,\ x)$. With $dx = 0$ and, since $\dfrac{\partial \lambda(i,\ x)}{\partial i} = L(x)$, (2.3-7) becomes

$$d\lambda = L(x)di \tag{2.3-17}$$

Hence, from (2.3-8),

$$W_f(i,\ x) = \int_0^i \xi L(x)d\xi = \frac{1}{2}L(x)i^2 \tag{2.3-18}$$

It is left to the reader to show that by a similar procedure $W_f(\lambda,\ x)$, $W_c(i,\ x)$, and $W_c(\lambda,\ x)$ are equivalent to (2.3-18) for this magnetically linear system.

The field energy is a state function and the expression describing the field energy in terms of system variables is valid regardless of the variations in the system variables. For example, (2.3-18) expresses the field energy regardless of the variations in $L(x)$ and i. The fixing of the mechanical system so as to obtain an expression for the field energy is a mathematical convenience and not a restriction upon the result.

In the case of a multiexcited electromagnetic system, an expression for the field energy may be obtained by evaluating the following relation with $dx = 0$:

$$W_f = \int \sum_{j=\mathrm{i}}^{J} i_j d\lambda_j \quad \text{with } dx = 0 \tag{2.3-19}$$

Since the coupling field is considered conservative, (2.3-19) may be evaluated independent of the order in which the flux linkages or currents are brought to their final values. To illustrate evaluation of (2.3-19) for a multiexcited system, we will allow the currents to establish their final states one at a time while all other currents are mathematically fixed either in their unexcited or final states. This procedure may be illustrated by considering a doubly excited electric system with one electrical input. An electromechanical system of this type could be constructed by placing a second winding, supplied from a second electric system, on either the stationary or movable member of the system shown in Fig. 2.2-3. In this evaluation, it is convenient to use currents and displacement as the independent variables. Hence, for a doubly excited electric system,

$$W_f(i_1,\ i_2,\ x) = \int [i_1 d\lambda_1(i_1,\ i_2,\ x) + i_2 d\lambda_2(i_1,\ i_2,\ x)] \quad \text{with } dx = 0 \tag{2.3-20}$$

In this determination of an expression for W_f, the mechanical displacement is held constant ($dx = 0$); thus (2.3-20) becomes

$$\begin{aligned} W_f(i_1,\ i_2,\ x) = \int i_1 &\left[\frac{\partial\lambda_1(i_1,i_2,x)}{\partial i_1}di_1 + \frac{\partial\lambda_1(i_1,i_2,x)}{\partial i_2}di_2\right] \\ +i_2 &\left[\frac{\partial\lambda_2(i_1,i_2,x)}{\partial i_1}di_1 + \frac{\partial\lambda_2(i_1,i_2,x)}{\partial i_2}di_2\right] \end{aligned} \tag{2.3-21}$$

We will evaluate the energy stored in the field by employing (2.3-21) twice. First, we will mathematically increase the current i_1 from zero to its desired final value while holding i_2 at zero. Thus, i_1 is the variable of integration and $di_2 = 0$. Energy is supplied to the coupling field from the source connected to winding 1. As the second evaluation of (2.3-21), i_2 is increased from zero to its desired final value while maintaining i_1 at the value attained in the preceding step. Hence, i_2 is the variable of integration and $di_1 = 0$. During this time, energy is supplied from both sources to the coupling field since $i_1 d\lambda_1$ is, in general, nonzero. The total energy stored in the coupling field is the sum of the two evaluations. Following this two-step procedure, the evaluation of (2.3-21) for the total field energy becomes

$$\begin{aligned} W_f(i_1,\ i_2,\ x) = &\int i_1\frac{\partial\lambda_1(i_1,0,x)}{\partial i_1}di_1 \\ &+ \int\left[i_1\frac{\partial\lambda_1(i_1,i_2,x)}{\partial i_2}di_2 + i_2\frac{\partial\lambda_2(i_1,i_2,x)}{\partial i_2}di_2\right] \end{aligned} \tag{2.3-22}$$

which should be written

$$\begin{aligned} W_f(i_1,\ i_2,\ x) = &\int_0^{i_1} \xi\frac{\partial\lambda_1(\xi,0,x)}{\partial \xi}d\xi \\ &+ \int_0^{i_2}\left[i_1\frac{\partial\lambda_1(i_1,\xi,x)}{\partial \xi} + \xi\frac{\partial\lambda_2(i_1,\xi,x)}{\partial \xi}d\xi\right] \end{aligned} \tag{2.3-23}$$

The first integral on the right-hand side of (2.3-22) or (2.3-23) results from the first step of the evaluation with i_1 as the variable of integration and with $i_2 = 0$ and $di_2 = 0$. The second integral comes from the second step of the evaluation with i_1 equal to its final value ($di_1 = 0$) and i_2 as the variable of integration. The order of allowing the currents to reach their final state is irrelevant; that is, as our first step, we could have made i_2 the variable of integration while holding i_1 at zero ($di_1 = 0$) and then let i_1 become the variable of integration while holding i_2 at its final value. The results would be the same. For three electric inputs, the evaluation procedure would require three steps, one for each current to be brought mathematically to its final state.

Let us now evaluate the energy stored in a magnetically linear system with two electric inputs and one mechanical input. For this, let

$$\lambda_1(i_1,\ i_2,\ x) = L_{11}(x)i_1 + L_{12}(x)i_2 \tag{2.3-24}$$

$$\lambda_2(i_1,\ i_2,\ x) = L_{21}(x)i_1 + L_{22}(x)i_2 \tag{2.3-25}$$

where the self-inductances $L_{11}(x)$ and $L_{22}(x)$ include the leakage inductances. With the mechanical displacement held constant ($dx = 0$),

$$d\lambda_1(i_1,\ i_2,\ x) = L_{11}(x)di_1 + L_{12}(x)di_2 \tag{2.3-26}$$

$$d\lambda_2(i_1,\ i_2,\ x) = L_{12}(x)di_1 + L_{22}(x)di_2 \tag{2.3-27}$$

The coefficients on the right-hand side of (2.3-26) and (2.3-27) are the partial derivatives. For example, $L_{11}(x)$ is the partial derivative of $\lambda_1(i_1,\ i_2,\ x)$ with respect to i_1. Appropriate substitution into (2.3-23) gives

$$W_f(i_1,\ i_2,\ x) = \int_0^{i_1} \xi L_{11}(x)d\xi + \int_0^{i_2} \left[i_1 L_{12}(x) + \xi L_{22}(x)\right] d\xi \tag{2.3-28}$$

which yields

$$W_f(i_1,\ i_2,\ x) = \frac{1}{2}L_{11}(x)i_1^2 + L_{12}(x)i_1 i_2 + \frac{1}{2}L_{22}(x)i_2^2 \tag{2.3-29}$$

It follows that the total field energy of a linear electromagnetic system with J electric inputs may be expressed as

$$W_f(i_1,\ \ldots,\ i_J,\ x) = \frac{1}{2}\sum_{p=1}^{J}\sum_{q=1}^{J} L_{pq} i_p i_q \tag{2.3-30}$$

Example 2A. Consider the magnetic system described by

$$\lambda(i, x) = (0.1 + kx^{-1})i \tag{2A-1}$$

Calculate W_f and W_c. Here, it is convenient to work with i and x as independent variables. Thus, from (2.3-8),

$$W_f = \int_0^{i} \xi(0.1 + kx^{-1})d\xi = \frac{1}{2}(0.1\ + kx^{-1})i^2 \tag{2A-2}$$

From (2.3-9),

$$W_c = \int_0^i (0.1 + kx^{-1})\xi d\xi = \frac{1}{2}(0.1 + kx^{-1})i^2 \tag{2A-3}$$

We see that $W_f = W_c$. Did you recognize the fact that this is a linear magnetic system with

$$L(x) = 0.1 + kx^{-1} \tag{2A-4}$$

where the first term on the right-hand side is analogous to the leakage inductance and kx^{-1} is the magnetizing inductance of the electromagnet treated in Chapter 1.

Let us make it a nonlinear system; in particular, let

$$\lambda(i,\ x) = (0.1\ + kx^{-1})i^2 \tag{2A-5}$$

From (2.3-8),

$$W_f = \int_0^i \xi 2(0.1 + kx^{-1})\xi d\xi = \frac{2}{3}(0.1 + kx^{-1})i^3 \tag{2A-6}$$

From (2.3-9),

$$W_c = \int_0^i (0.1 + kx^{-1})\xi^2 d\xi = \frac{1}{3}(0.1 + kx^{-1})i^3 \tag{2A-7}$$

We see that W_f and W_c are not equal; however, according to (2.3-4),

$$\lambda i = W_f + W_c \tag{2A-8}$$

Let us show that this is true.

$$[(0.1 + kx^{-1})i^2]i = \frac{2}{3}(0.1 + kx^{-1})i^3 + \frac{1}{3}(0.1 + kx^{-1})i^3$$

$$(0.1\ + kx^{-1})i^3 = (0.1 + kx^{-1})i^3 \tag{2A-9}$$

SP2.3-1 $\lambda = kx^2 i$. Calculate W_f and W_c when $kx^2 = 1$ V·s/A and $i = 2$ A. [$W_f = W_c = 2$ J]

SP2.3-2 $\lambda = kxi^2$. Calculate W_f and W_c when $kx = 1$ V·s/A^2 and $i = 2$ A. [$W_f = \frac{16}{3}$ J; $W_c = \frac{8}{3}$ J]

SP2.3-3 The current is increased from 2 to 3 A in SP2.3-2. Calculate the change in W_f and W_c. [$\Delta W_f = \frac{38}{3}$ J; $\Delta W_c = \frac{19}{3}$ J]

SP2.3-4 $i = b(x)\lambda^2$. Express $W_f(\lambda,\ x)$ and $W_c(\lambda,\ x)$. [$W_f(\lambda,\ x) = \frac{1}{3}b(x)\lambda^3$; $W_c(\lambda,\ x) = \frac{2}{3}b(x)\lambda^3$]

2.4 GRAPHICAL INTERPRETATION OF ENERGY CONVERSION

Before proceeding to the derivation of expressions for the electromagnetic force, it is instructive to consider briefly a graphical interpretation of the energy conversion process. For this purpose, let us again refer to the elementary system shown in Fig. 2.2-3 and assume that as the movable member moves from $x = x_a$ to $x = x_b$, where $x_b < x_a$, the λi characteristics are given by Fig. 2.4-1. Let us furthermore assume that, as the member moves from x_a to x_b, the λi trajectory moves from point A to point B. The exact trajectory from A to B is determined by the combined dynamics of the electrical and mechanical systems, and any variation in v and f which may occur. Now, the area $0AC0$ represents the original energy stored in the coupling field; area $0BD0$ represents the final energy stored in the field. Therefore, the change in field energy is

$$\Delta W_f = \text{area } 0BD0 - \text{area } 0AC0 \tag{2.4-1}$$

The change in W_e, denoted as ΔW_e, is

$$\Delta W_e = \int_{\lambda_A}^{\lambda_B} i d\lambda = \text{area } CABDC \tag{2.4-2}$$

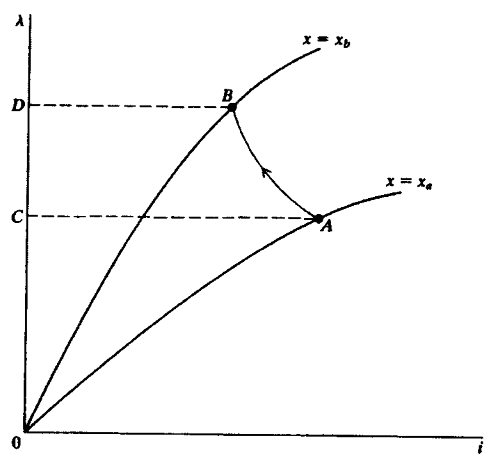

Figure 2.4-1: Graphical representation of electromechanical energy conversion for λi path A to B.

From (2.2-6),

$$\Delta W_m = \Delta W_f - \Delta W_e \tag{2.4-3}$$

Hence, by adding and subtracting the appropriate areas in Fig. 2.4-1, we can obtain ΔW_m. In particular,

$$\begin{aligned}\Delta W_m &= \text{area } 0BD0 - \text{area } 0AC0 - \text{area } CABDC \\ &= -\text{area } 0AB0 \end{aligned} \tag{2.4-4}$$

The energy contributed to the coupling field from the mechanical system ΔW_m is negative. Energy has been supplied to the mechanical system from the coupling field, part of which came from the energy stored in the field, and part of which came from the electric system. If the member is now moved back to x_a, the λi trajectory may be as shown in Fig. 2.4-2. Here, ΔW_m is still area $0AB0$, but it is positive, which means that energy was supplied from the mechanical system to the coupling field, part of which is stored in the field and part of which is transferred to the electric system.

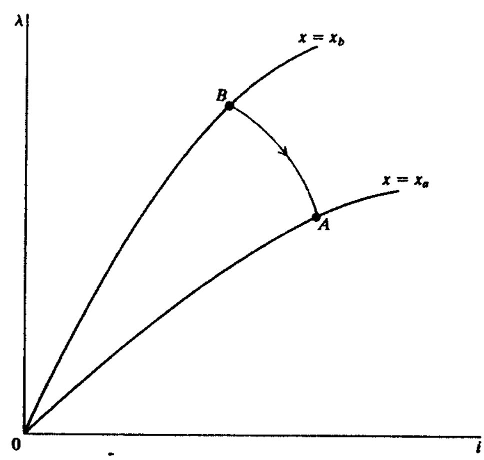

Figure 2.4-2: Graphical representation of electromechanical energy conversion for λi path B to A.

The energy supplied by the mechanical system during the motion from B to A (area $0AB0$ in Fig. 2.4-2) is larger than the energy supplied to the mechanical system during the original motion from A to B (area $0AB0$ in Fig. 2.4-1). Therefore, the net energy supplied by the mechanical system for the complete cycle is positive. The net ΔW_m for the cycle from A to B

back to A is the shaded area shown in Fig. 2.4-3. Since the coupling field energy at point A is uniquely determined from the mechanical displacement and current at point A, the net change in field energy is zero as we move from A to B and back to A. Since ΔW_f is zero for this cycle,

$$\Delta W_m = -\Delta W_e \tag{2.4-5}$$

For the cycle shown, the net ΔW_e is negative since the magnitude of the change in W_e is larger when we went from B to A than from A to B, and ΔW_e is negative from B to A. If the trajectory had been in the counterclockwise direction, the net ΔW_e would have been positive and the net ΔW_m negative.

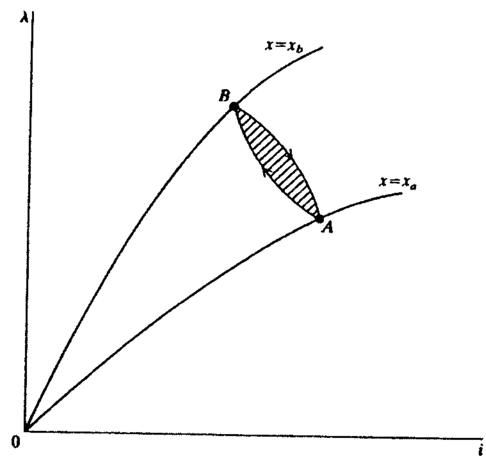

Figure 2.4-3: Graphical representation of electromechanical energy conversion for λi path A to B to A.

SP2.4-1 $\lambda = a(x)i^2$. The current is held constant at 2 A while $a(x)$ increases from 1 to 2. Calculate ΔW_m. [$\Delta W_m = -\frac{8}{3}$ J]

SP2.4-2 Repeat SP2.4-1 if it were possible for $a(x)$ to instantaneously increase from 1 to 2 while λ is held constant at 4 V·s followed by a current increase back to 2 A with $a(x) = 2$ (λ must change accordingly). [$\Delta W_m = \dfrac{-16 + 8\sqrt{2}}{3}$ J]

2.5 ELECTROMAGNETIC AND ELECTROSTATIC FORCES

The stage is set for us to obtain expressions for the electromagnetic and electrostatic forces in electromechanical devices. We will focus on electromagnetic devices. For this purpose, recall that e_{fj} in (2.2-21) may be expressed as

$$e_{fj} = \frac{d\lambda_j}{dt} \tag{2.5-1}$$

If we substitute (2.5-1) into (2.2-21) and if we solve for $f_e dx$, we obtain

$$f_e dx = \sum_{j=1}^{J} i_j d\lambda_j - dW_f \tag{2.5-2}$$

Although we will use (2.5-2), it is helpful to express (2.5-2) in an alternative form. For this purpose, let us first write (2.3-4) for multiple electrical inputs:

$$\sum_{j=1}^{J} \lambda_j i_j = W_c + W_f \tag{2.5-3}$$

If we take the total derivative of (2.5-3), we obtain

$$\sum_{j=1}^{J} \lambda_j di_j + \sum_{j=1}^{J} i_j d\lambda_j = dW_c + dW_f \tag{2.5-4}$$

We realize that when we evaluate the force f_e we must select the independent variables; that is, either the flux linkages and x or the currents and x. The flux linkages and the currents cannot simultaneously be considered independent variables when evaluating the force f_e. Nevertheless, (2.5-4), wherein both $d\lambda_j$ and di_j appear, is valid in general, before a selection of independent variables is made to evaluate f_e. If we solve (2.5-4) for the field energy dW_f and substitute the result into (2.5-2), we obtain

$$f_e dx = -\sum_{j=1}^{J} \lambda_j di_j + dW_c \tag{2.5-5}$$

Either (2.5-2) or (2.5-5) can be used to evaluate the electromagnetic force f_e. If flux linkages and x are selected as independent variables, (2.5-2) is the most direct, whereas (2.5-5) is the most direct if currents and x are selected.

With flux linkages and x as the independent variables, the currents are expressed functionally as

$$i_j(\lambda_1, \cdots, \lambda_j, x) \tag{2.5-6}$$

For the purpose of compactness, we will denote $(\lambda_1, ..., \lambda_j, x)$ as $(\boldsymbol{\lambda}, x)$, where $\boldsymbol{\lambda}$ is an abbreviation for the complete set of flux linkages associated with the J windings. Let us write (2.5-2) with flux linkages and x as independent variables:

$$f_e(\boldsymbol{\lambda}, x)dx = \sum_{j=1}^{J} i_j(\boldsymbol{\lambda}, x)d\lambda_j - dW_f(\boldsymbol{\lambda}, x) \tag{2.5-7}$$

If we take the total derivative of the field energy with respect to $\boldsymbol{\lambda}$ and x, and substitute that result into (2.5-7) we obtain

$$\begin{aligned} f_e(\boldsymbol{\lambda}, x)dx = &\sum_{j=1}^{J} i_j(\boldsymbol{\lambda}, x)d\lambda_j \\ &- \sum_{j=1}^{J} \frac{\partial W_f(\boldsymbol{\lambda}, x)}{\partial \lambda_j} d\lambda_j - \frac{\partial W_f(\boldsymbol{\lambda}, x)}{\partial x} dx \end{aligned} \tag{2.5-8}$$

Equating the coefficients of dx gives

$$f_e(\boldsymbol{\lambda}, x) = -\frac{\partial W_f(\boldsymbol{\lambda}, x)}{\partial x} \tag{2.5-9}$$

A second expression for $f_e(\boldsymbol{\lambda}, x)$ may be obtained by expressing (2.5-3) with flux linkages and x as independent variables, solving for $W_f(\boldsymbol{\lambda}, x)$, and then taking the partial derivative with respect to x. Thus,

$$f_e(\boldsymbol{\lambda}, x) = -\sum_{j=1}^{J} \left[\lambda_j \frac{\partial i_j(\boldsymbol{\lambda}, x)}{\partial x}\right] + \frac{\partial W_c(\boldsymbol{\lambda}, x)}{\partial x} \tag{2.5-10}$$

If we now select $\mathbf{i}$ and x as independent variables, where $(\mathbf{i}, x)$ is the abbreviated notation for $(i_1, ..., i_J, x)$, then (2.5-5) can be written as

$$f_e(\mathbf{i}, x)dx = -\sum_{j=1}^{J} \lambda_j(\mathbf{i}, x)di_j + dW_c(\mathbf{i}, x) \tag{2.5-11}$$

If we take the total derivative of $W_c(\mathbf{i}, x)$ with $\mathbf{i}$ and x as independent variables and substitute the result into (2.5-11), we obtain

$$f_e(\mathbf{i}, x)dx = -\sum_{j=1}^{J} \lambda_j(\mathbf{i}, x)di_j + \sum_{j=1}^{J} \frac{\partial W_c(\mathbf{i}, x)}{\partial i_j} di_j + \frac{\partial W_c(\mathbf{i}, x)}{\partial x} dx \quad (2.5\text{-}12)$$

Equating coefficients of dx yields

$$f_e(\mathbf{i}, x) = \frac{\partial W_c(\mathbf{i}, x)}{\partial x} \quad (2.5\text{-}13)$$

We will make extensive use of this expression. If we now solve (2.5-3) for $W_c(\mathbf{i}, x)$ and then take the partial derivative with respect to x we can obtain a second expression for $f_e(\mathbf{i}, x)$. That is,

$$f_e(\mathbf{i}, x) = \sum_{j=1}^{J} \left[i_j \frac{\partial \lambda_j(\mathbf{i}, x)}{\partial x} \right] - \frac{\partial W_f(\mathbf{i}, x)}{\partial x} \quad (2.5\text{-}14)$$

We have derived four expressions for the electromagnetic which are summarized in Table 2.5-1. Since we will generally use currents and x as independent variables, the two expressions for $f_e(\mathbf{i}, x)$ are listed first in Table 2.5-1.

Before proceeding to the next section, it is important to take a moment to look back. In order to obtain $f_e(\boldsymbol{\lambda}, x)$, we equated the coefficients of dx in (2.5-8). If, however, we equate the coefficients of $d\lambda_j$ in (2.5-8), we obtain

$$\sum_{j=1}^{J} \frac{\partial W_f(\boldsymbol{\lambda}, x)}{\partial \lambda_j} = \sum_{j=1}^{J} i_j(\boldsymbol{\lambda}, x) \quad (2.5\text{-}15)$$

Similarly, if we equate the coefficients of di_j in (2.5-12) we obtain

$$\sum_{j=1}^{J} \frac{\partial W_c(\mathbf{i}, x)}{\partial i_j} = \sum_{j=1}^{J} \lambda_j(\mathbf{i}, x) \quad (2.5\text{-}16)$$

Equations (2.5-15) and (2.5-16) are readily verified by recalling the definitions of W_f and W_c, (2.3-2) and (2.3-3), respectively, which were obtained by holding x fixed ($dx = 0$).

In Table 2.5-1, the independent variables to be used are designated in each equation by the abbreviated functional notation. Although only translational mechanical systems have been considered, all force relationships developed herein may be modified for the purpose of evaluating the torque in rotational systems. In particular, when considering a rotational system, f_e is replaced with the electromagnetic torque T_e and x with the angular displacement θ

Table 2.5-1: Electromagnetic forces at mechanical input. (For rotational systems, replace f_e with T_e and x with θ.)

$$f_e(\mathbf{i}, x) = \sum_{j=1}^{J} \left[i_j \frac{\partial \lambda_j(\mathbf{i}, x)}{\partial x} \right] - \frac{\partial W_f(\mathbf{i}, x)}{\partial x}$$

$$f_e(\mathbf{i}, x) = \frac{\partial W_c(\mathbf{i}, x)}{\partial x}$$

$$f_e(\boldsymbol{\lambda}, x) = -\frac{\partial W_f(\boldsymbol{\lambda}, x)}{\partial x}$$

$$f_e(\boldsymbol{\lambda}, x) = -\sum_{j=1}^{J} \left[\lambda_j \frac{\partial i_j(\boldsymbol{\lambda}, x)}{\partial x} \right] + \frac{\partial W_c(\boldsymbol{\lambda}, x)}{\partial x}$$

of the rotating member. These substitutions are justified since the change of mechanical energy in a rotational system is expressed as

$$dW_m = -T_e \, d\theta \tag{2.5-17}$$

The force equation for an electromechanical system with electric coupling fields may be derived by following a procedure similar to that used in the case of magnetic coupling fields. These relationships are given in Table 2.5-2 without explanation or proof.

Example 2B. We have mentioned that one may prefer to determine the electromagnetic force or torque by starting with the relationship $dW_f = dW_e + dW_m$ rather than by selecting a formula from a table. To illustrate this procedure, let

$$\lambda = [1 + a(x)]i^2 \tag{2B-1}$$

First, we must evaluate the field energy. Since losses in the coupling field are neglected, W_f is a function of state. Hence, W_f may be evaluated by fixing the mechanical displacement. This is done by setting $dx = 0$, whereupon

$$dW_f = dW_e = id\lambda \text{ with } dx = 0 \tag{2B-2}$$

Table 2.5-2: Electrostatic forces at mechanical input. (For rotational systems, replace f_e with T_e and x with θ.)

$$f_e(\mathbf{e}_f, x) = \sum_{j=1}^{J}\left[e_{fj}\frac{\partial q_j(\mathbf{e}_f, x)}{\partial x}\right] - \frac{\partial W_f(\mathbf{e}_f, x)}{\partial x}$$

$$f_e(\mathbf{e}_f, x) = \frac{\partial W_c(\mathbf{e}_f, x)}{\partial x}$$

$$f_e(\mathbf{q}, x) = -\frac{\partial W_f(\mathbf{q}, x)}{\partial x}$$

$$f_e(\mathbf{q}, x) = -\sum_{j=1}^{J}\left[q_j\frac{\partial e_{fj}(\mathbf{q}, x)}{\partial x}\right] + \frac{\partial W_c(\mathbf{q}, x)}{\partial x}$$

where dW_e is obtained from (2.2-13) with $e_f = d\lambda/dt$. From (2B-1) with $dx = 0$,

$$d\lambda = 2[1 + a(x)]idi \tag{2B-3}$$

Substituting (2B-3) into (2B-2) and solving for W_f yields

$$W_f = \int_0^i 2[1 + a(x)]\xi^2 d\xi = \frac{2}{3}[1 + a(x)]i^3 \tag{2B-4}$$

To obtain an expression for f_e, we go back to the basic relationship that $dW_f = dW_e + dW_m$; however, now $dx \neq 0$. Thus, from (2B-4),

$$dW_f = \frac{2}{3}i^3\frac{\partial a(x)}{\partial x}dx + 2[1 + a(x)]i^2 di \tag{2B-5}$$

Now,

$$dW_e = id\lambda = i[i^2\frac{\partial a(x)}{\partial x}dx + 2[1 + a(x)]idi \tag{2B-6}$$

and from (2.2-15),

$$dW_m = -f_e dx \tag{2B-7}$$

Substituting into $dW_f = dW_e + dW_m$ yields

$$\frac{2}{3}i^3\frac{\partial a(x)}{\partial x}dx + 2[1+a(x)]i^2di =$$

$$i^3\frac{\partial a(x)}{\partial x}dx + 2[1+a(x)]i^2di - f_e dx \qquad \text{(2B-8)}$$

Note the di terms cancel as (2.5-10) tells us they should, and by equating the coefficients of dx,

$$f_e = \frac{1}{3}i^3\frac{\partial a(x)}{\partial x} \qquad \text{(2B-9)}$$

Let us check our work by using information from Table 2.5-1. Since the system is magnetically nonlinear, $W_f \neq W_c$. Thus, knowing W_f, we can use the first entry in Table 2.5-1 or evaluate W_c and use the second entry. We shall do both. From Table 2.5-1 with one electric input ($J = 1$),

$$f_e(i,x) = i\frac{\partial \lambda(i,x)}{\partial x} - \frac{\partial W_f(i,x)}{\partial x} \qquad \text{(2B-10)}$$

Now, $\lambda(i,x)$ is expressed by (2B-1) and $W_f(i,x)$ by (2B-4), thus

$$\begin{aligned} f_e(i,x) &= i[i^2\frac{\partial a(x)}{\partial x}] - \frac{2}{3}i^3\frac{\partial a(x)}{\partial x} \\ &= \frac{1}{3}i^3\frac{\partial a(x)}{\partial x} \end{aligned} \qquad \text{(2B-11)}$$

which agrees with our previous result. Alternatively, from the second entry of Table 2.5-1,

$$f_e(i,x) = \frac{\partial W_c(i,x)}{\partial x} \qquad \text{(2B-12)}$$

Now, from (2.3-4),

$$W_c(i,x) = \lambda(i,x)i - W_f(i,x) = \frac{1}{3}[1+a(x)]i^3 \qquad \text{(2B-13)}$$

[Obtain this same expression by using (2.3-3) to evaluate W_c.] Substituting (2B-13) into (2B-12) yields

$$f_e(i,x) = \frac{1}{3}i^3\frac{\partial a(x)}{\partial x} \qquad \text{(2B-14)}$$

SP2.5-1 $\lambda = kx^2i^2$. Express f_e when $i = 2$ A and $x = 1$ m. [$f_e = (16k/3)$ N]
SP2.5-2 $\lambda = ki/x$. Express f_e if $i = \sqrt{2}I_s \cos\omega_e t$. [$f_e = -(ki_s^2/2x^2)(1 + \cos 2\omega_e t)$]
SP2.5-3 $i = a(x)\lambda^3$. Express f_e by using the third entry in Table 2.5-1. [$f_e = -\frac{1}{4}\lambda^4(da(x)/dx)$]
SP2.5-4 In a rotational system, $\lambda = ki^2 \sin\theta$. Express the torque T_e. [$T_e = \frac{1}{3}ki^3 \cos\theta$]

2.6 OPERATING CHARACTERISTICS OF AN ELEMENTARY ELECTROMAGNET

From our work in Section 1.7, we established that for $x > 0$ the inductance of the electromagnet shown in Fig. 2.2-3 may be adequately approximated by (1.7-21). That is,

$$L(x) = L_l + L_m(x) = L_l + \frac{k}{x} \tag{2.6-1}$$

Now,

$$\lambda(i, x) = L(x)i \tag{2.6-2}$$

and, since the system is magnetically linear,

$$W_f(i, x) = W_c(i, x) = \frac{1}{2}L(x)i^2 \tag{2.6-3}$$

From the second entry of Table 2.5-1,

$$f_e(i, x) = \frac{\partial W_c(i, x)}{\partial x} = \frac{1}{2}i^2\frac{dL(x)}{dx} \tag{2.6-4}$$

Substituting (2.6-1) into (2.6-4) yields

$$f_e(i, x) = -\frac{ki^2}{2x^2} \tag{2.6-5}$$

The force f_e is always negative in the system shown in Fig. 2.2-3; the electromagnetic force pulls the moving member to the stationary member. In other words, an electromagnetic force is set up so as to minimize the reluctance (maximize the inductance) of the magnetic system.

The differential equations that describe the electromagnet are given by (2.2-7) for the electric system and (2.2-8) for the mechanical system. If the applied voltage v and the applied mechanical force f are both constant, all derivatives with respect to time in (2.2-7) and (2.2-8) are zero during steady-state operation. Thus,

$$v = ri \tag{2.6-6}$$

$$f = K(x - x_0) - f_e \tag{2.6-7}$$

Equation (2.6-7) may be written as

$$-f_e = f - K(x - x_0) \tag{2.6-8}$$

A plot of (2.6-8), with f_e replaced by (2.6-5), is shown in Fig. 2.6-1 for the following system parameters: $r = 10\ \Omega$, $K = 2667$ N/m, $x_0 = 3$ mm, $k = 6.283\times\ 10^{-5}$ H · m.

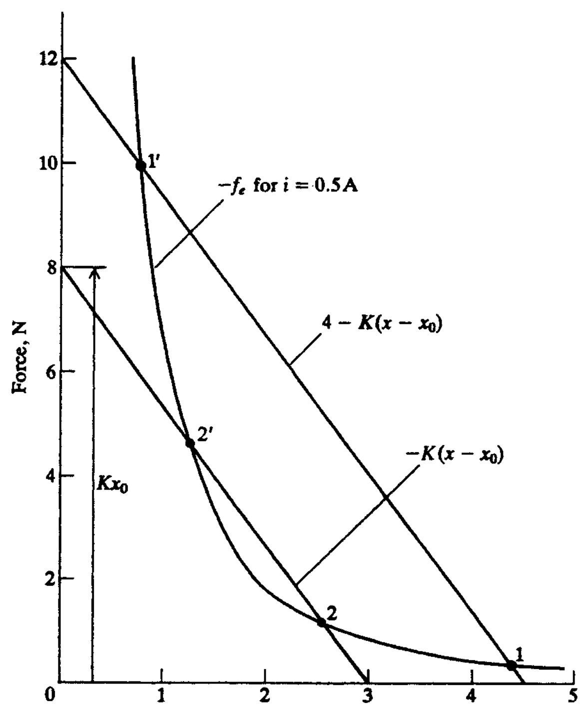

Figure 2.6-1: Steady-state operation of electromechanical system shown in Fig. 2.2-3.

In Fig. 2.6-1, the plot of the negative of the electromagnetic force is for an applied voltage of 5 V, whereupon the steady-state current is 0.5 A. The straight lines represent the right-hand side of (2.6-8) with $f = 0$ (lower straight line) and $f = 4\,\mathrm{N}$ (upper straight line). Both lines intersect the $-f_e$ curve at two points. In particular, the upper line intersects the $-f_e$ curve at 1 and 1′; the lower line intersects at 2 and 2′. Stable operation occurs at only points 1 and 2. The system will not operate stably at points 1′ and 2′. This can be explained by assuming the system is operating at one of these points (1′ and 2′) and then show that any system disturbance whatsoever will cause the system to move away from these points. If, for example, x increases slightly from its value corresponding to point 1′, the restraining force, $f - K(x - x_0)$, which is a force to pull the movable member to the right, is larger than the electromagnetic force to pull the movable member to the left. Hence, x will continue to increase until the system reaches operating point 1. If x increases beyond its value corresponding to operating point 1, the restraining force, $f - K(x - x_0)$, is less than the electromagnetic force. Therefore, the system will establish steady-state operation at 1. If, on the other hand, x decreases from point 1′, the electromagnetic force is larger than the restraining force. Therefore, the movable member will move until it comes in contact with the stationary member ($x = 0$). The restraining force that yields a straight line below the $-f_e$ curve will not permit stable operation with $x > 0$. Note also that, at point 2, x is less than x_0 and the spring is extended, exerting a force to the right on the movable member. At point 1, x is greater than x_0 and the spring is in compression, exerting a force to the left on the movable member. In fact, at 1 most of the force $4 - K(x - x_0)$ goes to compress the spring since $x > x_0$. This can be seen graphically by extending the $-K(x - x_0)$ line into the negative-force region and visualizing the intersection of this line and a vertical line through 1.

The dynamic behavior of the system during step changes in the source voltage v is shown in Fig. 2.6-2, and Figs. 2.6-3 and 2.6-4 for step changes in the applied force f. The following system parameters were used in addition to those given previously: $L_l = 0$, $l = 0$, $M = 0.055$ kg, $D = 4\,\mathrm{N} \cdot \mathrm{s/m}$. The computer traces shown in Fig. 2.6-2 depict the dynamic performance of the example system when the applied voltage is stepped from zero to 5 V and then back to zero, with the applied mechanical force f held equal to zero. The following system variables are plotted: e_f, λ, i, f_e, x, W_e, W_f, and W_m. The energies are plotted in millijoules (mJ). Initially, the mechanical system is at rest with $x = x_0$ (3 mm). When the source voltage is applied, x decreases

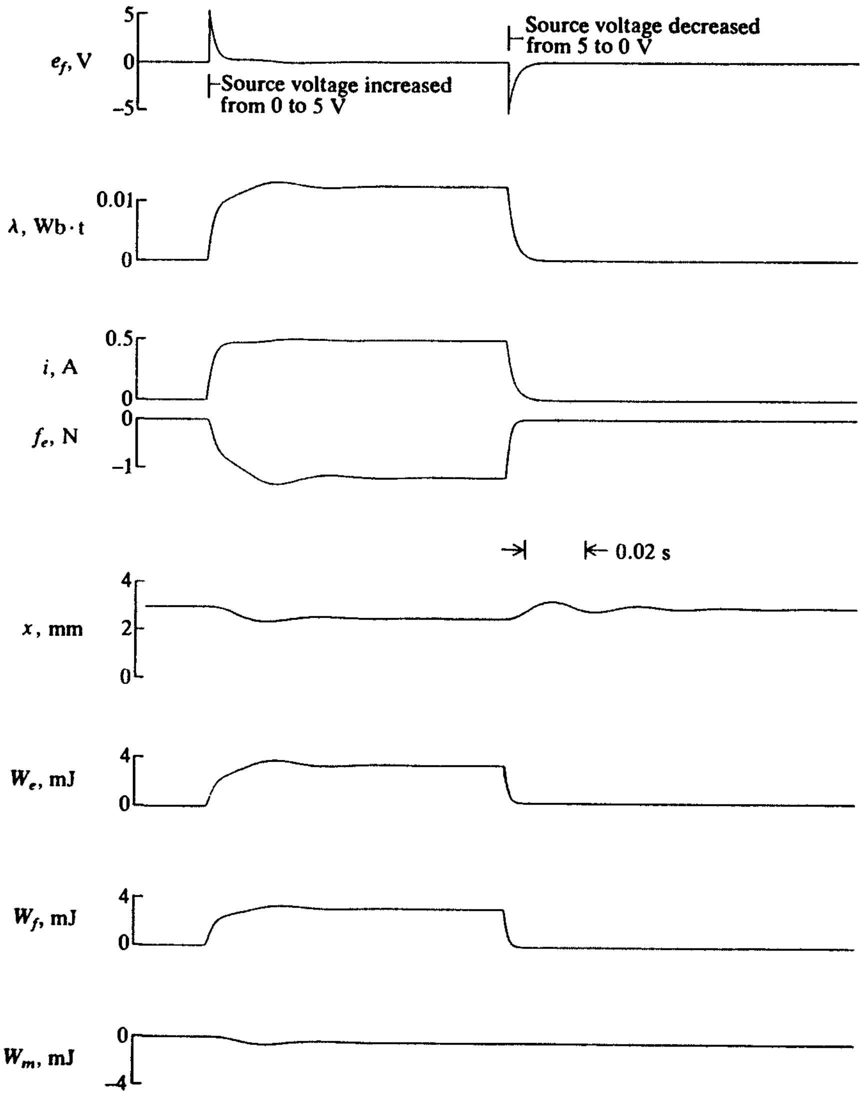

Figure 2.6-2: Dynamic performance of the electromechanical system shown in Fig. 2.2-3 during step changes in the source voltage.

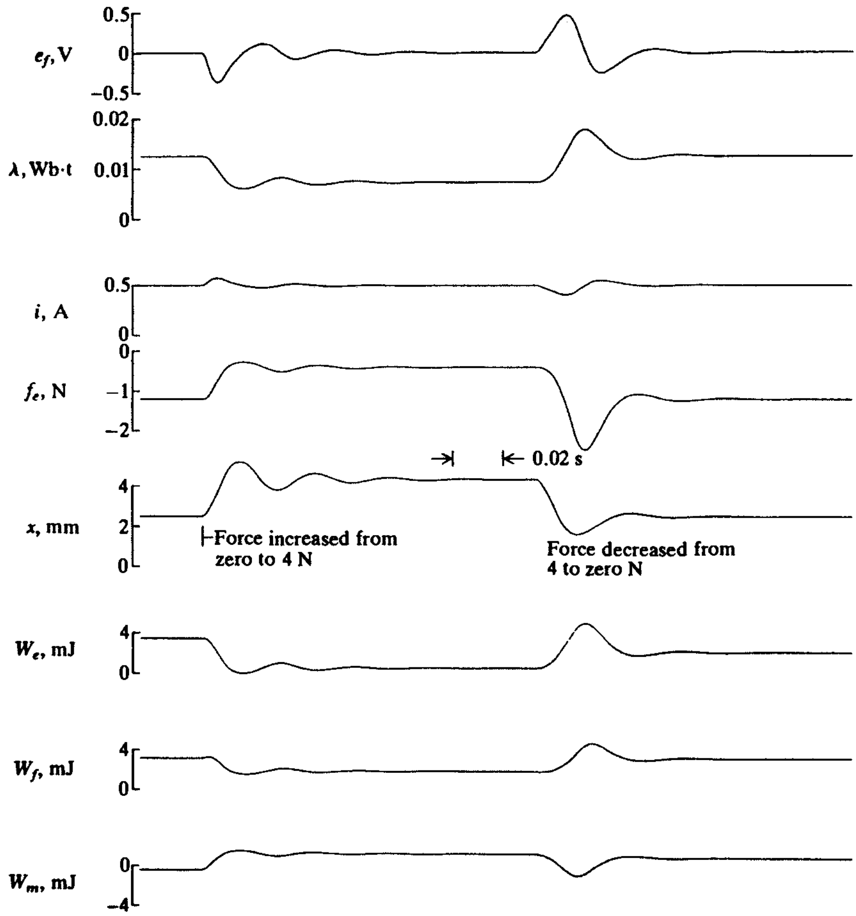

Figure 2.6-3: Dynamic performance of the electromechanical system shown in Fig. 2.2-3 during step changes in the applied force.

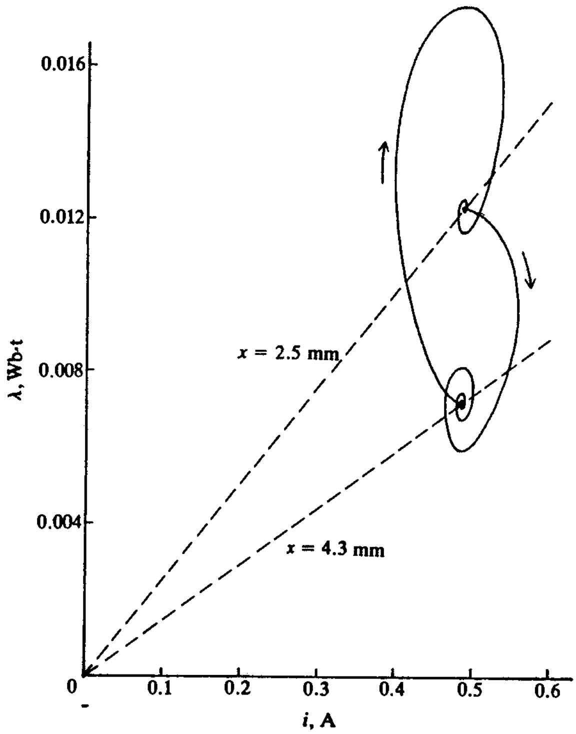

Figure 2.6-4: λ versus i plot of the system response shown in Fig. 2.6-3.

and, when steady-state operation is reestablished, x is approximately 2.5 mm, which is operating point 2 in Fig. 2.6-1. During the transient period, energy enters the coupling field via W_e. The bulk of this energy is stored in the field (W_f) with a smaller amount transferred to the mechanical system, some of which is dissipated in the damper during the transient period, and the remainder is stored in the spring. When the applied voltage is removed, the electric and mechanical systems return to their original states. The change in W_m is small, increasing only slightly. Hence, during the transient period, there is an interchange of energy between the spring and mass that is finally dissipated in the damper. The net change in W_f during the application and removal of the applied voltage is zero, hence the net change in W_e is positive and equal to the negative of the net change in W_m. The energy transferred to the mechanical system during this cycle is dissipated in the damper since f is fixed at zero and the mechanical system returns to its initial rest position with zero energy stored in the spring.

In Fig. 2.6-3, the initial state is that shown in Fig. 2.6-2 with 5 V applied to the electric system. The mechanical force f is increased from zero to 4 N, whereupon energy enters the coupling field from the mechanical system. Energy is transferred from the coupling field to the electric system and dissipated in the resistor, some coming from the mechanical system and some from the energy originally stored in the magnetic field. We have moved from point 2 to point 1 in Fig. 2.6-1. Next, the force is stepped back to zero from 4 N. The electric and mechanical systems return to their original states. During the cycle, a net energy has been transferred from the mechanical system to the electric system, which is dissipated in the resistance. This cycle is depicted in the λi plot shown in Fig. 2.6-4.

SP2.6-1 In Fig. 2.6-2, e_f jumps to 5 V when the source voltage is stepped from zero to 5 V and jumps from zero to -5 V when the source voltage is stepped from 5 V to zero. Why? [At first $t = 0^+$, $v = L(x)(di/dt)$; at second $t = 0^+$, $L(x)(di/dt) = -ir$]
SP2.6-2 Consider Fig. 2.6-1 with initial operation at point 2. Determine the final operating value of x (a) if f is stepped from zero to -1 N; (b) if f is zero but v is stepped from 5 V to 10 V [(a) and (b) $x = 0$]
SP2.6-3 Assume that the elementary electromagnet shown in Fig. 2.2-3 portrays the λi characteristics shown in Fig 2.4-1. As the system moves from x_a to x_b, the λi trajectory moves from A to B, as shown in Fig. 2.4-1. Assume steady-state operation exists at A and B. (a) Does the voltage v increase or decrease? (b) Does the applied force f increase or decrease? [(a) and (b) decrease]
SP2.6-4 Why does not $i(t)$ portray an exponential increase when the source voltage is increased from zero to 5 V in Fig. 2.6-2? [$L(x)$]

2.7 SINGLE-PHASE RELUCTANCE MACHINE

An elementary two-pole, single-phase reluctance machine, which was first shown in Fig. 1.7-2, is shown in a slightly different form in Fig. 2.7-1. In particular, the notation has been changed, that is, winding 1 is now winding *as*. We shall see the convenience of this notation as we go along. Next, the stator or stationary member has been changed to depict more accurately the configuration common for this device. The voltage equation may be written as

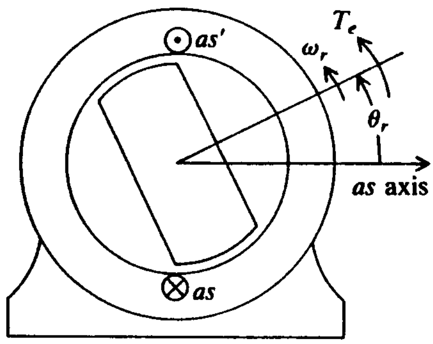

Figure 2.7-1: Elementary two-pole, single-phase reluctance machine.

$$v_{as} = r_s i_{as} + \frac{d\lambda_{as}}{dt} \tag{2.7-1}$$

where r_s is the resistance of the as winding and

$$\lambda_{as} = L_{asas} i_{as} \tag{2.7-2}$$

The self-inductance of the as winding, which is denoted L_{asas}, can be approximated by an expression of the same form as that for the device shown in Fig. 1.7-2. In particular, from (1.7-29),

$$L_{asas} = L_{ls} + L_A - L_B \cos 2\theta_r \tag{2.7-3}$$

where for constant rotor speed

$$\theta_r = \omega_r t + \theta_r(0) \tag{2.7-4}$$

and L_{ls} is the leakage inductance.

An expression for the electromagnetic torque may be obtained by using the information given in Table 2.5-1. The magnetic system is linear. Hence $W_f = W_c$. We will use the second entry to evaluate T_e; in particular,

$$T_e(i_{as}, \theta_r) = \frac{\partial W_c(i_{as}, \theta_r)}{\partial \theta_r} \tag{2.7-5}$$

where

$$W_c(i_{as}, \theta_r) = \frac{1}{2}(L_{ls} + L_A - L_B \cos 2\theta_r) i_{as}^2 \tag{2.7-6}$$

from which

$$T_e(i_{as}, \theta_r) = L_B i_{as}^2 \sin 2\theta_r \tag{2.7-7}$$

Although the expression for torque given by (2.7-7) is valid for transient and steady-state conditions, we shall consider only elementary modes of steady-state operation in this section.

As a first example, let i_{as} be a constant current. In this case, the torque may be expressed as

$$T_e = K \sin 2\theta_r \tag{2.7-8}$$

where K is a constant equal to $L_B I_{as}^2$. Equation (2.7-8) is plotted in Fig.2.7-2 with the position of the rotor shown for $\theta_r = 0, \frac{1}{4}\pi, \frac{1}{2}\pi, \ldots, 2\pi$. Let us assume that there is no external torque on the shaft; that is, there is no torque to twist the shaft one way or the other. We learned from the study of the electromagnet in the previous section that there is a force created to minimize the reluctance of the magnetic system. This would suggest that the rest position of the rotor with constant I_{as} would be at the minimum reluctance positions; either $\theta_r = \frac{1}{2}\pi$ or $\frac{3}{2}\pi$, depending upon the initial rotor position. For example, if $0 < \theta_r < \frac{1}{2}\pi$ at the time i_{as}, was increased from zero to a constant value (transients neglected), the torque T_e would immediately become $K \sin 2\theta_r$, which is a positive value. Recall that the positive assumed direction of the electromagnetic torque is in the positive direction of θ_r (Fig. 2.7-1). Thus, the electromagnetic torque would cause the rotor to rotate to $\theta_r = \frac{1}{2}\pi$. Is this a stable point of operation? Well, at $\theta_r = \frac{1}{2}\pi$, $T_e = 0$. This tells us that electromagnetic torque is not created to move the rotor if θ_r is exactly at $\frac{1}{2}\pi$. However, let us try the stability test that we used on the electromagnet. If we displace the rotor ever so slightly from this operating point, will it return to $\theta_r = \frac{1}{2}\pi$? If so, then $\theta_r = \frac{1}{2}\pi$ is a stable operating point for a constant stator current. Let θ_r decrease very slightly, whereupon T_e becomes positive; hence, an electromagnetic torque is developed to increase θ_r back to $\frac{1}{2}\pi$. Now let θ_r increase very slightly beyond $\frac{1}{2}\pi$; T_e now becomes negative which forces θ_r back to $\frac{1}{2}\pi$. Certainly, $\theta_r = \frac{1}{2}\pi$ is a stable operating point and we can see that $\theta_r = -\frac{1}{2}\pi$ would also be a stable operating point.

We still have some questions. What would happen if the rotor were initially positioned at $\theta_r = 0$ when we increased i_{as} from zero to a constant value? Well, from our previous discussion we know that the rotor would

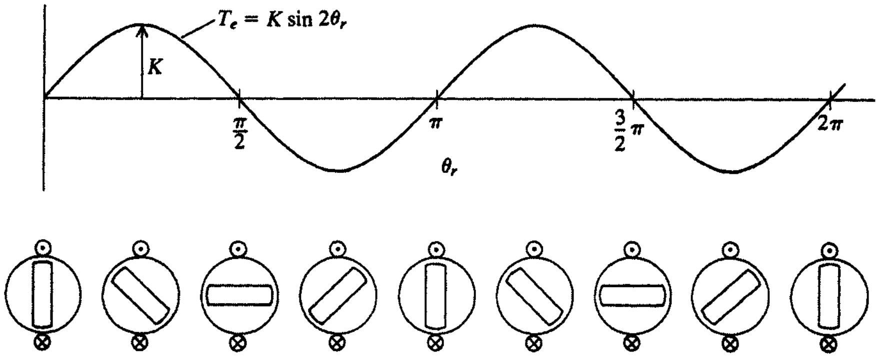

Figure 2.7-2: Electromagnetic torque versus angular displacement of a single-phase reluctance machine with constant stator current.

come to rest at $\theta_r = \frac{1}{2}\pi$ or $-\frac{1}{2}\pi$. However, since there is no external torque on the rotor and since (2.7-8) tells us that $T_e = 0$ at $\theta_r = 0$, why does it not remain at $\theta_r = 0$? The fact that the external torque is satisfied is certainly one condition for stable operation; however, let us try our stability test again. When we increase θ_r slightly from zero, T_e becomes positive, which would cause θ_r to increase even further. The rotor will move away from $\theta_r = 0$ to $\frac{1}{2}\pi$, a stable operating point. If we decrease θ_r slightly from zero, T_e becomes negative, decreasing θ_r even further, and the rotor will come to rest at $-\frac{1}{2}\pi$. Therefore, let us assume that, before increasing the current from zero to a constant value, we took great pains to set θ_r exactly at zero. If then we increased the current from zero to a constant value, the rotor would theoretically remain at $\theta_r = 0$. However, any disturbance, ever so slight, will cause the rotor to rotate away from $\theta_r = 0$ and there is a 50-50 chance as to the direction, counterclockwise or clockwise.

We have established that, with zero external torque on the shaft, $\theta_r = \frac{1}{2}\pi$ and $\frac{3}{2}\pi$ are stable points of operation for a constant stator current, and $\theta_r = 0$ and π are unstable. Let us see what happens when we apply an external torque. For this purpose, let us assume that initially the rotor is positioned at $\theta_r = \frac{1}{2}\pi$ with i_{as} a constant. Assume that we apply the torque to twist the shaft in the counterclockwise direction, increasing θ_r. An electromagnetic torque T_e will be developed to oppose the external torque in an attempt to maintain alignment with the as axis. When the T_e produced, in the attempt to align, is equal and opposite to the external torque, the rotor will stop advancing and come to rest with $\frac{1}{2}\pi < \theta_r < \frac{3}{4}\pi$. Now, the external torque must be less than the peak absolute value of T_e at $\theta_r = \frac{3}{4}\pi$ (K in Fig. 2.7-2). Otherwise, the torque to align cannot satisfy the external torque, whereupon the rotor would continue to advance counterclockwise as long as the external torque were present. If, instead of applying a torque to twist the rotor in the counterclockwise direction, the external torque is applied to twist the rotor in the opposite direction (clockwise), θ_r would decrease. If the electromagnetic torque developed in an attempt to maintain alignment with the *as* axis is large enough to satisfy the external torque, then the rotor will come to rest with $\frac{1}{4}\pi < \theta_r < \frac{1}{2}\pi$. With a little thought, we can convince ourselves that if T_e can satisfy the external torque requirements, then stable operation will occur only with $\frac{1}{4}\pi < \theta_r < \frac{3}{4}\pi$ or $\frac{5}{4}\pi < \theta_r < \frac{7}{4}\pi$, which represents the negative slope portions of the T_e versus θ_r characteristics.

We need to discuss the convention regarding the sign of T and T_e when dealing with rotational devices. In this chapter, it was established in Fig. 2.2-3 that f and f_e were both positive in the direction of positive displacement x. Therefore, for a rotational system, T and T_e would be positive in the direction of positive shaft displacement (counterclockwise θ_r). However, over the years it has become convention when considering motor action to let T_e be positive for counterclockwise shaft displacement but make the load torque, which we will denote T_L rather than T, positive for negative shaft displacement (clockwise θ_r). Starting in Chapter 3, we will follow this convention even when dealing with generator action where the input torque will be a negative T_L. Thus, in the above paragraph, the torque to twist the shaft in the counterclockwise direction is an input torque or a negative load torque ($-T_L$); the torque to twist the shaft in the clockwise direction is a positive load torque ($+T_L$). Hopefully, this will minimize the confusion that would certainly occur if we were to again change the sense to comply with the convention that is often used when analyzing generator action.

Although operation of a single-phase reluctance machine with a constant stator current is impracticable, it provides a basic understanding of reluctance torque, which is the operating principle of variable-reluctance stepper motors. We will find that, in its simplest form, a variable-reluctance stepper motor consists of three cascaded, single-phase reluctance motors with the rotors on a common shaft and arranged so that their minimum reluctance paths are displaced from each other. We shall talk more about stepper motors in a later chapter. Before leaving this brief encounter with the single-phase reluctance machine, it is instructive to look at an approximation of a practicable mode of operation of this device. To approximate the operation of a single-phase reluctance machine, we will assume that the steady-state stator current is sinusoidal. Thus,

$$I_{as} = \sqrt{2} I_s \cos\theta_{esi} \tag{2.7-9}$$

where, for steady-state operation,

$$\theta_{esi} = \omega_e t + \theta_{esi}(0) \tag{2.7-10}$$

In the above equations the electrical angular displacement has the subscript *esi*. The e denotes association with an electrical variable, s with a stator variable, and i with current. We know that θ_r, which is given by (2.7-4), may also be written in a form similar to (2.7-10) for steady-state operation. Substituting (2.7-9) into (2.7-7) and after using a few trigonometric identities from Appendix A, we have

$$\begin{aligned} T_e = {} & L_B I_s^2 \sin 2[\omega_r t + \theta_r(0)] \\ & + \frac{1}{2} L_B I_s^2 \{\sin 2[(\omega_r + \omega_e)t + \theta_r(0) + \theta_{esi}(0)] \\ & + \sin 2[(\omega_r - \omega_e)t + \theta_r(0) - \theta_{esi}(0)]\} \end{aligned} \tag{2.7-11}$$

We see from the first term that an average steady-state torque is produced when $\omega_r = 0$. More importantly, we see that either the second or the third term produces an average torque whenever $|\omega_r| = \omega_e$, where ω_e is the angular velocity of the electric system (synchronous speed). For this example, let $\omega_r = \omega_e$, then (2.7-11) becomes

$$\begin{aligned} T_e = {} & L_B I_s^2 \sin 2[\omega_e t + \theta_r(0)] \\ & + \frac{1}{2} L_B l_s^2 \sin 2[2\omega_e t + \theta_r(0) + \theta_{esi}(0)] \\ & + \frac{1}{2} L_B I_S^2 \sin 2[\theta_r(0) - \theta_{esi}(0)] \end{aligned} \tag{2.7-12}$$

Recall that $\theta_r(0)$ and $\theta_{esi}(0)$ are the time zero values of the displacement of the rotor and the current, respectively.

It appears from (2.7-12) that we should expect the steady-state torque to pulsate at $4\omega_e$ and $2\omega_e$, and the average torque is a double-angle sinusoidal function of $\theta_r(0) - \theta_{esi}(0)$. Although (2.7-12) illustrates that a reluctance machine develops an average torque, it is difficult to explain how this all takes place. Even though you probably have numerous questions regarding the operation of a single-phase reluctance machine, it is perhaps best to delay a more in-depth discussion until we have studied the material on the rotating magnetic field (rotating air gap mmf) in Chapter 4.

SP2.7-1 Initially, the rotor of a single-phase reluctance motor is positioned with $\theta_r = 0$. Instantaneously, i_{as} is stepped to 1 A and an external torque of 0.01 N·m is applied to rotate the rotor in the clockwise direction. $L_B = 0.02$ H. Neglect transients and determine the final value of θ_r. [$\theta_r = -105^\circ$]
SP2.7-2 The device in SP2.7-1 is operating steadily at $\theta_r = -105^\circ$ when i_{as} is reversed instantaneously ($I_{as} = -1$ A). Neglect the transients and determine the final value of θ_r. [$\theta_r = -105^\circ$]
SP2.7-3 The friction and windage losses of a reluctance motor appear as a retarding torque of 0.01 N · m at $\omega_r = \omega_e$. The steady-state current is $I_{as} = 2\cos\omega_e t$ and $L_B = 0.02$ H. Calculate $\theta_r(0) - \theta_{esi}(0)$ if the motor is rotating steadily at ω_e. [$\theta_r(0) = -105^\circ$]

2.8 WINDINGS IN RELATIVE MOTION

It is instructive to formulate an expression for the electromagnetic torque of the elementary rotational device shown in Fig. 1.7-4. The voltage equations are given by (1.7-30) and (1.7-31), the self-inductances L_{11} and L_{22} are constant as given by (1.7-34) and (1.7-35), and the mutual inductance is given by (1.7-38). Let us rewrite these equations here for convenience. The voltage equations may be written in matrix form as

$$\begin{bmatrix} v_1 \\ v_2 \end{bmatrix} = \begin{bmatrix} r_1 & 0 \\ 0 & r_2 \end{bmatrix} \begin{bmatrix} i_1 \\ i_2 \end{bmatrix} + \frac{d}{dt} \begin{bmatrix} \lambda_1 \\ \lambda_2 \end{bmatrix} \tag{2.8-1}$$

which may also be written as

$$\mathbf{v}_{12} = \mathbf{r}\mathbf{i}_{12} + \frac{d}{dt}\boldsymbol{\lambda}_{12} \tag{2.8-2}$$

All terms are defined by comparison with (2.8-1). The flux linkage equations are

$$\begin{bmatrix} \lambda_1 \\ \lambda_2 \end{bmatrix} = \begin{bmatrix} L_{l1} + L_{m1} & L_{sr}\cos\theta_r \\ L_{sr}\cos\theta_r & L_{l2} + L_{m2} \end{bmatrix} \begin{bmatrix} i_1 \\ i_2 \end{bmatrix} \tag{2.8-3}$$

From Table 2.5-1,

$$T_e(i_1, i_2, \theta_r) = \frac{\partial W_c(i_1, i_2, \theta_r)}{\partial \theta_r} \tag{2.8-4}$$

Since the magnetic system is assumed to be linear,

$$W_c(i_1, i_2, \theta_r) = \frac{1}{2}L_{11}i_1^2 + L_{12}i_1i_2 + \frac{1}{2}L_{22}i_2^2 \tag{2.8-5}$$

The self-inductances are constants and the mutual inductance is represented by the off-diagonal terms in (2.8-3). Thus,

$$T_e(i_1, i_2, \theta_r) = -i_1i_2L_{sr}\sin\theta_r \tag{2.8-6}$$

Although (2.8-6) is valid regardless of the form of i_1 and i_2, let us consider for a moment the form of the torque if i_1 and i_2 are both positive and constant. For the positive direction of current shown, the torque would then be of the form

$$T_e = -K\sin\theta_r \tag{2.8-7}$$

where K is a positive constant equal to $i_1i_2L_{sr}$.

A plot of (2.8-7) is shown in Fig. 2.8-1 with the position of the windings illustrated for $\theta_r = 0,\ \frac{1}{2}\pi,\ \dots,\ 2\pi$. Also shown are the positions of the poles of the magnetic systems created by constant positive current flowing in the windings. It may at first appear that the north (N^s) and south (S^s) poles produced by positive current flowing in the stator winding are positioned incorrectly. However, recall that flux issues from a north pole of a magnet into the air. Since the stator and rotor windings must each be considered as creating separate magnetic systems, we realize, by the right-hand rule, that flux issues from the north pole of the magnetic system established by the stator winding into the air gap. Similarly, the flux produced by positive current flowing in the rotor winding enters the air gap from the north pole of the magnetic system of the rotor.

Here, we see that an electromagnetic torque is produced in an attempt to align the magnetic systems established by currents flowing in the stator and rotor windings; in other words, to align the 1- and 2-axes. We can use our stability test, as we did in the case of the single-phase reluctance machine, to establish the fact that, with no external torque on the rotor, stable positioning occurs at $\theta_r = 0$, whereas unstable operation occurs at $\theta_r = \pi$. This, of course, assumes that i_1 and i_2 are positive constants. Also, stable operation with an external applied torque occurs over the range of $-\frac{1}{2}\pi < \theta_r < \frac{1}{2}\pi$, the negative slope portion of the T_e versus θ_r characteristic. Although op-

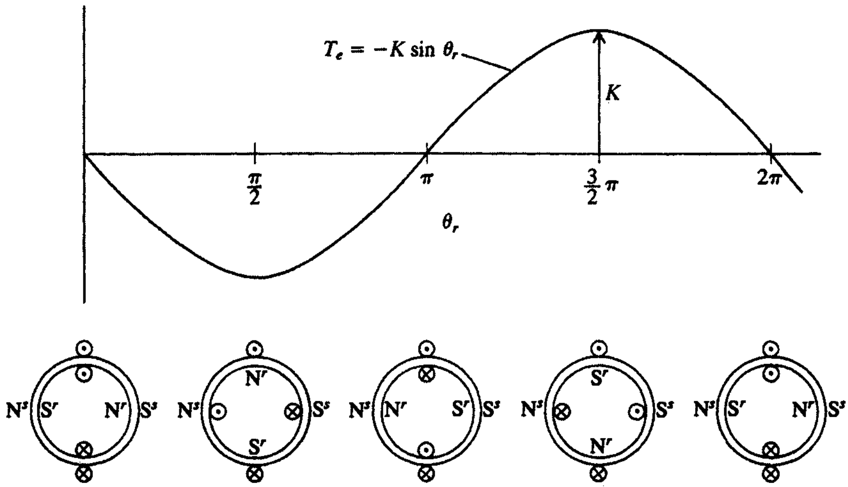

Figure 2.8-1: Electromagnetic torque versus angular displacement with constant winding currents.

eration with constant winding currents is somewhat impracticable, it does illustrate the principle of positioning of stepper motors with a permanent-magnet rotor which, in many respects, is analogous to holding i_2 constant in the elementary device considered here.

Before leaving this elementary device for good, let us assume that i_2 is constant ($i_2 = I_2$) and

$$I_1 = \sqrt{2} I \cos \theta_{esi} \tag{2.8-8}$$

where, for steady-state operation

$$\theta_{esi} = \omega_e t + \theta_{esi}(0) \tag{2.8-9}$$

Also,

$$\theta_r = \omega_r t + \theta_r(0) \tag{2.8-10}$$

Substituting into (2.8-6) yields

$$T_e = -\sqrt{2} I I_2 L_{sr} \cos[\omega_e t + \theta_{esi}(0)] \sin[\omega_r t + \theta_r(0)] \tag{2.8-11}$$

which can be expressed as

$$T_e = -\sqrt{2}II_2L_{sr}\{\frac{1}{2}\sin[(\omega_r + \omega_e)t + \theta_r(0) + \theta_{esi}(0)]$$

$$+\frac{1}{2}\sin[(\omega_r - \omega_e)t + \theta_r(0) - \theta_{esi}(0)]\} \qquad (2.8\text{-}12)$$

Here, we see that an average torque is produced if $|\omega_r| = \omega_e$. In particular, if $\omega_r = \omega_e$, (2.8-12) becomes

$$T_e = -\sqrt{2}II_2L_{sr}\times$$

$$\{\frac{1}{2}\sin[2\omega_e t + \theta_r(0) + \theta_{esi}(0)] + \frac{1}{2}\sin[\theta_r(0) - \theta_{esi}(0)]\} \quad (2.8\text{-}13)$$

From this brief analysis, we can see that an average torque will be produced with $|\omega_r| = \omega_e$. In fact, with i_2 constant and I_1 given by (2.8-8), this device is an elementary single-phase synchronous machine. However, as in the case of the single-phase reluctance machine, we do not really have all the tools at hand to provide an in-depth explanation of its operation. We will be able to do this once we have studied the material in Chapter 4.

SP2.8-1 In the system shown in Fig. 1.7-4, $L_{sr} = 0.1$ H, $i_1 = 2$ A, and $i_2 = 10$ A. (*a*) A torque of 1 N · m is applied in the clockwise direction. Calculate the steady-state value of θ_r. (*b*) Repeat with a torque of 2 N · m. [(*a*) $\theta_r = -30^\circ$; (*b*) unstable]

SP2.8-2 Reverse the direction of i_1 in Fig. 1.7-4 and determine the range of stable operation for constant, positive currents. [$\frac{1}{2}\pi < \theta_r < \frac{3}{2}\pi$]

SP2.8-3 In Fig. 1.7-4, winding 1 is moved so that $\otimes$ is at three o'clock and $\odot$ at nine. Express T_e. [$T_e = i_1 i_2 L_{sr}\cos\theta_r$]

SP2.8-4 The currents i_1 and i_2 are positive constants in the device shown in Fig. 1.7-4. (*a*) An external torque is applied to increase θ_r to 45° and then released. Assume damping exists. What is the final position of the rotor? Repeat for θ_r increased to (*b*) 90°, (*c*) 120°, (*d*) 180°, and (*e*) 210°. [(*a*) $\theta_r = 0$; (*b*) 0; (*c*) 0; (*d*) 0 or 2π; (*e*) 2π]

SP2.8-5 In the system shown in Fig. 1.7-4, $L_{sr} = 0.1$ H, $i_1 = 20\cos\omega_e t$, $i_2 = 2$ A, and $\omega_r = \omega_e$. Calculate $\theta_r(0) - \theta_{esi}(0)$ if an external torque of 1 N · m is applied in the clockwise direction. [$\theta_r(0) = -30^\circ$]

2.9 RECAPPING

The primary purpose of this chapter is to establish a means of expressing the force or torque in electromechanical devices. Therefore, an understanding of all relationships given in Table 2.5-1 is of importance. However, since the magnetic system of the devices that we will consider is assumed to be linear, we will make extensive use of the second entry of Table 2.5-1.

The detailed analysis of the elementary electromagnet and the associated problems at the end of the chapter warrant consideration since this material will not be revisited later in the text. You are now prepared to proceed to the study of dc machines (Chapter 3) or jump to Chapter 4 and begin study of the electromechanical motion devices that operate on the principle of a rotating magnetic field. This includes induction machines, synchronous machines, stepper motors, and the permanent-magnet ac machine.

2.10 PROBLEMS

1. A resistor and an inductor are connected as shown in Fig. 2.10-1 with $R = 15\,\Omega$ and $L = 250$ mH. Express the energy stored in the inductor and the energy dissipated by the resistor for $t > 0$ if $i(0) = 10$ A.

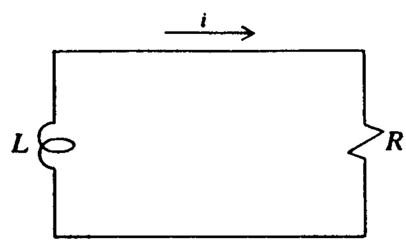

Figure 2.10-1: *RL* circuit.

2. Consider the spring-mass-damper system shown in Fig. 2.10-2. Let $x_0 = 0$ and assume $f = \cos \omega t$. Express the steady-state response $x(t)$ in the form $x = X_s \cos(\omega t + \phi)$.

* 3. Consider the spring-mass-damper system shown in Fig. 2.10-3. At $t = 0$, $x(0) = x_0$ (rest position), and $dx/dt = 1.5\,\text{m/s}$. Also, $M = 0.8$ kg, $D = 10\,\text{N}\cdot\text{s/m}$, and $K = 120\,\text{N}\cdot\text{m}$. For $t > 0$, express the energy

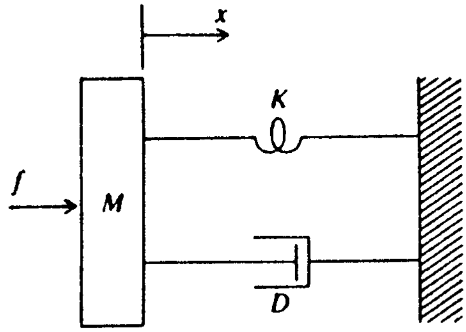

Figure 2.10-2: Spring-mass-damper system with applied force.

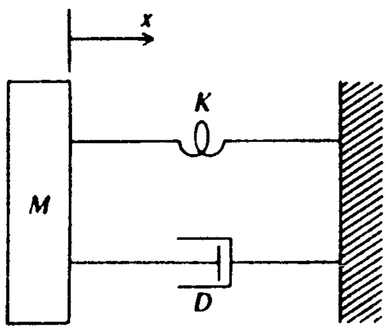

Figure 2.10-3: Spring-mass-damper system.

stored in the spring, W_{mS1}, the kinetic energy of the mass, W_{mS2}, and the energy dissipated by the damper, W_{mL}. You need not evaluate the integral expression for W_{mL}.

4. Express $W_f(i,x)$ and $W_c(i,x)$ for (a) $\lambda(i,x) = xi^3 + i$; (b) $\lambda(i,x) = -xi^2 + i\sin x$.

* 5. The energy stored in the coupling field of a magnetically linear system with two electric inputs may be expressed as

$$W_f(\lambda_1, \lambda_2, x) = \tfrac{1}{2}B_{11}\lambda_1^2 + B_{12}\lambda_1\lambda_2 + \tfrac{1}{2}B_{22}\lambda_2^2$$

Express B_{11}, B_{12}, and B_{22} in terms of inductances L_{11}, L_{12}, and L_{22}.

6. An electromechanical system has two electric inputs. The flux linkages

may be expressed as

$$\lambda_1(i_1, i_2, x) = x^2 i_1^2 + x i_2 + i_1$$

$$\lambda_2(i_1, i_2, x) = x^2 i_2^2 + x i_1 + i_2$$

Express $W_f(i_1, i_2, x)$ and $W_c(i_1, i_2, x)$ by first making i_2 the variable of integration with $di_1 = 0$ and $i_1 = 0$. Then let i_1 be the variable of integration with $di_2 = 0$ and i_2 at its final value.

7. The mechanical system moves from x_1 to x_2 along the λi path 1 to 2 in Fig. 2.10-4. Identify the following by areas: (*a*) ΔW_f, (*b*) ΔW_c, (*c*) ΔW_e, (*d*) ΔW_m.

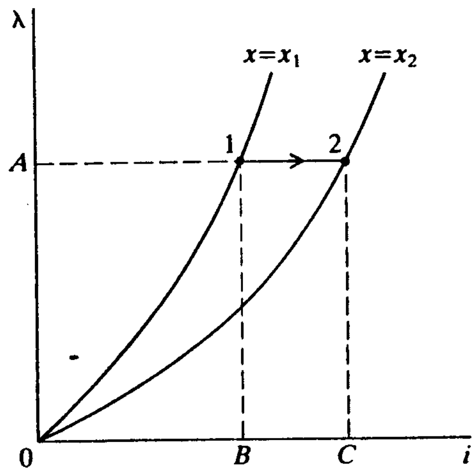

Figure 2.10-4: λi characteristics.

8. Let $i = k\lambda^2 e^{2x}$. Evaluate f_e when $\lambda = 2\ \mathrm{V \cdot s}$, $x = 1$ m, and $k = 1\ \mathrm{A/(V \cdot s)^2}$.

9. The plunger with mass M shown in Fig. 2.10-5 is free to move within an electromagnet. Although the winding of the electromagnet consists of many turns, only one is shown. The mechanical damping varies directly as the surface area of the plunger within the electromagnet. (*a*) Write the voltage equation for the electric system. (*b*) Write the dynamic equation for the mechanical system. Include the force of gravity. (*c*) Express the mechanical damping D. (*d*) Express the electromagnetic

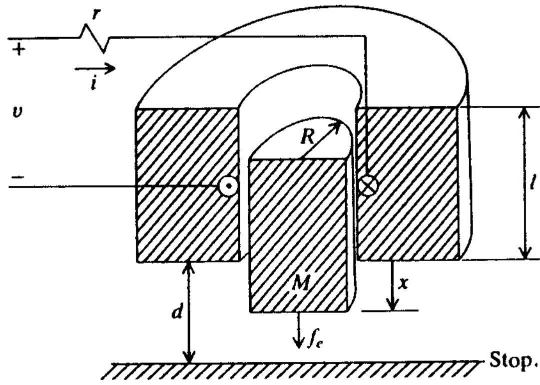

Figure 2.10-5: Cross section of plunger system.

force f_e if $i = a\lambda^2 + b\lambda(x-d)^2$. (*e*) Express the steady-state position x for a constant current flowing in the winding.

10. Express the force of attraction between the iron faces of the air gap in Fig. 1.3-1 in terms of N, the turns of the winding; i, the current flowing in the winding; μ_0; A_g, the cross-sectional area of the air gap; and g, the air gap length. Neglect the reluctance of the iron. (*Hint*: Express the energy in the air gap in terms of air gap length and allow an infinitesimal change in air gap length dg. This procedure is often referred to as "virtual displacement.")

11. Express $f_e(i_1, i_2, x)$ for λ_1 and λ_2 given in Prob. 6.

12. For the electromagnet shown in Fig. 2.2-3, let $L(x) = L_l + L_m(x)$, where L_l is constant and $L_m(x)$ is expressed by (1.7-17). Express f_e for $x = 0$.

13. Following the system transients due to the application of the source voltage in Fig. 2.6-2 ($v = 5\,\text{V}$), the system assumes steady-state operation. Calculate W_{eS}, W_f, and W_{mS} during steady-state operation. [*Hint*: The external inductance l is set equal to zero in this example and $W_{mS} = K\int_{x_0}^{x}(\xi - x_0)d\xi$].

14. Consider Fig. 2.6-3 wherein the force f is changed. The source voltage v is constant and the leakage inductance L_l and the external inductance l are both zero. As f is changed, e_f changes during the transient. Show

that, for transient and steady-state conditions, the energy dissipated in the resistor may be expressed as

$$W_{eL} = \frac{v^2}{r}\int dt - \frac{2v}{r}\int e_f dt + \frac{1}{r}\int e_f^2 dt$$

Also express W_E and W_e.

15. The dc source for the electromagnet considered in Section 2.6 is replaced with a 60-Hz source. With $f = 0$ and $i = \sqrt{2}\,0.5\cos\omega_e t$, it is found that the system operates with x constant at 2.5 mm. (a) Express f_e and justify this observation. (b) Calculate the applied voltage.

16. Assume that the steady-state current supplied to a single-phase reluctance motor is sinusoidal. The rotor speed is $\omega_r = \omega_e$. Determine the harmonics that must be present in the applied voltage V_{as} in order for $I_{as} = \sqrt{2}I_s\cos\omega_e t$.

* 17. The steady-state currents flowing in the conductors of the device shown in Fig. 1.7-4 are $I_1 = \sqrt{2}I_{s1}\cos\omega_1 t$ and $I_2 = \sqrt{2}I_{s2}\cos(\omega_2 t + \phi_2)$. Assume that during steady-state operation the rotor speed is constant; thus, $\theta_r = \omega_r t + \theta(0)$, where $\theta_r(0)$ is the rotor displacement at time zero. Determine the rotor speed(s) at which the device produces a nonzero average torque during steady-state operation if (a) $\omega_1 = \omega_2 = 0$, (b) $\omega_1 = \omega_2 \neq 0$, and ($c$) $\omega_1 \neq 0$, $\omega_2 = 0$.

18. In Fig. 2.10-6, θ_r and ω_r are positive in the clockwise direction. The peak amplitude of the mutual inductance is L_{sr}. Express (a) the mutual inductance L_{ab} and (b) the electromagnetic torque T_e.

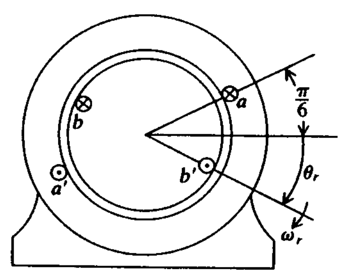

Figure 2.10-6: A 2-winding device with clockwise rotation.

19. Consider the electromechanical system shown in Fig. 2.10-7. Assume the peak amplitude of the mutual inductance is L_{sr}. (*a*) Express the mutual inductance. (*b*) Show the location of the north and south poles of the stator (N^s and S^s) and of the rotor (N^r and S^r) for positive i_1 and negative i_2. (*c*) Express the electromagnetic torque T_e.

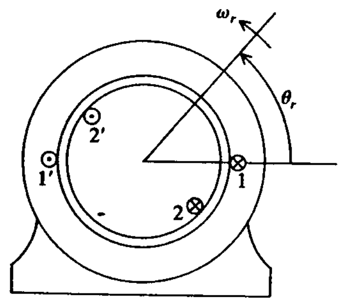

Figure 2.10-7: A 2-winding device with counterclockwise rotation.

20. The device shown in Fig. 2.10-8 has two stator windings. Winding 1 is fixed in the position shown. However, we are able to wind winding 2 at any angle α relative to winding 1. (*a*) Express the mutual inductance between windings 1 and 2 as a function of α. Let the peak amplitude be M. (*b*) Use the concept of virtual displacement to express the torque between the windings.

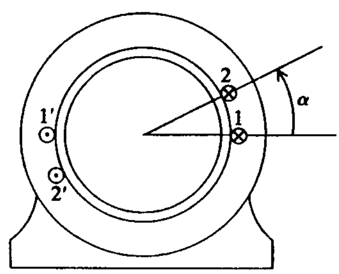

Figure 2.10-8: Two stator windings.

Chapter 3

DIRECT-CURRENT MACHINES

3.1 INTRODUCTION

The direct-current (dc) machine is not as widely used today as it was in the past. The dc generator has been replaced by solid-state rectifiers that convert alternating current into direct current with provisions to control the magnitude of the dc voltage, and, in drive applications, the dc motor is being replaced by the voltage-controlled, permanent-magnet ac machine (brushless dc motor) and/or the field-orientation-controlled induction motor. Nevertheless, it is still desirable to devote some time to the dc machine in an introductory course since it is still used as a low-power drive motor, especially in automotive applications. Although maintenance and environmental issues hamper the use of dc machines, this device is the only electric machine that inherently produces maximum torque per ampere. Thus, it is a highly efficient device. With the advent of electronic switching devices, there has become a huge effort to control the permanent-magnet ac and induction machines so as to emulate the performance characteristics of the dc motor without the maintenance and environmental problems inherent to the dc machines. This chapter is an attempt to treat dc machines sufficient to introduce the reader to the operating principles of dc machines with focus on the shunt-connected and permanent-magnet dc machines, thereby setting the stage for a comparison of the look-alike operating characteristics with the voltage-controlled, permanent-magnet ac machine and the field-orientation-controlled induction motor.

A simplified method of analysis is presented rather than an analysis wherein commutation is treated in detail. With this type of analytical approach, the dc machine is considered to be the most straightforward to analyze of all electromechanical devices. The dynamic characteristics of the permanent-magnet dc machine are illustrated and the time-domain block diagram and state equations are developed. A brief consideration of a dc converter used as a means of voltage control and thus speed control is presented as one of the final sections of the chapter.

3.2 ELEMENTARY DIRECT-CURRENT MACHINE

It is instructive to discuss the concept of commutation using the elementary machine shown in Fig. 3.2-1 prior to a formal analysis of the performance of a practical dc machine. The two-pole elementary machine is equipped with a field winding wound on the stator poles, a rotor coil $(a-a')$, and a commutator. The commutator is made up of two semicircular copper segments mounted on the shaft at the end of the rotor and insulated from one another as well as from the iron of the rotor. Each terminal of the rotor coil is connected to a copper segment. Stationary carbon brushes ride upon the copper segments, whereby the rotor coil is connected to a stationary circuit by a near frictionless contact.

The voltage equations for the field winding and rotor coil are

$$v_f = r_f i_f + \frac{d\lambda_f}{dt} \tag{3.2-1}$$

$$v_{a-a'} = r_a i_{a-a'} + \frac{d\lambda_{a-a'}}{dt} \tag{3.2-2}$$

where r_f and r_a are the resistance of the field winding and armature coil, respectively. The rotor of a dc machine is commonly referred to as the *armature;* rotor and armature will be used interchangeably. At this point in the analysis it is sufficient to express the flux linkages as

$$\lambda_f = L_{ff} i_f + L_{fa} i_{a-a'} \tag{3.2-3}$$

$$\lambda_{a-a'} = L_{af} i_f + L_{aa} i_{a-a'} \tag{3.2-4}$$

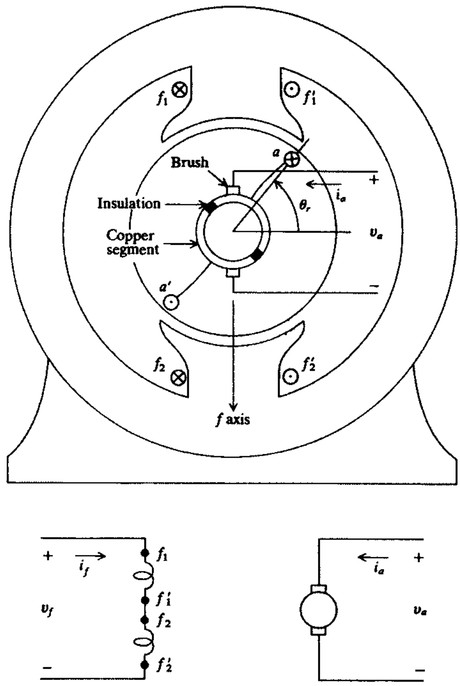

Figure 3.2-1: Elementary two-pole dc machine.

As a first approximation, the mutual inductance between the field winding and an armature coil may be expressed as a sinusoidal function of θ_r as

$$L_{af} = L_{fa} = -L\cos\theta_r \tag{3.2-5}$$

where L is a constant. As the rotor revolves, the action of the commutator is to switch the stationary terminals from one terminal of the rotor coil to the other. For the configuration shown in Fig. 3.2-1, this switching or commutation occurs at $\theta_r = 0,\ \pi,\ 2\pi,\ \ldots$. At the instant of switching, each brush is in contact with both copper segments, whereupon the rotor coil is short-circuited. It is desirable to commutate (short-circuit) the rotor coil at the instant the induced voltage is a minimum. The waveform of the voltage induced in the open-circuited armature coil, during constant-speed operation with a constant field-winding current, may be determined by setting $i_{a-a'} = 0$ and i_f equal to a constant. Substituting (3.2-4) and (3.2-5) into (3.2-2) yields the following expression for the open-circuit voltage of coil $a - a'$ with the field current i_f a constant:

$$v_{a-a'} = \omega_r L I_f \sin\theta_r \tag{3.2-6}$$

where $\omega_r = d\theta_r/dt$ is the rotor speed. The open-circuit coil voltage $v_{a-a'}$ is zero at $\theta_r = 0, \pi, 2\pi, \ldots$, which is the rotor position during commutation. Commutation is illustrated in Fig. 3.2-2. The open-circuit terminal voltage, v_a, corresponding to the rotor positions denoted as θ_{ra}, θ_{rb} ($\theta_{rb} = 0$), and θ_{rc}, are indicated. It is important to note that, during one revolution of the rotor, the assumed positive direction of armature current i_a is down coil side a and out of coil side a' for $0 < \theta_r < \pi$. For $\pi < \theta_r < 2\pi$, positive current is down coil side a and out of coil side a'. In Chaps. 1 and 2, we let positive current flow into the winding denoted without a prime and out the winding denoted with a prime. We will not be able to adhere to this relationship

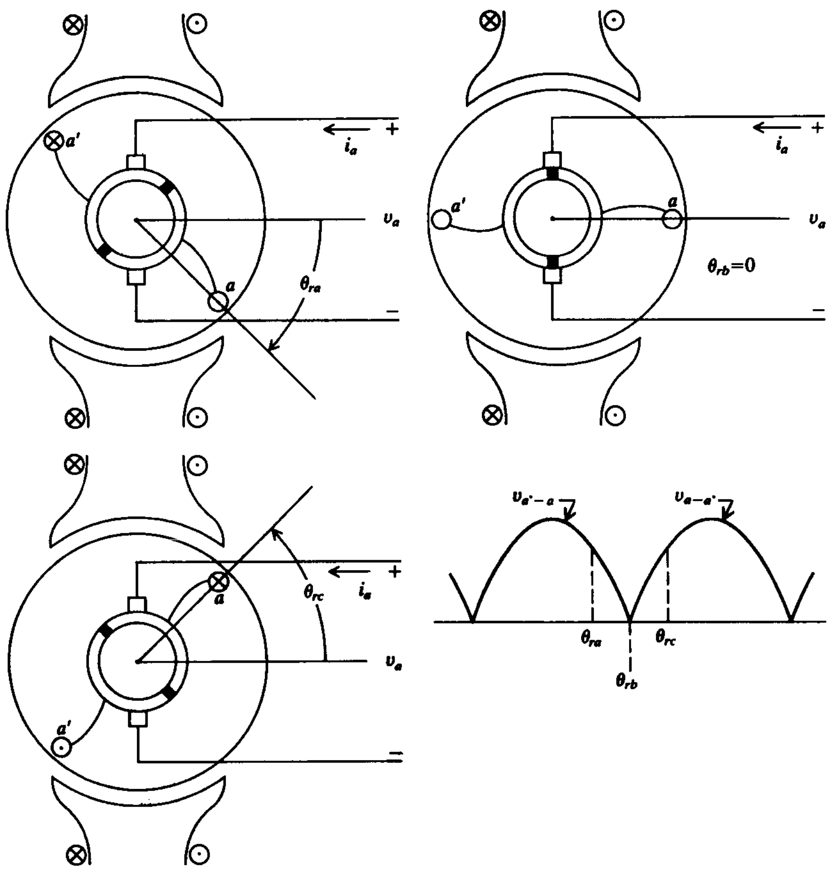

Figure 3.2-2: Commutation of the elementary dc machine.

in the case of the armature windings of a dc machine since commutation is involved. Although the machine shown in Fig. 3.2-1 could be operated as a generator supplying a resistive load, it could not be operated effectively as a motor supplied from a voltage source, owing to the short-circuiting of the armature coil at each commutation. Nevertheless, this impracticable device helps to illustrate two features of commutation; first, commutation takes place when the voltage induced in the rotor winding is ideally zero and, second, commutation can be thought of as a mechanical means of full-wave rectification. We will see another important feature that commutation provides when we consider the torque produced by the dc machine.

A practicable dc machine, with the rotor equipped with an a winding and an A winding, is shown schematically in Fig. 3.2-3. At the rotor position depicted, coils $a_4 - a_4'$ and $A_4 - A_4'$ are being commutated. The bottom brush short-circuits the $a_4 - a_4'$ coil while the top brush short-circuits the $A_4 - A_4'$ coil. Figure 3.2-3 illustrates the instant when the assumed direction of positive current is into the paper in coil sides a_1', A_1; a_2, A_2;..., and out in coil sides a_1', A_1'; a_2', A_2';.... It is instructive to follow the path of current through one of the parallel paths from one brush to the other. For the angular position shown in Fig. 3.2-3, positive current enters the top brush and flows down the rotor via a_1 and back through a_1'; down a_2 and back through a_2'; down a_3 and back through a_3' to the bottom brush. A parallel current path exists through $A_3 - A_3'$, $A_2 - A_2'$, and $A_1 - A_1'$. The open-circuit or induced armature voltage is also shown in Fig. 3.2-3; however, these idealized waveforms require additional explanation. As the rotor advances in the counterclockwise direction, the segment connected to a_1 and A_4 moves from under the top brush, as shown in Fig. 3.2-4. The top brush then rides only on the segment connecting A_3 and A_4'. At the same time, the bottom brush is riding on the segment connecting a_4 and a_3'. With the rotor so positioned, current flows in A_3 and A_4' and out a_4 and a_3'. In other words, current flows down the coil sides in the upper half of the rotor and out of the coil sides in the bottom half. Let us follow the current flow through the parallel paths of the armature windings shown in Fig. 3.2-4. Current now flows through the top brush into A_4' out A_4, into a_1 out a_1', into a_2, out a_2', into a_3 out a_3' to the bottom brush. The parallel path beginning at the top brush is $A_3 - A_3'$, $A_2 - A_2'$, $A_1 - A_1'$, and $a_4' - a_4$ to the bottom brush. The voltage induced in the coils is shown in Figs. 3.2-3 and 3.2-4 for the first parallel path described. It is noted that the induced voltage is plotted only when the coil is in this parallel path.

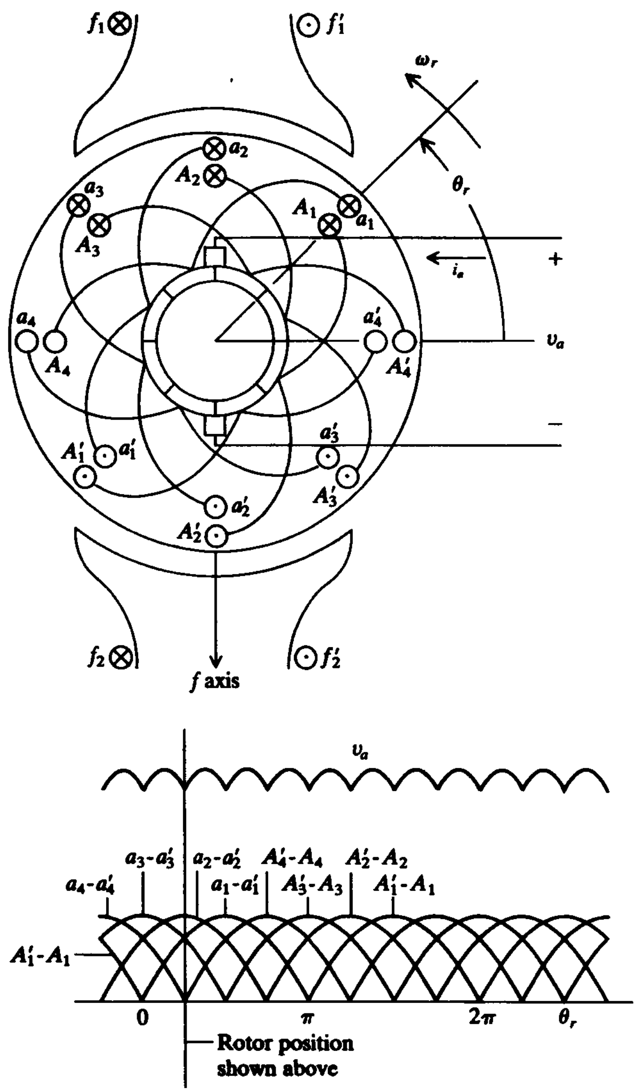

Figure 3.2-3: A dc machine with parallel armature windings.

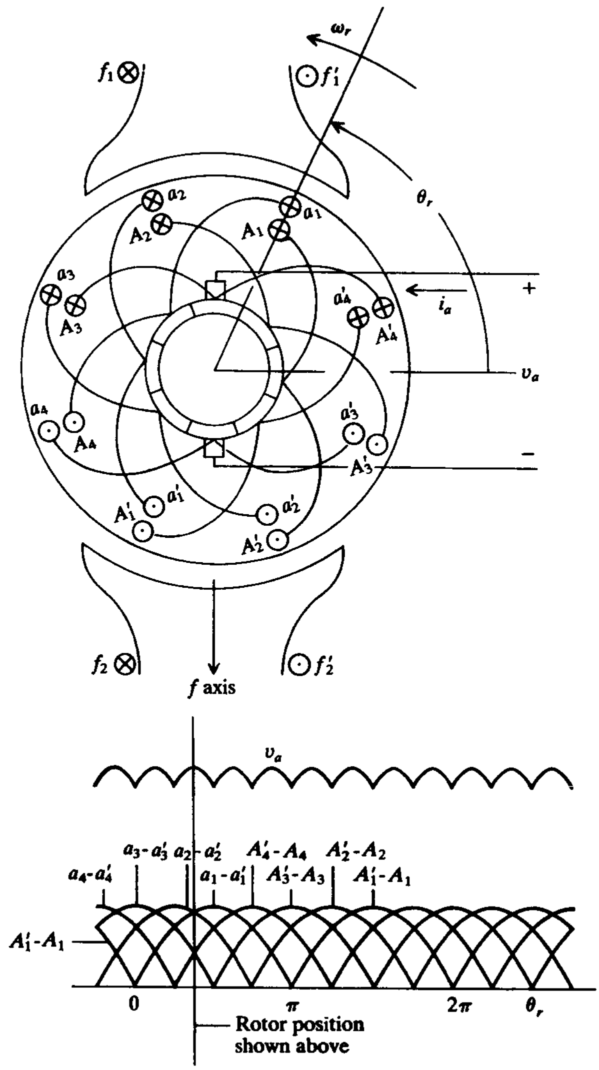

Figure 3.2-4: Same as Fig. 3.2-3 with rotor advanced approximately 22.5° counterclockwise.

In Figs. 3.2-3 and 3.2-4, the parallel windings consist of only four coils. Usually, the number of rotor coils is substantially more than four, thereby reducing the harmonic content of the open-circuit armature voltage. In this case, the rotor coils may be approximated as a uniformly distributed winding, as illustrated in Fig. 3.2-5. Therein the rotor winding is considered as current sheets that are fixed in space due to the action of the commutator and that establish a magnetic axis positioned orthogonal to the magnetic axis of the field winding. We will see the importance of this orthogonal positioning of the magnetic axes when derive the expression of the torque. The brushes are shown positioned on the current sheet for the purpose of depicting commutation. The small angular displacement, denoted by 2γ, designates the region of commutation wherein the coils are short-circuited. However, commutation cannot be visualized from Fig. 3.2-5; one must refer to Figs. 3.2-3 and 3.2-4.

Before proceeding to the development of the equations portraying the operating characteristics of the dc machine, it is instructive to take a brief look at the arrangement of the armature windings and the method of commutation used in many of the low-power, permanent-magnet dc motors. Small dc motors used in low-power control systems are often the permanent-magnet type, wherein a constant field flux is established by a permanent magnet rather than by a current flowing in a field winding.

Three rotor positions of a typical low-power, permanent-magnet dc motor are shown in Fig. 3.2-6. The rotor is turning in the counterclockwise direction and the rotor position advances from left to right. Physically, these devices may be an inch or less in diameter with brushes sometimes as small as a pencil lead. They are mass-produced and relatively inexpensive. Although the brushes actually ride on the outside of the commutator, for convenience they are shown on the inside in Fig. 3.2-6. The armature windings consist of a large number of turns of fine wire; hence, each circle shown in Fig. 3.2-6 represents many conductors. Note that the position of the brushes is shifted approximately 40° relative to a line drawn between the center of the north and south poles. This shift in the brushes was probably determined experimentally by minimizing brush arcing for normal load conditions. Note also that the windings do not span π radians but more like 140°, and there is an odd number of commutator segments.

In Fig. 3.2-6a, only winding 4 is being commutated. As the rotor advances from the position shown in Fig. 3.2-6a, both windings 4 and 1 are being commutated. In Fig. 3.2-6b, winding 1 is being commutated; then

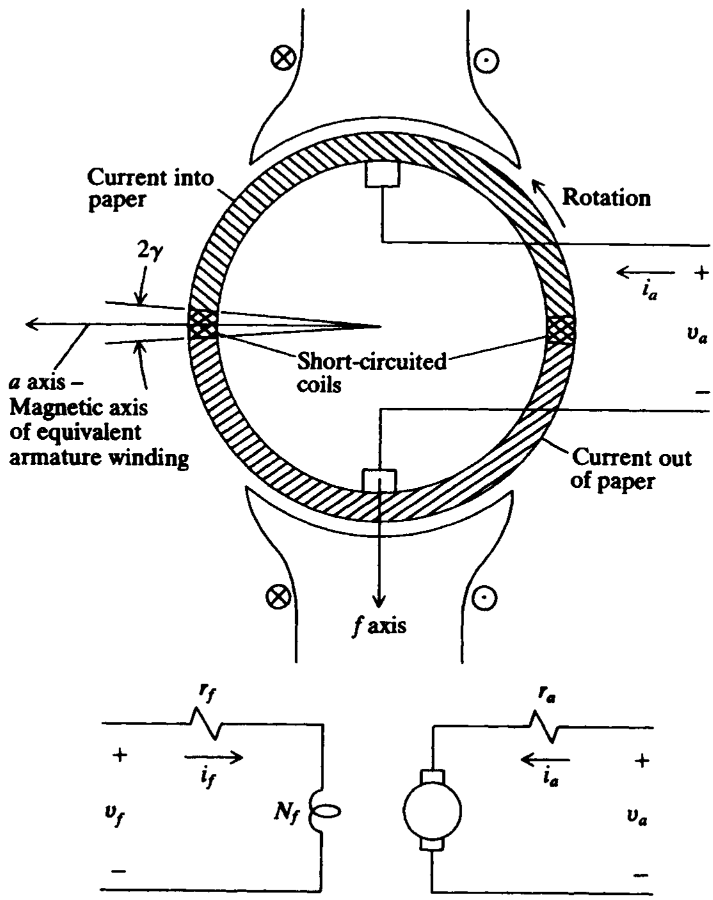

Figure 3.2-5: Idealized dc machine with uniformly distributed rotor winding.

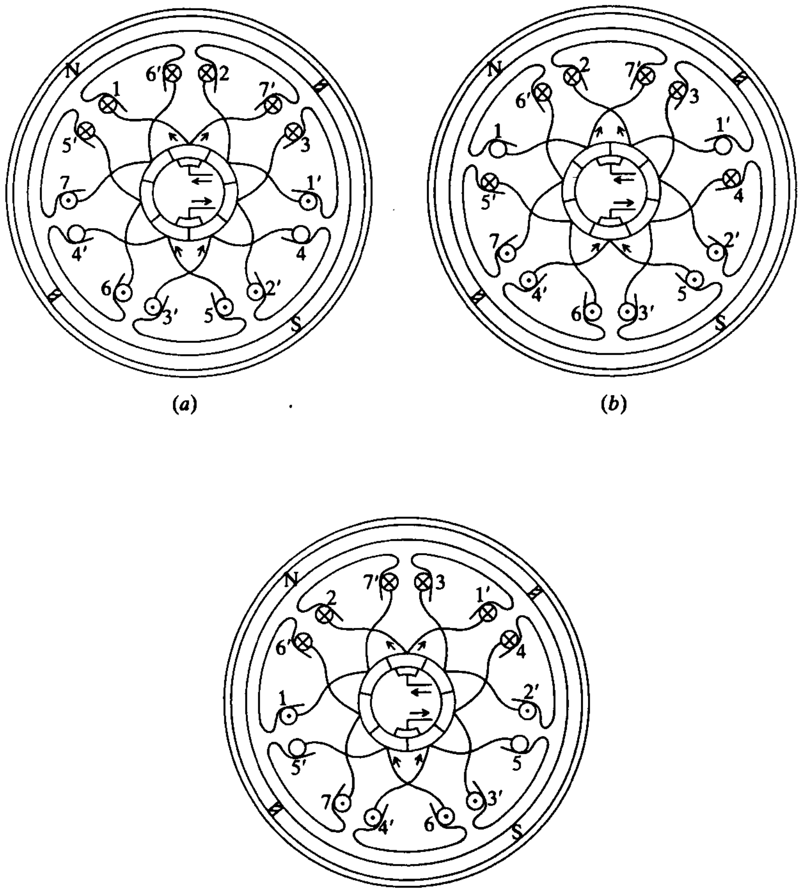

Figure 3.2-6: Commutation of a permanent-magnet dc motor.

windings 1 and 5, and, finally, in Fig. 3.2-6*c*, only winding 5 is being commutated. The windings are being commutated when the induced voltage is nonzero and one would expect some arcing to occur at the brushes. We must realize, however, that the manufacture and sale of these devices is very competitive, and one often must compromise when striving to produce an acceptable motor at the least cost possible. Although we realize that in some cases it may be a rather crude approximation, we will consider the permanent-magnet dc motor as having current sheets on the armature with orthogonal armature and field magnetic axes as shown in Fig. 3.2-5.

For purposes of illustration, a two-pole, general-purpose, shunt-field dc machine is shown in Fig. 3.2-7. A disassembled two-pole, 0.1-hp, 6-V, 12,000-r/min, permanent-magnet dc motor is shown in Fig. 3.2-8. The magnets are made from samarium cobalt and the device is used to drive hand-held battery-operated surgical instruments. Although some of these terms are new to us, they will be defined as we go along.

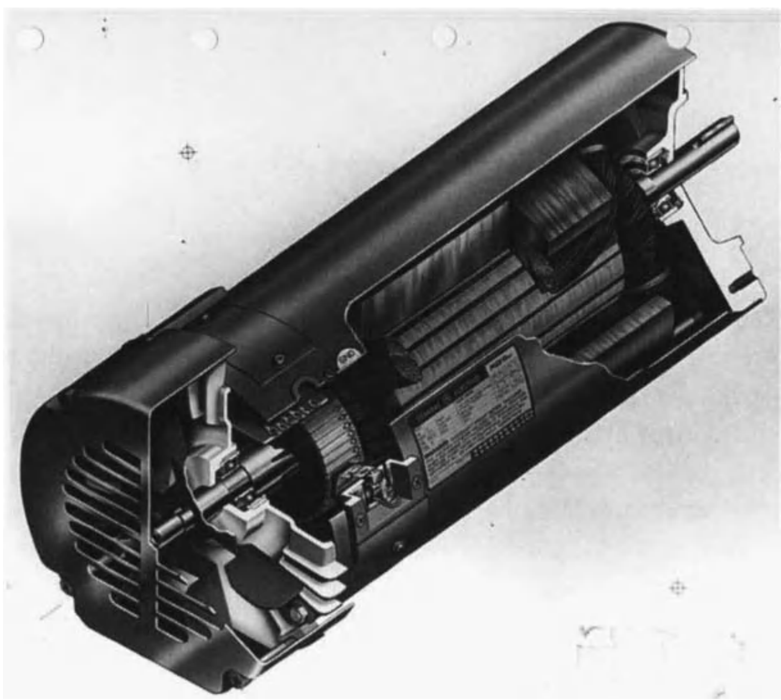

Figure 3.2-7: Cutaway view of two-pole, 3-hp, 180-V, 2500-r/min, shunt-field dc motor. (Courtesy of GE.)

Figure 3.2-8: Two-pole, 0.1-hp, 6-V, 12,000-r/min, permanent-magnet dc motor. (Courtesy of Vick ElectroMech.)

SP3.2-1 The peak value of the voltage induced in one coil shown in Fig. 3.2-3 is 1 V. Determine, from Fig. 3.2-3, the maximum and minimum value of v_a. [2.613 V; 2.414 V]

SP3.2-2 Consider Fig. 3.2-3. Indicate the two parallel paths immediately following commutation of $a_3 - a_3'$ and $A_3 - A_3'$. [$A_3' - A_3$, $A_4' - A_4$, $a_1 - a_1'$, and $a_2 - a_2'$; $A_2 - A_2'$, $A_1 - A_1'$, $a_4' - a_4$, and $a_3' - a_3$]

3.3 VOLTAGE AND TORQUE EQUATIONS

It is advantageous to first consider the dc machine with a field and armature winding before turning to the permanent-magnet device exclusively. Although rigorous derivation of the voltage and torque equations is possible, it is rather lengthy and little is gained since these relationships may be deduced. The armature coils revolve in a magnetic field established by a current flowing in the field winding. We have established that voltage is induced in these coils by virtue of this rotation. However, the action of the commutator causes the armature coils to appear as a stationary winding with its magnetic axis orthogonal to the magnetic axis of the field winding. Consequently, voltages are not induced in one winding due to the time rate of change of the current flowing in the other (transformer action). Mindful of these conditions, we can write the field and armature voltage equations in matrix form as

$$\begin{bmatrix} v_f \\ v_a \end{bmatrix} = \begin{bmatrix} r_f + pL_{FF} & 0 \\ \omega_r L_{AF} & r_a + pL_{AA} \end{bmatrix} \begin{bmatrix} i_f \\ i_a \end{bmatrix} \tag{3.3-1}$$

where L_{FF} and L_{AA} are the self-inductances of the field and armature windings, respectively, and p is the short-hand notation for the operator d/dt. The rotor speed is denoted as ω_r, and L_{AF} is the mutual inductance between the field and the rotating armature coils. The above equation suggests the equivalent circuit shown in Fig. 3.3-1. The voltage induced in the armature circuit, $\omega_r L_{AF} i_f$, is commonly referred to as the counter or back emf. It also represents the open-circuit armature voltage.

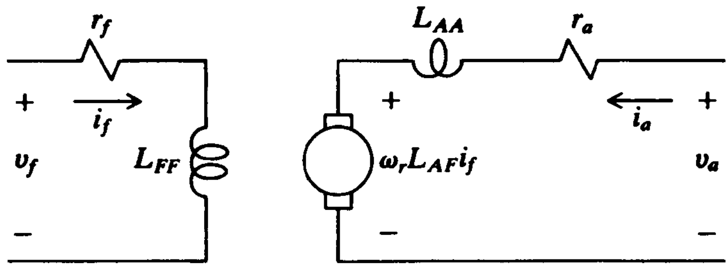

Figure 3.3-1: Equivalent circuit of dc machine.

There are several other forms in which the field and armature voltage equations are often expressed. For example, L_{AF} may also be written as

$$L_{AF} = \frac{N_a N_f}{\Re} \tag{3.3-2}$$

where N_a and N_f are the equivalent turns of the armature and field windings, respectively, and $\Re$ is the reluctance. Thus,

$$L_{AF} i_f = N_a \frac{N_f i_f}{\Re} \tag{3.3-3}$$

If we now replace $N_f i_f/\Re$ with Φ_f, the field flux per pole, then $N_a \Phi_f$ may be substituted for $L_{AF} i_f$ in the armature voltage equation.

Another substitute variable often used is

$$k_v = L_{AF} i_f \tag{3.3-4}$$

We will find that this substitute variable is particularly convenient and frequently used. Even though a permanent-magnet dc machine has no field circuit, the constant field flux produced by the permanent magnet is analogous to a dc machine with a constant k_v.

We can take advantage of previous work to obtain an expression for the electromagnetic torque. In particular, the expression for torque given by (2.8-6) may be used directly to express the torque for the dc machine. If we fix θ_r in Fig. 1.7-4 or Fig. 2.8-1 at $-\frac{1}{2}\pi$, the same relationship exists between the magnetic axes of a dc machine (Fig. 3.2-5) and the magnetic axes of the two-coil machine. Hence, (2.8-6) may be written for the dc machine as

$$T_e = L_{AF} i_f i_a \tag{3.3-5}$$

Here again, the variable k_v is often substituted for $L_{AF} i_f$. In some instances, k_v is multiplied by a factor less than unity when substituted into (3.3-5) so as to approximate the effects of rotational losses. It is interesting that the field winding produces a stationary mmf and, owing to commutation, the armature winding also produces a stationary mmf, which is displaced $\frac{1}{2}\pi$ electrical degrees from the mmf produced by the field winding. It follows then that the interaction of these two mmfs produces the electromagnetic torque and, due to the method of commutation, the mmfs are in quadrature, thereby producing the maximum torque possible for any field and armature currents. In other words, commutation positions the magnet fields stationary and orthogonal, which yields the maximum possible torque, a feature that we will find being emulated by modern-day control of *ac* machines.

The torque and rotor speed are related by

$$T_e = J\frac{d\omega_r}{dt} + B_m \omega_r + T_L \tag{3.3-6}$$

where J is the inertia of the rotor and, in some cases, the connected mechanical load. The units of the inertia are $\mathrm{kg \cdot m^2}$ or $\mathrm{J \cdot s^2}$. A positive electromagnetic torque T_e acts to turn the rotor in the direction of increasing θ_r. The load torque T_L is positive for a torque on the shaft of the rotor, which opposes a positive electromagnetic torque T_e. The constant B_m is a damping coefficient associated with the mechanical rotational system of the machine. It has the units of $\mathrm{N \cdot m \cdot s}$ and it is generally small and often neglected.

In the next section, we will focus on the permanent-magnet dc motor; however, it is worthwhile to take a moment to mention that we have established the basis for several types of dc machines. In particular, the machine shown in Fig. 3.3-1 is a separately excited dc machine. If we connect the field winding in parallel with the armature winding, it becomes a shunt-connected dc machine. If the field winding is connected in series with the armature winding, it is a series-connected dc machine. If two windings are used, one in parallel with and another in series with the armature, it is referred to as a compound-connected dc machine. Clearly, this is an overly simplistic description and the reader is referred to [1,2] for a more detailed consideration of these machine types.

SP3.3-1 When a 12-V, permanent-magnet dc motor is driven at 100 rad/s, the open-circuit voltage is 10 V. Calculate k_v. [$k_v = 0.1$ V · s/rad]

SP3.3-2 The armature applied voltage of a dc motor is 240 V; the rotor speed is constant at 50 rad/s. The steady-state armature current is 15 A, the armature resistance is 1 Ω, and $L_{AF} = 1$ H. Calculate the steady-state field current. [$I_f = 4.5$ A]

SP3.3-3 Calculate the no-load speed ($T_L = 0$) for the permanent-magnet dc motor in SP3.3-1 when rated voltage (12 V) is applied to the armature. [$\omega_r = 120$ rad/s]

SP3.3-4 Multiply the expression for v_a given in (3.3-1) by i_a and identify all terms. [$v_a i_a$ the input power to armature, $i_a^2 r_a$ the armature ohmic loss, $L_{AA} i_a p i_a$ the change of energy stored in L_{AA}, $L_{AF} i_f i_a \omega_r = T_e \omega_r$ the output power]

SP3.3-5 Is SP3.3-4 an alternate method of deriving an expression for torque? Why? [Yes; $L_{AF} i_f i_a$ is the coefficient of $p\theta_r$]

3.4 PERMANENT-MAGNET dc MACHINE

In the case of the permanent-magnet dc machine, $L_{AF} I_f$ is replaced with a constant k_v, whereupon the steady-state armature voltage equation becomes

$$V_a = r_a I_a + k_v \omega_r \tag{3.4-1}$$

If (3.4-1) is solved for I_a and substituted in to (3.3-5) with $L_{AF} I_f$ replaced by k_v, the steady-state torque may be expressed as

$$T_e = \frac{k_v V_a - k_v^2 \omega_r}{r_a} \tag{3.4-2}$$

The steady-state torque-speed characteristic is shown in Fig. 3.4-1.

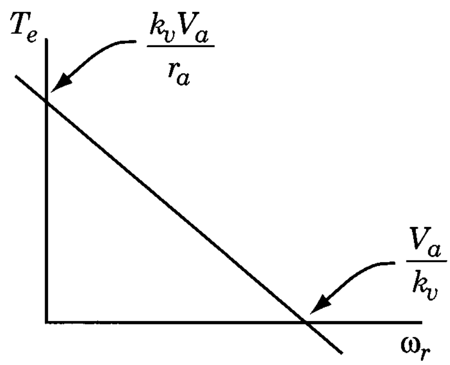

Figure 3.4-1: Steady-state torque-speed characteristic of a permanent-magnet dc machine.

It apparent from Fig.3.4-1, that the stall ($\omega_r = 0$) torque could be made larger for a given armature voltage by reducing r_a. Although the machine may be designed with a smaller armature resistance, there is a problem since, at stall, the steady-state armature current is limited by the armature resistance; hence, for a constant V_a, reducing r_a will result in a larger I_a, which can cause damage to the brushes. On the other hand, increasing the starting torque by reducing r_a causes the torque-speed characteristics to have a steeper slope, which results in a smaller change in speed for a given change in load torque during normal (near rated) operation. If, however, the armature voltage is reduced during the starting period to protect the brushes, the desirable characteristic of a small speed change during load torque variations during normal operation could be achieved. In fact, controlled regulation of the armature voltage is generally employed for large horsepower machines by using a converter; however, low-power, permanent-magnet dc machines are generally supplied from a battery, as in the case of the automobile, and, therefore, a large armature resistance is necessary in order to prevent brush damage during the early part of the starting period. Fortunately, a small speed variation during load torque changes is not required in many applications of the permanent-magnet dc machine; therefore, the steep torque-speed characteristics are not necessary. We will consider the dynamic performance of a permanent-magnet dc motor in the next section. In a later chapter, we will discover that the permanent-magnet ac machine can be controlled to have torque-speed characteristics similar to that of the permanent-magnet dc motor. This device is commonly referred to as a brushless dc machine.

Example 3A. A permanent-magnet dc motor similar to that shown in Fig. 3.2-8 is rated at 6 V with the following parameters: $r_a = 7\,\Omega$, $L_{AA} = 120$ mH, $k_T = 2$ oz·in/A, and $J = 150\ \mu$oz·in·s^2. According to the motor information sheet, the no-load speed is approximately 3350 r/min and the no-load armature current is approximately 0.15 A. Let us attempt to interpret this information.

First, let us convert k_T and J to units that we have been using in this text. In this regard, we will convert the inertia to kg·m^2, which is the same as N·m·s^2. To do this, we must convert ounces to Newtons and inches to meters (Appendix A). Thus,

$$J = \frac{150 \times 10^{-6}}{(3.6)(39.37)} = 1.06 \times 10^{-6}\ \mathrm{kg \cdot m^2} \tag{3A-1}$$

We have not seen k_T before. It is the torque constant and, if expressed in the appropriate units, it is numerically equal to k_v. When k_v is used in the expression for T_e ($T_e = k_v i_a$), it is often referred to as the *torque constant* and denoted k_T. When used in the voltage equation, it is always denoted k_v. Now we must convert oz·in to N·m, whereupon k_T equals our k_v; hence,

$$k_v = \frac{2}{(16)(0.225)(39.37)} = 1.41 \times 10^{-2}\mathrm{N \cdot m/A} = 1.41 \times 10^{-2}\mathrm{V \cdot s/rad} \tag{3A-2}$$

What do we do about the no-load armature current? What does it represent? Well, probably it is a measure of the friction and windage losses. We could neglect it, but we will not. Instead, let us include it as B_m. First, however, we must calculate the no-load speed. We can solve for the no-load rotor speed from the steady-state armature voltage equation (3.4-1):

$$\omega_r = \frac{V_a - r_a I_a}{k_v} = \frac{6 - (7)(0.15)}{1.41 \times 10^{-2}} = 351.1 \text{ rad/s}$$

$$= \frac{(351.1)(60)}{2\pi} = 3353 \text{ r/min} \tag{3A-3}$$

Now at this no-load speed,

$$T_e = k_v i_a = (1.41 \times 10^{-2})(0.15) = 2.12 \times 10^{-3} \text{ N} \cdot \text{m} \tag{3A-4}$$

Since T_L and $J(d\omega_r/dt)$ are zero for this steady-state no-load condition, (3.3-6) tells us that (3A-4) is equal to $B_m\omega_r$; hence,

$$B_m = \frac{2.12 \times 10^{-3}}{\omega_r} = \frac{2.12 \times 10^{-3}}{351.1} = 6.04 \times 10^{-6} \text{ N} \cdot \text{m} \cdot \text{s} \tag{3A-5}$$

Example 3B. The permanent-magnet dc machine described in Example 3A is operating with rated applied armature voltage and a load torque T_L of 0.5 oz · in. Our task is to determine the efficiency where percent eff = (power output/power input)100.

First let us convert oz · in to N · m:

$$T_L = \frac{0.5}{(16)(0.225)(39.37)} = 3.53 \times 10^{-3} \text{ N} \cdot \text{m} \tag{3B-1}$$

In Example 3A, we determined k_v to be 1.41×10^{-2} V · s/rad and B_m to be 6.04×10^{-6} N · m · s.

During steady-state operation, (3.3-6) becomes

$$T_e = B_m\omega_r + T_L \tag{3B-2}$$

From (3.3-5), with $L_{AF}i_f$ replaced by k_v, the steady-state electromagnetic torque is

$$T_e = k_v I_a \tag{3B-3}$$

Substituting (3B-3) into (3B-2) and solving for ω_r yields

$$\omega_r = \frac{k_v}{B_m} I_a - \frac{1}{B_m} T_L \tag{3B-4}$$

Repeating (3.4-1)

$$V_a = r_a I_a + k_v \omega_r \tag{3B-5}$$

Substituting (3B-4) into (3B-5) and solving for I_a yields

$$I_a = \frac{V_a + (k_v/B_m)T_L}{r_a + (k_v^2/B_m)}$$

$$= \frac{6 + [(1.41 \times 10^{-2})/(6.04 \times 10^{-6})](3.53 \times 10^{-3})}{7 + (1.41 \times 10^{-2})^2/(6.04 \times 10^{-6})} = 0.357 \text{ A} \tag{3B-6}$$

From (3B-4),

$$\omega_r = \frac{1.41 \times 10^{-2}}{6.04 \times 10^{-6}} 0.357 - \frac{1}{6.04 \times 10^{-6}}(3.53 \times 10^{-3})$$

$$= 249 \text{ rad/s} \tag{3B-7}$$

The power input is

$$P_{\text{in}} = V_a I_a = (6)(0.357) = 2.14 \text{ W} \tag{3B-8}$$

The power output is

$$P_{\text{out}} = T_L \omega_r = (3.53 \times 10^{-3})(249) = 0.88 \text{ W} \tag{3B-9}$$

The efficiency is

$$\text{Percent eff} = \frac{P_{\text{out}}}{P_{\text{in}}} 100$$

$$= \frac{0.88}{2.14} 100 = 41.1 \text{ percent} \tag{3B-10}$$

This low efficiency is characteristic of low-power dc motors due to the relatively large armature resistance. In this regard, it is interesting to determine the losses due to i^2r, friction, and windage:

$$P_{i^2r} = r_a I_a^2 = (70)(0.357)^2 = 0.89 \text{ W} \tag{3B-11}$$

$$P_{fw} = (B_m \omega_r)\omega_r = (6.04 \times 10^{-6})(249)^2 = 0.37 \text{ W} \tag{3B-12}$$

Let us check our work:

$$P_{\text{in}} = P_{i^2r} + P_{fw} + P_{\text{out}} = 0.89 + 0.37 + 0.88 = 2.14 \text{ W} \tag{3B-13}$$

which is equal to (3B-8).

SP3.4-1 A 12-V, permanent-magnet dc motor has an armature resistance of 12 Ω and $k_v = 0.01$ V · s/rad. Calculate the steady-state stall torque (T_e with $\omega_r = 0$). [$T_e = 0.01$ N · m]

SP3.4-2 Determine T_e in Example 3B. [$T_e = 0.713$ oz · in]

3.5 DYNAMIC CHARACTERISTICS OF A PERMANENT-MAGNET dc MOTOR

Two modes of dynamic operation are of interest; starting from stall and changes in load torque with the machine supplied from a constant-voltage source. The permanent-magnet dc machine considered in Examples 3A and 3B is used to demonstrate these modes of operation. It is important that the reader become familiar with the material in these examples before proceeding.

Dynamic Performance During Starting

In the previous section, it was pointed out that, if the armature resistance is small, damaging armature current could result if rated voltage is applied to the armature terminals when the machine is stalled ($\omega_r = 0$). With the machine at stall, the counter emf is zero; therefore, during the transient starting period, the armature current is opposed only by the voltage drop across the armature resistance ($r_a i_a$) and the armature inductance ($L_{AA} di_a/dt$). We have mentioned and also noted in Examples 3A and 3B that low-power permanent-magnet dc motors are designed with a large armature resistance, making it possible to "direct line" start these devices without damaging brushes or the stator windings. The no-load starting characteristics ($T_L = 0$) of the permanent-magnet dc motor described in Example 3A are shown in Fig. 3.5-1. The armature voltage v_a, the armature current i_a, and the rotor speed ω_r are plotted. Initially, the motor is at stall and, at time zero, 6 V is applied to the armature terminals. The peak transient armature current is limited to approximately 0.55 A due to the voltage drop across the inductance and resistance of the armature and the fact that the rotor is accelerating from stall, thereby developing the voltage $k_v\omega_r$, which also opposes the applied voltage. After about 0.25 s, steady-state operation is achieved with the no-load armature current of 0.15 A. (From Example 3A, $B_m = 6.04 \times 10^{-6}$ N · m · s.) It is noted that the rotor speed is slightly os-

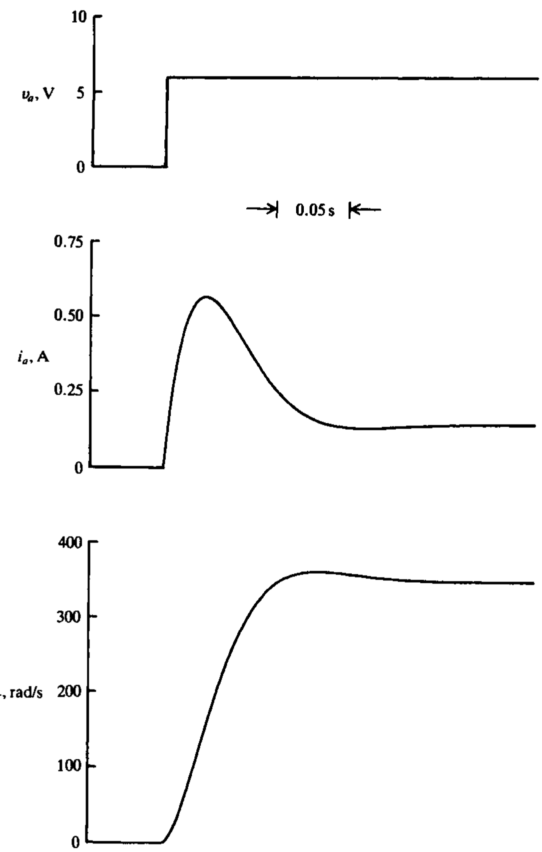

Figure 3.5-1: Starting characteristics of a permanent-magnet dc machine.

cillatory (underdamped), as illustrated by the small overshoot of the final, steady-state value.

Dynamic Performance During Sudden Changes in Load Torque

In Example 3B, we calculated the efficiency of the permanent-magnet dc motor given in Example 3A with a load torque of 0.5 oz·in (3.53×10^{-3}N·m). Let us assume that this load torque was suddenly applied with the motor initially operating at the no-load condition ($I_a = 0.15$ A). The dynamic characteristics following a step change in load torque T_L from zero to 0.5 oz · in are shown in Fig. 3.5-2. The armature current i_a and the rotor speed ω_r are plotted. Since $T_e = k_v i_a$ and since k_v is constant, T_e differs from i_a by a constant multiplier. It is noted that the system is slightly oscillatory. Also, it is noted that the change in the steady-state rotor speed is quite large.

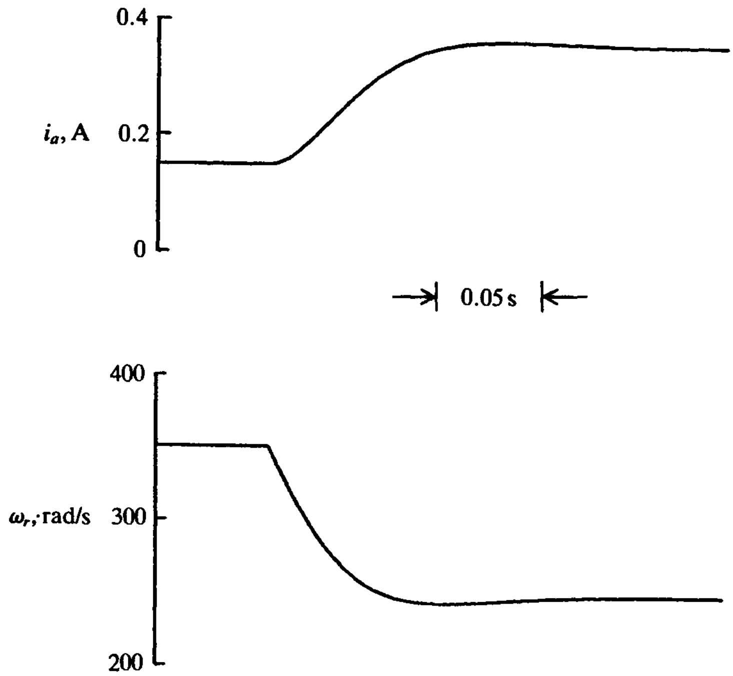

Figure 3.5-2: Dynamic performance of a permanent-magnet dc motor following a sudden increase in load torque from zero to 0.5 oz · in.

From Example 3A or Fig. 3.5-2, we see that no-load speed is 351.1 rad/s. With $T_L = 0.5$ oz · in, the rotor speed is 249 rad/s as calculated in Example 3B and noted from Fig. 3.5-2. There has been approximately a 30 percent decrease in speed for this increase in load torque. As we have mentioned, this is characteristic of a low-power permanent-magnet motor owing to the high armature resistance.

SP3.5-1 Plot the T_e versus ω_r characteristic for the permanent-magnet dc motor given in Example 3A. [A straight line between (12.1×10^{-3}, 0) and (0, 425.5)]

SP3.5-2 Assume that the peak value of i_a in Fig. 3.5-1 is 0.55 A. Calculate $k_v\omega_r$ at peak i_a. [$k_v\omega_r = 2.15\,\text{V}$]

3.6 INTRODUCTION TO CONSTANT-TORQUE AND CONSTANT-POWER OPERATION

If it were not for the frictional losses attributed to the sliding contact between the brushes and commutator segments and the arcing during commutation, the dc machine would be the ideal electromagnetic device. Due to commutation, the stator and rotor magnetic systems are orthogonal, thereby producing the maximum possible torque per ampere (per unit of field strength). We will find that this feature is the goal of many of the control methods used with the permanent-magnet ac machine and the induction machine.

Fortunately, the equations that describe the performance of a dc machine provide an excellent opportunity to introduce these control principles in a straightforward manner. In this section, we will attempt to take advantage of this opportunity and to do this without the complexities of converter switching or the details of the actual controls.

Let us start by repeating the steady-state voltage and torque equations for a permanent-magnet dc machine.

$$V_a = r_a I_a + k_v \omega_r \tag{3.6-1}$$

$$T_e = k_v I_a \tag{3.6-2}$$

Recall that if the device has a field winding rather than a permanent magnet, k_v is replaced by $L_{AF}I_f$. Also, the torque-speed characteristics shown in Fig. 3.4-1 are repeated in Fig. 3.6-1. It is noted that the y- or T_e-intercept is $k_v V_a / r_a$ and the x- or ω_r-intercept is V_a/k_v. The torque-speed characteristics shown in Fig. 3.6-1 are for rated V_a (V_{aR}); however, if we reduce V_a the torque-speed line would shift down toward the origin. Therefore, depending upon the load torque and the value of V_a, steady-state operation is possible without exceeding rated V_a anywhere in the region below the rated voltage torque-speed line. To illustrate this, three load-torque characteristics are shown in Fig. 3.6-1: T_{L1}, T_{L2}, and T_{L3}. It is assumed that the load-torque characteristics are approximated by a linear function of speed. Although this may be an over simplification, it is a convenient approximation.

Three operating points are shown in Fig. 3.6-1. The first is the intersection of the T_{L1} line and the torque-speed plot with $V_a = V_{aR}$. We will assume that rated conditions V_{aR}, I_{aR}, T_{eR}, and ω_{rR} all occur at this operating point.

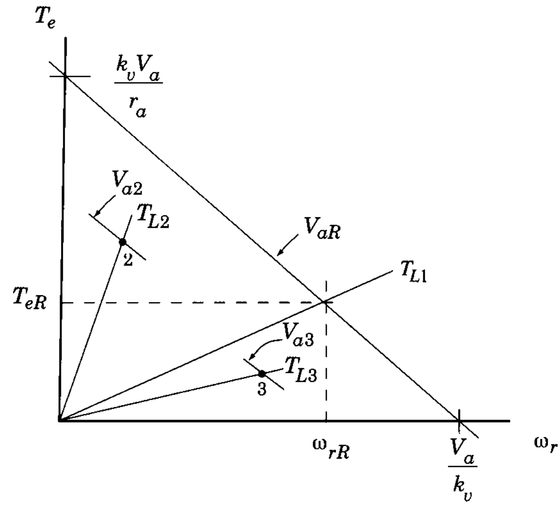

Figure 3.6-1: Torque-speed characteristics with voltage control.

The second operating point occurs at T_{L2} and V_{a2}, where $V_{a2} < V_{aR}$. The third operating point is at the intersection of the T_{L3} load line with the torque-speed plot with V_{a3}, where $V_{aR} > V_{a1} > V_{a3}$. Therefore, the region below the torque-speed plot with $V_a = V_{aR}$ is the region of the operation without exceeding V_{aR}. This is assuming that we have a means of reducing the voltage applied to the armature, which we will cover in a later section.

Constant-Torque Operation

There is something we are overlooking. What about rated armature current? Well, we know from (3.6-2), that I_{aR} occurs at T_{eR} and we see from Fig. 3.6-1 that operating point T_{L2} with V_{a2} occurs at more than twice rated torque (armature current). This operating point is not practical due to overheating and, moreover, the commutator may not be able to handle a continuous current of this magnitude. If the region of operation is controlled so that rated V_{aR} and I_{aR} are not exceeded, then the upper limit of the operating region is T_{eR}, shown by the dashed line in Fig. 3.6-1. This region or envelope of operation is shown again in Fig. 3.6-2 with solid-line boundaries. For speeds less than ω_{rR}, the maximum torque is determined by the rated current I_{aR}, whereas for speeds greater than ω_{rR}, the maximum torque is determined by the rated voltage V_{aR}. Also shown are three load-torque lines $\frac{5}{3}T_{L1}$, T_{L1}, and $\frac{2}{3}T_{L1}$. This figure is the same as the third trace in Fig. 3.6-3, where machine

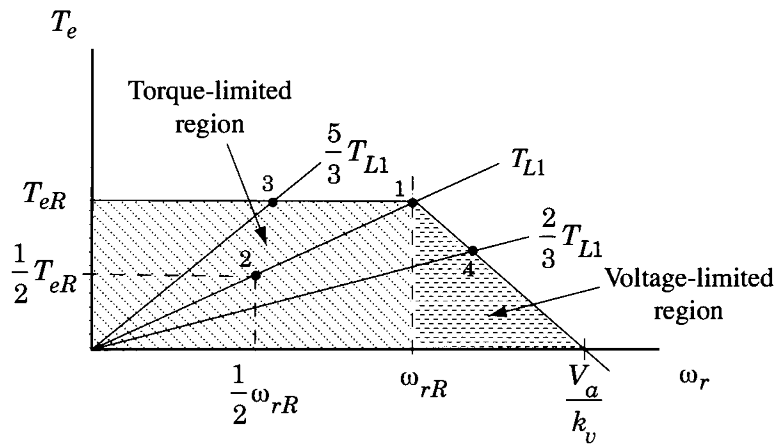

Figure 3.6-2: Torque control of a permanent-magnet dc machine for $\omega_r \leq \omega_{rR}$.

variables I_a, V_a, P_{in} and output power P_o are also plotted. The plots shown in Fig. 3.6-3 depict the values of the armature voltage V_a and current I_a necessary to produce the boundary or envelope of operation shown in Fig. 3.6-2. However, it is important to emphasize that the region of operation is defined by the envelope of the torque-versus-speed characteristics as shown by the shaded area in Fig. 3.6-2.

We have noticed the dots and numbers, which we assume represent operating points, in Figs. 3.6-2 and 3.6-3, and we have been waiting for an explanation. Depending on the type of control being implemented, the commanded values could be one or all of the desired values of armature voltage, torque (armature current), and/or rated speed. Also, depending upon the type of control, the sensed or measured machine variables could include armature voltage and/or current and rotor speed.

The schematic block diagram shown in Fig. 3.6-4 is sufficient to illustrate torque control for the points of operation shown in Figs. 3.6-2 and 3.6-3. As mentioned, three load-torque characteristics are shown in Figs. 3.6-2 and 3.6-3. The T_{L1} load-torque line intersects rated conditions. This operating point is indicated as "1" on the plots shown in Figs. 3.6-2 and 3.6-3. This would be the point of operation for this load-torque characteristic with commanded $T_e^* = T_{eR}$. Is it clear that operating point 1 would also be the normal (uncontrolled) intersection of the T_{L1} load-torque character-

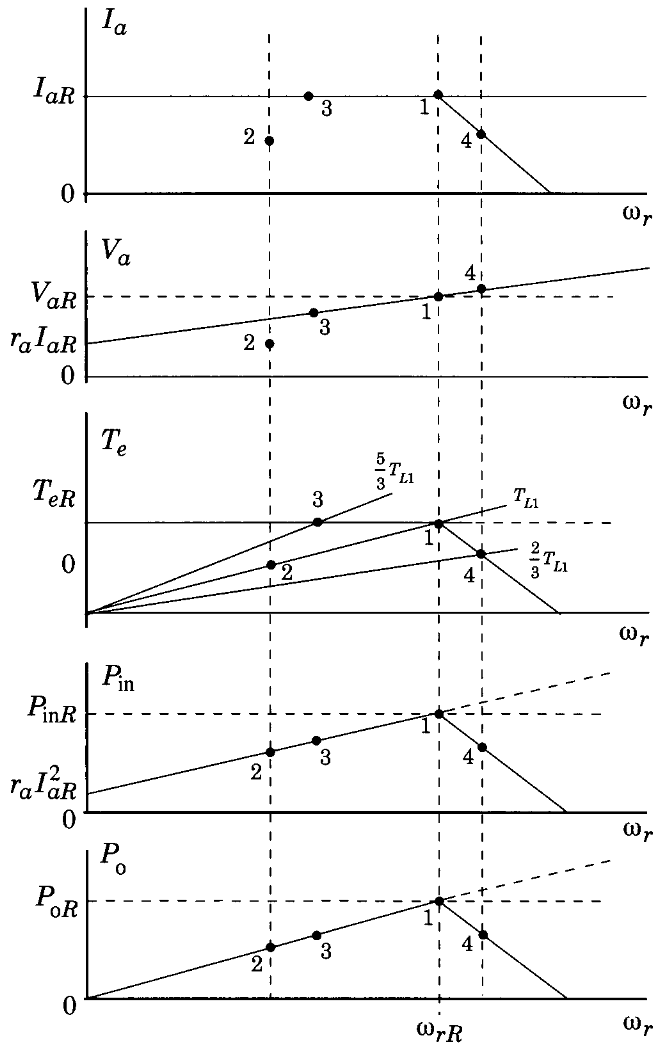

Figure 3.6-3: Machine variables for the controlled operating region depicted in Fig. 3.6-2.

istics and the torque-speed plot with V_{aR} applied to the terminals? Let us now command T_e^* to be $\frac{1}{2}T_{eR}$ with the same load-torque characteristics T_{L1}. Steady-state operation would occur at point 2. Since a linear load-torque characteristic is assumed, the rotor speed would be $\frac{1}{2}\omega_{rR}$. This operating point is indicated by "2" on the plots of the machine variables in Fig. 3.6-3. The machine is operating well within the operating envelope. If we assume that the load-torque characteristic is changed to $\frac{5}{3}T_{L1}$ and $T_e^* = T_{eR}$. Point 3 in Fig. 3.6-2 would be the controlled operating point. We see that the current limit for T_{eR}^* would be exceeded at higher rotor speeds. This operating point is shown as "3" on the plots in Fig. 3.6-3. Assume that the load-torque characteristic is changed to $\frac{2}{3}T_{L1}$ with $T_e^* = T_{eR}$. The steady-state operating point would be at "4." In this case, T_{eR} cannot be achieved without exceeding V_{aR}. We have reached the voltage limit and the control would be unable to maintain T_{eR} and with $V_a = V_{aR}$ point 4 would be the normal, uncontrolled intersection of the rated torque-speed characteristic. This operating point is also shown as "4" on the plots of machine variables in Fig. 3.6-3.

Constant-Power Operation

Before leaving this introductory discussion of controlled operation of a dc machine, let us consider one addition type of control referred to as *constant power* or *field weakening*. Although this control has limited application in the case of dc machines, the concept of this type of control, which is used in permanent-magnet ac machines, is readily explained for a dc machine. For this purpose, let us express the steady-state voltage and torque equations for the dc machine with a field winding:

$$V_a = I_a r_a + L_{AF} I_f \omega_r \tag{3.6-3}$$

$$V_f = I_f r_f \tag{3.6-4}$$

$$T_e = L_{AF} I_f I_a \tag{3.6-5}$$

The discussion presented thus far in this section applies not only to permanent-magnet dc machines but also to a dc machine with a field winding with the field current held constant. In fact, if $L_{AF}I_f$ is made equal to k_v there would be no difference; however, it is difficult to explain field weakening with a permanent-magnet dc machine. Therefore, it is convenient to change to a machine with a field winding for discussion purposes and let the rated field current I_{fR} occur at ω_{rR}.

The reason behind field weakening is to extend the speed range of the machine by reducing the back emf ($L_{AF}I_f\omega_r$) in (3.6-3), thereby allowing V_{aR} to maintain I_{aR} at rotor speeds higher than ω_{rR}. It must be assumed that higher rotor speeds can be achieved without mechanical damage.

Field weakening is illustrated in Figs. 3.6-5 and 3.6-6. The characteristics for operation below ω_{rR} are those discussed previously and shown in Figs. 3.6-2 and 3.6-3. Field weakening occurs at rotor speeds above ω_{rR}, wherein the field current is decreased as the rotor speed increases. In particular, it will be assumed that for $\omega_r > \omega_{rR}$, the field current for the boundary where $P_o^* = P_{oR}$ will be varied in accordance with

$$I_f = \frac{P_{oR}}{L_{AF}\omega_r I_{aR}} \qquad \text{for } \omega_r > \omega_{rR} \tag{3.6-6}$$

where

$$\begin{aligned} P_{oR} &= T_{eR}\omega_{rR} \\ &= L_{AF}I_{fR}I_{aR}\omega_{rR} \end{aligned} \tag{3.6-7}$$

The upper boundary of the region of operation (Fig. 3.6-5) during the field-weakening mode is obtained with $V_a = V_{aR}$ and $I_a = I_{aR}$. Thus, the input power and output power are constant at P_{inR} and P_{oR}, respectively.

Three load-torque characteristics are shown in Figs. 3.6-5 and 3.6-6: T_{L1}, $\frac{2}{3}T_{L1}$, and $\frac{1}{3}T_{L1}$. The load-torque line labeled T_{L1} is the same as used in previous figures and is indicated as operating point 1 in Figs. 3.6-5 and 3.6-6. Operating point 2 is for $\frac{2}{3}T_{L1}$ and operating point 3 for $\frac{1}{3}T_{L1}$. The schematic block diagram shown in Fig. 3.6-7 is a control method that could be used to achieve constant-power control.

The controlled-torque mode operation illustrated in Figs. 3.6-2 and 3.6-3 is often referred to as the constant-torque mode, whereas the field-weakening mode illustrated in Figs. 3.6-5 and 3.6-6 is often called the constant-power mode. One might confuse the boundary or envelope as a plot of the only operating points. Indeed, the boundaries shown in Figs. 3.6-5 and 3.6-6 form the envelope of an array of possible operating points within the envelope. It is interesting that the upper boundary of T_e during the constant-power (field-weakening) mode varies as I_f, (3.6-7), since $I_a = I_{aR}$.

When operating in the constant-power mode, it would be customary to command another operating condition in addition to P_o. If, for example, $P_o^* = \frac{1}{2}P_{oR}$ and $I_a^* = I_{aR}$, then V_f would be controlled so that I_f would be

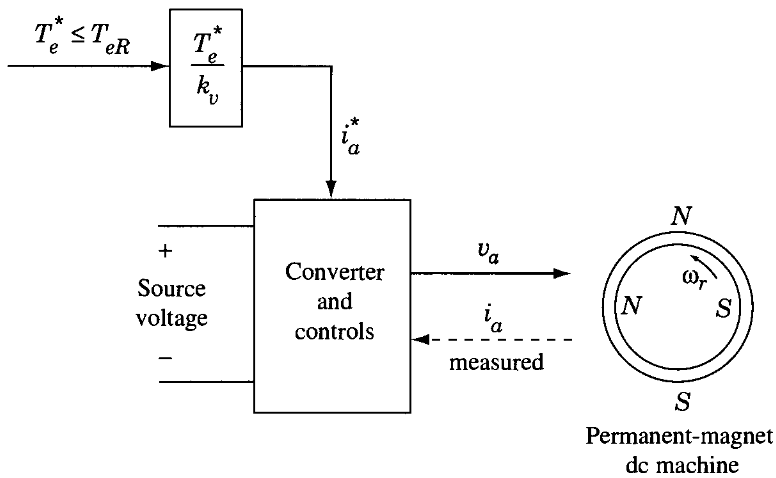

Figure 3.6-4: Torque control of a permanent-magnet dc machine for $\omega_r \leq \omega_{rR}$.

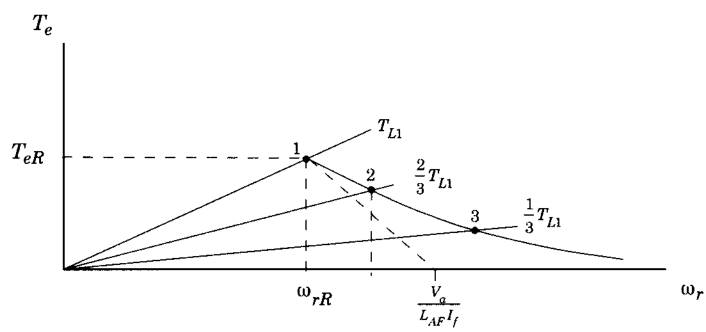

Figure 3.6-5: Controlled operating region with constant power (field weakening) added.

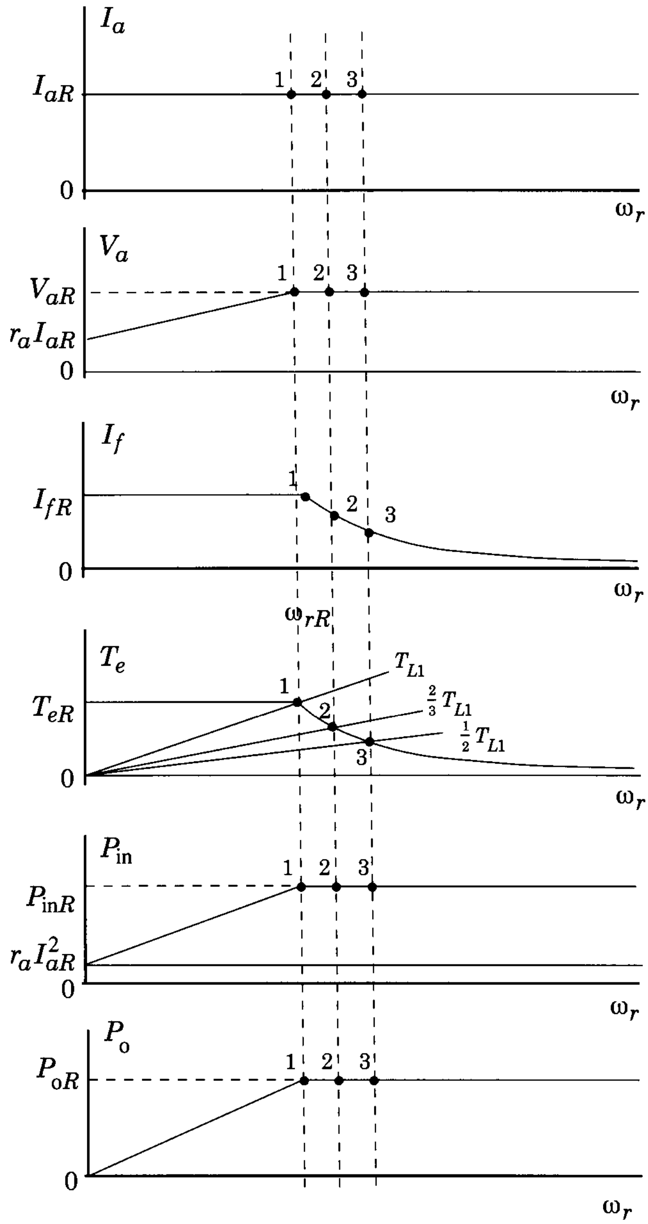

Figure 3.6-6: Machine variables for controlled operation depicted in Fig. 3.6-5.

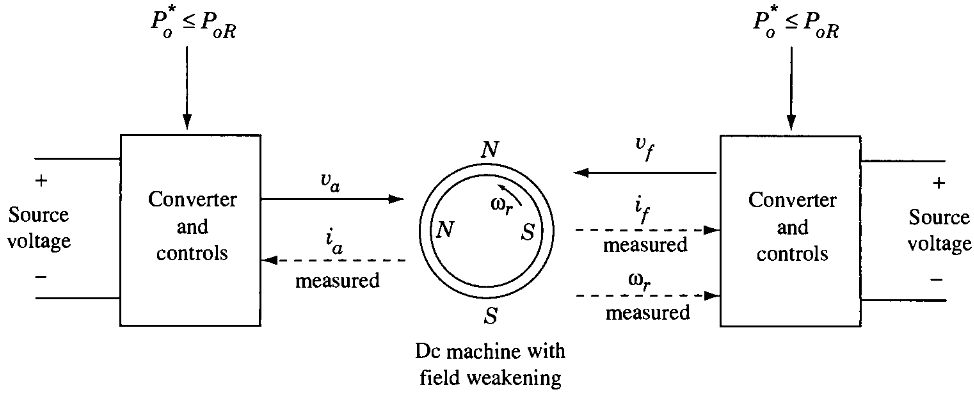

Figure 3.6-7: Power output control (field weakening) for dc machine with field winding and $\omega_r > \omega_{rR}$.

$$I_f = \frac{\omega_{rR}}{\omega_r} I_{fR} \tag{3.6-8}$$

The armature voltage would be regulated to

$$V_a = r_a I_a^* + \frac{P_o^*}{I_a^*} \tag{3.6-9}$$

wherein $I_a^* = I_{aR}$ and $P_o^* = \frac{1}{2} P_{oR}$.

SP3.6-1 If in Fig. 3.6-1 the load-torque characteristic is T_{L3} and $V_a = V_{aR}$, define the operating point. [Intersection of T_{L3} and the rated V_a torque-speed curve]

SP3.6-2 What would happen to the rotor speed if, during field weakening, the field current accidentally became zero? Why? [ω_r would accelerate to machine destruction; field flux would be only the residue]

SP3.6-3 For the operating points shown in Fig. 3.6-1, identify those that would fall within the constant-torque operating envelope. [All but operating point 2 in Fig. 3.6-1]

SP3.6-4 Verify (3.6-8) and (3.6-9).

3.7 TIME-DOMAIN BLOCK DIAGRAM AND STATE EQUATIONS FOR THE PERMANENT-MAGNET dc MACHINE

Although the analysis of control systems is not our intent, it is worthwhile to set the stage for this type of analysis by means of a first look at time-domain block diagrams and state equations. Block diagrams, which portray the interconnection of the system equations, are used extensively in control system analysis and design. Arranging the equations of a permanent-magnet dc machine into a block diagram representation is straightforward. The armature voltage equation, (3.3-1), and the relationship between torque and rotor speed, (3.3-6), may be written as

$$v_a = r_a(1 + \tau_a p)i_a + k_v\omega_r \tag{3.7-1}$$

$$T_e - T_L = (B_m + Jp)\omega_r \tag{3.7-2}$$

where the armature time constant is $\tau_a = L_{AA}/r_a$. Here, p denotes d/dt and $1/p$ denotes integration. Solving (3.7-1) for i_a, and (3.7-2) for ω_r yields

$$i_a = \frac{1/r_a}{\tau_a p + 1}(v_a - k_v\omega_r) \tag{3.7-3}$$

$$\omega_r = \frac{1}{Jp + B_m}(T_e - T_L) \tag{3.7-4}$$

A few comments are in order regarding these expressions. In (3.7-3), we see that $(v_a - k_v\omega_r)$ is multiplied by the operator $(1/r_a)/(\tau_a p + 1)$ to obtain the armature current i_a. The fact that we are multiplying the voltage by an operator to obtain current is in no way indicative of the procedure that we might actually use to calculate the current i_a given the voltage $(v_a - k_v\omega_r)$. We are simply expressing the dynamic relationship between voltage and current in a form convenient for drawing block diagrams. However, to calculate i_a, we may prefer to express (3.7-3) in its equivalent form (3.7-1) and solve the given first-order differential equation using standard techniques. The operator $(1/r_a)/(\tau_a p + 1)$ in (3.7-3) may also be interpreted as a transfer function relating the voltage and current. Those of you who are familiar with

Laplace transform methods are likely accustomed to seeing transfer functions expressed in terms of the Laplace operator s instead of the differentiation operator p. In fact, the same transfer functions are obtained by using Laplace transform theory with p replaced by s.

The time-domain block diagram portraying (3.7-3) and (3.7-4) with $T_e = k_v i_a$ is shown in Fig. 3.7-1. This diagram consists of a set of linear blocks, wherein the relationship between the input and corresponding output variable is depicted in transfer function form.

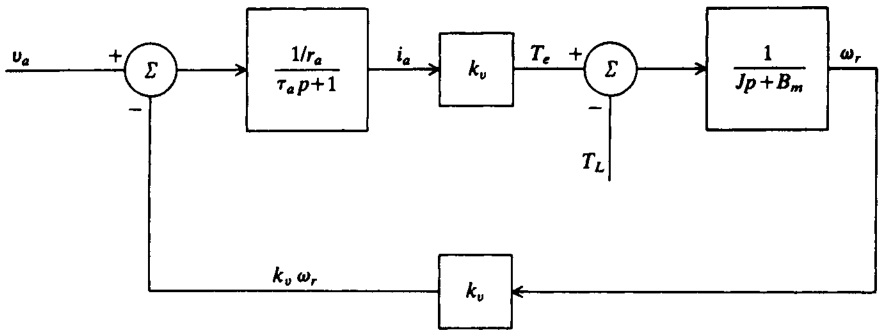

Figure 3.7-1: Time-domain block diagram of a permanent-magnet dc machine.

The so-called state equations of a system represent the formulation of the state variables into a matrix form convenient for computer implementation for linear systems. The state variables of a system are defined as a minimal set of variables such that knowledge of these variables at any initial time t_0 plus information on the input excitation subsequently applied is sufficient to determine the state of the system at any time $t > t_0$ [2]. In the case of the permanent-magnet dc machines, the armature current i_a, the rotor speed ω_r, and the rotor position θ_r are the state variables. However, since θ_r can be established from ω_r by using

$$\frac{d\theta_r}{dt} = \omega_r \tag{3.7-5}$$

and since θ_r is considered a state variable only when the shaft position is a controlled variable, we will omit θ_r from consideration in this development.

Solving the armature voltage equation, (3.7-1), for di_a/dt yields

$$\frac{di_a}{dt} = -\frac{r_a}{L_{AA}}i_a - \frac{k_v}{L_{AA}}\omega_r + \frac{1}{L_{AA}}v_a \tag{3.7-6}$$

From (3.7-2), with $k_v i_a$ substituted for T_e yields

$$\frac{d\omega_r}{dt} = -\frac{B_m}{J}\omega_r + \frac{k_v}{J}i_a - \frac{1}{J}T_L \tag{3.7-7}$$

The system is described by a set of linear differential equations. In matrix form, the state equations become

$$p\begin{bmatrix} i_a \\ \omega_r \end{bmatrix} = \begin{bmatrix} -\dfrac{r_a}{L_{AA}} & -\dfrac{k_v}{L_{AA}} \\ \dfrac{k_v}{J} & -\dfrac{B_m}{J} \end{bmatrix} \begin{bmatrix} i_a \\ \omega_r \end{bmatrix} + \begin{bmatrix} \dfrac{1}{L_{AA}} & 0 \\ 0 & -\dfrac{1}{J} \end{bmatrix} \begin{bmatrix} v_a \\ T_L \end{bmatrix} \tag{3.7-8}$$

The form in which the state equations are expressed in (3.7-8) is called the fundamental form. In particular, the previous matrix equation may be expressed symbolically as

$$p\mathbf{x} = \mathbf{A}\mathbf{x} + \mathbf{B}\mathbf{u} \tag{3.7-9}$$

which is called the fundamental form, where $\mathbf{x}$ is the state vector (column matrix of state variables), and $\mathbf{u}$ is the input vector (column matrix of inputs to the system). We see that (3.7-8) and (3.7-9) are identical in form. Methods of solving equations of the fundamental form given by (3.7-9) are well known. Consequently, it is used extensively in control system analysis. If we were to consider a dc machine with a field winding as shown in Fig. 3.3-1, the field current would be a state variable. In this case, the state equations become nonlinear due to the product of state variables in $L_{AF}i_f i_a$ and $L_{AF}i_f\omega_r$.

Example 3C. Once the permanent-magnet dc motor is portrayed in block diagram form (Fig. 3.6-1), it is often advantageous, for control design purposes, to express transfer functions between state and input variables. Our task is to derive transfer functions between the state variables (i_a and ω_r) and the input variables (v_a and T_L) for the permanent-magnet dc machine. Repeating (3.7-3) and (3.7-4)

$$i_a = \frac{1/r_a}{\tau_a p + 1}(v_a - k_v\omega_r) \tag{3C-1}$$

$$\omega_r = \frac{1}{Jp + B_m}(k_v i_a - T_L) \tag{3C-2}$$

If (3C-1) is substituted into (3C-2), we obtain, after considerable work,

$$\omega_r = \frac{(1/k_v\tau_a\tau_m)v_a - (1/J)(p + 1/\tau_a)T_L}{p^2 + (1/\tau_a + B_m/J)p + (1/\tau_a)(1/\tau_m + B_m/J)} \tag{3C-3}$$

where a new time constant has been introduced. The inertia time constant, which is what τ_m is called, is defined as

$$\tau_m = \frac{Jr_a}{k_v^2} \tag{3C-4}$$

The transfer function between ω_r and v_a may be obtained from (3C-3) by setting T_L equal to zero in (3C-3) and dividing both sides by v_a. Similarly, the transfer function between ω_r and T_L is obtained by setting v_a to zero and dividing by T_L. To calculate ω_r given v_a and T_L, we note that p is d/dt and p^2 is d^2/dt^2 and, if we multiply each side of (3C-3) by the denominator of the right-side of the equation, we would have a second-order differential equation in terms of the state variable ω_r.

The characteristic or force-free equation for this linear system is obtained by setting the denominator equal to zero. It is of the general form

$$p^2 + 2\alpha p + \omega_n^2 = 0 \tag{3C-5}$$

We are aware that α is the exponential damping coefficient and ω_n is the undamped natural frequency. The damping factor is defined as

$$\zeta = \frac{\alpha}{\omega_n} \tag{3C-6}$$

Let us denote b_1 and b_2 as the negative values of the roots of this second-order equation,

$$b_1, b_2 = \zeta\omega_n \pm \omega_n\sqrt{\zeta^2 - 1} \tag{3C-7}$$

If $\zeta > 1$, the roots are real and the natural response consists of two exponential terms with negative real exponents. When $\zeta > 1$, the roots are a conjugate complex pair and the natural response consists of an exponentially decaying sinusoid.

Now, the transfer function relationship between i_a and the input variables v_a and T_L may be obtained by substituting (3C-2) into (3C-1). After some work, we obtain

$$i_a = \frac{(1/\tau_a r_a)(p + B_m J)v_a + (1/k_v \tau_a \tau_m)T_L}{p^2 + (1/\tau_a + B_m/J)p + (1/\tau_a)(1/\tau_m + B_m/J)} \tag{3C-8}$$

SP3.7-1 Express the transfer function relationship between θ_r and the input variables v_a and T_L. [$\theta_r = (1/p)$ (3C-3)]

SP3.7-2 A permanent-magnet dc machine is operating without load torque ($T_L = 0$) and $B_m = 0$. Express the transfer function between i_a and v_a. [(3C-8) with T_L and B_m both zero]

3.8 AN INTRODUCTION TO VOLTAGE CONTROL

Although the dc machine is not used as extensively as in the past, the dc drive still plays a role in some drive applications and a brief look at a method of voltage control is appropriate. Our focus will be on the permanent-magnet dc machine supplied from a two-quadrant dc converter. Steady-state and dynamic performance are illustrated. An average value model is developed and a time-domain block diagram is given. This section is not a prerequisite for material in later chapters.

Since the dc converters used in dc drive systems are often called choppers, we will use dc converter and chopper interchangeably. In this section, we will analyze the operation and establish the average-value model for a two-quadrant chopper drive. A two-quadrant dc converter is depicted in Fig. 3.8-1. Each switch $S1$ or $S2$ is a transistor. It is assumed to be ideal; that is, if $S1$ or $S2$ is closed, current is allowed to flow in the direction of the arrow; current is not permitted to flow opposite to the arrow. If $S1$ or $S2$ is open, current is not allowed to flow in either direction regardless of the voltage across the switch. If $S1$ or $S2$ is closed and the current is positive, the voltage drop across the switch is assumed to be zero. Similarly, each diode $D1$ or $D2$ is ideal. Therefore, if the diode current i_{D1} or i_{D2} is greater than zero, the voltage across the diode is zero. The diode current can never be less than zero.

A voltage control scheme that is often used in dc drives is shown in Fig. 3.8-2. As illustrated, a ramp generator provides a sawtooth waveform of period T that ramps from zero to one. This ramp is compared to k, which is referred to as the duty cycle control signal. As the name implies, k is often the output variable of an open- or closed-loop control. The switches

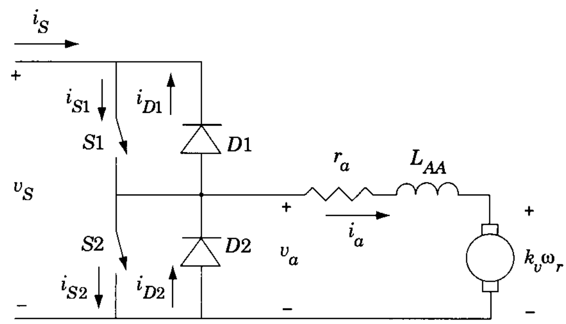

Figure 3.8-1: Two-quadrant chopper drive.

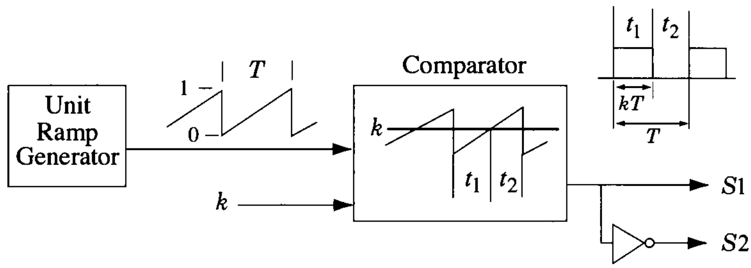

Figure 3.8-2: Pulse-width modulation voltage control.

are controlled by the output of the comparator. The duty cycle control signal may vary between zero and one ($0 \leq k \leq 1$). From Fig. 3.8-2, we see that whenever k is greater than the ramp signal, the logic output of the comparator is high. This corresponds to the time interval t_1 in Fig. 3.8-2. Now, since the ramp signal (sawtooth waveform) varies between zero and one, and since $0 \leq k \leq 1$, we can relate k, T, and t_1 as

$$t_1 = kT \tag{3.8-1}$$

which may be written

$$t_1 = \frac{k}{f_s} \tag{3.8-2}$$

where f_s is the switching or chopping frequency $\left(f_s = \dfrac{1}{T}\right)$.

When k is less than the ramp signal, the logic output is low. This corresponds to the time interval t_2. Thus, since

$$t_1 + t_2 = T \tag{3.8-3}$$

We can write

$$t_2 = (1-k)T = (1-k)\frac{1}{f_s} \tag{3.8-4}$$

It follows that if k is fixed at one, $S1$ is always closed ($S2$ is always open) and if k is fixed at zero, $S1$ is always open ($S2$ is always closed).

Waveforms of the converter variables during steady-state operation are shown in Fig. 3.8-3. Therein, the switching period T is large relative to the armature time constant τ_a for the purpose of depicting the transient of the armature current. Normally, the switching period is much smaller than the armature time constant and the switching segments of i_a are nearly sawtooth in shape. This is portrayed later in this section. With a two-quadrant chopper, the armature voltage cannot be negative ($v_a \geq 0$); however, the armature current can be positive or negative. That is, I_1 and I_2 (Fig. 3.8-3) can both be positive, or I_1 can be negative and I_2 positive, or I_1 and I_2 can both be negative. In Fig. 3.8-3, I_1 is negative and I_2 is positive and the average value of i_a is positive. Since the average value of v_a is positive, the mode of operation depicted is motor action if ω_r is positive (ccw).

In a two-quadrant chopper, the switching logic is generated from the duty cycle k, as shown in Fig. 3.8-2. When the comparator output signal is high, $S1$ is closed and $S2$ is open (interval A in Fig. 3.8-3); when it is low, $S1$ is open and $S2$ is closed (interval B in Fig. 3.8-3). When $S1$ is closed, current will flow either through $S1$ or $D1$; when $S2$ is closed current will flow either through $S2$ or $D2$. There is a practical consideration that must be mentioned. Electronic switches have finite turn-off and turn-on times. The turn-off time is generally longer than the turn-on time. Therefore, the switching logic must be arranged so that the turn-on signal is delayed in order to prevent short-circuiting the source, causing "shoot through." Although the delay is very short, it must be considered in the design; however, it does not make our analysis invalid, wherein we will assume instant-on, instant-off operation.

It is important to discuss the mode of operation depicted in Fig. 3.8-3. During interval A, $S1$ is closed and $S2$ is open and, at the start of interval A, $i_a = I_1$, which is negative. Since $S2$ is open, a negative i_a (I_1) can only flow through $D1$. It is important to note that $-i_{D1}$ and $-i_{S2}$ are plotted

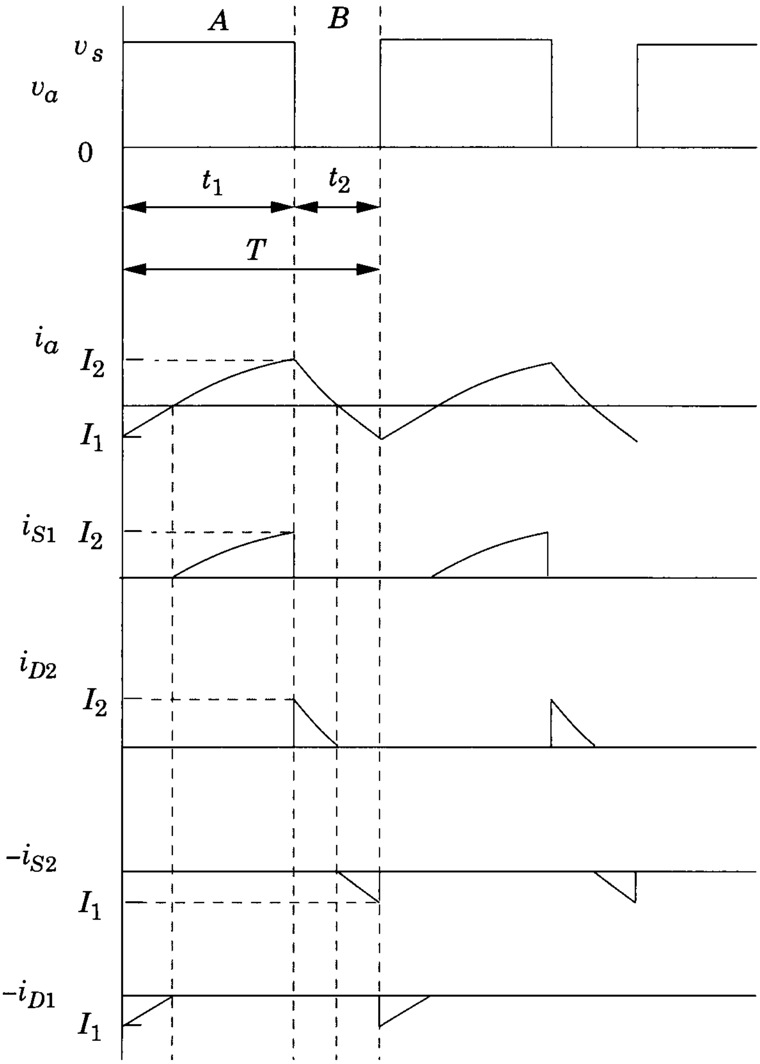

Figure 3.8-3: Steady-state operation of a two-quadrant dc converter drive.

in Fig. 3.8-3 to allow ready comparison with the waveform of i_a, since they are opposite to positive i_a. Let us go back to the start of interval A. How did i_a become negative? Well, during the interval B in the preceding period $S2$ was closed with $S1$ open. With $S2$ closed, the armature terminals are short-circuited and the counter emf has driven i_a negative. Therefore, when $S1$ is closed and $S2$ is opened at the start of interval A, the source voltage has to contend with this negative I_1. We see from Fig. 3.8-3 that the average value of i_a is slightly positive; therefore, v_S is larger than the counter emf and at the start of interval A when v_S is applied to the machine the armature current begins to increase toward zero from the negative value of I_1. Once i_a reaches zero, the diode D_1 blocks the current flow. That is, i_{D1} cannot become negative (cannot conduct positive i_a); however, $S1$ has been closed since the start of interval A and since i_{S1} can only be positive, $S1$ is ready to carry the positive i_a. The armature current, which is now i_{S1}, continues to increase until the end of interval A (I_2).

At the beginning of interval B, $S1$ is opened and $S2$ is closed; however, $S2$ cannot conduct a positive armature current. Therefore, the positive current (I_2) is diverted to diode $D2$ which is short-circuiting the armature terminals. Now, the counter emf has the positive current (I_2) with which to contend. It is clear that if the armature terminals were permanently short-circuited, the counter-emf would drive i_a negative. At the start of interval B, the counter-emf begins to do just that; however, when i_a becomes zero, diode $D2$ blocks i_{D2} and the negative armature current is picked up by $S2$, which has been closed since the beginning of interval B, waiting to be called upon to conduct a negative armature current. This continues until the end of interval B, whereupon we are back to where we started.

It is apparent that if the mode of operation is such that I_1 and I_2 are both positive, then the machine is acting as a motor with a substantial load torque if ω_r is positive (ccw). In this mode, either $S1$ or $D2$ will carry current during a switching period T. If both I_1 and I_2 are negative, the machine is operating as a generator, delivering power to the source if ω_r is positive (ccw). In this case, either $S2$ or $D1$ will carry current during a switching period.

It is instructive to derive expressions for I_1 and I_2. The period T in Fig. 3.8-3 is divided into interval A and interval B. During interval A, $v_a = v_S$, $i_a = i_S$, and $i_D = 0$. For interval A,

$$L_{AA}\frac{di_a}{dt} + r_a i_a = v_S - k_v\omega_r \tag{3.8-5}$$

If v_S and ω_r are assumed constant during this interval, the solution of (3.8-5) may be expressed in the form

$$i_a(t) = i_{a,ss} + i_{a,tr} \tag{3.8-6}$$

where $i_{a,ss}$ is the steady-state current that would flow if the given interval were to last indefinitely. This current can be calculated by assuming $di_a/dt = 0$, whereupon from (3.8-7) we obtain

$$i_{a,ss} = \frac{v_s - k_v\omega_r}{r_a} \tag{3.8-7}$$

The transient component ($i_{a,tr}$) of (3.8-6) is the solution of the homogeneous or force-free equation

$$L_{AA}\frac{di_a}{dt} + r_a i_a = 0 \tag{3.8-8}$$

Therefore,

$$i_{a,tr} = Ke^{-t/\tau_a} \tag{3.8-9}$$

where $\tau_a = L_{AA}/r_a$. Thus, during interval A, the armature current may be expressed as

$$i_a = \frac{1}{r_a}(v_s - k_v\omega_r) + Ke^{-t/\tau_a} \tag{3.8-10}$$

At $t = 0$ for interval A, $i_a(0) = I_1$ (Fig. 3.8-3); thus

$$I_1 = \frac{1}{r_a}(v_s - k_v\omega_r) + K \tag{3.8-11}$$

Solving for K and substituting the result into (3.8-10) yields the following expression for i_a:

$$i_a = I_1 e^{-t/\tau_a} + \frac{(v_s - k_v\omega_r)}{r_a}(1 - e^{-t/\tau_a}) \tag{3.8-12}$$

At $t = t_1$ or kT, $i_a = I_2$; from (3.8-12) we obtain

$$I_2 = I_1 e^{-kT/\tau_a} + \frac{(v_s - k_v\omega_r)}{r_a}(1 - e^{-kT/\tau_a}) \tag{3.8-13}$$

Equation (3.8-13) relates I_2, the current at the end of interval A, to I_1, the current at the beginning of interval A.

During interval B, we have

$$L_{AA}\frac{di_a}{dt} + r_a i_a = -k_v \omega_r \tag{3.8-14}$$

Solving for the steady-state current yields

$$i_{a,ss} = -\frac{k_v \omega_r}{r_a} \tag{3.8-15}$$

and $i_{a,tr}$ is still (3.8-9). Thus,

$$i_a = -\frac{k_v \omega_r}{r_a} + K e^{-t/\tau_a} \tag{3.8-16}$$

For convenience of analysis, we will define a "new" time zero at the beginning of interval B. Thus, at this new $t = 0$, we have $i_a = I_2$ and

$$I_2 = -\frac{k_v \omega_r}{r_a} + K \tag{3.8-17}$$

Therefore, during interval B, with $t = 0$ at the start of interval B, we have

$$i_a = I_2 e^{-t/\tau_a} - \frac{k_v \omega_r}{r_a}(1 - e^{-t/\tau_a}) \tag{3.8-18}$$

Equation (3.8-12) defines the current during interval A, assuming that the initial current, I_1, for this interval is known, whereas (3.8-18) defines the current during interval B, assuming the initial current, I_2, for interval B is known. How can we establish these currents? Well, the initial current during interval B is the final current in interval A. That is, I_2 is calculated from (3.8-12) by setting $t = kT$, giving an expression for I_2 in terms of I_1 (3.8-13). But what determines the value of I_1? At the end of interval B, when $t = t_2$ in (3.8-18), the current i_a must return to I_1 for steady-state operation. Now, from (3.8-4), $t_2 = (1 - k)T$. In other words, $i_a = I_1$ when t in (3.8-18) is $(1 - k)T$. Thus,

$$I_1 = I_2 e^{-(1-k)T/\tau_a} - \frac{k_v \omega_r}{r_a}(1 - e^{-(1-k)T/\tau_a}) \tag{3.8-19}$$

Equations (3.8-13) and (3.8-19) can be used to solve for I_1 and I_2 in terms of v_s, k, T, ω_r, and the machine parameters. In particular, with some work, we can write

$$I_1 = \frac{v_s}{r_a}\left[\frac{e^{-T/\tau_a}(e^{kT/\tau_a} - 1)}{1 - e^{-T/\tau_a}}\right] - \frac{k_v \omega_r}{r_a} \tag{3.8-20}$$

$$I_2 = \frac{v_s}{r_a}\left[\frac{1-e^{-kT/\tau_a}}{1-e^{-T/\tau_a}}\right] - \frac{k_v\omega_r}{r_a} \tag{3.8-21}$$

Average-Value Time-Domain Block Diagram

The average-value time-domain block diagram for the two-quadrant chopper drive system is shown in Fig. 3.8-4. From Fig. 3.8-3, the average armature voltage may be determined as

$$\bar{v}_a = \frac{1}{T}\left[\int_0^{t_1} v_s\,d\xi + \int_{t_1}^{T} 0\,d\xi\right] \tag{3.8-22}$$

Since $t_1 = kT$, the average armature voltage becomes

$$\bar{v}_a = kv_s \tag{3.8-23}$$

In Fig. 3.8-4, the bars over the variables denote average values. Other than depiction of (3.8-23) and the bar notation, the block diagram shown in Fig. 3.8-4 is the same as that shown in Fig. 3.6-1.

The starting characteristics of a permanent-magnet dc machine with a two-quadrant chopper drive are depicted in Fig. 3.8-5. The machine parameters are identical to those in Fig. 3.5-1. Here, the switching frequency f_s is set to 200 Hz and the source voltage to 10 V. Typically, the switching frequency is much higher, generally greater than 20 kHz. The frequency was selected to illustrate the dynamics introduced by the converter. Even at this low switching frequency, the switching period T is much less than the armature time constant τ_a. Thus, the armature current essentially consists of piecewise linear segments about an average response. In Fig. 3.8-5, the duty

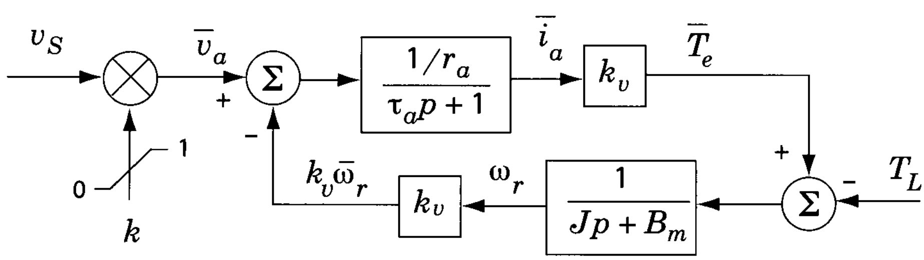

Figure 3.8-4: Average-value model of two-quadrant dc converter drive.

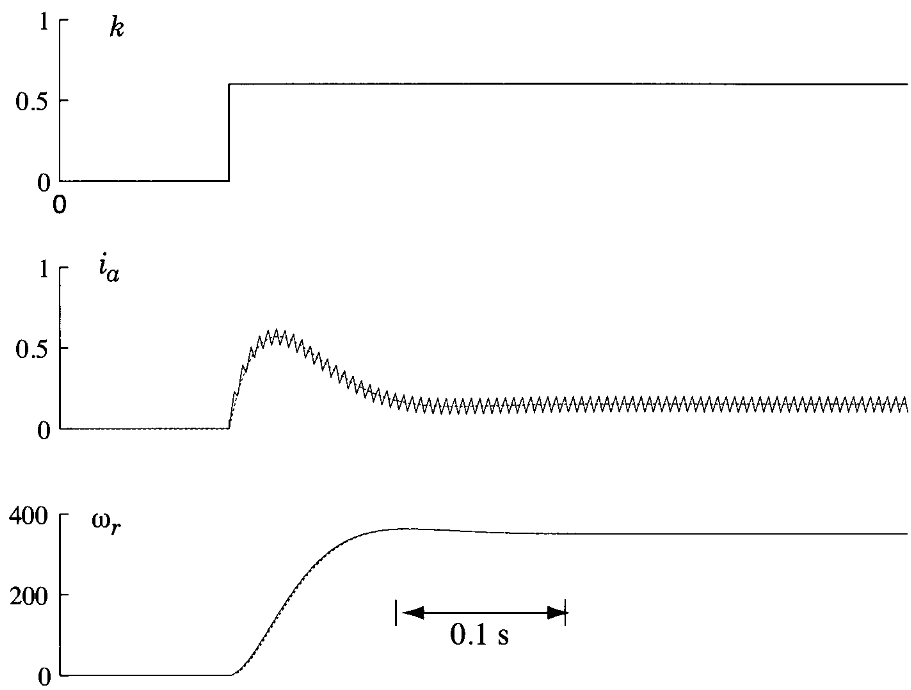

Figure 3.8-5: Starting characteristics of a permanent-magnet dc machine with a two-quadrant dc/dc converter drive.

cycle is stepped from 0 to 0.6, corresponding to a step increase in average applied voltage from 0 to 6 V. The start-up response established using the average-value model is superimposed for purposes of comparison. As shown, the only salient difference between the two responses is the "sawtooth" behavior of the armature current due to converter switching. The rotor speeds are indistinguishable.

3.9 RECAPPING

The dc machine is unique in that it exerts a torque on the rotating member as a result of the interaction of two stationary, orthogonal magnetic systems. One is produced by current flowing in the windings or a permanent magnet on the stationary member, and the other is caused by the current flowing in the windings of the rotating member. Direct current machines are being replaced by the converter-controlled permanent-magnet ac machine, which by modern control techniques is made to emulate the maximum torque-per-ampere characteristics of a dc machine. The equations that describe the dc machine offer a straightforward means of describing the modes of operation of this look-alike machine. Therefore, we are taking advantage of this to describe constant-torque and constant-power controlled modes of operation common to permanent-magnet ac machines. Since the dynamic characteristics of this device can be described by linear differential equations, we have also tried to set the stage for those who are interested in control system analysis by formulating the state equations of a permanent-magnet dc motor in fundamental form. Also, transfer functions have been developed with the control-systems student in mind. In a later chapter, we will consider the permanent-magnet ac machine operated as a brushless dc motor, which is rapidly replacing the permanent-magnet dc motor. The equations that describe the operation of these two devices are very similar. Hence, much of the material presented here for the permanent-magnet dc motor can be applied directly to the analysis of the brushless dc motor. In the last section of this chapter, a brief analysis of a converter used in dc-drive systems has been presented. An average-value block diagram for this converter supplying a permanent-magnet dc machine was derived.

3.10 REFERENCES

[1] P. C. Krause, O. Wasynczuk, S. D. Sudhoff, *Analysis of Electric Machinery and Drive Systems*, IEEE Press, 2002.

[2] S. J. Chapman, *Electric Machinery Fundamentals*, 3rd Edition, McGraw-Hill Book Company, New York, 1999.

3.11 PROBLEMS

1. A permanent-magnet dc motor has the following parameters: $r_a = 8\,\Omega$ and $k_v = 0.01$ V · s/rad. The shaft load torque is approximated as $T_L = K\omega_r$, where $K = 5 \times 10^{-6}$ N · m · s. The applied voltage is 6 V and $B_m = 0$. Calculate the steady-state rotor speed ω_r in rad/s.

2. A permanent-magnet dc motor is driven by a mechanical source at 3820 r/min. The measured open-circuit armature voltage is 7 V. The mechanical source is disconnected, and a 12-V electric source is connected to the armature. With zero-load torque, $I_a = 0.1$ A and $\omega_r = 650$ rad/s. Calculate k_v, B_m, and r_a.

3. Modify the state equations given by (3.7-8) for a permanent-magnet dc machine to include θ_r as a state variable.

* 4. Write the state equations in fundamental form for the coupled circuits considered in Section 1.5. Start with (1.5-37) and use λ_1 and λ_2' as state variables. Relate currents and flux linkages by (1.5-34) and (1.5-35).

5. Develop the time-domain block diagram for the coupled circuits considered in preceding problem.

6. The parameters of a permanent-magnet dc machine are $r_a = 6\,\Omega$ and $k_v = 2 \times 10^{-2}\,$V · s/rad. V_a can be varied from zero to 10 volts. The device is to be operated in the constant-torque mode with $T_e^* = 4 \times 10^{-3}\,$N · m. (a) Determine V_a for $\omega_r = 0$. (b) Determine maximum ω_r range of the constant-torque mode of operation.

7. A dc machine is rated 5 hp with $V_f = 240$ V, $V_a = 240$ V, $r_a = 0.63\,\Omega$, and $L_{AF} = 1.8$ H. At rated conditions $\omega_r = 127.7$ rad/s and the total resistance of the field circuit is $240\,\Omega$. (a) Calculate the rated armature

current. The machine is to be operated in the constant-power mode beyond rated speed. (b) Calculate I_f at four times rated speed. (c) Calculate the boundary value of T_e for (b).

8. The machine in Prob. 7 is operating at $2\omega_{rR}$ in the field-weakening mode. $V_a = V_{aR}$ and $I_a = I_{aR}$. The load torque is reduced by one-half. It is desirable to maintain the steady-state rotor speed at $\omega_r = 2\omega_{rR}$. (a) Calculate I_a if $V_a = V_{aR}$. (b) Calculate V_a if $I_a = I_{aR}$.

Electromechanical Motion Devices, Second Edition
by Paul Krause, Oleg Wasynczuk and Steven Pekarek

Chapter 4

WINDINGS AND ROTATING MAGNETOMOTIVE FORCE

4.1 INTRODUCTION

In the previous chapter, we found the dc machine to be a bit involved in that it has windings on both the stationary and rotating members, and these circuits are in relative motion whenever the armature (rotor) rotates. However, due to the action of the commutator, the resultant mmf produced by currents flowing in the rotating windings is stationary. In other words, the rotor windings appear to be stationary, magnetically. Therefore, with a constant current in the field (stator) winding, torque is produced and rotation results owing to the force established to align two stationary, orthogonal magnetic fields.

In rotational electromechanical devices other than dc machines, torque is produced as a result of one or more magnetic fields that rotate about the air gap of the device. Reluctance machines, induction machines, synchronous machines, stepper motors, and brushless dc motors, which are actually voltage-controlled permanent-magnet ac machines, all develop torque in this manner. There are features of these devices that are common to all. In particular, the winding arrangement of the stator and the method of producing a rotating magnctic field due to stator currents are the same for 2, 4, 6, ..., P-pole devices. It seems logical, therefore, to cover these common features once and for all rather than repeat this material for each electromechanical device covered in subsequent chapters.

In our analysis, we will assume that the arrangement of a stator winding may be approximated by a winding distributed sinusoidally in terms of displacement about the air gap. With a sinusoidally distributed winding, the resulting air-gap mmf will also be a sinusoidal function of displacement about the air gap. In this chapter, the sinusoidally distributed winding and the waveform of the resulting air-gap mmf (magnetic field) are considered from an empirical point of view. Once the expression for the rotating magnetic field (rotating air-gap mmf) is established, the concept of magnetic poles is discussed. Until this section, only two-pole devices are considered. Fortunately, we are able to show that, with a simple substitution of variables, P-pole devices, where P = 2, 4, 6, ... , may all be treated as if they had only two poles. In the final section of this chapter, some time is devoted to a non-analytical discussion of the operation of the reluctance, stepper, induction, and synchronous machines. Although some of this material may seem a bit premature and without theoretical basis, it is worthwhile in that it alerts us to the electromechanical devices that will be covered in later chapters.

4.2 WINDINGS

In Chaps. 1 and 2, we considered two windings in relative motion; one on the stator and one on the rotor (Fig. 1.7-4). When introducing this device in Sec. 1.7, we assumed the turns of the windings to be concentrated in one position even though, in practice, they would normally be distributed over a 30 to 60° arc. Let us redraw Fig. 1.7-4 with the following changes. First, we will disregard the rotor winding and focus our attention on the stator winding. We will see the reason for this when we discover that the arrangement of the stator winding(s) is common for the electromechanical-motion devices considered in subsequent chapters. Finally, we will call winding 1 of Fig. 1.7-4 winding *as,* and assume that it is distributed in slots over the inner circumference of the stator, as shown in Fig. 4.2-1. This is more characteristic of the stator winding of a single-phase electromechanical-motion device than is a concentrated winding.

The winding is depicted as a series of individual coils. Each coil is placed in a slot in the stator steel. If we follow the path of positive current i_{as} flowing in the *as* winding, we see that current enters as_1, depicted by $\otimes$, to indicate that the assumed direction of positive current is down the length of the stator in an axial direction (into the paper). Current flows down the length of the

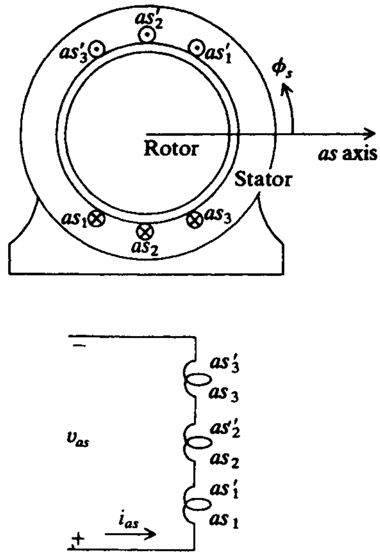

Figure 4.2-1: Elementary two-pole, single-phase stator winding.

stator, loops at the end (end turn, see Fig. 1.7-4), and flows back down the length of the stator and out at as_1', depicted by $\odot$. Note that as_1 and as_1' are placed in stator slots that span π radians. This is characteristic of a two-pole machine; we shall talk more about poles later. Now, as_1 around to as_1' is referred to as a *coil* and as_1 or as_1' is a coil side. In practice, a coil will contain more than one conductor. That is, current will flow into as_1 in a conductor and out as_1' via the same conductor. The conductor, which is, of course, insulated, may then be looped back to as_1 and the winding of the conductor around the $as_1 - as_1'$ path repeated, thereby forming a coil with numerous turns. The number of conductors in a coil side tells us the number of turns in this coil. This number will be denoted as nc_s.

Now then, once we have wound nc_s turns in the $as_1 - as_1'$ coil, we will take the same conductor and repeat this winding process to form the $as_2 - as_2'$ coil. We will assume that the same number of turns (nc_s) make up the $as_2 - as_2'$ coil as the $as_1 - as_1'$ coil and, similarly, for the $as_3 - as_3'$. We could have wound a different number of turns in each coil but we will assume that this was not done. With the same number of turns (nc_s) in each of the coils, the winding is said to be uniformly distributed over a span from as_1 to as_3, or 60°. Once the winding is wound, we can use the right-hand rule to give a meaning to the *as* axis shown in Fig. 4.2-1. It is, by definition, the principal direction of magnetic flux established by positive current flowing in the *as* winding. It is said to denote the positive direction of the magnetic axis of the *as* winding.

In Fig. 4.2-2, we have added a second stator winding—the *bs* winding. Note that its magnetic axis is displaced $\frac{1}{2}\pi$ from that of the *as* winding. Although it is a matter of choice, we will assume that the positive direction of i_{bs} is such that the positive magnetic axis of the *bs* winding is at $\phi_s = \frac{1}{2}\pi$ rather than at $\phi_s = -\frac{1}{2}\pi$. Actually, we have not defined ϕ_s yet, but we can see that it is an angular displacement about the stator, referenced to the *as* axis. Placing the *bs* winding $\frac{1}{2}\pi$ from the *as* winding makes this the stator configuration for a two-pole, two-phase electromechanical device. Unfortunately, this fact adds little to our present appreciation of the meaning of two-pole or two-phase; however, we can now establish the meaning of sym-

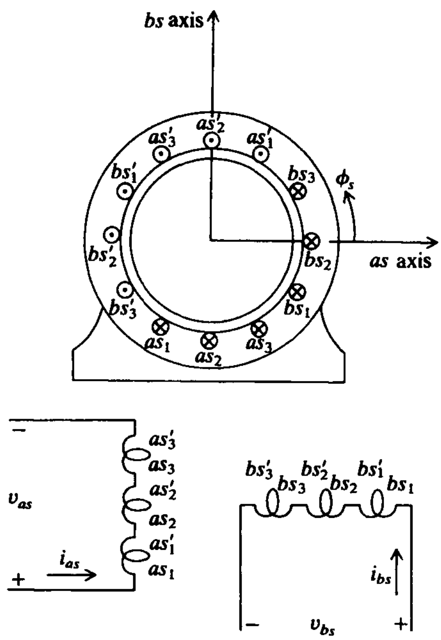

Figure 4.2-2: Elementary two-pole, two-phase stator winding.

metrical as it is used in electromechanical devices. If we wind the orthogonal *bs* winding exactly as we did the *as* winding, that is, the same number of turns per coil (nc_s) with the same size of wire, then the turns and resistance of the *as* and *bs* windings will be identical, whereupon the stator windings are said to be symmetrical. For a two-pole, three-phase, symmetrical electromechanical device, there are three identical stator windings, *as, bs,* and *cs,* displaced $\frac{2}{3}\pi$ from each other. Most multiphase electromechanical devices are equipped with symmetrical stators.

SP4.2-1 The total number of turns of the *as* winding in Fig. 4.2-2 is 15. The stator windings are symmetrical. For the *as* and *bs* windings, calculate (a) the turns per coil, nc_s and (b) the conductors per coil side. [(a) 5; (b) 5]

SP4.2-2 A fourth coil, $as_4 - as_4'$, with nc_s turns is placed in the same slot as the $as_2 - as_2'$ coil in Fig. 4.2-2. Is the stator symmetrical? A fourth coil, $bs_4 - bs_4'$, with nc_s turns, is placed in the same slot as the $bs_2 - bs_2'$ coil in Fig. 4.2-2. Is the stator now symmetrical? [no; yes]

4.3 AIR-GAP MMF–SINUSOIDALLY DISTRIBUTED WINDINGS

In the analysis of electromechanical motion devices, it is generally assumed that the stator windings and, in many cases, the rotor windings, may be approximated as sinusoidally distributed windings. That is, the distribution of a stator phase winding may be approximated as a sinusoidal function of ϕ_s, and the waveform of the resulting mmf dropped across the air gap (air-gap mmf) of the device may also be approximated as a sinusoidal function of ϕ_s. Actually, most electric machines, particularly large machines, are designed so that the windings, especially the stator windings, produce a relatively good approximation of a sinusoidally distributed air-gap mmf so as to minimize the voltage and current harmonics. To establish a truly sinusoidal air-gap mmf waveform (often referred to as a *space sinusoid*), the winding must also be distributed sinusoidally. Except in cases where the harmonics due to the winding configuration are of importance, it is typically assumed that all windings may be approximated as sinusoidally distributed windings. We will make this assumption in our analysis of the electromechanical motion devices considered in subsequent chapters.

For this discussion, let us add a few coils to the *as* winding shown in Fig. 4.2-1, whereupon we have Fig. 4.3-1. Although we may be going a bit far by adding coils that now span $\frac{2}{3}\pi$, it helps to illustrate our point. For the purpose of establishing an expression for the air-gap mmf, it is convenient to employ the so-called developed diagram of the cross-sectional view of the device shown in Fig. 4.3-1. This developed diagram is obtained by flattening out the rotor and stator as depicted in Fig. 4.3-2. To relate the developed diagram to the cross-sectional view of the device, it is helpful to define the displacement ϕ_s to the left of the *as* axis since this allows us to position the stator above the rotor.

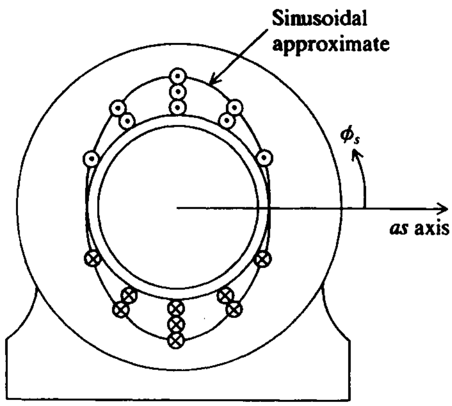

Figure 4.3-1: Approximate sinusoidal distribution of the *as* winding.

From Fig. 4.3-1 or the developed diagram in Fig. 4.3-2, we see that the winding distribution from $0 < \phi_s < \pi$ may be approximated by the expression

$$N_{as} = N_p \sin \phi_s \qquad \text{for } 0 < \phi_s < \pi \tag{4.3-1}$$

and from $\pi < \phi_s < 2\pi$ as

$$N_{as} = -N_p \sin \phi_s \qquad \text{for } \pi < \phi_s < 2\pi \tag{4.3-2}$$

where N_p is the peak turns density in turns/radian that could be determined from a Fourier analysis of the actual winding distribution. If N_s represents

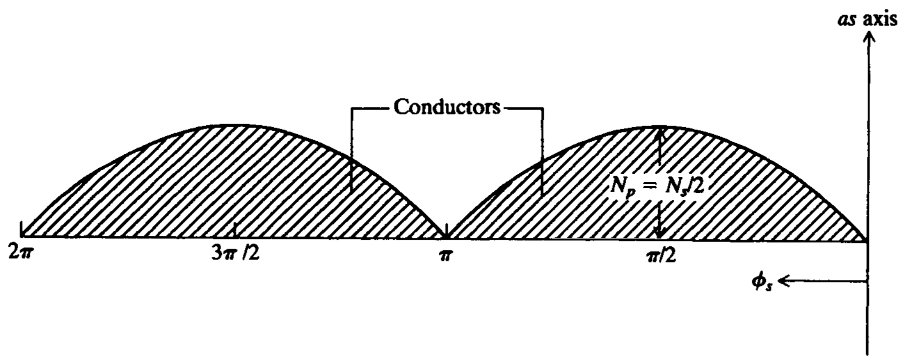

Figure 4.3-2: Developed diagram with sinusoidally distributed stator winding.

the number of turns of the equivalent sinusoidally distributed winding, then, using ξ as a dummy variable of integration,

$$N_s = \int_0^{\pi} N_p \sin \xi d\xi = 2N_p \tag{4.3-3}$$

It is important to note that the number of turns is obtained by integrating the turns density N_{as} from zero to π rather than from zero to 2π. Also, N_s represents not the total turns of the winding, but those of the equivalent sinusoidally distributed winding that corresponds to the fundamental component of the actual winding distribution.

Now, the sinusoidally distributed winding will produce an mmf that is positive in the direction of the *as* axis, to the right in Fig. 4.3-1, for positive i_{as}. Also, since the reluctance of the steel of this device is much smaller (neglecting saturation) than the reluctance of the air gap, it can be assumed that all of the mmf is dropped across the air gap. It seems logical that, if the windings are sinusoidally distributed in space (ϕ_s), then the mmf dropped across the air gap will also be sinusoidal in space.

For the purposes of establishing an expression for the air-gap mmf associated with the *as* winding, mmf_{as}, let us travel a closed path that starts at the center of the rotor as shown in Fig. 4.3-3*a*. From the center of the rotor, let us proceed to the right along the *as* axis, crossing the air gap at $\phi_s = 0$. Now that we are in the stator, we will turn to the right and proceed clockwise, encircling the lower windings until we get to $\phi_s = \pi$, whereupon

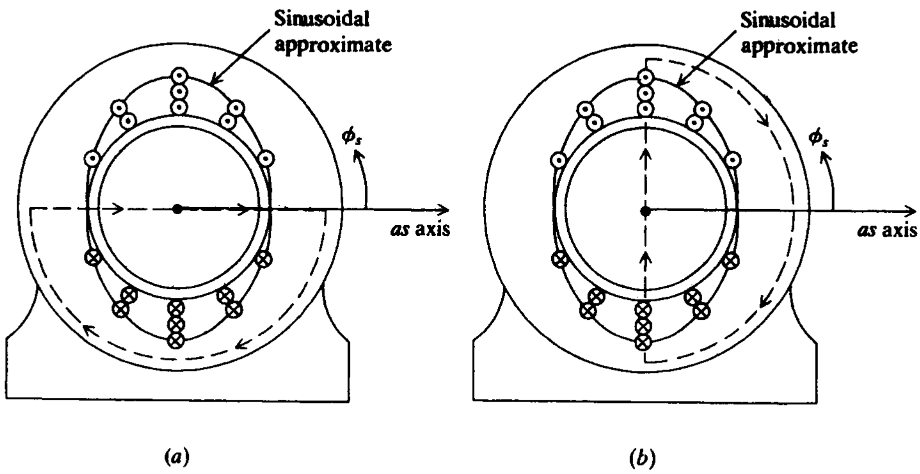

Figure 4.3-3: Closed paths used to establish mmf_{as}.

we will cross again the air gap and return to the center of the rotor. The total current enclosed is $N_s i_{as}$, which, by Ampere's law, is equal to the mmf drop ($\oint \mathbf{H} \cdot d\mathbf{L}$) around the given path. If the reluctance of the rotor and stator steel is small compared with the air gap reluctance, it can be assumed, for practical purposes, that one half of the mmf is dropped across the air gap at $\phi_s = 0$ and one half at $\phi_s = \pi$. By definition, mmf_{as} is positive for an mmf drop across the air gap from the rotor to the stator. Thus, mmf_{as} is positive at $\phi_s = 0$ and negative at $\phi_s = \pi$, assuming positive i_{as}. Moreover, since one half of this mmf ($N_s i_{as}$) is dropped at $\phi_s = 0$ and one half at $\phi_s = \pi$, $\text{mmf}_{as}(0) = (N_s/2)i_{as}$ and $\text{mmf}_{as}(\pi) = -(N_s/2)i_{as}$. This suggests that, for arbitrary ϕ_s, mmf_{as} might be expressed as

$$\text{mmf}_{as} = \frac{N_s}{2} i_{as} \cos \phi_s \tag{4.3-4}$$

Equation (4.3-4) tells us that the air-gap mmf is zero at $\phi_s = \pm\frac{1}{2}\pi$. Let us check this by traveling a path starting again at the center of the rotor, but this time we will go straight up, crossing the air gap at $\phi_s = \frac{1}{2}\pi$, as shown in Fig. 4.3-3*b*. Now that we are in the stator, we have two choices—we can go down the right side of the stator steel as in Fig. 4.3-2*b* or down the left side. In either case, we will cross the air gap into the rotor at $\phi_s = -\frac{1}{2}\pi$ and complete our closed path by ending up at the center of the rotor. Regardless of the path selected in Fig. 4.3-3*b*, we enclosed as much current going in one direction ⊙ as in the other ⊗. Since the net current enclosed is zero, the mmf drop is zero along the given path, implying that $\text{mmf}_{as} = 0$ at $\phi_s = \pm\frac{1}{2}\pi$. The fact that mmf_{as} is a positive (negative) maximum at $\phi_s = 0$ ($\phi_s = \pi$) and that $\text{mmf}_{as} = 0$ at $\phi_s = \pm\frac{1}{2}\pi$, together with the fact that the winding in Fig. 4.3-1 is sinusoidally distributed, strongly suggests that (4.3-4) is the correct expression of mmf_{as}. The mmf due to the sinusoidally distributed *as* winding is depicted in Fig. 4.3-4, where the locations of maximum turns density are depicted by ⊙ and ⊗. Hereafter, we will use this to depict a sinusoidally distributed winding.

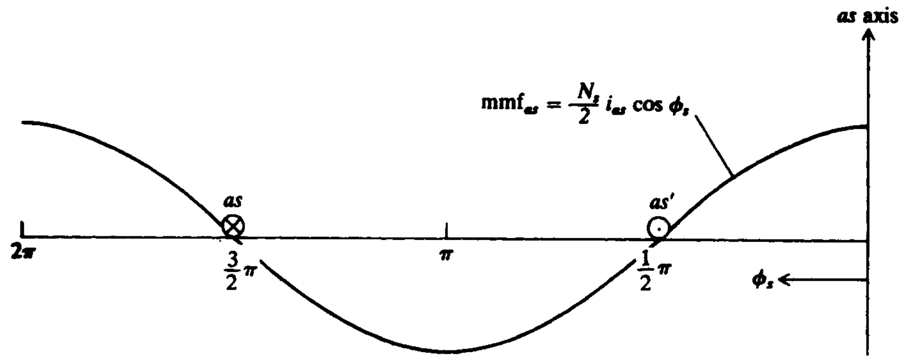

Figure 4.3-4: Stator mmf_{as} due to sinusoidally distributed *as* winding.

Let us now consider the *bs* winding of a two-phase device. Recall that it is an identical winding displaced $\frac{1}{2}\pi$ from the *as* winding, as shown in Fig. 4.2-2. It follows that the air-gap mmf due to a sinusoidally distributed *bs* winding may be expressed as

$$\text{mmf}_{bs} = \frac{N_s}{2} i_{bs} \sin \phi_s \tag{4.3-5}$$

Example 4A. The air-gap mmf of the elementary two-pole single-phase stator winding shown in Fig. 4.2-1 is established for those who wish to examine the mmf distribution associated with nonsinusoidally distributed windings. In Fig. 4.2-1, which is shown again in Fig. 4A-l, each of the three coils contains nc_s turns. We will apply Ampere's law to the closed path depicted in Fig. 4A-1. In particular,

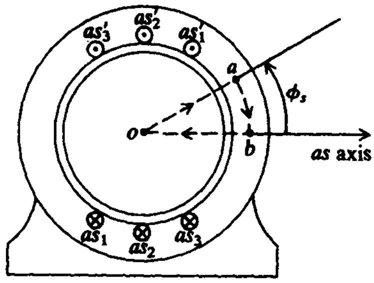

Figure 4A-1: Closed paths for evaluation of mmf_{as}.

$$\oint \mathbf{H} \cdot d\mathbf{L} = i_n \tag{4A-1}$$

where i_n is the current enclosed by the closed path. In Fig. 4A-l, the part of the closed path defined by the straight line from 0 to a is assumed to be at an angle ϕ_s measured from the as axis. If the reluctance of the rotor and stator steel is small, we can neglect the field intensity therein, whereupon (4A-l) becomes

$$H_r(\phi_s)g(\phi_s) - H_r(0)g(0) = i_n \tag{4A-2}$$

Here, $H_r(\phi_s)$ represents the radial component of the $\mathbf{H}$ field in the air gap and $g(\phi_s)$ is the air-gap length, which is constant in a uniform-air-gap machine. The stator mmf is defined as the line integral of $\mathbf{H}$. Therefore (4A-2) may be written as

$$\mathrm{mmf}_{as}(\phi_s) - \mathrm{mmf}_{as}(0) = i_n \tag{4A-3}$$

If, in Fig. 4A-l, $0 < \phi_s < \frac{1}{3}\pi$, then current is not enclosed by the closed path. If we assume that $\mathrm{mmf}_{as}(0) = 0$, then (4A-3) implies that $\mathrm{mmf}_{as}(\phi_s) = 0$ for $0 < \phi_s < \frac{1}{3}\pi$. On the other hand, if $\frac{1}{3}\pi < \phi_s < \frac{1}{2}\pi$, the enclosed current is $-n_c i_{as}$. The minus sign is needed since, in accordance with the right-hand rule, a positive enclosed current flows into the paper $\otimes$ for the selected clockwise path. In Fig. 4A-1, we have more enclosed positive current flowing out of the paper. Again, if we assume $\mathrm{mmf}_{as}(0) = 0$, then (4A-3) implies that $\mathrm{mmf}_{as} = -nc_s i_{as}$ for $\frac{1}{3}\pi < \phi_s < \frac{1}{2}\pi$. Continuing with this procedure results in the mmf distribution depicted in Fig. 4A-2.

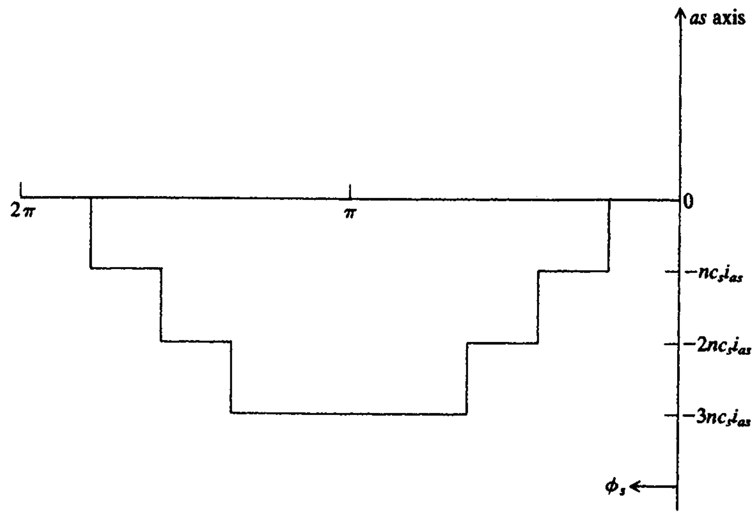

Figure 4A-2: Plot of air-gap mmf assuming $\text{mmf}_{as}(0) = 0$.

In Fig. 4A-2, the stator mmf has a nonzero average value. However, in obtaining the distribution of Fig. 4A-2, it was assumed, quite arbitrarily, that $\text{mmf}_{as}(0)$ is zero. If we had assumed a nonzero value, the distribution of Fig. 4A-2 would be shifted up or down. The question arises as to what value of $\text{mmf}_{as}(0)$ should we have assumed. The answer rests upon the fact that mmf_{as} must have zero average value to satisfy Gauss' law. In other words, the flux entering the stator from the air gap must equal the flux entering the air gap from the stator. The air-gap mmf depicted in Fig. 4A-2 would imply that all of the flux enters the air gap from the stator, which is an impossibility since a point source of flux does not exist. Hence, mmf_{as} in Fig. 4A-2 must be shifted upward by $\frac{3}{2}nc_si_{as}$ so that distribution has zero average value. The resulting air-gap mmf is depicted in Fig. 4A-3, which may be considered a coarse approximation of a sinusoidally distributed mmf. By Fourier analysis, which is an analytical method of expressing any periodic function in terms of sinusoidal components, it can be shown that the fundamental component of the resulting air-gap mmf has a peak amplitude of $1.74nc_si_{as}$.

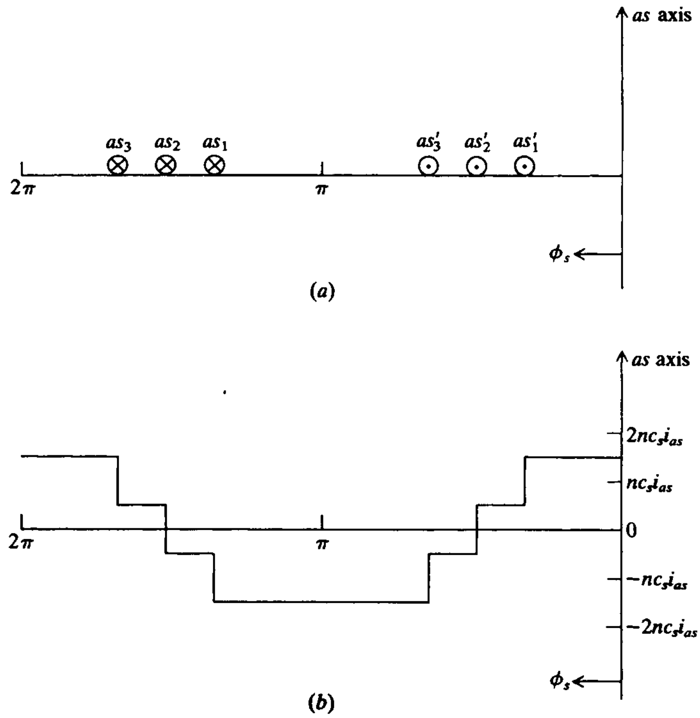

Figure 4A-3: The *as* winding with three coils. (a) Developed diagram; (b) air-gap mmf.

SP4.3-1 Express the sinusoidal approximation of mmf_{as} if the assumed positive direction of i_{as} is reversed in Fig. 4.2-1. [$\text{mmf}_{as} = -(4.3\text{-}4)$]
SP4.3-2 If $I_{as} = 1$ A, $I_{bs} = -1$ A, and $N_s = 10$ in Fig. 4.2-2, express the sum of the sinusoidal approximations of the two air-gap mmfs. [$\text{mmf}_{as} + \text{mmf}_{bs} = \sqrt{2}\, 5\cos(\phi_s + \pi/4)$]
SP4.3-3 Assume that winding 1 in Fig. 1.7-4 has one turn. Sketch the air-gap mmf due to current i_1 flowing in this winding. [$\frac{1}{2}i_1$ for $-\frac{1}{2}\pi < \phi_s < \frac{1}{2}\pi$ and $-\frac{1}{2}i_1$ for $\frac{1}{2}\pi < \phi_s < \frac{2}{3}\pi$]

4.4 ROTATING AIR-GAP MMF – TWO-POLE DEVICES

Considerable insight into the operation of electromechanical motion devices can be gained from an analysis of the air-gap mmf produced by current flowing in the stator winding(s). We will consider the rotating air-gap mmfs produced by currents flowing in the stator windings of single-, two-, and three-phase devices.

Single-Phase Devices

Let us first consider the device shown in Fig. 4.4-1, which illustrates a single-phase stator winding. We will assume that the *as* winding is sinusoidally distributed with *as* and *as'* placed at the point of maximum turns density. As mentioned previously, we will use this means of depicting a sinusoidally distributed winding. Actually, Fig. 4.4-1 is Fig. 4.2-1 with the winding assumed to be sinusoidally distributed.

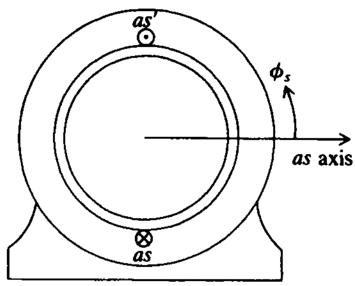

Figure 4.4-1: Elementary two-pole, single-phase, sinusoidally distributed stator winding.

If we assume that the current flowing in the *as* winding is a constant, then, as in our work in Sec. 2.8, the *as* winding would establish a stationary magnetic system with a north pole from $\frac{1}{2}\pi < \phi_s < \frac{3}{2}\pi$ and a south pole from $-\frac{1}{2}\pi < \phi_s < \frac{1}{2}\pi$. The air-gap mmf is directly related to these poles; indeed, the flux flowing from the north pole and into the south pole is caused by the air-gap mmf.

Let us see what happens when the current flowing in the *as* winding is a sinusoidal function of time. For this, we will assume steady-state operation with

$$I_{as} = \sqrt{2}\, I_s \cos[\omega_e t + \theta_{esi}(0)] \tag{4.4-1}$$

Recall that capital letters without a raised tilde are used to denote steady-state instantaneous variables. The current I_s is the rms value of the current,

ω_e is the electrical angular velocity, and $\theta_{esi}(0)$ is the angular position corresponding to the time-zero value of the instantaneous current. From Sec. 1.2, the phasor representation of I_{as} is $\tilde{I}_{as} = I_s \underline{/\theta_{esi}(0)}$.

The air-gap mmf is expressed for the *as* winding by (4.3-4). Substituting (4.4-1) into (4.3-4) yields

$$\text{mmf}_{as} = \frac{N_s}{2}\sqrt{2}\, I_s \cos[\omega_e t + \theta_{esi}(0)] \cos\phi_s \tag{4.4-2}$$

Let us consider this expression for a moment. If we stand at $\phi_s = 0$, we would see the air-gap mmf vary as a cosinusoidal function of time. In particular, if we selected $\theta_{esi}(0)$ to be zero, mmf_{as} at $\phi_s = 0$ would be a positive maximum (south pole) at $t = 0$ and a negative maximum (north pole) when $\omega_e t = \pi$. Recall that when positive flux enters the iron, where the winding exists, from the air gap, it is a south pole. When positive flux leaves the iron, where the windings exist, and enters the air gap, it is a north pole. Since we are interested in establishing a rotating air-gap mmf, this does not look too promising. It would appear that all we have is a stationary, pulsating magnetic field; however, let us use a trigonometric identity from Appendix A to write (4.4-2) as

$$\begin{aligned}\text{mmf}_{as} = \frac{N_s}{2}\sqrt{2}\, I_s \{&\tfrac{1}{2}\cos[\omega_e t + \theta_{esi}(0) - \phi_s] \\ &+ \tfrac{1}{2}\cos[\omega_e t + \theta_{esi}(0) + \phi_s]\}\end{aligned} \tag{4.4-3}$$

The arguments of the cosine terms are functions of time and displacement ϕ_s. If we can make an argument constant, then the cosine of this argument would be constant. Let us see if this is possible by setting both arguments equal to a constant. In particular, for the first term on the right-hand side of (4.4-3) let

$$\omega_e t + \theta_{esi}(0) - \phi_s = C_1 \tag{4.4-4}$$

For the second term,

$$\omega_e t + \theta_{esi}(0) + \phi_s = C_2 \tag{4.4-5}$$

Taking the derivative of (4.4-4) and (4.4-5) with respect to time yields, for the first term on the right-hand side,

$$\frac{d\phi_s}{dt} = \omega_e \tag{4.4-6}$$

and for the second term,

$$\frac{d\phi_s}{dt} = -\omega_e \tag{4.4-7}$$

What does this mean? Well, (4.4-6) tells us that, if we run around the air gap of Fig. 4.4-1 in the counterclockwise direction at an angular velocity of ω_e, the first term on the right-hand side of (4.4-3) will appear as a constant mmf, hence, a constant set of north and south poles. On the other hand, (4.4-7) tells us that, if we run clockwise at ω_e, the second term on the right-hand side of (4.4-3) will appear as a constant mmf. In other words, the pulsating air-gap mmf that we noted when standing at $\phi_s = 0$ can be thought of as two, one-half amplitude, oppositely rotating air-gap mmfs (magnetic fields), each rotating at the angular velocity of ω_e, which is the electrical angular velocity of the current. Since we have two oppositely rotating sets of north and south poles (magnetic fields), it would seem that the single-phase machine could develop an average torque as a result of interacting with either set. Indeed, we will find that a single-phase electromechanical device with the stator winding as shown in Fig. 4.4-1 can develop an average torque in either direction of rotation. It might appear that this is a four-pole device rather than a two-pole device, since there are two two-pole sets. However, only one set interacts with the rotor to produce a torque with a nonzero average.

Two-Phase Devices

Let us consider the two-pole two-phase stator shown in Fig. 4.4-2. The *as* and *bs* windings are shown with two circles for each winding, which is now our way of depicting sinusoidally distributed windings. For balanced steady-state conditions, the stator currents may be expressed as

$$I_{as} = \sqrt{2}\, I_s \cos[\omega_e t + \theta_{esi}(0)] \tag{4.4-8}$$

$$I_{bs} = \sqrt{2}\, I_s \sin[\omega_e t + \theta_{esi}(0)] \tag{4.4-9}$$

Here we see that $\tilde{I}_{bs} = -j\tilde{I}_{as}$. Actually, the set formed by (4.4-8) and (4.4-9) is but one of four possible two-phase balanced sets; that is, each expression for current could be preceded by a $\pm$ sign. The reason for selecting the set given by (4.4-8) and (4.4-9) will become apparent.

The total air-gap mmf due to both stator windings, which are assumed to be sinusoidally distributed, may be expressed by adding mmf_{as} and mmf_{bs} as given by (4.3-4) and (4.3-5), respectively. Thus, the total air-gap mmf due to the stator windings, denoted mmf_s is

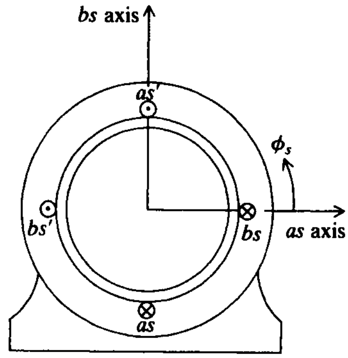

Figure 4.4-2: Elementary two-pole, two-phase, sinusoidally distributed stator windings.

$$\begin{aligned}\mathrm{mmf}_s &= \mathrm{mmf}_{as} + \mathrm{mmf}_{bs} \\ &= \frac{N_s}{2}(i_{as}\cos\phi_s + i_{bs}\sin\phi_s) \qquad (4.4\text{-}10)\end{aligned}$$

Substituting the expressions for the balanced steady-state stator currents, (4.4-8) and (4.4-9), into (4.4-10) and making use of the trigonometric relations given in Appendix A, yields

$$\mathrm{mmf}_s = \frac{N_s}{2}\sqrt{2}\, I_s \cos[\omega_e t + \theta_{esi}(0) - \phi_s] \qquad (4.4\text{-}11)$$

It is interesting that we have only one rotating air-gap mmf or rotating magnetic field. If we set the argument equal to a constant and take the derivative with respect to time, we find that the argument is constant if $d\phi_s/dt = \omega_e$. That is, if we travel around the air gap of Fig. 4.4-2 in the counterclockwise direction at ω_e, we will always see a constant mmf_s for the balanced set of stator currents given by (4.4-8) and (4.4-9). Hence, a single rotating air-gap mmf is produced. The actual value that we would see as we travel around the air gap at ω_e would depend upon the selection of time zero and our position on the stator at time zero. If, for example, $\theta_{esi}(0) = 0$ and if at $t = 0$ we are at $\phi_s = 0$, the magnitude of the total air-gap mmf that we would see would be $(N_s/2)\sqrt{2}I_s$, as determined from (4.4-11). If now, as time increases ($t > 0$), we immediately started running in the counterclockwise direction at ω_e, we would always see this same magnitude of mmf_s.

We can now answer a question raised earlier regarding the selection of the balanced set given by (4.4-8) and (4.4-9). With balanced steady-state stator currents, we want mmf_s to rotate in the counterclockwise direction for conventional purposes. With the assigned positive direction of current in the given arrangement of the *as* and *bs* windings shown in Fig. 4.4-1, the balanced set of stator currents given by (4.4-8) and (4.4-9) produces an mmf_s that rotates counterclockwise.

It is very important not to confuse the magnetic axes of the stator windings (*as* and *bs* axes), which are stationary with the phasors representing the stator currents ($\tilde{I}_{as}$ and $\tilde{I}_{bs}$). However, it is interesting to note the relative position of the *as* axis and *bs* axis versus the relative position of $\tilde{I}_{as}$ and $\tilde{I}_{bs}$ for a constant, counterclockwise mmf_s to occur. The *bs* axis is displaced $\frac{1}{2}\pi$ ahead of the *as* axis, as illustrated in Fig. 4.4-2; however, from (4.4-8) and (4.4-9) we see that $\tilde{I}_{bs}$ lags $\tilde{I}_{as}$ by $\frac{1}{2}\pi$. Note, that the negative of both (4.4-8) and (4.4-9) would also produce a counterclockwise mmf_s.

At $t = 0$ with $\theta_{esi}(0) = 0$, mmf_s is a cosine function of θ_s with the maximum value of $(N_s/2)\sqrt{2}I_s$ directed in the positive *as* axis (Fig. 4.4-2). As stated previously, a north pole is established over the area where the mmf due to the current flowing in the stator windings causes flux to enter the air gap from the stator. At $t = 0$ this would occur for $\frac{1}{2}\pi < \phi_s < \frac{3}{2}\pi$. Hence, at $t = 0$, a north pole caused by the currents flowing in the stator windings exists over the range $\frac{1}{2}\pi < \phi_s < \frac{3}{2}\pi$ with the maximum strength at $\phi_s = \pi$. Similarly, at $t = 0$, a south pole caused by stator currents exists over the range $-\frac{1}{2}\pi < \phi_s < \frac{1}{2}\pi$ with the maximum strength at $\phi_s = 0$. Note that there are two poles established, hence a two-pole machine, which rotate about the air gap at ω_e with mmf_s. The direction of rotation of the air-gap mmf (mmf_s) may readily be determined from the position of the poles when time has progressed to where I_{bs} is maximum and I_{as} is zero ($\omega_e t = \frac{1}{2}\pi$).

In the case of the single-phase stator winding with a sinusoidal current, the air-gap mmf can be thought of as two oppositely rotating, constant-amplitude mmfs. However, the instantaneous air-gap mmf is pulsating even when we are traveling with one of the rotating air-gap mmfs. Unfortunately, this pulsating air-gap mmf or set of poles gives rise to steady-state pulsating components of electromagnetic torque. In the case of the two-phase stator with balanced currents, only one rotating air-gap mmf exists. Hence, the steady-state electromagnetic torque will not contain a pulsating or time-varying component; it will be constant with the value determined by the operating conditions.

Three-Phase Devices

Although we will focus our attention upon two-phase devices in the following chapters, there is some time devoted to the three-phase version of each device. In preparation for this, it is worthwhile to consider briefly the arrangement of the stator windings of a two-pole, three-phase device shown in Fig. 4.4-3. The windings are shown connected in wye; however, a delta connection could also be used (Appendix C). The type of connection is irrelevant for this consideration. The windings are identical, sinusoidally distributed with N_s equivalent turns and with their magnetic axes displaced $\frac{2}{3}\pi$; the stator is symmetrical. The positive direction of the magnetic axes is selected so as to achieve counterclockwise rotation of the rotating air-gap mmf with balanced stator currents of the *abc* sequence (Appendix C). We shall see this in just a moment.

The air-gap mmfs established by the stator windings may be expressed by inspection of Fig. 4.4-3. In particular,

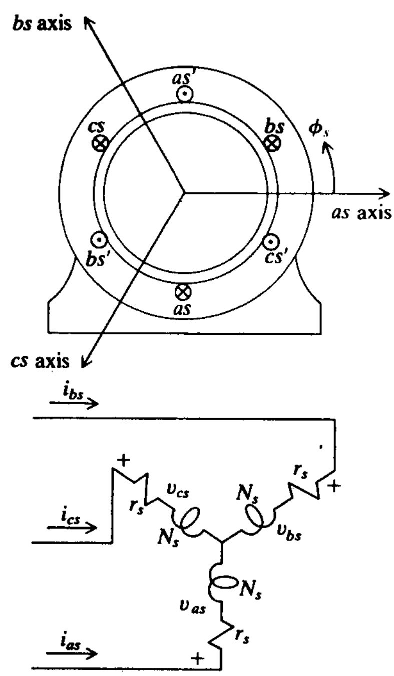

Figure 4.4-3: Elementary two-pole, three-phase, sinusoidally distributed stator windings.

$$\mathrm{mmf}_{as} = \frac{N_s}{2} i_{as} \cos \phi_s \tag{4.4-12}$$

$$\mathrm{mmf}_{bs} = \frac{N_s}{2} i_{bs} \cos(\phi_s - \tfrac{2}{3}\pi) \tag{4.4-13}$$

$$\mathrm{mmf}_{cs} = \frac{N_s}{2} i_{cs} \cos(\phi_s + \tfrac{2}{3}\pi) \tag{4.4-14}$$

As before, N_s is the number of turns of the equivalent sinusoidally distributed stator windings and ϕ_s is the angular displacement about the stator. For balanced steady-state conditions, the stator currents for an *abc* sequence may be expressed as

$$I_{as} = \sqrt{2} I_s \cos\left[\omega_e t + \theta_{esi}(0)\right] \tag{4.4-15}$$

$$I_{bs} = \sqrt{2} I_s \cos\left[\omega_e t - \tfrac{2}{3}\pi + \theta_{esi}(0)\right] \tag{4.4-16}$$

$$I_{cs} = \sqrt{2} I_s \cos\left[\omega_e t + \tfrac{2}{3}\pi + \theta_{esi}(0)\right] \tag{4.4-17}$$

Substituting (4.4-15) through (4.4-17) into (4.4-12) through (4.4-14) and adding the resulting expressions yields an expression for the rotating air-gap mmf established by balanced steady-state currents flowing in the stator windings:

$$\mathrm{mmf}_s = \frac{N_s}{2} \sqrt{2} I_s \tfrac{3}{2} \cos\left[\omega_e t + \theta_{esi}(0) - \phi_s\right] \tag{4.4-18}$$

The trigonometric relations given in Appendix A are helpful in obtaining (4.4-18). If mmf_s for the three-phase device given by (4.4-18) is compared with mmf_s for a two-phase device given by (4.4-11), we see that they are identical except that the amplitude of mmf_s for the three-phase device is $\frac{3}{2}$ times that of a two-phase device. Actually, it can be shown that this amplitude for multiphase devices changes from that of a two-phase device in proportion to the number of phases divided by two.

It is important to note that with the selected positive directions of the magnetic axes a counterclockwise rotating air-gap mmf is obtained with a three-phase set of balanced stator currents of the *abc* sequence. As in the two-phase case, it is also important to note the relative positions of the magnetic axes versus the relative positions of the phasors representing the currents in order to establish a constant amplitude counterclockwise rotating air-gap mmf. From (4.4-12) through (4.4-14) or Fig. 4.4-3, we see that the bs axis is stationary at 120°, whereas the cs axis is stationary at −120°. From (4.4-15) through (4.4-17), $\tilde{I}_{as}$, $\tilde{I}_{bs}$, and $\tilde{I}_{cs}$ are 120° out of phase; however, in order for the constant-amplitude air-gap mmf to rotate in the counterclockwise direction, $\tilde{I}_{bs}$ lags $\tilde{I}_{as}$ by 120° and $\tilde{I}_{cs}$ leads $\tilde{I}_{as}$ by 120°.

SP4.4-1 Assume I_{as} in Fig. 4.4-1 is $I_{as} = \sqrt{2}I_s \cos \omega_e t$. Express mmf$_{as}$ at $\phi_s = \pi$. [$\text{mmf}_{as}(\pi) = -(N_s/2)\sqrt{2}I_s \cos\, \omega_e t$]

SP4.4-2 When running counterclockwise at ω_e around the air gap of Fig. 4.4-1 with $I_{as} = \sqrt{2}I_s \cos[\omega_e t + \theta_{esi}(0)]$, what did the second term on the right-hand side of (4.4-3) appear as? [A one-half amplitude air-gap mmf pulsating at a frequency of ω_e/π Hz]

SP4.4-3 Determine the balanced sets that would produce a counterclockwise rotating mmf if the assigned positive direction of i_{bs} in Fig. 4.4-2 were reversed. [I_{as} =(4.4-8) and I_{bs} = −(4.4-9); I_{as} = − (4.4-8) and I_{bs} =(4.4-9)]

SP4.4-4 The rotor of the two-phase device shown in Fig. 4.4-2 is rotating at $0.9\omega_e$ in the counterclockwise direction. You are on the rotor. (a) Relative to you, what is the speed of the rotating air-gap mmf given by (4.4-11)? (b) If now you start running clockwise on the rotor at $2\omega_e$, what would be the speed of the rotating air-gap mmf relative to you? [$0.1\omega_e$, ccw; $2.1\omega_e$, ccw]

SP4.4-5 The steady-state stator currents flowing in the three-phase device shown in Fig. 4.4-3 are $\tilde{I}_{as} = I_s\underline{/-90^\circ}$, $\tilde{I}_{bs} = I_s\underline{/30^\circ}$, and $\tilde{I}_{cs} = I_s\underline{/150^\circ}$. Determine the direction of rotation of mmf$_s$. [cw]

4.5 *P*-POLE MACHINES

Thus far, we have considered only two-pole electromechanical motion devices. Actually, electromechanical devices may have any even number of poles (2, 4, 6, 8, ...) up to more than 100 in the case of large hydroturbine generators. We may at first be a little hesitant to tackle the analysis of machines with more than two poles, since it appears that this may complicate matters before we even get started. Fortunately, this is not the case. We will find that with a simple change of variables we can analyze all machines as if they were two-pole machines. We need only to modify the expression for evaluating torque and realize that, physically, the actual rotor speed of a machine with more than two poles will be a multiple less than that which we determine from our two-pole equivalent.

The characteristics of the rotating air-gap mmf of a machine with more than two poles can be determined by considering the four-pole device shown in Fig. 4.5-1. Here, the outer boundary of the stator is not depicted for purposes of convenience. We shall make this omission in many future drawings of rotational electromechanical devices. In Fig. 4.5-1, each phase winding consists of two series-connected windings, each of which is assumed to be sinusoidally distributed. For example, $as1'$ represents a group of conductors sinusoidally distributed over $0 < \phi_s < \frac{1}{2}\pi$, and so on. The phase windings consist of N_s turns, with $N_s/2$ turns in each of the series-connected windings. There may be some confusion in regard to notation. When considering the coils of a winding in Fig. 4.2-1, the notation as_1, bs_1, ... was used. In Fig. 4.5-1, the notation $as1$, $bs1$, ... is used to denote sinusoidally distributed windings. Thus, a subscripted number denotes a coil, whereas a number that is not a subscript denotes a sinusoidally distributed winding.

Note that each of the two series windings per phase spans $\frac{1}{2}\pi$ radians and each phase winding establishes two magnetic systems. For example, at the

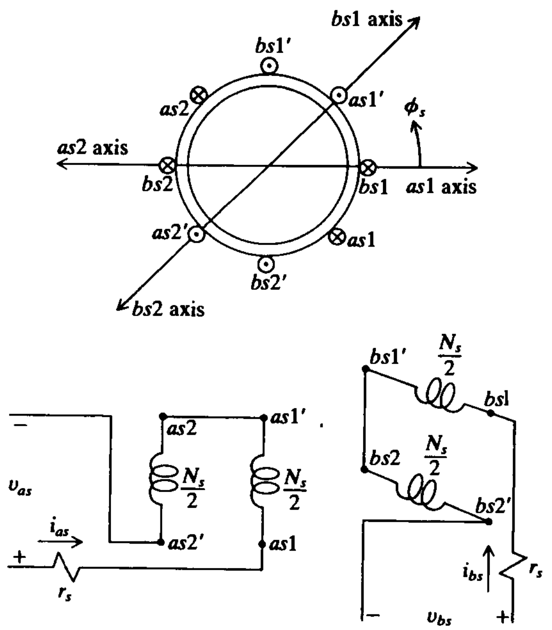

Figure 4.5-1: Stator winding arrangement of a four-pole, two-phase, symmetrical electromechanical device.

instant when $i_{bs} = 0$ and i_{as} is a positive maximum, the $as1 - as1'$ part of the as winding produces positive flux in the $as1$-axis direction whereas the $as2$-$as2'$ part of the as winding produces positive flux in the $as2$-axis direction. A south pole occurs for $-\frac{1}{4}\pi < \phi_s < \frac{1}{4}\pi$ and $\frac{3}{4}\pi < \phi_s < \frac{5}{4}\pi$. Now, one-half of the flux that enters the stator steel for $-\frac{1}{4}\pi < \phi_s < \frac{1}{4}\pi$ reenters the air gap between $\frac{5}{4}\pi < \phi_s < \frac{7}{4}\pi$ and the other one half between $\frac{1}{4}\pi < \phi_s < \frac{3}{4}\pi$. The flux that enters the stator for $\frac{3}{4}\pi < \phi_s < \frac{5}{4}\pi$ divides similarly. Hence, two north poles occur: one for $\frac{1}{4}\pi < \phi_s < \frac{3}{4}\pi$ and one for $\frac{5}{4}\pi < \phi_s < \frac{7}{4}\pi$.

The air-gap mmf established by each phase is a sinusoidal function of $2\phi_s$ for a four-pole machine or, in general, $(P/2)\phi_s$, where P is the number of poles. In particular,

$$\mathrm{mmf}_{as} = \frac{2}{P}\frac{N_s}{2} i_{as} \cos \frac{P}{2}\phi_s \tag{4.5-1}$$

$$\mathrm{mmf}_{bs} = \frac{2}{P}\frac{N_s}{2} i_{bs} \sin \frac{P}{2}\phi_s \tag{4.5-2}$$

where N_s is the total equivalent turns per stator phase. For balanced steady-state operation, the stator currents may be expressed as

$$I_{as} = \sqrt{2} I_s \cos[\omega_e t + \theta_{esi}(0)] \tag{4.5-3}$$

$$I_{bs} = \sqrt{2} I_s \sin[\omega_e t + \theta_{esi}(0)] \tag{4.5-4}$$

Equations (4.5-3) and (4.5-4) are the same expressions for the stator currents as given for the two-pole case. The air-gap mmf established by balanced steady-state stator currents (mmf_s) may be expressed by substituting (4.5-3) and (4.5-4) into (4.5-1) and (4.5-2), respectively, and by adding the resulting equations. Thus,

$$\mathrm{mmf}_s = \frac{N_s}{P}\sqrt{2} I_s \cos\left[\omega_e t + \theta_{esi}(0) - \frac{P}{2}\phi_s\right] \tag{4.5-5}$$

If the argument of (4.5-5) is set equal to a constant and if the derivative of this expression is taken with respect to time, we see that the four poles established by the balanced stator currents rotate about the air gap at $(2/P)\omega_e$, that is,

$$\frac{d\phi_s}{dt} = \frac{2}{P}\omega_e \tag{4.5-6}$$

Let us take a moment to review. With the stator arranged as in Fig. 4.5-1, balanced steady-state stator currents of frequency ω_e produce a four-pole (P-pole) magnetic system that rotates about the air gap at $(2/4)\omega_e$ or $(2/P)\omega_e$ relative to the stator windings. Synchronous speed, viewed from the rotor, is now $(2/P)\omega_e$; however, the stator variables are unaware of this. To the electric system, ω_e is synchronous speed.

The four-pole single-phase reluctance machine shown in Fig. 4.5-2 can be used to establish the change of variables necessary to allow us to consider P-pole machines as two-pole devices. In Fig. 4.5-2, θ_{rm} and ω_{rm} are the angular displacement and angular velocity, respectively, of the rotor. Recall that we used θ_r and ω_r for the two-pole device in our previous work. Now, let us write the self-inductance L_{asas}. If we follow the same procedure as we did to obtain (1.7-29), we will find that

$$L_{asas} = L_l + L_A - L_B \cos 2\left(\frac{4}{2}\theta_{rm}\right) \tag{4.5-7}$$

Generalizing for a P-pole machine,

$$L_{asas} = L_l + L_A - L_B \cos 2\left(\frac{P}{2}\theta_{rm}\right) \tag{4.5-8}$$

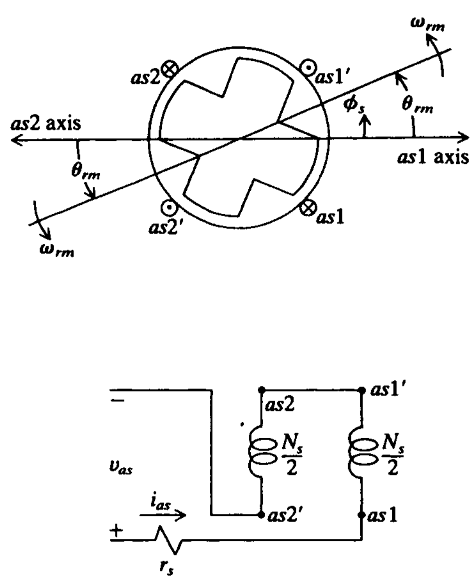

Figure 4.5-2: Elementary four-pole, single-phase, reluctance machine.

It is apparent that if we make the substitution of

$$\theta_r = \frac{P}{2}\theta_{rm} \tag{4.5-9}$$

then L_{asas} for the P-pole machine, (4.5-8), is identical in form to L_{asas} for the two-pole machine, (1.7-29). Also, (4.5-9) leads to

$$\omega_r = \frac{P}{2}\omega_{rm} \tag{4.5-10}$$

With the substitution of θ_r and ω_r for $(P/2)\theta_{rm}$ and $(P/2)\omega_{rm}$, respectively, the voltage equations for a P-pole machine are identical to those for a two-pole machine. Actually, the electric system can tell no difference. To the electric system, the angular position of the rotor is θ_r and its velocity is ω_r. For this reason, θ_r and ω_r are often called the electrical angular displacement of the rotor and the electrical angular velocity of the rotor, respectively.

One might be led to believe that the number of poles can be forgotten except when we want to know the actual physical rotor displacement θ_{rm} or angular velocity ω_{rm}. This is not quite the case. In the derivation for force (torque) in Chapter 2, the change of energy between the mechanical system and coupling fields was expressed for a rotational system as

$$dW_m = -T_e d\theta \tag{4.5-11}$$

where θ must be the actual displacement of the rotating member. Hence, for a P-pole machine,

$$dW_m = -T_e d\theta_{rm} \tag{4.5-12}$$

Since all electrical variables are expressed in terms of θ_r, it is convenient to replace $d\theta_{rm}$ in (4.5-12) with $d\theta_r$. Thus,

$$dW_m = -T_e \frac{2}{P} d\theta_r \tag{4.5-13}$$

Therefore, to calculate the electromagnetic torque of a P-pole machine, we simply multiply all terms on the right-hand side of Table 2.5-1 by $P/2$. For all other calculations, the P-pole machine may be considered as a two-pole device. This is true regardless of the number of phases.

Example 4B. A four-pole, two-phase reluctance machine is depicted in Fig. 4B-1. The stator currents are given by (4.5-3) and (4.5-4) with $\theta_{esi}(0) = 0$. The rotor is rotating in the counterclockwise direction at synchronous speed. The mechanical displacement θ_{rm} may be expressed as

$$\theta_{rm} = \omega_{rm}t + \theta_{rm}(0) \tag{4B-1}$$

where ω_{rm} is the mechanical speed of the rotor. In a four-pole machine, synchronous speed is $(2/P)\omega_e = \omega_e/2$. It is instructive to determine the time-zero position of the north and south magnetic poles associated with mmf_s.

From (4.5-5) with $P = 4$ and $\theta_{esi}(0) = 0$,

$$\mathrm{mmf}_s = \frac{N_s}{4}\sqrt{2}I_s \cos(\omega_e t - 2\phi_s) \tag{4B-2}$$

At $t = 0$, mmf_s is positive maximum at $\phi_s = 0$ and π, which define the median locations of the stator south poles at $t = 0$. Recall that if mmf_s is positive, the magnetic field is oriented from the rotor to the stator and magnetic flux enters the south poles. Also, from (4B-2) with t =0, mmf_s is a negative maximum at $\phi_s = \frac{1}{2}\pi$ and $\frac{3}{2}\pi$, which define the median locations of the stator north poles. The time-zero location of the stator north and south poles is depicted in Fig. 4B-2. Since the windings are assumed to be sinusoidally distributed, mmf_s is distributed sinusoidally. The placement of N^s and S^s in Fig. 4B-2 defines the locations of the positive and negative maximum values, respectively, of mmf_s at $t = 0$.

As time increases from zero, the stator mmf and, consequently, the stator poles (N^s and S^s) rotate at $\omega_e/2$ in the counterclockwise direction. For a constant electromagnetic torque to be produced, the rotor must also rotate at $\omega_{rm} = \omega_e/2$ (synchronous speed) in the counterclockwise direction. The electromagnetic torque acts to align the minimum reluctance paths of the rotor with the rotating stator poles.

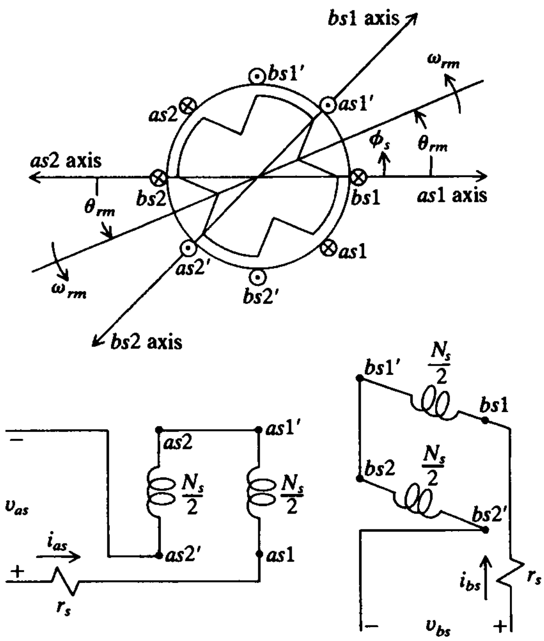

Figure 4B-1: Elementary four-pole, two-phase reluctance machine.

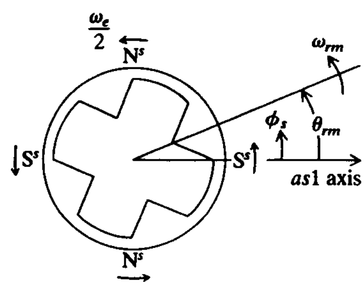

Figure 4B-2: Time-zero location of stator north and south poles.

SP4.5-1 If during steady-state operation, $\omega_r = \omega_e$, calculate the actual rotor speed in revolutions per minute of a 120-pole, 60-Hz hydroturbine synchronous generator. [$\omega_{rm} = 60$ r/min]

SP4.5-2 Suppose $\theta_{esi}(0) = 45°$ in (4.5-3) and (4.5-4). For a six-pole, two-phase stator, determine the location of the positive and negative maximum values of mmf$_s$ at time zero. [S^s at $\phi_s = 15°$, $135°$, $255°$; N^s at $\phi_s = 75°$, $195°$, $315°$]

4.6 INTRODUCTION TO SEVERAL ELECTROMECHANICAL MOTION DEVICES

We are at a point where it would be worthwhile to take a first look at the electromechanical devices that we will analyze in subsequent chapters. By introducing these devices here rather than waiting to introduce them individually at the beginning of the following appropriate chapters, you are able to study subsequent chapters in arbitrary order. For example, the chapter on induction machines is not a prerequisite to the chapter on synchronous machines, even though the principles involved when starting a synchronous motor are the same principles used to explain induction motor action. However, the introductory treatment of induction machines given in this section is sufficient for explaining how synchronous machines may be started. Similarly, the introductory treatment of the reluctance machine (a type of synchronous machine) given in this section enables you to study stepper motors (Chapter 9) without reading the material in Chapter 7 on synchronous machines. If, however, you choose to follow the subsequent chapters in the order in which they are presented, you may wish to bypass this section.

Rotational electromechanical devices fall into three general classes: direct-current, synchronous, and induction. The dc machine was treated in Chapter 3, and we have briefly considered the single-phase reluctance machine which is a type of synchronous machine. Synchronous machines are so called because they develop an average torque only when the rotor is rotating in synchronism (synchronous speed) with the rotating air-gap mmf established by currents flowing in the stator windings. Examples are reluctance machines, stepper motors, permanent-magnet ac machines such as brushless dc motors, and the machine that has become known as simply the synchronous machine. Even though these machines are of the synchronous type, the machine commonly referred to as the synchronous machine or synchronous generator is the device used to generate electric power. The vast majority of large electric power generators are synchronous generators and are so called.

On the other hand, the induction machine, which is the principal means of converting energy from electric to mechanical, cannot develop torque at synchronous speed in its normal mode of application. The windings on the rotor are short-circuited and, in order to cause current to flow in these windings that produce torque by interacting with the air-gap mmf established by the stator windings, the rotor must rotate at a speed other than synchronous speed. Although some synchronous machines are designed to start from stall and accelerate to near-synchronous speed as an induction motor, the induction machine family does not include a large number of relatives as does the synchronous machine group. There is, however, some differentiation made between a large, workhorse induction motor and induction motors used in lower-power, position-control systems.

In this section, we will show the winding arrangement for elementary versions of these electromechanical devices and describe briefly the principle of operation of each. In subsequent chapters, we will analyze these devices in detail.

Reluctance Devices

Elementary, single-, and two-phase, two-pole reluctance machines are shown in Fig. 4.6-1. The stator windings are assumed to be sinusoidally distributed. The two-phase reluctance motor is often used as a control motor. Moreover, the operation of these devices with constant stator currents provides an explanation of the positioning of reluctance-type stepper motors.

The principle of operation is quite straightforward. Recall from our work in Chapter 2 that in an electromagnetic system a force (torque) is produced in an attempt to minimize the reluctance of the magnetic system.

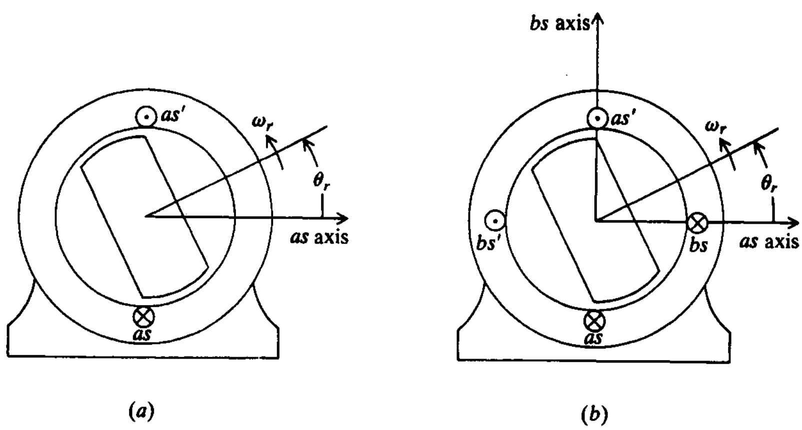

Figure 4.6-1: Elementary two-pole reluctance machines. (a) Single-phase; (b) two-phase.

We have established that, with an alternating current flowing in the winding of the single-phase stator, two oppositely rotating mmfs are produced, (4.4-3). Therefore, once the rotor is rotating in synchronism (remember, this is a type of synchronous machine) with either of the two oppositely rotating air-gap mmf's, there is a force (torque) created by the magnetic system in an attempt to align the minimum-reluctance path of the rotor with the rotating air-gap mmf. When there is no load torque on the rotor, the minimum-reluctance path of the rotor is in alignment with the rotating air-gap mmf. When a load torque is applied, the rotor slows ever so slightly, thereby creating a misalignment of the minimum-reluctance path and the rotating air-gap mmf. When the electromagnetic torque produced in an attempt to maintain alignment is equal and opposite to the load torque on the rotor, the rotor resumes synchronous speed. It follows that, if the load torque is larger than the torque that can be produced to align, the rotor will fall out of synchronism and, since the machine cannot develop an average torque at a speed other than synchronous, it will slow to stall.

The operation of the two-phase device differs from that of the single-phase device in that only one constant-amplitude, rotating air-gap mmf is produced during balanced steady-state conditions. Hence, a constant torque will be developed at synchronous speed rather than a torque that pulsates about an average value, as is the case with the single-phase machine. Although the reluctance motor can be started from a source that can be switched at a frequency corresponding to the rotor speed, as in the case of stepper or brushless dc motors, the devices, as shown in elementary form in Fig. 4.6-1, cannot develop an average starting torque when plugged into a household power outlet.

As a youngster, the oldest of the authors recalls that his parents had a small, old, mantle-type electric clock that was not self-starting. Although it was rather annoying to the rest of the family, it was extremely interesting and entertaining to spin the rotor from stall with the thumb wheel on the back of the clock. Spinning the rotor above synchronous speed would cause it to slow to synchronous speed and then "lock in" and operate normally. With a little practice you could spin the rotor so that it would come up to just slightly less than synchronous speed, whereupon you could see and hear it get pulled into step with the rotating air-gap mmf. However, the most interesting of all was the fact that the clock would operate in either direction. Moreover, once the device was operating at synchronous speed, you could pinch the thumb wheel very lightly between your thumb and index finger and feel the motor overcome the load torque you were applying. As you increased your hold on the thumb wheel, the motor would overcome this increased load and continue to run at synchronous speed until you exceeded the torque capability of the motor. Instantaneously, before you could release your hold on the thumb wheel, the motor torque would vanish and the clock would stop. Modern low-power reluctance motors are designed to self-start without a thumb wheel and, therefore, are not nearly as intriguing or instructive to a ten-year-old.

Some stepping or stepper motors are used to convert a digital input into a mechanical motion. Many stepper motors are of the reluctance type. In fact, some stepper motors are often called *variable-reluctance motors*. Operation of reluctance stepper motors is easily explained. For this purpose, let us assume that a constant current is flowing in the *bs* winding of Fig. 4.6-1*b* with the *as* winding open-circuited. The minimum-reluctance path of the rotor will be aligned with the *bs* axis, that is, assume $\theta_r = 0$. Now let us reduce the *bs* winding current to zero while increasing the current in the *as* winding to a constant value. There will be forces to align the minimum-reluctance path of the rotor with the *as* axis; however, this can be satisfied with $\theta_r = \pm\frac{1}{2}\pi$. Unfortunately, there is a 50-50 chance as to which way it will rotate. Although we see how stepping action can be accomplished from this explanation, we realize that we need a device different from a single- or two-phase reluctance machine to accomplish controlled stepping. There are two common techniques used to achieve controlled, bidirectional stepping with reluctance devices: Place more than two phase windings on the stator (generally, three are used) or cascade three or more single-phase reluctance machines on the same shaft with the minimum-reluctance paths displaced from each other. The first type is called a single-stack variable-reluctance stepper motor; the second, a multistack variable-reluctance stepper motor. The two-phase reluctance machine is treated in Chapter 7 and stepper motors in Chapter 9.

Induction Machines

Elementary single- and two-phase induction machines are shown in Fig. 4.6-2. The rotors of both devices are identical in configuration; each has the equivalent of two orthogonal windings, which are assumed to be sinusoidally distributed. In other words, the *ar* and *br* windings are equivalent to a symmetrical two-phase set of windings and, in the vast majority of applications,

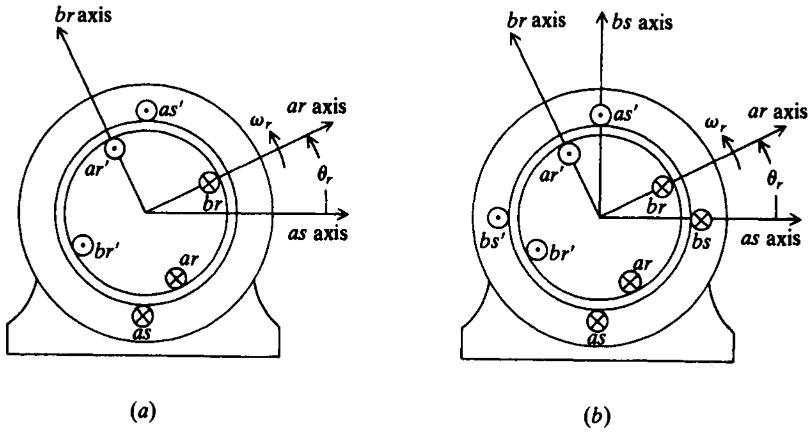

Figure 4.6-2: Elementary two-pole induction machines. (*a*) Single-phase; (*b*) two-phase.

these rotor windings are short-circuited.

It is perhaps a little more convenient to explain the operation of the two-phase device first. For balanced steady-state operation, the currents flowing in the stator windings produce an air-gap mmf that rotates about the air gap at an angular velocity of ω_e. With the rotor windings short-circuited, which is the only mode of operation we will consider, a voltage is induced in each of the rotor windings only if the rotor speed ω_r is different from ω_e. The currents flowing in the rotor circuits due to induction (thus, the name induction motor) will be a balanced set with a frequency equal to $\omega_e - \omega_r$, which will produce an air-gap mmf that rotates at $\omega_e - \omega_r$ relative to the rotor or ω_e relative to a stationary observer. Hence, the rotating air-gap mmf caused by the currents flowing in the stator windings induces currents in the short-circuited rotor windings which, in turn, establish an air-gap mmf that rotates in unison with the stator rotating air-gap mmf (mmf_s). Interaction of these magnetic systems (poles) rotating in unison provides the means of producing torque on the rotor.

Although the induction machine can operate as a motor or a generator, it is normally operated as a motor. As a motor, it can develop a torque from $0 < \omega_r < \omega_e$. At $\omega_r = \omega_e$, rotor currents are not present since the rotor is rotating at the speed of the stator rotating air-gap mmf and, therefore, the rotor windings do not experience a change of flux linkages, which is, of course, necessary to induce a current in the rotor windings. Large induction machines are designed to operate very close to synchronous speed.

The single-phase induction motor is, perhaps, the most widely used electromechanical device. Garbage disposals, washers, dryers, and furnace fans are but a few of the many applications of fractional-horsepower, single-phase induction motors. However, the device shown in Fig. 4.6-2a is not quite the whole picture of a single-phase induction motor. Recall that the single-phase stator winding produces oppositely rotating air-gap mmfs of equal amplitude. If the single-phase induction motor shown in Fig. 4.6-2a is stalled, $\omega_r = 0$, and if a sinusoidal current flows in the stator winding, the rotor will not move. This device does not develop a starting torque. Why? Well, the rotor cannot follow either of the rotating mmfs since it develops as much torque to go with one as it does to go with the other. If, however, you manually turn the rotor in either direction, it will accelerate in that direction and operate normally. Although single-phase induction motors normally operate with only one stator winding, it is necessary to include a second stator winding to start the device. Actually, the single-phase induction motors used in our homes are often two-phase induction motors with provisions to switch out one of the windings once the rotor accelerates to between 60 and 80 percent of synchronous speed. The next question is how do we get two phase voltages from a single-phase household supply? Well, we do not actually develop a two-phase supply, but we approximate one, as far as the two-phase motor is concerned, by placing a capacitor in series with one of the stator windings. This shifts the phase of one current relative to the other, thereby producing a larger rotating air-gap mmf in one direction than in the other. If you have looked closely at a single-phase induction motor, you probably noticed a cylinder 2 to 5 inches in length mounted on the housing of the motor and 9 times out of 10 it is painted black for some unknown reason. That is the capacitor, commonly called the *start capacitor,* for obvious reasons. Provisions to switch the capacitor out of the circuit are generally inside the housing of the motor. The induction machine is analyzed in Chaps. 6 and 10.

Synchronous Machines

Although the elementary single- and two-phase devices shown in Fig. 4.6-3 have become known as synchronous machines, they are but one of several devices that fall into the synchronous-machine category. Nevertheless, we will honor convention and refer to the devices in Fig. 4.6-3 as synchronous machines.

The single-phase synchronous machine has limited application. In fact,

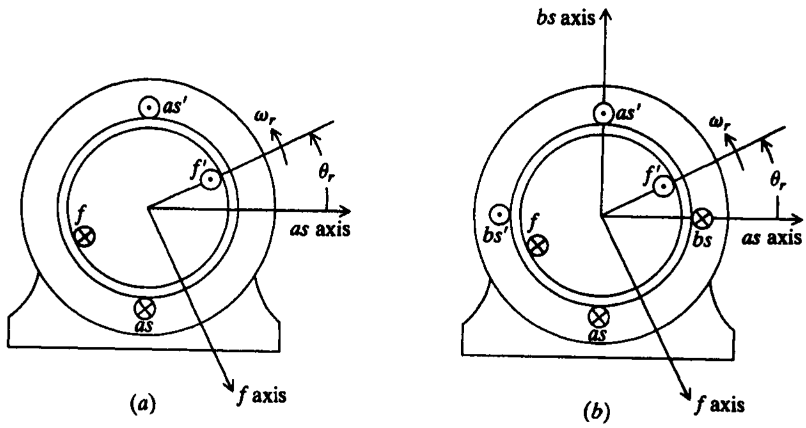

Figure 4.6-3: Elementary two-pole synchronous machines. (a) Single-phase; (b) two-phase.

the same can be said about the two-phase synchronous machine. It is the three-phase synchronous machine that is used to generate electric power in power systems such as in some automobiles, aircraft, utility systems, ships, and now, possibly, future spacecraft. Nevertheless, the theory of operation of synchronous machines is adequately introduced by considering the two-phase version.

The elementary devices shown in Fig. 4.6-3 have only one rotor winding, the field winding (f winding). In practical synchronous machines, the rotor is equipped with short-circuited windings in addition to the f winding, which help to damp oscillations about synchronous speed and, in some cases, these windings are used to start the unloaded synchronous machine from stall as an induction motor.

The principle of operation is apparent once we realize that the current flowing in the field winding is direct current. Although it may be changed in value by varying the applied field voltage, it is constant for steady-state operation of a balanced two-phase synchronous machine. When operated as a generator, the rotor is driven by some mechanical means. If the stator windings are connected to a balanced system, the stator currents produce a constant-amplitude, rotating air-gap mmf. A rotor air-gap mmf is produced by the direct current flowing in the field winding. To produce torque or transmit power, the air-gap mmf produced by the stator and that produced by the rotor must rotate in unison about the air gap of the machine. Hence,

$\omega_r = \omega_e$, that is, synchronous speed.

The synchronous machines shown in Fig. 4.6-3 are actually called round-rotor synchronous machines. A variation of this is the salient-pole synchronous machine used in low-speed multipole applications. A two-phase two-pole version is shown in Fig. 4.6-4. The principle of operation is identical to that of the round-rotor machine, except there are now two means of producing torque. One way is by the interaction of the rotating air-gap mmfs, as in the case of the round-rotor device, and, the other, normally much smaller, is a reluctance torque produced owing to the salient-pole configuration. Both torques are constant only when $\omega_r = \omega_e$. If ω_r is not equal to ω_e, the torques will pulsate with zero average. Although the synchronous machine is generally used as a generator, it can also be used as a motor. Synchronous machines are analyzed in Chapter 7.

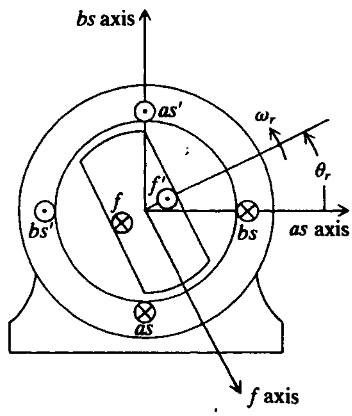

Figure 4.6-4: Elementary two-pole, two-phase, salient-pole synchronous machine.

Permanent-Magnet Devices

If we replace the rotor of the synchronous machines shown in Fig. 4.6-3 with a permanent-magnet rotor, we have the so-called permanent-magnet devices shown in Fig. 4.6-5. The operation of these devices is identical to that of the synchronous machine. Since the strength of the rotor field due to the permanent magnet cannot be controlled as in the case of the synchronous machine that has a field winding, it is not widely used as a means of generating power. It is, however, used widely as a drive motor. In particular, permanent-magnet motors are used as stepper motors and, extensively, as

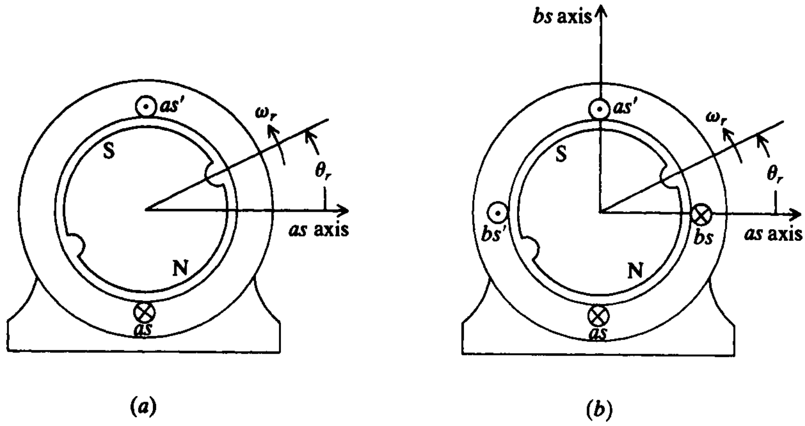

Figure 4.6-5: Elementary two-pole, permanent-magnet devices. (a) Single-phase; (b) two-phase.

brushless dc motors, wherein the voltages applied to the stator windings of a permanent-magnet device are switched electronically at a frequency corresponding to the speed of the rotor. We shall analyze the brushless dc motor in Chapter 8 and stepper motors in Chapter 9.

SP4.6-1 The *ar* winding of the two-phase induction machine shown in Fig. 4.6-2*b* is open-circuited and a negative direct current is supplied to the *br* winding. Find another machine in Sec. 4.6 that has the same winding configuration (active windings) and constraints and, thus, the same principles of operation. [Fig. 4.6-3*b*]

SP4.6-2 Repeat SP4.6-1 if the direct current in the *br* winding is held fixed by a current source. [Fig. 4.6-5*b*]

SP4.6-3 Which of the devices discussed in Sec. 4.6 can be operated as a generator supplying an *RL* static load? [Fig. 4.6-3 through Fig. 4.6-5]

SP4.6-4 We have two single-phase synchronous machines from which we want to generate two-phase voltages. What do we do? [Connect the shafts with fields displaced $\frac{1}{2}\pi$]

SP4.6-5 The current flowing in the *as* winding of the single-phase, round-rotor synchronous machine shown in Fig. 4.6-3*a* is fixed at $I_{as} = \sqrt{2}I_s \cos \omega_e t$. A dc voltage is applied to the field. The rotor is rotating counterclockwise at ω_e. The steady-state field current will consist of two components. Determine the frequency of these two components. [dc; $2\omega_e$]

SP4.6-6 The two-pole, two-phase, permanent-magnet machine shown in Fig. 4.6-5*b* is used as a stepper motor. Initially, $I_{as} = I$ and $I_{bs} = 0$. I_{as} is "stepped" to zero while I_{bs} is stepped to $-I$, where I is a positive current. Determine the initial and final values of θ_r. [$\frac{1}{2}\pi$; 0]

4.7 RECAPPING

We have seen that the electromechanical devices with rotating magnetic fields have a number of features in common. Perhaps most important of these features is the fact that the stator windings of all multiphase devices are arranged so that balanced, sinusoidal stator currents produce an air-gap mmf that rotates about the air gap at $(2/P)\omega_e$ rad/s, where ω_e is the electrical angular velocity of the stator currents and P is the number of poles. Also of importance is the observation that, by simple changes in the configuration of the windings and the constraints placed upon the electrical variables, we can readily identify, in elementary form, all of the electromechanical motion devices that we will consider in the remainder of this text.

4.8 PROBLEMS

1. A winding with five coils, each with nc_s conductors, is distributed over $\frac{1}{2}\pi$ of the stator. Sketch the configuration and indicate the direction of the positive magnetic axis of this single-phase stator winding.

2. The four coils, each with nc_s conductors, of the windings of a two-pole, two-phase, low-power device are concentrated so that four coil sides are placed in one slot per phase. Sketch the winding arrangement and show the *as* and *bs* axes.

3. Consider the two-phase device shown in Fig. 4.8-1. The windings are sinusoidally distributed, each with N equivalent turns. Express (*a*) N_{as} and N_{bs} and (*b*) mmf_{as} and mmf_{bs}.

* 4. Each stator coil in Fig. 4.8-2 contains nc_s turns. Using the information given in Example 4A as a guide, sketch the developed diagram for the *as* and *bs* windings and mmf_{as} and mmf_{bs}.

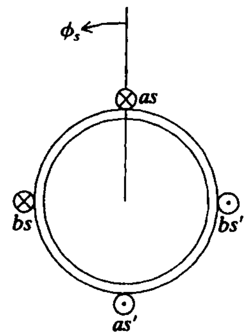

Figure 4.8-1: Elementary two-pole, two-phase electromechanical device.

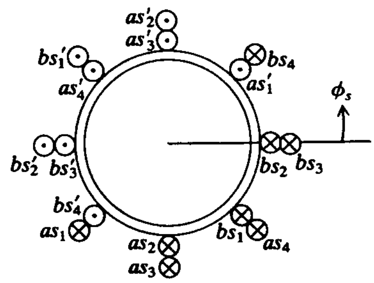

Figure 4.8-2: A two-pole, two-phase electromechanical device.

* 5. Consider Fig. 4.8-3, where a winding is formed by N conductors uniformly distributed over the regions shown. Each conductor carries the current i. Sketch the air-gap mmf. You will need the information in Example 4A as a guide.

6. Consider Fig. 4.8-1. (a) Express mmf$_s$. (b) Determine the phase relationship between $\tilde{I}_{as}$ and $\tilde{I}_{bs}$ that will produce counterclockwise rotation of mmf$_s$. That is, does $\tilde{I}_{as}$ lead or lag $\tilde{I}_{bs}$ by 90°? (c) Locate the positions of N^s and S^s when $\omega_e t = 30°$ with $I_{as} = \sqrt{2}I_s \cos\omega_e t$ and $I_{bs} = -\sqrt{2}I_s \sin\omega_e t$.

7. Consider the device shown in Fig. 4.4-2. Express mmf$_s$ for (a) $I_{as} = \sqrt{2}I_s \cos\omega_e t$, $I_{bs} = \sqrt{2}I_s \cos\omega_e t$; ($b$) $I_{as} = I_a \cos\omega_e t$, $I_{bs} = I_b \sin\omega_e t$, where $I_a \neq I_b$. Both (a) and (b) are unbalanced sets. Set (a) is

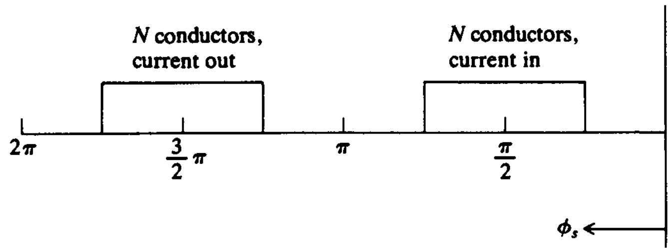

Figure 4.8-3: Uniformly distributed windings.

unbalanced since I_{as} and I_{bs} are not orthogonal; set (b) is unbalanced due to unequal amplitudes.

* 8. The windings of the device shown in Fig. 4.8-4 are sinusoidally distributed, each with N_s equivalent turns. The bs winding may be arranged so that the bs axis is at an arbitrary angle α with the as axis. Express i_{as} and i_{bs} so that mmf_s has a constant amplitude and rotates in the counterclockwise direction regardless of the value of α; in particular, $\text{mmf}_s = (N_s/2)\sqrt{2}I_s \cos(\omega_e t - \phi_s)$.

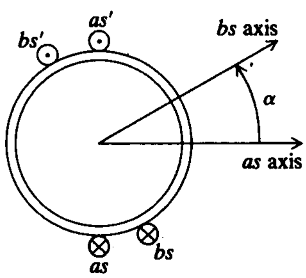

Figure 4.8-4: Magnetic axes displace by a mechanical angle α.

9. Sketch the stator windings and rotor configuration for a six-pole, two-phase, symmetrical-reluctance machine.

* 10. Show analytically that a single-phase reluctance motor does not produce an average starting torque when $I_{as} = \sqrt{2}I_s \cos[\omega_e t + \theta_{esi}(0)]$.

* 11. A two-pole, three-phase reluctance machine and the currents flowing in the stator windings are shown in Fig. 4.8-5. Sketch θ_r versus time,

assuming that the rotor oscillations are sufficiently damped and, at t_0^+, θ_r has a small positive value. Repeat if θ_r has a small negative value at t_0^+. Is there any advantage to make the necessary circuit provisions so that the stator currents can be made both positive and negative? Why?

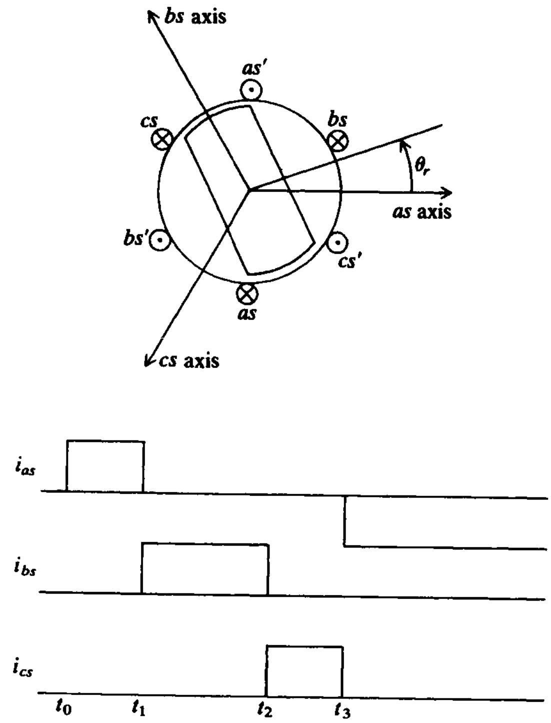

Figure 4.8-5: Two-pole, three-phase reluctance motor with switched phase currents.

* 12. A two-phase induction motor is operating at rated-load torque with balanced stator currents. The steady-state rotor speed is $\omega_r = 0.9\omega_e$. It is an eight-pole, 50-Hz device. Determine (a) the actual rotor speed, (b) the angular velocity of the rotor mmf relative to the rotor, and (c) the frequency of the rotor currents.

* 13. Determine the actual no-load and full-load rotor speeds (ω_{rm}) in revolutions per minute of the following devices: (a) A four-pole, three-phase,

100-hp, 60-Hz, round-rotor synchronous machine (*b*) A 120-pole, three-phase, 100-MW, 60-Hz, salient-pole synchronous machine (*c*) An eight-pole, two-phase, 1-hp, 60-Hz, reluctance machine supplied from a 5-Hz voltage source (*d*) A six-pole, three-phase, $\frac{1}{2}$-hp, permanent-magnet motor supplied from a 15-Hz source.

Chapter 5

INTRODUCTION TO REFERENCE-FRAME THEORY

5.1 INTRODUCTION

In recent years, there has been a steady evolution of the electric drive industry that began with the advent of the controlled rectifier. Controlled electric drives are being used in a wide range of applications such as maximizing the efficiency of air conditioning systems, brushless dc motors used in appliances, doubly-fed induction machines used in wind turbines, and drive motors in electric and hybrid vehicles, and now electric drives are replacing hydraulic drives in aircraft. As the applications for converter-controlled electric drives began to emerge, it became evident that the traditional steady-state approach to electric machine analysis and the machine characteristics as portrayed by this type of analysis were inadequate to analyze and understand most modern electric drive systems. In particular, rapid electronic switching enables control techniques that alter the characteristics of the electric machine beyond what one could envision from the traditional steady-state phasor analysis. It has become apparent that the transient characteristics of the electric machine must be considered and that computer simulations of the dynamic performance of converter-controlled electric drives are useful, if not necessary, in the design of these drives. Concurrently, it was shown that these needs could only be addressed through the appropriate application of reference-frame theory. In fact, reference-frame theory, which had been more or less considered an approach to electric-machine analysis reserved for graduate study, has become the basis of electric-drive simulation, analysis, and control design. Therefore, a modern introductory text on electric-machine analysis should also contain an introduction to reference-frame theory and, thereby, set the stage for the student to appreciate the role that reference-frame theory plays in the analysis of electric machines and drives. In fact, a basic concept of reference-frame theory is becoming as important as the concept of the steady-state characteristics of the electric machines for the analysis and understanding of modern electric drive systems.

This chapter is an attempt to familiarize the reader with reference-frame theory for two-phase systems. It would perhaps be more desirable to consider three-phase systems; however, the first-time reader tends to become overwhelmed with the trigonometry inherent to three-phase analysis and often misses the advantages and power of reference-frame theory. On the other hand, the trigonometry necessary for two-phase systems is not involved, and yet the main features of reference-frame theory are present in a two-phase analysis and are more obvious to the beginning electric-machine analyst. Moreover, the steady-state, torque-speed characteristics of the two-phase machine are the same in form as the three-phase machine. Therefore, the student is not missing the main steady-state features of the electric machine.

There are several changes of variables that are used and it was originally thought that each change of variables was different and, therefore, they were treated separately [1-4]. It was later learned that all changes of variables used to transform real variables are contained in one [5,6]. This general transformation refers machine variables to a frame of reference that rotates at an arbitrary angular velocity. All known real transformations are obtained from this transformation by simply assigning the speed of the rotation of the reference frame. In this chapter, this transformation is set forth and, since many of its properties can be studied without the complexities of the machine equations, it is applied to the equations that describe resistive, inductive, and capacitive circuit elements. By this approach, many of the basic concepts and interpretations of this general transformation are readily and concisely established. Extending the material presented in this chapter to the analysis of ac machines is straightforward, involving a minimum of trigonometric manipulations.

5.2 BACKGROUND

It seems appropriate to take a few moments to give a brief history of reference-frame theory. In the late 1920s, R. H. Park [1] introduced a new approach to electric-machine analysis. He formulated a change of variables that, in effect, replaced the variables (voltages, currents, and flux linkages) associated with the stator windings of a synchronous machine with variables associated with fictitious windings rotating at the electrical angular velocity of the rotor. This change of variables is often described as transforming or referring the stator variables to a frame of reference fixed in the rotor. Park's transformation revolutionized electric machine analysis.

In the late 1930s, H. C. Stanley [2] employed a change of variables in the analysis of induction machines. He showed that the rotor-position-dependent inductances in the voltage equations of an induction machine due to electric circuits in relative motion could be eliminated by transforming the variables associated with the rotor windings (rotor variables) to variables associated with fictitious stationary windings. This is often described as transforming or referring the rotor variables to a frame reference fixed in the stator.

G. Kron [3] introduced a change of variables that eliminated the rotor-position-dependent inductances of a symmetrical induction machine by transforming both the stator variables and the rotor variables to a reference frame rotating in synchronism with the fundamental angular velocity of the stator variables. This reference frame is commonly referred to as the synchronously rotating reference frame.

D. S. Brereton and coworkers [4] employed a change of variables that also eliminated the rotor-position-varying inductances of a symmetrical induction machine by transforming the stator variables to a reference frame rotating at the electrical angular velocity of the rotor. This is essentially Park's transformation applied to induction machines.

Park, Stanley, Kron, and Brereton and coworkers developed changes of variables each of which appeared to be uniquely suited for a particular application. Consequently, each transformation was derived and treated separately in the literature until it was noted in 1965 [5] that all known real transformations used in induction machine analysis are contained in one general transformation that eliminates all position-varying inductances by referring the stator and the rotor variables to a frame of reference that may rotate at any angular velocity or remain stationary. All known real transformations may then be obtained by simply assigning the appropriate speed of rotation, which may in fact be zero, to this so-called *arbitrary reference frame*. Later, it was noted that the stator variables of a synchronous machine could also be referred to the arbitrary reference frame [6]. However, we will find that the position-varying inductances of a synchronous machine are eliminated only if the reference frame is rotating at the electrical angular velocity of the rotor (Park's transformation); consequently, the arbitrary reference frame does not offer the advantages in the analysis of the synchronous machines that it does in the case of induction machines.

5.3 EQUATIONS OF TRANSFORMATION – CHANGE OF VARIABLES

Just as the concept of phasors is convenient for analyzing the steady-state performance of electromechanical motion devices, reference-frame theory is convenient, if not necessary, to simulate and analyze the transient performance of these devices. The change of variables, which is the basis of reference theory, allows us to rid the voltage equations of rotor-position-dependent inductances in ac machines. Although this will become apparent in later chapters when we consider each ac machine, many of the properties of the change of variables and the transformation involved can be illustrated by using a constant-parameter circuit. We will do this later in this chapter; however, first let us consider the transformation without regard to the type of circuit being analyzed.

The change of variables that formulates a transformation of a two-phase set of variables associated with a stationary circuit may be expressed as

$$\mathbf{f}_{qds} = \mathbf{K}_s \mathbf{f}_{abs} \tag{5.3-1}$$

where

$$(\mathbf{f}_{qds})^T = [f_{qs}, \ \ f_{ds}] \tag{5.3-2}$$

$$(\mathbf{f}_{abs})^T = [f_{as}, \ \ f_{bs}] \tag{5.3-3}$$

$$\mathbf{K}_s = \begin{bmatrix} \cos\theta & \sin\theta \\ \sin\theta & -\cos\theta \end{bmatrix} \tag{5.3-4}$$

where the superscript T denotes the transpose of a matrix and the angular position may be expressed as

$$\frac{d\theta}{dt} = \omega \tag{5.3-5}$$

We have a lot of things to define. First, f can denote voltage, current, flux linkage, or electric charge. That is, the same transformation is applied to all. The subscripts as and bs denote the variables associated the a and b phases of the stationary (stator) circuits; thus, the reason for adding s to the subscript. Now, qs and ds are the new or substitute variables that we are going to use in our analysis and the qs and ds variables are related to the as and bs variables by the transformation matrix $\mathbf{K}_s$. The subscript s is used in qs, ds, and $\mathbf{K}_s$ to distinguish these quantities from the variables associated with rotating (rotor) circuits of ac machines, which we will designate with an r in the subscript. Finally, the angular velocity and angular displacement are related by (5.3-5). It is left to the reader to show that $\mathbf{K}_s$ is equal to its inverse; $\mathbf{K}_s = (\mathbf{K}_s)^{-1}$.

Although it is not necessary, some prefer to attach a "physical" meaning to the transformation by casting (5.3-1) graphically as shown in Fig. 5.3-1. Therein, all variables associate with the as-circuit are considered to be "acting" in the horizontal direction (denoted f_{as}), and bs-circuit variables in the vertical direction (denoted by f_{bs}). We will find later that these directions can be thought of as directions of the magnetic axes of the stator windings of the ac machines that we will consider. Likewise, f_{qs} and f_{ds} are the directions associated with the substitute variables, which can also be thought of as the principal magnetic axes of the windings related to the substitute variables. Although a physical interpretation is not necessary, a change of variables can be interpreted by graphically projecting the "directions" of the variables associated with actual stationary circuits onto the "directions" of the variables associated with fictitious circuits rotating at an angular velocity of ω.

Please note that we have not assigned a value to ω or θ. The angular displacement θ must be continuous; however, the angular velocity associated with the change of variables is unspecified. The frame of reference may rotate at any constant or varying angular velocity or it may remain stationary. The connotation of arbitrary stems from the fact that the angular velocity of the transformation is unspecified and can be selected arbitrarily to expedite the solution of the system equations or to satisfy the system constraints. The change of variables may be applied to variables of any waveform and time sequence; however, we will find that the transformation given above is

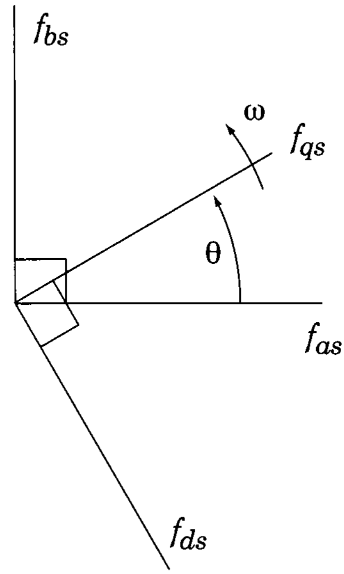

Figure 5.3-1: Transformation of stationary circuits portrayed by trigonometric relationships.

particularly appropriate for an *ab* sequence. Recall from Section 1.2 that in an *ab* sequence, the *a*-phase variables lead the *b*-phase variables by $\frac{1}{2}\pi$ for balanced steady-state conditions. However, as we just mentioned, this does not imply that the variables must be a balanced steady-state set in order for the transformation to be valid. Moreover, please be careful not to consider Fig. 5.3-1 as a phasor diagram, as one may be inclined to do. It is not; it is no more than a trigonometric relationship between f_{as}, f_{bs}, and f_{qs}, f_{ds} variables as stipulated by the transformation matrix $\mathbf{K}_s$ given by (5.3-4).

We have set forth the transformation for variables associated with stationary (stator) circuits. In a later chapter, we will set forth a transformation of rotating (rotor) circuits and we will see that it is very similar to that which we are using for stationary circuits. In fact, we will point out that we could have set forth just one transformation to a reference frame rotating at an arbitrary angular velocity, which could be used for any number of two-phase circuits each rotating at any arbitrary speed, whereupon we could consider one set of two-phase circuits as the stationary circuits by fixing its angular velocity at zero and set the angular velocity of a second set equal to the angular velocity of the rotor. Although this approach is quite elegant, it could be confusing. Therefore, stationary and rotor circuits will be treated separately.

Example 5A. Let us assume that $f_{as} = \cos\theta_e$ and $f_{bs} = \sin\theta_e$. From (5.3-1)

$$\begin{bmatrix} f_{qs} \\ f_{ds} \end{bmatrix} = \begin{bmatrix} \cos\theta & \sin\theta \\ \sin\theta & -\cos\theta \end{bmatrix} \begin{bmatrix} \cos\theta_e \\ \sin\theta_e \end{bmatrix} \tag{5A-1}$$

from which

$$f_{qs} = \cos(\theta_e - \theta) \tag{5A-2}$$

$$f_{ds} = -\sin(\theta_e - \theta) \tag{5A-3}$$

If, for example, $\theta = \omega t + \theta(0)$ and $\theta_e = \omega_e t + \theta_e(0)$, then f_{qs} and f_{ds} form a balanced two-phase set if $\omega \neq \omega_e$. If for this case, $\omega < \omega_e$, then f_{qs} leads f_{ds} by $\frac{1}{2}\pi$. If, however, $\omega > \omega_e$, f_{qs} lags f_{ds} by $\frac{1}{2}\pi$. If $\omega = \omega_e$, then f_{qs} and f_{ds} are constants; in particular,

$$f_{qs} = \cos[\theta_e(0) - \theta(0)] \tag{5A-4}$$

$$f_{ds} = -\sin[\theta_e(0) - \theta(0)] \tag{5A-5}$$

We see that if we have a balanced set, there is a reference frame where this balanced set appears as constants. If we think about all for this for just a minute, we can see that if in one reference frame a balanced set appears, then there is another reference frame in which this balanced set appears as constants and conversely.

Before leaving this example, let us assume that $\theta = 0$; then f_{qs} and f_{ds} in the stationary reference frame, (5A-2) and (5A-3), become

$$f_{qs} = \cos\theta_e \tag{5A-6}$$

$$f_{ds} = -\sin\theta_e \tag{5A-7}$$

Recall that at the beginning of this example we set $f_{as} = \cos\theta_e$ and $f_{bs} = \sin\theta_e$. It is important to note that f_{ds} in the stationary reference frame ($\omega = 0$) is the negative of f_{bs} if $\theta(0)$ is zero.

SP5.3-1 If $f_{as} = \cos\omega_e t$, $f_{bs} = \sin\omega_e t$, $f_{qs} = 1$, and $f_{ds} = 0$, determine $\theta_e(0)$, ω, and $\theta(0)$. [0, ω_e, 0]

SP5.3-2 Let $f_{as} = e^{-t}$ and $f_{bs} = 0$. Determine f_{qs} and f_{ds} in the arbitrary reference frame. $[f_{qs} = e^{-t}\cos\theta,\ f_{ds} = e^{-t}\sin\theta]$
SP5.3-3 Let $V_{as} = \cos\omega_e t$, $I_{as} = \cos\omega_e t$, $V_{bs} = \sin\omega_e t$, and $I_{bs} = \sin\omega_e t$. Determine V_{qs}, V_{ds}, I_{qs}, and I_{ds} when $\omega = \omega_e$ [(1, 0, 1, 0)].

5.4 TRANSFORMATION OF STATIONARY CIRCUIT VARIABLES TO THE ARBITRARY FRAME OF REFERENCE

In the case of a stationary resistive circuit,

$$\mathbf{v}_{abs} = \mathbf{r}_s\mathbf{i}_{abs} \tag{5.4-1}$$

where $\mathbf{r}_s$ is an equal-element diagonal matrix; the *as* and *bs* circuits have the same resistance. From (5.3-1),

$$\mathbf{v}_{qds} = \mathbf{K}_s\mathbf{v}_{abs} \tag{5.4-2}$$

Substituting (5.4-1) into (5.4-2) yields

$$\mathbf{v}_{qds} = \mathbf{K}_s\mathbf{r}_s\mathbf{i}_{abs} \tag{5.4-3}$$

Now, since $\mathbf{i}_{abs} = (\mathbf{K}_s)^{-1}\mathbf{i}_{qds}$ we can write (5.4-3) as

$$\mathbf{v}_{qds} = \mathbf{K}_s\mathbf{r}_s(\mathbf{K}_s)^{-1}\mathbf{i}_{qds} \tag{5.4-4}$$

Since $\mathbf{r}_s = r_s\mathbf{I}$,

$$\mathbf{K}_s\mathbf{r}_s(\mathbf{K}_s)^{-1} = r_s\mathbf{K}_s\mathbf{I}(\mathbf{K}_s)^{-1} = \mathbf{r}_s \tag{5.4-5}$$

Thus,

$$\mathbf{v}_{qds} = \mathbf{r}_s\mathbf{i}_{qds} \tag{5.4-6}$$

Therefore, if the phase resistances are equal, the form of the voltage equations is the same regardless of the frame of reference in which the equations are written. This, however, is not the case if the phase resistances are not equal. It is shown in Example 5B that when the phase resistances are not equal ($r_a \neq r_b$) the voltage equations, in all reference frames except the stationary frame of reference, become sinusoidal functions of the angular velocity of the reference frame. Hence, when the phase resistances are unequal it is best to analyze the circuits in the frame of reference where the asymmetry exists. In the case of the stationary asymmetric circuits, this is the stationary reference frame where the angular velocity of the reference frame is zero ($\omega = 0$).

Let us now consider a two-phase inductive circuit. In this case, the voltage equations become

$$\mathbf{v}_{abs} = p\boldsymbol{\lambda}_{abs} \tag{5.4-7}$$

For a linear magnetic system, one is tempted to express $\boldsymbol{\lambda}_{abs}$ in terms of inductances and currents; however, it is more convenient to transform flux linkages. Thus

$$\mathbf{v}_{qds} = \mathbf{K}_s p\boldsymbol{\lambda}_{abs} \tag{5.4-8}$$

In terms of qs and ds variables, (5.4-8) becomes

$$\mathbf{v}_{qds} = \mathbf{K}_s p\left[(\mathbf{K}_s)^{-1}\boldsymbol{\lambda}_{qds}\right] \tag{5.4-9}$$

using the chain rule

$$\mathbf{v}_{qds} = \mathbf{K}_s p\left[(\mathbf{K}_s)^{-1}\right]\boldsymbol{\lambda}_{qds} + \mathbf{K}_s(\mathbf{K}_s)^{-1}p[\boldsymbol{\lambda}_{qds}] \tag{5.4-10}$$

The last term on the right-hand side is, of course, $p\boldsymbol{\lambda}_{qds}$. The first term may be written as

$$\begin{aligned}\mathbf{K}_s p[(\mathbf{K}_s)^{-1}]\boldsymbol{\lambda}_{qds} &= \begin{bmatrix} \cos\theta & \sin\theta \\ \sin\theta & -\cos\theta \end{bmatrix} \omega \begin{bmatrix} -\sin\theta & \cos\theta \\ \cos\theta & \sin\theta \end{bmatrix} \begin{bmatrix} \lambda_{qs} \\ \lambda_{ds} \end{bmatrix} \\ &= \omega \begin{bmatrix} 0 & 1 \\ -1 & 0 \end{bmatrix} \begin{bmatrix} \lambda_{qs} \\ \lambda_{ds} \end{bmatrix} \end{aligned} \tag{5.4-11}$$

For a two-phase inductive circuit,

$$\mathbf{v}_{qds} = \omega \begin{bmatrix} \lambda_{ds} \\ -\lambda_{qs} \end{bmatrix} + p\boldsymbol{\lambda}_{qds} \tag{5.4-12}$$

The first term on the right-hand side is often written as $\omega\boldsymbol{\lambda}_{dqs}$. Equation (5.4-12) can be written in expanded form as

$$v_{qs} = \omega\lambda_{ds} + p\lambda_{qs} \tag{5.4-13}$$

$$v_{ds} = -\omega\lambda_{qs} + p\lambda_{ds} \tag{5.4-14}$$

For a linear magnetic system,

$$\boldsymbol{\lambda}_{abs} = \mathbf{L}_s \mathbf{i}_{abs} = \mathbf{L}_s (\mathbf{K}_s)^{-1} \mathbf{i}_{qds} \tag{5.4-15}$$

It follows that

$$\boldsymbol{\lambda}_{qds} = \mathbf{K}_s \mathbf{L}_s (\mathbf{K}_s)^{-1} \mathbf{i}_{qds} \tag{5.4-16}$$

Therefore, when $\mathbf{L}_s$ is known, for a linear magnetic system, λ_{qs} and λ_{ds} can be determined from (5.4-16) and substituted into (5.4-13) and (5.4-14).

It would appear that we have added complication to the situation since in all reference frames except the stationary reference frame, where $\omega = 0$, the voltage equations each have an additional term on the right-hand side. Let us consider the two-phase inductive circuits each having constant and equal self-inductance and without mutual coupling. In this simplistic case, $\mathbf{L}_s = diag\,[L_s,\ L_s]$. Therefore, $\mathbf{K}_s \mathbf{L}_s (\mathbf{K}_s)^{-1} = \mathbf{L}_s$ and from (5.4-16)

$$\boldsymbol{\lambda}_{qds} = \mathbf{L}_s \mathbf{i}_{qds} \tag{5.4-17}$$

and

$$v_{qs} = \omega L_s i_{ds} + L_s p i_{qs} \tag{5.4-18}$$

$$v_{ds} = -\omega L_s i_{qs} + L_s p i_{ds} \tag{5.4-19}$$

At this point, we should all be wondering why we have gone to all the trouble of a transformation since we have added a term on the right-side of the voltage equations even for $\mathbf{L}_s = diag\,[L_s,\ L_s]$. Perhaps we should give some justification for all this work. For this purpose, consider Fig. 4.6-1b, which depicts an elementary two-phase reluctance machine. We will find that the self-inductance of the *as*-winding is the same as that given by (1.7-29) and we will show, in a later chapter, that $\mathbf{L}_s$, the self-inductances of the stator windings of a two-phase reluctance machine, is

$$\mathbf{L}_s = \begin{bmatrix} L_l + L_A - L_B \cos 2\theta_r & -L_B \sin 2\theta_r \\ -L_B \sin 2\theta_r & L_l + L_A + L_B \cos 2\theta_r \end{bmatrix} \tag{5.4-20}$$

where θ_r is the rotor angular displacement. We will see (5.4-20) again in Chapter 7. Due to the salient rotor, there is a mutual coupling between the *as* and *bs* windings that is given by the off-diagonal elements in (5.4-20). It is not necessary to follow this explanation of the elements of (5.4-20); we will cover that later. The purpose here is to illustrate the facility of the change of variables. We are using the reference frame rotating at the angular velocity of the rotor. If (5.4-20) is substituted into (5.4-16) and if we set θ in $\mathbf{K}_s$

equal to θ_r and $\omega = \omega_r$ $[\theta(0) = \theta_r(0) = 0]$, it can be shown that

$$\mathbf{K}_s\mathbf{L}_s(\mathbf{K}_s)^{-1} = \begin{bmatrix} L_l + L_A - L_B & 0 \\ 0 & L_l + L_A + L_B \end{bmatrix} \tag{5.4-21}$$

whereupon

$$\lambda^r_{qs} = (L_l + L_A - L_B)i^r_{qs} \tag{5.4-22}$$

$$\lambda^r_{ds} = (L_l + L_A + L_B)i^r_{ds} \tag{5.4-23}$$

where the r superscript denotes variables in the reference frame rotating at ω_r. Obviously, the change of variables has eliminated the dependency of the inductances upon rotor position. Moreover, this transformation has decoupled the qs and ds circuits, that is, the qs and ds substitute circuits are not coupled magnetically. We will talk more about all this in a later chapter when we analyze the synchronous machine.

Although we will not find it necessary to consider capacitive elements, it is instructive to take a moment to derive the current equations in the arbitrary reference frame for capacitive elements. For this purpose, let

$$\mathbf{i}_{abs} = p\mathbf{q}_{abs} \tag{5.4-24}$$

where the charge vector is

$$(\mathbf{q}_{abs})^T = [q_{as},\ q_{bs}] \tag{5.4-25}$$

As mentioned previously, the transformation is valid for charge as well, thus

$$\mathbf{i}_{qds} = \mathbf{K}_s p\left[(\mathbf{K}_s)^{-1}\mathbf{q}_{qds}\right] \tag{5.4-26}$$

It is left to the reader to show that (5.4-26) can be written as

$$i_{qs} = \omega q_{ds} + pq_{qs} \tag{5.4-27}$$

$$i_{ds} = -\omega q_{qs} + pq_{ds} \tag{5.4-28}$$

For a linear, two-phase capacitive circuit

$$\mathbf{q}_{abs} = \mathbf{C}_s\mathbf{v}_{abs} \tag{5.4-29}$$

In the arbitrary reference

$$\mathbf{q}_{qds} = \mathbf{K}_s\mathbf{C}_s(\mathbf{K}_s)^{-1}\mathbf{v}_{qds} \tag{5.4-30}$$

It is interesting to note the analogy between (5.4-16) and (5.4-30).

There is an additional property of the transformation that should be mentioned, that is, power is invariant; it is the voltage times the current regardless of the reference frame. In as- and bs-variables,

$$P = (\mathbf{v}_{abs})^T \mathbf{i}_{abs} \tag{5.4-31}$$

Expressed in terms of qs- and ds-variables, (5.4-31) becomes

$$\begin{aligned}(\mathbf{v}_{abs})^T \mathbf{i}_{abs} &= \left[(\mathbf{K}_s)^{-1}\mathbf{v}_{qds}\right]^T (\mathbf{K}_s)^{-1}\mathbf{i}_{qds} \\ &= (\mathbf{v}_{qds})^T \left[(\mathbf{K}_s)^{-1}\right]^T (\mathbf{K}_s)^{-1}\mathbf{i}_{qds}\end{aligned} \tag{5.4-32}$$

Since $[(\mathbf{K}_s)^{-1}]^T = \mathbf{K}_s$,

$$(\mathbf{v}_{abs})^T \mathbf{i}_{abs} = (\mathbf{v}_{qds})^T \mathbf{i}_{qds} \tag{5.4-33}$$

In the case of electric machines, we will find that output power is the product of torque and rotor speed. Therefore, since power is invariant in all reference frames and since rotor speed is a scalar, the electromagnetic torque is also invariant.

Example 5B. Following (5.4-6) it was mentioned that voltage equations for a two-phase circuit were of the same form regardless of the frame of reference only if the resistances were equal. To illustrate this, let

$$\mathbf{r}_s = diag[r_a,\ r_b] \tag{5B-1}$$

where $r_a \neq r_b$. From (5.4-4),

$$\mathbf{K}_s \mathbf{r}_s (\mathbf{K}_s)^{-1} = \begin{bmatrix} \cos\theta & \sin\theta \\ \sin\theta & -\cos\theta \end{bmatrix} \begin{bmatrix} r_a & 0 \\ 0 & r_b \end{bmatrix} \begin{bmatrix} \cos\theta & \sin\theta \\ \sin\theta & -\cos\theta \end{bmatrix} \tag{5B-2}$$

After some work,

$$\begin{bmatrix} v_{qs} \\ v_{ds} \end{bmatrix} = \begin{bmatrix} \dfrac{r_a + r_b}{2} + \dfrac{r_a - r_b}{2}\cos 2\theta & \dfrac{r_a - r_b}{2}\sin 2\theta \\ \dfrac{r_a - r_b}{2}\sin 2\theta & \dfrac{r_a + r_b}{2} + \dfrac{r_a - r_b}{2}\cos 2\theta \end{bmatrix} \begin{bmatrix} i_{qs} \\ i_{ds} \end{bmatrix} \tag{5B-3}$$

It is clear from (5B-3) that we have complicated the situation beyond repair. Since $p\theta = \omega$, the sinusoidal functions in (5B-3) are time dependent. If however, $\omega = 0$ for the stationary reference frame, then the resistance matrix in (5B-3) is independent of time and if $\theta(0)$, which is the time-zero position of the reference frame, is selected to be zero, which is usually the case, then the resistance matrix becomes $diag[r_a,\ r_b]$.

SP5.4-1 If $\mathbf{r}_s = diag[r_s, r_s]$ and $\mathbf{L}_s = diag[L_s, L_s]$, determine v_{qs} and v_{ds} if $\mathbf{v}_{abs} = \mathbf{r}_s \mathbf{i}_{abs} + p\boldsymbol{\lambda}_{abs}$ and draw the equivalent qs- and ds-circuits. [$v_{qs} = r_s i_{qs} +$ right-hand side of (5.4-18); $v_{ds} = r_s i_{ds} +$ right-hand side of (5.4-19)]
SP5.4-2 If $\mathbf{L}_s = diag[L_a, L_b]$, where $L_a \neq L_b$, determine $\mathbf{K}_s \mathbf{L}_s (\mathbf{K}_s)^{-1}$. [The 2×2 matrix on the right-hand side of (5B-3) with all rs replaced by Ls]
SP5.4-3 If $\mathbf{C}_s$ is an equal-elements diagonal matrix, show that (5.4-28) may be expressed as $i_{ds} = C_s p v_{ds} - \omega C_s v_{qs}$.

5.5 TRANSFORMATION OF A BALANCED SET AND STEADY-STATE BALANCED OPERATION

A balanced two-phase set may be expressed as

$$f_{as} = \sqrt{2}\, f_s \cos \theta_{ef} \tag{5.5-1}$$

$$f_{bs} = \sqrt{2}\, f_s \sin \theta_{ef} \tag{5.5-2}$$

The above equations form an ab-sequence, balanced two-phase set where f_s may be a function of time. For steady-state conditions,

$$F_{as} = \sqrt{2}\, F_s \cos\left[\omega_e t + \theta_{ef}(0)\right] \tag{5.5-3}$$

$$F_{bs} = \sqrt{2}\, F_s \sin\left[\omega_e t + \theta_{ef}(0)\right] \tag{5.5-4}$$

where F_s, ω_e, and $\theta_{ef}(0)$ are all constants. The subscript f is used to denote the zero displacement of the voltage $[\theta_{ev}(0)]$ or current $[\theta_{ei}(0)]$. In phasor form,

$$\tilde{F}_{as} = F_s \underline{/\theta_{ef}(0)} \tag{5.5-5}$$

$$\tilde{F}_{bs} = F_s \underline{/\theta_{ef}(0) - \tfrac{1}{2}\pi} = -j\, \tilde{F}_{as} \tag{5.5-6}$$

For balanced steady-state conditions, it is unnecessary to consider both the *as* and *bs* phasors since the phasors of the two-phase set are orthogonal.

Transforming the balanced set given by (5.5-1) and (5.5-2) to the arbitrary reference frame using (5.3-1) yields

$$f_{qs} = \sqrt{2}\, f_s \cos(\theta_{ef} - \theta) \tag{5.5-7}$$

$$f_{ds} = -\sqrt{2}\, f_s \sin(\theta_{ef} - \theta) \tag{5.5-8}$$

Asynchrously Rotating Reference Frames

For steady-state conditions,

$$F_{qs} = \sqrt{2}\, F_s \cos\left[(\omega_e - \omega)t + \theta_{ef}(0) - \theta(0)\right] \tag{5.5-9}$$

$$F_{ds} = -\sqrt{2}\, F_s \sin\left[(\omega_e - \omega)t + \theta_{ef}(0) - \theta(0)\right] \tag{5.5-10}$$

where ω need not be constant. Let us consider all asynchronously rotating reference frames; that is, $\omega \neq \omega_e$. It is important to note that if $\omega \neq \omega_e$ and if $\theta(0) = 0$, then the phasors representations of (5.5-9) and (5.5-10) are

$$\tilde{F}_{qs} = F_s \underline{/\theta_{ef}(0)} = \tilde{F}_{as} \tag{5.5-11}$$

$$\tilde{F}_{ds} = F_s \underline{/\theta_{ef}(0) + \tfrac{1}{2}\pi} = j\tilde{F}_{qs} \tag{5.5-12}$$

Recall that F_{as} and F_{bs} can be obtained by rotating $\tilde{F}_{as}$ and $\tilde{F}_{bs}$ counterclockwise in the complex plane (muliplying $\tilde{F}_{as}$ by $e^{j\omega_e t}$) and taking the real component, for example, $F_{as} = Re\left(\tilde{F}_{as}e^{j\omega_e t}\right)$. Similarly, F_{qs} and F_{ds} can be obtained by multiplying $\tilde{F}_{qs}$ and $\tilde{F}_{ds}$ by $e^{j(\omega_e - \omega)t}$, which is rotation in the complex plane at $\omega_e - \omega$, and taking the real component. If $\omega < \omega_e$, $\omega_e - \omega$ is positive; hence, rotation is counterclockwise. However, if $\omega > \omega_e$, $\omega_e - \omega$ is negative, whereupon rotation is clockwise. Equations (5.5-11) and (5.5-12) hold in both cases, which implies that $\tilde{F}_{ds}$ (F_{ds}) leads $\tilde{F}_{qs}$ (F_{qs}) when rotation is counterclockwise ($\omega_e > \omega$) and lags it when rotation is clockwise ($\omega_e < \omega$).

From our work in Chapter 4, we know that applying a balanced set of currents to a symmetric set of windings produces a rotating magnetic field. Thus, it is sometimes useful to superimpose $\tilde{F}_{as}$ and $\tilde{F}_{bs}$ onto the *as* and *bs* magnetic axes of the electromechanical device. These phasors, when multiplied by $e^{j\omega_e t}$, rotate at the same speed as the resulting mmf (ω_e counterclockwise). Similarly, $\tilde{F}_{qs}$ and $\tilde{F}_{ds}$, when multiplied by $e^{j(\omega_e-\omega)t}$, rotate at $\omega_e - \omega$ relative to the qs and ds axes, which is counterclockwise when $\omega_e > \omega$ and clockwise otherwise.

Thus, in all reference frames except $\omega = \omega_e$, which is the synchronously rotating reference frame, $\tilde{F}_{qs}$ and $\tilde{F}_{as}$ are equal if $\theta(0) = 0$. Thus,

$$\tilde{V}_{qs} = \tilde{V}_{as} \tag{5.5-13}$$

$$\tilde{I}_{qs} = \tilde{I}_{as} \tag{5.5-14}$$

Therefore, the impedance in all asynchronously rotating reference frames is the same as the impedance of the real-life as and bs circuits. Although (5.5-13) and (5.5-14) tell us that this must be true, we are compelled to see this for ourselves. For this purpose, let us consider symmetrical, two-phase rL circuits.

From SP5.4-1, we know that for symmetrical two-phase rL circuits the steady-state voltage equations may be written as

$$V_{qs} = r_s I_{qs} + \omega L_s I_{ds} + L_s p I_{qs} \tag{5.5-15}$$

$$V_{ds} = r_s I_{ds} - \omega L_s I_{qs} + L_s p I_{ds} \tag{5.5-16}$$

Since $\tilde{F}_{as} = \tilde{F}_{qs}$, we need only to work with (5.5-15). The frequency of the F_{qs} and F_{ds} variables is $(\omega_e - \omega)$, and since $\tilde{I}_{ds} = j\tilde{I}_{qs}$ from (5.5-12) and I_{qs} is sinusoidal (5.5-10), we can write (5.5-15) in phasor form as

$$\tilde{V}_{qs} = r_s \tilde{I}_{qs} + j\omega L_s \tilde{I}_{qs} + jL_s(\omega_e - \omega)\tilde{I}_{qs} \tag{5.5-17}$$

which reduces to

$$\tilde{V}_{qs} = Z\,\tilde{I}_{qs} \tag{5.5-18}$$

where

$$Z = r_s + j\omega_e L_s \tag{5.5-19}$$

Synchronously Rotating Reference Frame

In the synchronous reference frame $\omega = \omega_e$ and with $\theta(0) = 0$, $\theta = \omega_e t$. For steady-state operation (5.5-9) and (5.5-10) become

$$F_{qs}^e = \sqrt{2}\,F_s \cos\theta_{ef}(0) \tag{5.5-20}$$

$$F_{ds}^e = -\sqrt{2}\,F_s \sin\theta_{ef}(0) \tag{5.5-21}$$

Here we have introduced a raised index e to signify variables in the synchronous reference frame. Later we will use a raised s (r) to denote variables in the stationary (rotor) reference frame. The as-phasor given by (5.5-5) can be written as

$$\tilde{F}_{as} = F_s \cos \theta_{ef}(0) + jF_s \sin \theta_{ef}(0) \tag{5.5-22}$$

which can be expressed in terms of F_{qs}^e and F_{ds}^e as

$$\sqrt{2}\,\tilde{F}_{as} = F_{qs}^e - jF_{ds}^e \tag{5.5-23}$$

We must be careful here; F_{qs}^e and F_{ds}^e are constants in the steady state. They are not phasors; nor do they represent sinusoidal variables. Clearly, $\tilde{F}_{as}$ is a complex number and it so happens that if $\omega = \omega_e$ and $\theta(0) = 0$, then $\tilde{F}_{as}$ can be expressed as (5.5-23). We will make use of this in later chapters.

For steady-state balanced conditions the qs- and ds-variables are constants; therefore, from (5.5-15) and (5.5-16) with $\omega = \omega_e$ and pI_{qs}^e and pI_{ds}^e both equal to zero,

$$V_{qs}^e = r_s I_{qs}^e + \omega_e L_s I_{ds}^e \tag{5.5-24}$$

$$V_{ds}^e = r_s I_{ds}^e - \omega_e L_s I_{qs}^e \tag{5.5-25}$$

Substituting (5.5-24) and (5.5-25) into (5.5-23) yields

$$\tilde{V}_{as} = \frac{1}{\sqrt{2}}(V_{qs}^e - jV_{ds}^e) = (r_s + j\omega_e L_s)\,\tilde{I}_{as} \tag{5.5-26}$$

Example 5C. Starting with the steady-state voltage equations in the synchronously rotating reference frame, derive the expression for the input impedance of each phase of a two-phase circuit where each phase consists of a resistance, r_s, in parallel with an inductance, L_s. Assume $\tilde{V}_{as} = j\tilde{V}_{bs}$ and θ in $\mathbf{K}_s^e$ is $\omega_e t$.

The steady-state voltage equations for the resistance branch from (5.4-6) are

$$V_{qs}^e = r_s I_{qs}^e \tag{5C-1}$$

$$V_{ds}^e = r_s I_{ds}^e \tag{5C-2}$$

For the inductance branch from (5.4-18) and (5.4-19),

$$V_{qs}^e = \omega_e L_s I_{ds}^e \tag{5C-3}$$

$$V_{ds}^e = -\omega_e L_s I_{qs}^e \tag{5C-4}$$

The total qs^e current, $I_{qs(T)}^e$, can be obtained from (5C-1) and (5C-4):

$$I_{qs(T)}^e = \frac{V_{qs}^e}{r_s} - \frac{V_{ds}^e}{\omega_e L_s} \tag{5C-5}$$

The total ds^e current is

$$I_{ds(T)}^e = \frac{V_{ds}^e}{r_s} + \frac{V_{qs}^e}{\omega_e L_s} \tag{5C-6}$$

Now from (5.5-23) since $\theta(0) = 0$,

$$\begin{aligned}\sqrt{2}\,\tilde{I}_{as} &= I_{qs(T)}^e - jI_{ds(T)}^e \\ &= \frac{V_{qs}^e}{r_s} - \frac{V_{ds}^e}{\omega_e L_s} - j\frac{V_{ds}^e}{r_s} - j\frac{V_{qs}^e}{\omega_e L_s}\end{aligned} \tag{5C-7}$$

Let us rearrange (5C-7) as

$$\sqrt{2}\,\tilde{I}_{as} = \frac{1}{r_s}(V_{qs}^e - jV_{ds}^e) - \frac{1}{\omega_e L_s}(V_{ds}^e + jV_{qs}^e) \tag{5C-8}$$

Using (5.5-23), we can write (5C-8) as

$$\tilde{I}_{as} = \left(\frac{1}{r_s} - \frac{j}{\omega_e L_s}\right)\tilde{V}_{as} \tag{5C-9}$$

which can be written as

$$\begin{aligned}\tilde{V}_{as} &= \left(\frac{j\,r_s\omega_e L_s}{r_s + j\omega_e L_s}\right)\tilde{I}_{as} \\ &= Z_p\tilde{I}_{as}\end{aligned} \tag{5C-10}$$

where Z_p is the phase impedance of the parallel rL-circuit.

SP5.5-1 If $\tilde{V}_{as} = r_s\tilde{I}_{as}$ and $\tilde{F}_{as} = j\tilde{F}_{bs}$, express (a) $\tilde{V}_{qs}$, (b) $\tilde{V}_{ds}$, (c) V_{qs}^e, and (d) V_{ds}^e. Are there any restrictions on your answers? [(a) $\tilde{V}_{qs} = r_s\tilde{I}_{qs}$; (b) $\tilde{V}_{ds} = r_s\tilde{I}_{ds}$; if $\omega \neq \omega_e$ and $\theta(0) = 0$; (c) $V_{qs}^e = r_s I_{qs}^e$; (d) $V_{ds}^e = r_s I_{ds}^e$; if $\omega = \omega_e$ and $\theta(0) = 0$]

SP5.5-2 Express F_{qs}^e and F_{ds}^e for balanced steady-state conditions if $\theta(0) = \frac{1}{2}\pi$. [$F_{qs}^e = \sqrt{2}F_s\cos(\theta_{ef}(0) - \frac{1}{2}\pi)$, $F_{ds}^e = -\sqrt{2}F_s\sin(\theta_{ef}(0) - \frac{1}{2}\pi)$]

SP5.5-3 Express $\tilde{F}_{as}$ in terms of F_{qs}^e and F_{ds}^e in SP5.5-2. [$\sqrt{2}\tilde{F}_{as} = -F_{ds}^e + jF_{qs}^e$]

5.6 VARIABLES OBSERVED FROM SEVERAL FRAMES OF REFERENCE

It is instructive to observe the waveform of the variables of a stationary, two-phase, series rL circuit in the arbitrary reference frame and in commonly used reference frames. For this purpose, we will assume that both r_s and L_s are diagonal matrices each with equal nonzero elements and the applied voltages are of the form

$$v_{as} = \sqrt{2}V_s \cos \omega_e t \tag{5.6-1}$$

$$v_{bs} = \sqrt{2}V_s \sin \omega_e t \tag{5.6-2}$$

where ω_e is an unspecified constant and $\theta_{ev}(0) = 0$. The currents, which are assumed to be zero at $t = 0$, may be expressed as

$$i_{as} = \frac{\sqrt{2}V_s}{|Z_s|}[-e^{-t/\tau} \cos \alpha + \cos(\omega_e t - \alpha)] \tag{5.6-3}$$

$$i_{bs} = \frac{\sqrt{2}V_s}{|Z_s|}\left[-e^{-t/\tau} \sin \alpha + \sin(\omega_e t - \alpha)\right] \tag{5.6-4}$$

where

$$Z_s = r_s + j\omega_e L_s \tag{5.6-5}$$

$$\tau = \frac{L_s}{r_s} \tag{5.6-6}$$

$$\alpha = \tan^{-1} \frac{\omega_e L_s}{r_s} \tag{5.6-7}$$

It may at first appear necessary to solve the voltage equations in the arbitrary reference frame in order to obtain the expression for the currents in the arbitrary reference frame. This is unnecessary since once the solution is known in one reference frame it is known in all reference frames. In the example at hand, this may be accomplished by transforming (5.6-3) and (5.6-4) to the arbitrary reference frame. For illustrative purposes, let ω be an unspecified constant with $\theta(0) = 0$, then $\theta = \omega t$ and, in the arbitrary reference frame,

$$i_{qs} = \frac{\sqrt{2}V_s}{|Z_s|}\{-e^{-t/\tau}\cos(\omega t - \alpha) + \cos[(\omega_e - \omega)t - \alpha]\} \tag{5.6-8}$$

$$i_{ds} = \frac{\sqrt{2}V_s}{|Z_s|}\{e^{-t/\tau}\sin(\omega t - \alpha) - \sin[(\omega_e - \omega)t - \alpha]\} \tag{5.6-9}$$

Clearly, the state of the electric system is independent of the frame of reference from which it is observed. Although the variables will appear differently in each reference frame, they will exhibit the same mode of operation (transient or steady state) regardless of the reference frame. In general, (5.6-8) and (5.6-9) contain two balanced sets. One, which represents the electric transient, decays exponentially at a frequency corresponding to the instantaneous angular velocity of the arbitrary reference frame. In this set, the qs variable leads the ds variable by 90° when $\omega > 0$, and lags by 90° when $\omega < 0$. The second balanced set, which represents the steady-state response, has a constant amplitude with a frequency corresponding to the difference in the angular velocity of the voltages applied to the stationary circuits and the angular velocity of the arbitrary reference frame. In this set, the qs-variable lags the ds-variables by 90° when $\omega < \omega_e$ and leads by 90° when $\omega > \omega_e$. This, of course, leads to the concept of negative frequency, previously mentioned, when relating phasors that represent qs- and ds-variables by (5.5-12).

There are two frames of reference that do not contain both balanced sets. In the stationary reference frame, $\omega = 0$ and $i_{qs} = i_{as}$. The exponentially decaying balanced set becomes an exponential decay and the constant-amplitude balanced set varies at ω_e. In the synchronously rotating reference frame where $\omega = \omega_e$, the electric transients are represented by an exponentially decaying balanced set varying at ω_e and the constant-amplitude balanced set is represented by constants.

The waveforms of the system variables in various reference frames are shown in Figs. 5.6-1 through 5.6-3. The voltages of the form given by (5.6-1) and (5.6-2) are applied to the two-phase system with $V_s = 10/\sqrt{2}$ V, $r_s = 0.216\ \Omega$, and $\omega_e L_s = 1.09\ \Omega$ with $\omega_e = 377$ rad/s. The response, for $t > 0$, of the electric system in the stationary reference frame is shown in Fig. 5.6-1. Since we have selected $\theta(0) = 0$, $f_{as} = f_{qs}^s$ and the plots of v_{qs}^s and i_{qs}^s are v_{as} and i_{as}, respectively. Note that we are using a raised s to denote qs- and ds-variables in the stationary reference frame. The variables for the same mode of operation are shown in the synchronously rotating reference frame in Fig. 5.6-2. Note from (5.6-1) and (5.6-3) that we have selected the time-zero position of the two-phase voltages to be zero; that is, $\theta_{ev}(0) = 0$; thus, from (5.5-7) and (5.5-8) with $\theta(0) = 0$, $v_{qs}^e = 10$ V and $v_{ds}^e = 0$. As mentioned previously, we are using the raised e to denote variables in the synchronously rotating reference frame. In Fig. 5.6-3 with $\theta(0) = 0$, the speed of the reference frame is switched from its original value of –377 rad/s to zero and then to 377 rad/s.

There are several features worthy of note. The waveform of the instantaneous electric power is the same in all cases. The electric transient is very evident in the waveforms of the instantaneous electric power and the currents in the synchronously rotating reference frame (Fig. 5.6-2), and since v_{ds}^e is zero, i_{qs}^e is related to the power by a constant (v_{qs}^e). In Fig. 5.6-3, we selected $\theta_{ev}(0) = 0$ and $\theta(0) = 0$. The voltages were applied and we observed the solution of the differential equations in the reference frame rotating clockwise at ω_e ($\omega = -\omega_e$). The reference-frame speed was then stepped from –377 rad/s to zero, whereupon the differential equations were solved in the stationary reference frame. However, when switching from one reference frame to another, the variables must be continuous. Therefore, after the switching occurs the solution continues using the stationary reference frame differential equations with the initial values determined by the instantaneous values of the variables in the previous reference frame ($\omega = -\omega_e$) at the time of switching. When the reference frame speed is switched to synchronous speed, the variables have reached steady state; therefore, they will be constant corresponding to their values at the instant ω is switched to ω_e. In essence, we have applied a balanced two-phase set of voltages to a symmetrical rL circuit, and in Fig. 5.6-3 we observed the actual variables from various reference frames by "jumping" from one reference frame to another.

SP5.6-1 In Fig. 5.6-1, qs^s- and ds^s-variables are plotted. Relabel the traces so that the traces are for as- and bs-variables. [$v_{qs}^s = v_{as}$, $i_{qs}^s = i_{as}$, $v_{ds}^s = -v_{bs}$, $i_{ds}^s = -i_{bs}$, power unchanged]

SP5.6-2 What restriction is associated with the plots in Fig. 5.6-2 other than $\omega = \omega_e$. [$\theta(0) = 0$]

SP5.6-3 Why is $v_{ds}^e = 0$ in Fig. 5.6-2? [$\theta_{ev}(0) = 0$, $\theta(0) = 0$]

SP5.6-4 There is a comparison between the plots in Fig. 5.6-1 and Fig. 5.6-3 when $\omega = 0$ in Fig. 5.6-3. Why isn't there a comparison between Fig. 5.6-2 and $\omega = \omega_e$ in Fig. 5.6-3? We selected $\theta_{ev}(0)$ and $\theta(0)$ as zero in both cases. [In Fig.5.6-1 we entered the synchronous reference frame at

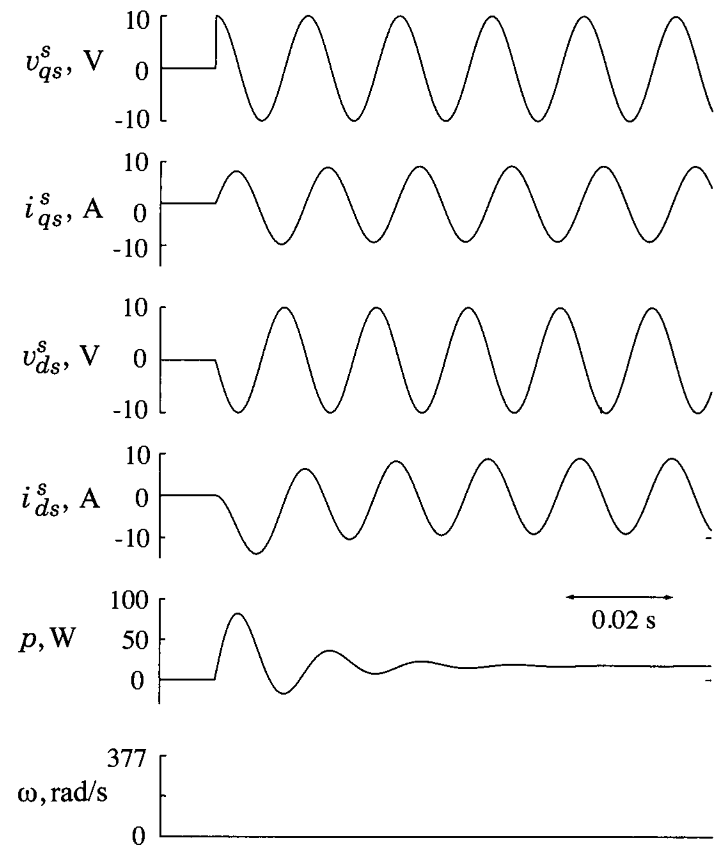

Figure 5.6-1: Variables of a stationary two-phase system in the stationary reference frame.

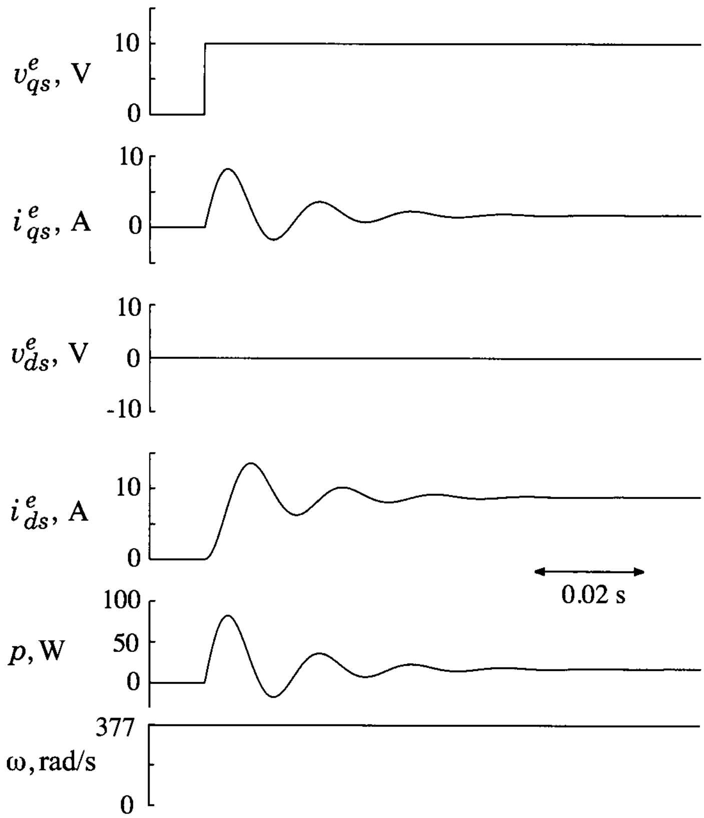

Figure 5.6-2: Variables of a stationary two-phase system in the synchronous reference frame.

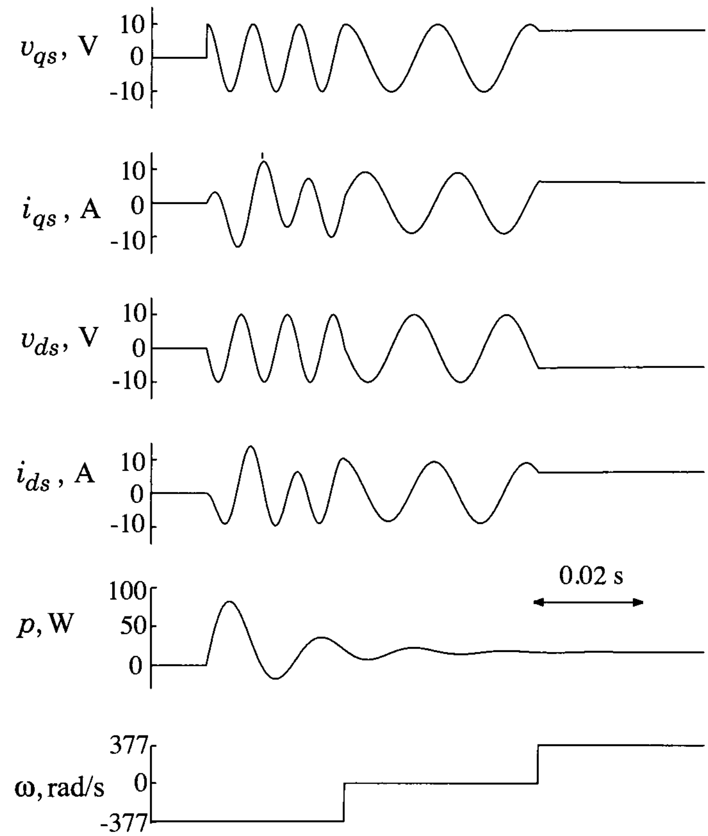

Figure 5.6-3: Variables of a stationary two-phase system. First $\omega = -\omega_e$, then ω is stepped to zero followed by a step change in reference frame speed to $\omega = \omega_e$.

$t = 0$ when v_{as} was maximum. In Fig. 5.6-3, we had to accept the values of the qs^e- and ds^e-variables at the instant we switched into the synchronously rotating reference frame ($\omega = \omega_e$).]

5.7 EQUATIONS OF TRANSFORMATION FOR THREE-PHASE SYSTEMS

Although we will not consider the transformation of a three-phase set of variables in detail, it is interesting to introduce this transformation for the purpose of comparing with the transformation we have used for a two-phase system. A change of variables that formulates a transformation of the three-phase variables of stationary circuit elements to the arbitrary reference frame may be expressed as

$$\mathbf{f}_{qd0s} = \mathbf{K}_s \mathbf{f}_{abcs} \tag{5.7-1}$$

where, for an abc-sequence (Appendix C),

$$(\mathbf{f}_{qd0s})^T = [f_{qs} \quad f_{ds} \quad f_{0s}] \tag{5.7-2}$$

$$(\mathbf{f}_{abcs})^T = [f_{as} \quad f_{bs} \quad f_{cs}] \tag{5.7-3}$$

$$\mathbf{K}_s = \frac{2}{3} \begin{bmatrix} \cos\theta & \cos(\theta - \frac{2}{3}\pi) & \cos(\theta + \frac{2}{3}\pi) \\ \sin\theta & \sin(\theta - \frac{2}{3}\pi) & \sin(\theta + \frac{2}{3}\pi) \\ \frac{1}{2} & \frac{1}{2} & \frac{1}{2} \end{bmatrix} \tag{5.7-4}$$

$$\frac{d\theta}{dt} = \omega \tag{5.7-5}$$

It can be shown that for the inverse transformation we have

$$(\mathbf{K}_s)^{-1} = \begin{bmatrix} \cos\theta & \sin\theta & 1 \\ \cos(\theta - \frac{2}{3}\pi) & \sin(\theta - \frac{2}{3}\pi) & 1 \\ \cos(\theta + \frac{2}{3}\pi) & \sin(\theta + \frac{2}{3}\pi) & 1 \end{bmatrix} \tag{5.7-6}$$

Since there are three variables, f_{as}, f_{bs}, and f_{cs}, we need three substitute variables f_{qs}, f_{ds}, and f_{0s}. It is important to note that the f_{0s} variables are independent of the angular displacement or angular velocity of the arbitrary reference frame. Let us assume that

$$v_{as} = r_s i_{as} + p\lambda_{as} \tag{5.7-7}$$

$$v_{bs} = r_s i_{bs} + p\lambda_{bs} \tag{5.7-8}$$

$$v_{cs} = r_s i_{cs} + p\lambda_{cs} \tag{5.7-9}$$

If (5.7-7) through (5.7-9) are transformed to the arbitrary reference frame, we obtain

$$v_{qs} = r_s i_{qs} + \omega\lambda_{ds} + p\lambda_{qs} \tag{5.7-10}$$

$$v_{ds} = r_s i_{ds} - \omega\lambda_{qs} + p\lambda_{ds} \tag{5.7-11}$$

$$v_{0s} = r_s i_{0s} + p\lambda_{0s} \tag{5.7-12}$$

Although the $0s$-voltage equation has been added, the v_{qs} and v_{ds} equations are identical in form to those for the two-phase systems.

The $0s$-variables are zero for a balanced three-phase system. Also, three-phase electric machines are often connection in wye (Y) without a neutral conductor. In this case, the fundamental phase currents sum to zero. If i_{0s} is zero, then v_{0s} is zero.

Let us consider a balanced, abc-sequence three-phase set of variables:

$$f_{as} = \sqrt{2} f_s \cos\theta_{ef} \tag{5.7-13}$$

$$f_{bs} = \sqrt{2} f_s \cos(\theta_{ef} - \tfrac{2}{3}\pi) \tag{5.7-14}$$

$$f_{cs} = \sqrt{2} f_s \cos(\theta_{ef} - \tfrac{2}{3}\pi) \tag{5.7-15}$$

Using (5.7-1) to transform to the arbitrary reference frame yields

$$f_{qs} = \sqrt{2}\, f_s \cos(\theta_{ef} - \theta) \tag{5.7-16}$$

$$f_{ds} = -\sqrt{2}\, f_s \sin(\theta_e - \theta) \tag{5.7-17}$$

$$f_{0s} = 0 \tag{5.7-18}$$

Please note that if f_{0s} is zero, the three-phase system becomes a two-phase system and (5.7-16) and (5.7-17) are (5.5-7) and (5.5-8), respectively. Therefore, the material in Section 5.5 and 5.6 also applies for a balanced three-phase system.

SP5.7-1 If a three-phase system had the same elements as the two-phase system in Section 5.6 and if balanced three-phase voltages are applied, the voltages and currents of all figures would be the same for the three-phase system. Why? [(5.5-7) = (5.7-16) and (5.5-8) = (5.7-17)]

SP5.7-2 A three-wire, three-phase system is magnetically linear. Do (5.7-16) through (5.7-18) apply if the applied voltages are unbalanced? [Only (5.7-18)]

SP5.7-3 In SP5.7-1, it was shown that the voltages and currents in the figures in Section 5.6 can apply to a balanced three-phase system. However, the trace of power in the figures in Section 5.6 must be multiplied by $\frac{3}{2}$. Why? [Three-phase power is being calculated with two-phase variables]

5.8 RECAPPING

Reference frame theory is indeed a different approach to circuit analysis than that taught in basic circuit courses. Nevertheless, it is convenient if not necessary in order to analyze ac electric machines and ac electric-drive systems. Although this chapter has been only a brief introduction to the concept of reference-frame theory, it sets the stage for the analysis to come. If we have been successful, the reader will be comfortable with the use of reference-frame theory in the coming chapters and, in fact, able to foresee the applications and advantages of reference-frame theory as the analysis tool of choice. We will make frequent use of material in this chapter and, hopefully, the reader will find this chapter a convenient and easily accessible reference.

The focus has been and will continue to be on two-phase systems. This allows the concept and advantage of reference-frame theory to be presented concisely without the cumbersome trigonometry inherent to three-phase systems. Those who have studied Section 5.7 on three-phase systems realize that the extension of reference-frame theory from the two-phase to the three-phase system is direct.

5.9 REFERENCES

[1] R. H. Park, "Two-Reaction Theory of Synchronous Machines – Generalized Method of Analysis – Part I," *AIEE Trans.*, Vol. 48, July 1929, pp. 716-727.

[2] H. C. Stanley, "An Analysis of the Induction Motor," *AIEE Trans.*, Vol. 57 (Supplement), 1938, pp. 751-755.

[3] G. Kron, Equivalent Circuits of Electric Machinery, John Wiley and Sons, Inc., New York, N.Y., 1951.

[4] D. S. Brereton, D. G. Lewis, and C. G. Young, "Representation of Induction Motor Loads During Power System Stability Studies," *AIEE Trans.*,Vol. 76, August 1957, pp. 451-461.

[5] P. C. Krause and C. H. Thomas, "Simulation of Symmetrical Induction Machinery," *IEEE Trans. Power Apparatus and Systems*, Vol.84, November 1965, pp. 1038-1053.

[6] P. C. Krause, F. Norari, T. L. Skvarenina, and D. W. Olive, "The Theory of Neglecting Stator Transients," *IEEE Trans. Power Apparatus and Systems*, Vol. 98, January/February 1979, pp. 141-148.

5.10 PROBLEMS

1. If $f_{as} = \cos \omega_e t$ and $f_{bs} = -\sin \omega_e t$, (a) express the relationships between $\tilde{F}_{as}$ and $\tilde{F}_{bs}$; (b) obtain f^e_{qs} and f^e_{ds} using (5.3-1) with $\theta(0) = 0$; (c) devise a transformation $\mathbf{T}(\theta)$ so that $f^e_{qs} = 1$ and $f^e_{ds} = 0$, where $\theta(0) = 0$.

2. If $\mathbf{f}^a_{qds}$ are the as- and bs-variables expressed in the a-reference frame, and $\mathbf{f}^b_{qds}$ are the as- and bs-variables expressed in the b-reference frame, determine ${}^a\mathbf{K}^b$ in terms of $\mathbf{K}^a_s$ and $\mathbf{K}^b_s$, where

$$\mathbf{f}^b_{qds} = {}^a\mathbf{K}^b \mathbf{f}^a_{qds}$$

3. Repeat Example 5C using the asynchronously rotating reference frame. Let $\theta(0) = 0$.

4. Repeat Example 5C for a two-phase parallel rC-circuit.

5. Assume that the as and bs phases are each series connected r_s and L_s. Let $V_{as} = \sqrt{2}\, V_s \cos \omega_e t$ and $V_{bs} = \sqrt{2}\, V_s \sin \omega_e t$. With $\theta(0) = 0$, express V^e_{qs} in terms of r_s, L_s, ω_e, and I^e_{qs}.

6. Assume a two-phase system with $\mathbf{r}_s$ and $\mathbf{L}_s$ equal-elements diagonal matrices. $v_{as} = \sqrt{2}V_s \cos\theta_{esv}$ and $v_{bs} = \sqrt{2}\,V_s \sin\theta_{esv}$, where $\theta_{esv} = \omega_e t + \theta_{esv}(0)$. Construct the qs^e and ds^e equivalent circuits where $\theta = \omega_e t + \theta(0)$ in $\mathbf{K}_s^e$. It is desirable to investigate variable-frequency operation. Thus, ω_e is a function of time. (a) What changes are necessary in the qs^e and ds^e equivalent circuits? (b) Are the equivalent circuits valid for $\omega_e = 0$?

7. Assume $f_{as} = 1$ and $f_{bs} = 1$. Determine θ in $\mathbf{K}_s$, where these constants will appear as a balanced two-phase set. Let $\theta(0) = 0$ and express v_{qs} and v_{ds} in this reference frame.

Electromechanical Motion Devices, Second Edition
by Paul Krause, Oleg Wasynczuk and Steven Pekarek

Chapter 6

SYMMETRICAL INDUCTION MACHINES

6.1 INTRODUCTION

Although the induction machine is used most often as a means to convert electric power to mechanical work, it can operate as either a motor or a generator. Three-phase induction motors are commonly used in large-horsepower applications. Pump drives, steel-mill drives, hoist drives, and vehicle drives are examples. On a smaller scale, the two- and three-phase induction motors are used extensively as control motors in low-power applications. They are also used as generators in wind turbine and low-head hydro applications. Single-phase induction motors, which develop torque in a manner similar to the multiphase induction motor, are used in many household appliances.

In order to conduct a rigorous analysis of an induction machine, it is necessary to perform a change of variables (transformation) that eliminates the position-varying mutual inductances that occur due to windings in relative motion, as witnessed in Section 1.7. We will show that there are numerous transformations that can be used in the case of the symmetrical induction machine to accomplish this goal. This analysis is somewhat involved; however, the resulting steady-state, single-phase equivalent circuit is similar to that of a transformer with one winding short-circuited.

The analysis of symmetrical two- and three-phase induction machines is essentially the same. Therefore, we will focus our attention on the two-phase machine, since this enables us to become familiar with the theory and performance of induction machines without becoming inundated with trigonometric manipulations. Once the theory has been established, induction-motor performance during balanced operation is illustrated by computer traces. The three-phase induction machine is treated in the last section of this chapter; single-phase and unbalanced operations of the two-phase symmetrical induction machine are covered in a later chapter.

6.2 TWO-PHASE INDUCTION MACHINE

A two-pole, two-phase induction machine is shown in Fig. 6.2-1. It is assumed that the stator windings may be portrayed by orthogonal, sinusoidally distributed windings as described in Chapter 4. It is convenient to assume that the rotor of the two-pole, two-phase induction machine may also be portrayed electrically by two sinusoidally distributed windings displaced 90°. We will talk about forged and squirrel cage rotors of induction motors later. Hence, for our present purposes, we will consider that the *ar* and *br* windings are sinusoidally distributed, each with the same total winding resistance. Thus, both the stator and rotor are symmetrical. For this reason, this device is often referred to as a *symmetrical induction machine.*

Note that the air gap distance between the stator and rotor is uniform. Also, the rotor windings of an induction machine are generally short-circuited ($v_{ar} = v_{br} = 0$). Most often, only the stator windings are connected to a source, whereupon the induction machine is said to be single-fed. In some special applications, such as wind turbines, both the rotor and stator windings are connected to sources, whereupon the induction machine is said to be double-fed. In this case, the rotor windings are connected to a stationary multiphase source by a brush and slip-ring arrangement. The slip ring is a solid copper ring and is not segmented as a commutator in a dc machine.

As established in Chapter 4, the angular displacement about the stator is denoted ϕ_s, and it is referenced to the *as* axis. We see from Fig. 6.2-1 that the angular displacement about the rotor is denoted ϕ_r and it is referenced to the *ar* axis. The angular velocity of the rotor is ω_r and θ_r is its angular displacement. In particular, θ_r is the angular displacement between the *ar* and *as* axes. Thus, a given point on the rotor surface at the angular position ϕ_r may be related to an adjacent point on the inside stator surface with the angular position ϕ_s as

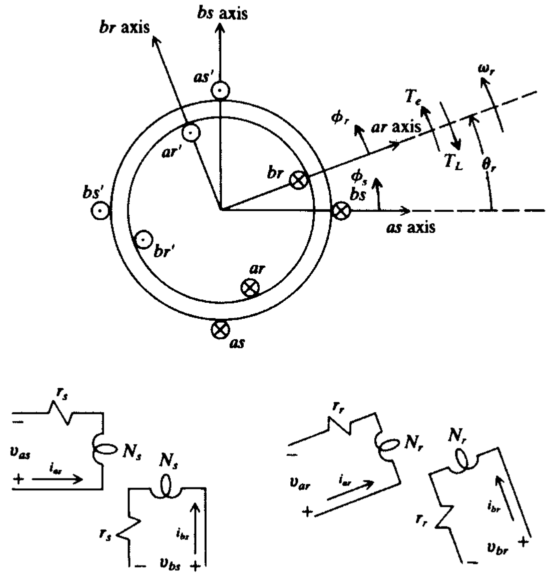

Figure 6.2-1: A two-pole, two-phase, symmetrical induction machine.

$$\phi_s = \phi_r + \theta_r \tag{6.2-1}$$

The electromechanical torque T_e and the load torque T_L are also indicated in Fig. 6.2-1. We are aware from Chapter 2 that T_e is assumed to be positive in the direction of increasing θ_r, whereas the load torque is positive in the opposite direction (opposing rotation).

The air-gap mmfs due to the *as* and *bs* windings are given by (4.3-4) and (4.3-5). From our work in Chapter 4, we are able to write the air-gap mmfs for the *ar* and *br* windings by inspection. In particular,

$$\text{mmf}_{ar} = \frac{N_r}{2} i_{ar} \cos \phi_r \tag{6.2-2}$$

$$\text{mmf}_{br} = \frac{N_r}{2} i_{br} \sin \phi_r \tag{6.2-3}$$

where N_r is the equivalent number of turns of the rotor windings.

In Chapter 4, we established that balanced two-phase currents flowing in the stator windings of a two-pole device produced a constant-amplitude rotating air-gap mmf_s during steady-state balanced operation (4.4-11). Two rotating poles are established as a result of this rotating air-gap mmf (mmf_s), and this magnetic system rotates about the air gap at the angular velocity ω_e of the stator currents. Let us consider the air-gap mmf established by the rotor currents. During balanced steady-state operation, the rotor speed is constant and the stator currents may be expressed by (4.4-8) and (4.4-9). For now, let us assume that the rotor currents may be expressed as

$$I_{ar} = \sqrt{2}\, I_r \cos[(\omega_e - \omega_r)t + \theta_{eri}(0)] \tag{6.2-4}$$

$$I_{br} = \sqrt{2}\, I_r \sin[(\omega_e - \omega_r)t + \theta_{eri}(0)] \tag{6.2-5}$$

Once time zero is selected, $\theta_{esi}(0)$ and $\theta_{eri}(0)$ are determined from the instantaneous values of the stator and rotor currents, respectively, at the assigned time zero. One wonders why the frequency of the rotor currents is the difference of the angular velocity ω_e of the stator currents and the angular velocity ω_r of the rotor. We will find that this must be the frequency of the rotor currents during balanced steady-state operation, regardless of whether the rotor circuits are short-circuited and only the stator windings are connected to a source (single-fed), or whether both the stator and rotor windings are connected to sources (double-fed).

An expression for the air-gap mmf due to the rotor currents is obtained by substituting (6.2-4) into (6.2-2) and (6.2-5) into (6.2-3), and adding the resulting expressions. Thus,

$$\begin{aligned} \text{mmf}_r &= \text{mmf}_{ar} + \text{mmf}_{br} \\ &= \frac{N_r}{2}\sqrt{2}\, I_r \cos[(\omega_e - \omega_r)t + \theta_{eri}(0) - \phi_r] \end{aligned} \tag{6.2-6}$$

Setting the argument equal to a constant and taking the derivative with respect to time yields

$$\frac{d\phi_r}{dt} = \omega_e - \omega_r \tag{6.2-7}$$

Here, mmf_r rotates relative to the rotor at $\omega_e - \omega_r$, and, if $\omega_e - \omega_r > 0$, the direction of rotation is counterclockwise relative to the rotor. Before proceeding, let us note the position of the poles. For purpose of this explanation, let $\theta_{esi}(0)$ and $\theta_{eri}(0)$ both be zero. Thus, at $t = 0$, mmf_r is the cosine of ϕ_r positioned about the *ar* axis. Flux due to mmf_r leaves the rotor and enters the air gap for $-\frac{1}{2}\pi < \phi_r < \frac{1}{2}\pi$, a north pole ($N^r$), and enters the rotor from the air gap for $\frac{1}{2}\pi < \phi_r < \frac{3}{2}\pi$, a south pole ($S^r$). Make sure you are aware of the location of N^s and S^s for this condition. Thus, we have a set of poles established by the stator mmf$_s$ that rotates at ω_e relative to the stator and another set of poles established by the rotor mmf$_r$ that rotates at $\omega_e - \omega_r$ relative to the rotor. If the stator poles and the rotor poles were to rotate at the same angular velocity about the air gap, the stage would be set for producing a constant electromagnetic torque due to the force exerted between the two magnetic systems rotating at the same angular velocity. Is it true that the two sets of poles rotate at the same angular velocity? To answer this question, we can relate a displacement on the rotor, ϕ_r, to a displacement on the stator, ϕ_s, by (6.2-1). Taking the derivative of (6.2-1) with respect to time yields

$$\frac{d\phi_s}{dt} = \frac{d\phi_r}{dt} + \frac{d\theta_r}{dt} \tag{6.2-8}$$

Now, (6.2-7) tells us that $d\phi_r/dt = \omega_e - \omega_r$ and we know that $d\theta_r/dt = \omega_r$; thus,

$$\frac{d\phi_s}{dt} = \omega_e - \omega_r + \omega_r = \omega_e \tag{6.2-9}$$

In other words, the air-gap mmf established by currents flowing in the rotor, mmf$_r$, rotates about the air gap at ω_e if observed from the stator. Hence, to a stationary observer, both the stator and rotor poles rotate about the air gap at ω_e. This, of course, makes sense from another point of view, The mmf$_r$ is rotating at $\omega_e - \omega_r$ relative to the rotor; that is, if we were riding on the rotor that is moving at ω_r, we would observe mmf$_r$ rotating at $\omega_e - \omega_r$ relative to us on the rotor. If we now jump off the rotor and look at mmf$_r$ as a stationary observer, we would see the rotor rotating at ω_r and mmf$_r$ rotating relative to the rotor at $\omega_e - \omega_r$; hence, $\omega_r + (\omega_e - \omega_r) = \omega_e$. While you were on the rotor, did you look at mmf$_s$? If so, at what speed was it rotating relative to you? ($\omega_e - \omega_r$.)

With mmf$_s$ and mmf$_r$ rotating at the same angular velocity, an average steady-state electromagnetic torque can be produced. This is not the case if they rotate at different angular velocities. How did we cause the angular velocities to be equal? We assumed that the frequency of the steady-state rotor currents was $\omega_e - \omega_r$, and we said that this had to be the case regardless whether the machine was single- or double-fed. Now we see why. We have also said that the induction machine is most often operated with the rotor windings short-circuited. Hence, currents are induced in the rotor circuits (thus the name *induction motor)* by the flux established by mmf$_s$. However, to induce a current in the rotor circuits, the rotor must rotate at a speed different from that of mmf_s in order for the rotor circuits to experience a change of flux.

We have said that an electromagnetic torque is exerted on the shaft because of the interaction of the poles established by stator currents and the poles established by the rotor currents. If the rotor currents are not present, then a torque does not exist. Thus, the induction motor has the capability of developing an average, steady-state electromagnetic torque at any rotor speed except when $\omega_r = \omega_e$. In other words, when the rotor is rotating in synchronism with the rotating magnetic field produced by the stator currents (mmf_s), rotor currents are not induced and, hence, an electromagnetic torque cannot be developed. We will find that this device with short-circuited rotor windings operates as a motor when $\omega_r < \omega_e$, and as a generator when the rotor is driven above ω_e by a torque input to the shaft.

One may, at first, choose to call this device a four-pole rather than a two-pole device since two poles are established by the stator currents and two poles are established by the rotor currents. We must realize, however, that even though we have considered the stator and rotor air-gap mmf separately, they combine to form one resultant two-pole magnetic system.

A cutaway of a four-pole, three-phase, 7.5-hp, 460-V, squirrel-cage induction motor is shown in Fig. 6.2-2. It is an enclosed, fan-cooled, severe-duty motor for use in the chemical, paper, cement, and mining industries. A disassembled four-pole, two-phase, $\frac{1}{10}$-hp, 115-V, induction motor, which is used in low-power control applications, is shown in Fig. 6.2-3. Also shown in Fig. 6.2-3 is the case that houses the speed-reduction gears.

SP6.2-1 Assume sinusoidally distributed windings on the stator and rotor of the machine shown in Fig. 6.2-1. Express (*a*) mmf_{as} in terms of θ_r and ϕ_r and (*b*) mmf_{ar} in terms of θ_r and ϕ_s. [(*a*) $\text{mmf}_{as} = (N_s/2)i_{as}\cos(\phi_r + \theta_r)$; (*b*) $\text{mmf}_{ar} = (N_r/2)i_{ar}\cos(\phi_s - \theta_r)$]

SP6.2-2 The frequency of the balanced stator currents of an induction machine is 60 Hz and mmf_s rotates counterclockwise. The device is operating as a motor, and the rotor of the two-pole machine is rotating counterclockwise at $0.9\omega_e$. (*a*) Determine the frequency of the balanced rotor currents. Determine the angular velocity of mmf_s and mmf_r relative to an observer sitting (*b*) on the rotor and (*c*) on the stator. [(*a*) 6 Hz; (*b*) 37.7 rad/s, ccw; (*c*) 377 rad/s, ccw]

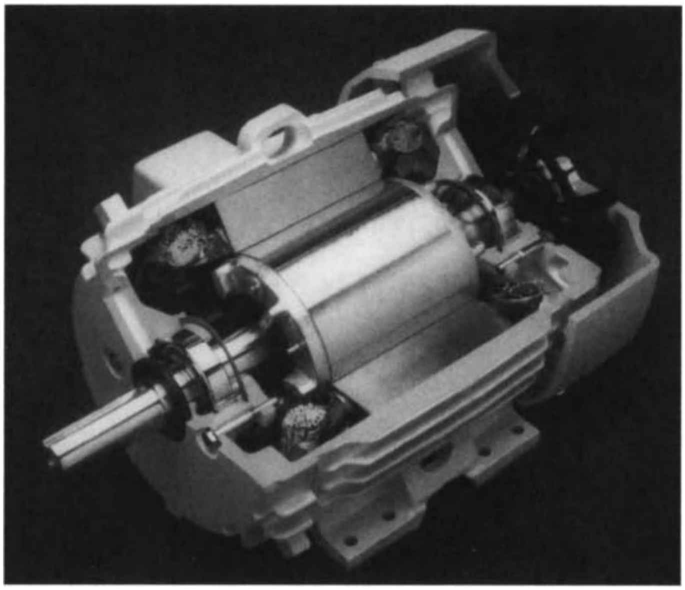

Figure 6.2-2: Four-pole, three-phase, 6.5-Hp, 460-V, severe-duty, squirrel-cage induction motor (courtesy of General Electric).

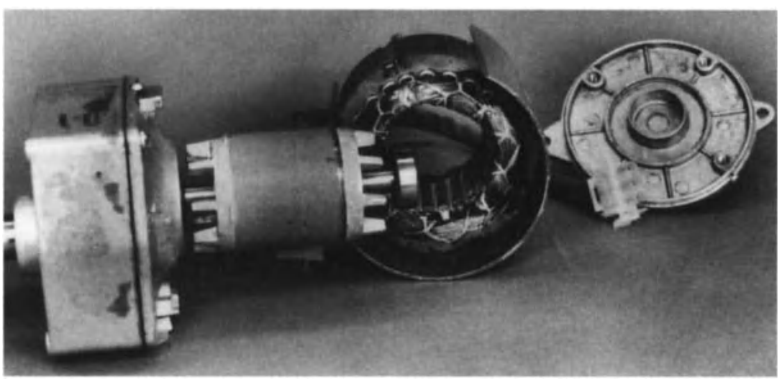

Figure 6.2-3: Four-pole, two-phase, 1/10-Hp, 115-V induction motor with reduction gear.

SP6.2-3 Repeat SP6.2-2 for a six-pole induction machine operating as a generator being driven at $\omega_r = 1.1\omega_e$. [(*a*) 6 Hz; (*b*) 37.7/3 rad/s, cw; (*c*) 377/3 rad/s, ccw]
SP6.2-4 Give the phase relationship of the rotor currents for (*a*) SP6.2-2 and (*b*) SP6.2-3. [(*a*) $\tilde{I}_{ar} = j\tilde{I}_{br}$; (*b*) $\tilde{I}_{ar} = -j\tilde{I}_{br}$]

6.3 VOLTAGE EQUATIONS AND WINDING INDUCTANCES

The voltage equations for the induction machine depicted in Fig. 6.2-1 may be expressed as

$$v_{as} = r_s i_{as} + \frac{d\lambda_{as}}{dt} \tag{6.3-1}$$

$$v_{bs} = r_s i_{bs} + \frac{d\lambda_{bs}}{dt} \tag{6.3-2}$$

$$v_{ar} = r_r i_{ar} + \frac{d\lambda_{ar}}{dt} \tag{6.3-3}$$

$$v_{br} = r_r i_{br} + \frac{d\lambda_{br}}{dt} \tag{6.3-4}$$

where r_s is the resistance of each of the stator windings and r_r is the resistance of each of the rotor windings. It is convenient, for future derivations, to write (6.3-1) through (6.3-4) in matrix form as

$$\mathbf{v}_{abs} = \mathbf{r}_s \mathbf{i}_{abs} + p\boldsymbol{\lambda}_{abs} \tag{6.3-5}$$

$$\mathbf{v}_{abr} = \mathbf{r}_r \mathbf{i}_{abr} + p\boldsymbol{\lambda}_{abr} \tag{6.3-6}$$

where

$$(\mathbf{f}_{abs})^T = [f_{as} \quad f_{bs}] \tag{6.3-7}$$

$$(\mathbf{f}_{abr})^T = [f_{ar} \quad f_{br}] \tag{6.3-8}$$

In (6.3-7) and (6.3-8), f can represent voltage, current, or flux linkages, and T denotes the transpose of a vector or matrix. In (6.3-5) and (6.3-6), p is the shorthand notation for the operator d/dt. Also,

$$\mathbf{r}_s = \begin{bmatrix} r_s & 0 \\ 0 & r_s \end{bmatrix} = r_s\mathbf{I} \tag{6.3-9}$$

and

$$\mathbf{r}_r = \begin{bmatrix} r_r & 0 \\ 0 & r_r \end{bmatrix} = r_r\mathbf{I} \tag{6.3-10}$$

where $\mathbf{I}$ is the identity matrix. A review of matrix algebra is given in Appendix B.

Although (6.3-5) and (6.3-6) are valid for a nonlinear magnetic system, we generally assume that the magnetic system is linear, whereupon the flux linkages may be expressed as functions of inductances and currents. In particular, we can write

$$\lambda_{as} = L_{asas}i_{as} + L_{asbs}i_{bs} + L_{asar}i_{ar} + L_{asbr}i_{br} \tag{6.3-11}$$

$$\lambda_{bs} = L_{bsas}i_{as} + L_{bsbs}i_{bs} + L_{bsar}i_{ar} + L_{bsbr}i_{br} \tag{6.3-12}$$

$$\lambda_{ar} = L_{aras}i_{as} + L_{arbs}i_{bs} + L_{arar}i_{ar} + L_{arbr}i_{br} \tag{6.3-13}$$

$$\lambda_{br} = L_{bras}i_{as} + L_{brbs}i_{bs} + L_{brar}i_{ar} + L_{brbr}i_{br} \tag{6.3-14}$$

The self- and mutual inductances given in (6.3-11) through (6.3-14) are defined by their subscripts. Reciprocity applies; thus, $L_{asbs} = L_{bsas}$, $L_{asar} = L_{aras}$, and so on. For future derivations, it is convenient to write (6.3-11) through (6.3-14) in matrix form as

$$\boldsymbol{\lambda}_{abs} = \mathbf{L}_s\mathbf{i}_{abs} + \mathbf{L}_{sr}\mathbf{i}_{abr} \tag{6.3-15}$$

$$\boldsymbol{\lambda}_{abr} = (\mathbf{L}_{sr})^T\mathbf{i}_{abs} + \mathbf{L}_r\mathbf{i}_{abr} \tag{6.3-16}$$

which may also be written as

$$\begin{bmatrix} \boldsymbol{\lambda}_{abs} \\ \boldsymbol{\lambda}_{abr} \end{bmatrix} = \begin{bmatrix} \mathbf{L}_s & \mathbf{L}_{sr} \\ (\mathbf{L}_{sr})^T & \mathbf{L}_r \end{bmatrix} \begin{bmatrix} \mathbf{i}_{abs} \\ \mathbf{i}_{abr} \end{bmatrix} \tag{6.3-17}$$

The inductance matrices are defined from (6.3-11) through (6.3-14) and the flux linkage and current vectors from (6.3-7) and (6.3-8).

Our job now is to express the self- and mutual inductances of all windings. As in the case of the transformer, the self-inductance of each winding is made up of a leakage inductance caused by the flux that fails to cross the air gap and a magnetizing inductance caused by the flux that traverses the air gap and circulates through the stator and rotor steel. For symmetrical stator windings, the self-inductances L_{asas} and L_{bsbs} are equal and will be denoted as L_{ss}, where

$$L_{ss} = L_{ls} + L_{ms} \tag{6.3-18}$$

In (6.3-18), L_{ls} is the leakage inductance and L_{ms} the magnetizing inductance. The machine is designed to minimize the leakage inductance; it generally makes up approximately 10 percent of the self-inductance. The self-inductance of the symmetrical rotor windings may be expressed similarly:

$$L_{rr} = L_{lr} + L_{mr} \tag{6.3-19}$$

The magnetizing inductances L_{ms} and L_{mr} may be expressed in terms of turns and reluctance. In particular,

$$L_{ms} = \frac{N_s^2}{\Re_m} \tag{6.3-20}$$

$$L_{mr} = \frac{N_r^2}{\Re_m} \tag{6.3-21}$$

The magnetizing reluctance $\Re_m$ is due primarily to the air gap and, since the winding is assumed to be an equivalent sinusoidally distributed winding, perhaps $\Re_m$ should be considered an equivalent magnetizing reluctance. Nevertheless, expressions for L_{ms} and L_{mr}, and thus $\Re_m$, as defined in (6.3-20) and (6.3-21), may be derived. In particular, it can be shown that [1]

$$L_{ms} = N_s^2 \frac{\pi \mu_0 r l}{4g} \tag{6.3-22}$$

$$L_{mr} = N_r^2 \frac{\pi \mu_0 r l}{4g} \tag{6.3-23}$$

where μ_0 is the permeability of free space, r is the mean radius of the air gap, l is the axial length of the air gap (rotor), and g is the radial length of the air gap. One must perform a rather involved and lengthy derivation to obtain (6.3-22) and (6.3-23). We will not do this derivation; instead, the use of an equivalent magnetizing reluctance $\Re_m$ without evaluation will be sufficient for our purposes.

Since the stator (rotor) windings are orthogonal as depicted in Fig. 6.2-1, it would seem that coupling does not exist between the *as* and *bs* windings

(L_{asbs} or L_{bsas}) or between the ar and br windings (L_{arbr} or L_{brar}). However, recall that the equivalent, sinusoidally distributed windings are depicted by one coil placed at the maximum turns density; the windings are actually distributed similar to that shown in Fig. 4.2-2. If we considered, for example, the coupling between the as and bs windings, one would be led to believe that coupling exists since current flowing in the $as_1 - as_1'$ coil in Fig. 4.2-2 would produce a flux that couples the bs winding. However, this same current flows through the $as_3 - as_3'$ coil, which produces a flux that couples the bs winding in a direction opposite to the flux established by the $as_1 - as_1'$ coil. Therefore, if the stator (rotor) windings are distributed symmetrically about orthogonal axes, a net coupling would not exist in this uniform-air-gap machine. Thus, L_{asbs}, L_{bsas}, L_{arbr}, and L_{brar} are all zero. We will find that, in a three-phase machine, where the stator (rotor) windings are displaced 120° magnetically in space, a net coupling exists between the stator (rotor) windings. However, for the two-phase machine we can write

$$\mathbf{L}_s = \begin{bmatrix} L_{ss} & 0 \\ 0 & L_{ss} \end{bmatrix} = L_{ss}\mathbf{I} \tag{6.3-24}$$

$$\mathbf{L}_r = \begin{bmatrix} L_{rr} & 0 \\ 0 & L_{rr} \end{bmatrix} = L_{rr}\mathbf{I} \tag{6.3-25}$$

The stator and rotor windings are in relative motion. Therefore, coupling will occur between the stator and rotor windings and this coupling will vary with the position (θ_r) of the rotor windings relative to the stator windings. For example, when the as and ar windings are aligned, $\theta_r = 0$, the magnitude of coupling between these windings is maximum and, with the assumed direction of positive i_{as} and i_{ar}, the right-hand rule tells us that the mutual fluxes are aiding. Hence, the mutual inductance at $\theta_r = 0$ is a positive maximum and can be expressed in terms of turns and $\Re_m$ as

$$L_{asar} = \frac{N_s N_r}{\Re_m} \qquad \text{for } \theta_r = 0 \tag{6.3-26}$$

Now, when $\theta_r = \frac{1}{2}\pi$, the as and ar windings are orthogonal and

$$L_{asar} = 0 \qquad \text{for } \theta_r = \tfrac{1}{2}\pi \tag{6.3-27}$$

For $\theta_r = \pi$ the windings are again aligned but now they oppose; thus,

$$L_{asar} = -\frac{N_s N_r}{\Re_m} \qquad \text{for } \theta_r = \pi \tag{6.3-28}$$

At $\theta_r = \frac{3}{2}\pi$, the windings are again orthogonal and

$$L_{asar} = 0 \qquad \text{for } \theta_r = \tfrac{3}{2}\pi \tag{6.3-29}$$

From (6.3-26) through (6.3-29), we see that mutual inductances might be approximated as a cosine function of θ_r. In particular, if we define L_{sr} as

$$L_{sr} = \frac{N_s N_r}{\Re_m} \tag{6.3-30}$$

we can approximate L_{asar} or L_{aras} as

$$L_{asar} = L_{sr} \cos \theta_r \tag{6.3-31}$$

If we were to carry out the derivation as in [1], we would find that (6.3-31) is, indeed, a valid expression for the mutual inductance between the *as* and *ar* windings. It follows by inspection of Fig. 6.2-1 that

$$L_{asbr} = -L_{sr} \sin \theta_r \tag{6.3-32}$$

$$L_{bsar} = L_{sr} \sin \theta_r \tag{6.3-33}$$

$$L_{bsbr} = L_{sr} \cos \theta_r \tag{6.3-34}$$

Hence,

$$\mathbf{L}_{sr} = L_{sr} \begin{bmatrix} \cos \theta_r & -\sin \theta_r \\ \sin \theta_r & \cos \theta_r \end{bmatrix} \tag{6.3-35}$$

One should now be able to write the mutual inductances by inspection. For practice, express the stator and rotor mutual inductances if the positive direction of i_{bs} is reversed. In this case, (6.3-31) and (6.3-32) remain unchanged; however, the sign of (6.3-33) and (6.3-34) would be changed.

Once the expressions for the mutual inductances are known, we begin to understand the complexities involved in the analysis of electric machines. The stator-to-rotor mutual inductances are sinusoidal functions of θ_r because of their relative motion. Hence, when in the voltage equations we take the derivative of the flux linkages with respect to time, we no longer obtain only the familiar $L(di/dt)$. Instead, two terms result; one due to the derivative of the mutual inductance, since θ_r is a function of time, and one due to the derivative of the current. For example,

$$\frac{d(L_{asar} i_{as})}{dt} = \frac{dL_{asar}}{dt} i_{as} + L_{asar} \frac{di_{as}}{dt} \tag{6.3-36}$$

Although we are going to have to deal with this problem, we shall not do it now. However, before leaving this work, let us incorporate a turns ratio into the equations as we did for the transformer. We may not see the purpose of this at this point since it cannot yield an equivalent T circuit, as in the case of the transformer, because of the variation of the mutual inductances. Later in this chapter, we will incorporate change of variables that will allow us to treat the induction machine from the standpoint of an equivalent T circuit with constant inductances. In preparation for this event, we will incorporate a turns ratio at this time. In particular, we will refer the rotor variables to a winding with N_s turns by the following turns ratios:

$$\mathbf{i}'_{abr} = \frac{N_r}{N_s}\mathbf{i}_{abr} \tag{6.3-37}$$

$$\mathbf{v}'_{abr} = \frac{N_s}{N_r}\mathbf{v}_{abr} \tag{6.3-38}$$

$$\boldsymbol{\lambda}'_{abr} = \frac{N_s}{N_r}\boldsymbol{\lambda}_{abr} \tag{6.3-39}$$

Thus (6.3-5) and (6.3-6) may be written as

$$\mathbf{v}_{abs} = \mathbf{r}_s\mathbf{i}_{abs} + p\boldsymbol{\lambda}_{abs} \tag{6.3-40}$$

$$\mathbf{v}'_{abr} = \mathbf{r}'_r\mathbf{i}'_{abr} + p\boldsymbol{\lambda}'_{abr} \tag{6.3-41}$$

where

$$\mathbf{r}'_r = \left(\frac{N_s}{N_r}\right)^2 \mathbf{r}_r \tag{6.3-42}$$

Substitution of (6.3-37) and (6.3-39) into (6.3-17) yields

$$\begin{bmatrix} \boldsymbol{\lambda}_{abs} \\ \boldsymbol{\lambda}'_{abr} \end{bmatrix} = \begin{bmatrix} \mathbf{L}_s & \dfrac{N_s}{N_r}\mathbf{L}_{sr} \\ \dfrac{N_s}{N_r}(\mathbf{L}_{sr})^T & \mathbf{L}'_r \end{bmatrix} \begin{bmatrix} \mathbf{i}_{abs} \\ \mathbf{i}'_{abr} \end{bmatrix} \tag{6.3-43}$$

where

$$\mathbf{L}'_r = \left(\frac{N_s}{N_r}\right)^2 \mathbf{L}_r = \begin{bmatrix} L'_{rr} & 0 \\ 0 & L'_{rr} \end{bmatrix} \tag{6.3-44}$$

Since L_{mr} and L_{ms} may be related from (6.3-20) and (6.3-21),

$$L'_{rr} = L'_{lr} + \left(\frac{N_s}{N_r}\right)^2 L_{mr} = L'_{lr} + L_{ms} \tag{6.3-45}$$

Note that

$$\frac{N_s}{N_r}\mathbf{L}_{sr} = \frac{N_s}{N_r}L_{sr}\begin{bmatrix} \cos\theta_r & -\sin\theta_r \\ \sin\theta_r & \cos\theta_r \end{bmatrix} \tag{6.3-46}$$

Comparing L_{ms}, (6.3-20), and L_{sr}, (6.3-30), we see that

$$\frac{N_s}{N_r}L_{sr} = L_{ms} \tag{6.3-47}$$

Hence, (6.3-46) may be expressed in terms of L_{ms} and, for compactness, we will define $\mathbf{L}'_{sr}$ as

$$\mathbf{L}'_{sr} = \frac{N_s}{N_r}\mathbf{L}_{sr} = L_{ms}\begin{bmatrix} \cos\theta_r & -\sin\theta_r \\ \sin\theta_r & \cos\theta_r \end{bmatrix} \tag{6.3-48}$$

Thus, (6.3-43) becomes

$$\begin{bmatrix} \boldsymbol{\lambda}_{abs} \\ \boldsymbol{\lambda}'_{abr} \end{bmatrix} = \begin{bmatrix} \mathbf{L}_s & \mathbf{L}'_{sr} \\ (\mathbf{L}'_{sr})^T & \mathbf{L}'_r \end{bmatrix} \begin{bmatrix} \mathbf{i}_{abs} \\ \mathbf{i}'_{abr} \end{bmatrix} \tag{6.3-49}$$

SP6.3-1 Assume that θ_r is positive in the clockwise direction in Fig. 6.2-1 rather than in the counterclockwise direction. Express all inductances. [$L_{asbr} = L_{sr}\sin\theta_r$; $L_{bsar} = -L_{sr}\sin\theta_r$; all others unchanged]

SP6.3-2 The *as* and *bs* windings in Fig. 6.2-1 are rotated $\frac{1}{4}\pi$ clockwise from the position shown. Express L_{asar} and L_{asbr}. [$L_{asar} = L_{sr}\cos(\theta_r + \frac{1}{4}\pi)$; $L_{asbr} = -L_{sr}\sin(\theta_r + \frac{1}{4}\pi)$]

SP6.3-3 Consider the device shown in Fig. 6.2-1. All windings are open-circuited except the *as* winding. $I_{as} = \sin t$, $L_{ms} = 0.1\,\text{H}$, $L_{rr} = \frac{1}{4}L'_{rr}$, $\omega_r = 0$, and $\theta_r = \frac{1}{3}\pi$. Determine V_{ar}. [$V_{ar} = 0.025\cos t$]

6.4 TORQUE

From Table 2.5-1 for a P-pole machine,

$$T_e(\mathbf{i}, \theta_r) = \frac{P}{2}\frac{\partial W_c(\mathbf{i}, \theta_r)}{\partial\theta_r} \tag{6.4-1}$$

Recall that in Chapter 2 we use $\mathbf{i}$ as a short-hand notation for $\mathbf{i} = (i_1, i_2, i_3, ...i_J)$. Here, $\mathbf{i} = (i_{as}, i_{bs}, i_{ar}, i_{br})$. Do not confuse this with $\mathbf{i}_{abs}$ and $\mathbf{i}_{abr}$, which are vectors. In a linear magnetic system, the energy in the coupling field W_f and the coenergy W_c are equal. The field energy can be expressed as

$$\begin{aligned} W_f(\mathbf{i}, \theta_r) = {} & \tfrac{1}{2}L_{ss}i_{as}^2 + \tfrac{1}{2}L_{ss}i_{bs}^2 + \tfrac{1}{2}L'_{rr}i'^2_{ar} + \tfrac{1}{2}L'_{rr}i'^2_{br} \\ & + L_{ms}i_{as}i'_{ar}\cos\theta_r - L_{ms}i_{as}i'_{br}\sin\theta_r \\ & + L_{ms}i_{bs}i'_{ar}\sin\theta_r + L_{ms}i_{bs}i'_{br}\cos\theta_r \end{aligned} \tag{6.4-2}$$

Since $W_f = W_c$ for a linear magnetic system, substituting (6.4-2) into (6.4-1) yields the electromagnetic torque for a magnetically linear P-pole, two-phase symmetrical induction machine. In particular,

$$T_e = -\frac{P}{2}L_{ms}\left[(i_{as}i'_{ar} + i_{bs}i'_{br})\sin\theta_r + (i_{as}i'_{br} - i_{bs}i'_{ar})\cos\theta_r\right] \tag{6.4-3}$$

The torque and rotor speed are related by

$$T_e = J\frac{d\omega_{rm}}{dt} + B_m\omega_{rm} + T_L \tag{6.4-4}$$

where ω_{rm} is the actual rotor speed. For a P-pole machine, since $\omega_{rm} = (2/P)\omega_r$,

$$T_e = J\frac{2}{P}\frac{d\omega_r}{dt} + B_m\frac{2}{P}\omega_r + T_L \tag{6.4-5}$$

where J is the inertia of the rotor and, in some cases, the connected load. The first term on the right-hand side is the inertial torque. The units of J are kilogram · meter^2 (kg · m^2) or joules · second^2 (J · s^2). Often, the inertia is given as a quantity called WR^2, expressed in units of pound-mass·feet^2 (lbm · ft^2). The load torque T_L is positive for a torque load on the shaft of the induction machine (motor action), as shown in Fig. 6.2-1. Since T_e is positive in the direction opposite to the positive direction for T_L, T_e is also positive for motor action. Generation occurs when both are negative. The constant B_m is a damping coefficient associated with the rotational system of the machine and mechanical load. It has the units of N · m · s/rad of mechanical rotation and it is generally small and often neglected.

SP6.4-1 Why is the sixth term on the right-hand side of (6.4-2) negative? [(6.3-32)]

6.5 VOLTAGE EQUATIONS IN THE ARBITRARY REFERENCE FRAME

In Chapter 5, we introduced the concept of reference frame theory wherein we set forth a change of variables that related the variables associated with symmetrical stationary circuits to variables associated with substitute circuits rotating at an arbitrary angular velocity. We mentioned that we would transform the variables of the rotor circuits to the arbitrary reference frame when considering the induction machine. The change of variables that transforms the rotor variables to the arbitrary reference frame is

$$\mathbf{f}'_{qdr} = \mathbf{K}_r \, \mathbf{f}'_{abr} \tag{6.5-1}$$

where

$$\left(\mathbf{f}'_{qdr}\right)^T = \left[f'_{qr},\ f'_{dr}\right] \tag{6.5-2}$$

$$\left(\mathbf{f}'_{abr}\right)^T = \left[f'_{ar},\ f'_{br}\right] \tag{6.5-3}$$

$$\mathbf{K}_r = \begin{bmatrix} \cos\beta & \sin\beta \\ \sin\beta & -\cos\beta \end{bmatrix} \tag{6.5-4}$$

where $\mathbf{K}_r = (\mathbf{K}_r)^{-1}$, T denotes the transpose of a matrix, and

$$\frac{d\beta}{dt} = \omega - \omega_r \tag{6.5-5}$$

where (6.5-2) and (6.5-3) can denote voltage, current, flux linkage, or charge. In the previous section, we used the turns ratio to set the stage for an equivalent T circuit. As in the analysis of the transformer, the raised prime denotes turns-ratio-referred variables.

We can save a lot of time if we take a moment to compare (6.5-1) through (6.5-5) with (5.3-1) through (5.3-5). Other than the subscript r rather than s, the raised prime, and β rather than θ, the equations are identical. Therefore, it would seem that qr'- and dr'-voltage equations can be written by replacing ω in the qs and ds voltage equation with β.

To show that this is the case, let us go back to Chapter 5 and consider the transformation of the stationary circuits, which we will now consider the stator circuits. From (5.4-6), (5.4-13), and (5.4-14), the qs- and ds-voltage equations in the arbitrary reference frame become

$$v_{qs} = r_s i_{qs} + \omega\lambda_{ds} + p\lambda_{qs} \tag{6.5-6}$$

$$v_{ds} = r_s i_{ds} - \omega\lambda_{qs} + p\lambda_{ds} \tag{6.5-7}$$

It follows that the qr'- and dr'-voltage equations in the arbitrary reference frame become

$$v'_{qr} = r'_r i'_{qr} + (\omega - \omega_r)\lambda'_{dr} + p\lambda'_{qr} \tag{6.5-8}$$

$$v'_{dr} = r'_r i'_{dr} - (\omega - \omega_r)\lambda'_{qr} + p\lambda'_{dr} \tag{6.5-9}$$

There are several things we should talk about. Equations (6.5-6) through (6.5-9) are the voltage equations for a symmetrical, two-phase induction machine in the arbitrary reference frame; they are symmetrical in that the two stator (rotor) windings are orthogonal magnetically with the same winding resistance, r_s (r_r), and the same number of equivalent turns, N_s (N_r). It is very important to realize that the machine need not be linear magnetically. The above voltage equations are valid for either a magnetically linear or a magnetically nonlinear symmetrical induction machine. Recall that we restrict the analysis to a linear magnetic system when we express the flux linkages in terms of inductances. There is one other thing to note before proceeding. We mentioned just prior to Example 5A, that we really need only one set of transformation equations for all symmetrical two-phase sets of windings. However, we refrained from doing that since it could add confusion. We now see that if in (6.5-5) we would have used ω_e, the arbitrary angular velocity of the circuits, rather than ω_r, then we could let $\omega_e = 0$ in (6.5-8) and (6.5-9) when dealing with stationary circuits and $\omega_e = \omega_r$ in (6.5-8) and (6.5-9) when dealing with rotor circuits. The confusion could arise since we would have two arbitraries: the reference frame speed and the speed of the rotating circuits.

Example 6A. Depending on the application, there are three reference frames that are commonly used in the analysis and control of induction machines: the stationary, the rotor, and the synchronously rotating. Let us write the voltage equations in each of these reference frames.

For the stationary reference frame with $\theta = 0$ and $\omega = 0$, (6.5-6) through (6.5-9) become

$$v^s_{qs} = r_s i^s_{qs} + p\lambda^s_{qs} \tag{6A-1}$$

$$v^s_{ds} = r_s i^s_{ds} + p\lambda^s_{ds} \tag{6A-2}$$

$$v_{qr}^{\prime s} = r_r' i_{qr}^{\prime s} - \omega_r \lambda_{dr}^{\prime s} + p\lambda_{qr}^{\prime s} \tag{6A-3}$$

$$v_{dr}^{\prime s} = r_r' i_{dr}^{\prime s} + \omega_r \lambda_{qr}^{\prime s} + p\lambda_{dr}^{\prime s} \tag{6A-4}$$

In the above equations, the raised s is used to denote variables in the stationary reference frame.

For the rotor reference frame with $\theta = \theta_r$ and $\omega = \omega_r$, (6.5-6) through (6.5-9) become

$$v_{qs}^{r} = r_s i_{qs}^{r} + \omega_r \lambda_{ds}^{r} + p\lambda_{qs}^{r} \tag{6A-5}$$

$$v_{ds}^{r} = r_s i_{ds}^{r} - \omega_r \lambda_{qs}^{r} + p\lambda_{ds}^{r} \tag{6A-6}$$

$$v_{qr}^{\prime r} = r_r' i_{qr}^{\prime r} + p\lambda_{qr}^{\prime r} \tag{6A-7}$$

$$v_{dr}^{\prime r} = r_r' i_{dr}^{\prime r} + p\lambda_{dr}^{\prime r} \tag{6A-8}$$

Here we have used the raised r to denote variables in the rotor reference frame.

For the synchronously rotating reference frame with $\theta = \theta_e$ and $\omega = \omega_e$, (6.5-6) through (6.5-9) become

$$v_{qs}^{e} = r_s i_{qs}^{e} + \omega_e \lambda_{ds}^{e} + p\lambda_{qs}^{e} \tag{6A-9}$$

$$v_{ds}^{e} = r_s i_{ds}^{e} - \omega_e \lambda_{qs}^{e} + p\lambda_{ds}^{e} \tag{6A-10}$$

$$v_{qr}^{\prime e} = r_r' i_{qr}^{\prime e} + (\omega_e - \omega_r)\lambda_{dr}^{\prime e} + p\lambda_{qr}^{\prime e} \tag{6A-11}$$

$$v_{dr}^{\prime e} = r_r' i_{dr}^{\prime e} - (\omega_e - \omega_r)\lambda_{qr}^{\prime e} + p\lambda_{dr}^{\prime e} \tag{6A-12}$$

The raised e denotes the variables in the synchronously rotating reference frame. It should be clear that all of the above equations are valid for linear or nonlinear magnetic systems.

Before leaving this example, let us note a property of reference frame theory: the speed voltages disappear from the q- and d-voltage equations if the reference frame is fixed where the windings physically exist. This occurs in (6A-1) and (6A-2) for the reference frame fixed in the stator and in (6A-7) and (6A-8) for the rotor reference frame. Unfortunately, the $\omega\lambda$ terms became known as the speed voltages probably as a result of Park's original work. He was working in the rotor reference frame and the voltage equations for the transformed stator circuits of the synchronous machine were essentially (6A-5) and (6A-

6), wherein the $\omega_r\lambda$ terms appeared. These terms were referred to as the speed voltages since rotor speed, ω_r, was present in these terms. We now know that the speed voltages are a function of the reference frame speed and appear whenever the reference frame angular velocity is different from that of the circuits being transformed.

Example 6B. A symmetrical two-phase induction machine is equipped with the terminals of the rotor windings available through a brush-slip-ring arrangement. Determine the reference frame that would appear to provide the most direct means of analyzing or implementing a computer simulation if (a) the stator voltages are unbalanced with the rotor windings short-circuited and (b) the stator voltages are balanced but an external rotor resistor is connected across the terminals of each rotor winding; however, the resistors are not equal.

Although it is not our intention, at this point, to become involved in either computer simulation or unbalanced or unsymmetrical operation of a symmetrical induction machine, it is instructive to consider the situations posed in this example since it helps to appreciate the facility of the arbitrary reference frame.

In (a) the stator applied voltages are unbalanced, meaning that they do not form an orthogonal, equal-amplitude, two-phase set. Generally, it is most convenient to select the reference frame where the asymmetry exists. Here, it is the stator or stationary reference frame. Therefore, we would use the voltage equations given by (6A-1) through (6A-4), and if we select $\theta = 0$ in (5.3-4), then $v_{qs}^s = v_{as}$ and $v_{ds}^s = -v_{bs}$. It is clear that since the rotor windings are short-circuited, $v_{qr}^{\prime s}$ and $v_{ds}^{\prime s}$ are both zero. If we would have selected any other reference frame, we would need to use (5.3-4) to transform v_{as} and v_{bs} to the reference frame selected. This would be more involved and would add complication to the analysis and/or simulation.

In (b), the asymmetry exists in the rotor, so we will select the rotor reference frame. In this case, the machine voltage equations given by (6A-5) through (6A-8) would be used and we will select $\theta = \theta_r$, whereupon β in (6.5-4) is zero and $v_{qr}^{\prime r} = v_{ar}^{\prime r}$, $v_{dr}^{\prime r} = -v_{br}'$, $i_{qr}^{\prime r} = i_{ar}'$, and $i_{dr}' = -i_{br}'$. Now $v_{qr}^{\prime r}$ and $v_{dr}^{\prime r}$ may now be expressed in terms of the unequal external resistors as

$$v'^r_{qr} = -i'^r_{qr} R'_a \tag{6B-1}$$

$$v'^r_{dr} = -i'^r_{dr} R'_b \tag{6B-2}$$

Equations (5.5-7) and (5.5-8) can be used to express v^r_{qs} and v^r_{ds} since the stator voltages are balanced; thus,

$$v^r_{qs} = \sqrt{2}\, v_s \cos(\theta_{esv} - \theta_r) \tag{6B-3}$$

$$v^r_{ds} = -\sqrt{2}\, v_s \sin(\theta_{esv} - \theta_r) \tag{6B-4}$$

Clearly, we have selected the reference frames in (a) and (b) so that we eliminated the complication of a time-dependent transformation in our analysis and simulation. The reader may wish to consider the problem at the end of the chapter wherein you are asked to reflect i^r_{qs} and i^r_{ds} to the source supplying the stator windings.

SP6.5-1 Are the voltage equations given in this section valid for a nonlinear magnetic system? Why? [yes; λ is not restricted to be a linear function of i]
SP6.5-2 When are (6A-5) through (6A-8) identical in form to (a) (6A-1) through (6A-4)? (b) to (6A-9) through (6A-12)? [(a) $\omega_r = 0$; (b) $\omega_r = \omega_e$]
SP6.5-3 You are given a set of four voltage equations in substitute variables; however, the raised indexes are missing. How can you tell if the reference frame is in either the stator or rotor? [speed voltages are absent in *qs* and *ds* or *qr* and *dr* equations]

6.6 MAGNETICALLY LINEAR FLUX LINKAGE EQUATIONS AND EQUIVALENT CIRCUITS

The flux linkage equations for a magnetically linear system given by (6.3-49) are in terms of *as*- *bs*- *ar'*- and *br'*-variables. In the arbitrary reference frame, (6.3-49) becomes

$$\begin{bmatrix} \boldsymbol{\lambda}_{qds} \\ \boldsymbol{\lambda}'_{qdr} \end{bmatrix} = \begin{bmatrix} \mathbf{K}_s \mathbf{L}_s (\mathbf{K}_s)^{-1} & \mathbf{K}_s \mathbf{L}'_{sr} (\mathbf{K}_r)^{-1} \\ \mathbf{K}_r (\mathbf{L}'_{sr})^T (\mathbf{K}_s)^{-1} & \mathbf{K}_r \mathbf{L}'_r (\mathbf{K}_r)^{-1} \end{bmatrix} \begin{bmatrix} \mathbf{i}_{qds} \\ \mathbf{i}'_{qdr} \end{bmatrix} \tag{6.6-1}$$

Since, from (6.3-24) and (6.3-44), respectively, $\mathbf{L}_s = diag[L_{ss}\ L_{ss}]$ and $\mathbf{L}'_r = diag[L'_{rr}\ L'_{rr}]$,

$$\mathbf{K}_s\mathbf{L}_s(\mathbf{K}_s)^{-1} = diag[L_{ss}\ L_{ss}] \tag{6.6-2}$$

$$\mathbf{K}_r\mathbf{L}'_r(\mathbf{K}_r)^{-1} = diag[L'_{rr}\ L'_{rr}] \tag{6.6-3}$$

Now let us work on the upper-right element of the 2×2 matrix:

$$\mathbf{K}_s\mathbf{L}'_{sr}(\mathbf{K}_r)^{-1} = \begin{bmatrix} \cos\theta & \sin\theta \\ \sin\theta & -\cos\theta \end{bmatrix} \times$$
$$L_{ms}\begin{bmatrix} \cos\theta_r & -\sin\theta_r \\ \sin\theta_r & \cos\theta_r \end{bmatrix}\begin{bmatrix} \cos(\theta-\theta_r) & \sin(\theta-\theta_r) \\ \sin(\theta-\theta_r) & -\cos(\theta-\theta_r) \end{bmatrix} \tag{6.6-4}$$

It is left to the reader to show that (6.6-4) reduces to

$$\mathbf{K}_s\mathbf{L}'_{sr}(\mathbf{K}_r)^{-1} = diag\,[L_{ms}\ L_{ms}] \tag{6.6-5}$$

and that

$$\mathbf{K}_s\mathbf{L}'_{sr}(\mathbf{K}_r)^{-1} = \mathbf{K}_r(\mathbf{L}'_{sr})^T(\mathbf{K}_s)^{-1} \tag{6.6-6}$$

Therefore,

$$\begin{bmatrix} \boldsymbol{\lambda}_{qds} \\ \boldsymbol{\lambda}'_{qdr} \end{bmatrix} = \begin{bmatrix} \mathbf{L}_{ss} & \mathbf{L}_{ms} \\ \mathbf{L}_{ms} & \mathbf{L}'_{rr} \end{bmatrix}\begin{bmatrix} \mathbf{i}_{qds} \\ \mathbf{i}'_{qdr} \end{bmatrix} \tag{6.6-7}$$

Since $L_{ss} = L_{ls} + L_{ms}$ and $L'_{rr} = L'_{lr} + L_{ms}$, (6.6-7) may be expressed as

$$\lambda_{qs} = L_{ls}i_{qs} + L_{ms}(i_{qs} + i'_{qr}) \tag{6.6-8}$$

$$\lambda_{ds} = L_{ls}i_{ds} + L_{ms}(i_{ds} + i'_{dr}) \tag{6.6-9}$$

$$\lambda'_{qr} = L'_{lr}i'_{qr} + L_{ms}(i_{qs} + i'_{qr}) \tag{6.6-10}$$

$$\lambda'_{dr} = L'_{lr}i'_{dr} + L_{ms}(i_{ds} + i'_{dr}) \tag{6.6-11}$$

Equations (6.5-6) through (6.5-9) and (6.6-8) through (6.6-11) suggest the equivalent circuits given in Fig. 6.6-1.

SP6.6-1 Starting with (6.6-8) through (6.6-11), express the flux linkage equations in the (*a*) stationary reference frame, (*b*) rotor reference frame, and (*c*) synchronously rotating reference frame. [All the same form; (*a*) place an s superscript on all flux linkages and currents; (*b*) an r, (*c*) an e]

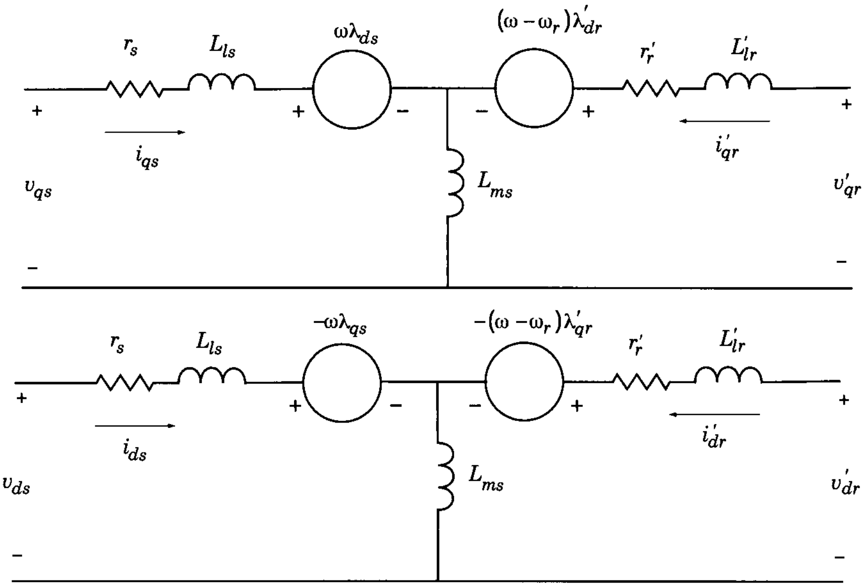

Figure 6.6-1: Arbitrary reference frame equivalent circuits for a two-phase, symmetrical induction machine.

6.7 TORQUE EQUATIONS IN ARBITRARY REFERENCE FRAME VARIABLES

In this section, two approaches to deriving expressions for torque are set forth. First, assuming a linear magnetic system as we have done thus far in this chapter and, second, assuming either a linear or a nonlinear magnetic system.

Linear Magnetic System

Equation (6.4-3) is an expression for the electromagnetic torque in machine currents i_{as}, i_{bs}, i'_{ar}, and i'_{br} for a linear magnetic system. If we express the torque in terms of the arbitrary reference frame currents, the electromagnetic torque may be expressed as

$$T_e = \frac{P}{2} L_{ms}(i_{qs}i'_{dr} - i_{ds}i'_{qr}) \tag{6.7-1}$$

where T_e is positive for motor action. Since we are dealing with a linear magnetic system, equivalent expressions for torque are

$$T_e = \frac{P}{2}\left(\lambda'_{qr} i'_{dr} - \lambda'_{dr} i'_{qr}\right) \tag{6.7-2}$$

$$T_e = \frac{P}{2}\left(\lambda_{ds} i_{qs} - \lambda_{qs} i_{ds}\right) \tag{6.7-3}$$

When the T_e is expressed in terms of flux linkages as in (6.7-2) and (6.7-3), it appears as if the leakage inductances play a role in the evaluation of torque. However, the product of leakage inductances times the currents cancel when the flux linkages are expressed in terms of inductances.

Nonlinear Magnetic System

In Chapter 2, we derived the expression for torque given in Table 2.5-1. In that derivation, we assumed a linear magnetic system and it was necessary to take the partial derivative of the field energy, W_f, or the coenergy, W_c, with respect to x in a translational system and θ in a rotational system in order to express torque for a linear magnetic system. It is interesting that once we have incorporated a change of variables, we open the door to another approach that can be used to derive an expression for torque that is valid for either a linear or nonlinear magnetic system.

The energy balance equation given in Chapter 2 is

$$W_f = W_e + W_m \tag{6.7-4}$$

where W_f is the energy stored in the coupling field, W_e is the energy entering the coupling field from the electrical system, and W_m is the energy entering the coupling field from the mechanical system. Let us do two things: solve for W_e and take the total derivative with respect to time of each term of (6.7-4),

$$pW_e = pW_f - pW_m \tag{6.7-5}$$

where pW_e is the power entering the coupling field. If, in order to follow the derivation in Chapter 2, we extract the ir terms from (6.5-6) through (6.5-9) we can express pW_e as

$$pW_e = e_{qs} i_{qs} + e_{ds} i_{ds} + e'_{qr} i'_{qr} + e'_{dr} i'_{dr} \tag{6.7-6}$$

where $e_{qs} = v_{qs} - r_s i_{qs}$, and so on. Substituting (6.5-6) through (6.5-9) minus the ir drops into (6.7-6) yields an expression for power into the coupling field in arbitrary reference frame variables:

$$\begin{aligned} pW_e = &\left(\lambda_{ds} i_{qs} - \lambda_{qs} i_{ds} + \lambda'_{dr} i'_{qr} - \lambda'_{qr} i'_{dr}\right) p\theta \\ &+ \left(i_{qs} p\lambda_{qs} + i_{ds} p\lambda_{ds} + i'_{qr} p\lambda'_{qr} + i'_{dr} p\lambda'_{dr}\right) \\ &+ \left(\lambda'_{qr} i'_{dr} - \lambda'_{dr} i'_{qr}\right) p\theta_r \end{aligned} \tag{6.7-7}$$

Recall, that pW_m in (6.7-5) is

$$pW_m = -T_e p\theta_{rm} \tag{6.7-8}$$

and since

$$\theta_{rm} = \frac{2}{P}\theta_r \tag{6.7-9}$$

in terms of the electrical angular velocity of the rotor, (6.7-8) becomes

$$pW_m = -\frac{2}{P} T_e\, p\theta_r \tag{6.7-10}$$

If we compare (6.7-5) with (6.7-7) and are aware of (6.7-10), we can equate coefficients of $p\theta_r$ and the expression for torque in all reference frames appears to be

$$T_e = \frac{P}{2}\left(\lambda'_{dr} i'_{qr} - \lambda'_{qr} i'_{dr}\right) \tag{6.7-11}$$

In a special case, when $\theta = \theta_r$ ($\omega = \omega_r$) and we are in the rotor reference frame, the λi products of the first term on the right-hand side of (6.7-7) are also coefficients of $p\theta_r$. In this case,

$$T_e = \frac{P}{2}\left(\lambda^r_{ds} i^r_{qs} - \lambda^r_{qs} i^r_{ds}\right) \tag{6.7-12}$$

where the raised r denotes variables in the rotor reference frame. This is the expression that Park derived in [2] for a synchronous machine; however, he did not use a true power balance since he did not include the rotor circuits. Nevertheless, his result is correct since none of the voltage equations of the rotor windings of the synchronous machine contain $p\theta_r$ in the rotor reference frame.

Significance of Two Torque Derivations

We have taken two different approaches to arrive at the same expressions for torque. That is, (6.7-2) and (6.7-11) are identical as are (6.7-3) and (6.7-12). One wonders why we have gone to the trouble of two derivations since, thus far, we have considered only a linear magnetic system and, therefore, we could have stopped with (6.7-3). This is true; however, the second approach is enlightening, albeit perhaps only of academic interest in an introductory treatment of electric machines. Nevertheless, let us talk about what has been done. Please note that we obtained (6.7-3), which is expressed in stator variables referred to the arbitrary reference frame, from (6.7-2), which is expressed in rotor variables referred to the arbitrary reference frame. We were able to do this only because those variables are related by the flux linkage equations of a linear magnetic system, (6.6-8) through (6.6-11).

What additional information does the derivation leading up to (6.7-11) and (6.7-12) offer? Well, since this deviation was carried out without using inductances, we can conclude that (6.7-11) is valid for both linear and nonlinear magnetic systems, except when the rotor reference frame is being used. In this case, (6.7-12), which is (6.7-3), must be used if the magnetic system is nonlinear. Although (6.7-3) is equivalent to (6.7-1) for a linear magnetic system, this cannot be shown to be true for a nonlinear magnetic system since there is not a relationship between rotor reference frame variables that come from the stator variables (f_{qs}^r and f_{ds}^r) and those that come from the rotor variables (f_{qr}^r and f_{dr}^r) as there is for a linear magnetic system.

In retrospect, we should have anticipated most of this without going through the second approach. To explain this, let us rewrite the voltage equations in the arbitrary reference frame. Thus, repeating (6.5-6) through (6.5-9),

$$v_{qs} = r_s i_{qs} + \omega\lambda_{ds} + p\lambda_{qs} \tag{6.7-13}$$

$$v_{ds} = r_s i_{ds} - \omega\lambda_{qs} + p\lambda_{ds} \tag{6.7-14}$$

$$v'_{qr} = r'_r i'_{qr} + (\omega - \omega_r)\lambda'_{dr} + p\lambda'_{qr} \tag{6.7-15}$$

$$v'_{dr} = r'_r i'_{dr} - (\omega - \omega_r)\lambda'_{qr} + p\lambda'_{dr} \tag{6.7-16}$$

Now, in a power-balance derivation we multiply each voltage equation with the corresponding current and then, since T_e is the coefficient of ω_r, we look for all ω_r terms. If the reference frame speed, ω, is not equal to ω_r then the qs- and ds-variables do not enter into the expression for torque if we assume that the magnetic system is nonlinear. If, however, $\omega = \omega_r$, the speed voltage disappears from the v'_{qr} and v'_{dr} voltage equations, (6.7-15) and (6.7-16), whereupon, we must look elsewhere for coefficients of ω_r. The qs-

and qs-voltage equations come to the rescue, and here and only here will the qs- and ds-variable appear in the expression for torque if we are dealing with a nonlinear magnetic system.

Although we will not dwell on other aspects of the power-balance derivation or on unbalanced or unsymmetrical conditions, it is important to mention that if either of the applied voltage vectors $\mathbf{v}_{qds}$ or $\mathbf{v}'_{qdr}$, or the current vectors $\mathbf{i}_{qds}$ or $\mathbf{i}'_{qdr}$, are unsymmetrical or unbalanced functions of θ_r then there could be additional terms in (6.7-7) that are coefficients of $p\theta_r$. In this case, (6.7-7) would not be valid and this approach becomes invalid. Although this situation can occur for either linear or nonlinear magnetic systems, it is uncommon and beyond the scope of this text and is covered in [3].

SP6.7-1 Why is (6.7-7) valid for magnetically nonlinear systems? [see SP6.5-1]

SP6.7-2 What does the second term on the right-hand side of (6.7-7) represent? [pW_f]

SP6.7-3 Show that (6.7-2) and (6.7-3) are equal for a linear magnetic system.

SP6.7-4 Show that the coefficient of $p\theta$ in (6.7-7) is zero for a linear magnetic system [(6.7-2) equals (6.7-3)]

6.8 ANALYSIS OF STEADY-STATE OPERATION

When analyzing steady-state balanced operation of an induction machine, it is convenient and customary to use the single-phase equivalent T circuit with the phasor quantities $\tilde{F}_{as}$ and $\tilde{F}'_{ar}$. Although we could use any reference frame to derive this equivalent circuit, we will use the synchronous rotating. To start this, let us recall from Chapter 5 that during steady-state balanced operation the variables in the synchronous rotating reference frame are constant. We also showed in Chapter 5 that in this case

$$\sqrt{2}\,\tilde{F}_{as} = F^{e}_{qs} - jF^{e}_{ds} \tag{6.8-1}$$

which is (5.5-23). By going through a similar procedure as in Section 5.5, it can be shown that

$$\sqrt{2}\,\tilde{F}'_{ar} = F'^{e}_{qr} - jF'^{e}_{dr} \tag{6.8-2}$$

Actually, we are not surprised by (6.8-2); however, we will derive it. In Chapter 5, we transform (5.5-3) and (5.5-4) to the arbitrary reference frame, that is, for steady-state conditions

$$F_{as} = \sqrt{2}\, F_s \cos\left[\omega_e t + \theta_{esf}(0)\right] \tag{6.8-3}$$

$$F_{bs} = \sqrt{2}\, F_s \sin\left[\omega_e t + \theta_{esf}(0)\right] \tag{6.8-4}$$

Equations (6.8-3) and (6.8-4) are a repeat of (5.5-3) and (5.5-4) with an s subscript added to $\theta_{ef}(0)$ to distinguish it from the zero position of the rotor variable. In the arbitrary reference frame

$$F_{qs} = \sqrt{2}\, F_s \cos\left[(\omega_e - \omega)t + \theta_{esf}(0) - \theta(0)\right] \tag{6.8-5}$$

$$F_{ds} = -\sqrt{2}\, F_s \sin\left[(\omega_e - \omega)t + \theta_{esf}(0) - \theta(0))\right] \tag{6.8-6}$$

Realizing that

$$\tilde{F}_{as} = F_s \cos\theta_{esf}(0) + jF_s \sin\theta_{esf}(0) \tag{6.8-7}$$

we see that if $\omega = \omega_e$ and $\theta(0) = 0$ in (6.8-5) and (6.8-6), then (6.8-1) results.

Now, for the rotor circuits the steady state rotor variables are expressed as

$$F'_{ar} = \sqrt{2}\, F'_r \cos\left[(\omega_e - \omega_r)t + \theta_{erf}(0)\right] \tag{6.8-8}$$

$$F'_{br} = \sqrt{2}\, F'_r \sin\left[(\omega_e - \omega_r)t + \theta_{erf}(0)\right] \tag{6.8-9}$$

Actually (6.8-8) and (6.8-9) are (6.2-4) and (6.2-5), respectively, written for any variable (voltage, current, flux linkage, or charge). If we use (6.5-1) to transform (6.8-8) and (6.8-9) to the arbitrary reference we have

$$F'_{qr} = \sqrt{2}\, F'_r \cos\left[(\omega_e - \omega)t + \theta_{erf}(0) - \theta(0) + \theta_r(0)\right] \tag{6.8-10}$$

$$F'_{dr} = \sqrt{2}\, F'_r \sin\left[(\omega_e - \omega)t + \theta_{erf}(0) - \theta(0) + \theta_r(0)\right] \tag{6.8-11}$$

If we select the synchronous rotating reference frame, $\omega = \omega_e$, and if we set $\theta(0)$ and $\theta_r(0)$ equal to zero, then since from (6.8-8)

$$\tilde{F}'_{ar} = F'_r \cos[\theta_{erf}(0)] + j\, F'_r \sin[\theta_{erf}(0)] \tag{6.8-12}$$

from which we can write (6.8-2).

In the synchronously rotating reference frame, the qs, ds, q'_r, and d'_r variables are all constant in the steady state, whereupon (6.5-6) through (6.5-9) may be written as

$$V_{qs}^e = r_s I_{qs}^e + \omega_e \lambda_{ds}^e \tag{6.8-13}$$

$$V_{ds}^e = r_s I_{ds}^e - \omega_e \lambda_{qs}^e \tag{6.8-14}$$

$$V_{qr}'^e = r_r' I_{qr}'^e + (\omega_e - \omega_r)\lambda_{dr}'^e \tag{6.8-15}$$

$$V_{dr}'^e = r_r' I_{dr}'^e - (\omega_e - \omega_r)\lambda_{qr}'^e \tag{6.8-16}$$

where the uppercase letters are used to denote constant voltages and currents. If we substitute (6.8-13) and (6.8-14) into (6.8-1) for V_{qs}^e and V_{ds}^e, respectively, and (6.8-15) and (6.8-16) into (6.8-2) for $V_{qr}'^e$ and $V_{dr}'^e$, and if we substitute (6.6-8) through (6.6-11) for the flux linkages in the synchronous rotating reference frame, we obtain

$$\tilde{V}_{as} = r_s \tilde{I}_{as} + j\omega_e(L_{ls} + L_{ms})\tilde{I}_{as} + j\omega_e L_{ms}\tilde{I}_{ar}' \tag{6.8-17}$$

$$\tilde{V}_{ar}' = r_r'\tilde{I}_{ar}' + j(\omega_e - \omega_r)(L_{lr}' + L_{ms})\tilde{I}_{ar}' + j(\omega_e - \omega_r)L_{ms}\tilde{I}_{as} \tag{6.8-18}$$

The so-called "slip" is

$$s = \frac{\omega_e - \omega_r}{\omega_e} \tag{6.8-19}$$

If we divided (6.8-18) by the slip, it becomes

$$\frac{\tilde{V}_{ar}'}{s} = \frac{r_r'}{s}\tilde{I}_{ar}' + j\omega_e(L_{lr}' + L_{ms})\tilde{I}_{ar}' + j\omega_e(L_{ms})\tilde{I}_{as}' \tag{6.8-20}$$

Equations (6.8-17) and (6.8-20) suggest the single-phase equivalent T circuit of a two-phase symmetrical induction machine during steady-state balanced operation shown in Fig. 6.8-1. It is important to note that this equivalent circuit includes the phasors of both stator and rotor currents, whose frequencies are, in general, different. This is not an error. We have previously shown that it is possible to relate the phasors of variables whose frequencies are not the same. Also, note that the inductive reactances are calculated as $X = \omega_e L$. One tends to want to calculate the inductive reactances of the rotor circuit as $X = (\omega_e - \omega_r)L$; however, (6.8-20) tells us that is not correct. We will find that, with a slight modification (X_{ms} becomes $\frac{3}{2}X_{ms}$),

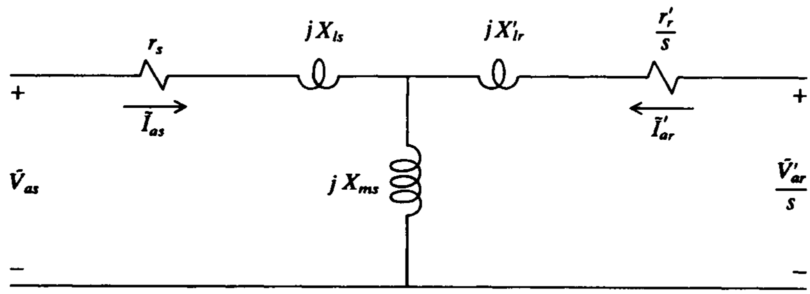

Figure 6.8-1: Equivalent circuit of a two-phase symmetrical induction machine for balanced steady-state operation.

this circuit may also be used to calculate the steady-state performance of a three-phase symmetrical induction machine.

An expression for the steady-state electromagnetic torque may be obtained by first writing (6.7-1) in terms of I^e_{qs}, I^e_{ds}, I'^e_{qr}, and I'^e_{dr}, and then use (6.8-1) and (6.8-2) to express $\tilde{I}_{as}$ and $\tilde{I}'_{ar}$. The expression may be reduced to

$$T_e = 2\left(\frac{P}{2}\right) L_{ms} Re[j\tilde{I}^*_{as}\tilde{I}'_{ar}] \tag{6.8-21}$$

where $\tilde{I}^*_{as}$ is the conjugate of $\tilde{I}_{as}$. Obtaining (6.8-21) is given as a problem at the end of this chapter.

The balanced steady-state torque-speed or torque-slip characteristic of a single-fed induction machine warrants discussion. The vast majority of induction machines in use today are single-fed, wherein electric power is transferred to or from the induction machine via the stator circuits with the rotor windings short-circuited. Moreover, the majority of the single-fed induction machines are of the squirrel-cage rotor type. In this type of rotor construction, copper or aluminum bars are uniformly distributed and embedded in a ferromagnetic material, with all bars terminated in a common ring at each end of the rotor. It may at first appear that the mutual inductance between a uniformly distributed rotor winding and a sinusoidally distributed stator winding would include more than just the fundamental component. In most cases, however, a uniformly distributed winding is adequately described by its fundamental sinusoidal component.

For single-fed machines, $\tilde{V}'_{ar}$ is zero, whereupon (6.8-20) may be written as

$$\tilde{I}'_{ar} = -\frac{jX_{ms}}{r'_r/s + jX'_{rr}}\tilde{I}_{as} \tag{6.8-22}$$

Substituting (6.8-22) into (6.8-21) yields the following expression for electromagnetic torque of a single-fed, two-phase symmetrical induction machine during balanced steady-state operation:

$$T_e = \frac{2(P/2)(X_{ms}^2/\ \omega_e)(r'_r/s)|\tilde{I}_{as}|^2}{(r'_r/s)^2 + X'^2_{rr}} \tag{6.8-23}$$

It is important to note from (6.8-23) that torque is positive (motor action) when slip is positive, which occurs when $\omega_r < \omega_e$, and negative (generator action) when the slip is negative, which occurs when $\omega_r > \omega_e$, and zero when the slip is zero ($\omega_r = \omega_e$). (Prove the last of these three statements.) In other words, the single-fed induction machine develops torque at all speeds except at synchronous speed.

With $\tilde{V}'_{ar} = 0$, the input impedance of the equivalent circuit shown in Fig. 6.8-1 is

$$Z = \frac{r_s r'_r/s + (X_{ms}^2 - X_{ss}X'_{rr} + j[(r'_r/s)X_{ss} + r_s X'_{rr}]}{r'_r/s + jX'_{rr}} \tag{6.8-24}$$

Now $|\tilde{I}_{as}|^2$ is I_s^2 and

$$I_s = \frac{|\tilde{V}_{as}|}{|Z|} \tag{6.8-25}$$

Hence, the expression for the steady-state electromagnetic torque for a single-fed, two-phase symmetrical induction machine becomes

$$T_e = \frac{2(P/2)(X_{ms}^2/\omega_e)r'_r s|\tilde{V}_{as}|^2}{[r_s r'_r + s(X_{ms}^2 - X_{ss}X'_{rr})]^2 + (r'_r X_{ss} + s r_s X'_{rr})^2} \tag{6.8-26}$$

Thus, for a given set of parameters and source frequency ω_e, the steady-state torque varies as the square of the magnitude of the applied voltages. The steady-state torque-speed characteristics typical of many single-fed, two-phase induction machines are shown in Fig. 6.8-2. The parameters of the machine are often selected so that, for rated frequency operation, the maximum torque occurs between 80 and 90 percent of synchronous speed. Generally, the maximum torque is two or three times the rated torque of the machine.

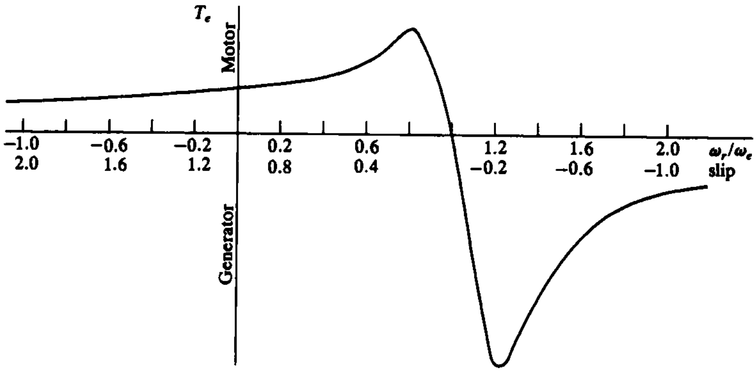

Figure 6.8-2: Steady-state torque-speed characteristics of a two-phase symmetrical induction machine.

Although we are considering a two-phase machine, the general shape of the torque-speed characteristic is similar for multiphase induction machines.

Let us take a moment to consider stable, steady-state operation of an induction machine. Consider (6.4-5); for steady-state operation $d\omega_r/dt$ is zero since the speed is constant. Thus, $T_e = T_L$. From Fig. 6.8-2, it would appear that, for a given load torque T_L there could be two operating points on the T_e versus ω_r plot. When we calculate the steady-state torque, we are assuming, in the calculation, that the speed is constant without regard to whether or not it is a stable operating point. Let us consider the T_e versus ω_r plot shown in Fig. 6.8-3. Since induction machines are used primarily as motors, the characteristic shown in Fig. 6.8-3 is the range of speeds over which motors operate. For the load torque T_L, shown in Fig. 6.8-3, there appear to be two operating points, 1 and 1′. If we assume stable steady-state operation occurs at either point 1 or 1′, then, if the system is displaced from this operating point, there will be a torque established to return the system to this operating point. This, of course, is the same procedure used to determine the stable operating points of the relay in Chapter 2.

Consider operation at point 1. If the speed ω_r were to increase ever so slightly, T_e would become less than T_L. In other words, the load torque (T_L) requirements are larger than the electromagnetic torque (T_e) that can be developed by the machine. Consequently, the machine will slow down due to the fact that $T_L > T_e$. Hence, the machine will return to operation at point

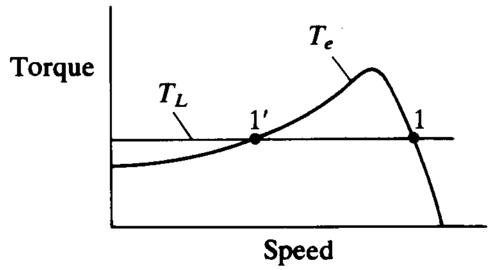

Figure 6.8-3: Stable operation of an induction motor.

1. If, instead, the speed decreased from operating point 1, T_e is greater than T_L. Hence, the machine will accelerate back to point 1. It follows that point 1 is a stable steady-state operating point.

Now consider operation at point 1′. An increase in ω_r causes T_e to become greater than T_L, hence, the machine will accelerate and move away from point 1′. In fact, the machine will accelerate to point 1, where it will operate stably. If ω_r decreases slightly from point 1′, T_e becomes less than T_L. The machine decelerates to stall and, if T_L remains applied to the shaft, the rotor will reverse direction and accelerate forever in the opposite direction. Point 1′ is an unstable operating point. It follows that stable operation, for either motor or generation operation, occurs on the negative-slope portion of the T_e versus ω_r characteristic.

Looking at Fig. 6.8-3, one may wonder how operation could be established at point 1 since T_L is larger than T_e at stall and the machine could not develop a large enough starting torque to accelerate the machine up to operation at point 1. In most cases, the load torque is a function of ω_r, say $T_L = K\omega_r^2$, for example. In these cases, the machine can develop sufficient starting torque and, if T_L and T_e match on the negative-slope portion, stable operation will occur. If, on the other hand, T_L is constant and greater than T_e at $\omega_r = 0$, we have at least three choices: (1) increase the stator voltage, (2) increase the rotor resistance, or (3) use a different machine. Increasing the rotor resistance to increase the starting torque is something that we have not yet discussed. We will now.

An expression for the slip at maximum torque may be obtained by taking the derivative of (6.8-26) with respect to slip and setting the result equal to zero. In particular,

$$s_m = r_r' G \tag{6.8-27}$$

where

$$G = \pm \sqrt{\frac{r_s^2 + X_{ss}^2}{(X_{ms}^2 - X_{ss}X_{rr}')^2 + r_s^2 X_{rr}'^2}} \tag{6.8-28}$$

Two values of slip at maximum torque, s_m, are obtained, one for motor action and one for generator action. It is important to note that G is not a function of r_r'; thus, the slip at maximum torque, (6.6-28), is directly proportional to r_r'. Consequently, since all other machine parameters are constant, the speed at which maximum steady-state torque occurs may be varied by inserting external rotor resistance. This feature is often used when starting large motors which have coil-wound rotor windings with slip rings. In this application, balanced external rotor resistances are placed across the terminals of the rotor windings so that maximum torque occurs near stall. As the machine speeds up, the external resistors are short-circuited. On the other hand, some two-phase induction machines are designed with high-resistance rotor windings so that maximum torque is available at or near stall to provide fast response in position-follow-up systems.

It may at first appear that the magnitude of the maximum torque would be influenced by r_r'. However, if (6.6-27) is substituted into (6.6-26), the maximum torque may be expressed as

$$T_{e,\max} = \frac{2(P/2)(X_{ms}^2/\omega_e)G|\tilde{V}_{as}|^2}{[r_s + G(X_{ms}^2 - X_{ss}X_{rr}')]^2 + (X_{ss} + Gr_s X_{rr}')^2} \tag{6.8-29}$$

Equation (6.8-29) is independent of r_r'. Thus, the maximum torque remains constant if only r_r' is varied; however, the slip at which maximum torque is produced varies in accordance with (6.8-27). Figure 6.8-4 illustrates the effect of changing r_r'. Therein $r_{r3}' > r_{r2}'$ and $r_{r2}' > r_{r1}'$.

In variable-frequency drive systems, the operating speed of the electromechanical device (reluctance, synchronous, or induction machine) is controlled by changing the frequency of the applied voltages by either an inverter (solid-state dc-to-ac converter) or a cycloconverter (ac frequency changer) arrangement. The phasor voltage equations are applicable regardless of the frequency of operation. It is only necessary to keep in mind that the reactances given in the steady-state equivalent circuit (Fig. 6.8-1) are defined as the product of ω_e and the inductances. As the frequency is decreased, the time rate of change of the steady-state variables is decreased proportionally. Thus, the

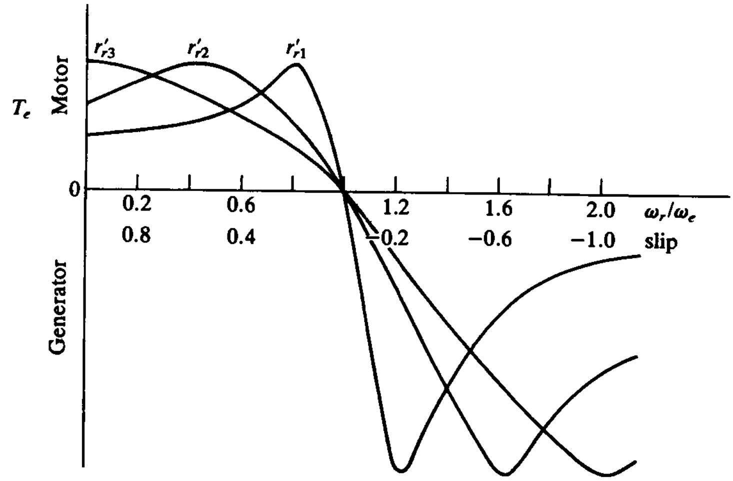

Figure 6.8-4: Steady-state torque-speed characteristics of a two-phase symmetrical induction machine for different values of r'_r.

reactances decrease linearly with frequency. If the amplitude of the applied voltages is maintained at the rated value, the currents will become excessive. To prevent large currents, the magnitude of the stator voltages is decreased as the frequency is decreased. In many applications, the voltage magnitude is reduced linearly with frequency until a low frequency is reached, whereupon the decrease in voltage is programmed in a manner to compensate for the effects of the stator resistance.

The influence of frequency upon the steady-state torque-speed characteristics is illustrated in Fig. 6.8-5. These characteristics are for a linear relationship between the magnitude of the applied voltages and frequency. This machine is designed to operate at $\omega_e = \omega_b$, where ω_b corresponds to the rated frequency. Rated voltage is applied at rated frequency; that is, when $\omega_e = \omega_b$, $|\tilde{V}_{as}| = V_B$, where V_B is the base or rated voltage. Since the reactances ($\omega_e L$) decrease with frequency, the voltage is reduced as frequency is reduced to avoid large stator currents. The maximum torque is reduced markedly at $\omega_e/\omega_b = 0.1$. At this frequency, the voltage would probably be increased somewhat so as to obtain a higher torque. Perhaps a voltage of, say, $0.15V_B$ or $0.2V_B$ would be used rather than 0.1 V_B. Saturation of the stator or rotor steel may, however, cause the stator currents to be excessive

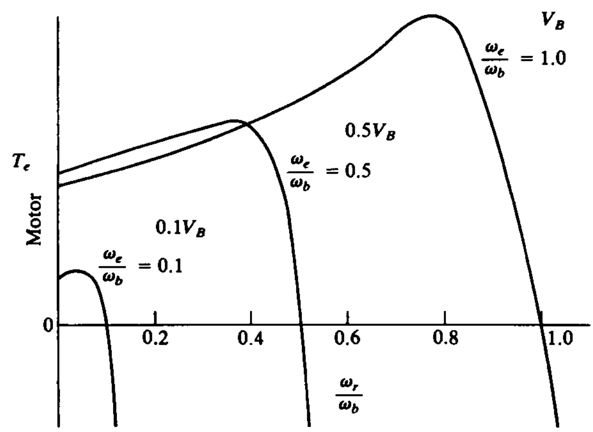

Figure 6.8-5: Steady-state torque-speed characteristics of a two-phase symmetrical induction machine for different operating frequencies.

at this higher voltage. These practical considerations of variable-frequency drives are of major importance but well beyond the scope of this text.

Example 6C. The parameters for the equivalent circuit shown in Fig. 6.8-1 may be calculated by using electromagnetic field theory or determined from tests. The tests generally performed are a dc test, a no-load test, and a blocked-rotor test. The following test data are given for a 3-hp, four-pole, 110-V (rms), two-phase, 60-Hz, induction machine, where all ac voltages and currents are in rms values:

DC test	No-load test	Blocked-rotor test
$V_{dc} = 6.9$ V $I_{dc} = 13.0$ A	$V_{nl} = 110$ V $I_{nl} = 3.86$ A $P_{nl} = 134$ W $f = 60$ Hz	$V_{br} = 23.5$ V $I_{br} = 16.1$ A $P_{br} = 469$ W $f = 15$ Hz

During the dc test, a dc voltage is applied to one phase while the machine is at standstill. Thus,

$$r_s = \frac{V_{dc}}{I_{dc}} = \frac{6.9}{13} = 0.531\ \Omega \tag{6C-1}$$

The no-load test, which is analogous to the transformer open-circuit test, is performed with balanced two-phase 60-Hz voltages applied to the stator windings without mechanical load on the rotor (no load). The total power input during this test is the sum of the stator ohmic losses per phase, the core losses due to hysteresis and eddy currents, and rotational losses due to friction and windage. The total stator ohmic losses (two phases) are

$$P_r = 2I_{n1}^2 r_s = 2(3.86)^2 0.531 = 15.8 \text{ W} \tag{6C-2}$$

Therefore, the power loss due to friction, windage, and core losses is

$$P_{fWC} = P_{nl} - P_r = 134 - 15.8 = 118.2 \text{ W} \tag{6C-3}$$

In the equivalent circuit shown in Fig. 6.8-1, the core loss is neglected. It is generally small and, in most cases, little error is introduced by neglecting it. It can be taken into account by placing a resistor in shunt with the magnetizing reactance X_{ms}. The friction and windage losses may be approximated with B_m in (6.4-5).

It is noted from the no-load test data that the power factor is very small since the total apparent power input to the motor is

$$|S_{nl}| = 2V_{nl}I_{nl} = 2(110)(3.86) = 849.2 \text{ VA} \tag{6C-4}$$

Therefore, the no-load impedance is highly inductive, and its magnitude is assumed to be the sum of the stator leakage reactance and the magnetizing reactance since the rotor speed is essentially synchronous, whereupon r_r'/s is much larger than X_{ms} in Fig. 6.8-1. Thus,

$$X_{ls} + X_{ms} \cong \frac{V_{n1}}{I_{n1}} = \frac{110}{3.86} = 28.5 \ \Omega \tag{6C-5}$$

During the blocked-rotor test, which is analogous to the transformer short-circuit test, the rotor is locked by some mechanical means and balanced two-phase stator voltages are applied. The frequency of the applied voltages is often less than rated in order to obtain a representative value of r_r', since during normal operation the frequency of the rotor currents is low and the rotor resistance of some induction machines vary considerably with frequency. During stall ($s = 1$), the rotor impedance $r_r'/s + jX_{lr}'$ is much smaller in magnitude than X_{ms}, whereupon the current flowing in the magnetizing reactance may be neglected in these calculations. Hence, the total power input to the motor during the blocked-rotor test is

$$P_{\rm br} = 2I_{\rm br}^2(r_s + r_r') \tag{6C-6}$$

From which

$$r_r' = \frac{P_{\rm br}}{2I_{\rm br}^2} - r_s = \frac{469}{(2)(16.1)^2} - 0.531 = 0.374\,\Omega \tag{6C-7}$$

The magnitude of the blocked-rotor input impedance is

$$|Z_{\rm br}| = \frac{V_{\rm br}}{I_{\rm br}} = \frac{23.5}{16.1} = 1.46\,\Omega \tag{6C-8}$$

Thus,

$$|(r_s + r_r') + j\tfrac{15}{60}(X_{ls} + X_{lr}')| = 1.46\,\Omega \tag{6C-9}$$

from which

$$\begin{aligned}\left[\tfrac{15}{60}(X_s + X_{lr}')\right]^2 &= (1.46)^2 - (r_s + r_r')^2 \\ &= 1.46^2 - (0.531 + 0.374)^2 = 1.31\,\Omega^2\end{aligned} \tag{6C-10}$$

Thus,

$$X_{ls} + X_{lr}' = 4.58\,\Omega \tag{6C-11}$$

Generally, X_{ls} and X_{lr}' are assumed equal; however, in some types of induction machines a different ratio is suggested. We will assume $X_{ls} = X_{lr}'$, whereupon we have determined the machine parameters. In particular, for $\omega_e = 377$ rad/s, the parameters are $r_s = 0.531\,\Omega$, $X_{ls} = 2.29\,\Omega$, $X_{ms} = 26.2\,\Omega$, $r_r' = 0.374\,\Omega$, and $X_{lr}' = 2.29\,\Omega$.

Example 6D. A four-pole, 110-V (rms), 28-A, 7.5-hp, two-phase, induction motor has the following parameters: $r_s = 0.3\,\Omega$, $L_{ls} = 0.0015$ H, $L_{ms} = 0.035$ H, $r_r' = 0.15\,\Omega$, and $L_{lr}' = 0.0007$ H. The machine is supplied from a 110-V, 60-Hz source. Calculate the starting torque and starting current.

It would be necessary to use a computer to solve for the starting current and torque if the electrical and mechanical transients are to be considered. However, an approximation of the actual starting characteristics may be obtained from a constant-speed, steady-state analysis. For this purpose, it is assumed that the speed is fixed at zero and the electric system has established steady-state operation:

$$X_{ss} = \omega_e(L_{ls} + L_{ms}) = 377(0.0015 + 0.035) = 13.76\ \Omega \tag{6D-1}$$

$$X'_{rr} = \omega_e(L'_{lr} + L_{ms}) = 377(0.0007 + 0.035) = 13.46\ \Omega \tag{6D-2}$$

$$X_{ms} = \omega_e L_{ms} = 377(0.035) = 13.2\ \Omega \tag{6D-3}$$

The steady-state torque with $\omega_r = 0$ ($s = 1$) may be calculated from (6.8-26):

$$\begin{aligned} T_e &= \frac{2(P/2)X_{ms}^2/\omega_e)r'_r s|\tilde{V}_{as}|^2}{[r_s r'_r + s(X_{ms}^2 - X_{ss}X'_{rr})]^2 + (r'_r X_{ss} + s r_s X'_{rr})^2} \\ &= \frac{2(\frac{4}{2})(13.2^2/377)(0.15)(1)(110)^2}{\{(0.3)(0.15)+(1)[13.2^2-(13.76)(13.46)]\}^2+[(0.15)(13.76)+(1)(0.3)(13.46)]^2} \\ &= 21.4\ \text{N}\cdot\text{m} \end{aligned} \tag{6D-4}$$

Since $s = 1$, the rotor impedance in parallel with X_{ms} is much smaller than X_{ms}. Thus, for this mode of operation the input impedance is approximately

$$\begin{aligned} Z &= (r_s + r'_r) + j(X_{ls} + X'_{lr}) \\ &= (0.30 + 0.15) + j377(0.0015 + 0.0007) \\ &= 0.45 + j0.83\ \Omega \end{aligned} \tag{6D-5}$$

Assuming $\tilde{V}_{as}$ as the reference phasor, then

$$\tilde{I}_{as} = \frac{\tilde{V}_{as}}{Z} = \frac{110\underline{/0^\circ}}{0.944\underline{/61.5^\circ}} = 117\underline{/-61.5^\circ}\,A \tag{6D-6}$$

The stall or starting current is over four times larger than the rated current. In some large machines, the starting current with rated voltage applied may be ten times the rated current. This high value of current may cause overheating and damage to the windings. Consequently, reduced voltage is applied to many large machines during the starting period, and rated voltage is not applied until the machine has accelerated to near rated speed. This is generally accomplished by closed-transition transformer switching, wherein the voltage is increased by switching from a lower to a higher transformer tap without opening the stator circuits.

SP6.8-1 The rotor speed ω_{rm} of a six-pole, two-phase induction motor is $0.3\omega_e$. Express (a) I'_{ar}, (b) I'^s_{qr}, and (c) $\tilde{I}'_{ar}$ for balanced steady-state operation with $\tilde{I}'^s_{qr} = I'_r\underline{/30^\circ}$. [(a) $I'_{ar} = \sqrt{2}\, I'_r \cos(0.1\omega_e t + 30^\circ)$; (b) $I'^s_{qr} = \sqrt{2}\, I'_r \cos(\omega_e t + 30^\circ)$; (c) $\tilde{I}'_{ar} = \tilde{I}'^s_{qr}$]

SP6.8-2 Neglecting the current flowing in X_{ms} is generally an acceptable approximation when calculating the machine parameters from the blocked-rotor test (Example 6C). However, this approximation is not valid when calculating the blocked-rotor torque. Use (6.8-21) to show that T_e is zero regardless of the rotor speed if the current flowing in X_{ms} is assumed to be negligibly small. [Let $\tilde{I}_{as} = a + jb$]

SP6.8-3 Neglect the core losses and assume that the friction and windage losses P_{fWC}, calculated in Example 6B, are to be represented by $B_m\omega_{rm}$, with B_m selected so that a load equivalent to 118.2 W occurs at $\omega_r = 0.9\omega_e$. Determine B_m. [$B_m = 4.11 \times 10^{-3}$ N · m · s/rad]

SP6.8-4 The parameters of a 60-Hz, four-pole, two-phase induction motor are $r_s = r'_r = 20\ \Omega$, $L_{ls} = L'_{lr} = 25$ mH, and $L_{ms} = 0.3$ H. Calculate $\tilde{I}_{as}$ for (a) no-load conditions and (b) blocked-rotor conditions ($\omega_r = 0$), with $\tilde{V}_{as} = 115\underline{/0^\circ}$. Approximate the blocked-rotor current. [(a) $\tilde{I}_{as} = 0.927\underline{/-80.75^\circ}$A; (b) $\tilde{I}_{as} = 2.6\underline{/-25.2^\circ}$A]

6.9 DYNAMIC AND STEADY-STATE PERFORMANCE–MACHINE VARIABLES

It is instructive to observe the machine variables during transient and steady-state operation. For this purpose, the nonlinear differential equations that describe the induction machine were programmed on a computer. Two induction machines are considered; a 5-hp, general-purpose machine with characteristics typical of many two- and three-phase, squirrel-cage, industrial-type induction motors and a $\frac{1}{10}$-hp, two-phase, induction motor with high-resistance rotor windings to produce a relatively large starting torque. The majority of the performance characteristics given in this and the following section are for the single-fed, two-pole, two-phase, 5-hp, 110-V (rms), 60-Hz, induction machine with the following parameters: $r_s = 0.295\ \Omega$, $L_{ls} = 0.944$ mH, $L_{ms} = 35.15$ mH, $r'_r = 0.201\ \Omega$, and $L'_{lr} = 0.944$ mH.

The inertia of the rotor and connected mechanical load is $J = 0.026\ \mathrm{kg \cdot m^2}$.

The four-pole, two-phase, $\frac{1}{10}$-hp, 115-V(rms), 60-Hz, induction motor has the following parameters: $r_s = 24.5\ \Omega$, $L_{ls} = 27.06$ mH, $L_{ms} = 273.7$ mH, $r'_r = 23\ \Omega$, and $L'_{lr} = 27.06$ mH. The inertia of the rotor and connected mechanical load is $J = 1 \times 10^{-3}\ \mathrm{kg \cdot m^2}$. This device is shown in Fig. 6.2-3.

Free Acceleration from Stall

The free-acceleration characteristics are depicted in Figs. 6.9-1 and 6.9-2 for the 5-hp machine and in Figs. 6.9-3 and 6.9-4 for the $\frac{1}{10}$-hp motor. At $t = 0$, rated voltages are applied of the form $v_{as} = \sqrt{2}\, V_s \cos 377t$ and $v_{bs} = \sqrt{2} V_s \sin 377t$, where $V_s = 110$ V for the 5-hp machine and $V_s = 115$ V for the $\frac{1}{10}$-hp motor. The machines accelerate from stall with zero load torque and, since friction and windage losses are not taken into account, the simulated machine accelerates to synchronous speed. In practice, friction and windage losses would exist and the machines would not reach synchronous speed. Instead, they will operate at a speed slightly less than synchronous, developing an electromagnetic torque T_e sufficient to satisfy the small torque load due to friction and windage. For the two-pole machine (5 hp), synchronous speed is 3600 r/min, where $\omega_{rm} = 377$ rad/s. For the four-pole $\frac{1}{10}$-hp motor, synchronous speed is 1800 r/min, where $\omega_{rm} = 188.5$ rad/s. In both cases, ω_r, the electrical angular velocity of the rotors, is 377 rad/s at synchronous speed.

We will find that rated current (rms) for the 5-hp machine is on the order of 20 A and 1.5 A for the $\frac{1}{10}$-hp motor. The starting current for the 5-hp machine (Fig. 6.9-1) is approximately 120 A (rms) or on the order of six times the rated current. This ratio is typical of industrial-type induction motors, which, depending upon the load, may require reduced-voltage starting, as mentioned in Example 6C. The starting current for the $\frac{1}{10}$-hp motor is about 2 A (rms) or less than twice the rated current. These devices are designed to withstand full-voltage starting since they are often used in position- or motion-control systems requiring rapid, short-duration acceleration from stall and, depending upon the application, may seldom reach rated speed.

The transient offset of the stator and rotor currents, characteristic of rL circuits, is evident in Figs. 6.9-1 and 6.9-3. This transient or dc offset in the stator and rotor currents give rise to the transient pulsation in the electromagnetic torque. Note that the pulsation in torque, which is the frequency of the stator source voltages (60 Hz), disappears when the transient offsets in the stator and rotor currents disappear. Also apparent in the stator

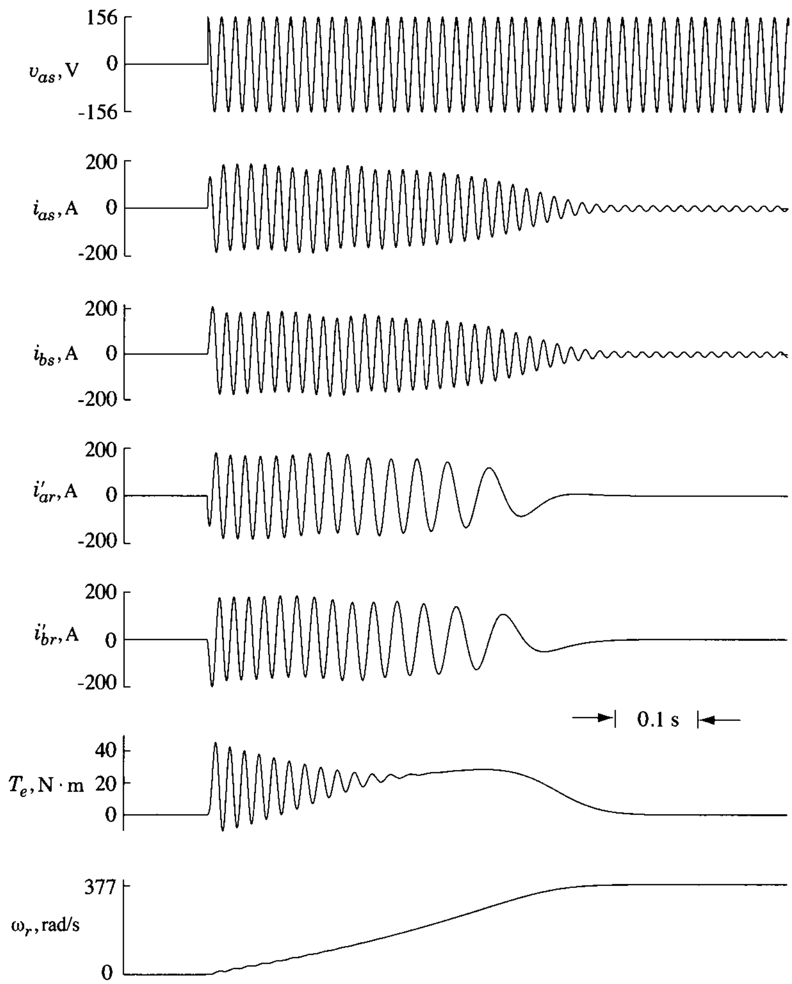

Figure 6.9-1: Free-acceleration characteristics of a two-pole, three-phase, 5-Hp induction motor – machine variables.

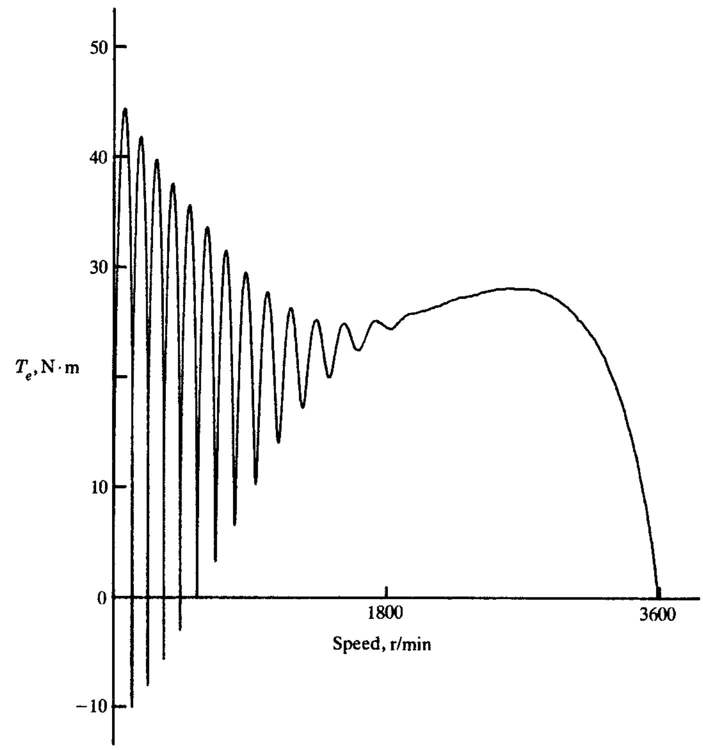

Figure 6.9-2: Torque versus speed during free-acceleration shown in Fig. 6.9-1.

and rotor currents, especially in the case of the 5-hp machine, is the variation in the envelope of the currents during the transient period, This is caused by the interaction of the transient offset in the stator currents with the transient offset in the rotor currents and the fact that the stator and rotor circuits are in relative motion [1].

For small-horsepower induction machines, the steady-state torque-speed characteristic is essentially the average of the transient torque-speed curve during the time the transient pulsating torque exists, The inertia of the rotor and connected load is generally large enough to prevent this pulsating torque from causing significant variations in rotor speed. This is not the case, however, if the induction machine is operated with stator voltages of low frequencies, as may occur in variable-frequency drive systems. Although we will not explore a detailed comparison between transient and steady-

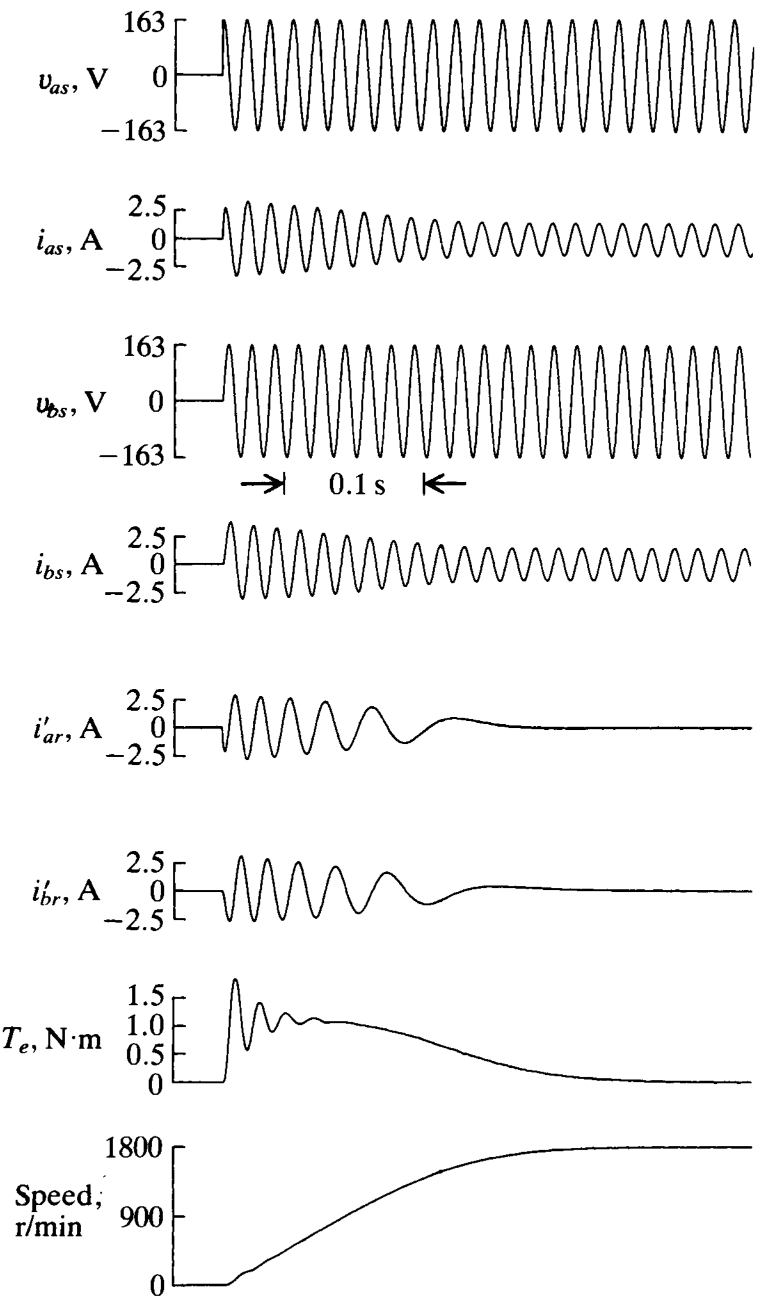

Figure 6.9-3: Free-acceleration characteristics of a four-pole, two-phase, 1/10-Hp induction motor – machine variables.

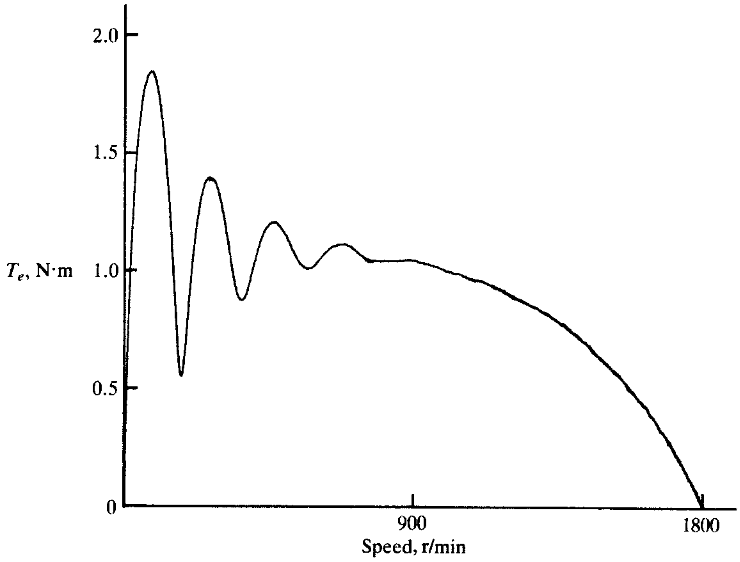

Figure 6.9-4: Torque versus speed during free-acceleration shown in Fig. 6.9-3.

state torque speed characteristics for rated frequency, it is worth mentioning in passing that the transient torque-speed characteristic of large-horsepower machines (larger than, say, 500 hp) may differ considerably from the steady-state characteristics, particularly at rotor speeds above 60 to 80 percent of synchronous speed [1].

Acceleration from Stall with Load Torque

The acceleration characteristics of the 5-hp motor with a load torque are shown in Figs. 6.9-5 and 6.9-6. Here, the load torque is $T_L = K\omega_{rm}^2$, where K is selected as $10/(377)^{-2}$ $\text{N} \cdot \text{m} \cdot \text{s}^2/\text{rad}^2$. A load torque characteristic of this type is typical of a fan load. Rated torque load is approximately 10 N · m. The constant K is selected so that a load torque of 10 N · m occurs at synchronous speed. In Fig. 6.9-6, the difference between the average value of the electromagnetic torque T_e and the load torque T_L is the torque that accelerates the rotor, commonly referred to as the accelerating torque. Acceleration occurs until $T_e = T_L$.

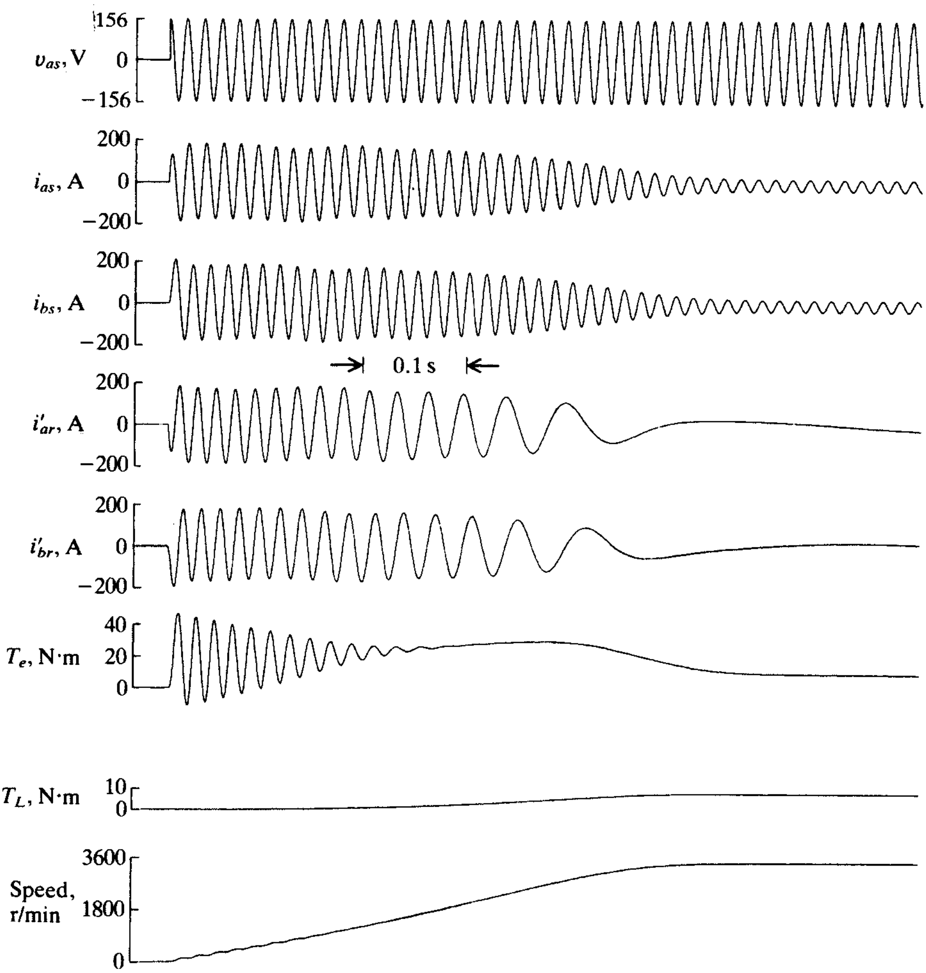

Figure 6.9-5: Acceleration from stall of a 5-Hp induction motor with $T_L = K\omega_{rm}^2$, where $K = 10(377)^{-2}\text{N} \cdot \text{m} \cdot \text{s}^2/\text{rad}^2$.

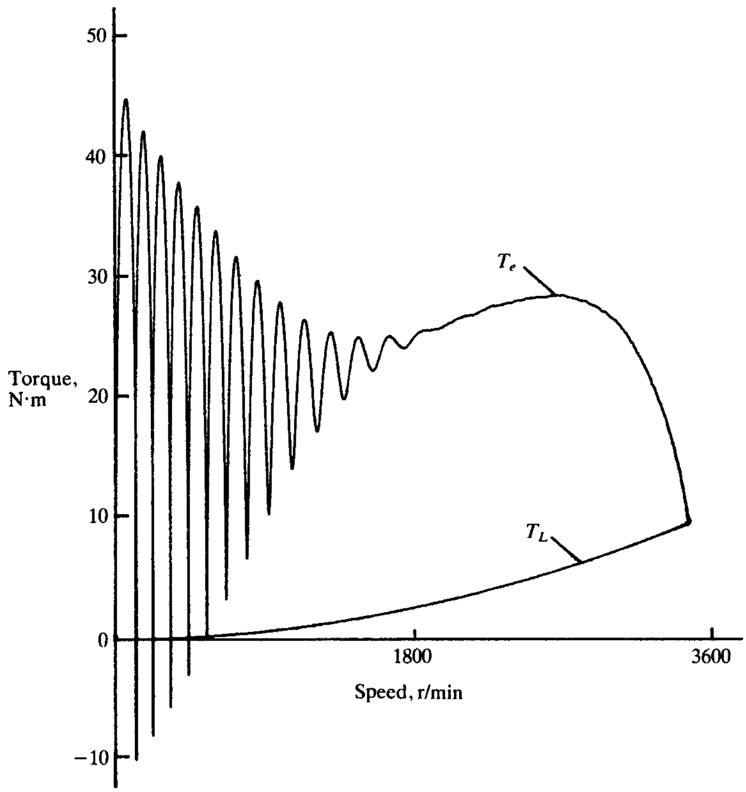

Figure 6.9-6: Torque versus speed during acceleration shown in Fig. 6.9-5.

Step Changes in Load Torque

The dynamic performance of the 5-hp motor during load torque changes are shown in Fig. 6.9-7. Initially, the machine is operating with a constant load torque of 5 N · m. The load torque is stepped to 10 N · m and the machine is allowed to reach steady-state operation, whereupon the load torque is stepped back to 5 N · m. You should be able to calculate the rotor speed for $T_L = 5$ N · m and $T_L = 10$ N · m from the frequency of the rotor currents shown in Fig. 6.9-7. (For $T_L = 5$ N · m, $\omega_{rm} \cong 370$ rad/s; $T_L = 10$ N · m, $\omega_{rm} \cong 362$ rad/s.)

Step Changes in Stator Frequency

In Fig. 6.9-8, the 5-hp induction machine is operating in the steady state with $T_L = 10$ N · m. The frequency of the stator voltages is stepped to 50 Hz, and, at the same time, the amplitude of the stator voltages is decreased

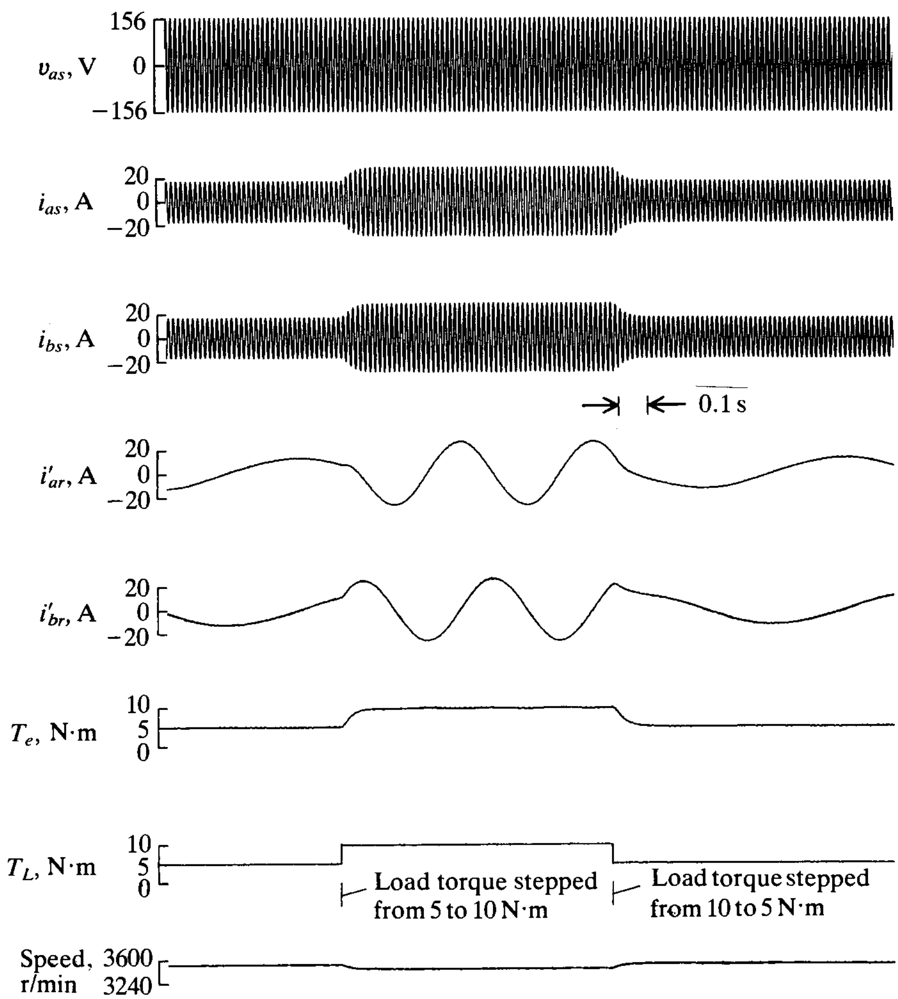

Figure 6.9-7: Step changes in load torque of a 5-Hp induction motor.

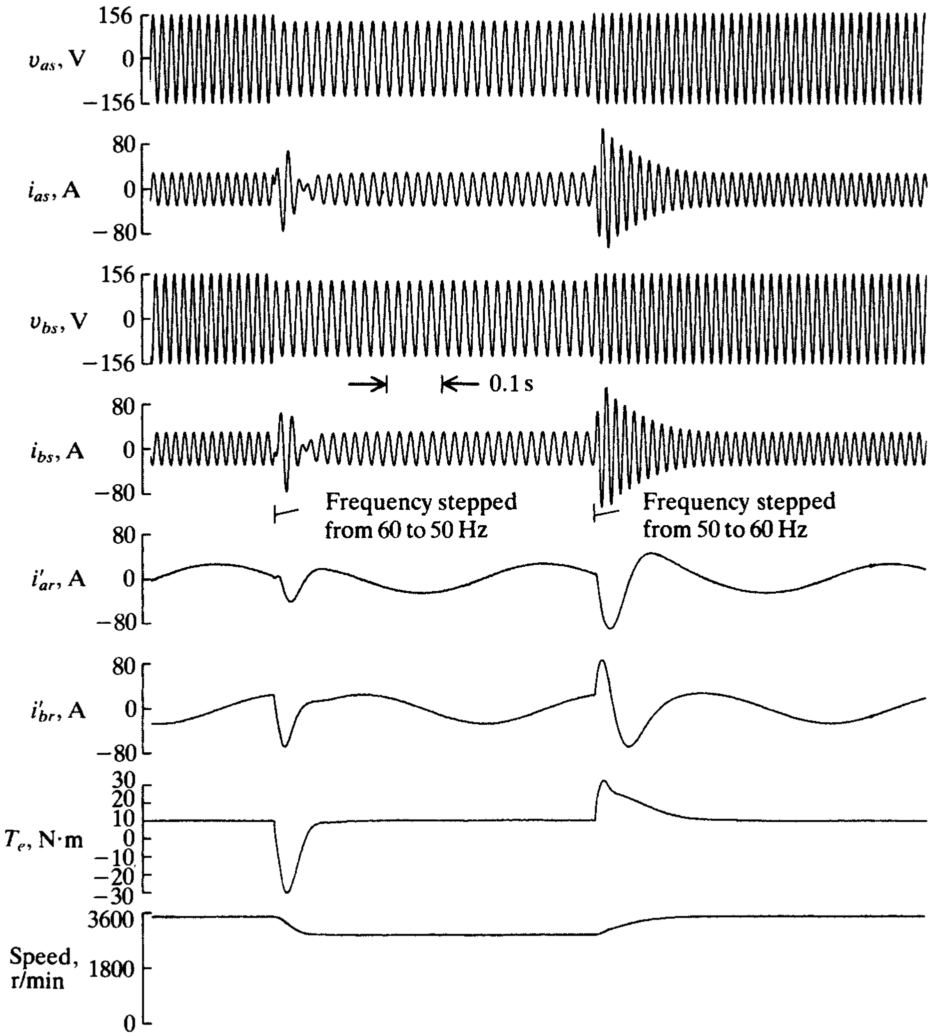

Figure 6.9-8: Step changes in the frequency of the stator voltages of a 5-Hp induction motor.

to $(\frac{5}{6})(110)$ V. Once the system has reached steady-state operation, the frequency and amplitude of the stator voltages are stepped back to rated (60 Hz and 110 V). The load torque was held fixed at 10 N · m during this change in stator frequency. This type of operation is possible when the induction machine is supplied from a variable-frequency inverter, whereby the frequency and amplitude of the fundamental component of the stator voltages may be rapidly changed by controlling the switching of the inverter which converts a dc voltage to a variable-frequency ac voltage.

The dynamic torque-speed characteristics during these step changes in frequency are shown in Fig. 6.9-9. Therein, the steady-state torque-speed characteristics for 50- and 60-Hz operations are also shown. Initially, operation is at point 1. When the frequency and voltage amplitude are changed, the instantaneous torque decreases, whereupon the rotor slows down and

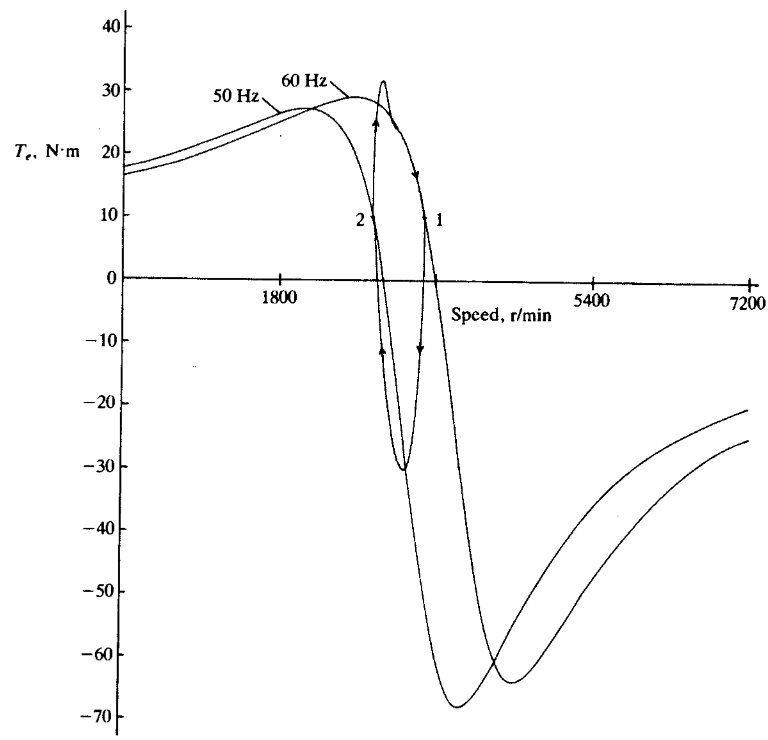

Figure 6.9-9: Torque vesus speed for step changes in the stator frequency shown in Fig. 6.9-8.

steady-state operation finally occurs at point 2. When the stator voltages are stepped back to rated conditions, the instantaneous torque increases, the rotor accelerates, and the original operating condition is reestablished.

SP6.9-1 Approximate the accelerating torque from Fig. 6.9-6 when the rotor speed is 280 rad/s. [$\cong$ 23 N · m]
SP6.9-2 In going from point 1 to point 2 in Fig. 6.9-9, the induction machine acts as a generator supplying energy to the electric system. What is the source of this energy. [Rotor]

6.10 FREE ACCELERATION VIEWED FROM STATIONARY, ROTOR, AND SYNCHRONOUSLY ROTATING REFERENCE FRAMES

It is instructive to view the free acceleration of the 5-hp, two-phase induction motor in the reference frames commonly used for induction-machine analysis and control. Free acceleration portrayed in stationary reference frame variables is shown in Fig. 6.10-1, rotor reference frame variables in Fig. 6.10-2, and synchronously rotating reference frame variables in Fig. 6.10-3. Each of these traces should be compared to Fig. 6.9-1, which depicts the same free acceleration in machine (actual) variables.

SP6.10-1 Determine the steady-state frequency of (a) i'_{ar} and i'_{br} in Fig. 6.9-1, (b) i'^{s}_{qr} and i'^{s}_{dr} in Fig. 6.10-1, (c) i'^{r}_{qr} and i'^{r}_{dr} in Fig. 6.10-2, and (d) i^{e}_{qr} and i^{e}_{dr} in Fig. 6.10-3. [(a) $\omega_e - \omega_r$, (b) ω_e, (c) $\omega_e - \omega_r$, (d) constant]
SP6.10-2 Repeat SP 6.10-1 for the stator related variables. [(a) ω_e, (b) ω_e, (c) $\omega_e - \omega_r$, (d) constant]

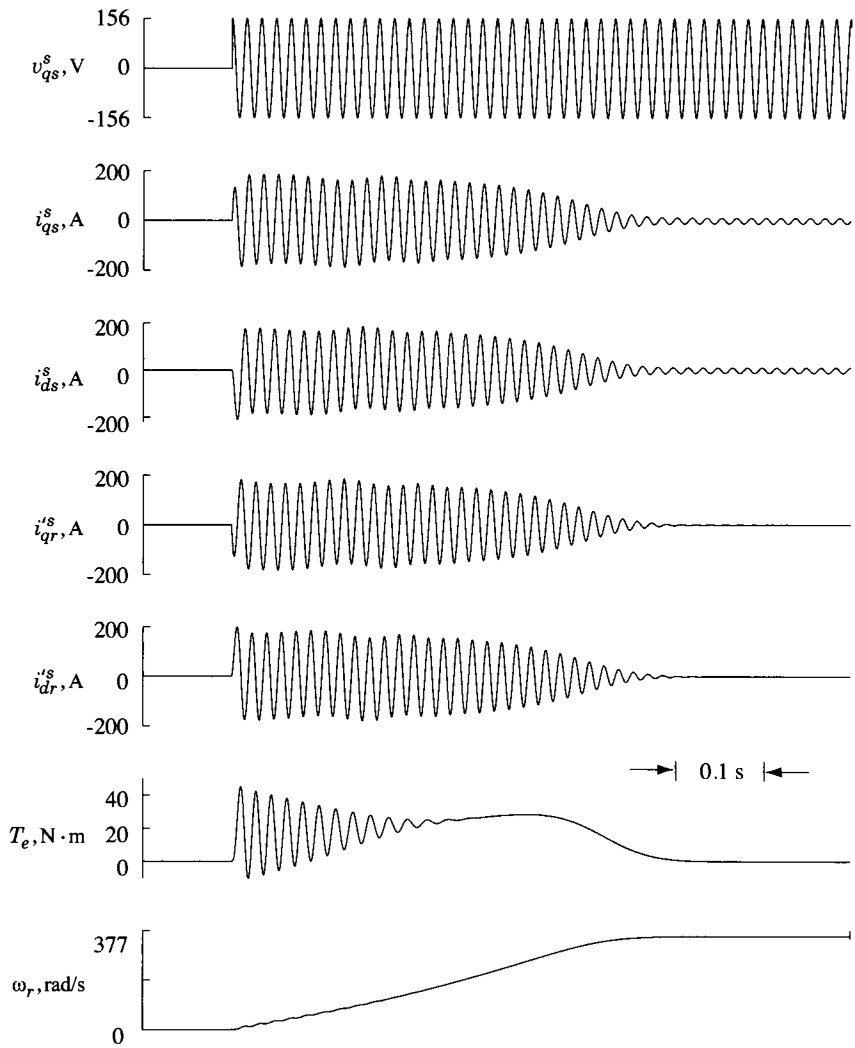

Figure 6.10-1: Same as Fig. 6.9-1 – stationary reference frame variables.

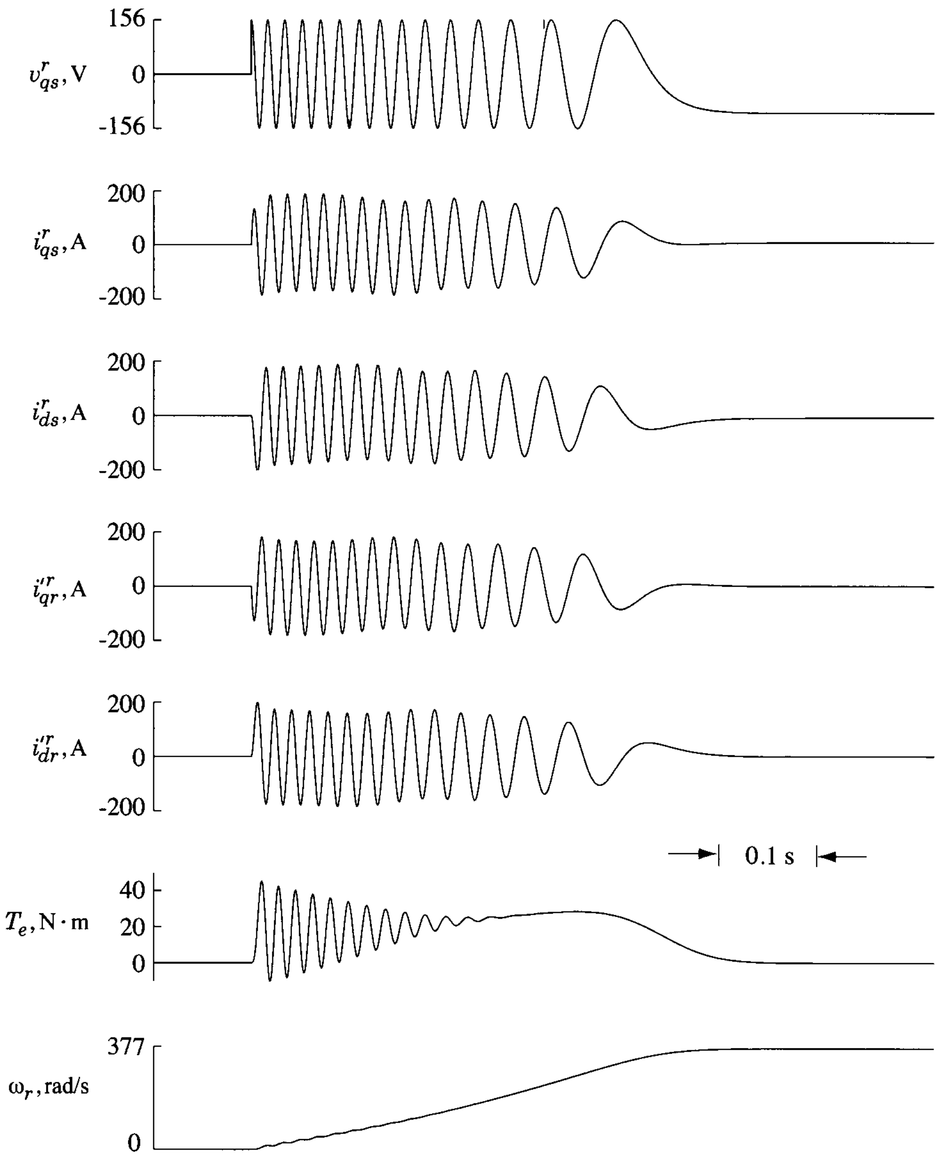

Figure 6.10-2: Same as Fig. 6.9-1 – rotor reference frame variables.

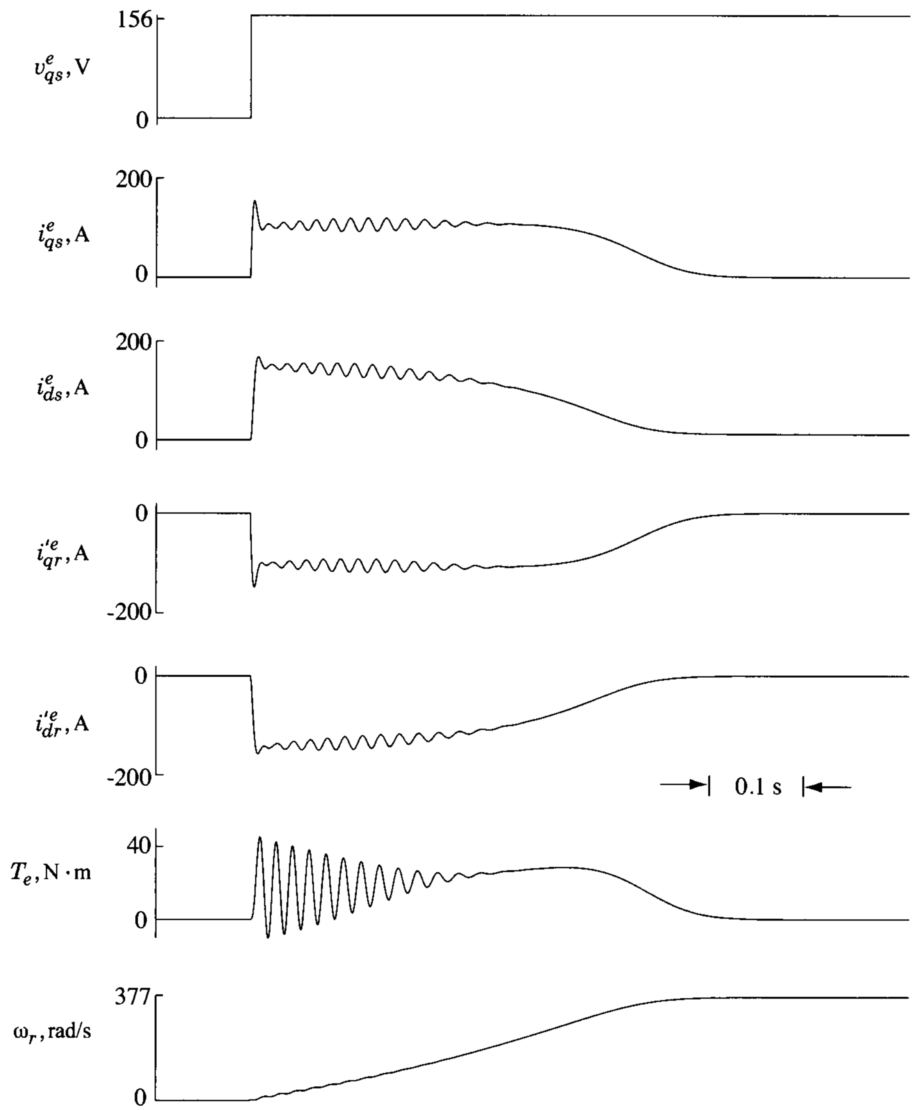

Figure 6.10-3: Same as Fig. 6.9-1 – synchronous reference frame variables.

6.11 INTRODUCTION TO FIELD-ORIENTED CONTROL

As has been mentioned, the advent and the ever-increasing sophistication of controlled electronic switching devices has opened the door to an array of various performance controls of electric machines, field-oriented control being one that is widely used. In Chapter 3, constant torque and power modes of control of a permanent-magnet dc machine were described. It was pointed out that since the magnetic fields of the dc machine are orthogonal, the device develops the maximum torque possible for given field strengths. Therefore, orthogonal magnetic systems is often the goal of the modern control of ac machinery.

Since the goal of field-oriented control is to control the ac machine to emulate a dc machine, it seems very logical that this control technique is most directly analyzed and implemented using the variables of the ac machine in a reference frame where the variables resemble those of a dc machine, that is, constant during steady-state operation. In the case of the symmetrical induction machine, this is the synchronously rotating reference frame ($\omega = \omega_e$). Also, the variables to be controlled should be readily accessible or accurately calculated from accessible machine variables. Therefore, we should not be surprised if we find it necessary to incorporate the transformation $\mathbf{K}_s^e$ in the control.

The voltage equations of an induction machine in the synchronously rotating reference frame are given by (6A-9) through (6A-12) and repeated here:

$$v_{qs}^e = r_s i_{qs}^e + \omega_e \lambda_{ds}^e + p\lambda_{qs}^e \tag{6.11-1}$$

$$v_{ds}^e = r_s i_{ds}^e - \omega_e \lambda_{qs}^e + p\lambda_{ds}^e \tag{6.11-2}$$

$$v_{qr}'^e = r_r' i_{qr}'^e + (\omega_e - \omega_r)\lambda_{dr}'^e + p\lambda_{qr}'^e \tag{6.11-3}$$

$$v_{dr}'^e = r_r' i_{dr}'^e - (\omega_e - \omega_r)\lambda_{qr}'^e + p\lambda_{dr}'^e \tag{6.11-4}$$

The flux-linkage equations may be obtained by rearranging (6.6-8) through (6.6-11) and adding the superscript e. Thus,

$$\lambda_{qs}^e = L_{ss} i_{qs}^e + L_{ms} i_{qr}'^e \tag{6.11-5}$$

$$\lambda_{ds}^{e} = L_{ss} i_{ds}^{e} + L_{ms} i_{dr}^{\prime e} \tag{6.11-6}$$

$$\lambda_{qr}^{\prime e} = L_{rr}^{\prime} i_{qr}^{\prime e} + L_{ms} i_{qs}^{e} \tag{6.11-7}$$

$$\lambda_{dr}^{\prime e} = L_{rr}^{\prime} i_{dr}^{\prime e} + L_{ms} i_{ds}^{e} \tag{6.11-8}$$

The torque equation for a linear magnetic system may be expressed from (6.7-2) with the superscript e added:

$$T_e = \frac{P}{2} \left(\lambda_{qr}^{\prime e} i_{dr}^{\prime e} - \lambda_{dr}^{\prime e} i_{qr}^{\prime e} \right) \tag{6.11-9}$$

The torque of a dc machine is the cross product of orthogonal magnetic systems. We see from (6.11-9) that the two terms within the parentheses each satisfy this cross-product requirement since each is flux linkage times an orthogonally directed current; however, the two terms are not additive. It is customary in field-oriented control to align the d axis of the synchronous reference frame with the north pole of the synchronously rotating magnetic field established by the rotor currents. In this case, $\lambda_{qr}^{\prime e}$ is identically zero [4]. From (6.11-7) with $\lambda_{qr}^{\prime e} = 0$,

$$i_{qr}^{\prime e} = -\frac{L_{ms}}{L_{rr}^{\prime}} i_{qs}^{e} \tag{6.11-10}$$

Substituting (6.11-10) into (6.11-9) with $\lambda_{qr}^{\prime e} = 0$, yields

$$T_e = \frac{P}{2} \frac{L_{ms}}{L_{rr}^{\prime}} \lambda_{dr}^{\prime e} i_{qs}^{e} \tag{6.11-11}$$

Since $\lambda_{qr}^{\prime e}$ is identically zero, then $p\lambda_{qr}^{\prime e} = 0$. Therefore, since $v_{qr}^{\prime e}$ and $v_{dr}^{\prime e}$ are both zero in the case of a single-fed induction machine, (6.11-3) becomes

$$0 = r_r^{\prime} i_{qr}^{\prime e} + (\omega_e - \omega_r) \lambda_{dr}^{\prime e} \tag{6.11-12}$$

Substituting (6.11-10) into (6.11-12) and solving for $\omega_e - \omega_r$ yields

$$\omega_e - \omega_r = r_r^{\prime} \frac{L_{ms}}{L_{rr}^{\prime}} \frac{i_{qs}^{e}}{\lambda_{dr}^{\prime e}} \tag{6.11-13}$$

Let us take a minute to recall that ω_e is two things: the frequency of the stator variables and the electrical angular velocity of the synchronously rotating reference frame. Equation (6.11-13) makes us wonder if it is necessary to vary frequency of the stator variables in order to implement field-oriented control. It is; but, we have not shown that quite yet.

Let us now solve (6.11-8) for $i_{dr}'^{e}$:

$$i_{dr}'^{e} = \frac{1}{L_{rr}'}(\lambda_{dr}'^{e} - L_{ms} i_{ds}^{e}) \tag{6.11-14}$$

If we substitute (6.11-14) into (6.11-4) with $\lambda_{qr}'^{e} = 0$, and since $v_{dr}'^{e}$ is zero, we can solve for $\lambda_{dr}'^{e}$. Thus,

$$\lambda_{dr}'^{e} = \frac{L_{ms}}{\tau_r p + 1} i_{ds}^{e} \tag{6.11-15}$$

where $\tau_r = L_{rr}'/r_r'$. Finally, if we substitute (6.11-15) into the expression for torque given by (6.11-11),

$$T_e = \left(\frac{P}{2}\right) \frac{(L_{ms}^2/L_{rr}')}{\tau_r p + 1} i_{ds}^{e} i_{qs}^{e} \tag{6.11-16}$$

Equation (6.11-16) is an expression for torque as a product of two orthogonally directed currents, much as in the case of the dc machine with a field winding. More important, however, is that the two currents are related to stator currents i_{as} and i_{bs} by the transformation $\mathbf{K}_s^e$. In other words, the torque is expressed in terms of variables that are related to accessible machine variables.

Our goal is to control the torque that is produced. We will denote the commanded stator currents with an asterisk. That is, i_{qs}^{e*} and i_{ds}^{e*} are the commanded values of the q and d components of stator current, whereas i_{qs}^{e} and i_{ds}^{e} are the actual values. We will assume that we have the means to set the stator currents to any value that we command: $i_{qs}^{e} = i_{qs}^{e*}$ and $i_{ds}^{e} = i_{ds}^{e*}$. Equation (6.11-15) becomes

$$\lambda_{dr,\text{calc}}'^{e} = \frac{L_{ms}}{\tau_r p + 1} i_{ds}^{*e} \tag{6.11-17}$$

and from (6.11-13)

$$(\omega_e - \omega_r)_{\text{calc}} = r_r' \frac{L_{ms}}{L_{rr}'} \frac{i_{qs}^{e*}}{\lambda_{dr,\text{calc}}'^{e}} \tag{6.11-18}$$

The subscript "calc" has been added in (6.11-17) and (6.11-18) to emphasize that these quantities are calculated from commanded values using machine paramaters L_{ms}, L_{rr}', and r_r'. This method of field-oriented control is often referred to as the indirect method of control [4-6]. If the equations and the values of the parameters are correct for all operating conditions, then these calculated values would be the same as the corresponding machine quantities. In addition, it the measured rotor speed is exact and the inverter is designed such that the commanded i_{as}^* and i_{bs}^* are tracked at the commanded frequency ω_e^*, then the slip frequency $(\omega_e - \omega_r)$ will be indistinguishabe from the calculated slip frequency $(\omega_e - \omega_r)_{\text{calc}}$.

The block diagram shown in Fig. 6.11-1 illustrates the basic concepts of field-oriented control of an induction machine. It is important to note that the calculated (commanded) slip frequency is added to the measured rotor speed, ω_r, and the output of this summation is denoted ω_e, which is the commanded (and actual) electrical angular velocity of the stator variables and, therefore, the speed of the synchronously rotating reference frame. When the rotor is stalled ($\omega_r = 0$) the electrical angular velocity of the stator variables is equal to the commanded slip frequency, which is generally the slip frequency at rated conditions. The electrical angular velocity is then integrated to obtain θ_e, which is the angular displacement of the transformation $(\mathbf{K}_s^e)^{-1}$.

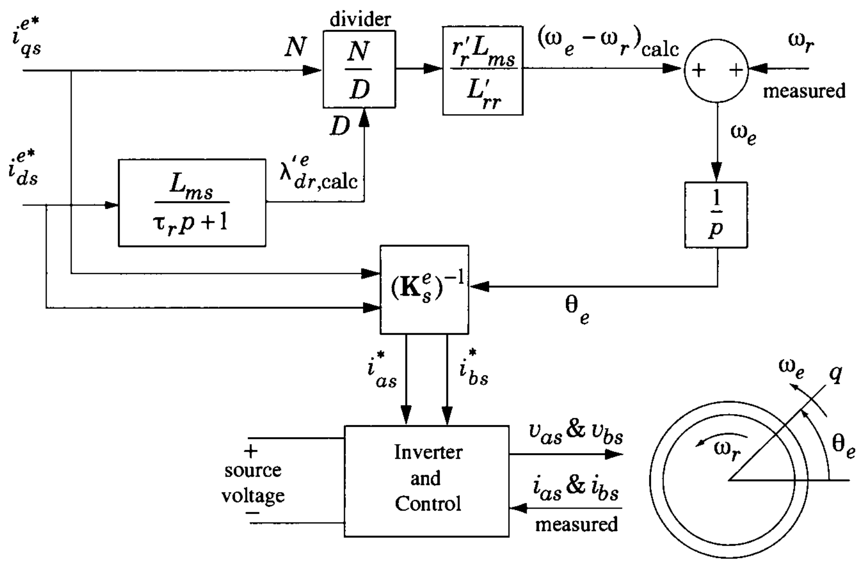

Figure 6.11-1: Block diagram of field-oriented control of an induction machine.

The commanded currents i_{qs}^{e*} and i_{ds}^{e*} are used to calculate $(\omega_e - \omega_r)_{\text{calc}}$ as shown in Fig. 6.11-1. Generally, i_{ds}^{e*} is held constant or varied slightly to maintain rated flux and i_{qs}^{e*} is then determined from (6.11-16) depending upon the output torque desired. These commanded currents are also supplied to the transformation $(\mathbf{K}_s^e)^{-1}$ to make up i_{as}^* and i_{bs}^*, which are the reference (command) currents for the control of the stator currents i_{as} and i_{bs}.

Our purpose now is to establish the performance boundaries of the induction machine with field-oriented control, assuming ideal conditions in which all machine parameters are constant and correctly determined, and the field-oriented control and the converter are properly designed. Let us also assume that the control is designed so that rated voltage, current, torque, speed, and power all occur together. In addition, we will assume that the output torque T_e is controlled to rated T_{eR} for $0 < \omega_r < \omega_{rR}$, which establishes the boundary operating points. Figure 6.11-2 depicts this type of operation with a load torque T_{L1}, which is assumed to be a linear function of rotor speed and intersects the torque-speed characteristics at rated conditions (point 1).

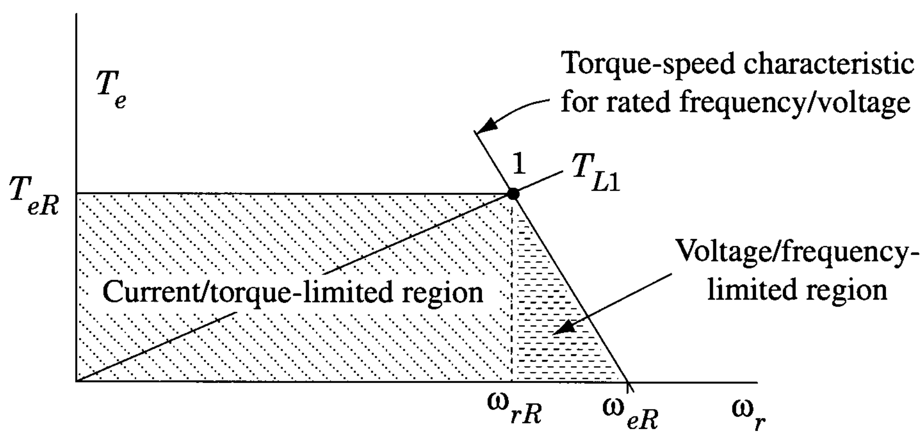

Figure 6.11-2: Region of operation during constant (rated) torque operation.

To ensure rated conditions at point 1 in Fig. 6.11-2, i_{qs}^{e*} and i_{ds}^{e*} can be calculated from the rated conditions, and we will assume that i_{ds}^{e*} is held fixed at this calculated value; i_{qs}^{e*} will also be fixed at the value to give rated torque. For this condition, $(\omega_e - \omega_r)_{\text{calc}}$ becomes $\omega_{eR} - \omega_{rR}$, the slip frequency at rated conditions.

At stall, $\omega_r = 0$ and $T_e = T_{eR}$:

$$\omega_e = \omega_{eR} - \omega_{rR} \quad \text{for } \omega_r = 0 \tag{6.11-19}$$

This is the electrical angular velocity of the stator variables at stall, which is the slip frequency at rated conditions. Figure 6.11-3 shows the electrical angular rotor speed and the electrical angular velocity of the stator variables during acceleration from stall with the torque output controlled at rated.

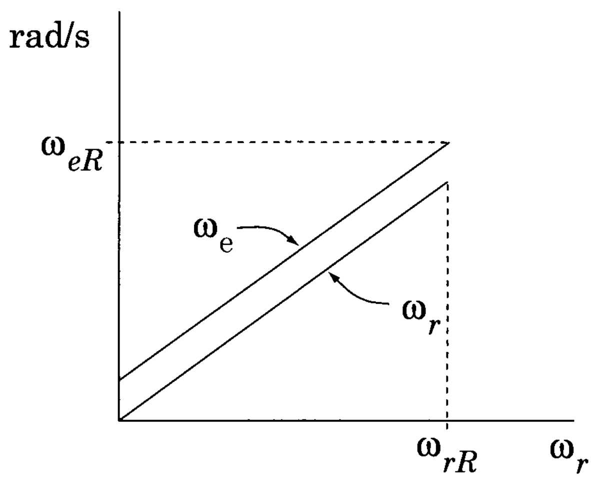

Figure 6.11-3: Electrical frequency of stator variables and rotor speed for rated torque.

At this time, it would be helpful for the reader to revisit the torque-speed plots for variable frequency operation shown in Fig. 6.8-5. At stall, ω_e is the slip frequency with $T_e = T_{eR}$. As the rotor speed increases, ω_e increases (Fig. 6.11-3), whereupon the torque-speed plot is shifting to the right. Recall that zero torque occurs at ω_e. Therefore, one should visualize the steep negative slope portion of the torque-speed characteristics shifting toward the right (Fig. 6.8-5) as ω_e increases. In Fig. 6.11-2, the intersection of the steep negative-slope portion of the rated torque-speed characteristics (shown as a straight line with $T_e = 0$ occurring at ω_{eR}) with the load torque-speed plot is point 1. The region of possible operating points falls within the shaded area shown in Fig. 6.11-2. It is clear that the right boundary is the normal rated torque-speed characteristics, which are limited by rated voltage.

Operation of an induction machine with field-oriented control with different load-torque characteristics is shown in Fig. 6.11-4. Operating point 1 is the same as that in Fig. 6.11-2. If operation is at point 1 and the load torque is increased such that the load torque-versus-speed characteristic becomes T_{L2}, the rotor speed will start decreasing and, since the slip frequency is commanded constant, ω_e will decrease and operation will occur at point 2. The steep negative-slope line intersecting point 2 is the torque-speed characteristics for the new operating frequency. If initial operation is again at point 1 and the load torque is decreased to T_{L3}, the voltage limitation would prevent operation at rated torque and the load-torque characteristics would intersect the rated torque-speed characteristic at point 3.

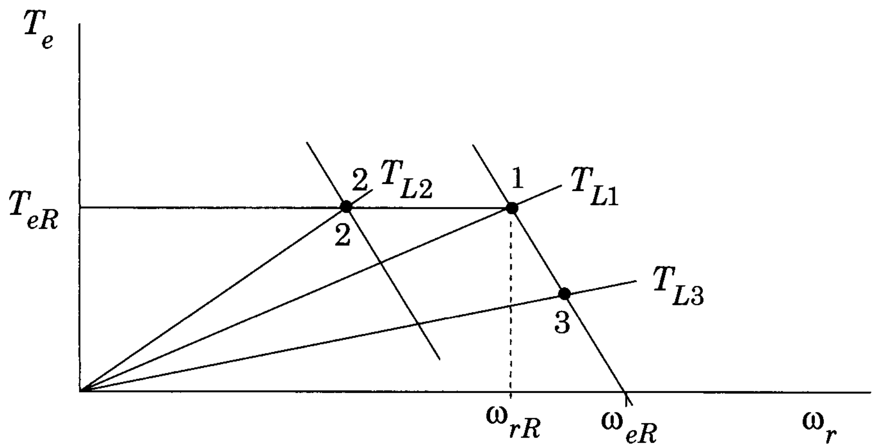

Figure 6.11-4: Operation with field-oriented control for different load torques.

Various field-oriented control strategies and designs have been set forth in the recent past [4, 5] and there are many practical issues that we have only mentioned in passing in this text. However, our purpose has been to introduce the concepts of field-oriented control and the factors that affect performance characteristics. If we have done our job, you should be prepared to address these practical issues in subsequent courses or as practicing engineers.

SP6.11-1 Verify (6.11-15).
SP6.11-2 What would cause inaccuracies in (6.11-17) and (6.11-17)? [Increase in r'_r due to heating]
SP6.11-3 The starting current of an induction motor can be less with field-oriented control than without. Why? [T_e is controlled]

6.12 THREE-PHASE INDUCTION MACHINE

A two-pole, three-phase symmetrical induction machine is shown in Fig. 6.12-1. The three-phase machine has three identical, sinusoidally distributed stator (rotor) windings, the magnetic axes of that are displaced 120° from each other. For the most part, the analysis of a three-phase machine is a direct extension of that of a two-phase machine. Therefore, it is unnecessary to repeat many of the details set forth thus far in this chapter. In fact, once we are acquainted with the two-phase symmetrical induction machine, the analysis of the three-phase symmetrical induction machine is straightforward and is more involved only because of the trigonometry necessary to deal with three-phase variables to transform rather than two. Perhaps the only aspect that may cause some study is the addition of the third fictitious variable in the transformation. However, these so-called zero variables or zero quantities play no role in the analysis of balanced operation of three-phase symmetrical induction machines. We will not consider unbalanced operation; a detailed analysis of unbalanced operation is found in [1].

Voltage Equations and Winding Inductances
For the three-phase symmetrical induction machine,

$$v_{as} = r_s i_{as} + \frac{d\lambda_{as}}{dt} \tag{6.12-1}$$

$$v_{bs} = r_s i_{bs} + \frac{d\lambda_{bs}}{dt} \tag{6.12-2}$$

$$v_{cs} = r_s i_{cs} + \frac{d\lambda_{cs}}{dt} \tag{6.12-3}$$

$$v_{ar} = r_r i_{ar} + \frac{d\lambda_{ar}}{dt} \tag{6.12-4}$$

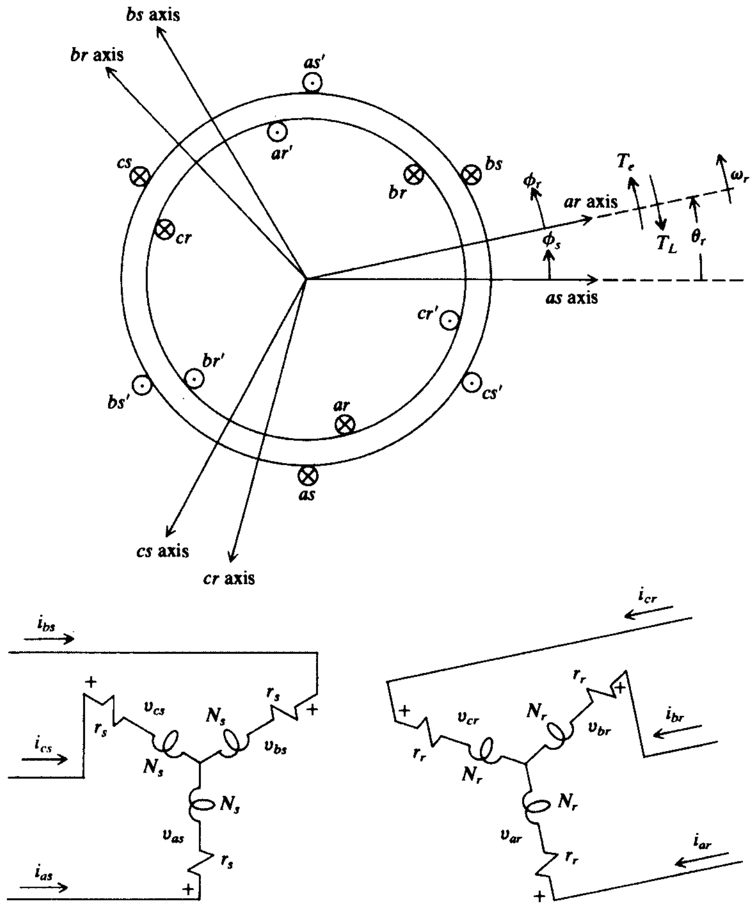

Figure 6.12-1: A two-pole, three-phase symmetrical induction machine.

$$v_{br} = r_r i_{br} + \frac{d\lambda_{br}}{dt} \tag{6.12-5}$$

$$v_{cr} = r_r i_{cr} + \frac{d\lambda_{cr}}{dt} \tag{6.12-6}$$

where $r_s(r_r)$ is the resistance of the stator (rotor) windings. In matrix form,

$$\mathbf{v}_{abcs} = \mathbf{r}_s \mathbf{i}_{abcs} + p\boldsymbol{\lambda}_{abcs} \tag{6.12-7}$$

$$\mathbf{v}_{abcr} = \mathbf{r}_r \mathbf{i}_{abcr} + p\boldsymbol{\lambda}_{abcr} \tag{6.12-8}$$

where

$$(\mathbf{f}_{abcs})^T = [f_{as} \quad f_{bs} \quad f_{cs}] \tag{6.12-9}$$

$$(\mathbf{f}_{abcr})^T = [f_{ar} \quad f_{br} \quad f_{cr}] \tag{6.12-10}$$

and

$$\mathbf{r}_s = r_s \mathbf{I} \tag{6.12-11}$$

$$\mathbf{r}_r = r_r \mathbf{I} \tag{6.12-12}$$

As in the two-phase case, (6.11-9) and (6.11-10) can represent voltage, current, or flux linkage, the superscript T denotes the transpose, p is d/dt, and $\mathbf{I}$ a 3×3 identity matrix.

The flux-linkage equations may be written as

$$\begin{bmatrix} \boldsymbol{\lambda}_{abcs} \\ \boldsymbol{\lambda}_{abcr} \end{bmatrix} = \begin{bmatrix} \mathbf{L}_s & \mathbf{L}_{sr} \\ (\mathbf{L}_{sr})^T & \mathbf{L}_r \end{bmatrix} \begin{bmatrix} \mathbf{i}_{abcs} \\ \mathbf{i}_{abcr} \end{bmatrix} \tag{6.12-13}$$

Although the same notation is used for the inductance matrices as for the two-phase case, they are not the same. The self-inductances are all constant and can be expressed as in the case of the two-phase machine; however, a mutual coupling exists between stator (rotor) phases. To determine this mutual inductance, let us consider the coupling between the as and bs windings, and let us imagine that we can take a hold of the bs winding and rotate it 120° in a clockwise direction. If this were possible, then the as and bs windings would be on top of each other and, thus, tightly coupled with a mutual inductance of

$$L = \frac{N_s N_s}{\Re_m} = L_{ms} \tag{6.12-14}$$

If now we rotate the bs winding back to its original position and if we assume that the mutual inductance varies in proportion to $\cos\phi_s$ as the bs winding is rotated, then

$$L_{asbs} = L_{ms}\cos\phi_s\big|_{\phi_s=2\pi/3} = -\tfrac{1}{2}L_{ms} \tag{6.12-15}$$

It follows that

$$\mathbf{L}_s = \begin{bmatrix} L_{ss} & -\frac{1}{2}L_{ms} & -\frac{1}{2}L_{ms} \\ -\frac{1}{2}L_{ms} & L_{ss} & -\frac{1}{2}L_{ms} \\ -\frac{1}{2}L_{ms} & -\frac{1}{2}L_{ms} & L_{ss} \end{bmatrix} \tag{6.12-16}$$

$$\mathbf{L}_r = \begin{bmatrix} L_{rr} & -\frac{1}{2}L_{mr} & -\frac{1}{2}L_{mr} \\ -\frac{1}{2}L_{mr} & L_{rr} & -\frac{1}{2}L_{mr} \\ -\frac{1}{2}L_{mr} & -\frac{1}{2}L_{mr} & L_{rr} \end{bmatrix} \tag{6.12-17}$$

where $L_{ss} = L_{ls} + L_{ms}$ and $L_{rr} = L_{lr} + L_{mr}$. Also,

$$\mathbf{L}_{sr} = L_{sr}\begin{bmatrix} \cos\theta_r & \cos(\theta_r + \frac{2}{3}\pi) & \cos(\theta_r - \frac{2}{3}\pi) \\ \cos(\theta_r - \frac{2}{3}\pi) & \cos\theta_r & \cos(\theta_r + \frac{2}{3}\pi) \\ \cos(\theta_r + \frac{2}{3}\pi) & \cos(\theta_r - \frac{2}{3}\pi) & \cos\theta_r \end{bmatrix} \tag{6.12-18}$$

where

$$L_{sr} = \frac{N_s N_r}{\Re_m} \tag{6.12-19}$$

All rotor variables may be referred to the stator windings by the following turns ratios:

$$\mathbf{i}'_{abcr} = \frac{N_r}{N_s}\mathbf{i}_{abcr} \tag{6.12-20}$$

$$\mathbf{v}'_{abcr} = \frac{N_s}{N_r}\mathbf{v}_{abcr} \tag{6.12-21}$$

$$\boldsymbol{\lambda}'_{abcr} = \frac{N_s}{N_r}\boldsymbol{\lambda}_{abcr} \tag{6.12-22}$$

Thus, (6.12-7) and (6.12-8) become

$$\mathbf{v}_{abcs} = \mathbf{r}_s\mathbf{i}_{abcs} + p\boldsymbol{\lambda}_{abcs} \tag{6.12-23}$$

$$\mathbf{v}'_{abcr} = \mathbf{r}'_r\mathbf{i}'_{abcr} + p\boldsymbol{\lambda}'_{abcr} \tag{6.12-24}$$

where

$$\mathbf{r}'_r = \left(\frac{N_s}{N_r}\right)^2 \mathbf{r}_r \tag{6.12-25}$$

The flux linkage equations may now be written as

$$\begin{bmatrix} \boldsymbol{\lambda}_{abcs} \\ \boldsymbol{\lambda}'_{abcr} \end{bmatrix} = \begin{bmatrix} \mathbf{L}_s & \mathbf{L}'_{sr} \\ (\mathbf{L}'_{sr})^T & \mathbf{L}'_r \end{bmatrix} \begin{bmatrix} \mathbf{i}_{abcs} \\ \mathbf{i}'_{abcr} \end{bmatrix} \tag{6.12-26}$$

where, by definition,

$$\mathbf{L}'_{sr} = \frac{N_s}{N_r}\mathbf{L}_{sr} = \frac{L_{ms}}{L_{sr}}\mathbf{L}_{sr} \tag{6.12-27}$$

and

$$\mathbf{L}'_r = \begin{bmatrix} L'_{lr} + L_{ms} & -\frac{1}{2}L_{ms} & -\frac{1}{2}L_{ms} \\ -\frac{1}{2}L_{ms} & L'_{lr} + L_{ms} & -\frac{1}{2}L_{ms} \\ -\frac{1}{2}L_{ms} & -\frac{1}{2}L_{ms} & L'_{lr} + L_{ms} \end{bmatrix} \tag{6.12-28}$$

In (6.12-28),

$$L'_{lr} = \left(\frac{N_s}{N_r}\right)^2 L_{lr} \tag{6.12-29}$$

Torque

The electromagnetic torque, positive for motor action, may be expressed by using the second entry in Table 2.5-1. In particular,

$$\begin{aligned} T_e = -\frac{P}{2}L_{ms}\{[\, &i_{ar}(i'_{ar} - \tfrac{1}{2}i'_{br} - \tfrac{1}{2}i'_{cr}) + i_{bs}(i'_{br} - \tfrac{1}{2}i'_{ar} - \tfrac{1}{2}i'_{cr}) \\ &+ i_{cs}(i'_{cr} - \tfrac{1}{2}i'_{br} - \tfrac{1}{2}i'_{ar})] \sin\theta_r \\ &+ \tfrac{\sqrt{3}}{2}[i_{as}(i'_{br} - i'_{cr}) + i_{bs}(i'_{cr} - i'_{ar}) + i_{cs}(i'_{ar} - i'_{br})] \cos\theta_r\} \end{aligned} \tag{6.12-30}$$

The torque and rotor speeds are related by (6.4-5), which is repeated for convenience:

$$T_e = J\left(\frac{2}{P}\right)\frac{d\omega_r}{dt} + B_m\left(\frac{2}{P}\right)\omega_r + T_L \tag{6.12-31}$$

where J is the inertia of the rotor and, in some cases, the connected load. The units of J and the damping coefficient B_m are discussed following (6.4-5). The load torque T_L is positive for a torque load (motor action) on the shaft of the induction machine and T_e is also positive for motor action, as indicated in Fig. 6.12-1.

Voltage Equations in the Arbitrary Reference Frame

A change of variables which formulates a transformation of the three-phase variables of stationary (stator) circuits to the arbitrary reference frame may by expressed as

$$\mathbf{f}_{qd0s} = \mathbf{K}_s \mathbf{f}_{abcs} \tag{6.12-32}$$

where

$$(\mathbf{f}_{qd0s})^T = [\, f_{qs} \quad f_{ds} \quad f_{0s} \,] \tag{6.12-33}$$

$$(\mathbf{f}_{abcs})^T = [\, f_{as} \quad f_{bs} \quad f_{cs} \,] \tag{6.12-34}$$

$$\mathbf{K}_s = \frac{2}{3}\begin{bmatrix} \cos\theta & \cos\left(\theta - \frac{2}{3}\pi\right) & \cos\left(\theta + \frac{2}{3}\pi\right) \\ \sin\theta & \sin\left(\theta - \frac{2}{3}\pi\right) & \sin\left(\theta + \frac{2}{3}\pi\right) \\ \frac{1}{2} & \frac{1}{2} & \frac{1}{2} \end{bmatrix} \tag{6.12-35}$$

$$p\theta = \omega \tag{6.12-36}$$

It can be shown that for the inverse

$$(\mathbf{K}_s)^{-1} = \begin{bmatrix} \cos\theta & \sin\theta & 1 \\ \cos\left(\theta - \frac{2}{3}\pi\right) & \sin\left(\theta - \frac{2}{3}\pi\right) & 1 \\ \cos\left(\theta + \frac{2}{3}\pi\right) & \sin\left(\theta + \frac{2}{3}\pi\right) & 1 \end{bmatrix} \tag{6.12-37}$$

In the above equations, f can represent either voltage, current, flux linkage, or electric charge. The superscript T denotes the transpose of a matrix. The s subscript indicates the variables, parameters, and transformation associated with stationary circuits. The angular displacement θ must be continuous; however, the angular velocity associated with the change of variables is unspecified. The frame of reference may rotate at any constant or varying angular velocity or it may remain stationary.

A change of variables that formulates a transformation of the three-phase variables of the rotor circuits to the arbitrary reference frame is

$$\mathbf{f}'_{qd0r} = \mathbf{K}_r \mathbf{f}'_{abcr} \tag{6.12-38}$$

where

$$(\mathbf{f}'_{qd0r})^T = [f'_{qr} \quad f'_{dr} \quad f'_{0r}] \tag{6.12-39}$$

$$(\mathbf{f}'_{abcr})^T = [f'_{ar} \quad f'_{br} \quad f'_{cr}] \tag{6.12-40}$$

$$\mathbf{K}_r = \frac{2}{3}\begin{bmatrix} \cos\beta & \cos\left(\beta - \frac{2}{3}\pi\right) & \cos\left(\beta + \frac{2}{3}\pi\right) \\ \sin\beta & \sin\left(\beta - \frac{2}{3}\pi\right) & \sin\left(\beta + \frac{2}{3}\pi\right) \\ \frac{1}{2} & \frac{1}{2} & \frac{1}{2} \end{bmatrix} \tag{6.12-41}$$

$$\beta = \theta - \theta_r \tag{6.12-42}$$

where the angular displacement is defined by (6.12-36) and

$$p\theta_r = \omega_r \tag{6.12-43}$$

The inverse is

$$(\mathbf{K}_r)^{-1} = \begin{bmatrix} \cos\beta & \sin\beta & 1 \\ \cos\left(\beta - \frac{2}{3}\pi\right) & \sin\left(\beta - \frac{2}{3}\pi\right) & 1 \\ \cos\left(\beta + \frac{2}{3}\pi\right) & \sin\left(\beta + \frac{2}{3}\pi\right) & 1 \end{bmatrix} \tag{6.12-44}$$

The r subscript indicates the variables, parameters, and transformation associated with rotating circuits. Transforming the voltage equations given by (6.12-7) and (6.12-8) yields

$$v_{qs} = r_s i_{qs} + \omega\lambda_{ds} + p\lambda_{qs} \tag{6.12-45}$$

$$v_{ds} = r_s i_{ds} - \omega\lambda_{qs} + p\lambda_{ds} \tag{6.12-46}$$

$$v_{0s} = r_s i_{0s} + p\lambda_{0s} \tag{6.12-47}$$

$$v'_{qr} = r'_r i'_{qr} + (\omega - \omega_r)\lambda'_{dr} + p\lambda'_{qr} \tag{6.12-48}$$

$$v'_{dr} = r'_r i'_{dr} - (\omega - \omega_r)\lambda'_{qr} + p\lambda'_{dr} \tag{6.12-49}$$

$$v'_{0r} = r'_r i'_{0r} + p\lambda'_{0r} \tag{6.12-50}$$

Transforming (6.12-26) yields

$$\lambda_{qs} = L_{ls} i_{qs} + M(i_{qs} + i'_{qr}) \tag{6.12-51}$$

$$\lambda_{ds} = L_{ls} i_{ds} + M(i_{ds} + i'_{dr}) \tag{6.12-52}$$

$$\lambda_{0s} = L_{ls} i_{0s} \tag{6.12-53}$$

$$\lambda'_{qr} = L'_{lr} i'_{qr} + M(i_{qs} + i'_{qr}) \tag{6.12-54}$$

$$\lambda'_{dr} = L'_{lr} i'_{dr} + M(i_{ds} + i'_{dr}) \tag{6.12-55}$$

$$\lambda'_{0r} = L'_{lr} i'_{0r} \tag{6.12-56}$$

where

$$M = \tfrac{3}{2} L_{ms} \tag{6.12-57}$$

Equations (6.12-45) through (6.12-57) suggest the equivalent circuits shown in Fig. 6.12-2.

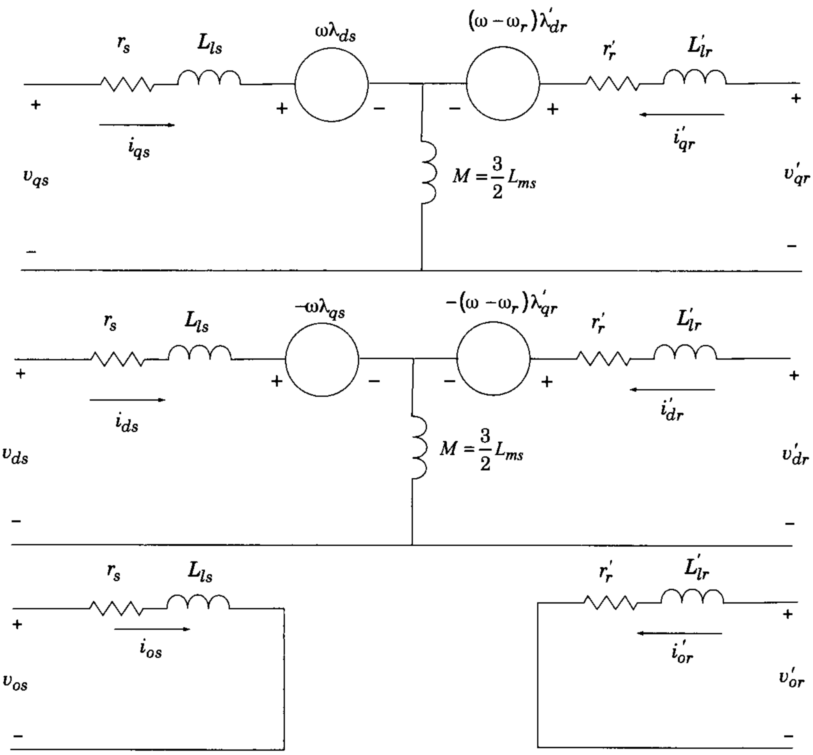

Figure 6.12-2: Arbitrary reference frame equivalent circuits for a three-phase, symmetrical induction machine.

Other than the zero-voltage equations (6.12-47) and (6.12-50) and the $\frac{3}{2}$ factor in (6.12-57), the voltage equations are the same as those for a two-phase induction machine. Moreover, if the three-phase induction machine is connected in wye without a neutral connection as shown in Fig. 6.12-1, the currents i_{0s} and i'_{0r} are zero since the sum of the three-phase currents must be zero. Therefore, v_{0s} and v'_{0r} are zero since the sum of the three-phase stator and rotor flux linkages must also be zero. We begin to see that the analysis and performance of the two-phase induction machine tells us a lot (in fact, nearly everything) about its bigger, three-phase brother.

Torque Equation in Arbitrary Reference Frame Variables

Since the voltage equations for v_{0s} and v'_{0r} given by (6.12-47) and (6.12-50) do not contain a speed voltage term, the expression for torque can be determined from (6.7-7) if we realize that power input to the coupling field is $\frac{3}{2}$ of the sum of the instantaneous phase power. Hence, the analysis set forth in Section 6.7 can be applied to a three-phase induction machine with or without a neutral connection. We need only to multiply the torque expressions in Section 6.7 by $\frac{3}{2}$. Thus, for a three-phase machine, (6.7-11) would become

$$T_e = \left(\frac{3}{2}\right)\left(\frac{P}{2}\right)(\lambda'_{dr}i'_{qr} - \lambda'_{qr}i'_{dr}) \tag{6.12-58}$$

Please recall that this equation has not been shown to be valid for a nonlinear magnetic system in the rotor reference frame ($\omega = \omega_r$).

6.13 RECAPPING

There are at least two aspects of the material presented in this chapter that are worth reemphasizing. First, to analyze a symmetrical induction machine, it is necessary to incorporate a change of variables so that the resulting variables (windings) are not in relative motion. Second, even though this change of variables is somewhat involved, the resulting steady-state equivalent circuit is very easy to work with, making it an invaluable tool for predicting and understanding the operation of symmetrical induction machines. It has also become very apparent that, in order to investigate the dynamic characteristics of the induction machine, it is necessary to use a computer. Although the implementation of a computer simulation of an induction machine is beyond the scope of this text, the computer traces obtained from such an implementation are instructive, not only to portray the dynamic characteristics of this device but also to illustrate the change of variables used in the analysis.

Unbalanced operation of two-phase symmetrical induction motors is analyzed in a later chapter. This sets the stage for the analysis of induction motors used for single-phase operation of a two-phase induction machine. The material that has been presented in this chapter is prerequisite for this later chapter.

6.14 REFERENCES

[1] P. C. Krause, O. Wasynczuk, and S. D. Sudhoff, *Analysis of Electric Machinery*, 1^{st} Edition, IEEE Press, 1994.

[2] R. H. Park, "Two-Reaction Theory of Synchronous Machines – Generalized Method of Analysis – Part I," *AIEE Trans.*, Vol. 48, July 1929, pp. 716-727.

[3] P. C. Krause, O. Wasynczuk, and S. D. Sudhoff, *Analysis of Electric Machinery and Drive Systems*, 2^{nd} Edition, IEEE Press, 2002.

[4] A. M. Trzynadlowski, *The Field Orientation Principle in Control of Induction Motors*, Kluwer Academic Publishers, 1994.

[5] F. Blaschke, *Das Verfahren der Feldorientierung zur Regelung der Drehfeldmaschine*, Ph. D. thesis, TU Braunschweig, 1974.

6.15 PROBLEMS

1. Consider the two-pole, two-phase induction machine shown in Fig. 6.2-1. The device is operating as a motor at $\omega_r = 95\pi$ rad/s with $I'_{ar} = \cos 5\pi t$ and $I'_{br} = -\sin 5\pi t$. Determine the angular velocity and direction of mmf_r relative to (a) an observer on the rotor and (b) an observer on the stator. Also determine (c) angular velocity of the stator currents and (d) the direction of rotation of the rotor.

2. The windings shown in Fig, 6.15-1 are sinusoidally distributed and the device is symmetrical. The amplitude of the stator-to-rotor mutual inductance is L_{sr}. Express all mutual inductances as functions of L_{sr} and θ_r.

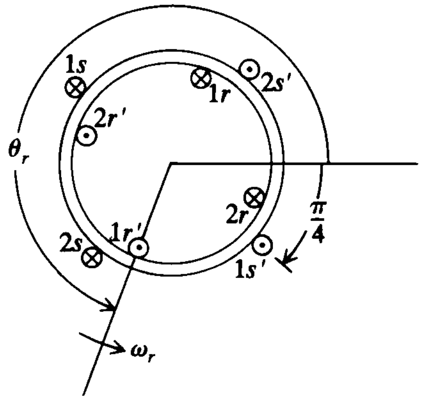

Figure 6.15-1: Coupled windings.

3. Consider the two-pole, two-phase symmetrical induction machine shown in Fig. 6.2-1. For steady-state operation, let $I_{as} = \sqrt{2}I_s \cos\omega_e t$, $I_{bs} = \sqrt{2}I_s \sin\omega_e t$, $I'_{ar} = \sqrt{2}I'_r \cos[(\omega_e - \omega_r)t + \alpha]$, and $I'_{br} = \sqrt{2}I'_r \sin[(\omega_e - \omega_r)t + \alpha]$, where $\alpha = \theta_{eri}(0)$. Assume the rotor speed is constant and $V'_{ar} = V'_{br} = 0$. Use v_{as} of (6.3-40) and λ_{as} (6.3-49) to express V_{as} in the form A cos $\omega_e t + B$ sin $\omega_e t$.

4. The rotor windings of the two-pole, two-phase symmetrical induction machine shown in Fig. 6.2-1 are open-circuited. $I_{as} = \sqrt{2}I_s \cos\omega_e t$ and $I_{bs} = -\sqrt{2}I_s \sin\omega_e t$. The rotor is driven at $\omega_r = \omega_e$ in the counterclockwise direction. Express V_{ar}.

* 5. For the devices shown in Fig. 6.2-1, let $r_s = r'_r = 0.5\,\Omega$, $L_{ss} = L'_{rr} = 0.1$ H, and $L_{ms} = 0.09$ H. With $V_{as} = \sqrt{2}\cos\, t$, $\omega_r = 0$, $\theta_r = \frac{1}{4}\pi$, and the bs and br windings are open-circuited. The ar winding is short-circuited, Calculate $\tilde{I}_{as}$.

6. Derive the expression for the electromagnetic torque T_e given by (6.4-3), starting with (6.4-1) and (6.4-2).

7. It is often convenient to express the voltage and flux linkage equations in the arbitrary reference frame, and the torque in terms of flux linkages per second rather than flux linkages. To do this, a base electrical angular velocity (ω_b) is defined, say 377 rad/s for a 60-Hz machine, and

the flux linkage equations are multiplied by ω_b. For example, (6.6-8) would become

$$\psi_{qs} = X_{ls} i_{qs} + X_{ms}(i_{qs} + i'_{qr})$$

where $X_{ls} = \omega_b L_{ls}$ and $X_{ms} = \omega_b L_{ms}$. Rewrite (6.5-6) through (6.5-9) and (6.6-8) through (6.6-11) in terms of flux linkages per second.

8. Synchronously rotating variables may be related to rotor reference variables by $\mathbf{f}^e_{qds} = {}^r\mathbf{K}^e \mathbf{f}^r_{qds}$. Determine ${}^r\mathbf{K}^e$ in terms of $\mathbf{K}^e_s$ and $\mathbf{K}^r_s$.

9. Start with (6.8-21) and obtain (6.7-1). Hint: (6.7-1) is valid in all reference frames for a linear magnetic system.

10. Obtain (6.8-26) from (6.8-23).

11. Verify (6.8-27) and (6.8-29).

12. Repeat SP6.8-4*b* without approximation.

13. A four-pole, two phase induction machine has the following parameters: $r_s = 0.3\,\Omega$, $L_{ls} = 1$ mH, $L_{ms} = 20$ mH, $r'_r = 0.2\,\Omega$, and $L'_{lr} = 1$ mH. The device is supplied from a 60–Hz source; the rotor speed is $\omega_r = 360$ rad/s. In this mode of operation, $\tilde{I}_{as} = 28.8\underline{/-36.1^\circ}$ and $\tilde{I}'_{ar} = 23.9\underline{/173.2^\circ}$. Calculate (*a*) T_e, (*b*) the total ohmic loss in the rotor windings, (*c*) the mechanical power delivered to the load, and (*d*) express I_{as}, I'_{ar}, I^s_{qs}, and I'^s_{qr}.

14. Consider Example 6B. Relate $\mathbf{i}^r_{qds}$ to $\mathbf{i}_{abs}$ in part (*b*).

*15. Calculate the actual rotor speed, in rad/s, at maximum steady-state torque for the machine given in Example 6C for operation as a motor when connected to an electric source of (*a*) 120 Hz with twice rated voltage, (*b*) 60 Hz with rated voltage, (*c*) 30 Hz with one-half rated voltage, and (*d*) 6 Hz with 10 percent rated voltage.

*16. The induction machine described in Example 6D is operating steadily at no load. The polarity of the applied voltage of one stator winding is suddenly reversed. Assume that the electric system establishes steady-state operation before the speed of the rotor has changed appreciably. Calculate the torque. Describe the behavior of the machine.

17. Select two identical capacitors so that when they are connected in parallel with each phase (one capacitor per phase) of the induction machine described in Example 6C. The no-load capacitor–induction machine combination operates at unity power factor. Assume the capacitors are ideal (zero resistance).

* 18. Assume that the current at rated load of a 110-V (rms), 60-Hz machine is $20 - j10$ A (rms). Select two identical capacitors so that the parallel combination of the capacitors and the induction machine (one capacitor per phase) has a power factor of 0.95 (current lagging the voltage) when the machine is operating at rated load. Assume the capacitors are ideal (zero resistance).

* 19. Consider the 5- and $\frac{1}{10}$-hp machines described in Section 6.9. Make reasonable approximations and determine the blocked-rotor and no-load, steady-state stator phase currents $\tilde{I}_{as}$, and compare them with the starting current and current at synchronous speed depicted in Figs. 6.9-1 and 6.9-3 for the 5- and $\frac{1}{10}$-hp machines, respectively.

20. Assume the torque load on the 5-hp machine described in Section 6.9 is $T_L = K\omega_r^2$. At a rotor speed of 1800 r/min, T_L is 22 N·m. Calculate K. Use the plot of T_e for 60 Hz in Fig. 6.9-9 to approximate the speed at which $T_L = T_e$. Will the machine operate at this speed? Explain. Use Fig. 6.9-1 to approximate $\tilde{I}_{as}$ for this speed.

21. A four-pole, 7.5-hp, three-phase, symmetrical induction motor has the following parameters: $r_s = 0.3\,\Omega$, $L_{ls} = 1.5$ mH, $L_{ms} = 35$ mH, $r_r' = 0.15\,\Omega$, and $L_{lr}' = 0.7$ mH. The machine is supplied from a 110-V line-to-neutral 60-Hz source. (a) Calculate the steady-state starting torque and current. Make valid approximations. (b) Calculate the no-load current. Neglect friction and windage losses.

22. Repeat Prob. 21 with the machine supplied from an 11-V line-to-neutral 6-Hz source.

Electromechanical Motion Devices, Second Edition
by Paul Krause, Oleg Wasynczuk and Steven Pekarek

Chapter 7

SYNCHRONOUS MACHINES

7.1 INTRODUCTION

Nearly all electric power is generated by synchronous machines driven either by hydroturbines, steam turbines, or combustion engines. Just as the induction machine is the workhorse when it comes to converting energy from electric to mechanical, the synchronous machine is the principal means of converting energy from mechanical to electric. Although nearly all electric power is generated with three-phase synchronous machines, their electrical and electromechanical behavior can be predicted from the equations that describe the two-phase, salient-pole synchronous machine. In particular, with only slight modifications, these equations can be used to predict the performance of large hydroturbine and steam turbine synchronous generators, synchronous motors, and reluctance motors used in low-power drive systems. It is for this reason that we will focus our attention on the two-phase machine since the work involved is much less than with the three-phase device. However, those who wish to extend their study to the three-phase synchronous machine may do so since there is a section devoted to it near the end of the chapter.

The rotor of a synchronous machine is equipped with a field winding and one or more short-circuited windings, which we will refer to as *damper windings*. In general, the rotor windings have different electrical characteristics. Moreover, the rotor of a salient-pole synchronous machine is magnetically asymmetrical. Owing to these rotor asymmetries, a change of variables offers no advantage in the case of the rotor variables. However, we will find it beneficial to define a change of variables or transformation for the voltages, currents, and flux linkages of the stator circuits. In effect, this transformation replaces these stator variables with variables associated with fictitious circuits rotating with the rotor.

In this chapter, the voltage and electromagnetic torque equations are first established for the synchronous machine in machine variables. Reference frame theory is then used to establish the machine equations with the stator variables transformed to a reference frame fixed in the rotor (Park's equations). The equations that describe the steady-state behavior are then derived from these equations. Attention is also given to the two-phase reluctance motor that is used in control system applications.

7.2 TWO-PHASE SYNCHRONOUS MACHINE

A two-pole, two-phase, salient-pole synchronous machine is shown in Fig. 7.2-1. The stator windings are identical, sinusoidally distributed windings, as described in Chapter 4. The electrical characteristics of the rotor of a synchronous machine may be approximated by a field winding (*fd* winding) and short-circuited damper or amortisseur windings (*kq* and *kd* windings). Although the damper windings are shown with provisions to apply a voltage, they are, in fact, short-circuited windings that represent the paths for induced rotor currents. In particular, these short-circuited windings represent squirrel-cage-type windings (short-circuited copper bars) forged below the surface of the rotor or current paths in the iron of solid-iron rotors. Laminated salient-pole rotors with cage-damper windings are used in machines with a large number of poles, whereas solid-iron round rotors with or without cage-type damper windings are used in high-speed (two- or four-pole) machines. In any event, the electrical characteristics of the equivalent damper windings may be determined by test. We will assume that the damper windings are approximated by two sinusoidally distributed windings displaced 90°. The *kd* winding has the same magnetic axis as the *fd* winding, it has N_{kd} equivalent turns with resistance r_{kd}. The magnetic axis of the *kq* winding is 90° ahead of the magnetic axis of the *fd* and *kd* windings. It has N_{kq} equivalent turns and r_{kq} resistance. It is important to mention that the rotor configuration shown in Fig. 7.2-1 for a two-phase machine is the same for

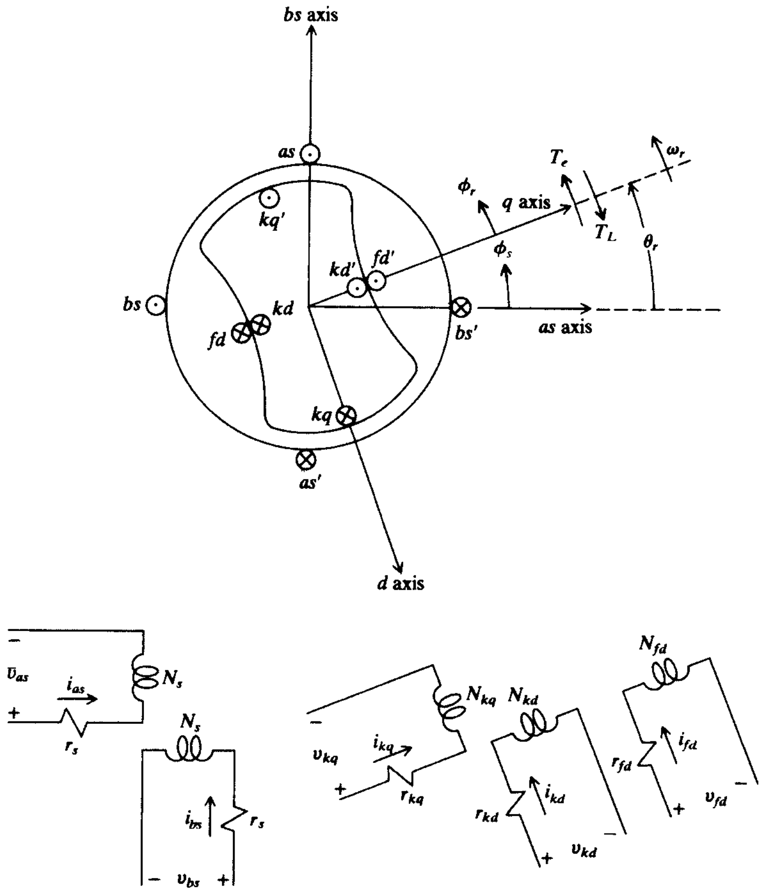

Figure 7.2-1: Two-pole, two-phase synchronous machine.

any multiphase, two-pole synchronous machine. In some cases, a more accurate representation of the electrical characteristics of the rotor is achieved by assuming that two or more damper windings exist in each axis (i.e., $kq1$, $kq2$, ... and $kd1$, $kd2$, ...). We will consider only the kq and kd windings; the modifications and extensions necessary to accommodate any number of rotor windings are straightforward [1].

The quadrature axis (q axis) and direct axis (d axis) are introduced in Fig. 7.2-1. The q axis is the magnetic axis of the kq winding, whereas the d axis is the magnetic axis for the fd and kd windings. The q and d axes are reserved to denote the rotor magnetic axes of a synchronous machine since, over the years, they have been associated with the physical structure of the rotor quite independent of any transformation. The angular displacement about the stator is denoted ϕ_s and it is referenced to the *as* axis. The angular displacement about the rotor is ϕ_r, which is referenced to the q axis. The electrical angular velocity of the rotor is ω_r and θ_r is the electrical angular displacement of the rotor measured from the *as* axis to the q axis. Thus, a given point on the rotor surface at the angular position may be ϕ_r related to an adjacent point on the inside stator surface with angular position ϕ_s as

$$\phi_s = \phi_r + \theta_r \tag{7.2-1}$$

The electromechanical torque T_e and the load torque T_L are also shown in Fig. 7.2-1. We are aware from Chapter 2 that T_e is assumed to be positive in the positive direction of θ_r. The load torque is positive in the opposite direction, opposing rotation.

The stator of a synchronous machine is symmetrical; however, the rotor is asymmetrical from two standpoints. The rotor windings are not identical since, in general, they do not have the same number of turns and the same value of resistance. Also, owing to the nonuniform air gap of the salient-pole synchronous machine, the magnetic characteristics of the q and d axes are not the same.

With balanced steady-state stator currents, an air-gap mmf (mmf_s) is established that rotates about the air gap of a two-pole machine at ω_e, the angular velocity of the stator currents (4.4-11). Now, the damper windings are short-circuited and, for the machine to operate as a synchronous machine, a dc voltage is applied to the *fd* (field) winding (often by a brush-and-slip-ring arrangement). The resulting field current i_{fd} establishes an air-gap mmf (mmf_r) that is fixed with respect to the rotor. The air-gap mmf (poles) established by the field winding must rotate at the same angular velocity as the rotating air-gap mmf (poles) established by the stator windings in order to produce a nonzero average electromagnetic torque during steady-state operation. Therefore, the rotor must rotate in synchronism with the air-gap mmf established by the stator windings ($\omega_r = \omega_e$); hence, the name synchronous machine. The main torque production mechanism is this interaction of the air-gap mmf established by the stator currents (mmf_s) and the air-gap mmf due to the direct current flowing in the field winding (mmf_r). However, electromagnetic torque (reluctance torque) is also developed at synchronous speed due to the nonuniform air gap (salient-pole rotor). The so-called salient-pole construction is common for slower-speed machines (large number of poles) such as hydroturbine generators. In this type of rotor construction, the field winding is wound upon the rotor surface, as shown in Fig. 7.2-1, and the air gap is nonuniform to make room for the placement of the field winding. Therefore, the q-axis magnetic path has a higher reluctance than the d-axis magnetic path. Now, in Chapter 2 we learned that torque is produced in a reluctance machine to align the minimum-reluctance path of the rotor with the mmf produced by the stator. Let us apply this principle to the salient-pole synchronous machine. There is an electromagnetic torque developed to align the minimum-reluctance path (d axis) with the resultant air-gap mmf ($\text{mmf}_s + \text{mmf}_r$). We will find that in the case of salient-pole synchronous machines, the reluctance torque is a small part of the total torque developed. However, two facts warrant mentioning. First, in high-speed synchronous machines (two-, four-, and six-pole machines) the field windings are generally embedded in rotor slots and the air gap is, for the most part, uniform (round rotor). It is apparent that, in the case of a round-rotor synchronous machine, the reluctance torque is not present. Second, if the field winding (fd winding) is removed from the salient-pole synchronous machine shown in Fig. 7.2-1, it would be a two-phase reluctance machine, which is used in low-power drive systems.

We have yet to discuss the damper windings. It was found early on that a synchronous machine with only a field winding, and without provisions for induced currents to circulate in the rotor iron, would tend to oscillate about synchronous speed in a slowly damped manner following any slight disturbance. Adding damper windings (short-circuited rotor windings) provided the desired damping. To explain this damping action, let us compare the torque developed by the damper windings to that developed by an induction motor. The damper windings are short-circuited as are the rotor windings of an induction motor and, as we discussed in Section 4.6 and Chapter 6, currents are induced in these rotor (damper) windings whenever the speed of the rotor differs from the angular velocity of the rotating air-gap mmf established by the stator currents (mmf_s). Since the damper windings are not symmetrical and since the air gap is not uniform, the steady-state torque due to the interaction of the currents induced in the damper windings and mmf_s will pulsate; however, an average torque will occur. Now, the main torque of a synchronous machine is developed at synchronous speed because of the interaction of mmf_s and mmf_r. At synchronous speed, current is not induced in the damper windings and, hence, induction-motor torque is not developed. However, if for any reason the speed of the rotor should vary around synchronous speed because of a disturbance, currents will be induced in the damper windings and the torque developed due to induction-motor action, although small, will damp oscillations of the rotor speed. That is, a slight slowing down (speeding up) of the rotor will produce an induction-motor torque to accelerate (decelerate) the rotor back to synchronous speed.

Although it is generally necessary to start large synchronous machines by auxiliary means, smaller-horsepower synchronous machines and reluctance motors develop sufficient induction-motor torque because of the damper windings to accelerate the machine to near-synchronous speed. During this starting period, the field winding of the synchronous machine is also short-circuited, hence, it too provides some induction-motor torque. The synchronous machine will accelerate to near-synchronous speed, whereupon it will operate as an induction machine developing the average torque necessary to satisfy the no-load losses. The field winding is then open-circuited and a dc voltage is applied to its terminals by means of a brush-and-slip-ring combination. The machine then pulls in to synchronism with the rotating air-gap mmf established by the stator currents and, thus, operates as a synchronous machine.

The damper windings of reluctance motors are often designed so that the device will develop sufficient induction-motor torque to accelerate the rotor, sometimes under load, from stall to near-synchronous speed. If the load is not too large, the reluctance torque will then pull the rotor in step with the rotating air-gap mmf established by the stator currents and the device will operate as a reluctance machine.

Torque is torque by whatever means it is developed and, perhaps, we should not emphasize the separation of torque into three types since the system is nonlinear and superposition cannot be applied. Nevertheless, this separation is helpful and, as we proceed, we will be able to identify what we have called the induction-motor torque, the reluctance torque, and the torque due to the interaction of mmf_s and mmf_r, all of which can occur in the machine shown in Fig. 7.2-1.

A four-pole, three-phase, salient-pole synchronous machine is shown in Fig. 7.2-2. Note the dc machine connected to the shaft for purposes of supplying voltage to the field winding of the synchronous machine. Note also the squirrel-cage damper windings embedded in the pole faces. Figure 7.2-3 shows the stator and rotor of a miniature two-pole, three-phase alternator with an alnico permanent-magnet rotor. This device produces 12 W at 4200 r/min to supply aircraft instruments. It mounts on an aircraft engine auxiliary drive pad where temperatures can be as high as 350°F.

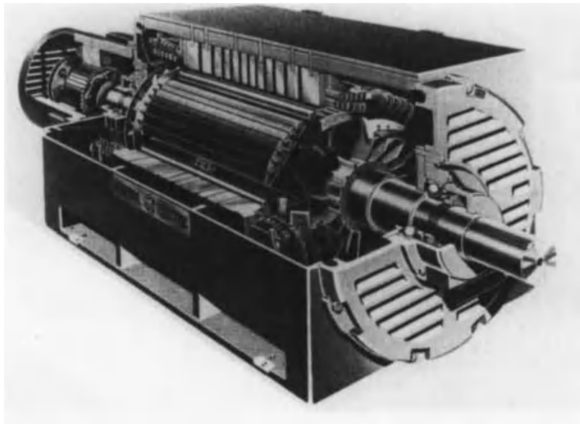

Figure 7.2-2: Four-pole, three-phase, salient-pole synchronous machine.

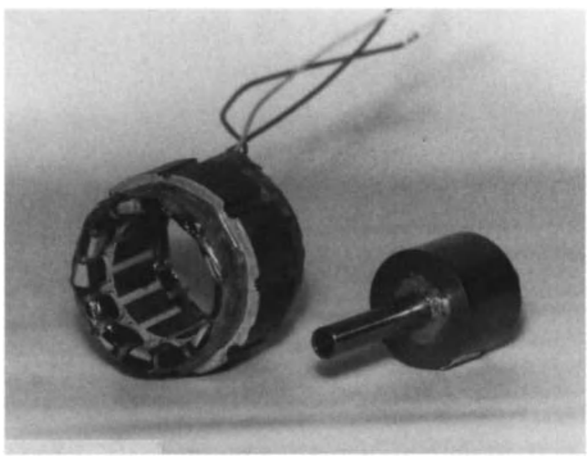

Figure 7.2-3: Stator and rotor of a two-pole, 12-W, 4200 r/min, permanent-magnet, synchronous machine (Courtesy of Vickers Electromech.).

SP7.2-1 Express mmf_r for the two-pole, two-phase synchronous machine shown in Fig. 7.2-1. [$\text{mmf}_r = -(N_{fd}/2)i_{fd}\sin(\phi_s - \theta_r)$]

SP7.2-2 A dc voltage is applied to the *fd* winding of the machine shown in Fig. 7.2-1. The damper windings are short-circuited and the machine is driven at ω_r, counterclockwise. Assume that the stator currents are balanced 60-Hz currents with $\tilde{I}_{as} = -j\tilde{I}_{bs}$. Determine the frequency of the currents flowing in the damper windings. [$\omega_r + \omega_e$]

7.3 VOLTAGE EQUATIONS AND WINDING INDUCTANCES

The voltage equations for the two-pole, two-phase, salient-pole synchronous machine shown in Fig. 7.2-1 may be expressed as

$$v_{as} = r_s i_{as} + \frac{d\lambda_{as}}{dt} \tag{7.3-1}$$

$$v_{bs} = r_s i_{bs} + \frac{d\lambda_{bs}}{dt} \tag{7.3-2}$$

$$v_{kq} = r_{kq} i_{kq} + \frac{d\lambda_{kq}}{dt} \tag{7.3-3}$$

$$v_{fd} = r_{fd} i_{fd} + \frac{d\lambda_{fd}}{dt} \tag{7.3-4}$$

$$v_{kd} = r_{kd} i_{kd} + \frac{d\lambda_{kd}}{dt} \tag{7.3-5}$$

The above equations may be written in matrix form as

$$\mathbf{v}_{abs} = \mathbf{r}_s \mathbf{i}_{abs} + p\boldsymbol{\lambda}_{abs} \tag{7.3-6}$$

$$\mathbf{v}_{qdr} = \mathbf{r}_r i_{qdr} + p\boldsymbol{\lambda}_{qdr} \tag{7.3-7}$$

where

$$(\mathbf{f}_{abs})^T = [f_{as} \quad f_{bs}] \tag{7.3-8}$$

$$(\mathbf{f}_{qdr})^T = [f_{kq} \quad f_{fd} \quad f_{kd}] \tag{7.3-9}$$

In the above equations, the s and r subscripts denote variables associated with the stator and rotor windings, respectively, and p is the operator d/dt. Also,

$$\mathbf{r}_s = \begin{bmatrix} r_s & 0 \\ 0 & r_s \end{bmatrix} \tag{7.3-10}$$

$$\mathbf{r}_r = \begin{bmatrix} r_{kq} & 0 & 0 \\ 0 & r_{fd} & 0 \\ 0 & 0 & r_{kd} \end{bmatrix} \tag{7.3-11}$$

A review of matrix algebra is given in Appendix B. If we assume a linear magnetic system, the flux linkage equations may be expressed as

$$\lambda_{as} = L_{asas}i_{as} + L_{asbs}i_{bs} + L_{askq}i_{kq} + L_{asfd}i_{fd} + L_{askd}i_{kd} \tag{7.3-12}$$

$$\lambda_{bs} = L_{bsas}i_{as} + L_{bsbs}i_{bs} + L_{bskq}i_{kq} + L_{bsfd}i_{fd} + L_{bskd}i_{kd} \tag{7.3-13}$$

$$\lambda_{kq} = L_{kqas}i_{as} + L_{kqbs}i_{bs} + L_{kqkq}i_{kq} + L_{kqfd}i_{fd} + L_{kqkd}i_{kd} \tag{7.3-14}$$

$$\lambda_{fd} = L_{fdas}i_{as} + L_{fdbs}i_{bs} + L_{fdkq}i_{kq} + L_{fdfd}i_{fd} + L_{fdkd}i_{kd} \tag{7.3-15}$$

$$\lambda_{kd} = L_{kdas}i_{as} + L_{kdbs}i_{bs} + L_{kdkq}i_{kq} + L_{kdfd}i_{fd} + L_{kdkd}i_{kd} \tag{7.3-16}$$

In the case of a salient-pole device (nonuniform air gap), the self-inductances of the stator windings and the mutual inductances between stator windings are functions of θ_r. Although this is a review of the material in Chapter 1, let us consider L_{asas}. With $\theta_r = 0$, we see from Fig. 7.2-1 that the magnetizing inductance of L_{asas} is less than it would be when $\theta_r = \frac{1}{2}\pi$. Let the magnetizing inductance of the as winding be denoted L_{mq} when $\theta_r = 0$ since the q axis (high-reluctance path) is aligned with the magnetic axis of the as winding. Thus,

$$L_{asas} = L_{ls} + L_{mq} \qquad \theta_r = 0 \tag{7.3-17}$$

where L_{ls} is the leakage inductance of the stator windings and

$$L_{mq} = \frac{N_s^2}{\Re_{mq}} \tag{7.3-18}$$

where $\Re_{mq}$ is an equivalent reluctance of the magnetic path in the q axis. We called this $\Re_m(0)$ in (1.7-24). Now, at $\theta_r = \frac{1}{2}\pi$ the d axis (low-reluctance path) is aligned with the magnetic axis of the *as* winding. Hence, denoting this magnetizing inductance as L_{md}, we can write

$$L_{asas} = L_{ls} + L_{md} \qquad \theta_r = \tfrac{1}{2}\pi \tag{7.3-19}$$

where

$$L_{md} = \frac{N_s^2}{\Re_{md}} \tag{7.3-20}$$

where $\Re_{md}$ is an equivalent reluctance of the magnetic path in the d axis. This is $\Re_m(\frac{1}{2}\pi)$ in (1.7-25).

Since $\Re_{mq} > \Re_{md}$, $L_{mq} < L_{md}$, and we see that a minimum L_{asas} occurs at $\theta_r = 0$ and also again at $\theta_r = \pi$. Therefore, (7.3-17) is valid for $\theta_r = 0$ and π. Similarly, maximum L_{asas} occurs at $\theta_r = \frac{1}{2}\pi$; and again at $\theta_r = \frac{3}{2}\pi$; hence (7.3-19) applies for $\theta_r = \frac{1}{2}\pi$ and $\frac{3}{2}\pi$. The magnetizing inductance varies about an average value (which must be positive) and if we assume this variation to be sinusoidal, it would vary as a function of $2\theta_r$ (Fig. 1.7-3). Let L_A be the average value and L_B the amplitude of the sinusoidal variation about this average value. In this case,

$$L_{mq} = L_A - L_B \tag{7.3-21}$$

$$L_{md} = L_A + L_B \tag{7.3-22}$$

Substituting (7.3-18) and (7.3-20) for L_{mq} and L_{md}, respectively, into (7.3-21) and (7.3-22), and solving for L_A and L_B yields

$$L_A = \frac{N_s^2}{2}\left(\frac{1}{\Re_{md}} + \frac{1}{\Re_{mq}}\right) \tag{7.3-23}$$

$$L_B = \frac{N_s^2}{2}\left(\frac{1}{\Re_{md}} - \frac{1}{\Re_{mq}}\right) \tag{7.3-24}$$

Assuming a sinusoidal variation, we can write (Fig. 1.7-3) as

$$L_{asas} = L_{ls} + L_A - L_B \cos 2\theta_r \tag{7.3-25}$$

If the air gap were uniform, as is the case in a round-rotor synchronous machine, $\Re_{mq} = \Re_{md}$ and, hence, from (7.3-24), $L_B = 0$.

By a similar procedure, it follows that, for the salient-pole device,

$$L_{bsbs} = L_{ls} + L_A + L_B \cos 2\theta_r \tag{7.3-26}$$

Note that when $\theta_r = 0$, L_{asas} is a minimum according to (7.3-25) and, according to (7.3-26), L_{bsbs} is a maximum. This, of course, corresponds to that which is portrayed in Fig. 7.2-1.

The mutual inductance $L_{asbs}(L_{bsas})$ is next. One would think that since the windings are orthogonal, the mutual coupling would always be zero. However, this is not the case due to the fact that the air gap is not uniform. Let us consider Fig. 7.3-1, where various rotor positions are shown with only the flux paths of the *as* winding illustrated. Coupling occurs when flux produced by one winding links the other winding; in particular, when the flux of the *as* winding links the *bs* winding. This will give us L_{bsas} and we know that $L_{asbs} = L_{bsas}$.

Note that, when $\theta_r = 0$, π, and 2π as shown in Fig. 7.3-1*a* or when $\theta_r = \frac{1}{2}\pi$ and $\frac{3}{2}\pi$ as shown in Fig. 7.3-1*b*, L_{bsas} is zero. In these positions, there is no channeling of the flux of one winding through the other. However, let the rotor start to turn counterclockwise from zero toward $\frac{1}{2}\pi$ and consider the flux produced by positive current flowing the *as* winding. As the rotor turns, the configuration of the rotor provides a low-reluctance path to the flux produced in the *as* winding and the flux is channeled across the *bs* winding with maximum coupling occurring at $\theta_r = \frac{1}{4}\pi$, as illustrated in Fig. 7.3-1*c*. We see that this same rotor position relative to the windings occurs also at $\theta_r = \frac{5}{4}\pi$. Maximum coupling will again occur at $\theta_r = \frac{3}{4}\pi$ and $\frac{7}{4}\pi$, as illustrated by Fig. 7.3-1*d*. Now, what is the sign of the mutual inductance? With the assumed direction of positive currents, the right-hand rule tells us that L_{bsas} (or L_{asbs}) is negative at $\theta_r = \frac{1}{4}\pi$, $\frac{5}{4}\pi, \ldots$ (the fluxes of the windings oppose each other for positive currents) and positive for $\theta_r = \frac{3}{4}\pi$, $\frac{7}{4}\pi, \ldots$ (the fluxes aid each other). If we sketch L_{bsas} versus θ_r using the above information, we see, from Fig. 7.3-1*e*, that, as a first approximation, L_{bsas} or L_{asbs} may be expressed as

$$L_{bsas} = L_{asbs} = -L_B \sin 2\theta_r \tag{7.3-27}$$

In order for us to prove that the coefficient is L_B, it would be necessary to become quite involved [1]. We will accept this without proving it.

Let us now go back to the flux linkage equations, (7.3-12) through (7.3-16), and write these equations in matrix form as

$$\begin{bmatrix} \boldsymbol{\lambda}_{abs} \\ \boldsymbol{\lambda}_{qdr} \end{bmatrix} = \begin{bmatrix} \mathbf{L}_s & \mathbf{L}_{sr} \\ (\mathbf{L}_{sr})^T & \mathbf{L}_r \end{bmatrix} \begin{bmatrix} \mathbf{i}_{abs} \\ \mathbf{i}_{qdr} \end{bmatrix} \tag{7.3-28}$$

The matrix $\mathbf{L}_s$ can now be written as

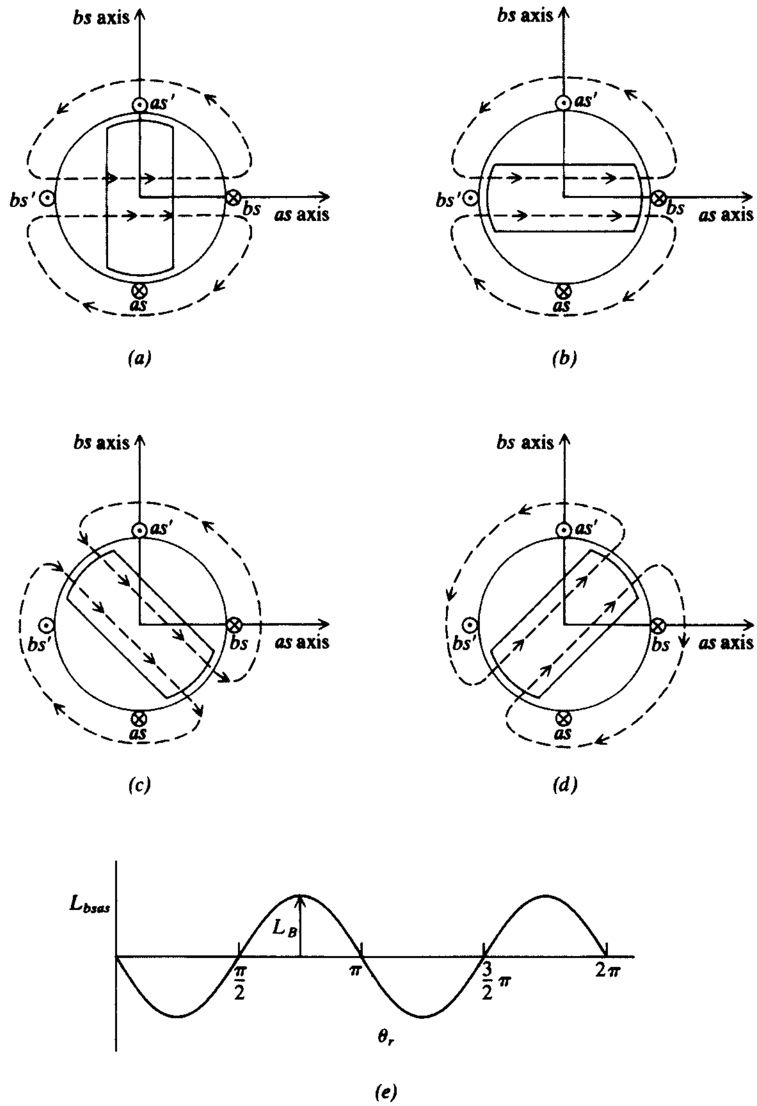

Figure 7.3-1: Flux path of *as* winding illustrating the mutual coupling between stator windings to determine L_{bsas} and L_{asbs}. (*a*) $\theta_r = 0$, π, and 2π; (*b*) $\theta_r = \frac{1}{2}\pi$ and $\frac{3}{2}\pi$; (*c*) $\theta_r = \frac{1}{4}\pi$ and $\frac{5}{4}\pi$; (*d*) $\theta_r = \frac{3}{4}\pi$ and $\frac{7}{4}\pi$; and (*e*) approximation of L_{bsas} and L_{asbs}.

$$\mathbf{L}_s = \begin{bmatrix} L_{asas} & L_{asbs} \\ L_{bsas} & L_{bsbs} \end{bmatrix}$$

$$= \begin{bmatrix} L_{ls} + L_A - L_B \cos 2\theta_r & -L_B \sin 2\theta_r \\ -L_B \sin 2\theta_r & L_{ls} + L_A + L_B \cos 2\theta_r \end{bmatrix} \tag{7.3-29}$$

By inspection of Fig. 7.2-1, we can write

$$\mathbf{L}_{sr} = \begin{bmatrix} L_{askq} & L_{asfd} & L_{askd} \\ L_{bskq} & L_{bsfd} & L_{bskd} \end{bmatrix}$$

$$= \begin{bmatrix} L_{skq} \cos \theta_r & L_{sfd} \sin \theta_r & L_{skd} \sin \theta_r \\ L_{skq} \sin \theta_r & -L_{sfd} \cos \theta_r & -L_{skd} \cos \theta_r \end{bmatrix} \tag{7.3-30}$$

$$\mathbf{L}_r = \begin{bmatrix} L_{kqkq} & L_{kqfd} & L_{kqkd} \\ L_{fdkq} & L_{fdfd} & L_{fdkd} \\ L_{kdkq} & L_{kdfd} & L_{kdkd} \end{bmatrix}$$

$$= \begin{bmatrix} L_{lkq} + L_{mkq} & 0 & 0 \\ 0 & L_{lfd} + L_{mfd} & L_{fdkd} \\ 0 & L_{kdfd} & L_{lkd} + L_{mkd} \end{bmatrix} \tag{7.3-31}$$

In the above inductance matrices, the leakage inductances are denoted with an l in the subscript. The *skq, sfd,* and *skd* subscripts denote the peak mutual inductances between stator and rotor windings. The following equations define the inductances used in (7.3-30) and (7.3-31):

$$L_{skq} = \frac{N_{kq}}{N_s} L_{mq} \tag{7.3-32}$$

$$L_{sfd} = \frac{N_{fd}}{N_s} L_{md} \tag{7.3-33}$$

$$L_{skd} = \frac{N_{kd}}{N_s} L_{md} \tag{7.3-34}$$

$$L_{mkq} = \left(\frac{N_{kq}}{N_s} \right)^2 L_{mq} \tag{7.3-35}$$

$$L_{mfd} = \left(\frac{N_{fd}}{N_s} \right)^2 L_{md} \tag{7.3-36}$$

$$L_{mkd} = \left(\frac{N_{kd}}{N_s}\right)^2 L_{md} \tag{7.3-37}$$

$$L_{fdkd} = L_{kdfd} = \frac{N_{kd}}{N_{fd}} L_{mfd} = \frac{N_{fd}}{N_{kd}} L_{mkd} \tag{7.3-38}$$

As in the case of the induction machine, it is convenient to refer the rotor variables to a winding with N_s turns. Thus,

$$i'_j = \frac{N_j}{N_s} i_j \tag{7.3-39}$$

$$v'_j = \frac{N_s}{N_j} v_j \tag{7.3-40}$$

$$\lambda'_j = \frac{N_s}{N_j} \lambda_j \tag{7.3-41}$$

where j may be *kq, fd,* or *kd.* The flux linkage equations given by (7.3-28) may now be written as

$$\begin{bmatrix} \boldsymbol{\lambda}_{abs} \\ \boldsymbol{\lambda}'_{qdr} \end{bmatrix} = \begin{bmatrix} \mathbf{L}_s & \mathbf{L}'_{sr} \\ (\mathbf{L}'_{sr})^T & \mathbf{L}'_r \end{bmatrix} \begin{bmatrix} \mathbf{i}_{abs} \\ \mathbf{i}'_{qdr} \end{bmatrix} \tag{7.3-42}$$

where

$$\mathbf{L}'_{sr} = \begin{bmatrix} L_{mq}\cos\theta_r & L_{md}\sin\theta_r & L_{md}\sin\theta_r \\ L_{mq}\sin\theta_r & -L_{md}\cos\theta_r & -L_{md}\cos\theta_r \end{bmatrix} \tag{7.3-43}$$

$$\mathbf{L}'_r = \begin{bmatrix} L'_{lkq} + L_{mq} & 0 & 0 \\ 0 & L'_{lfd} + L_{md} & L_{md} \\ 0 & L_{md} & L'_{lkd} + L_{md} \end{bmatrix} \tag{7.3-44}$$

The voltage equations expressed in terms of machine variables referred by a turns ratio to the stator windings are

$$\mathbf{v}_{abs} = \mathbf{r}_s \mathbf{i}_{abs} + p\boldsymbol{\lambda}_{abs} \tag{7.3-45}$$

$$\mathbf{v}'_{qdr} = \mathbf{r}'_r \mathbf{i}'_{qdr} + p\boldsymbol{\lambda}'_{qdr} \tag{7.3-46}$$

In terms of inductances, (7.3-45) and (7.3-46) become

$$\begin{bmatrix} \mathbf{v}_{abs} \\ \mathbf{v}'_{qdr} \end{bmatrix} = \begin{bmatrix} \mathbf{r}_s + p\mathbf{L}_s & p\mathbf{L}'_{sr} \\ p(\mathbf{L}'_{sr})^T & \mathbf{r}'_r + p\mathbf{L}'_r \end{bmatrix} \begin{bmatrix} \mathbf{i}_{abs} \\ \mathbf{i}'_{qdr} \end{bmatrix} \tag{7.3-47}$$

where in the matrices $\mathbf{r}'_r$ and $\mathbf{L}'_r$

$$r'_j = \left(\frac{N_s}{N_j}\right)^2 r_j \tag{7.3-48}$$

$$L'_{lj} = \left(\frac{N_s}{N_j}\right)^2 L_{lj} \tag{7.3-49}$$

where, as before, j may be *kq, fd,* or *kd.*

Since the synchronous machine is generally operated as a generator, it is often considered more convenient to assume positive current out of the machine. This may be done in the above equations by simply placing a negative sign preceding $\mathbf{i}_{abs}$.

SP7.3-1 Express L_{asbs} for positive θ_r in the clockwise direction in Fig. 7.2-1 with (a) positive direction of i_{as} reversed, (b) positive direction of i_{bs} reversed, and (c) positive direction of both i_{as} and i_{bs} reversed. [(a) and (b) L_{asbs} = (7.3-27); (c) L_{asbs} = -(7.3-27)]

SP7.3-2 The current i_{fd} in Fig. 7.2-1 is 1 A, $L_{sfd} = 0.1$ H, and $\theta_r = 10t$. Determine the open-circuited steady-state voltages V_{as} and V_{bs}. [$V_{as} = \cos 10t$; $V_{bs} = \sin 10t$]

SP7.3-3 The current i'_{fd} in a round-rotor synchronous machine is 1 A, $L_{mq} = 0.1$ H, $L_{asfd} = \sin\theta_r$, and $\theta_r = 10t$. Determine the open-circuited steady-state voltages V_{as} and V_{bs}. [SP7.3-2]

7.4 TORQUE

The electromagnetic torque may be evaluated from Table 2.5-1:

$$T_e = \frac{P}{2}\frac{\partial W_c(\mathbf{i}, \theta_r)}{\partial \theta_r} \tag{7.4-1}$$

For a magnetically linear system, this yields

$$T_e = \frac{P}{2}\{\frac{L_{md}-L_{mq}}{2}[(i_{as}^2 - i_{bs}^2)\sin 2\theta_r - 2i_{as}i_{bs}\cos 2\theta_r]$$
$$-L_{mq}i'_{kq}(i_{as}\sin\theta_r - i_{bs}\cos\theta_r)$$
$$+L_{md}(i'_{fd}+i'_{kd})(i_{as}\cos\theta_r + i_{bs}\sin\theta_r)\} \quad (7.4\text{-}2)$$

The above expression for torque is positive for motor action. Obtaining (7.4-2) from (7.4-1) is a problem at the end of the chapter.

The torque and rotor speed are related by

$$T_e = J\left(\frac{2}{P}\right)\frac{d\omega_r}{dt} + B_m\left(\frac{2}{P}\right)\omega_r + T_L \quad (7.4\text{-}3)$$

where J is the inertia expressed in kilogram·meter^2 (kg·m^2) or joule·second^2 (J · s^2). Often, the inertia is given as WR^2 in units of pound-mass·feet^2 (lbm · ft^2). As indicated in Fig. 7.2-1, T_L is positive for a torque load when the machine is operated as a motor and negative when torque is supplied to the shaft of the machine by a prime mover (generator action). Since T_e is positive in the direction opposite to the positive direction of T_L, T_e is also positive for motor action and negative for generator action. The constant B_m is a damping coefficient associated with the rotational system of the machine and mechanical load. It has the units N · m · s/rad of mechanical rotation, and it is generally small and often neglected in the case of the machine but may be considerable for the mechanical load.

SP7.4-1 Which of the terms on the right-hand side of (7.4-2) can be thought of as the reluctance torque? $\left\{\left(\frac{P}{2}\right)\left(\frac{L_{md}-L_{mq}}{2}\right)[...]\right\}$
SP7.4-2 Repeat SP7.4-1 for the damping (induction motor) torque. [Terms with i'_{kq} or i'_{kd}]
SP7.4-3 Repeat SP7.4-1 for the torque due to the interaction of mmf$_s$ and the fd current. [Terms with i'_{fd}]

7.5 MACHINE EQUATIONS IN THE ROTOR REFERENCE FRAME

The mutual inductances between the stator and rotor windings vary sinusoidally with θ_r. Moreover, the self-inductances of the stator windings are sinusoidal functions of $2\theta_r$ and the rotor is unsymmetrical since the rotor windings are not identical. From our work in Chapter 5 and 6, we realize that the position-varying parameters disappear if we select the arbitrary reference frame fixed to the member where the unsymmetrical windings exist, in this case the rotor. One might argue that the stator windings are not symmetrical due to saliency of the rotor that led to (7.3-29), which has position-varying terms and unequal diagonal elements. Recall that our definition of symmetrical windings is that the magnetic axes of the windings are electrically orthogonal for a two-phase machine ($\frac{2}{3}\pi$ for three-phase) and have the same resistance and number of turns. By this definition, the stator of a synchronous machine is symmetrical but the rotor is not. There is another way to look at this. If the system of windings is transformable to the arbitrary reference frame, we should select the reference frame wherein the position-varying coefficients, which can occur due to the position of either the rotor or the reference frame, are not present. Recall that in Example 5B we showed that the stationary reference frame was the reference frame of choice if the resistances of the stationary circuits were unequal. Also recall that in Chapter 5 we transform (7.3-29) to the rotor reference frame to illustrate that, as a result of this transformation, the inductances were not rotor-position dependent as shown by (5.4-21).

Without further ado, we are ready to express the voltage equations of the synchronous machine in the rotor referene frame. From (5.4-6), (5.4-13), and (5.4-14) for the transformation of the stator variables to the rotor reference frame ($\omega = \omega_r$), and if we use (7.3-46) for the voltage equations of the rotor windings, we have

$$v_{qs}^r = r_s i_{qs}^r + \omega_r \lambda_{ds}^r + p\lambda_{qs}^r \tag{7.5-1}$$

$$v_{ds}^r = r_s i_{ds}^r - \omega_r \lambda_{qs}^r + p\lambda_{ds}^r \tag{7.5-2}$$

$$v_{kq}^{\prime r} = r_{kq}^{\prime} i_{kq}^{\prime r} + p\lambda_{kq}^{\prime r} \tag{7.5-3}$$

$$v_{fd}^{\prime r} = r_{fd}^{\prime} i_{fd}^{\prime r} + p\lambda_{fd}^{\prime r} \tag{7.5-4}$$

$$v_{kd}^{\prime r} = r_{kd}^{\prime} i_{kd}^{\prime r} + p\lambda_{kd}^{\prime r} \tag{7.5-5}$$

where the raised r is used to denote variables in the rotor reference frame.

Before considering a linear magnetic system wherein we will express flux linkages in terms of inductances and currents, let us obtain an expression for the torque. [If you are familiar with Section 6.7, you can skip to (7.5-11), which is (6.7-12).] To do this, we will use a power balance in which the power entering the coupling field from the electric system is

$$pW_e = e_{qs}^r i_{qs}^r + e_{ds}^r i_{ds}^r + e_{kq}'^r i_{kq}'^r + e_{fd}'^r i_{fd}'^r + e_{kd}'^r i_{kd}'^r \tag{7.5-6}$$

where, from (7.5-1) through (7.5-5), $e_{qs}^r = v_{qs}^r - r_s i_{qs}^r$ and so on. Although moving the resistances external to the coupling field is not necessary, it is done here in order to be consistent with our work in Chapter 2. Appropriate substitution of (7.5-1) through (7.5-5) into (7.5-6) yields

$$\begin{aligned} pW_e = {} & i_{qs}^r p\lambda_{qs}^r + +i_{ds}^r p\lambda_{ds}^r \\ & +i_{kq}'^r p\lambda_{kq}'^r + i_{fd}'^r p\lambda_{fd}'^r + i_{kd}'^r p\lambda_{kd}'^r \\ & +(\lambda_{ds}^r i_{qs}^r - \lambda_{qs}^r i_{ds}^r) p\theta_r \end{aligned} \tag{7.5-7}$$

The equation given by (2.2-6) can be written as a power-balance equation by taking the total derivative with respect to time; thus,

$$pW_e = pW_f - pW_m \tag{7.5-8}$$

Recall that the energy entering the coupling field from the mechanical system is

$$W_m = -T_e d\theta_{rm} \tag{7.5-9}$$

In terms of electrical angular velocity of the rotor, (7.5-9) becomes

$$pW_m = -T_e \left(\frac{2}{P}\right) p\theta_r \tag{7.5-10}$$

If we substitute (7.5-7) and (7.5-10) into (7.5-8), and if we then equate coefficients, we have

$$T_e = \frac{P}{2}(\lambda_{ds}^r i_{qs}^r - \lambda_{qs}^r i_{ds}^r) \tag{7.5-11}$$

This equation is valid for linear or nonlinear systems. The above derivation for T_e was first done by Park in his 1929 paper [2]. Note that neither field energy, W_f, nor coenergy, W_c, was used in this derivation. This is another benefit of the change of variables. Although the derivation in Chapter 2 is necessary to obtain an expression for torque when the voltage equations are expressed in machine variables, it is not necessary once a change of variables has been implemented and the reference frame selected, wherein the coefficients are not rotor-position dependent.

Equations (7.5-1) through (7.5-5) are valid for a linear or nonlinear magnetic system. For a linear magnetic system, we can express $\boldsymbol{\lambda}_{abs}$ and $\boldsymbol{\lambda}'_{qdr}$ from (7.3-42) as

$$\boldsymbol{\lambda}_{abs} = \mathbf{L}_s\mathbf{i}_{abs} + \mathbf{L}'_{sr}\mathbf{i}'_{qdr} \tag{7.5-12}$$

$$\boldsymbol{\lambda}'_{qdr} = (\mathbf{L}'_{sr})^T\mathbf{i}_{abs} + \mathbf{L}'_r\mathbf{i}'_{qdr} \tag{7.5-13}$$

where $\mathbf{L}_s$, $\mathbf{L}'_{sr}$, and $\mathbf{L}'_r$ are given by (7.3-29), (7.3-43), and (7.3-44), respectively. If in (5.3-4) we set $\theta = \theta_r$ and place a superscript r on $\mathbf{f}_{qds}$ and $\mathbf{K}_s$, we can then use (5.3-1) to transform (7.5-12), and if we add the r superscript to $\boldsymbol{\lambda}'_{qdr}$ and $\mathbf{i}'_{qdr}$ in (7.5-13), we can write

$$\boldsymbol{\lambda}^r_{qds} = \mathbf{K}^r_s\mathbf{L}_s(\mathbf{K}^r_s)^{-1}\mathbf{i}^r_{qds} + \mathbf{K}^r_s\mathbf{L}'_{sr}\mathbf{i}'^r_{qdr} \tag{7.5-14}$$

$$\boldsymbol{\lambda}'^r_{qdr} = (\mathbf{L}'_{sr})^T(\mathbf{K}^r_s)^{-1}\mathbf{i}^r_{qds} + \mathbf{L}'_r\mathbf{i}'^r_{qdr} \tag{7.5-15}$$

We can show that

$$\mathbf{K}^r_s\mathbf{L}_s(\mathbf{K}^r_s)^{-1} = \begin{bmatrix} L_{ls}+L_{mq} & 0 \\ 0 & L_{ls}+L_{md} \end{bmatrix} \tag{7.5-16}$$

$$\mathbf{K}^r_s\mathbf{L}'_{sr} = \begin{bmatrix} L_{mq} & 0 & 0 \\ 0 & L_{md} & L_{md} \end{bmatrix} \tag{7.5-17}$$

$$(\mathbf{L}'_{sr})^T(\mathbf{K}^r_s)^{-1} = \begin{bmatrix} L_{mq} & 0 \\ 0 & L_{md} \\ 0 & L_{md} \end{bmatrix} \tag{7.5-18}$$

where L_{mq} and L_{md} are defined by (7.3-21) and (7.3-22), respectively. In a problem at the end of the chapter, you are asked to obtain (7.5-16) through (7.5-18). The flux-linkage equations may now be written as

$$\begin{bmatrix} \lambda^r_{qs} \\ \lambda^r_{ds} \\ \lambda'^r_{kq} \\ \lambda'^r_{fd} \\ \lambda'^r_{kd} \end{bmatrix} = \begin{bmatrix} L_{ls}+L_{mq} & 0 & L_{mq} & 0 & 0 \\ 0 & L_{ls}+L_{md} & 0 & L_{md} & L_{md} \\ L_{mq} & 0 & L'_{lkq}+L_{mq} & 0 & 0 \\ 0 & L_{md} & 0 & L'_{lfd}+L_{md} & L_{md} \\ 0 & L_{md} & 0 & L_{md} & L'_{lkd}+L_{md} \end{bmatrix} \begin{bmatrix} i^r_{qs} \\ i^r_{ds} \\ i'^r_{kq} \\ i'^r_{fd} \\ i'^r_{kd} \end{bmatrix} \tag{7.5-19}$$

We have accomplished our goal; the self- and mutual inductances in (7.5-19) are constant. Moreover, all q circuits are magnetically decoupled from

d circuits. We now see that the fictitious windings are indeed fixed in the rotor reference frame. Since the mutual inductances between the fictitious windings ($^r_{qs}$ and $^r_{ds}$ windings) and the rotor windings are all constant, the fictitious windings and the rotor windings are not in relative motion. Hence, the $^r_{qs}$ and $^r_{ds}$ windings are rotating with the rotor.

The inductance $L_{ls} + L_{mq}$ is commonly called the q-axis inductance and denoted L_q. Similarly, $L_{ls} + L_{md}$ is called the d-axis inductance and denoted L_d. That is,

$$L_q = L_{ls} + L_{mq} \tag{7.5-20}$$

$$L_d = L_{ls} + L_{md} \tag{7.5-21}$$

If the air gap is uniform, $L_q = L_d$. Otherwise, $L_q < L_d$.

For a linear magnetic system, the flux linkage equations may be written from (7.5-19) as

$$\begin{aligned} \lambda^r_{qs} &= L_{ls} i^r_{qs} + L_{mq}(i^r_{qs} + i'^r_{kq}) \\ &= L_q i^r_{qs} + L_{mq} i'^r_{kq} \end{aligned} \tag{7.5-22}$$

$$\begin{aligned} \lambda^r_{ds} &= L_{ls} i^r_{ds} + L_{md}(i^r_{ds} + i'^r_{fd} + i'^r_{kd}) \\ &= L_d i^r_{ds} + L_{md}(i'^r_{fd} + i'^r_{kd}) \end{aligned} \tag{7.5-23}$$

$$\begin{aligned} \lambda'^r_{kq} &= L'_{lkq} i'^r_{kq} + L_{mq}(i^r_{qs} + i'^r_{kq}) \\ &= L'_{kq} i'^r_{kq} + L_{mq} i^r_{qs} \end{aligned} \tag{7.5-24}$$

$$\begin{aligned} \lambda'^r_{fd} &= L'_{lfd} i'^r_{fd} + L_{md}(i^r_{ds} + i'^r_{fd} + i'^r_{kd}) \\ &= L'_{fd} i'^r_{fd} + L_{md}(i^r_{ds} + i'^r_{kd}) \end{aligned} \tag{7.5-25}$$

$$\begin{aligned} \lambda'^r_{kd} &= L'_{lkd} i'^r_{kd} + L_{md}(i^r_{ds} + i'^r_{fd} + i'^r_{kd}) \\ &= L'_{kd} i'^r_{kd} + L_{md}(i^r_{ds} + i'^r_{fd}) \end{aligned} \tag{7.5-26}$$

where L_q and L_d are defined by (7.5-20) and (7.5-21), respectively, and

$$L'_{kq} = L'_{lkq} + L_{mq} \tag{7.5-27}$$

$$L'_{fd} = L'_{lfd} + L_{md} \tag{7.5-28}$$

$$L'_{kd} = L'_{lkd} + L_{md} \tag{7.5-29}$$

The voltage equations given by (7.5-1) through (7.5-5) and flux-linkage equations given by (7.5-22) through (7.5-26) suggest the equivalent circuits shown in Fig. 7.5-1. Substituting (7.5-22) through (7.5-26) into (7.5-1) through (7.5-5) yields the voltage equations in terms of currents:

$$\begin{bmatrix} v_{qs}^r \\ v_{ds}^r \\ v_{kq}^{\prime r} \\ v_{fd}^{\prime r} \\ v_{kd}^{\prime r} \end{bmatrix} = \begin{bmatrix} r_s + pL_q & \omega_r L_d & pL_{mq} & \omega_r L_{md} & \omega_r L_{md} \\ -\omega_r L_q & r_s + pL_d & -\omega_r L_{mq} & pL_{md} & pL_{md} \\ pL_{mq} & 0 & r'_{kq} + pL'_{kq} & 0 & 0 \\ 0 & pL_{md} & 0 & r'_{fd} + pL'_{fd} & pL_{md} \\ 0 & pL_{md} & 0 & pL_{md} & r'_{kd} + pL'_{kd} \end{bmatrix} \begin{bmatrix} i_{qs}^r \\ i_{ds}^r \\ i_{kq}^{\prime r} \\ i_{fd}^{\prime r} \\ i_{kd}^{\prime r} \end{bmatrix} \tag{7.5-30}$$

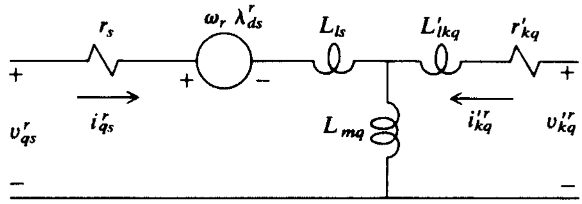

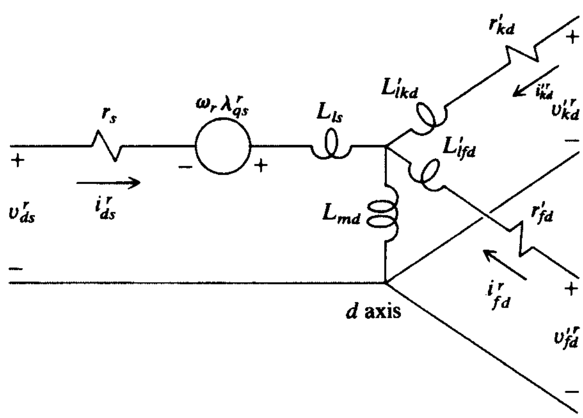

Figure 7.5-1: Equivalent circuits of a two-phase synchronous machine in the rotor reference frame.

Although (7.5-11) is most often used to calculate torque, the torque can be expressed in terms of rotor reference frame currents for a linear magnetic system by substituting (7.5-22) and (7.5-23) into (7.5-11). Thus,

$$T_e = \frac{P}{2}\left[L_{md}(i_{ds}^r + i_{fd}'^r + i_{kd}'^r)i_{qs}^r - L_{mq}(i_{qs}^r + i_{kq}'^r)i_{ds}^r\right] \qquad (7.5\text{-}31)$$

It is helpful to review what has been done thus far in this chapter. Since the stator and rotor windings of a synchronous machine are in relative motion, it is necessary to implement a change of variables, which, in effect, eliminates the relative motion between circuits. However, the synchronous machine is not too cooperative. Not only are there circuits in relative motion, but also the rotor of the salient-pole synchronous machine gives rise to sinusoidal variations of $2\theta_r$ in the self-inductances of the stator windings. To make matters worse, the rotor windings are not symmetrical.

As we think about this situation, we conclude that Park [2] really had no choice but to devise a change of variables that would transform the stator variables to fictitious circuits in the rotor reference frame. First, the air gap of a salient-pole synchronous machine is not uniform; hence, only circuits rotating with the rotor would experience a constant self-inductance. Yes, that is right. But what about a round-rotor synchronous machine? Why, in the case of a round-rotor machine, would it be necessary to transform the stator variables to fictitious rotor reference frame circuits? The windings must be symmetrical to benefit from a change of variables, which is a function of an angular displacement. The rotor windings of a synchronous, salient-pole, or round-rotor machine, are, in general, asymmetrical. We are unaware of a change of variables that provides an advantage in transforming the variables of asymmetrical windings to a reference frame other than that where the windings physically exist. Therefore, the stator variables must be transformed to the rotor reference frame even for the round-rotor machine.

Example 7A. A two-pole, two-phase reluctance machine is identical in configuration to the synchronous machine shown in Fig. 7.2-1 with the field winding (*fd* winding) absent. It is our job to derive the equivalent circuits for the reluctance machine in the rotor reference frame.

Actually, we need not do any derivation; it has already been done. We need only to eliminate the field winding from the equivalent circuits shown in Fig. 7.5-1. In particular, Fig. 7A-1 shows equivalent circuits in the rotor reference frame for a two-phase reluctance machine, wherein the damper windings are shown short-circuited as they are in real life.

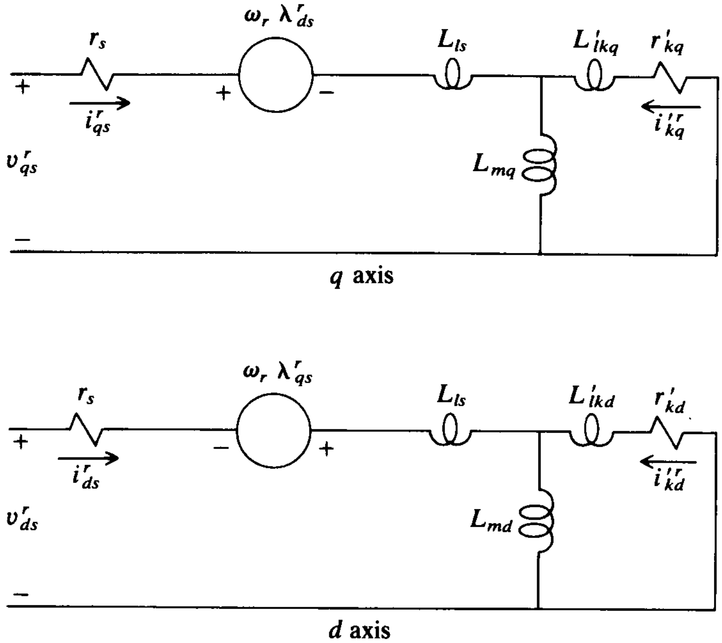

Figure 7A-1: Rotor reference frame equivalent circuits for a reluctance machine.

SP7.5-1 $f_{as} = \cos\omega_e t$ and $f_{bs} = \sin\omega_e t$. Determine f_{qs}^r and f_{ds}^r if $\theta_r = \omega_r t$ and $\omega_r = \omega_e$. $[f_{qs}^r = 1;\ f_{ds}^r = 0]$
SP7.5-2 Determine $\theta_r(0)$ so that $f_{qs}^r = f_{ds}^r$ in SP7.5-1, where here $\theta_r = \omega_r t + \theta_r(0)$. $[\theta_r(0) = \frac{1}{4}\pi$ and $-\frac{3}{4}\pi]$
SP7.5-3 Determine $\theta_{ef}(0)$ so that $f_{qs}^r = f_{ds}^r$ in SP7.5-1, where $\theta_{ef} = \omega_e t + \theta_{ef}(0)$. $[\theta_{ef}(0) = -\frac{1}{4}\pi$ and $\frac{3}{4}\pi]$
SP7.5-4 Repeat SP7.5-1 for $\omega_r = -\omega_e$. $[f_{qs}^r = \cos 2\omega_e t;\ f_{ds}^r = -\sin 2\omega_e t]$

7.6 ROTOR ANGLE

It would seem that we have already done our share of defining concepts and terms that we have not seen or used before; the sinusoidally distributed winding, self- and mutual inductances that vary, changes of variables that give rise to fictitious windings, and a machine that develops three types of torque. We cannot help but wonder when these new concepts are going to stop. Unfortunately, we are now faced with another definition that has evolved over the years to become deeply ingrained in synchronous-machine theory. The rotor angle is the case in point.

In its broadest definition, the rotor angle δ is

$$\delta = \theta_r - \theta_{esv} \tag{7.6-1}$$

where θ_r is the electrical angular position of the rotor and θ_{esv} is the angular displacement of a stator phase voltage, generally v_{as}. The time-zero position is generally selected so that the fundamental component of v_{as} is maximum at $t = 0$; for example, a cosine with $\theta_{esv}(0) = 0$. Although the above definition of δ is valid regardless of the mode of operation (either or both ω_r and ω_e may vary), a physical interpretation is most easily visualized during balanced steady-state operation. It is, however, important to mention in passing that here we see the mixing of a variable associated with the electric system, $\theta_e(\omega_e)$, and a variable associated with the mechanical system, $\theta_r(\omega_r)$. Fortunately, good will come from this, even though it can be somewhat confusing when, in the next section, we superimpose a phasor diagram that rotates at ω_e upon the rotor, which also rotates at ω_e during steady-state operation, and then note that the angle between $\tilde{V}_{as}$ and the q axis is δ, the rotor angle.

SP7.6-1 Calculate δ for SP7.5-1, SP7.5-2, and SP7.5-4. Assume f_{as} and f_{bs} are v_{as} and v_{bs}, respectively. [$\delta = 0$; $\delta = \frac{1}{4}\pi$ and $-\frac{3}{4}\pi$; $\delta = -2\omega_e t$]
SP7.6-2 Why did we not ask you to calculate δ for SP7.5-3? [We could have, but $\theta_{esv}(0)$ is generally selected to be zero.]

7.7 ANALYSIS OF STEADY-STATE OPERATION

In the case of the synchronous machine, we have found it necessary to refer the stator variables to the rotor reference frame. What will be the frequency of the variables in the rotor reference frame during balanced steady-state operation? Actually, we have our answer from SP7.5-1, but let us think more about this before doing anything analytical. First, we know that, during steady-state operation, the electrical angular velocity of the rotor, ω_r, is equal to ω_e. Hence, the circuits that physically exist on the rotor (*kq, fd,* and *kd* windings) or the fictitious windings (qs^r and ds^r windings) do not experience a change of flux linkages. How do we know this? Well, the air-gap mmf established by the constant (dc) field current is, of course, constant relative to the windings on the rotor. Now, what about mmf_s, the rotating air-gap mmf established by the balanced, sinusoidal stator currents? It rotates at ω_e, which is also the speed ω_r of the rotor. Hence, since neither mmf_s nor mmf_r is changing relative to the rotor, the windings in the rotor reference frame will not experience a change in flux linkages. At this point, we can forget about the short-circuited damper windings since, without a change of flux linkages, there can be no induced voltage and, thus, i'^r_{kq} and i'^r_{kd} must be zero for balanced steady-state operation where $\omega_r = \omega_e$. Actually, if we accept the fact that there is not a change of flux linkages relative to the rotor circuits, then there can be no induced voltage due to transformer action in any of the circuits on the rotor or in the rotor reference frame. One would then guess that, in the steady state, the currents and voltages associated with all rotor windings, actual or fictitious, would have to be constant (i'^r_{kq} and i'^r_{kd} are constant at zero). This seems logical, but what has happened to the balanced, sinusoidal stator variables? Remember that the balanced, steady-state sinusoidal stator currents give rise to a constant mmf_s rotating at ω_e. But, if mmf_s, which rotates at ω_e, is now to be produced by currents flowing in fictitious windings ($i^r_{qs}$and i^r_{ds}), that are mathematically fixed in the rotor reference frame which is rotating at ω_e during steady-state operation, what must be the frequency of these currents flowing in the fictitious windings? They must be constant (dc).

Now that we know what to expect, let us proceed. During balanced steady-state operation, the stator variables may be expressed as

$$F_{as} = \sqrt{2}F_s \cos[\omega_e t + \theta_{esf}(0)] \tag{7.7-1}$$

$$F_{bs} = \sqrt{2}F_s \sin[\omega_e t + \theta_{esf}(0)] \tag{7.7-2}$$

Substituting F_{as}, and F_{bs}, into the equations of transformation, (5.3-1), with $\omega = \omega_r$, which is ω_e, and the zero position of the rotor reference frame $\theta(0) = \theta_r(0)$ yields

$$F^r_{qs} = \sqrt{2}F_s \cos[\theta_{esf}(0) - \theta_r(0)] \tag{7.7-3}$$

$$F^r_{ds} = -\sqrt{2}F_s \sin[\theta_{esf}(0) - \theta_r(0)] \tag{7.7-4}$$

Clearly, $\theta_{esf}(0)$ and $\theta_r(0)$ are constants and, thus, F^r_{qs} and F^r_{ds} are constants. In other words, a balanced set of sinusoidal stator variables become constants in the rotor reference frame during steady-state conditions where $\omega_r = \omega_e$. Actually, we expected this from our work in Chapter 5.

Let us now go back to the voltage equations in the rotor reference frame, (7.5-1) through (7.5-5). As we have agreed, for balanced steady-state operation we can forget about the damper windings. Hence, (7.5-3) and (7.5-5) play no role in the analysis of steady-state operation of a synchronous machine. Moreover, since the voltages and currents in the rotor reference frame are constants during balanced steady-state operation, we can apply dc circuit theory to solve the $^r_{qs}$, $^r_{ds}$, and $^r_{fd}$ voltage equations. In particular, since all variables are constant during steady-state operation, all variables multiplied by the operator p are zero. Hence, (7.5-1), (7.5-2), and (7.5-4) may be written as

$$V_{qs}^r = r_s I_{qs}^r + \omega_r \lambda_{ds}^r \tag{7.7-5}$$

$$V_{ds}^r = r_s I_{ds}^r - \omega_r \lambda_{qs}^r \tag{7.7-6}$$

$$V_{fd}'^r = r_{fd}' I_{fd}'^r \tag{7.7-7}$$

where capital letters have been used to denote steady-state voltages and currents. Now λ_{qs}^r and λ_{ds}^r are (7.5-22) and (7.5-23), respectively, wherein the damper winding currents are set equal to zero. Appropriate substitution of (7.5-22) and (7.5-23) into (7.7-5) and (7.7-6), wherein ω_r is set equal to ω_e, yields

$$V_{qs}^r = r_s I_{qs}^r + X_d I_{ds}^r + X_{md} I_{fd}'^r \tag{7.7-8}$$

$$V_{ds}^r = r_s I_{ds}^r - X_q I_{qs}^r \tag{7.7-9}$$

Note that these are dc voltage equations and, yet, we have reactances X_d, X_q, and X_{md} without js. We are not dealing with phasors, yet X times I is a voltage, regardless. Actually, we saw this in (5.5-24) and (5.5-25) when we selected the synchronously rotating reference frame.

The above voltage equations can be used in their present form to analyze the synchronous machine; however, it is convenient and customary to relate the F_{qs}^r and F_{ds}^r quantities, which are constants, to $\tilde{F}_{as}$, which is a phasor representing a sinusoidal voltage. To accomplish this goal, let us first look at δ for steady-state operation. In particular, if we arbitrarily select or "call" time zero with $\omega_r = \omega_e$, the steady-state rotor angle from (7.6-1) becomes

$$\delta = \theta_r(0) - \theta_{esv}(0) \tag{7.7-10}$$

Later, we will set $\theta_{esv}(0) = 0$, but for now we will let it be. If (7.7-10) is solved for $\theta_r(0)$ and the result substituted into (7.7-3) and (7.7-4), we obtain

$$F_{qs}^r = \sqrt{2}F_s \cos[\theta_{esf}(0) - \theta_{esv}(0) - \delta] \tag{7.7-11}$$

$$F_{ds}^r = -\sqrt{2}F_s \sin[\theta_{esf}(0) - \theta_{esv}(0) - \delta] \tag{7.7-12}$$

Now, let us leave these equations for just a moment. From (7.7-1) and (7.7-2), we know that F_{as} and F_{bs} may be written as

$$F_{as} = Re[\sqrt{2}\tilde{F}_{as}e^{j\omega_e t}] \tag{7.7-13}$$

$$F_{bs} = Re[\sqrt{2}\tilde{F}_{bs}e^{j\omega_e t}] \tag{7.7-14}$$

where

$$\tilde{F}_{as} = F_s e^{j\theta_{esf}(0)} \tag{7.7-15}$$

and $\tilde{F}_{bs} = -j\tilde{F}_{as}$. If each side of (7.7-15) is multiplied by $\sqrt{2}e^{-j\delta}$, we will obtain

$$\sqrt{2}\tilde{F}_{as}e^{-j\delta} = \sqrt{2}F_s \cos[\theta_{esf}(0) - \delta] + j\sqrt{2}F_s \sin[\theta_{esf}(0) - \delta] \tag{7.7-16}$$

We will now do what we promised. We will select time zero at the maximum positive value of V_{as}. That is, $\theta_{esv}(0) = 0$, whereupon

$$V_{as} = \sqrt{2}V_s \cos \omega_e t \tag{7.7-17}$$

$$V_{bs} = \sqrt{2}V_s \sin \omega_e t \tag{7.7-18}$$

and $\tilde{V}_{as}$ is at zero degrees. Let us remember that from now on whenever we conduct an analysis of steady-state operation of synchronous machines, $\theta_{esv}(0) = 0$. With this restriction, compare the right-hand terms of (7.7-16) with (7.7-11) and (7.7-12). From this comparison and with $\theta_{esv}(0) = 0$, we can write

$$\sqrt{2}\tilde{F}_{as}e^{-j\delta} = F_{qs}^r - jF_{ds}^r \tag{7.7-19}$$

We have only a few more steps. From (7.7-19) we can write

$$\sqrt{2}\tilde{V}_{as}e^{-j\delta} = V_{qs}^r - jV_{ds}^r \tag{7.7-20}$$

Substituting (7.7-8) and (7.7-9) into (7.7-20) yields

$$\sqrt{2}\tilde{V}_{as}e^{-j\delta} = r_s I_{qs}^r + X_d I_{ds}^r + X_{md} I_{fd}^{\prime r} + j(-r_s I_{ds}^r + X_q I_{qs}^r) \tag{7.7-21}$$

If $X_q I_{ds}^r$ is added to and subtracted from the right-hand side of (7.7-21), and if it is noted from (7.7-19) that

$$j\sqrt{2}\tilde{I}_{as}e^{-j\delta} = I_{ds}^r + jI_{qs}^r \tag{7.7-22}$$

then (7.7-21) may be written as

$$\tilde{V}_{as} = (r_s + jX_q)\tilde{I}_{as} + \frac{1}{\sqrt{2}}[(X_d - X_q)I_{ds}^r + X_{md}I_{fd}^{\prime r}]e^{j\delta} \tag{7.7-23}$$

It is convenient to define the last term of (7.7-23) as

$$\tilde{E}_a = \frac{1}{\sqrt{2}}[(X_d - X_q)I_{ds}^r + X_{md}I_{fd}^{\prime r}]e^{j\delta} \tag{7.7-24}$$

which is often referred to as the *excitation voltage*. Thus, (7.7-23) becomes

$$\tilde{V}_{as} = (r_s + jX_q)\tilde{I}_{as} + \tilde{E}_a \tag{7.7-25}$$

Equation (7.7-25) is used widely in the analysis of steady-state operation of synchronous machines. It is very compact and easy to use, far more reduced than one would have expected at the outset of this development. However, there is something more involved here than first meets the eye. Note that the angle of the phasor $\tilde{E}_a$ is δ, but δ has to do with the rotor. In particular, from (7.7-10) with $\theta_{esv}(0) = 0$ ($\tilde{V}_{as}$ is at zero degrees) the steady-state value of δ is $\theta_r(0)$, which is also the zero position of the rotor reference frame. In other words, if we look back to Fig. 7.2-1, we see that δ or $\theta_r(0)$ is the position of the q axis at the instant we called time zero, which was at the positive maximum value of V_{as}. In the end, we will have superimposed the phasor diagram upon the rotor. To start, consider Fig. 7.7-1. In Fig. 7.7-1*a* we see the position of the rotor at $t = 0$. However, we know that the rotor is rotating at ω_r (ω_e). Now, because at time zero $\theta_{esv}(0) = 0$, $\tilde{V}_{as}$ is at zero degrees, and the phase angle of $\tilde{E}_a$ is equal to δ, as shown in Fig. 7.7-1*b*, where we have assumed $\tilde{I}_{as}$ leading $\tilde{V}_{as}$ to illustrate generator operation. How can *a* and *b* of Fig. 7.7-1 be superimposed? Well, the rotor is rotating counterclockwise at ω_e and, although we generally do not think of it in this way, the phasors are also rotating counterclockwise at ω_e. Thus, we can superimpose Fig. 7.7-1*a* and Fig. 7.7-1*b* as shown in Fig. 7.7-1*c*.

We can now express the electromagnetic torque for a linear magnetic

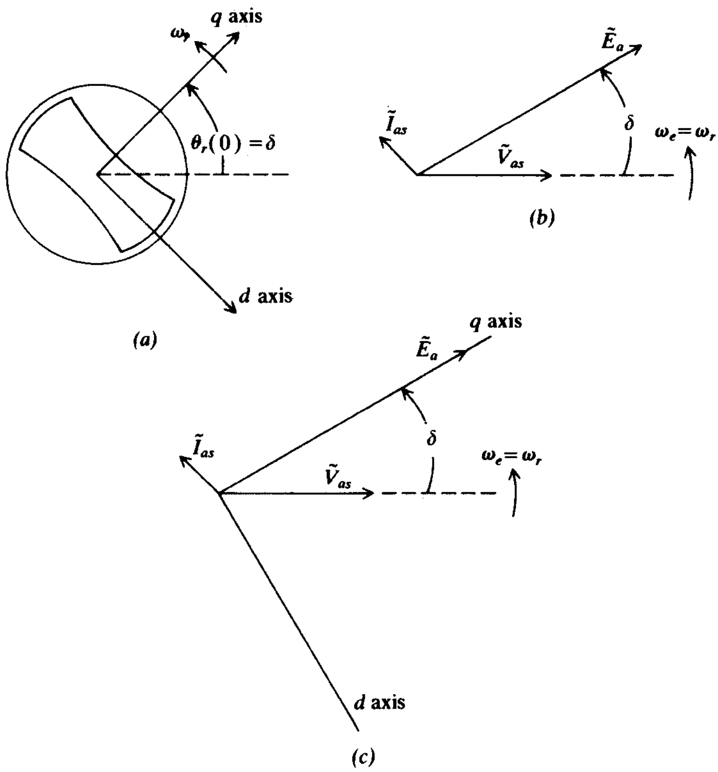

Figure 7.7-1: Superimposing the phasor diagram on the rotor of a synchronous machine $[\theta_{esv}(0) = 0]$. (a) Rotor at $t = 0$, (b) phasor at $t = 0$, (c) together at $t = 0$.

system in terms of the rotor angle. If (7.7-8) and (7.7-9) are solved for I_{qs}^r and I_{ds}^r and the results substituted into (7.5-31), we obtain

$$T_e = -\frac{P}{2}\frac{1}{\omega_e}\left\{\frac{r_s X_{md} I_{fd}'^r}{r_s^2 + X_q X_d}\left(V_{qs}^r - X_{md} I_{fd}'^r - \frac{X_d}{r_s} V_{ds}^r\right)\right.$$
$$+\frac{X_d - X_q}{(r_s^2 + X_q X_d)^2}[r_s X_q (V_{qs}^r - X_{md} I_{fd}'^r)^2$$
$$\left. +(r_s^2 - X_q X_d) V_{ds}^r (V_{qs}^r - X_{md} I_{fd}'^r) - r_s X_d (V_{ds}^r)^2]\right\} \qquad (7.7\text{-}26)$$

Note that, if we want to use (7.7-11) and (7.7-12), respectively, to express V_{qs}^{r} and $V_{ds}^{\prime r}$ then $\theta_{esv} = \theta_{esf}$ and

$$\begin{aligned} V_{qs}^{r} &= \sqrt{2}V_s \cos[\theta_{esv}(0) - \theta_{esv}(0) - \delta] \\ &= \sqrt{2}V_s \cos\delta \end{aligned} \tag{7.7-27}$$

$$\begin{aligned} V_{ds}^{r} &= -\sqrt{2}V_s \sin[\theta_{esv}(0) - \theta_{esv}(0) - \delta] \\ &= \sqrt{2}V_s \sin\delta \end{aligned} \tag{7.7-28}$$

We should mention in passing that (7.7-27) and (7.7-28) are valid for transient as well as steady-state operation. Although this fact is interesting, we will use the equations only for steady-state operation in this section. For compactness, we will define

$$E_{xfd}^{\prime r} = X_{md} I_{fd}^{\prime r} \tag{7.7-29}$$

If (7.7-27) through (7.7-29) are substituted into (7.7-26) and if the resistance r_s of the stator windings is neglected, the steady-state electromagnetic torque may be written as

$$T_e = -\frac{P}{2}\frac{1}{\omega_e}\left[\frac{E_{xfd}^{\prime r}\sqrt{2}V_s}{X_d}\sin\delta + \frac{1}{2}\left(\frac{1}{X_q} - \frac{1}{X_d}\right)(\sqrt{2}V_s)^2 \sin 2\delta\right] \tag{7.7-30}$$

Neglecting r_s is justified if its ohmic value is small relative to the magnetizing reactances (X_{mq} and X_{md}) of the machine. In variable-frequency drive systems, this is not the case at low frequencies, whereupon (7.7-26) must be used to calculate the steady-state torque rather than (7.7-30). The electromagnetic torque evaluated by (7.7-26) or (7.7-30) is positive for motor action (torque load; δ negative) and negative for generator action (torque input; δ positive).

Although (7.7-30) is a valid expression for the electromagnetic torque during balanced steady-state operation only if the stator winding resistance is small relative to the magnetizing reactances, it permits a quantitative description of two of the three torques produced by a salient-pole synchronous machine. Since $\omega_r = \omega_e$, the damper winding currents are zero and, hence, induction-motor torque is not present. The first term on the right-hand side of (7.7-30) is due to the interaction of the mmf produced by the stator currents and the mmf produced by the field current. The second term is the reluctance torque that occurs owing to the forces set up to attempt to align the minimum-reluctance path of the rotor with the resultant air-gap mmf.

A word of caution seems appropriate. With the advent of controlled electronic switching devices, electric machines are often operated in systems where the frequency and amplitude of applied stator voltages can be varied. In the above steady-state voltage equations, (7.7-24), (7.7-25), and (7.7-29), and steady-state torque equations, (7.7-26) and (7.7-30), inductive reactances are used. Therein, reactances are calculated by using the frequency of the applied stator voltages. Therefore, the ω_e in the reactances as well as the ω_e that appears in the torque equations must be changed as frequency changes.

Let us return to the expression for steady-state electromagnetic torque given by (7.7-30). Remember that it is valid only if r_s is small relative to X_{mq} and X_{md}. The first term on the right side of (7.7-30) is plotted in Fig. 7.7-2a, the second in Fig 7.7-2b, and the total or sum of the two components is plotted in Fig. 7.7-2c. (We shall talk about the points 1 and 1′ appearing in Fig. 7.7-2c a little later.) It is noted that, for a given frequency of the applied stator voltages and for a given machine design, the amplitude of the first term (denoted as A in Fig. 7.7-2a) is proportional to the product of the amplitude of the stator voltages ($\sqrt{2}V_s$) and the field voltage $V_{fd}^{\prime r}$ since, from (7.7-29), during steady-state operation

$$E_{xfd}^{\prime r} = \frac{X_{md}}{r_{fd}} V_{fd}^{\prime r} \tag{7.7-31}$$

When synchronous machines are used as motors in variable-frequency drive systems, both V_s and $E_{xfd}^{\prime r}$ can be varied. However, in applications where the synchronous machine is used as a generator to produce electric power, such as in a power system, the stator voltage (V_s) is generally regulated and, consequently, it is not allowed to vary more than, say, 1 to 3 percent during normal steady-state operation. In this case, the amplitude of the first term, which is the main torque component in generators, is changed by changing the field voltage $V_{fd}^{\prime r}$.

The amplitude of the second term, the reluctance torque, is denoted as B in Fig. 7.7-2b. For a fixed frequency of operation and a given machine design, the reluctance torque varies as the square of the amplitude of the applied stator voltages ($\sqrt{2}V_s$). In variable-frequency drive systems, the reluctance torque may be changed by changing V_s for a given frequency of operation. However, in a power system where both the frequency and amplitude of the stator voltages are essentially constant, the amplitude of the reluctance torque is also essentially constant.

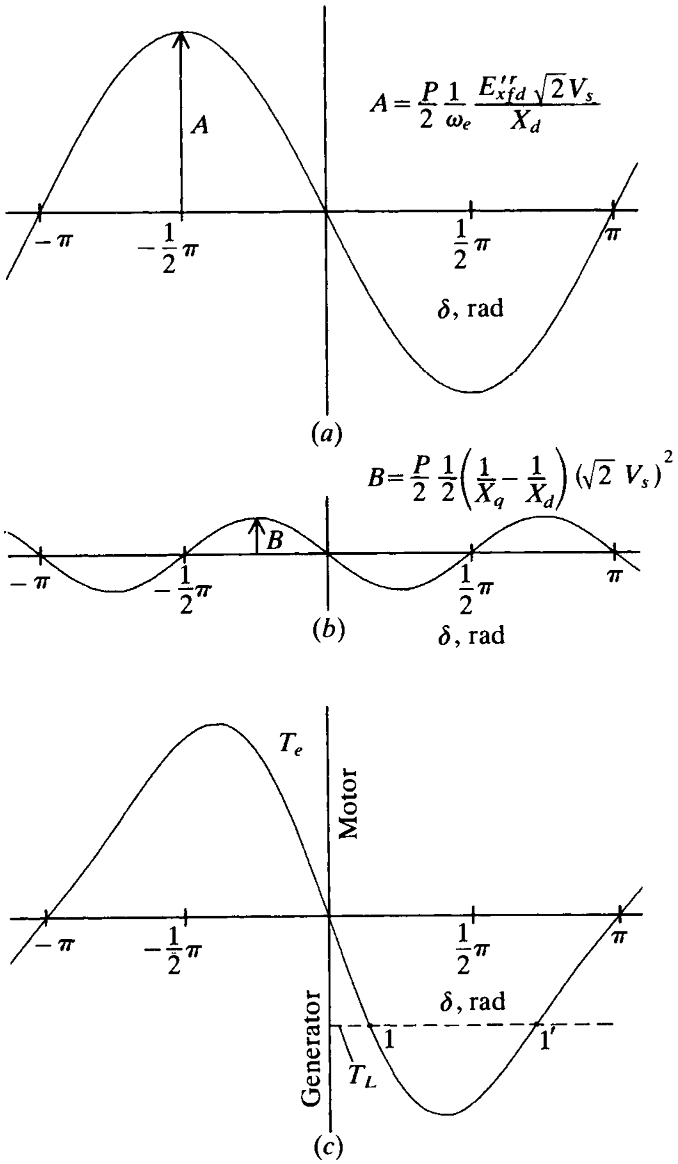

Figure 7.7-2: Steady-state electromagnetic torque of a synchronous machine.

Recall that the rotor angle δ is the angle between the phasor $\tilde{E}_a$ that lays along the q axis and the phasor $\tilde{V}_{as}$. Also, for a given load or input torque, the rotor angle is constant during steady-state operation and, since T_e versus δ is periodic, we need only consider the plot for $-\pi < \delta < \pi$. Now, the load torque and the electromagnetic torque are related by (7.4-3), from which it is clear that during steady-state operation $T_e = T_L$. Recall that T_e and T_L are positive in opposite directions. For illustrative purposes, let the synchronous machine be connected to an electric system and let the load torque be negative. That is, torque is applied to the shaft by some external means such as a steam- or hydro-turbine, a combustion engine, or, perhaps a wind turbine. Regardless of how the applied torque is developed, it is an input torque to the generator shaft and the steady-state T_e is negative. Let us think about this for a minute. The machine is connected to an electric system. If a torque is applied to the shaft, and since torque times rotor speed is equal to power, the synchronous machine must deliver an equal amount of power (neglecting friction, windage, and ohmic losses) to the electric system. Otherwise, there would be a torque or power imbalance and, if T_e is not equal to T_L, the synchronous machine would accelerate for $T_e - T_L > 0$ and decelerate for $T_e - T_L < 0$.

In the next section, we will discuss the dynamic performance of the synchronous machine. It is interesting, however, to continue our example of steady-state operation to determine the stable operating region. We can do as we did in the case of the relay back in Chapter 2. With T_L negative, there are two possible operating points between $-\pi < \delta < \pi$. They are denoted 1 and 1′ in Fig. 7.7-2*c*. Now, we must remember that T_L is constant. First, assume that steady-state operation occurs at point 1. This is a valid operating point if the system will return to this point when distributed from it. To test this, let δ decrease ever so slightly. In this case $T_e - T_L > 0$ and the rotor will accelerate, thereby increasing δ, (7.6-1); hence, a torque is developed to move the system back to operating point 1. If now δ increases ever so slightly, $T_e - T_L < 0$, and the system will again move back to point 1. Hence, point 1 is a stable operating point.

Although we all suspect what is going to happen at point 1′, let us go through the exercise anyway. If we assume that the system is operating stably at point 1′, then a displacement in δ from this operating point should cause a torque to restore the system to this operating point. If δ decreases slightly from point 1′, $T_e - T_L < 0$ and the machine would decelerate, which would further decrease δ. The system would move away from point 1′ and, after all transients have subsided, the system would operate stably at point 1. If, instead, δ increases from point $1'$, $T_e - T_L > 0$, whereupon the machine will accelerate, moving away from point $1'$. We can conclude that, although point $1'$ satisfies the torque-balance equation (7.4-3), it is not a stable operating condition. Let us go back a step. If δ increases from point $1'$ and the rotor accelerates, where will it end up? At point $1 + 2\pi$ if it does not go unstable dynamically. We really cannot appreciate the meaning of "unstable dynamically" until we can study the dynamic characteristics in the next section. It is sufficient here to say that we are dealing with steady-state characteristics, and one can get into trouble using steady-state characteristics to explain the large-excursion, dynamic (transient) characteristics of a system.

It is apparent that the only way that the steady-state electric power output or input can be changed is to change the torque T_L. However, the electrical characteristics of a synchronous machine connected to a system can be changed by changing the field voltage $V_{fd}'^r$. Although the following is, perhaps, of most interest to power-system engineers, it is worth a passing consideration by all. To explain the influence of $E_{xfd}'^r$ ($V_{fd}'^r$), we will assume that the machine is connected to a large system so that, regardless what we do with the synchronous machine, it will not change the magnitude or phase of the system voltage, $\tilde{V}_{as}$. This is commonly called an *infinite bus* in power-system language. If we now assume that the load torque T_L is zero and if we neglect friction and windage losses along with the stator resistance, then T_e and δ are also zero and the machine will run at synchronous speed without absorbing energy from either the electric or mechanical systems.

Although this mode of operation is not feasible in practice, since the machine will actually absorb a small amount of power to satisfy the ohmic, friction, and windage losses, and, thus, a small δ would exist at no load, it is convenient for purposes of explanation. With the machine floating on the line, the field voltage can be adjusted to establish the desired terminal conditions. Three situations may exist:

1. $|\tilde{E}_a| = |\tilde{V}_{as}|$, whereupon $\tilde{I}_{as} = 0$.

2. $|\tilde{E}_a| > |\tilde{V}_{as}|$, whereupon $\tilde{I}_{as}$ leads $\tilde{V}_{as}$ and the synchronous machine appears as a capacitor supplying reactive power to the system.

3. $|\tilde{E}_a| < |\tilde{V}_{as}|$ with $\tilde{I}_{as}$ lagging $\tilde{V}_{as}$, whereupon the machine is absorbing reactive power, appearing as an inductor to the system.

We should define reactive power, which is generally denoted as Q. In particular, the reactive power per phase is

$$Q = |\tilde{V}_{as}||\tilde{I}_{as}| \sin[\theta_{esv}(0) - \theta_{esi}(0)]$$

$$= |\tilde{V}_{as}||\tilde{I}_{as}| \sin \phi_{\text{pf}} \tag{7.7-32}$$

where ϕ_{pf} is the power-factor angle and the units of Q are var (volt ampere reactive). An inductance is said to absorb reactive power and thus, by definition, Q is positive for an inductor and negative for a capacitor. Actually, Q is a measure of the cyclic exchange of energy stored in the electric (capacitor) and magnetic (inductance) fields; however, there is no average power interchanged between these energy storage devices.

Now, to maintain the voltage in an actual power system at rated value, the synchronous generators are normally operated in the overexcited mode, $|\tilde{E}_a| > |\tilde{V}_{as}|$, since the generators are the main source of reactive power for the inductive loads throughout the system. In the past, synchronous machines have been placed in the power system for the sole purpose of supplying reactive power without any provision to absorb or provide real power. During peak load conditions when the system voltage starts to become depressed, these so-called *synchronous condensers* are brought on line and the field voltage is adjusted to help increase the system voltage. In this mode of operation, the synchronous machine behaves like an adjustable capacitor. On the other hand, it may be necessary for a generator to absorb reactive power in order to regulate voltage in a high-voltage transmission system during light-load conditions. This mode of operation is, however, not desirable and should be avoided since machine oscillations become less damped as the reactive power required is decreased. The influence of the field voltage during motor operation is illustrated in Example 7B.

As a finale to the analysis of steady-state operation of synchronous machines, let us consider the procedure by which generator action is established and then look at the phasor diagram for this mode of operation. A prime mover is mechanically connected to the shaft of the synchronous generator. As mentioned, this prime mover can be either a steam or wind turbine, a hydroturbine, or a combustion engine. If initially the torque input to the shaft due to the prime mover is zero, the synchronous machine is essentially floating on the line. If now the input torque is increased to some value (T_L negative), for example, by supplying steam to the turbine blades, a torque imbalance occurs since T_e must remain at its original value (zero) until δ

changes. Hence, the rotor will temporarily accelerate slightly above synchronous speed, whereupon δ will increase in accordance with (7.6-1). Thus, T_e increases negatively and a new operating point will be established with a positive δ where T_L is equal to T_e. The rotor will again rotate at synchronous speed. The actual dynamic response of the electric and mechanical systems during this loading process is illustrated by computer traces in the following section. If, during generator operation, the torque input from the prime mover is increased (T_L negative) to a value greater than the maximum possible value of T_e, the machine will be unable to maintain steady-state operation since it cannot electrically transmit the power supplied to the shaft. In this case, the device will accelerate above synchronous speed theoretically without bound. However, protection is normally provided in power systems that disconnects the machine from the system and reduces the input torque to zero by closing the steam valves of the steam turbine, for example, when it exceeds synchronous speed by 3 to 5 percent.

Normally, steady-state generator operation is depicted by the phasor diagram shown in Fig. 7.7-3. Here $\theta_{esi}(0)$ is the angle between the voltage and the current since the time-zero position is $\theta_{esv}(0) = 0$. Since the phasor diagram and the q and d axes of the machine may be superimposed, the rotor reference frame voltages and currents are also shown. If we wish to show each component of V_{qs}^r and V_{ds}^r, they can be broken up according to (7.7-8) and (7.7-9), and each term added algebraically along the appropriate axes.

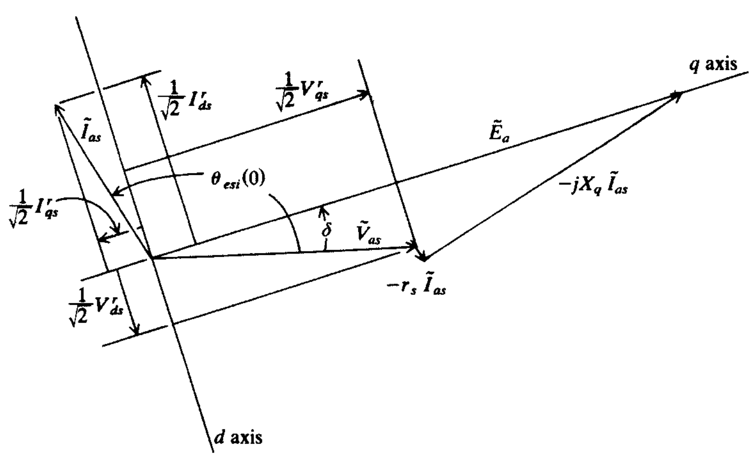

Figure 7.7-3: Phasor diagram for generator operation.

However, care must be taken when interpreting this diagram. $\tilde{V}_{as}$, $\tilde{I}_{as}$, and $\tilde{E}_a$ are phasors representing sinusoidal quantities. On the other hand, all rotor reference frame quantities are constants. They do not represent phasors in the rotor reference frame even though we have displayed them on a phasor diagram.

Example 7B. A six-pole, two-phase, salient-pole synchronous machine is supplied from a 440-V (rms) 60-Hz source. The machine is operated as a motor with a total power input of 40 kW at the terminals. The parameters of the machine are $r_s = 0.3\,\Omega$, $L_{ls} = 0.001$ H, $L_{md} = 0.015$ H, $L_{mq} = 0.008$ H, $r'_{fd} = 0.03\,\Omega$, and $L'_{lfd} = 0.001$ H. (a) The excitation is adjusted so that $\tilde{I}_{as}$ lags $\tilde{V}_{as}$ by 30°. Calculate $\tilde{E}_a$. (b) Repeat (a) with the excitation adjusted so that $\tilde{I}_{as}$, is in phase with $\tilde{V}_{as}$. (c) Repeat (a) with the excitation adjusted so that $\tilde{I}_{as}$ leads $\tilde{V}_{as}$ by 30°.

(a) The phase current may be calculated from the power as

$$|\tilde{I}_{as}| = \frac{\frac{1}{2}(40 \times 10^3)}{440 \cos 30^\circ} = 52.5 \text{ A} \tag{7B-1}$$

Note that the 40×10^3 is the total power, which is the sum of the two phases, and from (1.2-31) $\phi_{pf} = 30°$. With $\tilde{V}_{as} = 440\underline{/0^\circ}$,

$$\tilde{I}_{as} = 52.5\underline{/-30^\circ} \text{ A} \tag{7B-2}$$

From (7.7-25),

$$\begin{aligned}\tilde{E}_a &= \tilde{V}_{as} - (r_s + jX_q)\tilde{I}_{as} \\ &= 440\underline{/0^\circ} - [0.3 + j377(0.001 + 0.008]52.5\underline{/-30^\circ} \\ &= 368\underline{/-23.4^\circ} \text{ V}\end{aligned} \tag{7B-3}$$

(b) The phase current is

$$|\tilde{I}_{as}| = \frac{20 \times 10^3}{440} = 45.4 \text{ A} \tag{7B-4}$$

From (7.7-25),

$$\begin{aligned}\tilde{E}_a &= 440\underline{/0^\circ} - (0.3 + j3.39)45.4\underline{/0^\circ} \\ &= 453\underline{/-19.9^\circ} \text{ V}\end{aligned} \tag{7B-5}$$

(c) The phase current is

$$|\tilde{I}_{as}| = \frac{20 \times 10^3}{440\cos(-30°)} = 52.5 \text{ A} \tag{7B-6}$$

From (7.7-25),

$$\tilde{E}_a = 440\underline{/0°} - (0.3 + j3.39)52.5\underline{/30°}$$

$$= 540\underline{/-17.4°} \text{ V} \tag{7B-7}$$

It is important to note that the characteristics of the reactive component of the input power of the machine may be changed by changing the magnitude of $\tilde{E}_a$. If r_s is negligibly small, the power output is determined entirely by the input torque and, therefore, it is the same in (a), (b), and (c). It is left to the reader to construct the phasor diagram for each case.

Example 7C. A two-pole, 60-Hz, 110-V (rms), $\frac{3}{4}$-hp, two-phase reluctance machine has the following parameters: $r_s = 1\,\Omega$, $L_{ls} = 0.005$ H, $L_{md} = 0.10$ H, and $L_{mq} = 0.02$ H. The machine is operating at rated torque output. Calculate δ and $\tilde{I}_{as}$.

With the machine operating at rated conditions, the power output is

$$P_{\text{out}} = (0.75)(746) = 559.5 \text{ W} \tag{7C-1}$$

Therefore, the electromagnetic torque is

$$T_e = \frac{P_{\text{out}}}{(2/P)\omega_r} = \frac{559.5}{(\frac{2}{2})377} = 1.484 \text{ N} \cdot \text{m} \tag{7C-2}$$

Substituting into (7.7-30) and noting that I'^r_{fd} is zero, we can solve for δ. In particular,

$$\sin 2\delta = \frac{-(2/P)\omega_e T_e(2)(1/X_q - 1/X_d)^{-1}}{(\sqrt{2}V_s)^2}$$

$$= \frac{-(\frac{2}{2})(377)(1.484)(2)[1/(377)(0.025) - 1/(377)/(0.105)]^{-1}}{(2)(110)^2}$$

$$= \frac{-(377)(1.484)(0.0808)^{-1}}{(110)^2} = -0.572 \tag{7C-3}$$

Therefore, $\delta = -17.4°$.

Although we could use (7.7-25) to obtain $\tilde{I}_{as}$, it is more straightforward to use (7.7-8) and (7.7-9). We know from (7.7-27) and (7.7-28) that

$$\begin{aligned} V_{qs}^r &= \sqrt{2}V_s \cos\delta \\ &= \sqrt{2}\,110\cos(-17.4°) = 148.4 \text{ V} \qquad (7\text{C-}4) \\ V_{ds}^r &= \sqrt{2}\,110\sin(-17.4°) = -46.5 \text{ V} \qquad (7\text{C-}5) \end{aligned}$$

Therefore, we can write (7.7-8) and (7.7-9) as

$$\begin{bmatrix} V_{qs}^r \\ V_{ds}^r \end{bmatrix} = \begin{bmatrix} r_s & X_d \\ -X_q & r_s \end{bmatrix} \begin{bmatrix} I_{qs}^r \\ I_{ds}^r \end{bmatrix} \qquad (7\text{C-}6)$$

which may be written as

$$\begin{bmatrix} 148.4 \\ -46.5 \end{bmatrix} = \begin{bmatrix} 1 & (377)(0.105) \\ -(377)(0.025) & 1 \end{bmatrix} \begin{bmatrix} I_{qs}^r \\ I_{ds}^r \end{bmatrix} \qquad (7\text{C-}7)$$

Solving for I_{qs}^r and I_{ds}^r yields

$$I_{qs}^r = 5.32 \text{ A} \qquad (7\text{C-}8)$$

$$I_{ds}^r = 3.61 \text{ A} \qquad (7\text{C-}9)$$

From (7.7-19),

$$\begin{aligned} \tilde{I}_{as} &= \frac{1}{\sqrt{2}}(I_{qs}^r - jI_{ds}^r)e^{j\delta} \\ &= \frac{1}{\sqrt{2}}(5.32 - j3.61)e^{-j17.4°} = 4.55\underline{/-51.6°} \text{ A} \qquad (7\text{C-}10) \end{aligned}$$

If we calculate the input power from the voltage and current, we obtain approximately 620 W. If we add the output power to the ohmic losses, we obtain approximately 601 W. Why the discrepancy? [*Hint:* What are the restrictions on (7.7-30)?]

SP7.7-1 A two-pole, two-phase synchronous machine is operated as a generator with $\tilde{V}_{as} = 110\underline{/0°}$ and $\tilde{I}_{as} = 5\underline{/150°}$. Calculate (*a*) total real power and (*b*) total reactive power. [(*a*) $P = -952.6$ W; (*b*) $Q = -550$ var]

SP7.7-2 The machine in SP7.7-1 is a round-rotor device with $\omega_r = 377$ rad/s. $L_{ls} = 4$ mH, $L_{md} = 50$ mH, and $r_s \cong 0$. Calculate δ. [$\delta = 28.7°$]

SP7.7-3 Calculate I'^r_{fd} for SP7.7-2. [$I'^r_{fd} = 13.76$ A]
SP7.7-4 The reluctance machine in Example 7C is operating as a motor with $\delta = -30°$. Calculate T_e. Neglect r_s. [$T_e = 2.25$ N · m]
SP7.7-5 Determine the approach in SP7.7-4 if we are to take the stator resistance into account. [(7.7-26) with $I^r_{fd} = 0$]

7.8 DYNAMIC AND STEADY-STATE PERFORMANCE

It is instructive to observe the variables of the synchronous machine during dynamic and steady-state operation. In this section, generator operation of a synchronous machine is illustrated by computer traces as well as motor operation of a reluctance machine. Although a two-phase reluctance machine is used in practice, a two-phase synchronous generator would not normally be used. Instead, the three-phase synchronous machine is the device normally used for generating electric power. Nevertheless, our purpose is to understand the theory and principles of operation of a synchronous machine. A two-phase machine is just as applicable in this regard as a three-phase machine. The following section on the three-phase synchronous machine provides the information necessary for the power-system engineer to make the straightforward transformation from a two-phase to a three-phase machine.

Two-Phase Synchronous Machine

The two-phase synchronous machine that we will consider is a four-pole, 150-hp, 440-V (rms), 60-Hz machine with the following parameters: $r_s = 0.26\,\Omega$, $L_{ls} = 1.14$ mH, $r'_{kq} = 0.02\,\Omega$, $L'_{lkq} = 1$ mH, $L_{mq} = 11$ mH, $L_{md} = 13.7$ mH, $r'_{fd} = 0.013\,\Omega$, $L'_{lfd} = 2.1$ mH, $r'_{kd} = 0.0224\,\Omega$, and $L'_{lkd} = 1.4$ mH. The inertia of the rotor and connected mechanical load is $J = 16.6$ kg · m^2 and B_m is assumed to be zero.

The dynamic performance of this synchronous machine during a step decrease in load torque from zero to -400 N · m is illustrated in Fig. 7.8-1. Since we are considering generator operation, perhaps it is more appropriate to consider this as a step increase in input torque from zero to 400 N · m. In any event, the machine is initially operating at synchronous speed with the field voltage adjusted so that the open-circuit voltage of the stator windings is equal to the rated voltage of the machine (440 V). Therefore, the stator currents are very small since $T_L = 0$. Plotted are v_{as}, i_{as}, v_{bs}, i_{bs}, T_e, ω_r (electrical angular velocity), δ, and T_L.

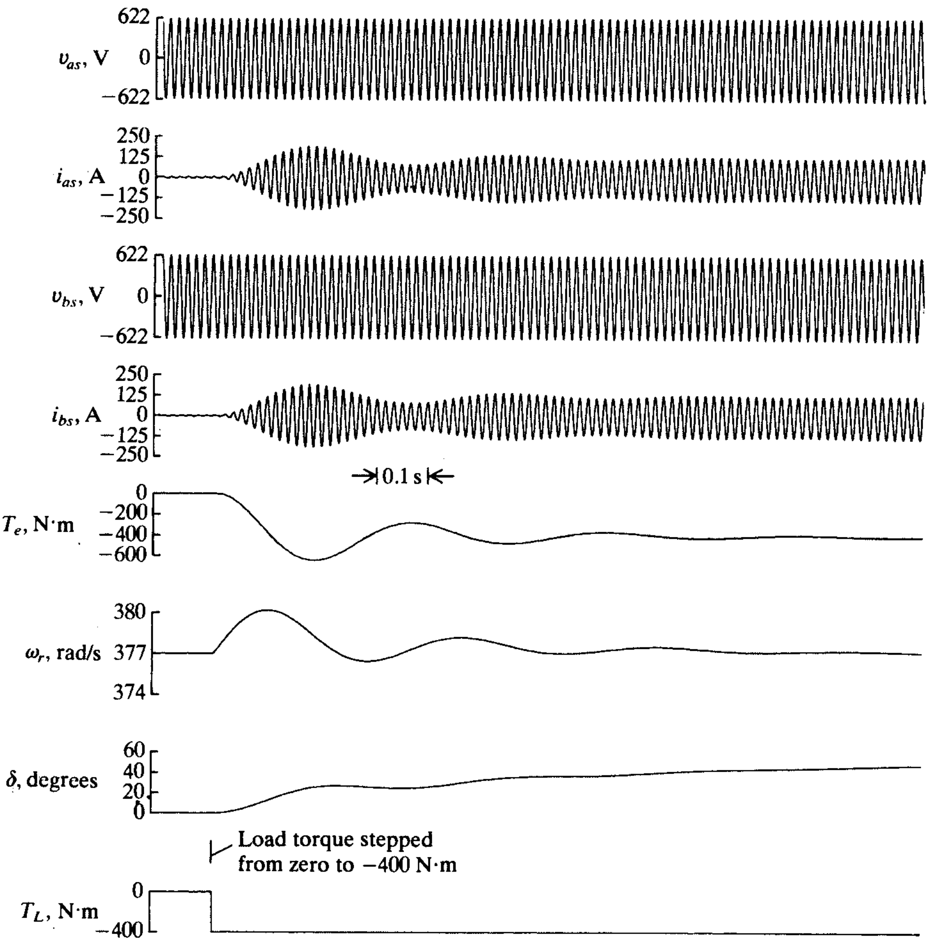

Figure 7.8-1: Dynamic performance of a two-phase synchronous generator during a step decrease in load torque (step increase in input torque).

Immediately upon the application of the input torque $(-T_L)$, the machine accelerates above synchronous speed as predicted by (7.4-3) and the rotor angle increases in accordance with (7.6-1). The rotor continues to speed up until the accelerating torque on the rotor is zero. This occurs when T_e is equal in magnitude to the input torque. As noted in Fig. 7.8-1, the speed increases to approximately 380 rad/s (electrical angular velocity). Even though the accelerating torque on the rotor is zero at this time, the rotor is still running above synchronous speed. Hence, δ will continue to increase and, consequently, T_e will continue to decrease (increase negatively). The decrease in T_e causes the rotor to decelerate and the speed of the rotor decreases toward synchronous speed. Note that at the first synchronous speed crossing of ω_r after the torque disturbance, the rotor angle is approximately 28 electrical degrees and T_e is approximately –600 N · m. The rotor speed decreases below synchronous speed, whereupon the integrand of (7.6-1) becomes negative and the rotor angle will begin to decrease. Damped oscillations of the rotor about synchronous speed continue until the new steady-state operating point is attained. We might wish to think of the instantaneous electromagnetic torque during this disturbance resulting from the interaction between (1) the stator and field currents, (2) the stator currents and saliency of the rotor, and (3) the stator and damper winding currents. Although this line of thinking may be helpful in visualizing what is going on, we must be careful when separating T_e into these three different torques during this transient period.

The dynamic torque versus rotor-angle characteristics during and following the step change in input torque is shown in Fig. 7.8-2. It is interesting to note that it requires considerable time before the machine establishes steady-state operation at $T_L = -400$ N · m. The steady-state torque-angle curve, which is also shown, in part, in Fig. 7.8-2, will pass through $T_e = 0$ at $\delta \cong 0$ and $T_L = -400$ N · m at $\delta = 68°$; however, it is much different from the T_e versus δ during the transient period.

Recall that, if we slowly increase the input torque in small increments, theoretically we could reach the maximum value of T_e shown in Fig. 7.7-2c before the machine would fall out of synchronism. The machine is generally rated at 50 to 70 percent of maximum torque capability. It is interesting to mention in passing that the maximum value of input torque (or load torque) that can be applied, with T_L initially zero and with the machine still being able to return to synchronous speed, is referred to as the *transient stability limit.*

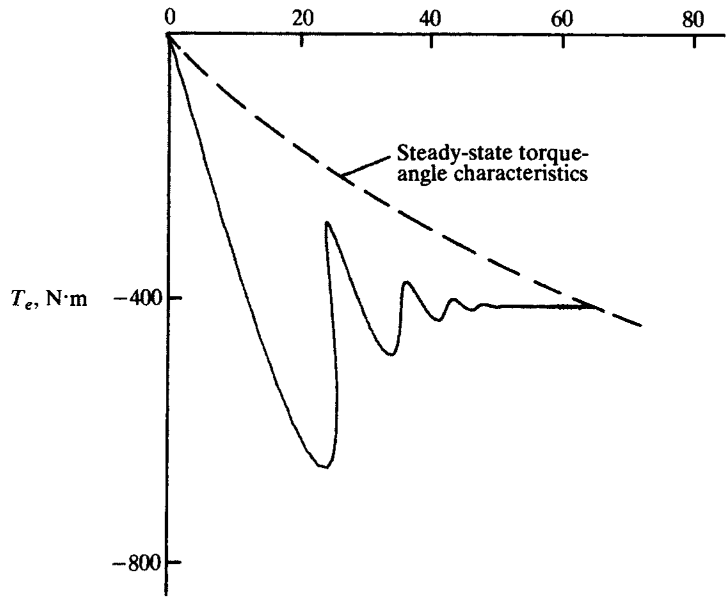

Figure 7.8-2: Dynamic torque versus rotor-angle characteristic for Fig. 7.8-1.

It is necessary to employ a computer to predict the dynamic torque-angle characteristics as shown in Fig. 7.8-2 and to determine the transient stability limit. However, before computers, the dynamic torque-angle characteristics were approximated for the "first swing" of the rotor by replacing X_d in (7.7-30) with X'_d, the so-called *transient reactance*, and E'^r_{xfd} with a voltage behind this transient reactance [1]. The transient reactance X'_d is always smaller than X_d and approximately equal to the sum of X_{ls} and X'_{lfd}. Also, the voltage behind this reactance that replaces E'^r_{xfd} is always larger than its steady-state value. It is shown in [1] that the resulting approximate, dynamic torque-angle characteristic is quite accurate during the first swing of the rotor. We shall leave this all to the power-system engineer because it is, indeed, a topic that should be studied by one working in the area of power-system stability. However, our purpose here is to make the first-time reader aware that the steady-state and dynamic torque versus rotor-angle characteristics are different, sometimes markedly different, as illustrated here.

Figure 7.8-3 is a repeat of Fig. 7.8-1 with the rotor reference frame variables plotted rather than the stator or machine variables. Also plotted is the field current i'^r_{fd}. Although for this machine the field current changed only slightly owing to a change in flux linkages, this is not typical of all machines. In some cases, depending upon the parameters and the type of the disturbance, a considerable voltage may be induced in the field winding, resulting in a marked change in field current during the transient period [1].

Two-Phase Reluctance Machine

As we have mentioned, the two-phase reluctance machine is a two-phase, salient-pole, synchronous machine without a field winding. It is instructive to observe the steady-state and dynamic performance of a low-power two-phase reluctance motor. The parameters of a 115-V (rms), 60-Hz, two-pole, two-phase, $\frac{1}{10}$-hp reluctance motor are: $r_s = 10\,\Omega$, $L_{ls} = 26.5$ mH, $r'_{kq} = 2\,\Omega$, $L'_{lkq} = 26.5$ mH, $J = 1 \times 10^{-3}$ kg $\cdot$ m^2, $L_{mq} = 132.6$ mH, $L_{md} = 318.3$ mH, $r'_{kd} = 4\,\Omega$, $L'_{lkd} = 26.5$ mH, and $B_m = 0$.

The dynamic performance when T_L is stepped from zero to 0.2 N $\cdot$ m is shown in Fig. 7.8-4. The following variables are plotted: v_{as}, i_{as}, v_{bs}, T_e, ω_r, δ, and T_L. The steady-state torque versus rotor-angle characteristic is shown in Fig. 7.8-5. It is interesting to note that this characteristic does not pass through the origin as does the reluctance component of the steady-state torque portrayed in Fig. 7.7-2*b*. Recall that the characteristics plotted in Fig. 7.7-2 were calculated by using (7.7-30), wherein the stator resistance is neglected. The stator resistance of this small reluctance motor is relatively large. The characteristics shown in Fig. 7.8-5 are calculated without neglecting r_s.

We understand that a reluctance or synchronous machine is equipped with short-circuited rotor windings for the purpose of damping rotor oscillations about synchronous speed and that is why we call them damper windings. Also, we understand that this damping torque occurs because of currents induced in the rotor circuits whenever $\omega_r \neq \omega_e$. As we have mentioned, this is often called induction-motor action since, with the short-circuited rotor windings, the reluctance machine produces an average torque-speed characteristic similar to an induction machine. If the rotor should slow down ever so slightly from synchronous speed, the induction-motor torque would become positive, which would tend to accelerate the rotor back to synchronous speed. Likewise, if the rotor should speed up from synchronous speed, the induction-motor torque would be negative, which would tend to slow the

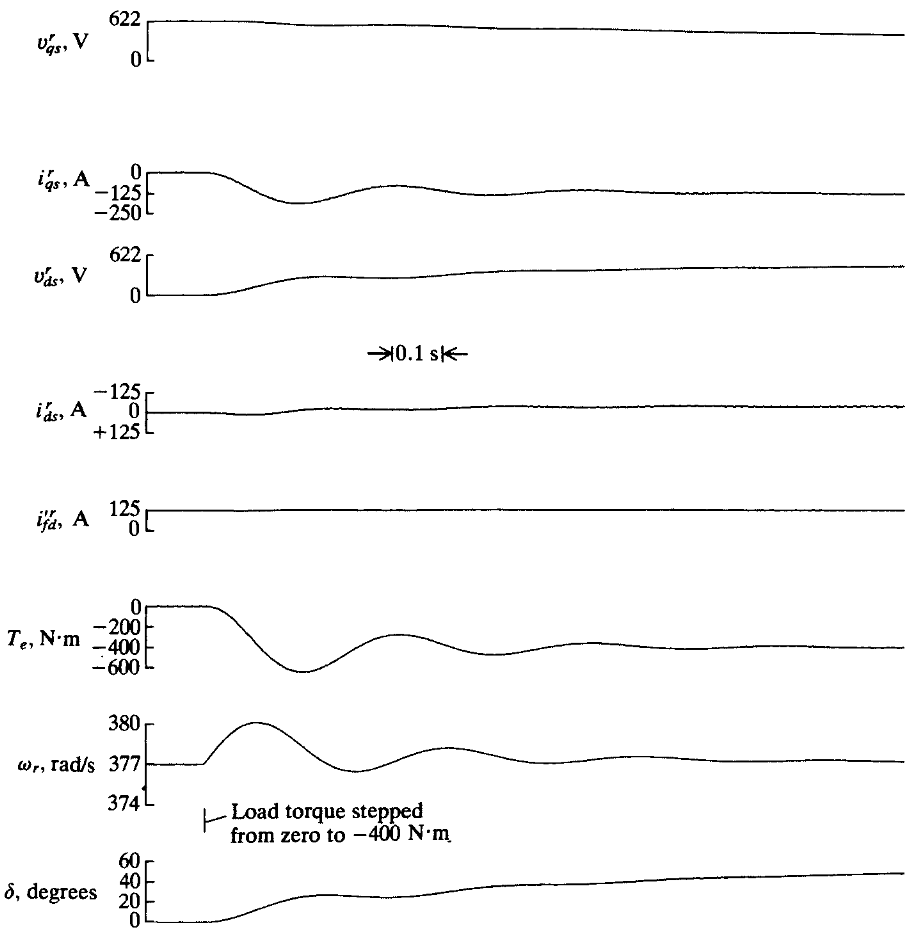

Figure 7.8-3: Same as Fig. 7.8-1 with rotor reference frame variables plotted.

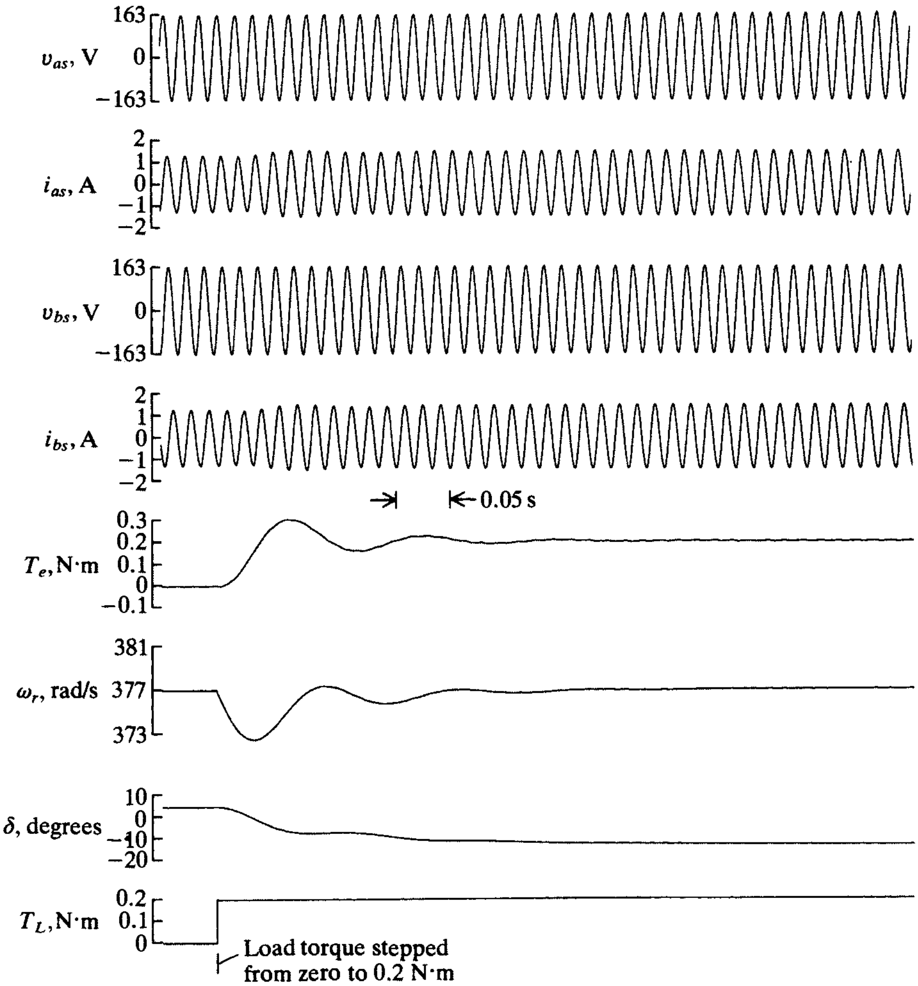

Figure 7.8-4: Dynamic performance of a two-pole, two-phase, $\frac{1}{10}$-hp reluctance motor when T_L is stepped from zero to 0.2 N · m.

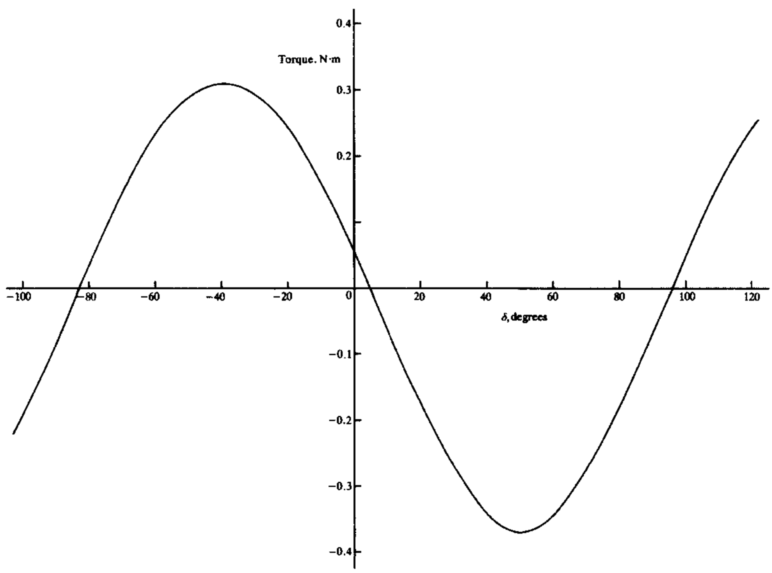

Figure 7.8-5: Steady-state torque versus rotor angle for a two-pole, two-phase, $\frac{1}{10}$-hp reluctance machine.

rotor speed. One wonders then if it is possible for the reluctance machine, with damper windings, to produce a starting torque by induction-motor action. Yes; in most cases the machine is designed so that it can accelerate from stall and pull in to synchronous-speed operation, often under 50 to 70 percent of rated load. Actually, we are not too surprised at this since we expected that somehow the reluctance motors of the world would be started by some means other than physically twisting each by its shaft in order to get it up to synchronous speed.

The acceleration torque-versus-speed characteristics are shown in Fig. 7.8-6. The load torque during acceleration is $T_L = K\omega_{rm}^2$, where $K = 0.2(377)^{-2}\,\mathrm{N\cdot m\cdot s^2/rad^2}$. The electromagnetic torque pulsates until synchronous speed is reached, whereupon the device operates as a reluctance motor producing a constant torque. But what causes the pulsating torque? Well, immediately following the application of the stator voltages, the pulsation in torque appears to be 60-Hz. This is caused by the transient dc offset in the stator currents, similar to what we saw in Chapter 6; however, as this 60-Hz pulsation decays in amplitude, a higher frequency pulsation starts to appear. As the rotor accelerates, this pulsation in torque increases

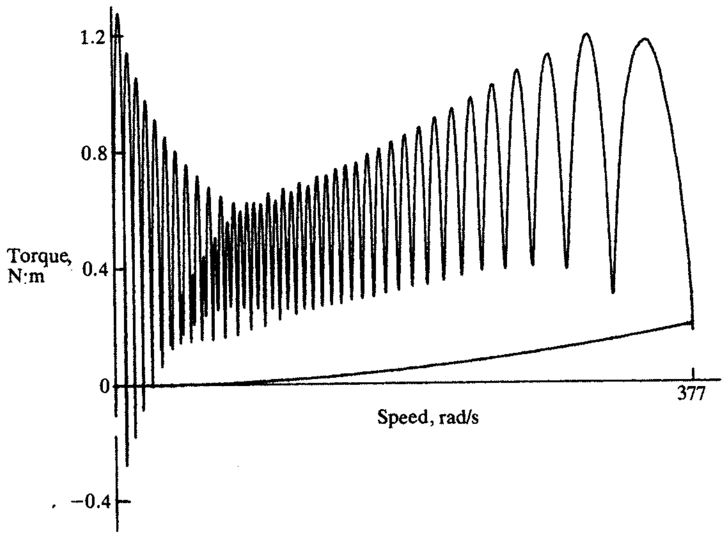

Figure 7.8-6: Acceleration from stall of the $\frac{1}{10}$-hp reluctance machine with $T_L = K\omega_{rm}^2$, where $K = 0.2(377)^{-2}$ N · m · s^2/rad^2.

in amplitude while decreasing in frequency. Actually, the frequency of this pulsating component is $2(\omega_e - \omega_r)$ and it is due to the saliency of the rotor (instantaneous reluctance torque) and to the fact that the *kq* and *kd* windings have different resistances. The pulsating reluctance torque is understandable; however, the fact that a pulsating torque with a frequency of $2(\omega_e - \omega_r)$ occurs because of unequal r'_{kq} and r'_{kd} is not at all apparent. It requires considerable work to prove that it exists; however, the interested reader will find this proof in [1].

SP7.8-1 From the steady-state voltage and current waveforms given in Fig. 7.8-1, approximate the power input from the electric system and compare this value to the shaft power ($T_L\omega_{rm}$). [$\tilde{V}_{as} = 440\underline{/0^\circ}$, $\tilde{I}_{as} \cong 111\underline{/-135^\circ}$, $P_{\text{in}} \cong -69$ kW, $P_{\text{shaft}} \cong -75$ kW]

SP7.8-2 Why is there a difference between P_{in} and P_{shaft} in SP7.8-1? Check your answer. [Ohmic loss]

SP7.8-3 Use Fig. 7.8-1 to determine each term of (7.4-3) at the first time $\omega_r = \omega_e$ after the step in T_L from zero to –400 N · m. [$T_L = -400$ N · m, $T_e = -570$ N · m, $J\frac{2}{P}\frac{d\omega_r}{dt} = -170$ N · m]

7.9 THREE-PHASE SYNCHRONOUS MACHINE

A two-pole, three-phase, salient-pole synchronous machine is shown in Fig. 7.9-1. The stator windings are identical and sinusoidally distributed with their magnetic axes displaced $\frac{2}{3}\pi$ from each other. The extension from the analysis of a two-phase machine to a three-phase machine is straightforward. However, it is worthwhile to note the expressions of the mutual inductances of the stator windings. Also, the addition of a third substitute variable, the zero variable, is necessary since we have three stator variables *as*, *bs*, and *cs*.

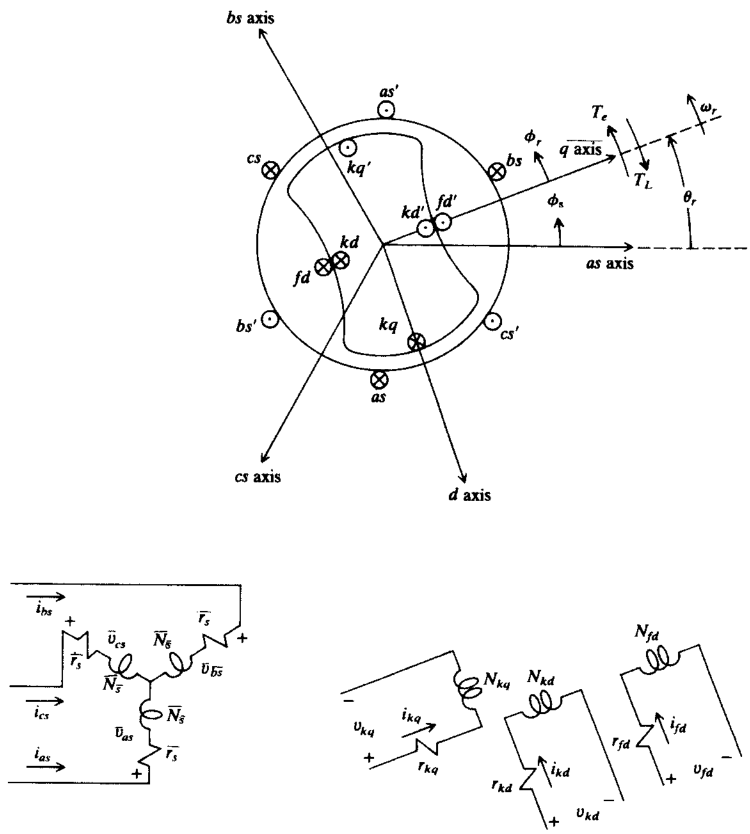

Figure 7.9-1: Two-pole, three-phase, salient-pole synchronous machine.

Voltage Equations and Winding Inductances

The voltage equations for the three-phase synchronous machine are those given by (7.3-1) through (7.3-5) for the two-phase machine, with the voltage equation for the cs phase added. In matrix form,

$$\mathbf{v}_{abcs} = \mathbf{r}_s \mathbf{i}_{abcs} + p\boldsymbol{\lambda}_{abcs} \tag{7.9-1}$$

$$\mathbf{v}_{qdr} = \mathbf{r}_r \mathbf{i}_{qdr} + p\boldsymbol{\lambda}_{qdr} \tag{7.9-2}$$

where

$$(\mathbf{f}_{abcs})^T = [f_{as} \quad f_{bs} \quad f_{cs}] \tag{7.9-3}$$

$$(\mathbf{f}_{qdr})^T = [f_{kq} \quad f_{fd} \quad f_{kd}] \tag{7.9-4}$$

The matrix $\mathbf{r}_s$ is an equal-element diagonal matrix and $\mathbf{r}_r$ is defined by (7.3-11).

The flux-linkage equations may be written as

$$\begin{bmatrix} \boldsymbol{\lambda}_{abcs} \\ \boldsymbol{\lambda}_{qdr} \end{bmatrix} = \begin{bmatrix} \mathbf{L}_s & \mathbf{L}_{sr} \\ (\mathbf{L}_{sr})^T & \mathbf{L}_r \end{bmatrix} \begin{bmatrix} \mathbf{i}_{abcs} \\ \mathbf{i}_{qdr} \end{bmatrix} \tag{7.9-5}$$

where

$\mathbf{L}_s =$

$$\begin{bmatrix} L_{ls} + L_A - L_B \cos 2\theta_r & -\frac{1}{2}L_A - L_B \cos 2(\theta_r - \frac{1}{3}\pi) & -\frac{1}{2}L_A - L_B \cos 2(\theta_r + \frac{1}{3}\pi) \\ -\frac{1}{2}L_A - L_B \cos 2(\theta_r - \frac{1}{3}\pi) & L_{ls} + L_A - L_B \cos 2(\theta_r - \frac{2}{3}\pi) & -\frac{1}{2}L_A - L_B \cos 2(\theta_r + \pi) \\ -\frac{1}{2}L_A - L_B \cos 2(\theta_r + \frac{1}{3}\pi) & -\frac{1}{2}L_A - L_B \cos 2(\theta_r + \pi) & L_{ls} + L_A - L_B \cos 2(\theta_r + \frac{2}{3}\pi) \end{bmatrix} \tag{7.9-6}$$

where L_{ls} is the leakage inductance, and L_A and L_B are defined by (7.3-23) and (7.3-24), respectively. The matrix $\mathbf{L}_{sr}$ is an extension of (7.3-30) to account for a three-phase stator:

$$L_{sr} = \begin{bmatrix} L_{skq} \cos \theta_r & L_{sfd} \sin \theta_r & L_{skd} \sin \theta_r \\ L_{skq} \cos(\theta_r - \frac{2}{3}\pi) & L_{sfd} \sin(\theta_r - \frac{2}{3}\pi) & L_{skd} \sin(\theta_r - \frac{2}{3}\pi) \\ L_{skq} \cos(\theta_r + \frac{2}{3}\pi) & L_{sfd} \sin(\theta_r + \frac{2}{3}\pi) & L_{skd} \sin(\theta_r + \frac{2}{3}\pi) \end{bmatrix} \tag{7.9-7}$$

The matrix $\mathbf{L}_r$ is (7.3-31).

The $\mathbf{L}_s$ given by (7.9-6) requires some discussion. The expressions for the self-inductances, which are the diagonal terms in (7.9-6), are apparent from our explanation for the self-inductances of a two-phase machine. Also the $-\frac{1}{2}L_A$ factor in the off-diagonal terms of (7.9-6) seems logical since the mutual inductance between two sinusoidally distributed windings of the stator can be adequately portrayed by the cosine of the angle between their magnetic axes (120°). Therefore, if the air gap were uniform, as in the case of the round-rotor synchronous machine, the off-diagonal terms (mutual inductances) would be $-\frac{1}{2}L_A$. However, as in the case of the two-phase synchronous machine, it is not clear that the variation of the mutual inductance would be L_B, nor is it immediately obvious that maximum coupling between the *as* and *bs* phase, for example, would occur at $\theta_r = \frac{1}{3}\pi$ and $\frac{3}{4}\pi$, and minimum coupling at $\theta_r = \frac{5}{6}\pi$ and $\frac{11}{6}\pi$. We will accept (7.9-6) without proof. A derivation is given in [1] for those who wish additional information.

In the case of the three-phase synchronous machine, the stator magnetizing inductances are defined as $\frac{3}{2}$ times the magnetizing inductances of a two-phase machine. In particular,

$$L_{mq} = \tfrac{3}{2}(L_A - L_B) \tag{7.9-8}$$

$$L_{md} = \tfrac{3}{2}(L_A + L_B) \tag{7.9-9}$$

With the above definition of L_{mq} and L_{md}, the right-hand sides of (7.3-32) through (7.3-37) must be multiplied by $\frac{2}{3}$ in order to define the amplitudes of the stator-to-rotor mutual inductances used in $\mathbf{L}_{sr}$ and the rotor magnetizing inductances used in $\mathbf{L}_r$. With the selection of (7.9-8) and (7.9-9) as the stator magnetizing inductances, the turns ratio for the rotor currents is two-thirds that given by (7.3-39); however, the turns ratio for the rotor voltages and flux linkages are unchanged from (7.3-40) and (7.3-41). The flux linkage equations can now be written as

$$\begin{bmatrix} \boldsymbol{\lambda}_{abcs} \\ \boldsymbol{\lambda}'_{qdr} \end{bmatrix} = \begin{bmatrix} \mathbf{L}_s & \mathbf{L}'_{sr} \\ \frac{2}{3}(\mathbf{L}'_{sr})^T & \mathbf{L}'_r \end{bmatrix} \begin{bmatrix} \mathbf{i}_{abcs} \\ \mathbf{i}'_{qdr} \end{bmatrix} \tag{7.9-10}$$

where

$$\mathbf{L}_{sr} = \begin{bmatrix} L_{mq}\cos\theta_r & L_{md}\sin\theta_r & L_{md}\sin\theta_r \\ L_{mq}\cos(\theta_r - \frac{2}{3}\pi) & L_{md}\sin(\theta_r - \frac{2}{3}\pi) & L_{md}\sin(\theta_r - \frac{2}{3}\pi) \\ L_{mq}\cos(\theta_r + \frac{2}{3}\pi) & L_{md}\sin(\theta_r + \frac{2}{3}\pi) & L_{md}\sin(\theta_r + \frac{2}{3}\pi) \end{bmatrix} \tag{7.9-11}$$

The matrix $\mathbf{L}'_r$ is (7.3-44) with our new definition of L_{mq} and L_{md}.

The voltage equations become

$$\mathbf{v}_{abcs} = \mathbf{r}_s\mathbf{i}_{abcs} + p\boldsymbol{\lambda}_{abcs} \tag{7.9-12}$$

$$\mathbf{v}'_{qdr} = \mathbf{r}'_r \mathbf{i}'_{qdr} + p\boldsymbol{\lambda}'_{qdr} \tag{7.9-13}$$

In terms of inductances,

$$\begin{bmatrix} \mathbf{v}_{abcs} \\ \mathbf{v}'_{qdr} \end{bmatrix} = \begin{bmatrix} \mathbf{r}_s + p\mathbf{L}_s & p\mathbf{L}'_{sr} \\ \frac{2}{3}p(\mathbf{L}'_{sr})^T & \mathbf{r}'_r + p\mathbf{L}'_r \end{bmatrix} \begin{bmatrix} \mathbf{i}_{abcs} \\ \mathbf{i}'_{qdr} \end{bmatrix} \tag{7.9-14}$$

where r'_j and L'_{lj} are $\frac{3}{2}$ times (7.3-48) and (7.3-49), respectively.

Torque

The electromagnetic torque, positive for motor action, may be expressed by using the second entry in Table 2.5-1. In particular,

$$\begin{aligned} T_e = \frac{P}{2}\Bigg\{ & \frac{L_{md} - L_{mq}}{3}\Big[\big(i_{as}^2 - \tfrac{1}{2}i_{bs}^2 - \tfrac{1}{2}i_{cs}^2 - i_{as}i_{bs} - i_{as}i_{cs} + 2i_{bs}i_{cs}\big)\sin 2\theta_r \\ & + \frac{\sqrt{3}}{2}\big(i_{bs}^2 + i_{cs}^2 - 2i_{as}i_{bs} + 2i_{as}i_{cs}\big)\cos 2\theta_r\Big] \\ & - L_{mq}i'_{kq}\left[\big(i_{as} - \tfrac{1}{2}i_{bs} - \tfrac{1}{2}i_{cs}\big)\sin\theta_r - \tfrac{\sqrt{3}}{2}\big(i_{bs} - i_{cs}\big)\cos\theta_r\right] \\ & + L_{md}(i'_{fd} + i'_{kd})\left[\big(i_{as} - \tfrac{1}{2}i_{bs} - \tfrac{1}{2}i_{cs}\big)\cos\theta_r + \tfrac{\sqrt{3}}{2}\big(i_{bs} - i_{cs}\big)\sin\theta_r\right]\Bigg\} \end{aligned} \tag{7.9-15}$$

The torque and rotor speed are related by (7.4-3), which is repeated here for convenience:

$$T_e = J\left(\frac{2}{P}\right)\frac{d\omega_r}{dt} + B_m\left(\frac{2}{P}\right)\omega_r + T_L \tag{7.9-16}$$

where J is the inertia and B_m is the damping coefficient, the units of which are discussed following (7.4-3). The load torque T_L is positive for a torque load (motor action) and negative for a torque input (generator action), as shown in Fig. 7.9-1.

Machine Equations in the Rotor Reference Frame

Since there are three stator variables (f_{as}, f_{bs}, f_{cs}), we must use three substitute variables in the transformation of the stator variables to the rotor reference frame. In particular, from (5.7-1) through (5.7-4) with a raised r,

$$\mathbf{f}^r_{qd0s} = \mathbf{K}^r_s \mathbf{f}_{abcs} \tag{7.9-17}$$

$$(\mathbf{f}^r_{qd0s})^T = [f^r_{qs} \quad f^r_{ds} \quad f_{0s}] \tag{7.9-18}$$

$$\mathbf{K}_s^r = \frac{2}{3}\begin{bmatrix} \cos\theta_r & \cos(\theta_r - \frac{2}{3}\pi) & \cos(\theta_r + \frac{2}{3}\pi) \\ \sin\theta_r & \sin(\theta_r - \frac{2}{3}\pi) & \sin(\theta_r + \frac{2}{3}\pi) \\ \frac{1}{2} & \frac{1}{2} & \frac{1}{2} \end{bmatrix} \tag{7.9-19}$$

where the rotor displacement θ_r is defined by (7.5-4). The inverse of $\mathbf{K}_s^r$ is

$$(\mathbf{K}_s^r)^{-1} = \begin{bmatrix} \cos\theta_r & \sin\theta_r & 1 \\ \cos(\theta_r - \frac{2}{3}\pi) & \sin(\theta_r - \frac{2}{3}\pi) & 1 \\ \cos(\theta_r + \frac{2}{3}\pi) & \sin(\theta_r + \frac{2}{3}\pi) & 1 \end{bmatrix} \tag{7.9-20}$$

It is important to note that the same notation ($\mathbf{K}_s^r$) is used for the transformation for both the two- and three-phase of variables.

As in the case of the induction machine, the zero variable ($0s$ variable) is the third substitute variable. We note that f_{0s} is zero for balanced conditions and that f_{0s} is not a function of θ_r and, therefore, the $0s$ quantities (voltage, current, and flux linkage) are associated with stationary circuits. For this reason, a raised index is not incorporated with the zero variables.

If the above change of variables is substituted into the stator-voltage equations and the flux-linkage equations, the resulting q and d voltage equations are identical to (7.5-1) through (7.5-5). The voltage equation for the 0s variables must be added. In particular,

$$v_{0s} = r_s i_{0s} + p\lambda_{0s} \tag{7.9-21}$$

For a linear magnetic system, the q and d flux-linkage equations for a three-phase synchronous machine are identical to those given by (7.5-22) through (7.5-26) for the two-phase machine. One must remember, however, that for a three-phase machine L_{mq} and L_{md} are defined by (7.9-8) and (7.9-9), respectively. The expression for λ_{0s} is

$$\lambda_{0s} = L_{ls} i_{0s} \tag{7.9-22}$$

Hence, the voltage equations in the rotor reference frame may be written in terms of inductances as

$$\begin{bmatrix} v_{qs}^r \\ v_{ds}^r \\ v_{0s}^r \\ v_{kq}'^r \\ v_{fd}'^r \\ v_{kd}'^r \end{bmatrix} = \begin{bmatrix} r_s + pL_q & \omega_r L_d & 0 & pL_{mq} & \omega_r L_{md} & \omega_r L_{md} \\ -\omega_r L_q & r_s + pL_d & 0 & -\omega_r L_{mq} & pL_{md} & pL_{md} \\ 0 & 0 & r_s + pL_{ls} & 0 & 0 & 0 \\ pL_{mq} & 0 & 0 & r'_{kq} + pL'_{kq} & 0 & 0 \\ 0 & pL_{md} & 0 & 0 & r'_{fd} + pL'_{fd} & pL_{md} \\ 0 & pL_{md} & 0 & 0 & pL_{md} & r'_{kd} + pL'_{kd} \end{bmatrix} \begin{bmatrix} i_{qs}^r \\ i_{ds}^r \\ i_{0s} \\ i_{kq}'^r \\ i_{fd}'^r \\ i_{kd}'^r \end{bmatrix} \tag{7.9-23}$$

where L_q and L_d are defined by (7.5-20) and (7.5-21), whereas L'_{kq}, L'_{fd}, and L'_{fd} are defined by (7.5-27) through (7.5-29), respectively. Again, we must realize that L_{mq} and L_{md} in all of these equations are defined by (7.9-8) and (7.9-9), respectively, for the three-phase machine.

The q and d equivalent circuits given in Fig. 7.5-1 for a two-phase machine are valid for the three-phase machine if L_{mq} and L_{md} are defined by (7.9-8) and (7.9-9), respectively, and the approximate turns ratio is used for the rotor currents [$\frac{3}{2}$ times (7.3-39)]. The equivalent circuit for the 0s quantities is a series rL circuit.

The expression for the electromagnetic torque for a three-phase synchronous machine in terms of q and d variables is identical to (7.5-11) and (7.5-31) if each expression is multiplied by $\frac{3}{2}$, and, of course, with the appropriate expression for L_{mq} and L_{md}. It follows that the steady-state voltage and torque equations given for the two-phase machine are also valid for the three-phase machine with the $\frac{3}{2}$ factor properly taken into account in the torque equation and in L_{mq} and L_{md}.

SP7.9-1 The parameters of a three-phase synchronous machine are identical to those for the two-phase synchronous machine given in Section 7.8. What must J and T_L be to make the dynamic and steady-state response of v^r_{qs}, i^r_{qs}, v^r_{ds}, and i^r_{ds} shown in Fig. 7.8-3 the same for the two- and three-phase machine? [$J_3 = \frac{3}{2}J_2$; $T_{L3} = \frac{3}{2}T_{L2}$]

SP7.9-2 The values of L_A and L_B are identical for two machines. One is a two-phase reluctance motor, the other a three-phase reluctance motor; otherwise, the parameters are identical. Will v^r_{qs}, i^r_{qs}, v^r_{ds}, and i^r_{ds} be identical for steady-state operation with $T_{L3} = \frac{3}{2}T_{L2}$? Why? [No; $L_{mq3} = \frac{3}{2}L_{mq2}$, $L_{md3} = \frac{3}{2}L_{md2}$]

7.10 RECAPPING

To conduct a rigorous analysis of a synchronous machine, it was necessary to incorporate a change of variables. In effect, this change of variables replaces the stator variables (voltages, currents, and flux linkages) with variables that are associated with fictitious windings fixed in the rotor reference frame. In this way, the time-varying stator self- and mutual inductances as well as the time-varying stator-to-rotor mutual inductances are eliminated and all inductances are constant. Although this analysis is rather involved, the resulting equations form the basis for analysis and the computer simulation of synchronous machines. Also, we found that, for steady-state operation, the voltage equations reduce to a single phasor equation, making steady-state motor or generator operation readily analyzable.

Since the equations that describe the dynamic behavior of synchronous machines are nonlinear, it is necessary to use a computer to solve these equations. Computer traces are given to illustrate the dynamic and steady-state performance of a synchronous generator and a reluctance motor. Although implementation of a computer simulation that can be used for these calculations is beyond the goals of this text, the advantage of portraying machine variables by computer simulation is vividly illustrated by the dynamic response of the synchronous generator. These traces not only give meaning to the dynamic behavior of a single synchronous machine but also they set the stage for studying the dynamic characteristics of a power system containing hundreds of such machines.

Our purpose has been to establish a method of analysis that is valid for synchronous machines ranging from a large synchronous generator to a small, low-power reluctance motor and to illustrate, by computer traces, the dynamic and steady-state behavior of these devices. Hopefully, we have been successful.

7.11 REFERENCES

[1] P. C. Krause, O. Wasynczuk, and S. D. Sudhoff, *Analysis of Electric Machinery and Drive Systems*, 2nd Edition, IEEE Press, 2002.

[2] R. H. Park, "Two Reaction Theory of Synchronous Machines – Generalized Method of Analysis – Part I," *AIEE Trans.*, vol. 48, July 1929, pp. 716-727.

7.12 PROBLEMS

1. Express all self- and mutual inductances for the synchronous machine shown in Fig. 7.12-1. Note that θ_r is referenced to the d axis.

* 2. Obtain (7.4-2) from (7.4-1).

3. Write Park's transformation ($\mathbf{K}_s^r$) with θ_r referenced to the d axis as in Fig. 7.12-1.

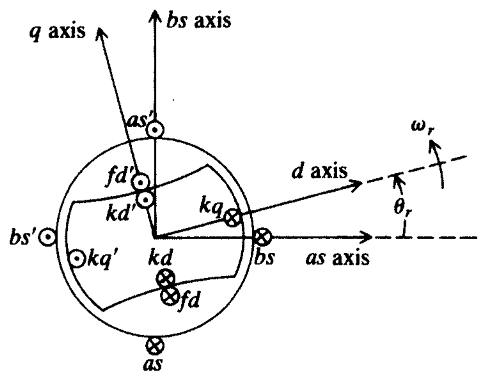

Figure 7.12-1: Two-pole, two-phase, salient-pole synchronous machine.

* 4. Derive the inductance matrices given by (7.5-16) through (7.5-18).

5. Derive the expression for torque given by (7.5-31).

6. It is often convenient to express the flux-linkage equations given by (7.5-22) through (7.5-26) in terms of flux linkages per second rather than flux linkages. This is accomplished by multiplying the flux linkage equations by a base electrical angular velocity ω_b. For example, ω_b for a 60-Hz machine would be 377 rad/s. In terms of flux linkages per second, (7.5-22) would become

$$\psi_{qs}^r = X_{ls} i_{qs}^r + X_{mq}(i_{qs}^r + i_{kq}'^r)$$

$X_{ls} = \omega_b L_{ls}$ and $X_{mq} = \omega_b L_{mq}$. Rewrite the voltage equations (7.5-1) through (7.5-5) and the expression for torque given by (7.5-11) in terms of flux linkages per second.

7. Rewrite the steady-state voltage equations, (7.7-24) and (7.7-25), and the steady-state torque equations, (7.7-26) and (7.7-30), for the reluctance machine.

8. A four-pole, 2-hp, two-phase, round-rotor synchronous machine is connected to a 110-V, 60-Hz source. The machine is operating as a generator with a total steady-state power output of 1 kW at the terminals.

The phase current lags the phase voltage by 160°. The parameters are $r_s = 0.5\,\Omega$, $L_{ls} = 0.005$ H, and $L_{mq} = L_{md} = 0.005$ H. Calculate $\tilde{E}_a$ and draw the phasor diagram showing $\tilde{V}_{as}$, $\tilde{I}_{as}$, $\tilde{E}_a$, and $(r_s + jX_q)\tilde{I}_{as}$.

9. Refer to Example 7B. Calculate I_{ds}^r, $I_{fd}^{\prime r}$, and the torque output in N·m for each mode of operation described.

10. Refer to Example 7C. Calculate $\tilde{E}_a$ and draw the phasor diagram showing $\tilde{V}_{as}$, $\tilde{I}_{as}$, $\tilde{E}_a$, and $(r_s + jX_q)\tilde{I}_{as}$.

11. In Fig. 7.8-1, the field voltage is adjusted so that the open-circuit stator phase voltage would be equal to rated voltage if the rotor were driven at synchronous speed. Calculate $V_{fd}^{\prime r}$ and $E_{fd}^{\prime r}$ for this condition.

*12. A three-phase, sixty-four-pole hydroturbine generator is rated at 325 MVA, with a 20-kV line-to-line voltage, and the generator delivers reactive power with a power factor of 0.85. In this case, the power factor is determined by the cosine of the angle between the voltage and the current with the positive direction of current out of the machine. In our work, we have assumed positive current into the machine; thus, the power factor would be −0.85. The machine parameters in ohms at 60 Hz are $r_a = 0.0023$, $X_q = 0.591$, and $X_d = 1.047$. For balanced steady-state rated conditions, calculate (*a*) $\tilde{E}_a$, (*b*) $E_{xfd}^{\prime r}$, and (*c*) T_e.

*13. A two-pole, 220-V (rms, line-to-line), 5-hp, three-phase reluctance machine has the following parameters: $r_s = 1\,\Omega$, $L_{ls} = 0.005$ H, $L_{md} = 0.10$ H, and $L_{mq} = 0.02$ H. (*a*) The machine is supplied from a 60-Hz, 220-V source with zero load torque. Calculate δ and $\tilde{I}_{as}$. (*b*) Repeat (*a*) with the machine connected to a 6-Hz, 22-V source.

Electromechanical Motion Devices, Second Edition
by Paul Krause, Oleg Wasynczuk and Steven Pekarek

Chapter 8

PERMANENT-MAGNET ac MACHINE

8.1 INTRODUCTION

The permanent-magnet ac machine supplied from a controlled voltage or current source inverter is becoming widely used as a low-power control motor. Depending upon the control strategies and inverters used, the performance of this inverter-machine combination can be made, for example, to (1) emulate the performance of a permanent-magnet dc motor, (2) operate in a maximum torque per ampere mode, (3) provide a field-weakening technique to increase the speed range for constant-power operation, and (4) shift the phase of the stator applied voltages to obtain the maximum possible torque at any given rotor speed. As all of these and other methods of controlled operation evolved, the inverter-machine combination has acquired various names, for example: (1) brushless dc machine, (2) controlled permanent-magnet ac machine, (3) controlled permanent-magnet synchronous machine, and (4) vector-controlled brushless dc machine. Identifying similar modes of operation with different names is to be expected as a technique or a technology evolves. The dynamo which became better known as a dc generator, and the rotating transformer, which we now know as the induction machine, are examples. Even the authors are guilty of name changing; in the first edition, this chapter was entitled "Brushless dc Machines."

Although there are probably many good reasons to do otherwise, in this introductory treatment of this emerging technology we will try to adhere to the following nomenclature. When referring to a brushless dc motor, the inverter is controlled so that the frequency of the voltages applied to the stator windings is equal to the speed of the rotor of the machine and these voltages are positioned in time so that maximum voltage applied to the as-winding occurs $\frac{1}{2}\pi$ electrical degrees ahead of the north pole of the permanent-magnet rotor. In all other applications or modes of operation, the inverter-machine combination will be referred to as a voltage- or current-controlled permanent-magnet ac machine. However, in an effort to avoid mass confusion we will make every effort to cite references and provide alternative nomenclature that might be used in the literature.

There are numerous types of inverters; however, we are able to become quite familiar with the operating features without getting involved with the actual inverter and the control thereof. In particular, if we assume that the stator variables (voltages and currents) are sinusoidal and balanced with the same angular velocity as the rotor speed, we are able to predict the predominant operating features of all modes of operation without becoming involved with the actual switching or control of the inverter. Therefore, except for the final section of this chapter, we will focus on the performance of the inverter-machine combination, assuming that the inverter is designed and controlled appropriately, and not how this is done.

As in the case of the synchronous machine, we will use the rotor reference frame to perform the analysis. For this purpose, it is convenient for us to deal first with the two-phase device since we are familiar with a two-phase system. We will find that after all these new concepts are out of the way, it is then rather easy for us to step up to the three-phase device.

If you have studied Chapter 7 on synchronous machines, you will be able to move rapidly through the introductory material. However, do not feel that you need to study the material in Chapter 7 to follow the presentation in this chapter. It is written assuming that the reader does not have a background in synchronous machines.

8.2 TWO-PHASE PERMANENT-MAGNET ac MACHINE

A two-pole two-phase permanent-magnet ac machine is shown in Fig. 8.2-1. The stator windings are identical, sinusoidally distributed windings each with N_s equivalent turns and resistance r_s as described in Chapter 4. The angular displacement about the stator is denoted ϕ_s, referenced to the *as* axis. The angular displacement about the rotor is ϕ_r, referenced to the q axis. The angular velocity of the rotor is ω_r and θ_r is the angular displacement of the rotor measured from the *as* axis to the q axis. Thus, a given point on the rotor surface at the angular position ϕ_r may be related to an adjacent point on the inside stator surface with angular position ϕ_s as

$$\phi_s = \phi_r + \theta_r \tag{8.2-1}$$

The d axis is fixed at the center of the north pole of the permanent-magnet rotor and the q axis is displaced $\frac{1}{2}\pi$ counterclockwise from the d axis. The electromechanical torque T_e and the load torque T_L are also indicated in Fig. 8.2-1. As defined in Chapter 2, T_e is assumed positive in the direction of increasing θ_r; T_L is positive in the opposite direction.

In the following analysis, it is assumed that:

1. The magnetic system is linear.

2. It is assumed that the q- and d-axis reluctances are equal. Unequal reluctance is treated briefly in Section 8.11. The slight rotor indentation in the q axis is shown in Fig. 8.2-1 to indicate separation of the N and S poles.

3. The open-circuit stator voltages, induced by rotating the permanent-magnet rotor at a constant speed, are sinusoidal.

4. Large stator currents can be tolerated without significant demagnetization of the permanent magnet.

5. Damper windings (short-circuited rotor windings) are not considered.

Although these assumptions may be somewhat oversimplifying, this type of analysis is convenient while still portraying the main operating features of the device. For example, neglecting damper windings, in effect, neglects currents circulating in the surface of the rotor (eddy currents), which are induced by harmonics in the applied voltages and/or oscillations in rotor speed (induction-motor action). For permanent-magnet machines with surface-mounted magnets of low permeability, neglecting circulating rotor currents appears to be justified. However, in the buried-magnet type of rotor construction, eddy current effects occur and it may be necessary to include

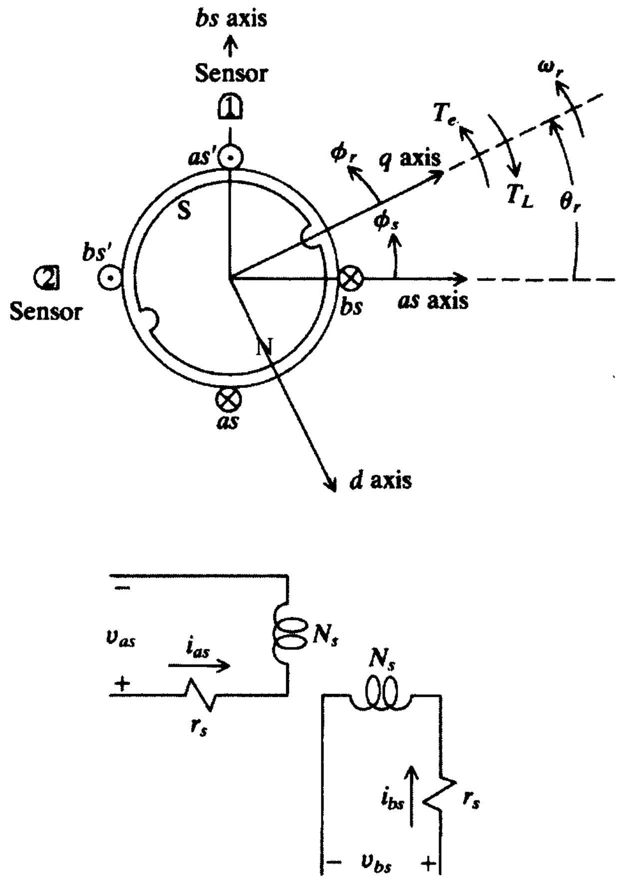

Figure 8.2-1: Two-pole, two-phase, permanent-magnet ac machine.

short-circuited rotor windings in the analysis. If so, this may be readily achieved by application of the material presented in Chapter 7. In the following sections, we will establish the voltage and torque equations that can be used to describe the behavior of the permanent-magnet ac machine. This chapter is written with the assumption that the reader is not familiar with synchronous machine theory. Hence, those who have studied the material in Chapter 7 may find most of the material in the next two sections a review, offering little challenge. In this chapter, as in previous chapters, we will consider the two-phase machine before the three-phase counterpart for convenience of analysis. Even though most brushless dc machines are three-phase devices, from an analytical standpoint, it is to our advantage to consider the two-phase device and then extend our work to the three-phase system.

In Fig. 8.2-1, the magnetic axes of the stator windings are denoted as the *as* and *bs* axes. The d axis (direct axis) is used to denote the magnetic axis of the permanent-magnet rotor and the q axis (quadrature axis) is used to denote an axis $\frac{1}{2}\pi$ ahead of the d axis. The concept of the q axis and d axis is reserved for association with the rotor magnetic axes of synchronous machines since, over the years, this association has become convention. Electromagnetic torque is produced by the interaction of the poles of the permanent-magnet rotor and the poles resulting from the rotating air-gap mmf established by currents flowing in the stator windings. The rotating mmf (mmf_s) established by symmetrical two-phase stator windings carrying balanced two-phase currents is given by (4.4-11).

The two sensors shown in Fig. 8.2-1 may be Hall-effect devices. When the north pole is under a sensor, its output is nonzero; with a south pole under the sensor, its output is zero. The stator of the permanent-magnet ac machine is supplied from a dc-to-ac inverter, the frequency of which corresponds to the rotor speed. The states of the sensors are used to determine the switching logic for the inverter, which, in turn, determines the output frequency of the inverter. In the actual machine, the sensors are not positioned over the rotor as shown in Fig. 8.2-1. Instead, they are placed over a ring that is mounted on the shaft external to the stator and magnetized as the rotor. We will return to these sensors and the roles they play later.

A four-pole, three-phase, 28-V, $\frac{1}{3}$-hp, permanent-magnet ac machine is shown in Fig. 8.2-2. The disassembled motor is shown in Fig. 8.2-2*a*, wherein the stator windings are visible. The opposite end of the stator housing is shown in Fig. 8.2-2*b*. Housed therein are the Hall-effect sensors, which are used to determine rotor position, the drive inverter, the filter capacitor, and the logic circuitry. The stator and rotor of a ten-pole, three-phase, 28-V, 0.63-hp, 4500-r/min, permanent-magnet ac machine is shown in Fig. 8.2-3. The magnets are samarium cobalt and the drive inverter is supplied from a 28-V dc source. The magnetic end cap is used in conjunction with Hall-effect sensors mounted in the stator housing (not shown) to determine the rotor position.

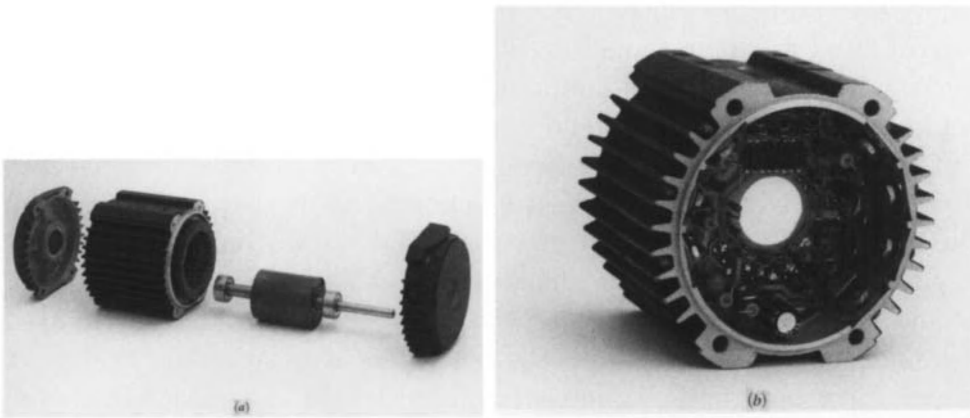

Figure 8.2-2: Four-pole, three-phase, 28-V, $\frac{1}{3}$-hp, permanent-magnet ac machine (courtesy of EG and G Rotron).

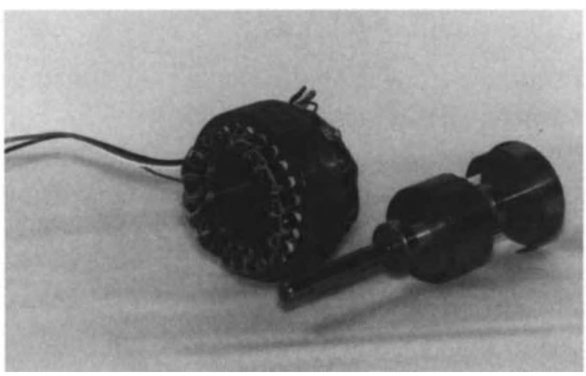

Figure 8.2-3: Two-pole, three-phase, 28-V, 0.63-hp, 4500-r/min, permanent-magnet ac machine (courtesy of Vickers Electromech).

SP8.2-1 Express mmf_r for the two-pole, two-phase, permanent-magnet ac machine shown in Fig. 8.2-1. Let F_p denote the peak value. [$\text{mmf}_r = -F_p \sin(\phi_s - \theta_r)$]

8.3 VOLTAGE EQUATIONS AND WINDING INDUCTANCES OF A PERMANENT-MAGNETIC ac MACHINE

The voltage equations for the two-pole, two-phase, permanent-magnet ac machine shown in Fig. 8.2-1 may be expressed as

$$v_{as} = r_s i_{as} + \frac{d\lambda_{as}}{dt} \tag{8.3-1}$$

$$v_{bs} = r_s i_{bs} + \frac{d\lambda_{bs}}{dt} \tag{8.3-2}$$

In matrix form,

$$\mathbf{v}_{abs} = \mathbf{r}_s \mathbf{i}_{abs} + p\boldsymbol{\lambda}_{abs} \tag{8.3-3}$$

where p is the operator d/dt, and for voltages, currents, and flux linkages,

$$(\mathbf{f}_{abs})^T = [f_{as} \quad f_{bs}] \tag{8.3-4}$$

with

$$\mathbf{r}_s = \begin{bmatrix} r_s & 0 \\ 0 & r_s \end{bmatrix} \tag{8.3-5}$$

A review of matrix algebra is given in Appendix B. The flux-linkage equations may be expressed as

$$\lambda_{as} = L_{asas} i_{as} + L_{asbs} i_{bs} + \lambda_{asm} \tag{8.3-6}$$

$$\lambda_{bs} = L_{bsas} i_{as} + L_{bsbs} i_{bs} + \lambda_{bsm} \tag{8.3-7}$$

In matrix form,

$$\boldsymbol{\lambda}_{abs} = \mathbf{L}_s \mathbf{i}_{abs} + \boldsymbol{\lambda}'_m \tag{8.3-8}$$

where $\boldsymbol{\lambda}_m'$ is the column vector:

$$\boldsymbol{\lambda}_m' = \begin{bmatrix} \lambda_{asm} \\ \lambda_{bsm} \end{bmatrix} = \lambda_m' \begin{bmatrix} \sin\theta_r \\ -\cos\theta_r \end{bmatrix} \tag{8.3-9}$$

In (8.3-9), λ_m' is the amplitude of the flux linkages established by the permanent magnet as viewed from the stator phase windings. In other words, the magnitude of λ_m' is proportional to the magnitude of the open-circuit sinusoidal voltage induced in each stator phase winding. It may be helpful to visualize the permanent-magnet rotor as a rotor with a winding carrying a constant current and in such a position to cause the north and south poles to appear as shown in Fig. 8.2-1. The rotor displacement θ_r is expressed as

$$\frac{d\theta_r}{dt} = \omega_r \tag{8.3-10}$$

We will assume that the reluctance of the rotor of the permanent-magnet ac machine is the same in the q- and d-axes. Actually, this assumption may be an oversimplification in some cases; however, it markedly reduces our work and allows us to establish directly the basic principles of the controlled permanent-magnet ac machine without significant error. Unequal q- and d-axes reluctances is considered briefly in Section 8.11 and is taken into account in more detail in [1].

With the assumption of a uniform air gap, the mutual inductance between the *as* and *bs* windings is zero. Since the windings are identical, the self-inductances L_{asas} and L_{bsbs} are equal and denoted as L_{ss}. As in the case of a transformer, the self-inductance is made up of a leakage L_{ls} and a magnetizing inductance L_{ms}. Thus,

$$L_{ss} = L_{ls} + L_{ms} \tag{8.3-11}$$

The machine is designed to minimize the leakage inductance; it generally makes up approximately 10 percent of L_{ss}. The magnetizing inductances may be expressed in terms of turns and reluctance. In particular,

$$L_{ms} = \frac{N_s^2}{\Re_m} \tag{8.3-12}$$

The magnetizing reluctance $\Re_m$ is an equivalent reluctance due to the stator steel, the permanent magnet, and the air gap. We will assume that $\Re_m$ is independent of rotor position θ_r, whereupon, the self-inductance matrix $\mathbf{L}_s$ may be expressed as

$$\mathbf{L}_s = \begin{bmatrix} L_{ss} & 0 \\ 0 & L_{ss} \end{bmatrix} \tag{8.3-13}$$

Example 8A. The parameters of a four-pole, two-phase, permanent-magnet ac machine are $r_s = 3.4\,\Omega$, $L_{ls} = 1.1$ mH, and $L_{ms} = 11$ mH. When the device is driven at 1000 r/min, the open-circuit phase voltage is sinusoidal with a peak-to-peak value of 34.6 V. Determine λ'_m. The actual rotor speed at which the measurement was taken is

$$\begin{aligned}\omega_{rm} &= \frac{(\text{r/min})(\text{rad/r})}{\text{s/min}} \\ &= \frac{(1000)(2\pi)}{60} = \frac{100}{3}\pi \text{ rad/s}\end{aligned} \tag{8A-1}$$

From (4.5-10), the electrical angular velocity is

$$\begin{aligned}\omega_r &= \frac{P}{2}\omega_{rm} \\ &= \frac{4}{2}\frac{100\pi}{3} = \frac{200}{3}\pi \text{ rad/s}\end{aligned} \tag{8A-2}$$

With the phases open-circuited, $i_{as} = i_{bs} = 0$. Thus, from (8.3-1) and (8.3-9),

$$v_{as} = \frac{d(\lambda'_m \sin\theta_r)}{dt} = \lambda'_m \omega_r \cos\theta_r \tag{8A-3}$$

Now the peak-to-peak voltage is 34.6 V; hence, from (8A-3), with the peak-to-peak voltage divided by 2, we have

$$\frac{34.6}{2} = \lambda'_m\left(\frac{200}{3}\pi\right) \tag{8A-4}$$

Solving for λ'_m yields

$$\lambda'_m = \frac{(34.6)(3)}{(2)(200\pi)} = 0.0826 \text{ V}\cdot\text{s/rad} \tag{8A-5}$$

SP8.3-1 The stator windings of the permanent-magnet ac machine shown in Fig. 8.2-1 are open-circuited. The rotor is driven clockwise and $V_{as} = -10\sin 100t$. Determine V_{bs}. [$V_{bs} = -10\cos 100t$]
SP8.3-2 Determine λ'_m for SP8.3-1. [$\lambda'_m = 0.1\text{ V}\cdot\text{s/rad}$]
SP8.3-3 During steady-state operation, (8.3-10) becomes $\theta_r = \omega_r t + \theta_r(0)$. What is $\theta_r(0)$ in SP8.3-1? [$\theta_r(0) = -\frac{1}{2}\pi$]

8.4 TORQUE

An expression for the electromagnetic torque may be obtained by using the second entry in Table 2.5-1. Since we are assuming a linear magnetic system, the coenergy may be expressed as

$$W_c = \frac{1}{2}L_{ss}(i_{as}^2 + i_{bs}^2) + \lambda_m' i_{as} \sin\theta_r - \lambda_m' i_{bs} \cos\theta_r + W_{pm} \tag{8.4-1}$$

where W_{pm} is the energy associated with the permanent magnet, which is constant for the device shown in Fig. 8.2-1. Taking the partial derivative with respect to θ_r yields

$$T_e = \frac{P}{2}\lambda_m'(i_{as}\cos\,\theta_r + i_{bs}\sin\,\theta_r) \tag{8.4-2}$$

The above expression is positive for motor action. The torque and speed may be related as

$$T_e = J\left(\frac{2}{P}\right)\frac{d\omega_r}{dt} + B_m\left(\frac{2}{P}\right)\omega_r + T_L \tag{8.4-3}$$

where J is in kg $\cdot$ m^2; it is the inertia of the rotor and the connected mechanical load. Since we will be concerned primarily with motor action, the load torque T_L is assumed positive, as indicated in Fig. 8.2-1. The constant B_m is a damping coefficient associated with the rotational system of the machine and mechanical load. It has the units N $\cdot$ m $\cdot$ s/rad and it is generally small and often neglected in the case of the machine but may be considerable for the mechanical load.

SP8.4-1 Calculate T_e for a two-pole permanent-magnet ac motor if $i_{as} = \cos\,\theta_r$, and $i_{bs} = \sin\,\theta_r$. $\lambda_m' = 0.1$ V $\cdot$ s/rad. [$T_e = 0.1$ N $\cdot$ m]
SP8.4-2 Repeat SP8.4-1 with $\theta_r = \omega_r t$ and $i_{as} = \cos(\omega_r t + \frac{1}{2}\pi)$ and $i_{bs} = \sin(\omega_r t + \frac{1}{2}\pi)$. [$T_e = 0$]

8.5 MACHINE EQUATIONS OF A PERMANENT-MAGNETIC ac MACHINE IN THE ROTOR REFERENCE FRAME

For the permanent-magnet ac machine, the reference frame fixed in the rotor is the reference frame of choice. The voltage equations may be written directly from the work in Chapter 5. In particular, if we select $\theta = \theta_r$ and $\omega = \omega_r$ and combine (5.4-6), (5.4-13), and (5.4-14), the stator voltage equations transformed to the rotor reference frame, expressed in expanded form, become

$$v_{qs}^r = r_s i_{qs}^r + \omega_r \lambda_{ds}^r + p\lambda_{qs}^r \tag{8.5-1}$$

$$v_{ds}^r = r_s i_{ds}^r - \omega_r \lambda_{qs}^r + p\lambda_{ds}^r \tag{8.5-2}$$

where the raised r is used to denote the variables in the rotor reference frame.

For a magnetically linear system, the stator flux linkages are expressed by (8.3-8). Substituting the change of variables into (8.3-8) yields

$$(\mathbf{K}_s^r)^{-1}\boldsymbol{\lambda}_{qds}^r = \mathbf{L}_s(\mathbf{K}_s^r)^{-1}\mathbf{i}_{qds}^r + \boldsymbol{\lambda}_m' \tag{8.5-3}$$

where, from (5.3-4)

$$\mathbf{K}_s^r = (\mathbf{K}_s^r)^{-1} = \begin{bmatrix} \cos\theta_r & \sin\theta_r \\ \sin\theta_r & -\cos\theta_r \end{bmatrix} \tag{8.5-4}$$

Premultiplying by $\mathbf{K}_s^r$ and substituting (8.3-13) and (8.3-11) for $\mathbf{L_s}$ yields

$$\begin{bmatrix} \lambda_{qs}^r \\ \lambda_{ds}^r \end{bmatrix} = \begin{bmatrix} L_{ls} + L_{ms} & 0 \\ 0 & L_{ls} + L_{ms} \end{bmatrix} \begin{bmatrix} i_{qs}^r \\ i_{ds}^r \end{bmatrix} + \lambda_m'^r \begin{bmatrix} 0 \\ 1 \end{bmatrix} \tag{8.5-5}$$

To be consistent with our previous notation, we have added the superscript r to λ_m'. We see from (8.5-5) that, in our new system of variables, the flux linkage created by the permanent magnet appears constant. Hence, our fictitious circuits are fixed relative to the permanent magnet and, therefore, fixed in the rotor reference frame. We have accomplished the goal of eliminating flux linkages that vary with θ_r. From (8.5-5)

$$\lambda_{qs}^r = L_{ss} i_{qs}^r \tag{8.5-6}$$

$$\lambda_{ds}^{r} = L_{ss}i_{ds}^{r} + \lambda_{m}^{\prime r} \tag{8.5-7}$$

and, as before,

$$L_{ss} = L_{ls} + L_{ms} \tag{8.5-8}$$

Substituting (8.5-6) and (8.5-7) into (8.5-1) and (8.5-2) and, since $\lambda_{m}^{\prime r}$ is constant, $p\lambda_{m}^{\prime r} = 0$:

$$v_{qs}^{r} = (r_s + pL_{ss})i_{qs}^{r} + \omega_r L_{ss} i_{ds}^{r} + \omega_r \lambda_{m}^{\prime r} \tag{8.5-9}$$

$$v_{ds}^{r} = (r_s + pL_{ss})i_{ds}^{r} - \omega_r L_{ss} i_{qs}^{r} \tag{8.5-10}$$

Let us assume that the applied stator voltages are

$$v_{as} = \sqrt{2}\, v_s \cos\theta_{esv} \tag{8.5-11}$$

$$v_{bs} = \sqrt{2}\, v_s \sin\theta_{esv} \tag{8.5-12}$$

where

$$\omega_e = \frac{d\theta_{esv}}{dt} \tag{8.5-13}$$

Transforming these voltages to the rotor reference frame yields

$$v_{qs}^{r} = \sqrt{2}\, v_s \cos\phi_v \tag{8.5-14}$$

$$v_{ds}^{r} = -\sqrt{2}\, v_s \sin\phi_v \tag{8.5-15}$$

where

$$\phi_v = \theta_{esv} - \theta_r \tag{8.5-16}$$

The expression for electromagnetic torque is obtained from (8.4-2) (see Prob. 3 in Section 8.16):

$$T_e = \frac{P}{2}\lambda_{m}^{\prime r} i_{qs}^{r} \tag{8.5-17}$$

which is positive for motor action.

SP8.5-1 Let $f_{as} = -\cos\theta_r$ and $f_{bs} = -\sin\theta_r$. Determine f_{qs}^{r} and f_{ds}^{r}. [$f_{qs}^{r} = -1$; $f_{ds}^{r} = 0$]

SP8.5-2 Let $f_{as} = \cos\theta_{esf}$, $f_{bs} = \sin\theta_{esf}$, and $\theta_r = \omega_r t$. Determine θ_{esf} for $f_{qs}^{r} = 0$ and $f_{ds}^{r} = 1$.[$\theta_{esf} = \omega_r t - \frac{1}{2}\pi$]

SP8.5-3 If the speed ω_r is constant and if $V_{as} = \cos\theta_r$ and $V_{bs} = \sin\theta_r$, what will be the waveform of I_{qs}^r and I_{ds}^r (steady-state currents)? [dc]
SP8.5-4 Start with $T_e = \frac{P}{2}(\lambda_{ds}^r i_{qs}^r - \lambda_{qs}^r i_{ds}^r)$, which was derived in Chapter 7 for a synchronous machine, and derive (8.5-17).
SP8.5-5 Determine ϕ_v if $\theta_{esv} = \omega_r t + \theta_{esv}(0)$ and $\theta_r = \omega_r t$. $[\phi_v = \theta_{esv}(0)]$

8.6 TWO-PHASE BRUSHLESS dc MACHINE

We are now ready to turn the permanent-magnetic ac machine into what we will call a brushless dc machine. To do this, we must implement a method of sensing the position of the rotor poles and the rotor electrical angular velocity. Although we have mentioned that this can be achieved in several ways, we will not become involved in this detail in this introductory treatment of a brushless dc machine since our purpose is to portray the operating characteristics of the machine and not the detailed design of the inverter control. With the rotor speed and position available, the dc-to-ac inverter is controlled so that the frequency of the fundamental component of the voltages applied to the stator windings is equal instantaneously to the electrical angular velocity of the rotor ω_r. Also, the switching of the inverter can be advanced or retarded, thereby shifting the phase or time position of the phase voltages by changing θ_{esv} relative to the rotor position θ_r. In the case of the brushless dc machine θ_{esv} is shifted such that ϕ_v (8.5-16) is zero, whereupon the peak positive values of v_{as} occur at every instant the q axis (Fig. 8.2-1) is horizontal and directed to the right. With $\phi_v = 0$, $v_{qs}^r = \sqrt{2}\, v_s$ and $v_{ds}^r = 0$. This angular relationship between the stator voltages and the magnetic poles of the rotor is tightly maintained by control of the inverter during steady-state operation as well as during transient changes in rotor speed ω_r due to changes in torque load T_L and/or the dc voltage of the inverter v_s.

Let us explain the action of the dc-to-ac inverter in a slightly different way. To do this, let us fix time at the instant v_{as} is at its peak value. If we looked at the q axis at this instant, it would be horizontal and to the right, whereupon, the N pole would be at $\phi_r = -\frac{1}{2}\pi$ and the S pole at $\phi_r = \frac{1}{2}\pi$ (Fig. 8.2-1). Now with $\phi_v = 0$ and for steady-state operation, $V_{as} = \sqrt{2}\, V_s \cos\omega_r t$ and $\theta_r = \omega_r t$, and we have fixed time at zero in order to portray the situation described above, where the positive peak value of V_{as}

occurs when the q axis is horizontal to the right. Now let time proceed and when $\theta_r = 2\pi$ the q axis is again horizontal and to the right and V_{as} has also advanced 2π and it is again at its positive peak. Ideally, the dc-to-ac inverter is designed to maintain this relative position between the rotor and the peak value of v_{as} during transient and steady-state operation.

Let us now see what this has done for us. For this purpose, let us consider steady-state operation with $\phi_v = 0$, whereupon $V_{qs}^r = \sqrt{2}\, V_s$ and $V_{ds}^r = 0$. Now since V_{qs}^r and V_{ds}^r are constants, pI_{qs}^r and pI_{ds}^r, in (8.5-9) and (8.5-10), are zero, and we can write (8.5-9) and (8.5-10) as

$$V_{qs}^r = r_s I_{qs}^r + \omega_r L_{ss} I_{ds}^r + \omega_r \lambda_m'^r \tag{8.6-1}$$

$$0 = r_s I_{ds}^r - \omega_r L_{ss} I_{qs}^r \tag{8.6-2}$$

From (8.6-2)

$$I_{ds}^r = \frac{\omega_r L_{ss}}{r_s} I_{qs}^r \tag{8.6-3}$$

Substituting (8.6-3) into (8.6-1) yields

$$V_{qs}^r = r_s I_{qs}^r + \frac{L_{ss}^2}{r_s} \omega_r^2 I_{qs}^r + \lambda_m'^r \omega_r \tag{8.6-4}$$

where $V_{qs}^r = \sqrt{2}\, V_s$, a constant.

Recall from Chapter 3 that the steady-state armature voltage of a permanent-magnet dc machine was given by (3.4-1) and repeated here:

$$V_a = r_a I_a + k_v \omega_r \tag{8.6-5}$$

where V_a is the armature dc voltage, I_a is the armature current, ω_r is the rotor speed, and k_v is proportional to the field flux produced by the permanent magnet.

Note that there is a marked similarly between (8.6-4) and (8.6-5). In fact, if the second term on the right-hand side of (8.6-4) were not present, the two equations would be identical in form. There is another similarity. The torque expression for a permanent-magnet dc machine was given by (3.3-5) with $L_{AF} i_f$ replaced by k_v:

$$T_e = k_v i_a \tag{8.6-6}$$

which is identical in form to (8.5-17).

Without Park's transformation [2], we would not have been able to formalize these similarities between the dc machine and the permanent-magnet ac machine with the applied phase voltages controlled so that $\phi_v = 0$. Thank you Mr. Park. However, we do wonder about the influence of the second term on the right-hand side of (8.6-4). Before we look into this, let us summarize what we have found so far in Table 8.6-1.

For the purpose of comparison let us assume that the $\omega_r = 0$ and $T_e = 0$ intercepts are equal for the permanent-magnet dc machine and the brushless dc machine as shown in Fig. 8.6-1. The reason for referring to the inverter/permanent-magnet ac machine combination as a brushless dc machine is clear. If $\phi_v = 0$, the torque speed characteristic of the brushless dc machine during motor action is nearly identical in form to that of a permanent-magnet dc machine. Although this comparison will vary depending upon the parameters of the machines, the comparison as shown in Fig. 8.6-1 is not uncommon. The influence of the $L_{ss}^2\omega_r^2/r_s$ term in (8.6-4) is minor when T_e and ω_r are both positive (motor action); however, it has a marked influence at other speeds. Although this nonmenclature is logical, it can be misleading since there is no such machine as a brushless dc machine; it is an inverter-controlled, permanent-magnet ac machine. Moreover,

Table 8.6-1: Comparison of voltage and torque equations of a permanent-magnet dc machine and a brushless dc machine.

Permanent-magnet dc machine	Brushless dc machine
$V_a = r_a I_a + k_v \omega_r$	$V_{qs}^r = r_s I_{qs}^r + \dfrac{L_{ss}^2}{r_s}\omega_r^2 I_{qs}^r + \lambda_m'^r \omega_r$
$T_e = k_v I_a$	$T_e = \dfrac{P}{2}\lambda_m'^r I_{qs}^r$
$T_e = \dfrac{k_v V_a}{r_a} - \dfrac{k_v^2}{r_a}\omega_r$	$T_e = \dfrac{P}{2}\dfrac{r_s \lambda_m'^r}{r_s^2 + \omega_r^2 L_{ss}^2}(\sqrt{2}\, V_s - \omega_r \lambda_m'^r)$
$T_e(\text{stall}) = \dfrac{k_v V_a}{r_a}$	$T_e(\text{stall}) = \left(\dfrac{P}{2}\right)\dfrac{\lambda_m'^r V_{qs}^r}{r_s}$
$\omega_r(T_e = 0) = \dfrac{V_a}{k_v}$	$\omega_r(T_e = 0) = \left(\dfrac{P}{2}\right)\dfrac{V_{qs}^r}{\lambda_m'^r}$

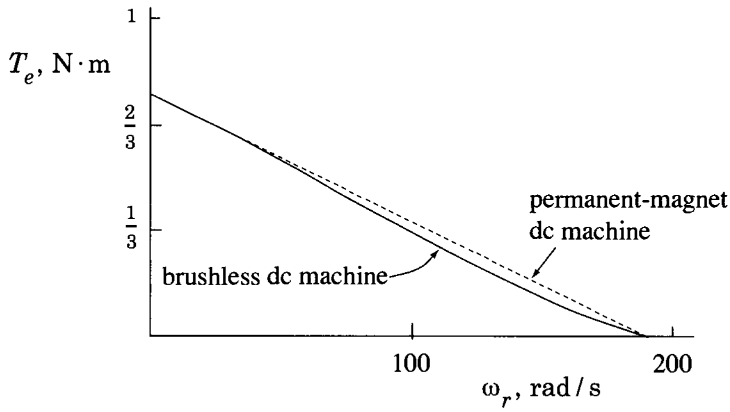

Figure 8.6-1: Comparison of torque-speed characteristics of a permanent-magnet dc motor and a brushless dc motor ($\phi_v = 0$) with identical $\omega_r = 0$ and $T_e = 0$ intercepts.

in a later section we will see that there are numerous modes of operation of the inverter-machine combination other than that with $\phi_v = 0$. In fact, only when $\phi_v = 0$ are the torque-speed characteristics similar to that of a permanent-magnet dc motor.

Example 8B. Consider the permanent-magnet ac machine the parameters of which are given in Example 8A. Assume that the applied stator voltages form a balanced two-phase set with $V_{as} = \sqrt{2}\,11.25\cos\omega_r t$ and $\phi_v = 0$. The machine is operating as a brushless dc motor, and the steady-state rotor speed is 600 r/min. Calculate T_e and $\tilde{I}_{as}$. Also, express $\tilde{V}_{as}$ from information given in Section 5.5.

From (4.5-10),

$$\omega_r = \frac{P}{2}\omega_{rm} = \frac{4}{2}\frac{(600)(2\pi)}{60} = 40\pi\,\text{rad/s} \tag{8B-1}$$

We can calculate the torque from T_e given in Table 8.6-1:

$$\begin{aligned} T_e &= \frac{P}{2}\frac{r_s\lambda_m'^r}{r_s^2+\omega_r^2L_{ss}^2}(\sqrt{2}\,V_s - \omega_r\lambda_r'^r) \\ &= \frac{4}{2}\frac{(3.4)(0.0826)}{(3.4)^2+(40\pi)^2(12.1\times10^{-3})^2}[\sqrt{2}\,(11.25)-(40\pi)(0.0826)] \\ &= 0.224\,\text{N}\cdot\text{m} \end{aligned} \tag{8B-2}$$

If B_m is small, which it often is, then from (8.4-3) $T_e = T_L$; thus, T_L is 0.224 N · m.

We need to calculate I_{qs}^r, which we can do by substituting into (8.6-4) or, since we know T_e, we can calculate I_{qs}^r from (8.5-17) or Table 8.6-1:

$$\begin{aligned} I_{qs}^r &= \frac{2}{P}\frac{T_e}{\lambda_m'^r} \\ &= \frac{2}{4}\frac{0.224}{0.0826} \\ &= 1.36 \text{ A} \end{aligned} \tag{8B-3}$$

Now, I_{ds}^r may be calculated from (8.6-3):

$$\begin{aligned} I_{ds}^r &= \frac{\omega_r L_{ss}}{r_s} I_{qs}^r \\ &= \frac{40\pi(12.1 \times 10^{-3})}{3.4}(1.36) \\ &= 0.606 \text{ A} \end{aligned} \tag{8B-4}$$

Thus, from (5.5-23) since $\omega_r = \omega_e$ and $\theta_r(0) = 0$,

$$\begin{aligned} \tilde{I}_{as} &= \frac{1}{\sqrt{2}}(I_{qs}^r - jI_{ds}^r) \\ &= \frac{1}{\sqrt{2}}(1.36 - j0.606) \\ &= 1.05 \underline{/ - 26.4^\circ} \end{aligned} \tag{8B-5}$$

From (5.5-23),

$$\tilde{V}_{as} = \frac{1}{\sqrt{2}}\left(V_{qs}^r - jV_{ds}^r\right) \tag{8B-6}$$

Substituting (8.6-1) and (8.6-2) into (8B-6) yields

$$\tilde{V}_{as} = (r_s + j\omega_r L_{ss})\tilde{I}_{as} + \frac{1}{\sqrt{2}}\omega_r \lambda_m'^r e^{j0} \tag{8B-7}$$

It is left to the reader to verify (8B-7) by substituting in numerical values given and/or calculated in this example and to draw the phase diagram. (See Prob. 5 in Section 8.16.)

SP8.6-1 A synchronous machine with a field winding is used rather than a permanent-magnet ac machine in an inverter-machine combination. What would differ from the equation given in Table 8.6-1? [Replace $\lambda_m'^r$ with $L_{md}I_{fd}'^r$]

SP8.6-2 Repeat SP8.6-1 for a dc machine with a field winding rather than a permanent magnet. [Replace k_v with $L_{AF}I_f$]

SP8.6-3 If V_a in Fig. 8.6-1 were doubled, what changes in the brushless dc machine would be necessary to maintain the intercepts the same as in the permanent-magnet dc machine? [Double number of poles or double V_{qs}^r]

SP8.6-4 A four-pole, two-phase, brushless dc motor is operating with $\theta_r(0) = 0$, $V_{as} = 10\cos\omega_r t$, and $I_{as} = \cos(\omega_r t - 20^o)$. Calculate $\lambda_m'^r$ if $r_s = 4\,\Omega$, $L_{ss} = 0.01$ H, and $\omega_r = 146$ rad/s. [$\lambda_m'^r = 0.0393$ V · s/rad]

SP8.6-5 Calculate the torque of the machine given in SP8.6-1 with $\omega_r = 0$ and $V_{as} = 10\cos\omega_r t$. [$T_e = 0.191$ N · m]

SP8.6-6 Repeat SP8.6-4 neglecting $\omega_r^2 L_{ss}^2$. [$\lambda_m'^r = 0.0427$ V · s/rad]

SP8.6-7 Calculate (a) the input power, (b) T_e, and (c) efficiency for the operating conditions given in SP8.6-4. [(a) $P_{\text{in}} = 9.4$ W; (b) $T_e = 0.074$ N·m; (c) eff. = 57.4 percent]

8.7 DYNAMIC PERFORMANCE OF A BRUSHLESS dc MACHINE

It is instructive to observe the variables of the brushless dc motor during free acceleration from stall and step changes in load torque with sinusoidal applied stator voltages. The machine parameters used during the free acceleration studies are those given in Example 8A with $J = 5 \times 10^{-4}$ kg · m^2, which includes the rotor and mechanical load, and $B_m = 0$. The free-acceleration characteristics are shown in Fig. 8.7-1. The applied stator phase voltages are of the form given by (8.5-14) and (8.5-15) with ϕ_v equal to zero; therefore, $v_{ds}^r = 0$ and $V_s = 11.25$ V. The phase voltage v_{as}, phase current i_{as}, q-axis voltage v_{qs}^r, q-axis current i_{qs}^r, d-axis current i_{ds}^r, electromagnetic torque T_e, and rotor speed ω_r (in electrical rad/s) are plotted in Fig. 8.7-1. Since the device is a four-pole machine, 200 electrical rad/s is equivalent to 955 r/min. A plot of T_e versus ω_r is shown in Fig. 8.7-2 for the free acceleration depicted in Fig. 8.7-1. The steady-state torque-speed characteristic is superimposed for purposes of comparison.

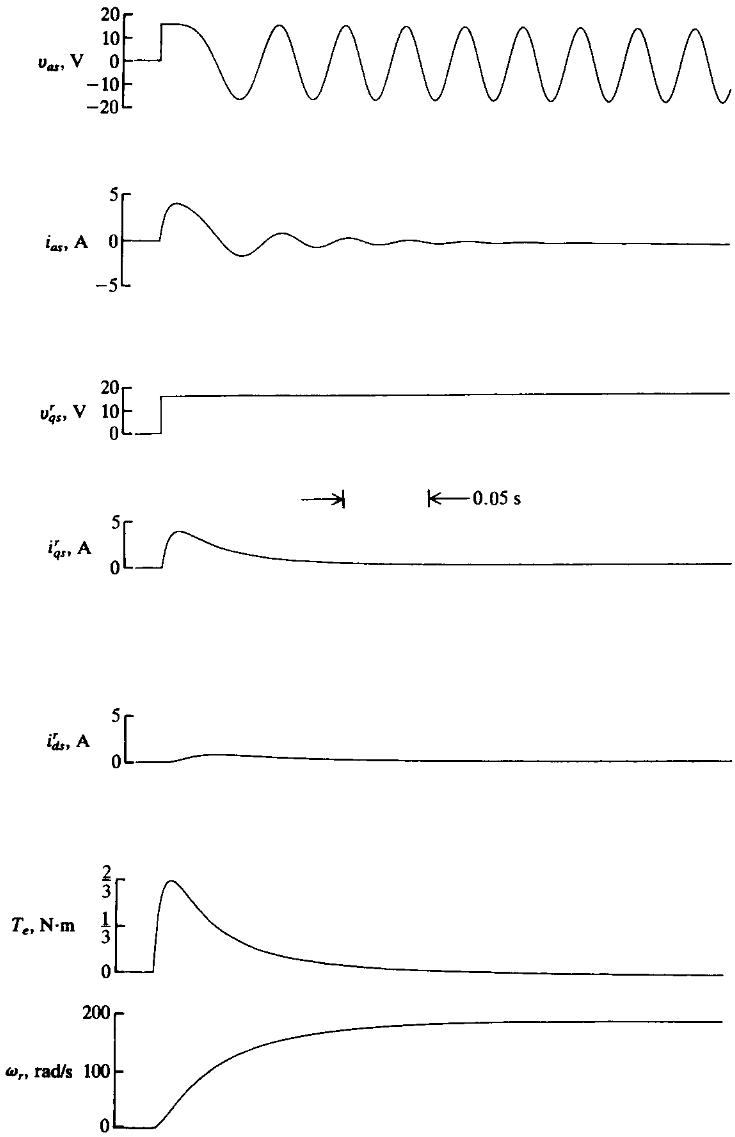

Figure 8.7-1: Free-acceleration characteristics of a brushless dc motor.

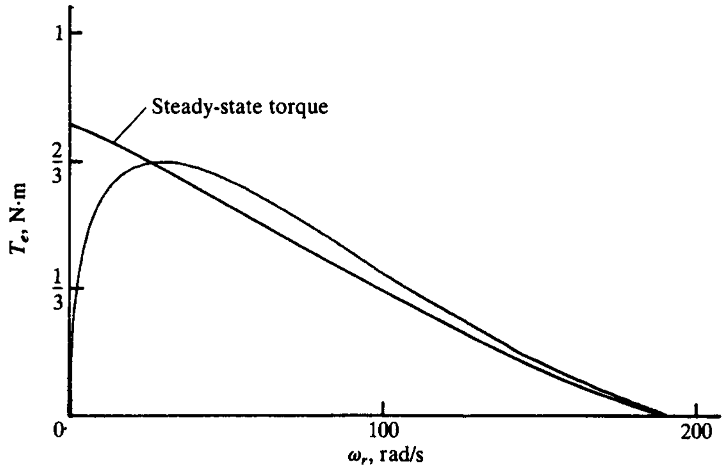

Figure 8.7-2: Torque-speed characteristics for free acceleration shown in Fig. 8.7-1.

The rapid acceleration of the brushless dc motor is apparent. In fact, the rotor reaches full speed in less than 0.15 s. Nevertheless, one can observe the change in frequency of the applied voltage v_{as} as the motor accelerates from stall. It is important to note that the dynamic torque-speed characteristics shown in Fig. 8.7-2 differ from the steady-state torque-speed characteristics. One must be aware of this discrepancy if one chooses to use the expression for the steady-state torque in a transfer function formulation describing the dynamic characteristics of a brushless dc motor. Also, recall that, with $\phi_v = 0$, v_{ds}^r is zero; however, from (8.6-3), steady-state i_{ds}^r is zero only if either ω_r or i_{qs}^r is zero. From Fig. 8.7-1, we see that the magnitude of i_{qs}^r is less than the amplitude of the phase currents. Although v_{qs}^r is equal to the peak value of a phase voltage, i_{qs}^r is not, in general, equal to the peak value of phase current.

The performance during step changes in load torque is illustrated in Fig. 8.7-3. Initially, the machine is operating with $T_L = 0.067$ N $\cdot$ m. The load torque is suddenly stepped to 0.267 N $\cdot$ m. The machine slows down, and once steady-state operation is established, the load torque is stepped back to 0.067 N $\cdot$ m. In these studies, the inertia is 2×10^{-4} kg $\cdot$ m^2, which is 40% of the inertia used in Figs. 8.7-1 and 8.7-2.

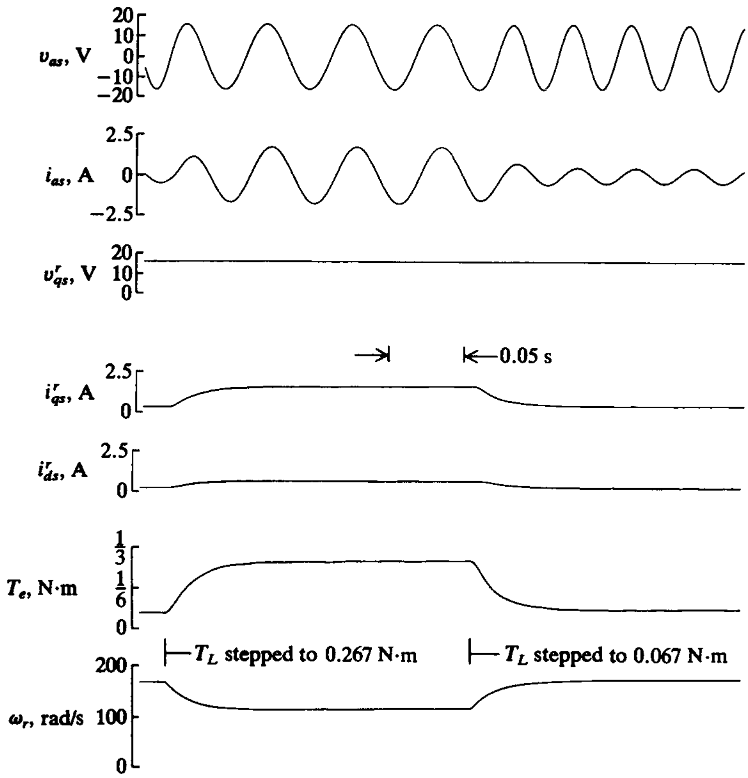

Figure 8.7-3: Dynamic performance of a brushless dc motor during step changes in load torque with total inertia 40% of that used in Figs. 8.7-1 and 8.7-2.

SP8.7-1 Consider Fig. 8.7-1. Express ω_r by assuming that it may be approximated by an exponential increase. $[\omega_r \cong 193\,(1 - e^{-25t})]$
SP8.7-2 Approximate T_e in Fig. 8.7-2 by a straight line between $T_e = 0.75$ N $\cdot$ m at $\omega_r = 0$ and $T_e = 0$ at $\omega_r = 193$ rad/s. Express ω_r for free acceleration with $J = 5 \times 10^{-4}$ kg $\cdot$ m^2. Compare with SP8.7-1.

8.8 PHASE SHIFTING OF STATOR VOLTAGES OF PERMANENT-MAGNET ac MACHINE

Let us repeat (8.5-14) through (8.5-16):

$$v_{qs}^r = \sqrt{2}\, v_s \cos\phi_v \tag{8.8-1}$$

$$v_{ds}^r = -\sqrt{2}\, v_s \sin\phi_v \tag{8.8-2}$$

where

$$\phi_v = \theta_{esv} - \theta_r \tag{8.8-3}$$

Now, we know that if the angular velocity associated with θ_{esv} and θ_r is controlled equal and if ϕ_v is also controlled to be equal to zero, then we have what we referred to as a brushless dc machine. However, there is a huge array of other modes of operation possible by shifting the phase of θ_{esv} relative to the q axis (north and south poles) by appropriate shifting of the firing of the inverter. This then allows ϕ_v to be varied between $-2\pi < \phi_v < 2\pi$. Moreover, ϕ_v may be constant over this range or varied to maintain prescribed or controlled v_{qs}^r and v_{ds}^r.

It is very instructive to consider steady-state operation of the inverter-controlled, permanent-magnetic ac machine with ϕ_v and v_s both constants. Thus for steady-state operation, $p = 0$ in (8.5-9) and (8.5-10), thus

$$V_{qs}^r = r_s I_{qs}^r + \omega_r L_{ss} I_{ds}^r + \omega_r \lambda_m'^r \tag{8.8-4}$$

$$V_{ds}^r = r_s I_{ds}^r - \omega_r L_{ss} I_{qs}^r \tag{8.8-5}$$

where capital letters denote steady-state (constant) quantities, except for $\lambda_m'^r$ which is assumed to be always constant. If (8.8-4) and (8.8-5) are solved for

I_{qs}^r and the result substituted into the expression for electromagnetic torque given by (8.5-17), we obtain

$$T_e = \frac{P}{2}\frac{\lambda_m'^r r_s}{r_s^2 + \omega_r^2 L_{ss}^2}\left(V_{qs}^r - \frac{\omega_r L_{ss} V_{ds}^r}{r_s} - \omega_r \lambda_m'^r\right) \tag{8.8-6}$$

Here we have not set V_{ds}^r equal to zero as in the case of the brushless dc machine since $-2\pi < \phi_v < 2\pi$. Please note that T_e for the brushless dc machine ($\phi_v = 0$) in Table 8.6-1 is (8.8-6) with $V_{ds}^r = 0$. When considering phase shifting of θ_{esv} relative to θ_r, it is convenient to use phasors to analyze steady-state operation. With $\omega_e = \omega_r$, and with

$$\theta_{esf} = \omega_r t + \theta_{esf}(0) \tag{8.8-7}$$

where θ_{esf} can represent θ_{esv} or θ_{esi}. We can now write

$$F_{as} = \sqrt{2}\, F_s \cos[\omega_r t + \theta_{esf}(0)] \tag{8.8-8}$$

$$F_{bs} = \sqrt{2}\, F_s \sin[\omega_r t + \theta_{esf}(0)] \tag{8.8-9}$$

From (5.5-9) and (5.5-10) with $\omega = \omega_r$ and $\theta(0) = \theta_r(0)$,

$$F_{qs}^r = \sqrt{2} F_s \cos[\theta_{esf}(0) - \theta_r(0)] \tag{8.8-10}$$

$$F_{ds}^r = -\sqrt{2} F_s \sin[\theta_{esf}(0) - \theta_r(0)] \tag{8.8-11}$$

The phasor that represents F_{as} given by (8.8-8) is

$$\tilde{F}_{as} = F_s e^{j\theta_{esf}(0)} \tag{8.8-12}$$

which may be written as

$$\tilde{F}_{as} = F_s \cos\theta_{esf}(0) + jF_s \sin\theta_{esf}(0) \tag{8.8-13}$$

Now, since we can choose our time zero as we wish, let us select it so that $\theta_r(0) = 0$. In other words, our time zero will always be selected at the time the q axis in Fig. 8.2-1 is horizontal to the right. For those of you who have read Chapter 7 on synchronous machines, you will note a difference; there we selected time zero so that $\theta_{esv}(0) = 0$.

If $\theta_r(0) = 0$, then F_{qs}^r, (8.8-10) and $-F_{ds}^r$, (8.8-11) are, respectively, the same as $\sqrt{2}$ times the real and imaginary parts of (8.8-13). Thus, for $\theta_r(0) = 0$,

$$\sqrt{2}\, \tilde{F}_{as} = F_{qs}^r - jF_{ds}^r \tag{8.8-14}$$

As in Chapter 5 and Example 8B, we have equated a phasor, which represents a sinusoidal quantity, to F_{qs}^r and F_{ds}^r, which are constants. Substituting (8.8-4) and (8.8-5) into (8.8-14) yields

$$\begin{aligned}\sqrt{2}\,\tilde{V}_{as} &= V_{qs}^r - jV_{ds}^r \\ &= r_s I_{qs}^r + \omega_r L_{ss} I_{ds}^r + \omega_r \lambda_m'^r - j(r_s I_{ds}^r - \omega_r L_{ss} I_{qs}^r) \end{aligned} \tag{8.8-15}$$

From (8.8-14),

$$j\sqrt{2}\,\tilde{F}_{as} = F_{ds}^r + jF_{qs}^r \tag{8.8-16}$$

Hence, (8.8-15) may be written as

$$\tilde{V}_{as} = (r_s + j\omega_r L_{ss})\tilde{I}_{as} + \frac{1}{\sqrt{2}}\omega_r \lambda_m'^r e^{j0^\circ} \tag{8.8-17}$$

We can define

$$\tilde{E}_a = \frac{1}{\sqrt{2}}\,\omega_r \lambda_m'^r e^{j0} \tag{8.8-18}$$

and write (8.8-17) as

$$\tilde{V}_{as} = (r_s + j\omega_r L_{ss})\,\tilde{I}_{as} + \tilde{E}_a \tag{8.8-19}$$

One should not confuse $\tilde{E}_a$ given by (8.8-18) with $\tilde{E}_a$ defined for a synchronous machine in Chapter 7.

Since $\theta_r(0) = 0$, $\phi_v = \theta_{esv}(0)$. Thus, the phase angle of $\tilde{V}_{as}$ is $\theta_{esv}(0)$ or ϕ_v, which could be written $\phi_v(0)$; also, we know that the phase angle of $\tilde{E}_a$ is zero. We have selected $\theta_r(0) = 0$, as shown in Fig. 8.8-1*a*. At $t = 0$ the phasor diagram for a given mode of operation would be as shown in Fig. 8.8-1*b*. During steady-state operation, the rotor instantaneously rotates at ω_r in the counterclockwise direction, and to portray the instantaneous electrical variables the phasor diagram rotates in the counterclockwise direction at ω_e. However, since $\omega_e = \omega_r$, it follows that Fig. 8.8-1*a* and Fig. 8.8-1*b* may be superimposed, as shown in Fig. 8.8-1*c*. If we substitute the steady-state version of (8.8-1) and (8.8-2) for V_{qs}^r and V_{ds}^r, respectively, into (8.8-6), the electromagnetic torque may be expressed as

$$T_e = \frac{P}{2}\frac{r_s \lambda_m'^r}{r_s^2 + \omega_r^2 L_{ss}^2}\left(\sqrt{2}\,V_s \cos\phi_v + \frac{\omega_r L_{ss}}{r_s}\sqrt{2}\;V_s \sin\phi_v - \omega_r \lambda_m'^r\right) \tag{8.8-20}$$

Time constants are not generally used in steady-state equations, however, we will do so here. Let

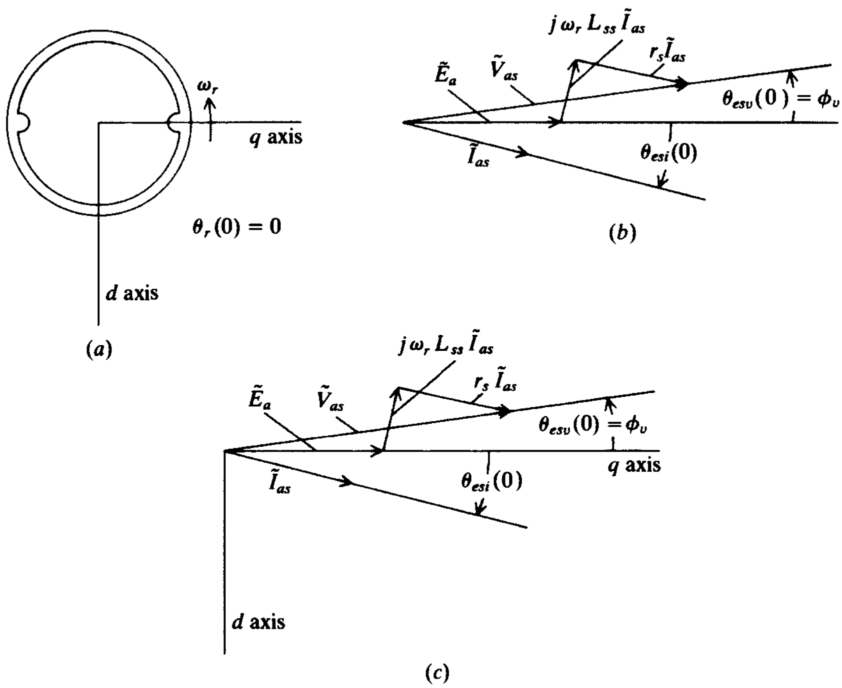

Figure 8.8-1: Superimposing the phasor diagram on the rotor of a permanent-magnet ac machine.

$$\tau_s = \frac{L_{ss}}{r_s} \tag{8.8-21}$$

$$\tau_v = \frac{\lambda'^r_m}{\sqrt{2}\,V_s} \tag{8.8-22}$$

Although both τ_s and τ_v have the units of seconds, τ_v is not a constant defined by the machine parameters; nevertheless, we will find these quantities very useful as we go along. If we substitute (8.8-21) and (8.8-22) into (8.8-20), T_e can be expressed as

$$T_e = \frac{P}{2}\left\{\frac{2V_s^2\tau_v}{r_s(1+\tau_s^2\omega_r^2)}[\cos\phi_v + (\tau_s\sin\phi_v - \tau_v)\omega_r]\right\} \tag{8.8-23}$$

Although (8.8-20) is valid for all rotor speeds, positive values of ω_r and T_e are of primary interest. From (8.8-23), we see that for the electromagnetic torque to be positive for positive values of rotor speed,

$$\cos\phi_v + \tau_s\omega_r\sin\phi_v > \tau_v\omega_r \tag{8.8-24}$$

The torque is zero when (8.8-24) is an equality. Therefore, if $\phi_v = 0$, T_e is positive if $\tau_v\omega_r < 1$ and T_e is zero when $\omega_r = \tau_v^{-1}$; however, we already knew this latter relationship from Fig. 8.6-1. When $\phi_v = \frac{1}{2}\pi$, T_e is positive for all positive values of ω_r, provided that $\tau_s > \tau_v$. Also, with $\phi_v = \frac{1}{2}\pi$, T_e is zero for all values of ω_r if $\tau_s = \tau_v$.

What can we do with ϕ_v in regard to the effect it might have on T_e? Can it be used to maximize T_e? Yes! The value of ϕ_v at which a maximum or minimum electromagnetic torque occurs for a given rotor speed may be obtained by taking the derivative of T_e, given by (8.8-23), with respect to ϕ_v, setting the result equal to zero, and then solving for ϕ_v. In particular,

$$\phi_{vMT} = \tan^{-1}(\tau_s\omega_r) \tag{8.8-25}$$

where ϕ_{vMT} is the shift in the phase voltages (v_{as} relative to the q axis), which will yield maximum or minimum steady-state torque at a given rotor speed. It is interesting to note that this phase shift angle is the angle of the impedance of the machine. That is, since $\omega_e = \omega_r$, $\tau_s\omega_r = \omega_e L_{ss}/r_s$. That is somewhat surprising.

The maximum or minimum steady-state electromagnetic torque may be determined by substituting (8.8-25) into (8.8-23). This gives

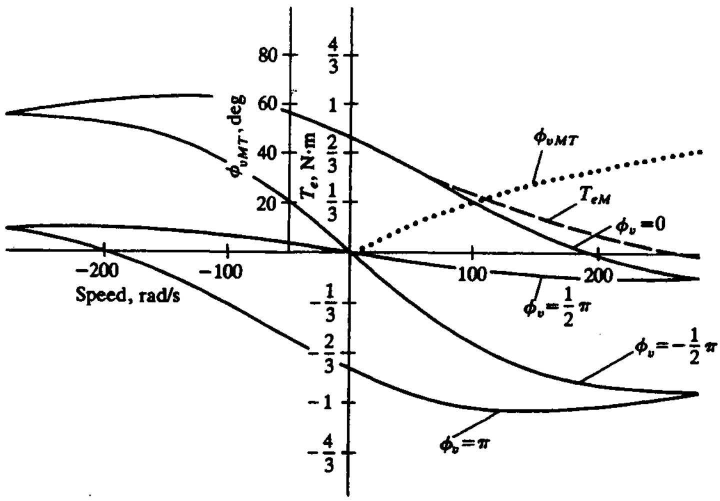

Figure 8.8-2: Torque-speed characteristics of a permanent magnet ac machine with controlled applied voltages.

$$T_{eM} = \frac{P}{2}\frac{2V_s^2\tau_v}{r_s(1+\tau_s^2\omega_r^2)}(\sqrt{1+\tau_s^2\omega_r^2} - \tau_v\omega_r) \qquad \text{for } \phi_v = \phi_{vMT} \qquad (8.8\text{-}26)$$

The steady-state torque-speed characteristics of a permanent-magnet ac machine with controlled applied voltages are shown in Fig. 8.8-2. The parameters, from Example 8A, are $r_s = 3.4\,\Omega$, $L_{ls} = 1.1$ mH, and $L_{ms} = 11.0$ mH; thus $L_{ss} = 12.1$ mH. The motor is a four-pole device and $\lambda_m'^r$, determined from the open-circuit voltage, is 0.0826 V · s/rad. The voltage V_s is 11.25 V. For this machine, $\tau_s = 3.56$ ms and $\tau_v = 5.2$ ms. In Fig. 8.8-2, plots of the steady-state electromagnetic torque are shown for $\phi_v = 0, \pm\frac{1}{2}\pi, \pi$, and ϕ_{vMT}. The maximum torque T_{eM} for $\omega_r > 0$ is also plotted along with the angle ϕ_{vMT}, which yields maximum torque. For $\omega_r > 0$, maximum torque occurs between $\phi_v = 0$ and $\phi_v = \frac{1}{2}\pi$. Note the fact that we can increase the torque considerably at higher rotor speeds compared to that with $\phi_v = 0$.

The influence of τ_s upon the steady-state torque-speed characteristics is illustrated in Figs. 8.8-3 and 8.8-4, wherein T_{eM} is shown for $\omega_r > 0$. In Fig. 8.8-3, τ_s is increased by a factor of three times by decreasing r_s. In Fig. 8.8-4, τ_s is increased by a factor of three by increasing L_{ss}. Note that in these cases $\tau_s > \tau_v$. Thus, with $\phi_v = \frac{1}{2}\pi$, maximum torque is always positive for $\omega_r > 0$, as shown in Figs. 8.8-3 and 8.8-4. A comparison of Figs. 8.8-2 through 8.8-4

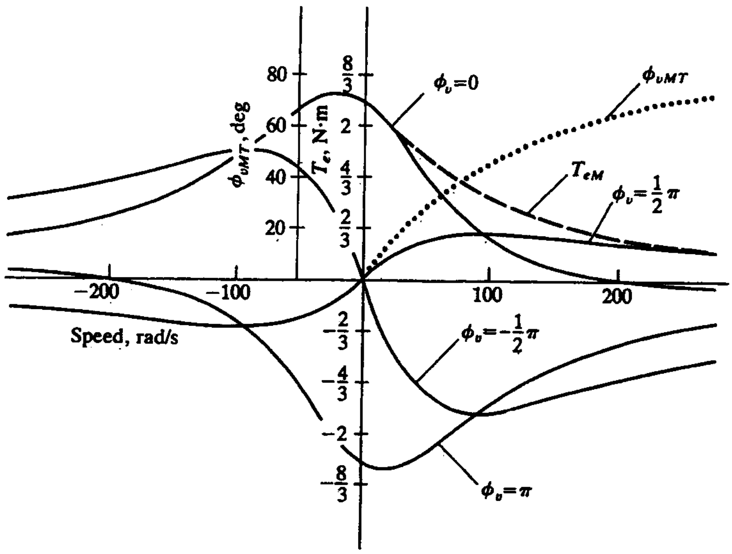

Figure 8.8-3: Same as Fig. 8.8-2 with τ_s increased by a factor of three by decreasing r_s.

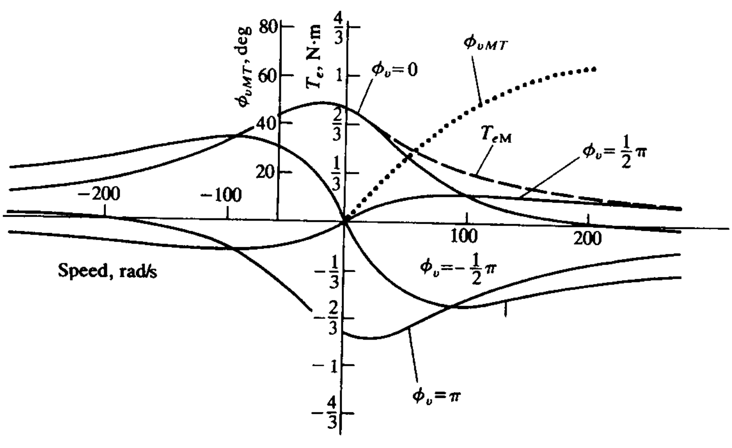

Figure 8.8-4: Same as Fig. 8.8-2 with τ_s increased by a factor of three by increasing L_{ss}.

reveals that a significantly larger torque can be achieved if the angle ϕ_v is maintained at the value to produce maximum torque, ϕ_{vMT}. The increase in torque is particularly significant if $\tau_s > \tau_v$. Considerable insight may be gained regarding the maximum-torque capability of the machine simply by comparing τ_s and τ_v. We may calculate τ_s from the machine parameters and τ_v from $\lambda_m'^r$ and V_s or from the inverse of the no-load speed. Thus, τ_s and τ_v may be readily determined, whereupon the torque characteristics caused by shifting the phase of the applied voltages may be anticipated without further calculation. However, in [1] it is shown that the increase in average torque due to shifting of the phase is achieved at the expense of an increase in the level of the harmonic torque, which comes about because of the harmonics introduced by the inverter. This may be prohibitive in some applications such as very precise speed control. Also, increased torque comes at the expense of increased current, which may become a limiting factor due to increased losses.

Example 8C. Repeat the calculation of $\tilde{I}_{as}$ in Example 8B using (8.8-19). From (8.8-18),

$$\begin{aligned}\tilde{E}_a &= \frac{1}{\sqrt{2}}\omega_r \lambda_m'^r \underline{/0^\circ} \\ &= \frac{1}{\sqrt{2}}(40\pi)(0.0826)\underline{/0^\circ} = 7.34\underline{/0^\circ}\end{aligned} \tag{8C-1}$$

From (8.8-19),

$$\begin{aligned}\tilde{I}_{as} &= \frac{1}{r_s + j\omega_r L_{ss}}(\tilde{V}_{as} - \tilde{E}_a) \\ &= \frac{1}{3.4 + j(40\pi)(12.1 \times 10^{-3})}(11.25\underline{/0^\circ} - 7.34\underline{/0^\circ}) \\ &= \frac{3.91\underline{/0^\circ}}{3.72\underline{/26.4^\circ}} = 1.05\underline{/-26.4^\circ}\text{A}\end{aligned} \tag{8C-2}$$

From (8.8-14),

$$\sqrt{2}\,\tilde{I}_{as} = I_{qs}^r - jI_{ds}^r$$

$$\sqrt{2}\,1.05\underline{/-26.4^\circ} = 1.36 - j0.606 \tag{8C-3}$$

Thus $I_{qs}^r = 1.36$ A and $I_{ds}^r = 0.606$ A. It is left to the reader to draw the phasor diagram. Recall when $\phi_v = 0$, $\tilde{V}_{as}$ and $\tilde{E}_a$ are both at zero degrees.

Example 8D. Consider the situation given in Example 8B and 8C. The load torque is removed. Calculate the value of ϕ_v so that the steady-state rotor speed is still 600 r/min.

We know from Example 8B that for a rotor speed of 600 r/min the electrical angular velocity of the rotor, ω_r, is 40π rad/s and $T_L = 0.224\,\text{N}\cdot\text{m}$. Now, what shift in phase ϕ_v must occur to maintain this speed in steady-state operation with $T_e = T_L = 0$? From (8.8-23) and (8.8-24), we know that for $T_e = 0$,

$$\cos\phi_v + \tau_s\omega_r \sin\phi_v = \tau_v\omega_r \tag{8D-1}$$

An analogous relationship may be obtained by setting the torque given by (8.8-6) equal to zero and substituting (8.5-14) and (8.5-15) for v_{qs}^r and v_{ds}^r. That is,

$$0 = V_s \cos\phi_v + \frac{\omega_r L_{ss}}{r_s} V_s \sin\phi_v - \frac{1}{\sqrt{2}}\omega_r \lambda_m'^r \tag{8D-2}$$

In any event, we are faced with a trial-and-error type of a solution. From (8.8-21) and (8.8-22), respectively,

$$\tau_s = \frac{L_{ss}}{r_s} = \frac{12.1 \times 10^{-3}}{3.4} = 3.56\text{ ms} \tag{8D-3}$$

$$\tau_v = \frac{\lambda_m'^r}{\sqrt{2}\,V_s} = \frac{0.0826}{\sqrt{2}\,11.25} = 5.2\text{ ms} \tag{8D-4}$$

Substituting (8D-3) and (8D-4) into (8D-1) with $\omega_r = 40\pi$ rad/s, we have

$$\cos\phi_v + (3.56 \times 10^{-3})(40\pi)\sin\phi_v = (5.2 \times 10^{-3})(40\pi)$$

$$\cos\phi_v + 0.447\sin\phi_v = 0.653 \tag{8D-5}$$

After a little work, we conclude that there are two values of ϕ_v that will satisfy this condition: $\phi_v = -29.3°$ or $77.5°$.

SP8.8-1 Calculate the current $\tilde{I}_{as}$ at T_{eM} for the permanent-magnet ac machine given in SP8.6-4. Assume $V_{as} = 10\cos(\omega_r t + \phi_{vMT})$ and $\omega_r = 146$ rad/s. [$\tilde{I}_{as} = 0.84\underline{/23.8°}$ A]

SP8.8-2 The parameters of the permanent-magnet ac machine are those given in SP8.6-4. Let $\theta_r(0) = 0$ and $V_{as} = \sqrt{2}\, V_s \cos(\omega_r t + \frac{1}{2}\pi)$. Determine a nonzero value of V_s so that $T_e = 0$ for $\omega_r > 0$. [$V_s = 11.1$ V]
SP8.8-3 Calculate (a) the input power, (b) T_e, and (c) the efficiency for the operating conditions given in SP8.8-1. (d) Why could the efficiency calculation be misleading? [(a) $P_{\text{in}} = 11.8\,\text{W}$; ($b$) $T_e = 0.085\,\text{N} \cdot \text{m}$; ($c$) eff.= 52.9 percent; ($d$) harmonics neglected]
SP8.8-4 Why are the $\omega_r = 0$ intercepts for $\phi_v = 0$ in Figs. 8.8-2 and 8.8-4 equal? [$T_e = \frac{P}{2}\lambda_m'^r \frac{V_{qs}^r}{r_s}$]
SP8.8-5 Why are the $T_e = 0$ intercepts for $\phi_v = 0$ the same in Fig. 8.8-2 through Fig. 8.8-4? [Following (8.8-24) $T_e = 0$ when $\omega_r = \tau_v^{-1} = \frac{\sqrt{2}V_s}{\lambda_m'^r}$]

8.9 INTRODUCTION TO CONSTANT-TORQUE AND CONSTANT-POWER OPERATION

In Chapter 3, we discussed constant-torque and constant-power operation of a dc machine. The equations that describe the dc machine permit a relatively straightforward presentation of the concepts of these modes of operation and control requirements. The reader may wish to review the material in Section 3.6 before proceeding.

In Section 8.6, it was shown that if the switching of the converter is fixed so that $V_{ds}^r = 0$, the torque-speed characteristics are similar to the dc machine during motor operation (Fig. 8.6-1). Although this type of control can be implemented quite easily, the controls necessary for the constant-torque and constant-power modes of operation of the permanent-magnet ac machine are somewhat more involved.

The goal is to control the permanent-magnet ac machine to have torque-speed capabilities similar to that of the dc machine. Therefore, it is convenient to analyze and design the control in a reference frame where the substitute variables resemble those of the dc machine – the rotor reference frame. Therefore, the transformation $\mathbf{K}_s^r$ must be embedded within the control. As we have mentioned, our purpose is not to become involved in the details of the controls but rather to set down the steady-state requirements of the control objectives and to describe the performance of the converter-machine drive, assuming the control objectives are met. Therefore, we will establish the ideal operating boundaries of these modes and leave the methods of control within these boundaries to the controls engineer [1].

For convenience, the voltage and torque equations for steady-state operation from Section 8.5 are repeated here:

$$V_{qs}^r = r_s I_{qs}^r + \omega_r L_{ss} I_{ds}^r + \omega_r \lambda_m'^r \tag{8.9-1}$$

$$V_{ds}^r = r_s I_{ds}^r - \omega_r L_{ss} I_{qs}^r \tag{8.9-2}$$

$$T_e = \frac{P}{2} \lambda_m'^r I_{qs}^r \tag{8.9-3}$$

Torque Operation with $I_{ds}^r = 0$

It is common in permanent-magnet ac machines with equal q- and d-axis inductances to control the machine so that $I_{ds}^r = 0$, since a d-axis current does not produce torque. Under such control, (8.9-1) and (8.9-2) become

$$V_{qs}^r = r_s I_{qs}^r + \omega_r \lambda_m'^r \tag{8.9-4}$$

$$V_{ds}^r = -\omega_r L_{ss} I_{qs}^r \tag{8.9-5}$$

At rated source voltage (V_{sR}),

$$\sqrt{2}\, V_{sR} = \sqrt{(V_{qs}^r)^2 + (V_{ds}^r)^2} \tag{8.9-6}$$

Substituting (8.9-4) and (8.9-5) into (8.9-6), solving for I_{qs}^r, and substituting the result in (8.9-3) yields the near-straight-line torque-speed curve shown in Fig. 8.9-1. From (8.9-5), V_{ds}^r will be zero when $\omega_r = 0$ and when $I_{qs}^r = 0$ ($T_e = 0$), which occurs when $\omega_r = V_{qs}^r / \lambda_m'$. It is noted that the torque-speed curve will be linear only if V_{qs}^r is constant for all speeds, which will not be the case when operating under the constraint of (8.9-6). However, V_{ds}^r is typically small and thus, for convenience, the torque-speed plot in Fig. 8.9-1 is shown as a straight line.

In practice, for $\omega_r \leq \omega_{rR}$, the current obtained by applying rated voltage V_{sR} will exceed its rated value. To avoid this situation, for $\omega_r < \omega_{rR}$, a current limit is imposed, wherein $I_{ds}^r = 0$ and $I_{qs}^r \leq \sqrt{2} I_{sR}$. For $I_{qs}^r = \sqrt{2} I_{sR}$, the upper boundary of operation becomes T_{eR}, which is depicted as a horizontal line in Fig. 8.9-1. The shaded area in Fig. 8.9-1 depicts the obtainable region of operation. In the literature, this region is often cited as the constant-torque region since, regardless of speed, the torque limit is constant. A

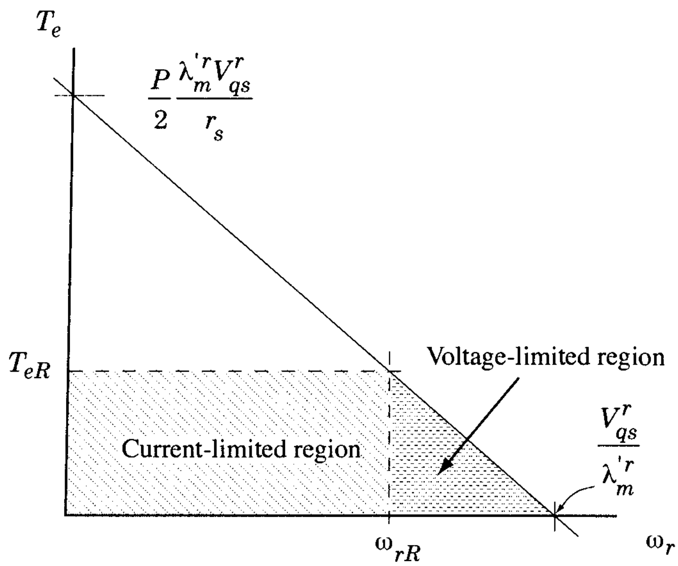

Figure 8.9-1: Torque-speed boundary for torque- and voltage-limited operation.

similar constant-torque region was shown for the dc machine in Chapter 3.

As ω_r increases beyond ω_{rR}, the voltage required to maintain $I^r_{ds} = 0$ and $I^r_{qs} = \sqrt{2}I_{sR}$ will, in general, exceed its rated value. This is due to the fact that as ω_r increases, the back-emf $\omega_r\lambda'_m$ increases, thus requiring a larger source voltage to maintain rated current. Therefore, for $\omega_r > \omega_{rR}$, the boundary of operation is the near-straight-line curve obtained from (8.9-6), which is often referred to as a voltage-limited region. It is rare to operate a machine with $I^r_{ds} = 0$ for $\omega_r > \omega_{rR}$. Rather, a negative I^r_{ds} is typically used to counteract the back-emf, enabling a so-called constant-power region that is described in the following section.

A block diagram of the constant-torque control of a permanent-magnet ac machine is shown in Fig. 8.9-2. For the boundary conditions of constant-torque operation where rated torque is commanded ($T^*_e = T_{eR}$), the commanded currents are $I^{r*}_{qs} = \sqrt{2}\ I_{sR}$ and $I^{r*}_{ds} = 0$ in Fig. 8.9-2. These commanded currents are transformed from the rotor reference frame to com-

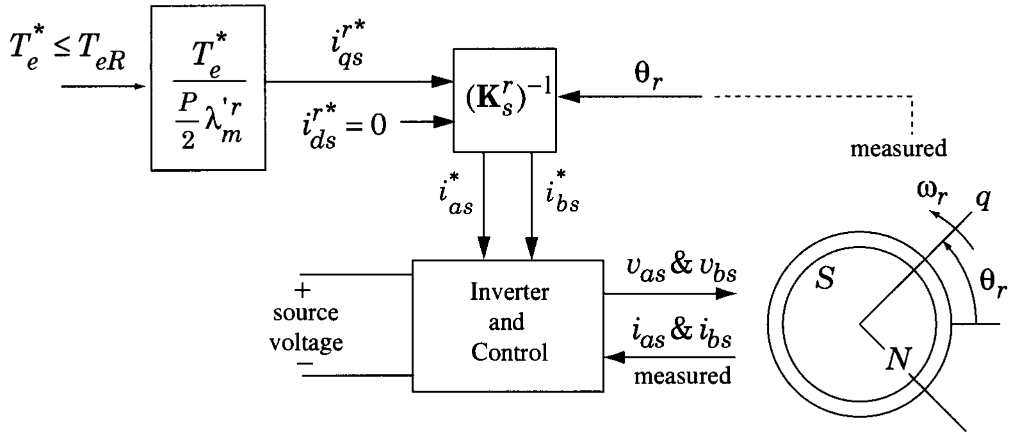

Figure 8.9-2: Block diagram of constant-torque control of a permanent-magnet ac machine for $\omega_r < \omega_{rR}$.

manded stator currents I_{as}^* and I_{bs}^* by $(\mathbf{K}_s^r)^{-1}$. In this transformation, it is necessary to ensure that the zero positions of the electrical angular displacement of the rotor and the rotor reference frame are equal and correlated with the zero position of the electrical angular displacement of the stator currents so that I_{as}^* is maximum and equal to $\sqrt{2}\, I_{sR}$ when the electrical angular displacement of the rotor and rotor reference frame are 0, 2π, 4π,.... We will leave this job to the control's engineer as well as the job of implementing the converter and converter controls to ensure that the voltages applied to the machine will maintain I_{as} and I_{bs} at the commanded values, thus, ensuring that $I_{qs}^r = \sqrt{2}\, I_{sR}$ and $I_{ds}^r = 0$.

It is important to mention that the concept of constant-torque mode of operation has been presented using steady-state electrical machine variables and yet, in Fig. 8.9-2, instantaneous currents and voltages (lower case) are shown for the actual machine applied voltages and measured currents. This is somewhat of a violation of our established notation rules; however, we will allow it, since the electric transients need only be considered when designing the actual converter controls. Also, it is important to note that in Fig. 8.9-2 θ_r is shown to be measured. In practice, the actual rotor position θ_{rm} would be measured, which is related to θ_r by the number of poles, $\theta_r = (\frac{P}{2})\theta_{rm}$. Once we have discussed the constant-power mode of operation, we will show a plot of the machine variables for the boundary operating points for both constant-torque and constant-power modes of operation.

Constant-Power Operation

Assuming that the constant-power mode occurs when $\omega_r > \omega_{rR}$, then at ω_{rR} the boundary operating conditions are T_{eR}, P_{inR}, and rated output power P_{oR}. From (8.9-4) and (8.9-5), the voltage equations at this entering boundary point of operation are

$$V_{qs}^r = r_s\sqrt{2}\, I_{sR} + \omega_{rR}\lambda_m'^r \tag{8.9-7}$$

$$V_{ds}^r = -\omega_{rR}L_{ss}\sqrt{2}\, I_{sR} \tag{8.9-8}$$

Let us take a moment to recall that we can select the zero position of the reference frame to facilitate our analysis. Here, it is convenient to select $\theta_r(0) = 0$, whereupon, from (8.9-7) and (8.9-8),

$$\begin{aligned}\tan^{-1}\phi_v &= \frac{|V_{ds}^r|}{|V_{qs}^r|}\\ &= \frac{\omega_{rR}L_{ss}}{r_s + \omega_{rR}\lambda_m'^r/\sqrt{2}\, I_{sR}}\end{aligned} \tag{8.9-9}$$

which, depending upon the parameters of the machine, is generally small. Now, since $I_{qs}^r = \sqrt{2}\ I_{sR}$ the power factor angle, $\phi_{pf} = (\theta_{ev} - \theta_{ei})$ at the beginning of the constant-power mode is ϕ_v (since θ_{ei} is zero).

At this operating point, where the constant-torque mode ends and the constant-power mode begins, the total input power for the two-phase machine is

$$\begin{aligned}P_{inR} &= 2\, I_{sR}^2\, r_s + P_{oR}\\ &= 2\, V_{sR}\, I_{sR}\cos\phi_{pf}\end{aligned} \tag{8.9-10}$$

where $\phi_{pf} = \phi_v$. The output power is

$$P_{oR} = \omega_{rmR}\left(\frac{P}{2}\right)\lambda_m'^r\sqrt{2}\, I_{sR} \tag{8.9-11}$$

Equations (8.9-10) and (8.9-11) define the boundary constraints that must exist throughout the constant-power mode of operation. In particular, in the constant-power mode, the boundary conditions are determined by the constraint that the output power is constant. Therefore, at the operating boundary, the output power must be equal to (8.9-11), and since both V_s and I_s are restricted to V_{sR} and I_{sR}, respectively, the $2\,I_{sR}^2\,r_s$ term in (8.9-10) is constant and, therefore, the input power at the boundary must be constant.

We are now ready to enter the constant-power mode, which in Chapter 3 is also referred to as the field- or flux-weakening mode of operation. Let us take a moment to think about this; the objective in the constant-power mode is to maintain the output power constant. At the boundary, this is P_{oR}. Now, as speed increases above ω_{rR}, T_e must be reduced in order to maintain P_{oR} constant. In the case of the permanent-magnet ac machine, the torque, with equal qs^r- and ds^r-winding self-inductances, L_{ss}, is reduced by reducing I_{qs}^r since torque is proportional to the product of $\lambda_m'^r$ and I_{qs}^r and input power is determined by the amplitude of the ac voltage (V_s), the ac current (I_s), and the power factor. However, both V_s and I_s are related to qs^r- and ds^r-variables as

$$\sqrt{2}\,V_s = \sqrt{(V_{qs}^r)^2 + (V_{ds}^r)^2} \tag{8.9-12}$$

$$\sqrt{2}\,I_s = \sqrt{(I_{qs}^r)^2 + (I_{ds}^r)^2} \tag{8.9-13}$$

It is clear that (8.9-12) and (8.9-13) are valid at all operating conditions; however, for the constant-power boundary conditions, V_s and I_s are rated values, V_{sR} and I_{sR}.

The power output is

$$P_o = \omega_{rm}\left(\frac{P}{2}\right)\lambda_m'^r I_{qs}^r \tag{8.9-14}$$

Since the output power must be controlled constant, then the upper boundary must be equal to (8.9-11). Equating (8.9-14) to (8.9-11) and solving for I_{qs}^r yields

$$I_{qs}^r = \frac{\omega_{rR}\sqrt{2}\,I_{sR}}{\omega_r} \qquad \text{(boundary conditions)} \tag{8.9-15}$$

From (8.9-13), the magnitude of I_{ds}^r at the boundary may be expressed as

$$I_{ds}^r = \pm\sqrt{(\sqrt{2}\,I_{sR})^2 - (I_{qs}^r)^2} \qquad \text{(boundary conditions)} \tag{8.9-16}$$

A negative I_{ds}^r is taken so as to reduce V_{qs}^r in (8.9-1). I_{ds}^r does not influence the torque when the self-inductances of the qs^r- and ds^r- windings are equal (L_{ss}). In Section 8.11, voltage and torque equations are given for unequal self-inductances. In this case, a reluctance torque occurs that is proportional to the difference in self-inductances [1].

We can now determine the boundary of the torque-speed characteristics during the constant-output-power mode of operation. In particular, for a given value of $\omega_r > \omega_{rR}$, I_{qs}^r for boundary conditions is determined from (8.9-15) and I_{ds}^r from (8.9-16) for boundary conditions. Now these boundary values are substituted into (8.9-1) and (8.9-2), with I_{ds}^r the negative value calculated from (8.9-16), to determine the boundary values of V_{qs}^r and V_{ds}^r.

Constant-Torque and Constant-Power Regions of Operation

The torque-speed operating regions for the constant-torque mode followed by the constant-power mode are shown as the shaded area in Fig. 8.9-3. Since rated conditions established the limits of operation, the boundary of the operating region for the constant-torque and constant-power modes can be explained and established. However, to illustrate operation within the boundaries is not as straightforward. Within the region of operation, all machine variables are within their permissible limits of operation. For example, commanded torque or power less than rated could be satisfied at any rotor speed within the region of operation and neither voltage nor current need be fixed or restricted. Clearly, the application will generally dictate the variable(s) other than torque or power to be commanded or limited. Appli-

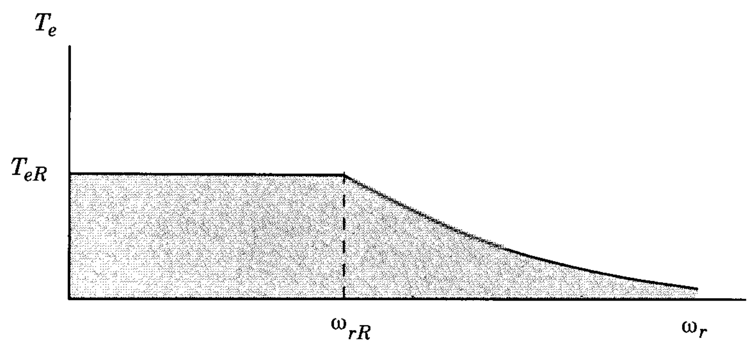

Figure 8.9-3: Torque-speed operating region for the constant-torque followed by the constant-power modes.

cations and the design of controls to meet the application requirements are well beyond this first look at controlled performance of a permanent-magnet ac machine. Our goal has been to introduce modes of operation and to establish the boundary of the torque-speed characteristics. A more extensive treatment is found in [4].

Before leaving this brief consideration of performance control of a permanent-magnet ac machine, two things are worth mentioning. First, this analysis has been carried out assuming the self-inductances of the *qs*- and *ds*-windings are the same (L_{ss}). In a following section, the voltage and torque equations are given for unequal qs^r- and ds^r self-inductances. This inequality markedly complicates the analysis of the constant-torque and constant-power modes; however, the basic concepts that have been established in this section are still valid. Second, in the case of the dc machine, field weakening directly influenced the torque and the armature current through demagnetization of the field flux. In the case of the permanent-magnet ac machine, field weakening by injecting a negative I_{ds}^r during the constant-power mode of operation does not directly influence the torque when the self-inductances are equal. However, it does permit a larger I_{qs}^r by demagnetizing the V_{qs}^r voltage equation.

Figure 8.9-4 is helpful in summarizing the concepts that have been introduced. The machine variables for boundary operation with constant-torque and constant-power modes of the machine considered in Example 8A and throughout this chapter are shown in Fig. 8.9-4. Rated conditions were assumed to occur at $\omega_{rR} = 135$ rad/sec with $\sqrt{2}\ V_{sR} = \sqrt{2}\ 11.25$ V and $\sqrt{2}\ I_{sR} = 1.5$ A. Albeit small, $\sqrt{2}\ V_{sR}$ was exceeded soon after entering the constant-power mode. This was done to achieve a torque-speed operating region that closely resembles that of a permanent-magnet dc machine. In practice, the torque-speed operating region is dependent on machine parameters as shown in [4].

SP8.9-1 Refer to Fig. 8.9-4. Calculate V_{qs}^r at ω_{rR} at the start of the constant-power mode for (a) $L_{ss} = 12.1$ mH and (b) $L_{ss} = 2(12.1)$ mH. [(a) 16.25 V, (b) 16.25 V]

SP8.9-2 Calculate $\tilde{E}_a$ at the end of the constant-torque mode of operation in Fig. 8.9-4. [7.89 $\underline{/0^\circ}$ V]

SP8.9-3 Describe how operation at $\frac{1}{2}T_{eR}$ and $\omega_r = \frac{1}{2}\omega_{rR}$ might be achieved. [Command $I_{qs}^{r*} = \frac{1}{2}T_{eR}^*/\frac{P}{2}\lambda_m'$]

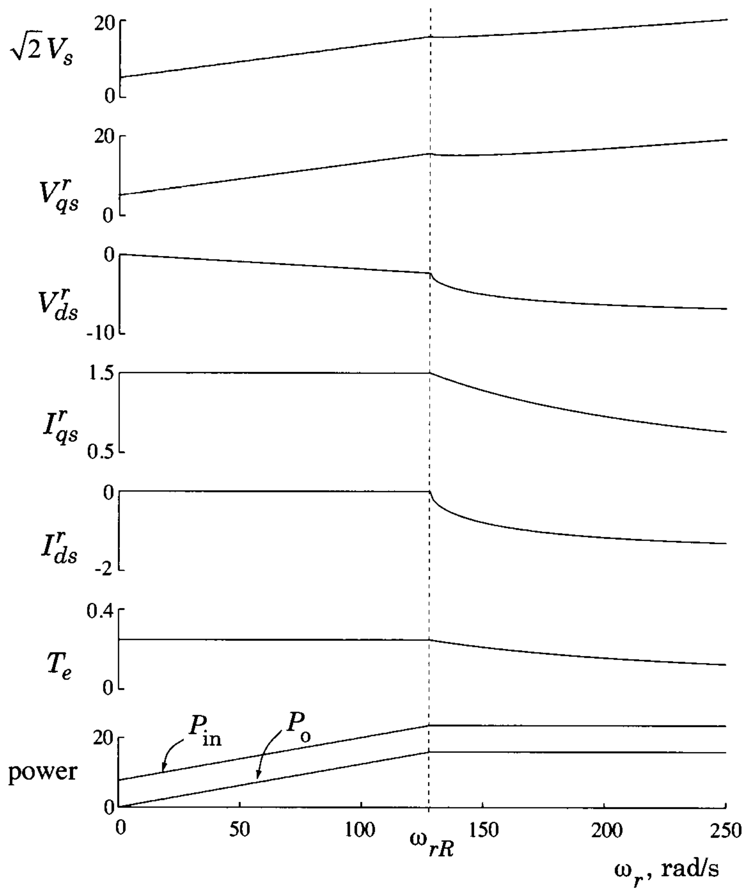

Figure 8.9-4: Constant-torque and constant-power modes of operation for $\sqrt{2}I_{sR} = 1.5$ A and machine parameters given in Example 8A.

8.10 TIME-DOMAIN BLOCK DIAGRAMS AND STATE EQUATIONS

Although the analysis of control systems is not our intent, it is worthwhile to set the stage for this type of analysis by briefly considering time-domain block diagrams and state equations. In this section, we will consider the permanent-magnet ac machine first described by the general nonlinear differential equations and then with $\phi_v = 0$ and i_{ds}^r neglected, whereupon the differential equations become linear. Some of the descriptive information regarding block diagrams and state variables given here is a repeat of that given in Section 3.7.

Nonlinear System Equations

Block diagrams, which portray the interconnection of the system equations, are used extensively in control system analysis and design. We will work with the time-domain equations by using the p operator to denote differentiation with respect to time and the operator $1/p$ to denote integration. Those familiar with Laplace transformations will have no trouble converting the time-domain block diagrams to transfer functions by using the Laplace operator.

Arranging the equations into block diagram representation is straightforward. From the voltage equations given by (8.5-9) and (8.5-10) and the relationship between torque and rotor speed, (8.4-3), we can write

$$v_{qs}^r = r_s(1 + \tau_s p)i_{qs}^r + r_s\tau_s\omega_r i_{ds}^r + \lambda_m^{\prime r}\omega_r \tag{8.10-1}$$

$$v_{ds}^r = r_s(1 + \tau_s p)i_{ds}^r - r_s\tau_s\omega_r i_{qs}^r \tag{8.10-2}$$

$$T_e - T_L = \frac{2}{P}(B_m + Jp)\omega_r \tag{8.10-3}$$

where $\tau_s = L_{ss}/r_s$. Solving (8.10-1) for i_{qs}^r, (8.10-2) for i_{ds}^r, and (8.10-3) for ω_r yields

$$i_{qs}^r = \frac{1/r_s}{\tau_s p + 1}(v_{qs}^r - r_s\tau_s\omega_r i_{ds}^r - \lambda_m^{\prime r}\omega_r) \tag{8.10-4}$$

$$i_{ds}^r = \frac{1/r_s}{\tau_s p + 1}(v_{ds}^r + r_s\tau_s\omega_r i_{qs}^r) \tag{8.10-5}$$

$$\omega_r = \frac{P/2}{Jp + B_m}(T_e - T_L) \tag{8.10-6}$$

A few comments are in order regarding these expressions. In (8.10-4), we see that the three voltage terms are multiplied by the operator $(1/r_s)/(\tau_s p+1)$ to obtain i_{qs}^r. The fact that we are multiplying the voltages by an operator to obtain current is in no way indicative of the procedure that we might actually use to calculate i_{qs}^r. We are simply expressing the dynamic relationship between the voltage terms and the current i_{qs}^r in a form convenient for drawing block diagrams.

The time-domain block diagram portraying (8.10-4) through (8.10-6) with $T_e = (P/2)\lambda_m'^r i_{qs}^r$ is shown in Fig. 8.10-1. This diagram consists of a set of linear blocks, wherein the relationship between the input and corresponding output variable is depicted in transfer function form, and two multipliers that represent nonlinear blocks. Since the system is nonlinear, it is not possible to apply previously used techniques (or, for that matter, Laplace transform methods) for solving the differential equations implied by this block diagram. For this, we would use a computer; however, if we neglect i_{ds}^r as we will later, we will find that the multipliers in Fig. 8.10-1 are no longer needed and conventional methods of analyzing linear systems may be applied with relative ease.

The so-called state equations of a system are the formulation of the state variables into a matrix form convenient for computer implementation, particularly for linear systems. The state variables of a system are defined as a minimal set of variables such that knowledge of these variables at any initial time t_0 and information on the input excitation subsequently applied are sufficient to determine the state of the system at any time $t > t_0$ [3]. In the case of the permanent-magnet ac machine, the stator currents i_{qs}^r and i_{ds}^r, the rotor speed ω_r, and the rotor position θ_r are the state variables. However, since θ_r can be established from ω_r using

$$\omega_r = \frac{d\theta_r}{dt} \tag{8.10-7}$$

and since θ_r is considered a state variable only when shaft position is a controlled variable, we will omit θ_r from consideration in this development.

The formulation of the state equations for the permanent-magnet ac machine can be readily achieved by straightforward manipulation of the voltage equations given by (8.5-9) and (8.5-10) and the equation relating torque and rotor speed given by (8.4-3). In particular, solving the v_{qs}^r voltage equation (8.5-9) for pi_{qs}^r yields

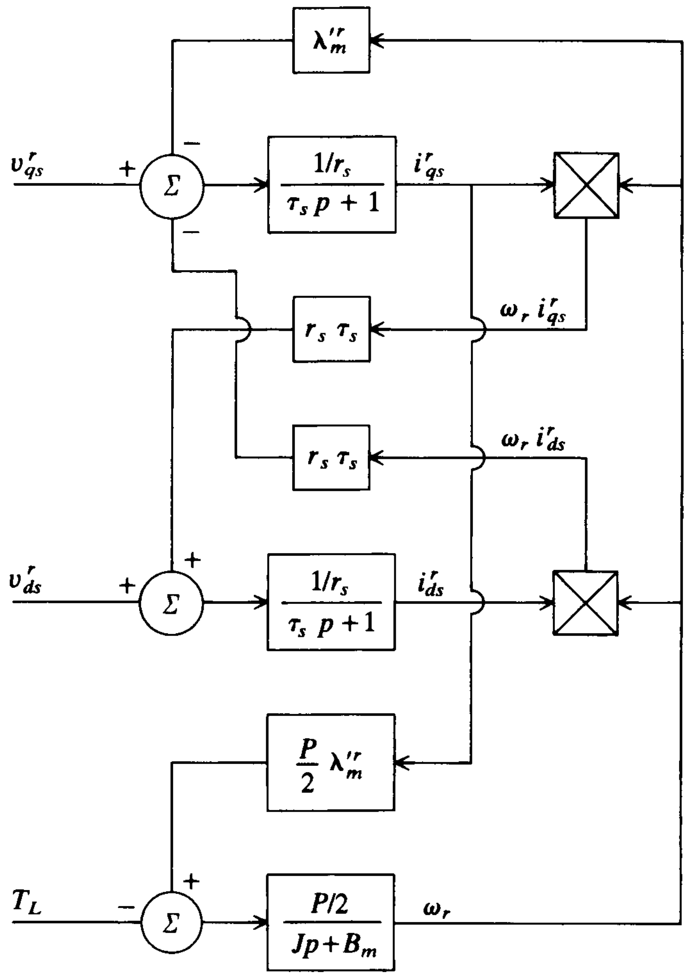

Figure 8.10-1: Time-domain block diagram of a permanent-magnet ac machine.

$$\frac{di_{qs}^r}{dt} = -\frac{r_s}{L_{ss}} i_{qs}^r - \omega_r i_{ds}^r - \frac{\lambda_m'^r}{L_{ss}} \omega_r + \frac{1}{L_{ss}} v_{qs}^r \tag{8.10-8}$$

Solving the v_{ds}^r voltage equation, (8.5-10), for pi_{ds}^r yields

$$\frac{di_{ds}^r}{dt} = -\frac{r_s}{L_{ss}} i_{ds}^r + \omega_r i_{qs}^r + \frac{1}{L_{ss}} v_{ds}^r \tag{8.10-9}$$

Solving (8.4-3) for $p\omega_r$ with $T_e = (P/2)\lambda_m'^r i_{qs}^r$ yields

$$\frac{d\omega_r}{dt} = -\frac{B_m}{J}\omega_r + \left(\frac{P}{2}\right)^2 \frac{\lambda_m'^r}{J} i_{qs}^r - \frac{P}{2}\frac{1}{J} T_L \tag{8.10-10}$$

All we have done is to solve the equations for the highest derivative of the state variables while substituting $T_e = (P/2)\lambda_m'^r i_{qs}^r$ into (8.4-3). The state equations in matrix or vector matrix form are

$$p\begin{bmatrix} i_{qs}^r \\ i_{ds}^r \\ \omega_r \end{bmatrix} = \begin{bmatrix} -\dfrac{r_s}{L_{ss}} & 0 & -\dfrac{\lambda_m'^r}{L_{ss}} \\ 0 & -\dfrac{r_s}{L_{ss}} & 0 \\ \left(\dfrac{P}{2}\right)^2 \dfrac{\lambda_m'^r}{J} & 0 & -\dfrac{B_m}{J} \end{bmatrix} \begin{bmatrix} i_{qs}^r \\ i_{ds}^r \\ \omega_r \end{bmatrix} + \begin{bmatrix} -\omega_r i_{ds}^r \\ \omega_r i_{qs}^r \\ 0 \end{bmatrix} +$$

$$\begin{bmatrix} \dfrac{1}{L_{ss}} & 0 & 0 \\ 0 & \dfrac{1}{L_{ss}} & 0 \\ 0 & 0 & -\dfrac{P}{2}\dfrac{1}{J} \end{bmatrix} \begin{bmatrix} v_{qs}^r \\ v_{ds}^r \\ T_L \end{bmatrix} \tag{8.10-11}$$

Equation (8.10-11) is the state equation; note, however, that the second term (vector) on the right-hand side contains the products of state variables, causing the state equation to be nonlinear.

Linear System Equations

As we know, if ϕ_v is set equal to zero and if i_{ds}^r is neglected, the brushless dc motor is described by equations identical in form to those of a permanent-magnet dc motor. In particular, the time-domain block diagram for the brushless dc motor with $\phi_v = 0$ and i_{ds}^r neglected is obtained from (8.10-4) and (8.10-6) with i_{ds}^r neglected in (8.10-4). The time-domain block diagram is shown in Fig. 8.10-2.

Usually, machine constants are given by the manufacturer. The voltage

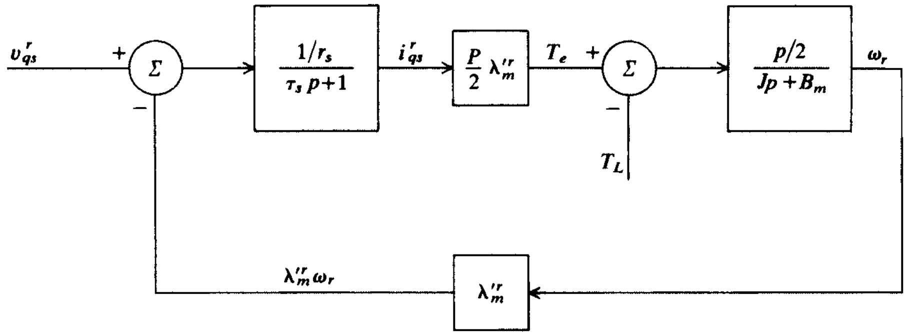

Figure 8.10-2: Time-domain block diagram of a brushless dc motor ($\phi_v = 0$) with i_{ds}^r neglected.

constant, often denoted k_e or k_v, is our $\lambda_m'^r$. It is given either as a peak phase (winding) voltage or as an rms voltage. A torque constant k_t is also given. It is in the units of N · m/A and, hence, one would be led to believe from the torque equation (8.5-17) that

$$k_t = \frac{P}{2}\lambda_m'^r = \frac{P}{2}k_e \tag{8.10-12}$$

Unfortunately, k_t may be given with or without the number of poles taken into account.

A mechanical or inertia time constant is often used as in the case of dc machines. In the case of the brushless dc motor, we will define it as

$$\tau_m = \frac{Jr_s}{(P/2)^2(\lambda_m'^r)^2} \tag{8.10-13}$$

This constant is often given by the manufacturers; however, one must realize that the manufacturer's value of τ_m will include the inertia of only the rotor, whereas the J in (8.10-13) is, by our definition, the inertia of the rotor and connected load.

Let us return to the block diagram given in Fig. 8.10-2. As in Example 3C for a permanent-magnet dc machine, we can write the following transfer function for the brushless dc machine with $i_{ds}^r = 0$:

$$\omega_r = \frac{\dfrac{1}{\lambda_m'^r \tau_s \tau_m} v_{qs}^r - \dfrac{P}{2}\dfrac{1}{J}\left(p + \dfrac{1}{\tau_s}\right) T_L}{p^2 + \left(\dfrac{1}{\tau_s} + \dfrac{B_m}{J}\right) p + \dfrac{1}{\tau_s}\left(\dfrac{1}{\tau_s} + \dfrac{B_m}{J}\right)} \tag{8.10-14}$$

The current i_{qs}^r can be expressed as

$$i_{qs}^r = \frac{\dfrac{1}{\tau_s r_s}\left(p + \dfrac{B_m}{J}\right) v_{qs}^r + \dfrac{1}{\lambda_m'^r \tau_s \tau_m} T_L}{p^2 + \left(\dfrac{1}{\tau_s} + \dfrac{B_m}{J}\right) p + \dfrac{1}{\tau_s}\left(\dfrac{1}{\tau_m} + \dfrac{B_m}{J}\right)} \tag{8.10-15}$$

With $\phi_v = 0$ and i_{ds}^r neglected, i_{qs}^r and ω_r are now the only state variables. Thus, from (8.10-8),

$$\frac{di_{qs}^r}{dt} = -\frac{r_s}{L_{ss}} i_{qs}^r - \frac{\lambda_m'^r}{L_{ss}} \omega_r + \frac{1}{L_{ss}} v_{qs}^r \tag{8.10-16}$$

Equation (8.10-10) still applies for ω_r. The system is described by a set of linear differential equations. In matrix form, the state equations become

$$p\begin{bmatrix} i_{qs}^r \\ \omega_r \end{bmatrix} = \begin{bmatrix} -\dfrac{r_s}{L_{ss}} & -\dfrac{\lambda_m'^r}{L_{ss}} \\ \left(\dfrac{P}{2}\right)^2 \dfrac{\lambda_m'^r}{J} & -\dfrac{B_m}{J} \end{bmatrix} \begin{bmatrix} i_{qs}^r \\ \omega_r \end{bmatrix} + \begin{bmatrix} \dfrac{1}{L_{ss}} & 0 \\ 0 & -\dfrac{P}{2}\dfrac{1}{J} \end{bmatrix} \begin{bmatrix} v_{qs}^r \\ T_L \end{bmatrix} \tag{8.10-17}$$

The state equations expressed in the form of (8.10-17) is called the *fundamental form.* In particular, it may be expressed symbolically as

$$p\mathbf{x} = \mathbf{A}\mathbf{x} + \mathbf{B}\mathbf{u} \tag{8.10-18}$$

which is the fundamental form, where p is the operator d/dt, $\mathbf{x}$ is the state vector (column matrix of state variables), and $\mathbf{u}$ is the input vector (column matrix of inputs to the system). We see that (8.10-17) and (8.10-18) are identical in form. Methods of solving equations of the fundamental form given by (8.10-18) are well known. Consequently, they are used extensively in control system analysis [3]. Before leaving this work, let us repeat the restrictions upon the linear differential equations given in this section. First, v_{ds}^r must be zero, that is, $\phi_v = 0$. Second, i_{ds}^r is neglected, which means that v_{qs}^r, ω_r, and T_e should not be negative. This latter restriction is rather severe since it can easily be violated if the system variables are subjected to large excursions. One last comment. The stator time constant τ_s is often neglected and the steady-state torque-speed characteristic is used in the transfer function. It was illustrated in Fig. 8.7-2 that this can lead to error in calculating the response of the rotor speed if the inertia of the mechanical system is small.

SP8.10-1 If $\phi_v = 0$ and i_{ds}^r is not neglected, are the system differential equations linear? Is i_{ds}^r a state variable? [No; yes, if state equations are written as (8.10-11)]

SP8.10-2 What is the difference between neglecting i_{ds}^r and neglecting the term $\omega_r^2 L_{ss}^2$ as we did in the analysis of steady-state operation with $\phi_v = 0$. [None]

SP8.10-3 Is Fig. 8.10-2 valid for the constant-torque mode of operation described in Section 8.9? Why? [No; $V_{ds}^r = 0$ ($\phi_v = 0$) only at $\omega_r = 0$ for constant-torque mode]

8.11 DIRECT AND QUADRATURE AXIS INDUCTANCES

Thus far in our analysis of the permanent-magnet ac machine, we have assumed that L_{md} and L_{mq} are equal and, thus,

$$L_s = \begin{bmatrix} L_{\ell s} + L_{ms} & 0 \\ 0 & L_{\ell s} + L_{ms} \end{bmatrix} \tag{8.11-1}$$

which is (8.3-13). However, the reluctances of the direct and quadrature axes can be different due to rotor saliency or due to the type of ferromagnetic material in each axes. In fact, due to the placing of permanent magnets, the direct-axis reluctance can be greater than the quadrature-axis reluctance. Although in most designs the reluctances are not radically different, unequal q- and d-axes reluctances can be treated by starting with (1.7-29) and then following the discussion surrounding (5.4-20) through (5.4-23). In particular, let us write (5.4-22) and (5.4-23) in a slightly different form while adding $\lambda_m'^r$ to (5.4-23):

$$\lambda_{qs}^r = (L_{ls} + L_{mq}) i_{qs}^r \tag{8.11-2}$$

$$\lambda_{ds}^r = (L_{ls} + L_{md}) i_{ds}^r + \lambda_m'^r \tag{8.11-3}$$

which can also be written

$$\lambda_{qs}^{r} = L_q i_{qs}^{r} \tag{8.11-4}$$

$$\lambda_{ds}^{r} = L_d i_{ds}^{r} + \lambda_m'^{r} \tag{8.11-5}$$

Equations (8.11-4) and (8.11-5) should be compared to (8.5-6) and (8.5-7). Clearly, if L_q and L_d are equal then $L_{mq} = L_{md}$ and we are back to (8.5-6) and (8.5-7).

It is not our purpose to rederive all of equations set forth in this chapter using (8.11-4) and (8.11-5) with unequal L_q and L_d; this is done in [1]. It is interesting, however, to point out a few of the differences. The qs^r- and ds^r-voltage equations become

$$v_{qs}^{r} = (r_s + pL_q)i_{qs}^{r} + \omega_r L_d i_{ds}^{r} + \omega_r \lambda_m'^{r} \tag{8.11-6}$$

$$v_{ds}^{r} = (r_s + pL_d)i_{ds}^{r} - \omega_r L_q i_{qs}^{r} \tag{8.11-7}$$

The torque may be expressed

$$T_e = \frac{P}{2}(\lambda_{ds}^{r} i_{qs}^{r} - \lambda_{qs}^{r} i_{ds}^{r}) \tag{8.11-8}$$

For a linear magnetic system

$$T_e = \frac{P}{2}\left[\lambda_m'^{r} i_{qs}^{r} + (L_d - L_q) i_{qs}^{r} i_{ds}^{r}\right] \tag{8.11-9}$$

It is important to note that, if L_q and L_d are markedly different, the form of the torque for motor action could be somewhat different from that of a permanent-magnet dc machine when the controlled permanent-magnet ac machine is operated as a brushless dc machine ($\phi_v = 0$).

The steady-state voltage equation becomes

$$\tilde{V}_{as} = (r_s + j\omega_r L_q)\tilde{I}_{as} + \tilde{E}_a \tag{8.11-10}$$

where

$$\tilde{E}_a = \frac{1}{\sqrt{2}}\left[\omega_r (L_d - L_q) I_{ds}^{r} + \omega_r \lambda_m'^{r}\right] e^{j0^\circ} \tag{8.11-11}$$

SP8.11-1 Express V_{qs}^{r} and V_{ds}^{r} for $L_q \neq L_d$. [$V_{qs}^{r} = r_s I_{qs}^{r} + \omega_r L_d I_{ds}^{r} + \omega_r \lambda_m'^{r}$; $V_{ds}^{r} = r_s I_{ds}^{r} - \omega_r L_q I_{qs}^{r}$]

SP8.11-2 A permanent-magnet ac machine is controlled to operate with $I_{ds}^r = 0$. $L_q = 1.5L_d$. Express T_e. $[T_e = \frac{P}{2}\lambda_m'^r I_{qs}^r]$
SP8.11-3 The machine given in SP8.11-1 is controlled to operate in the constant-power mode. The torque is expressed by (8.11-9). Why? [I_{ds}^r is not zero in the constant-power mode]

8.12 THREE-PHASE PERMANENT-MAGNET ac MACHINE

A two-pole, three-phase, permanent-magnet ac machine is shown in Fig. 8.12-1. The stator windings are identical windings, displaced by $\frac{2}{3}\pi$. The windings are sinusoidally distributed, each with N_s equivalent turns and resistance r_s. Electromagnetic torque is produced by the interaction of the poles of the permanent-magnet rotor and the poles resulting from the rotating air-gap mmf established by currents flowing in the stator windings. The rotating air-gap mmf (mmf_s) established by symmetrical three-phase stator windings carrying balanced three-phase currents is given by (4.4-18).

Voltage Equations and Winding Inductances

The voltage equations for the two-pole, three-phase, permanent-magnet ac machine shown in Fig. 8.12-1 may be expressed as

$$v_{as} = r_s i_{as} + \frac{d\lambda_{as}}{dt} \tag{8.12-1}$$

$$v_{bs} = r_s i_{bs} + \frac{d\lambda_{bs}}{dt} \tag{8.12-2}$$

$$v_{cs} = r_s i_{cs} + \frac{d\lambda_{cs}}{dt} \tag{8.12-3}$$

In matrix form,

$$\mathbf{v}_{abcs} = \mathbf{r}_s \mathbf{i}_{abcs} + p\boldsymbol{\lambda}_{abcs} \tag{8.12-4}$$

For voltages, currents, and flux linkages,

$$(\mathbf{f}_{abcs})^T = [f_{as} \quad f_{bs} \quad f_{cs}] \tag{8.12-5}$$

and

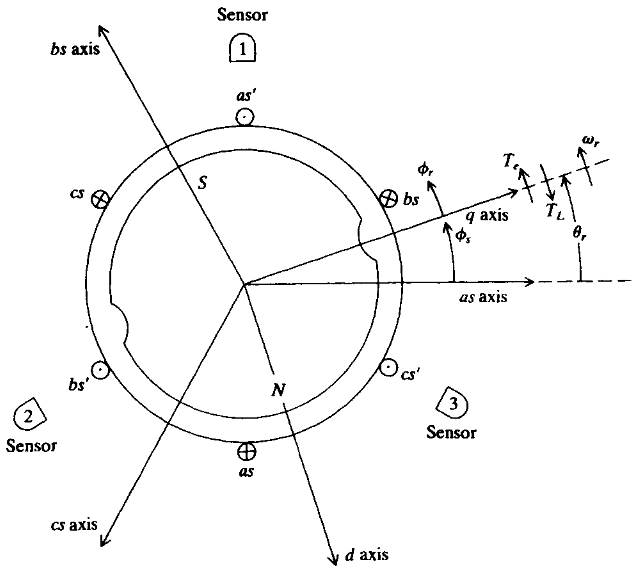

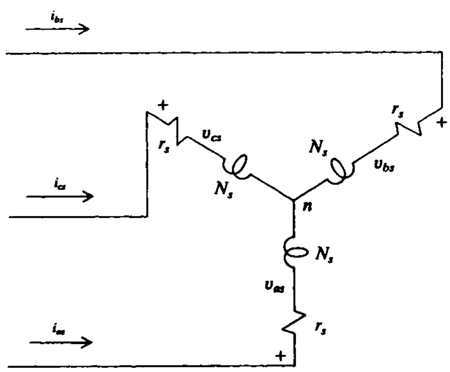

Figure 8.12-1: Two-pole, three-phase, permanent-magnet ac machine.

$$\mathbf{r}_s = \begin{bmatrix} r_s & 0 & 0 \\ 0 & r_s & 0 \\ 0 & 0 & r_s \end{bmatrix} \tag{8.12-6}$$

The flux linkage equations may be expressed as

$$\lambda_{as} = L_{asas}i_{as} + L_{asbs}i_{bs} + L_{ascs}i_{cs} + \lambda_{asm} \tag{8.12-7}$$

$$\lambda_{bs} = L_{bsas}i_{as} + L_{bsbs}i_{bs} + L_{bscs}i_{cs} + \lambda_{bsm} \tag{8.12-8}$$

$$\lambda_{cs} = L_{csas}i_{as} + L_{csbs}i_{bs} + L_{cscs}i_{cs} + \lambda_{csm} \tag{8.12-9}$$

In matrix form,

$$\boldsymbol{\lambda}_{abcs} = \mathbf{L}_s\mathbf{i}_{abcs} + \boldsymbol{\lambda}'_m \tag{8.12-10}$$

where $\boldsymbol{\lambda}'_m$ is the column vector:

$$\boldsymbol{\lambda}'_m = \begin{bmatrix} \lambda_{asm} \\ \lambda_{bsm} \\ \lambda_{csm} \end{bmatrix} = \lambda'_m \begin{bmatrix} \sin\theta_r \\ \sin(\theta_r - \frac{2}{3}\pi) \\ \sin(\theta_r + \frac{2}{3}\pi) \end{bmatrix} \tag{8.12-11}$$

In (8.12-11), λ'_m is the amplitude of the flux linkages established by the permanent magnet as viewed from the stator phase windings. In other words, the magnitude of $p\lambda_{asm}$, $p\lambda_{bsm}$, and $p\lambda_{csm}$ would be the magnitude of the open-circuit voltage induced in the respective stator phase windings. The rotor displacement θ_r is defined by (8.3-10).

For our purposes, we will assume that $L_q = L_d$, whereupon $\mathbf{L}_s$ may be written as

$$\mathbf{L}_s = \begin{bmatrix} L_{ls} + L_{ms} & -\frac{1}{2}L_{ms} & -\frac{1}{2}L_{ms} \\ -\frac{1}{2}L_{ms} & L_{ls} + L_{ms} & -\frac{1}{2}L_{ms} \\ -\frac{1}{2}L_{ms} & -\frac{1}{2}L_{ms} & L_{ls} + L_{ms} \end{bmatrix} \tag{8.12-12}$$

where L_{ls} represents the leakage inductance and L_{ms} the magnetizing inductance. The off-diagonal terms are $-\frac{1}{2}L_{ms}$ since the mutual inductance between two stator windings displaced $\frac{2}{3}\pi$ is $\cos\frac{2}{3}\pi$ times the mutual inductance if they were placed one on top of the other (L_{ms}).

Torque

An expression for the electromagnetic torque may be obtained by using the second entry in Table 2.5-1. Since the magnetic system is assumed to be linear, the field and coenergy are equal:

$$W_c = \frac{1}{2}L_{ss}(i_{as}^2 + i_{bs}^2 + i_{cs}^2) - \frac{1}{2}L_{ms}(i_{as}i_{bs} + i_{as}i_{cs} + i_{bs}i_{cs}) + \lambda'_m i_{as}\sin\theta_r$$

$$+ \lambda'_m i_{bs}\sin(\theta_r - \tfrac{2}{3}\pi) + \lambda'_m i_{cs}\sin(\theta_r + \tfrac{2}{3}\pi) + W_{pm} \qquad (8.12\text{-}13)$$

where W_{pm} relates to the energy associated with the permanent magnet, which is constant for the machine shown in Fig. 8.12-1. Taking the partial derivative with respect to θ_r yields

$$T_e = \frac{P}{2}\lambda'_m\left[(i_{as} - \frac{1}{2}i_{bs} - \frac{1}{2}i_{cs})\cos\theta_r + \frac{\sqrt{3}}{2}(i_{bs} - i_{cs})\sin\theta_r\right] \qquad (8.12\text{-}14)$$

The above expression is positive for motor action. The torque and speed may be related as given by (8.4-3).

Machine Equations in the Rotor Reference Frame

Since there are three stator variables (f_{as}, f_{bs}, and f_{cs}), we must use three substitute variables in the transformation of the stator variables to the rotor reference frame. In particular,

$$\mathbf{f}_{qd0s}^r = \mathbf{K}_s^r \mathbf{f}_{abcs} \qquad (8.12\text{-}15)$$

where

$$(\mathbf{f}_{qd0s}^r)^T = [f_{qs}^r \quad f_{ds}^r \quad f_{0s}] \qquad (8.12\text{-}16)$$

$$\mathbf{K}_s^r = \frac{2}{3}\begin{bmatrix} \cos\theta_r & \cos(\theta_r - \frac{2}{3}\pi) & \cos(\theta_r + \frac{2}{3}\pi) \\ \sin\theta_r & \sin(\theta_r - \frac{2}{3}\pi) & \sin(\theta_r + \frac{2}{3}\pi) \\ \frac{1}{2} & \frac{1}{2} & \frac{1}{2} \end{bmatrix} \qquad (8.12\text{-}17)$$

where the rotor displacement θ_r is defined by (8.3-10). The inverse of $\mathbf{K}_s^r$ is

$$(\mathbf{K}_s^r)^{-1} = \begin{bmatrix} \cos\theta_r & \sin\theta_r & 1 \\ \cos(\theta_r - \frac{2}{3}\pi) & \sin(\theta_r - \frac{2}{3}\pi) & 1 \\ \cos(\theta_r + \frac{2}{3}\pi) & \sin(\theta_r + \frac{2}{3}\pi) & 1 \end{bmatrix} \qquad (8.12\text{-}18)$$

It is important to note that the same notation ($\mathbf{K}_s^r$) used for the two-phase transformation is used here for the three-phase transformation. Equation (8.12-17) is Park's original transformation for synchronous machines [2]. The zero variable f_{0s} is the third substitute variable, and it is zero for balanced conditions. Also, f_{0s} is not a function of θ_r; therefore, the $0s$ variables are associated with stationary circuits. For this reason, a raised index is not incorporated with the zero variables.

Substituting the change of variables into the stator voltage equations given by (8.12-4) yields

$$(\mathbf{K}_s^r)^{-1}\mathbf{v}_{qd0s}^r = \mathbf{r}_s(\mathbf{K}_s^r)^{-1}\mathbf{i}_{qd0s}^r + p[(\mathbf{K}_s^r)^{-1}\boldsymbol{\lambda}_{qd0s}^r] \tag{8.12-19}$$

Premultiplying each side by $\mathbf{K}_s^r$ yields

$$\mathbf{v}_{qd0s}^r = \mathbf{r}_s\mathbf{i}_{qd0s}^r + \omega_r\boldsymbol{\lambda}_{dqs}^r + p\boldsymbol{\lambda}_{qd0s}^r \tag{8.12-20}$$

where

$$(\boldsymbol{\lambda}_{qds}^r)^T = [\lambda_{ds}^r \quad -\lambda_{qs}^r \quad 0] \tag{8.12-21}$$

If one wishes to work through the steps necessary to go from (8.12-19) to (8.12-20), the trigonometric relations given in Appendix A will be very helpful.

For a magnetically linear system, the stator flux linkages are expressed by (8.12-10). Substituting the change of variables into (8.12-10) yields

$$(\mathbf{K}_s^r)^{-1}\boldsymbol{\lambda}_{qd0s}^r = \mathbf{L}_{ss}(\mathbf{K}_s^r)^{-1}\mathbf{i}_{qd0s}^r + \boldsymbol{\lambda}_m' \tag{8.12-22}$$

Premultiplying by $\mathbf{K}_s^r$ yields

$$\boldsymbol{\lambda}_{qd0s}^r = \begin{bmatrix} L_{ls}+\frac{3}{2}L_{ms} & 0 & 0 \\ 0 & L_{ls}+\frac{3}{2}L_{ms} & 0 \\ 0 & 0 & L_{ls} \end{bmatrix} \begin{bmatrix} i_{qs}^r \\ i_{ds}^r \\ i_{0s} \end{bmatrix} + \lambda_m'^r \begin{bmatrix} 0 \\ 1 \\ 0 \end{bmatrix} \tag{8.12-23}$$

To be consistent with our previous notation we have added the superscript r to λ_m'. In expanded form,

$$v_{qs}^r = r_s i_{qs}^r + \omega_r\lambda_{ds}^r + p\lambda_{qs}^r \tag{8.12-24}$$

$$v_{ds}^r = r_s i_{ds}^r - \omega_r\lambda_{qs}^r + p\lambda_{ds}^r \tag{8.12-25}$$

$$v_{0s} = r_s i_{0s} + p\lambda_{0s} \tag{8.12-26}$$

where

$$\lambda_{qs}^r = L_{ss} i_{qs}^r \tag{8.12-27}$$

$$\lambda_{ds}^r = L_{ss} i_{ds}^r + \lambda_m^r \tag{8.12-28}$$

$$\lambda_{0s} = L_{ls} i_{0s} \tag{8.12-29}$$

where

$$L_{ss} = L_{ls} + \tfrac{3}{2} L_{ms} \tag{8.12-30}$$

We must be careful here. When dealing with the two-phase machine, we also used L_{ss}; however, there it was $L_{ls} + L_{ms}$ rather than $L_{ls} + \frac{3}{2}L_{ms}$. Although we should probably use a different notation for the two- and three-phase machines, we will not. Instead we will call attention to this difference as we go along.

Substituting (8.12-27) through (8.12-29) into (8.12-24) through (8.12-26) and since $\lambda_m'^r$ is constant, $p\lambda_m'^r = 0$, and we can write

$$v_{qs}^r = (r_s + pL_{ss}) i_{qs}^r + \omega_r L_{ss} i_{ds}^r + \omega_r \lambda_m'^r \tag{8.12-31}$$

$$v_{ds}^r = (r_s + pL_{ss}) i_{ds}^r - \omega_r L_{ss} i_{qs}^r \tag{8.12-32}$$

$$v_{0s} = (r_s + pL_{ls}) i_{0s} \tag{8.12-33}$$

Note that v_{qs}^r and v_{ds}^r, (8.12-31) and (8.12-32), are identical in form to v_{qs}^r and v_{ds}^r for the two-phase machine given by (8.5-9) and (8.5-10), respectively. The above equations may be written in matrix form as

$$\begin{bmatrix} v_{qs}^r \\ v_{ds}^r \\ v_{0s} \end{bmatrix} = \begin{bmatrix} r_s + pL_{ss} & \omega_r L_{ss} & 0 \\ -\omega_r L_{ss} & r_s + pL_{ss} & 0 \\ 0 & 0 & r_s + pL_{ls} \end{bmatrix} \begin{bmatrix} i_{qs}^r \\ i_{ds}^r \\ i_{0s} \end{bmatrix} + \begin{bmatrix} \omega_r \lambda_m'^r \\ 0 \\ 0 \end{bmatrix} \tag{8.12-34}$$

The expression for electromagnetic torque is obtained by expressing i_{as}, i_{bs}, and i_{cs}, in (8.12-14) in terms of i_{qs}^r and i_{ds}^r, or more simply by following the power-balance approach set forth in Section 6.7 or Section 7.5:

$$T_e = \frac{3}{2}\frac{P}{2} \lambda_m'^r i_{qs}^r \tag{8.12-35}$$

which is positive for motor action.

Example 8E. The parameters of a four-pole permanent-magnet ac machine are $r_s = 3.4\,\Omega$, $L_{ls} = 1.1$ mH, and $L_{ms} = 7.33$ mH. When the device is driven at 1000 r/min, the open-circuit winding-to-winding voltage is sinusoidal with a peak-to-peak value of 60 V. Let us determine L_{ss} and $\lambda_m'^r$.

The first of these is obtained by straightforward substitution into (8.12-30):

$$\begin{aligned} L_{ss} &= L_{ls} + \tfrac{3}{2} L_{ms} \\ &= 1.1 + \tfrac{3}{2}(7.33) = 12.1 \text{ mH} \end{aligned} \tag{8E-1}$$

Note that here we have selected L_{ms} so that L_{ss} is the same as in Example 8A. This will allow us to make a direct comparison between a two- and three-phase machine with essentially the same parameters.

Calculation of $\lambda_m'^r$ is a bit involved. The actual rotor speed in rad/s at which the measurement was taken is

$$\begin{aligned} \omega_{rm} &= \frac{(\text{r/min})(\text{rad/r})}{\text{s/min}} \\ &= \frac{(1000)(2\pi)}{60} = \frac{100}{3}\pi \text{ rad/s} \end{aligned} \tag{8E-2}$$

The electrical angular velocity is

$$\begin{aligned} \omega_r &= \frac{P}{2}\omega_{rm} \\ &= \frac{4}{2}\frac{100\pi}{3} = \frac{200}{3}\pi \text{ rad/s} \end{aligned} \tag{8E-3}$$

Let us assume that the open-circuit voltage is measured between a and b terminals; thus, from (8.12-1) and (8.12-2) and Appendix C, with i_{as} and $i_{bs} = 0$,

$$v_{ab} = v_{as} - v_{bs} = \frac{d\lambda_{as}}{dt} - \frac{d\lambda_{bs}}{dt} \tag{8E-4}$$

From (8.12-7), (8.12-8), and (8.12-11), and recalling that λ_m' and $\lambda_m'^r$ are the same quantity, we can write (8E-4) as

$$\begin{aligned} v_{ab} &= \frac{d}{dt}\{\lambda_m'^r[\sin\theta_r - \sin(\theta_r - \tfrac{2}{3}\pi)]\} \\ &= \lambda_m'^r\omega_r[\cos\theta_r - \cos(\theta_r - \tfrac{2}{3}\pi)] \\ &= \lambda_m'^r\omega_r(\cos\theta_r - \cos\theta_r\cos\tfrac{2}{3}\pi - \sin\theta_r\sin\tfrac{2}{3}\pi) \\ &= \lambda_m'^r\omega_r\left(\tfrac{3}{2}\cos\theta_r - \tfrac{\sqrt{3}}{2}\sin\theta_r\right) \\ &= \sqrt{2}\,\lambda_m'^r\omega_r\cos(\theta_r + \tfrac{1}{6}\pi) \end{aligned} \tag{8E-5}$$

We could have used phasor concepts after taking the derivative. That is, from the second line of (8E-5) we can write

$$\tilde{V}_{ab} = \frac{\lambda_m'^r \omega_r}{\sqrt{2}}(1\underline{/0^\circ} - 1\underline{/-120^\circ})$$

$$= \frac{\lambda_m'^r \omega_r}{\sqrt{2}}\left(\frac{3}{2} + j\frac{\sqrt{3}}{2}\right) = \frac{\sqrt{3}\,\lambda_m'^r \omega_r}{\sqrt{2}}\underline{/30^\circ} \tag{8E-6}$$

Now the peak-to-peak voltage is 60 V; hence, from either (8E-5) or (8E-6),

$$\frac{60}{2} = \sqrt{3}\,\lambda_m'^r \frac{200}{3}\pi \tag{8E-7}$$

The voltage must be divided by 2 since it is peak to peak. Solving for $\lambda_m'^r$ yields

$$\lambda_m'^r = \frac{\frac{60}{2}}{\sqrt{3}(\frac{200}{3}\pi)} = 0.0826 \text{ V} \cdot \text{s/rad} \tag{8E-8}$$

Stator Voltages for Balanced Operation

When the three-phase permanent-magnet ac machine is supplied from a balanced three-phase voltage source, the phase voltages may be expressed as

$$v_{as} = \sqrt{2}\,v_s \cos\theta_{esv} \tag{8.12-36}$$

$$v_{bs} = \sqrt{2}\,v_s \cos(\theta_{esv} - \tfrac{2}{3}\pi) \tag{8.12-37}$$

$$v_{cs} = \sqrt{2}\,v_s \cos(\theta_{esv} + \tfrac{2}{3}\pi) \tag{8.12-38}$$

The fundamental components of the stator applied voltages form a balanced three-phase set of *abc* sequence, where the amplitude v_s may be a function of time. In (8.12-36) through (8.12-38),

$$\omega_e = \frac{d\theta_{esv}}{dt} \tag{8.12-39}$$

$\theta_{esv}(0)$ is the time-zero position of the applied voltages. If these voltages are substituted into the equation of transformation, (8.12-15), with $\omega_e = \omega_r$, we obtain

$$v_{qs}^r = \sqrt{2}\, v_s \cos\phi_v \tag{8.12-40}$$

$$v_{ds}^r = -\sqrt{2}\, v_s \sin\phi_v \tag{8.12-41}$$

and v_{0s} is zero for balanced conditions. For compactness,

$$\phi_v = \theta_{esv} - \theta_r \tag{8.12-42}$$

where $\theta_r(0)$ is generally selected to be zero. Note that (8.12-40) through (8.12-42) are identical to (8.5-14) through (8.5-16), respectively, for the two-phase machine. It is interesting to note that the $\frac{2}{3}$ factor in $\mathbf{K}_s^r$, (8.12-17), makes the maximum amplitude of v_{qs}^r and v_{ds}^r the same as v_{as}, v_{bs}, and v_{cs}.

It is important to be aware that, as in the case of the two-phase machine, v_{qs}^r and v_{ds}^r may be changed in two ways. In particular, consider v_{qs}^r and v_{ds}^r given by (8.12-40) and (8.12-41), respectively. The amplitude of both v_{qs}^r and v_{ds}^r may be changed by changing v_s and the relative magnitude of v_{qs}^r and v_{ds}^r may be changed by changing ϕ_v.

Comparison of Equations for Two- and Three-Phase Machines

It seems appropriate to set out the important differences and similarities in the voltage and torque equations for the two- and three-phase permanent-magnet ac machines. First we note that the torque equation for the three-phase machine has the coefficient of $\frac{3}{2}$, whereas this coefficient is unity for the two-phase machine. Actually, it can be shown that this multiplier is $n_p/2$, where n_p is the number of stator phases.

Next, we introduced the $0s$ variables when defining the change of variables for the three-phase machine. However, these variables are zero when the stator variables are balanced or when a three-wire stator is being considered, wherein $i_{as} + i_{bs} + i_{cs} = 0$ [1].

Even though we introduced a 0s variable, this did not change the form of the voltage equations in the rotor reference frame. We noted that (8.12-31) and (8.12-32) were identical to (8.5-9) and (8.5-10), respectively. Hence, with $0s$ variables equal to zero, the voltage equations that describe the two- and three-phase machines are identical.

Moreover, when we transformed a two-phase balanced set by using the two-phase $\mathbf{K}_s^r$, we noted that we obtained the same expressions as when we transformed a three-phase balanced set by using the three-phase $\mathbf{K}_s^r$. Compare (8.12-40) and (8.12-41) with (8.5-14) and (8.5-15), respectively.

Perhaps the difference that is most easily overlooked is the fact that for a two-phase machine $L_{ss} = L_{ls} + L_{ms}$; but for a three-phase machine $L_{ss} = L_{ls} + \frac{3}{2}L_{ms}$. We saw a similar thing in the case of the two- and three-phase induction and/or synchronous machine.

Well, by this time you have most likely realized that we need not continue with a parallel development of the three-phase machine. Clearly, the material presented on the analysis and performance of the two-phase machine can be applied to a three-phase machine with little modification. These modifications for the three-phase machine are: (1) When you see L_{ss}, use $L_{ls} + \frac{3}{2}L_{ms}$; and (2) multiply all torque (T_e) equations by $\frac{3}{2}$.

SP8.12-1 The voltage equations given for v_{qs}^r and v_{ds}^r for the two-phase permanent-magnet ac machine, (8.5-9) and (8.5-10), appear to be identical in form to those for a three-phase machine, (8.12-34). Is there a difference other than the zero variables? [Yes, L_{ss}]

SP8.12-2 Make a two-phase and a three-phase machine identical as far as T_e is concerned for a given peak phase voltage. [$L_{ms2} = \frac{3}{2}L_{ms3}$, $\lambda_{m2}'^r = \frac{3}{2}\lambda_{m3}'^r$]

8.13 THREE-PHASE BRUSHLESS dc MACHINE

Speed control of a brushless dc machine is achieved by varying the amplitude of the phase voltages or by pulse-width modulation (PWM), which is accomplished by electronically switching the phase voltages to zero at a high frequency relative to the fundamental frequency of the phase voltages. Before considering pulse-width modulation in its elementary form, we will consider the operation of a three-phase brushless dc motor supplied from a six-step continuous-current inverter, where each phase of the machine is always connected to either the positive or negative terminal of the dc source.

The circuit configuration of the inverter is shown in Fig. 8.13-1 with the switching logic shown in Fig. 8.13-2. It is clear that in the case of the brushless dc motor inverter drive, the angular displacement of the applied stator voltages is θ_r defined by (8.3-10). Let us consider the action of one leg (phase) of the inverter shown in Fig. 8.13-1. The logic signals for the switching (commutation) of the transistors are shown in Fig. 8.13-2. $T1$ is turned on at $\theta_r = -90°$ and turned off at $\theta_r = 90°$, at which time $T4$ is turned on. It is assumed that the turn-off time of the transistors is negligible, whereupon the transistors become ideal switches. At the instant $T1$ is turned

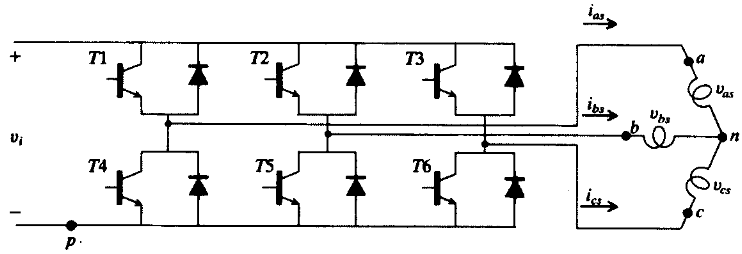

Figure 8.13-1: Six-step inverter-machine configuration.

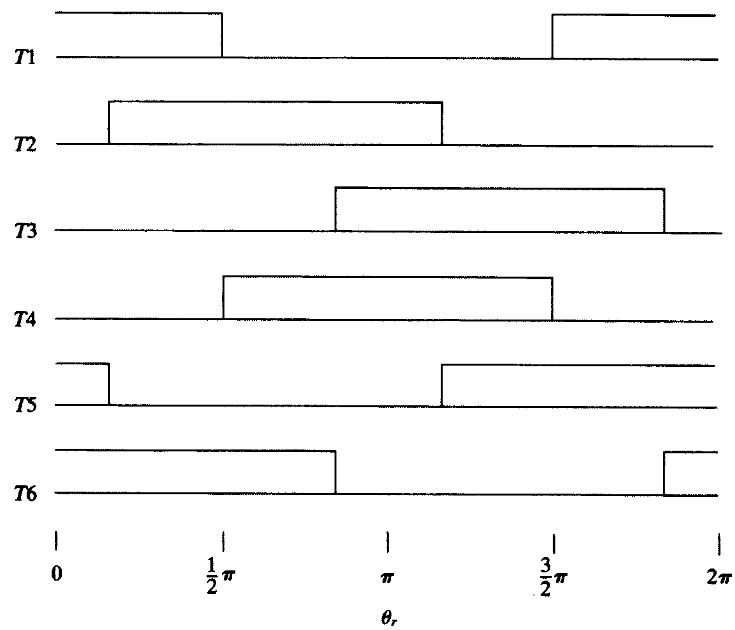

Figure 8.13-2: Transistor switching logic.

off, the current it was carrying is diverted to the diode in parallel with $T4$. The diode continues to conduct until the current decreases to zero. Once the current i_{as} reverses direction, it is carried by $T4$. This mode of inverter operation is generally referred to as the continuous voltage or continuous-current mode and, sometimes, the 180° conduction mode. We will consider the current flow in the transistor and diodes in more detail in a minute.

The following voltage equations may be written from Fig. 8.13-1:

$$v_{ap} = v_{as} + v_{np} \tag{8.13-1}$$

$$v_{bp} = v_{bs} + v_{np} \tag{8.13-2}$$

$$v_{cp} = v_{cs} + v_{np} \tag{8.13-3}$$

The stator is connected as a three-wire system, where $i_{as} + i_{bs} + i_{cs} = 0$ and, hence, the sum of v_{as}, v_{bs}, and v_{cs} is zero. Thus, by adding (8.13-1) through (8.13-3), we obtain

$$v_{np} = \tfrac{1}{3}(v_{ap} + v_{bp} + v_{cp}) \tag{8.13-4}$$

Hence

$$v_{as} = \tfrac{2}{3}v_{ap} - \tfrac{1}{3}(v_{bp} + v_{cp}) \tag{8.13-5}$$

$$v_{bs} = \tfrac{2}{3}v_{bp} - \tfrac{1}{3}(v_{ap} + v_{cp}) \tag{8.13-6}$$

$$v_{cs} = \tfrac{2}{3}v_{cp} - \tfrac{1}{3}(v_{ap} + v_{bp}) \tag{8.13-7}$$

where v_{ap}, v_{bp}, and v_{cp} are either v_i or zero depending upon the state of $T1$ through $T6$. We will consider the waveform of the voltages in more detail later.

The free-acceleration characteristics of this type of brushless dc motor-inverter drive is shown in Fig. 8.13-3. The machine parameters are those given previously, with the exception that $L_{ms} = 7.3$ mH for the three-phase machine, which makes L_{ss} the same for the two- and three-phase example machines. For purposes of comparison, the inverter voltage is 25 V, where the constant component of v_{qs}^r is equal to the value used in the case of sinusoidal applied stator voltages. (We shall see this in a minute.) In addition to the variables plotted in Fig. 8.7-1, the winding-to-winding voltage v_{ab} and the d axis voltage v_{ds}^r are also shown in Fig. 8.13-3. The torque-versus-speed characteristics for this free acceleration are shown in Fig. 8.13-4. The dynamic performance of this system during load-torque switching is shown in Fig. 8.13-5. As in Fig. 8.7-3, the inertia is 40% of that used in Figs. 8.13-3 and 8.13-4, and the load torque is switched from $0.1\,\mathrm{N\cdot m}$ to $0.4\,\mathrm{N\cdot m}$ and then back to $0.1\,\mathrm{N\cdot m}$. Note that T_L for the three-phase machine is $\frac{2}{3}$ times that of the two-phase machine. The steady-state and dynamic characteristics of the brushless dc motor driven from a continuous-current inverter are quite

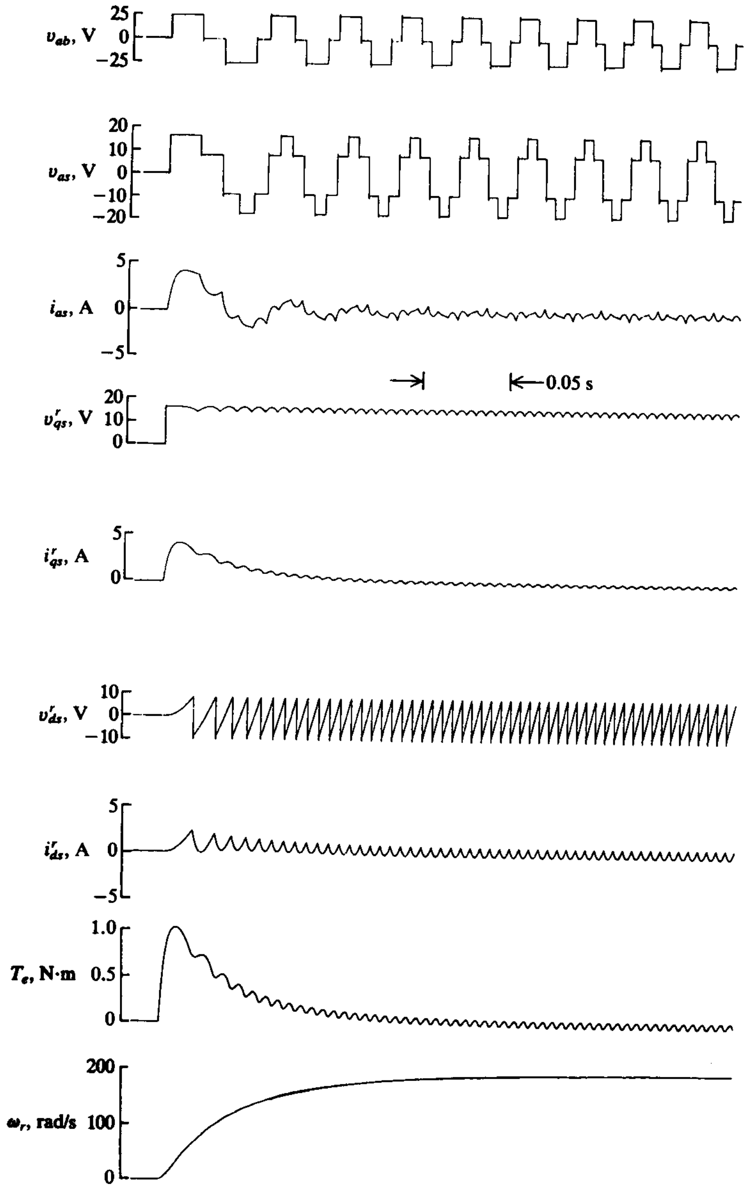

Figure 8.13-3: Free-acceleration characteristics of a three-phase brushless dc motor supplied by a six-step inverter; compare to Fig. 8.7-1.

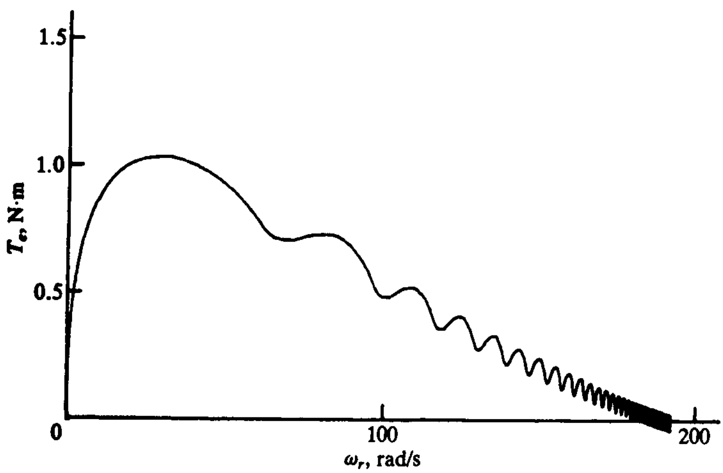

Figure 8.13-4: Torque-speed characteristics for free acceleration shown in Fig. 8.13-3; compare to Fig. 8.7-2.

similar to those when two-phase sinusoidal voltages are applied to the two-phase machine.

Let us take a little closer look at the voltage and current waveforms of the continuous-current inverter. For this purpose, it is sufficient to consider only v_{as} and i_{as}. The voltage v_{as} is given by (8.13-5), wherein v_{ap} is equal to v_i when $T1$ is on and $T4$ is off, and zero when $T4$ is on and $T1$ is off. A similar situation exists for v_{bp} with regard to the states of $T2$ and $T5$ and for v_{cp} with regard to $T3$ and $T6$. A plot of v_{as} as given by (8.13-5) for the switching logic given in Fig. 8.13-2 is shown in Fig. 8.13-6. Plotted below v_{as} in this figure is i_{as}. This waveform of i_{as} was taken from Fig. 8.13-5 with $T_L = 0.4\,\mathrm{N\cdot m}$. Plotted directly below i_{as} are the components of i_{as} that flow in $T1$, i_{aT1}; in $D1$, i_{aD1}; in $T4$, i_{aT4}; and in $D4$, i_{aD4}. $D1$ and $D4$ are the diodes in parallel with $T1$ and $T4$, respectively.

We have one more thing left to do. With $\phi_v = 0$, v_{qs}^r can be approximated as $2v_i/\pi$ for a continuous-current inverter. To show this, let us assume that time zero is selected in Fig. 8.13-6 at the center of the maximum value of v_{as} and let us also assume that $\theta_r(0)$ is zero. Here, $\phi_v = 0$ since this selection of time zero will make $\theta_{esv}(0)$ of the fundamental component of v_{as} equal to zero. We can express v_{as} by Fourier series expansion as

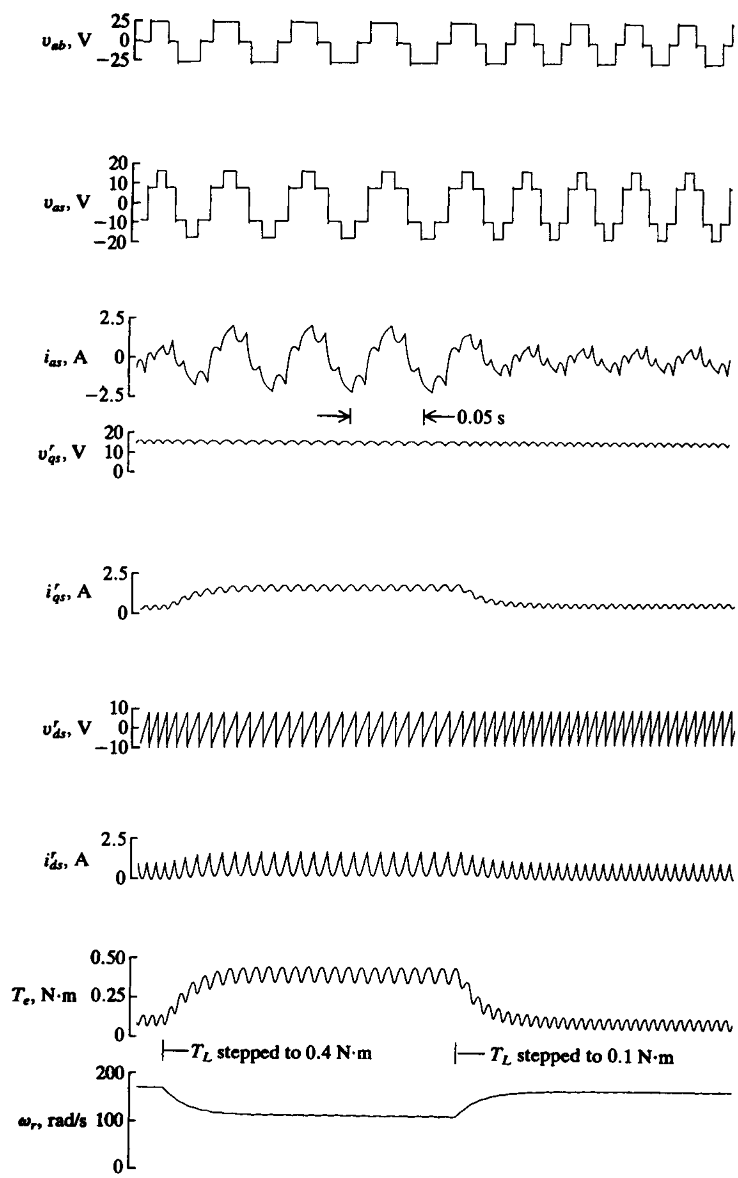

Figure 8.13-5: Dynamic performance during step changes in load torque of a three-phase, brushless dc motor supplied by an inverter; compare with Fig. 8.7-3.

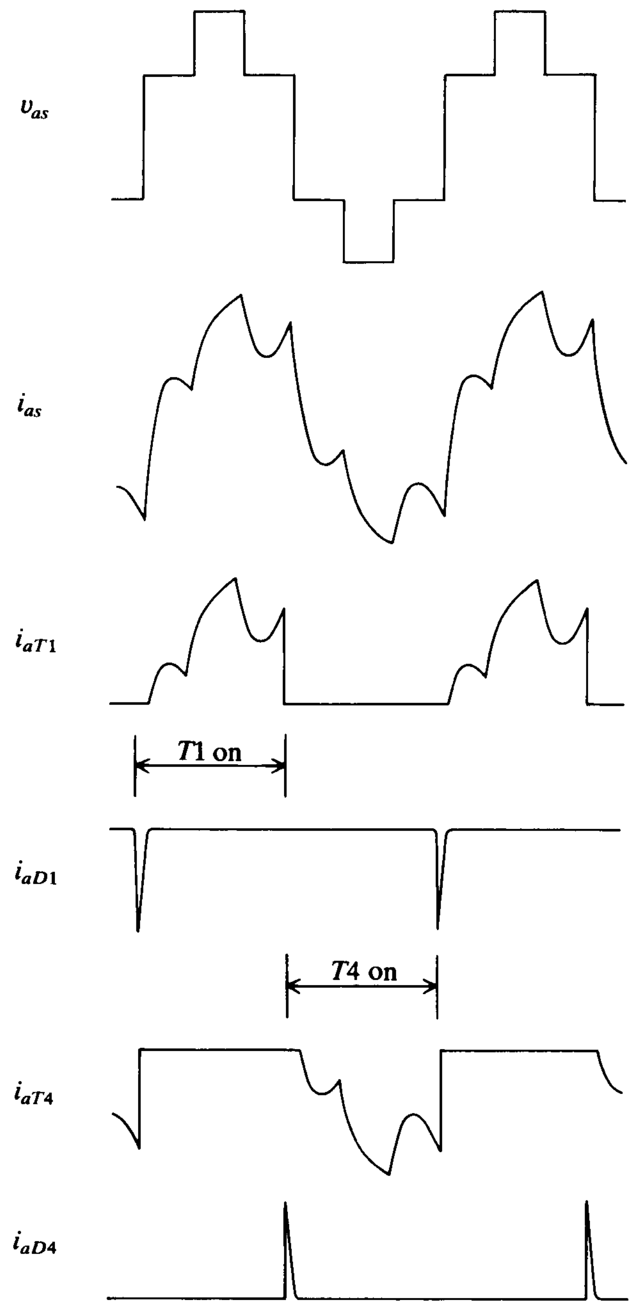

Figure 8.13-6: Plots of v_{as} and i_{as} and the components of i_{as}.

$$v_{as} = \frac{2v_i}{\pi}(\cos\omega_r t + \frac{1}{5}\cos 5\omega_r t - \frac{1}{7}\cos 7\omega_r t + \cdots) \tag{8.13-8}$$

(You are asked to prove this in a problem at the end of the chapter.) The voltages v_{bs} and v_{cs} may be expressed by substituting $\omega_r t - \frac{2}{3}\pi$ and $\omega_r t + \frac{2}{3}\pi$, respectively, for $\omega_r t$ in (8.13-8). If now v_{as}, v_{bs}, and v_{cs} are substituted into the equation of transformation, (8.12-15), we obtain

$$v_{qs}^r = \frac{2v_i}{\pi}(1 + \frac{2}{35}\cos 6\omega_r t - \frac{2}{143}\cos 12\omega_r t + \cdots) \tag{8.13-9}$$

$$v_{ds}^r = \frac{2v_i}{\pi}(\frac{12}{35}\sin 6\omega_r t - \frac{24}{143}\sin 12\omega_r t + \cdots) \tag{8.13-10}$$

We see from (8.13-9) and (8.13-10) that if we neglect the harmonics, v_{qs}^r becomes $2v_i/\pi$ and v_{ds}^r becomes zero. Take a minute to go back and look at the plots of v_{qs}^r and v_{ds}^r in Figs. 8.13-3 and 8.13-5. Is the average value of $v_{qs}^r = 2v_i/\pi$ and is the average value of $v_{ds}^r = 0$? Is the dominant harmonic the sixth harmonic?

Although we are not going to go through the details, it can be shown [1] that, with the provision for phase shifting incorporated, v_{as} may be expressed as

$$v_{as} = \frac{2v_i}{\pi}[\cos(\omega_r t + \phi_v) + \frac{1}{5}\cos 5(\omega_r t + \phi_v) - \frac{1}{7}\cos 7(\omega_r t + \phi_v) + \cdots] \tag{8.13-11}$$

If the harmonics are neglected, v_{qs}^r and v_{ds}^r become

$$v_{qs}^r = \frac{2v_1}{\pi}\cos\phi_v \tag{8.13-12}$$

$$v_{ds}^r = -\frac{2v_i}{\pi}\sin\phi_v \tag{8.13-13}$$

By now we are well aware that the brushless dc motor operates much the same as a dc shunt motor with constant field current or a permanent-magnet dc motor. Speed control can be achieved for both devices by varying the amplitude of the applied voltage. Consider, for a moment, the expression for steady-state electromagnetic torque of a brushless dc motor given in Table 8.6-1. If we neglect the $\omega_r^2 L_{ss}^2$ term in the denominator, the torque is proportional to the difference between V_{qs}^r and $\omega_r \lambda_m'^r$. The voltage V_{qs}^r is directly related to the dc voltage of the inverter, (8.13-8). Hence, the control of rotor speed can be accomplished by changing v_{qs}^r so that load torque requirements, within the capability of the machine, may be satisfied while maintaining a constant rotor speed. Clearly, v_{qs}^r may be changed by changing the inverter dc voltage v_i, which can be done if the inverter voltage is supplied from a phase-controlled rectifier, for example. In most cases, however, the inverter voltage is supplied from a constant source such as a battery. In this case, voltage control and, thus, speed control are achieved by pulse-width modulation (PWM) of the inverter.

Although pulse-width modulation may be incorporated into the inverters considered in the previous section, it is sufficient to consider only one phase to explain this technique. For this purpose, the operation of the continuous-current inverter with pulse-width modulation incorporated is shown in Fig. 8.13-7. Therein, i_i, v_{as}, and i_{as} are plotted. The current i_i is the current flowing into the inverter from the dc source. In a PWM system, all three of the applied stator phase voltages (v_{bs} and v_{cs} not shown) are simultaneously switched to zero. The effective value of the phase voltages is controlled by setting the time the voltages are held at zero. The zero-voltage mode is achieved by instantaneously connecting all three phases of the machine to the same side of the dc source by appropriate switching of the transistors. During normal operation of the inverter, two phases of the machine are connected to one terminal of the dc source while the third is connected to the other terminal. With all three phases connected to the same side of the dc source, the stator phases of the electric machine are short-circuited and the inverter current i_i is zero since the machine is effectively disconnected from the inverter.

The method of pulse-width modulation depicted in Fig. 8.13-7 is one wherein the on and off times of the transistors are equal. Hence, to change the effective value of the stator phase voltages, it is necessary to change the rate or frequency of the pulse-width modulation. Another common method is to maintain the frequency of the pulse-width modulation constant, generally at a high frequency, and the effective value of the stator voltages is controlled by controlling the time that the phase voltages are held at zero during one cycle of the pulse-width modulating frequency. There are many other aspects of pulse-width modulation and speed control that are very important and interesting but well beyond the scope of this text.

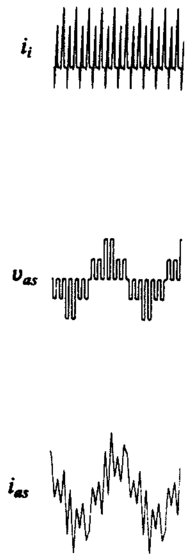

Figure 8.13-7: Pulse-width modulation of an inverter.

SP8.13-1 Express v_{ab} with v_{as}, as given by (8.13-8). $\{v_{ab} = \sqrt{3}\, 2v_i/\pi[\cos(\omega_r t + 30°) + \frac{1}{5}\cos(5\omega_r t + 30°) - \frac{1}{7}\cos(7\omega_r t + 30°) + \cdots]\}$
SP8.13-2 Express v_{as} with $i_{as} = 0$ and i_{bs} and i_{cs} nonzero. $[v_{as} = \omega_r \lambda_m'^r \cos\theta_r]$

8.14 RECAPPING

We have been able to analyze the permanent-magnet ac machine, including its operation as a brushless dc machine, from a very simplified point of view. Although this simplified analysis has limitations, it provides an excellent means of portraying the salient features of all operating modes of the voltage-controlled, permanent-magnet ac machine.

There is little doubt that the controlled permanent-magnet ac machine will be used in an ever-broadening range of applications. In fact, it will replace the permanent-magnet dc machine and the two-phase servomotor (induction motor) in many of their present-day applications. Although one reason for replacing the dc machine is that it does away with the brushes, we can see from the simplified analysis presented in this chapter that the voltage-controlled permanent-magnet ac machine has a much broader range of operating modes than does a dc motor. We will revisit the permanent-magnet ac machine when we study stepper motors in Chapter 9. As a stepper motor, the permanent-magnet ac machine is used widely as the positioning device in position-control systems.

8.15 REFERENCES

[1] P. C. Krause, O. Wasynczuk, and S. D. Sudhoff, *Analysis of Electric Machinery and Drive Systems*, 2^{nd} Edition, IEEE Press, 2002.

[2] R. H. Park, "Two-Reaction Theory of Synchronous Machines – Generalized Method of Analysis – Part I," *AIEE Trans.*, Vol. 48, July 1929, pp. 716-727.

[3] B. C. Kuo, *Automatic Control Systems,* Prentice-Hall Inc., Englewood Cliffs, N.J., 1987.

[4] W. L. Soong and T. J. E. Miller, "Field-Weakening Performance of Brushless Synchronous AC Motor Drives," *IEEE Proceedings Electric Power Application*, Vol, 141, No. 6, Nov. 1994.

8.16 PROBLEMS

1. It is found that $\lambda_m' = 0.1\,\mathrm{V\cdot s}$ for a permanent-magnet, six-pole, two-phase ac machine. Calculate the amplitude (peak value) of the open-circuit phase voltage measured when the rotor is turned at 60 revolutions per second (r/s).

2. Starting with (8.5-3), obtain (8.5-5).

3. Derive (8.5-17) from (8.4-2). (Hint: express i_{qs}^r in terms of i_{as} and i_{bs}.)

4. In the analysis of the brushless dc motor, we have selected $\theta_r(0) = 0$, where $\sqrt{2}\,\tilde{F}_{as} = F_{qs}^r - jF_{ds}^r$. Express the relationship between these same variables if we had selected $\theta_r(0) = \frac{1}{2}\pi$.

5. Refer to Example 8B. Verify (8B-7) and construct the phasor diagram showing $\tilde{V}_{as}$, $\tilde{E}_a$, $r_s\tilde{I}_{as}$, $j\omega_r L_{ss}\tilde{I}_{as}$, and $\tilde{I}_{as}$.

6. A four-pole, two-phase, permanent-magnet ac machine is driven by a mechanical source at $\omega_{rm} = 3600$ r/min. The open-circuit voltage across one of the phases is 50 V (rms). (a) Calculate λ'_m. The mechanical source is removed and the following voltages are applied: $V_{as} = \sqrt{2}\,25\cos\theta_r$; $V_{bs} = \sqrt{2}\,25\sin\theta_r$, where $\theta_r = \omega_r t$. (b) Neglect friction ($B_m = 0$) and calculate the no-load rotor speed ω_r in rad/s.

7. Consider the permanent-magnet ac machine motor described in Example 8C. Calculate the (a) steady-state starting torque by assuming $v^r_{ds} = 0$ and (b) steady-state no-load speed in r/min.

8. The parameters of a two-pole, two-phase permanent-magnet ac machine are as follows: $r_s = 2\,\Omega$, $\lambda'^r_m = 0.0707$ V · s/rad, $L_{ls} = 1$ mH, and $L_{ms} = 9$ mH. The applied voltages are $V_{as} = \sqrt{2}\,20\cos\theta_r$ and $V_{bs} = \sqrt{2}\,20\sin\theta_r$, where $\theta_r = 200t$. (a) Calculate the steady-state electromagnetic torque T_e. (b) Determine I_{as}.

* 9. For the two values of ϕ_v determined in Example 8D, calculate (a) $\tilde{I}_{as}$ and (b) the steady-state starting torque.

10. Consider the permanent-magnet ac machine described in Prob. 8. Assume that the applied stator voltages are $V_{as} = \sqrt{2}\,20\cos(\omega_r t + \phi_{vMT})$ and $V_{bs} = \sqrt{2}\,20\sin(\omega_r t + \phi_{vMT})$. Calculate $\tilde{V}_{as}$, $\tilde{I}_{as}$, and T_e when $\omega_r = 200$ rad/s.

11. Speed control is to be achieved by voltage control with $\phi_v = 0$. Consider Example 8D, where the load is removed and the speed of $\omega_r = 40\pi$ rad/s is to be maintained. Calculate V_s necessary to achieve this and the no-load current $\tilde{I}_{as}$.

12. Calculate ω_r, $\tilde{E}_a$, and $\tilde{I}_{as}$ and construct the phasor diagram showing $\tilde{V}_{as}$, $\tilde{E}_a$, $r_s\tilde{I}_{as}$, $j\omega_r L_{ss}\tilde{I}_{as}$, and $\tilde{I}_{as}$ for the load conditions portrayed in Fig. 8.7-3. Neglect $\omega_r^2 L_{ss}^2$ in these calculations.

13. For the load conditions given in Fig. 8.7-3, determine ω_r without neglecting $\omega_r^2 L_{ss}^2$. Compare with the values of ω_r calculated in Prob. 12.

14. In Fig. 8.9-1, the constant-torque region was maintained from stall to rated ω_r. Consider the permanent-magnet ac machine with the parameters given in Example 8A. Calculate the maximum ω_r that rated T_e can be maintained before $V_s = 11.25$ V is exceeded.

15. Refer to Prob. 14. Determine the minimum ω_r that can be achieved in the constant-power mode.

16. Draw the time-domain block diagram of a permanent-magnet ac machine with provisions to shift the phase. Use ϕ_v as an input. Do not neglect i_{ds}^r.

17. Derive (8.10-14) and (8.10-15).

18. Draw the time-domain block diagram with $\phi_v = 0$ and i_{ds}^r not neglected.

19. Write the state equations for Prob. 18.

20. Plot v_{as}, v_{bs}, v_{cs}, v_{ab}, and v_{np} for the 180° continuous-current inverter for $0 < \theta_r < 2\pi$ with the transistor switching shown in Fig. 8.13-2. Assume the inverter voltage v_i is constant.

*21. Derive (8.13-9) and (8.13-10).

Chapter 9

STEPPER MOTORS

9.1 INTRODUCTION

Stepper motors are electromechanical motion devices that are used primarily to convert information in digital form to mechanical motion. Although stepper motors were used as early as the 1920s, their use has skyrocketed with the advent of the digital computer. Whenever stepping from one position to another is required, whether the application is industrial, military, or medical, the stepper motor is often the motor of choice. Stepper motors come in various sizes and shapes but most fall into two types – the variable-reluctance stepper motor and the permanent-magnet stepper motor. Both types are considered in this chapter. We shall find that the operating principle of the variable-reluctance stepper motor is much the same as that of the reluctance machine that we have already discussed in earlier chapters, and the permanent-magnet stepper motor is similar in principle to the permanent-magnet synchronous machine.

9.2 BASIC CONFIGURATIONS OF MULTISTACK VARIABLE-RELUCTANCE STEPPER MOTORS

There are two general types of variable-reluctance stepper motors: single-stack and multistack. As a first approximation, the behavior of both types may be described from similar equations. Actually, the principle of operation of variable-reluctance stepper motors is the same as the reluctance machine that we considered in earlier chapters; only the mode of operation differs. There are, however, some new terms to define, and it is necessary for us to extend some of our previous definitions to fit the stepper motor. First, we will look at the multistack device in some detail, followed by a brief discussion of the single-stack, variable-reluctance stepper motor.

In its most basic form, the multistack variable-reluctance stepper motor consists of three or more single-phase reluctance motors on a common shaft with their stator magnetic axes displaced from each other. The rotor of an elementary three-stack device is shown in Fig. 9.2-1. It has three cascaded two-pole rotors with a minimum-reluctance path of each aligned at the angular displacement θ_{rm}. In stepper motor language, each of the two-pole rotors is said to have two teeth. Now, visualize that each of these rotors has its own, separate, single-phase stator with the magnetic axes of the stators displaced from each other. In Fig. 9.2-1 we have labeled the individual rotors *a, b,* and *c*. The corresponding stators are shown in Fig. 9.2-2; the stator with the *as* winding is associated with the *a* rotor, the *bs* winding with the *b* rotor, and so on. There are several things to note. First, we see that each of the single-phase stators has two poles, much the same in configuration as the dc machine, with the stator winding wound around both poles. In particular, positive current flows into as_1 and out as_1'; as_1' is connected to as_2 so that positive current flows into as_2 and out as_2'. Although we have shown only one circle for as_1,...,as_2', we realize that each would represent several turns, and that the number of turns from $as_1$to as_1' (indicated by $N_s/2$ in Fig. 9.2-2) is the same as from as_2 to as_2'. Let us note one more thing. Heretofore, we have referenced θ_{rm} (or θ_r) from the *as* axis to the maximum-reluctance path of a salient-pole rotor (Figs. 4.6-1, 4.6-4, and 7.2-1, for example). In Fig. 9.2-2, θ_{rm} is referenced to the minimum-reluctance path of the rotor. Since this is more or less standard in stepper motor analysis, we will deviate from the convention we have established for reluctance and synchronous machines.

Each stack is often called a phase. In other words, a three-stack machine is a three-phase machine. This nomenclature can be misleading since we generally think of a three-phase ac device when we hear the words three-phase machine. We will find that a stepper motor is a discrete device, operated by switching a dc voltage from one stator winding to the other. Although more than three stacks (phases) may be used, perhaps as many as seven, three-stack variable-reluctance stepper motors are quite common. Our previous meaning of phase must be modified to accommodate the stepper motor.

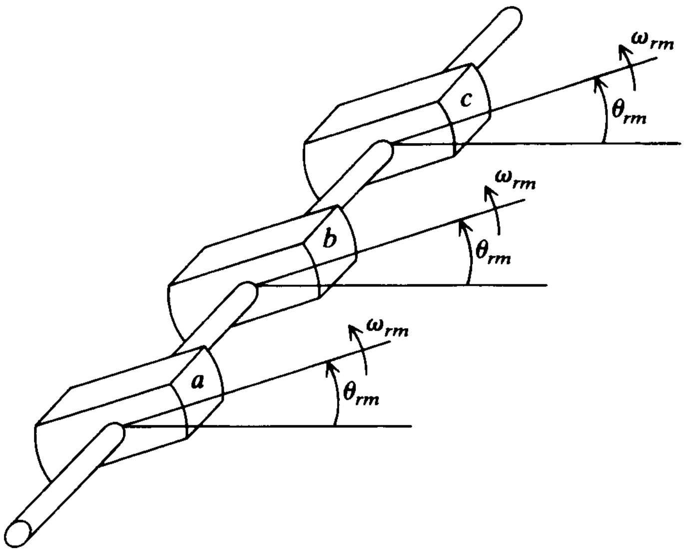

Figure 9.2-1: Rotor of an elementary two-pole, three-stack, variable-reluctance stepper motor.

Before writing any equations, let us see if we can gain some insight in regard to the operation of this device. To start, let the *bs* and *cs* windings in Fig. 9.2-2 be open-circuited, and let us apply a dc voltage to the *as* winding, whereupon we will assume that a constant i_{as} is immediately established. Now, since the magnetic systems of the three single-phase stators are separate, flux set up by one winding does not link the other windings. Hence, with only the *as* winding energized, flux exists only in the *as* axis. We know from our work back in Chapter 2 that the minimum-reluctance path of the *a* part of the rotor (see Fig. 9.2-2) will align with the *as* axis. That is, at equilibrium with zero load torque, θ_{rm}, in all parts of Fig. 9.2-2 is the same: either zero or 180°. Let us say it is zero to make our discussion easier. (What would the rotor do if we could instantaneously reverse the direction of i_{as}?)

Stepper motors are used to convert digital or discrete information into a change in angular position. Let us see how positioning (stepping) is achieved. For this, let us instantaneously deenergize the *as* winding and immediately establish a direct current in the *bs* winding. The minimum reluctance path of the rotor will align itself with the *bs* axis. To do this, the rotor would rotate

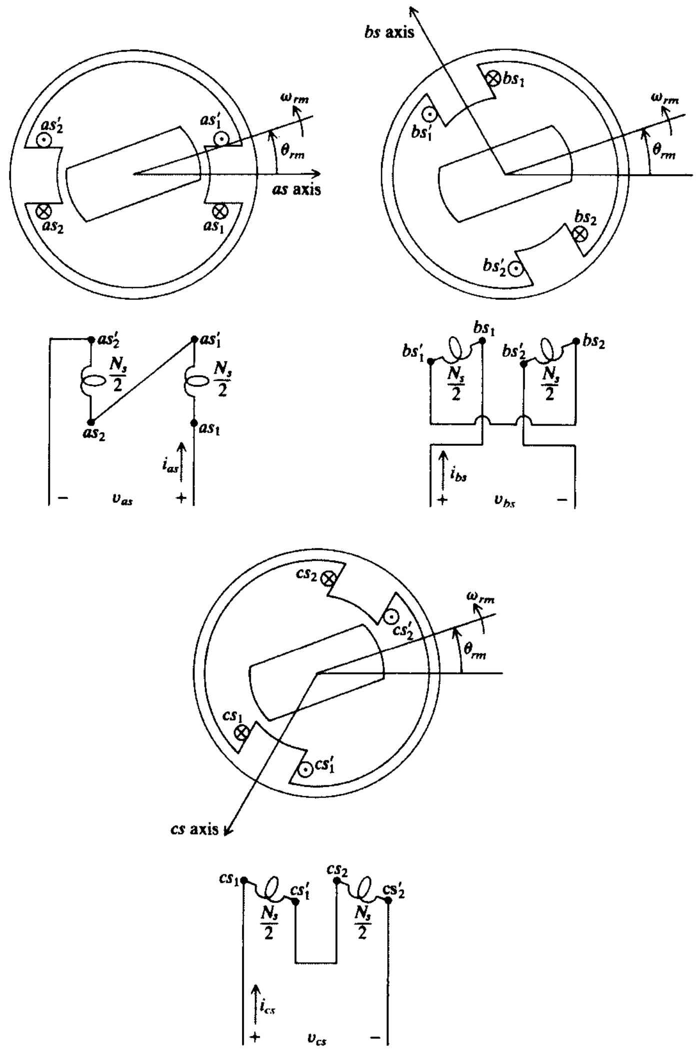

Figure 9.2-2: Stator configuration for an elementary two-pole, three-stack, variable-reluctance stepper motor.

clockwise from $\theta_{rm} = 0$ to $\theta_{rm} = -60°$. Note that by advancing the mmf from the positive *as* axis to the positive *bs* axis, 120° counterclockwise, we have caused a 60° clockwise rotation of the rotor. There must be something wrong here. We recall from our work with rotating magnetic fields in Chapter 4 that, with the magnetic axes as shown in Fig. 9.2-2, an *abc* sequence of balanced sinusoidal currents will yield operation at synchronous speed with the rotor rotating counterclockwise. Therefore, it would seem that rotating the air-gap mmf from the positive *as* axis to the positive *bs* axis would cause rotation in the counterclockwise direction. In the case of variable-reluctance stepper motors, we will find that the direction of stepping can be either in the same or opposite direction of the rotation of the air-gap mmf depending upon the number of phases (stacks), the number of poles created by the stator windings, and the number of rotor teeth.

If, instead of energizing the *bs* winding, we energize the *cs* winding in Fig. 9.2-2, the rotor would have stepped counterclockwise from $\theta_{rm} = 0$ to $\theta_{rm} = 60°$. Thus, applying a dc voltage separately in the sequences *as, bs, cs, as, ...* produces 60° steps in the clockwise direction, whereas the sequence *as, cs, bs, as, ...* produces 60° steps in the counterclockwise direction. We need at least three stacks to achieve rotation (stepping) in both directions.

Before defining some stepper motor terms, let us think of one more thing. What if we energized the *as* and *bs* windings with the same current? That is, assume that initially the *as* winding is energized with $\theta_{rm} = 0$ and the *bs* winding is energized without deenergizing the *as* winding. What happens? Well, the rotor rotates clockwise from $\theta_{rm} = 0$ to $\theta_{rm} = -30°$. We have reduced our step length by one half. This is referred to as *half-step operation.*

It is time to define terms. Let RT denote the number of rotor teeth per stack and ST the number of stator teeth per stack. The elementary device shown in Figs. 9.2-1 and 9.2-2 has two poles, two rotor teeth, and two stator teeth per stack; thus, $RT = ST = 2$. In fact, RT (rotor teeth per stack) always equals ST (stator teeth per stack) in a multistack variable-reluctance stepper motor. The number of stacks (phases) is denoted as N; here $N = 3$. Now, the tooth pitch, which we will denote as TP, is the angular displacement between rotor teeth. In this case, $TP = 180°$. We can write

$$TP = \frac{2\pi}{RT} \tag{9.2-1}$$

We have one more term to define: the step length, denoted as SL. It is the angular rotation of the rotor as we change the excitation (dc voltage) from one phase to the other. In this case, the step length is 60°, $SL = 60°$. If we energize each stack separately, then going from as to bs to cs back to as causes the rotor to rotate one tooth pitch. In other words, the number of stacks (phases) times the step length is a tooth pitch. That is,

$$TP = N\,SL \tag{9.2-2}$$

We can substitute (9.2-1) into (9.2-2) and obtain

$$SL = \frac{TP}{N} = \frac{2\pi}{RT\,N} \tag{9.2-3}$$

We shall find use for all of these new terms as we go along.

Although the elementary device shown in Figs. 9.2-1 and 9.2-2 offers a good starting point in our analysis of stepper motors, it has limited application owing to its large step length. Let us consider the four-pole, three-stack, variable-reluctance stepper motor with four rotor teeth, as illustrated in Fig. 9.2-3. Here, $RT = 4$ and $N = 3$; therefore, from (9.2-1) the tooth pitch is $TP = 2\pi/RT = 90°$. From (9.2-2), the step length is $SL = TP/N = 30°$ and an as, bs, cs, as, ... sequence produces 30° steps in the clockwise direction.

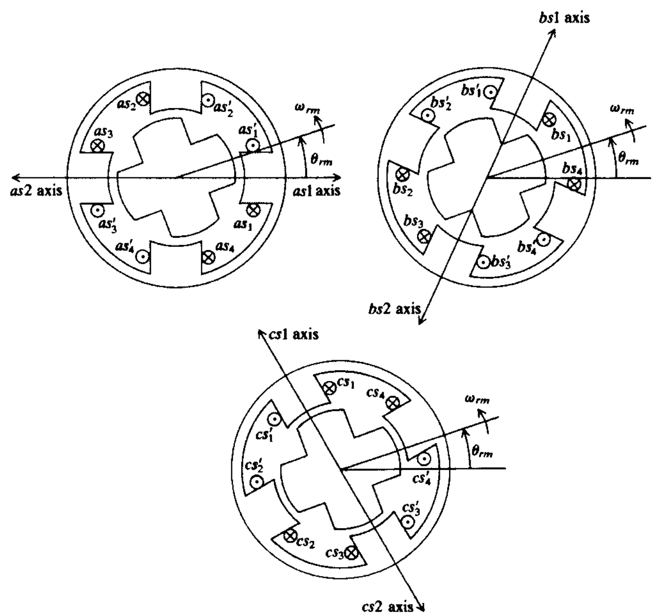

Figure 9.2-3: Four-pole, three-stack, variable-reluctance stepper motor with four rotor teeth.

The device shown in Fig. 9.2-4 is a four-pole, three-stack variable-reluctance stepper motor with eight rotor teeth. In this case, $RT = 8$ and $N = 3$, thus, $TP = 45°$ and $SL = 15°$. However, in this device an *as, bs, cs, as,...* sequence produces 15° steps in the counterclockwise direction. The pattern is clear; by increasing the number of rotor teeth we reduce the step length. The step lengths of multistack variable-relucance stepping motors typically range from 2 to 15°.

There appears to be an inconsistency in Fig. 9.2-4. In particular, θ_{rm} is referenced from the *as* axis to a position between rotor teeth. Earlier in this section, we established that, in the case of stepper motors, we would reference θ_{rm} from the *as* axis to the minimum-reluctance path of the rotor, whereupon the reluctance of the magnetic system associated with the *as* winding would be minimum when $\theta_{rm} = 0$. At first glance it appears that we have violated this stepper motor convention. However, when θ_{rm} is zero in Fig. 9.2-4, the reluctance of the magnetic system associated with the *as* winding is minimum. Hence, we must reference θ_{rm} from a position between rotor teeth

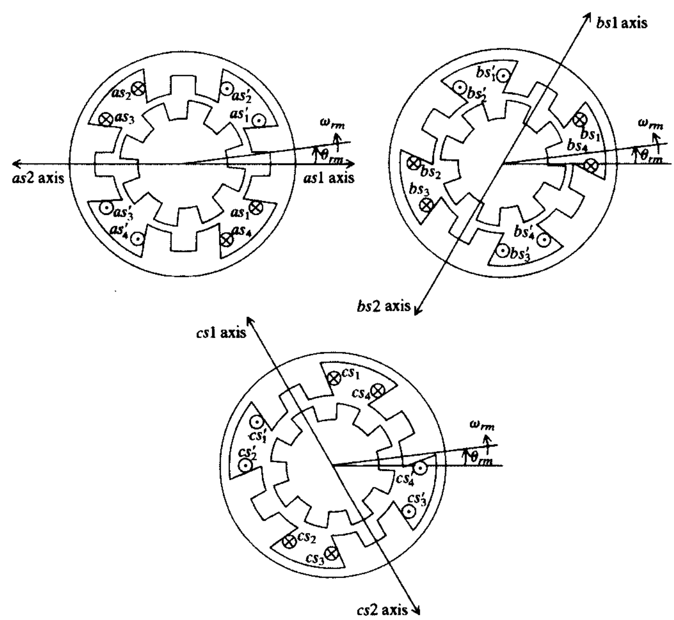

Figure 9.2-4: Four-pole, three-stack, variable-reluctance stepper motor with eight rotor teeth.

to maintain the convention that we established earlier in this section. A cutaway view of a four-pole, three-stack variable-reluctance stepper motor with 16 rotor teeth is shown in Fig. 9.2-5.

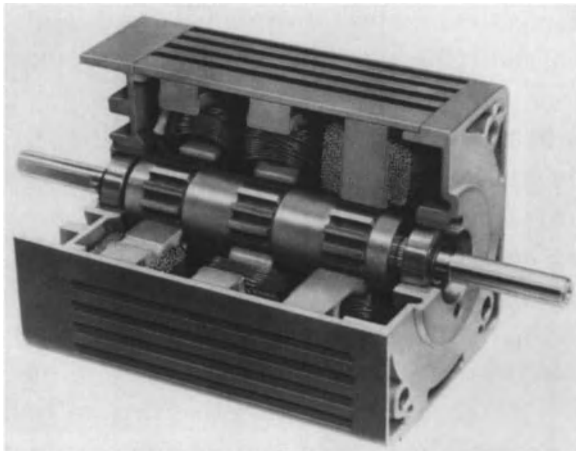

Figure 9.2-5: Cutaway view of four-pole, three-stack, variable-relucance stepper motor with sixteen rotor teeth. (Courtesy of Warner Electric.)

SP9.2-1 Calculate the step length for an eight-pole, three-stack, variable-reluctance stepper motor with 16 rotor teeth. [$SL = 7.5°$]

SP9.2-2 Consider the two-pole, two-phase reluctance motor shown in Fig. 4.6-1*b*. Calculate (*a*) *TP*, (*b*) *SL*, and (*c*) determine the direction of rotation when a dc voltage is switched from the *as* winding to the *bs* winding. [(*a*) $TP = 180°$; (*b*) $SL = 90°$; (*c*) either ccw or cw]

9.3 EQUATIONS FOR MULTISTACK VARIABLE-RELUCTANCE STEPPER MOTORS

The voltage equations for a three-stack, variable-reluctance stepper motor may be written as

$$v_{as} = r_s i_{as} + \frac{d\lambda_{as}}{dt} \tag{9.3-1}$$

$$v_{bs} = r_s i_{bs} + \frac{d\lambda_{bs}}{dt} \tag{9.3-2}$$

$$v_{cs} = r_s i_{cs} + \frac{d\lambda_{cs}}{dt} \tag{9.3-3}$$

In matrix form,

$$\mathbf{v}_{abcs} = \mathbf{r}_s \mathbf{i}_{abcs} + p\boldsymbol{\lambda}_{abcs} \tag{9.3-4}$$

where p is the operator d/dt and, for voltages, currents, and flux linkages

$$(\mathbf{f}_{abcs})^T = [f_{as} \quad f_{bs} \quad f_{cs}] \tag{9.3-5}$$

with

$$\mathbf{r}_s = \begin{bmatrix} r_s & 0 & 0 \\ 0 & r_s & 0 \\ 0 & 0 & r_s \end{bmatrix} \tag{9.3-6}$$

Since magnetic coupling does not exist between phases, we can write the flux linkages as

$$\begin{bmatrix} \lambda_{as} \\ \lambda_{bs} \\ \lambda_{cs} \end{bmatrix} = \begin{bmatrix} L_{asas} & 0 & 0 \\ 0 & L_{bsbs} & 0 \\ 0 & 0 & L_{cscs} \end{bmatrix} \begin{bmatrix} i_{as} \\ i_{bs} \\ i_{cs} \end{bmatrix} \tag{9.3-7}$$

For the purpose of expressing the self-inductances L_{asas}, L_{bsbs}, and L_{cscs}, let us first consider the elementary two-pole device illustrated in Fig. 9.2-2. With our work from Chapter 1, we can write as a first approximation,

$$L_{asas} = L_{ls} + L_A + L_B \cos 2\theta_{rm} \tag{9.3-8}$$

$$L_{bsbs} = L_{ls} + L_A + L_B \cos 2(\theta_{rm} - \tfrac{2}{3}\pi) \tag{9.3-9}$$

$$L_{cscs} = L_{ls} + L_A + L_B \cos 2(\theta_{rm} - \tfrac{4}{3}\pi) \tag{9.3-10}$$

From our previous work, we are aware that L_{ls} is the leakage inductance, whereas L_A and L_B are constants with $L_A > L_B$. For constant rotor speed, the rotor displacement can be expressed as

$$\theta_{rm} = \omega_{rm} t + \theta_{rm}(0) \tag{9.3-11}$$

We will use θ_{rm}, the actual rotor displacement, rather than θ_r, the electrical angular displacement. Although θ_{rm} and θ_r are related, $\theta_r = (P/2)\theta_{rm}$, where P is the number of poles, we will find it more convenient to use θ_{rm} in the analysis of stepper motors. We see that (9.3-8) is similar to (1.7-29) or (2.7-3), with θ_{rm} referenced to the minimum reluctance path of the rotor. Equation (9.3-9) is easily developed once we realize that the self-inductance of the bs winding is the same as that of the as winding. However, since θ_{rm} is referenced from the as axis, the angular displacement to the bs axis from the as axis must be subtracted from θ_{rm} so that, when $\theta_{rm} = \frac{2}{3}\pi$, the argument of (9.3-9) is zero and (9.3-9) with $\theta_{rm} = \frac{2}{3}\pi$ becomes the same as (9.3-8) with $\theta_{rm} = 0$. Following this same line of reasoning, we would determine that the angular displacement of (9.3-10) is $-\frac{4}{3}\pi$. However, since $\cos 2(\theta_{rm} - \frac{4}{3}\pi) = \cos 2(\theta_{rm} + \frac{2}{3}\pi)$, we can use $\frac{2}{3}\pi$ as the angular displacement for L_{cscs}. It is obvious that we can express (9.3-8) through (9.3-10) in various forms. By adding the appropriate multiple of 2π from the arguments in (9.3-8) through (9.3-10), we can also express the inductances as

$$L_{asas} = L_{ls} + L_A + L_B \cos 2\theta_{rm} \tag{9.3-12}$$

$$L_{bsbs} = L_{ls} + L_A + L_B \cos 2(\theta_{rm} + \tfrac{1}{3}\pi) \tag{9.3-13}$$

$$L_{cscs} = L_{ls} + L_A + L_B \cos 2(\theta_{rm} + \tfrac{2}{3}\pi) \tag{9.3-14}$$

The self-inductances of the four-pole, three-stack, variable-reluctance device with four rotor teeth shown in Fig. 9.2-3 can be approximated as

$$L_{asas} = L_{ls} + L_A + L_B \cos 4\theta_{rm} \tag{9.3-15}$$

$$L_{bsbs} = L_{ls} + L_A + L_B \cos 4(\theta_{rm} + \tfrac{1}{6}\pi) \tag{9.3-16}$$

$$L_{cscs} = L_{ls} + L_A + L_B \cos 4(\theta_{rm} + \tfrac{2}{6}\pi) \tag{9.3-17}$$

Although we are using the same L_{ls}, L_A, and L_B to denote constants, we realize that these are not equal for the various machines.

For the four-pole, three-stack, variable-reluctance stepper motor with eight rotor teeth shown in Fig. 9.2-4, we can approximate the self-inductances as

$$L_{asas} = L_{ls} + L_A + L_B \cos 8\theta_{rm} \tag{9.3-18}$$

$$L_{bsbs} = L_{ls} + L_A + L_B \cos 8(\theta_{rm} - \tfrac{1}{12}\pi) \tag{9.3-19}$$

$$L_{cscs} = L_{ls} + L_A + L_B \cos 8(\theta_{rm} - \tfrac{2}{12}\pi) \tag{9.3-20}$$

It may be observed that for the devices shown in Figs. 9.2-2 and 9.2-3, where we have previously noted that a counterclockwise rotation of the stator mmf and stepping are in opposite directions, the inductances may be expressed as

$$L_{asas} = L_{ls} + L_A + L_B \cos(RT\,\theta_{rm}) \tag{9.3-21}$$

$$L_{bsbs} = L_{ls} + L_A + L_B \cos[RT(\theta_{rm} + SL)] \tag{9.3-22}$$

$$L_{cscs} = L_{ls} + L_A + L_B \cos[RT(\theta_{rm} + 2SL)] \tag{9.3-23}$$

For the device shown in Fig. 9.2-4, where rotation of the stator mmf and stepping are in the same direction, the self-inductances may be expressed as

$$L_{asas} = L_{ls} + L_A + L_B \cos(RT\,\theta_{rm}) \tag{9.3-24}$$

$$L_{bsbs} = L_{ls} + L_A + L_B \cos[RT(\theta_{rm} - SL)] \tag{9.3-25}$$

$$L_{cscs} = L_{ls} + L_A + L_B \cos[RT(\theta_{rm} - 2SL)] \tag{9.3-26}$$

For each additional phase (stack), the self-inductance is offset by the appropriate multiple of SL. An expression for the electromagnetic torque may be obtained from Table 2.5-1:

$$T_e = \frac{\partial W_c(\mathbf{i}, \theta_{rm})}{\partial \theta_{rm}} \tag{9.3-27}$$

Since we are assuming a linear magnetic system, the field energy and coenergy are equal. Thus, since the mutual inductances are zero,

$$W_c = \frac{1}{2} L_{asas} i_{as}^2 + \frac{1}{2} L_{bsbs} i_{bs}^2 + \frac{1}{2} L_{cscs} i_{cs}^2 \tag{9.3-28}$$

Substituting the self-inductances given by (9.3-21) through (9.3-23) into (9.3-28) and taking the partial derivative with respect to θ_{rm} yields

$$\begin{aligned} T_e = -\frac{RT}{2} L_B \{ i_{as}^2 \sin(RT\,\theta_{rm}) &+ i_{bs}^2 \sin[RT(\theta_{rm} + SL)] \\ &+ i_{cs}^2 \sin[RT\,(\theta_{rm} + 2SL)] \} \end{aligned} \tag{9.3-29}$$

An alternate form of (9.3-29) using the tooth pitch TP is

$$T_e = -\frac{RT}{2}L_B\left\{i_{as}^2\sin(\frac{2\pi}{TP}\theta_{rm}) + i_{bs}^2\sin\left[\frac{2\pi}{TP}(\theta_{rm}+\frac{TP}{N})\right]\right.$$
$$\left. + i_{cs}^2\sin\left[\frac{2\pi}{TP}(\theta_{rm}+\frac{2TP}{N})\right]\right\} \tag{9.3-30}$$

It is important to note that (9.3-29) and (9.3-30) are written for rotation of the stator mmf and stepping of the rotor in opposite directions. For stepping in the same direction, the sign preceding both SLs in (9.3-29) and both (TP/N)s in (9.3-30) must be changed. Note also that the magnitude of the torque is proportional to the number of rotor teeth RT.

The torque and rotor angular position are related as

$$T_e = J\frac{d^2\theta_{rm}}{dt^2} + B_m\frac{d\theta_{rm}}{dt} + T_L \tag{9.3-31}$$

where J is the total inertia in $\mathrm{kg}\cdot\mathrm{m}^2$and B_m is a damping coefficient associated with the mechanical rotational system in $\mathrm{N}\cdot\mathrm{m}\cdot\mathrm{s}$. The electromagnetic torque T_e is positive in the counterclockwise direction (positive direction of θ_{rm}), whereas the load torque T_L is positive in the clockwise direction.

SP9.3-1 The stator currents of a three-stack, variable-reluctance machine are $i_{as} = I$, $i_{bs} = -1$, and $i_{cs} = 0$. Determine the no-load rotor position. $[\theta_{rm} = \pm TP/6]$

SP9.3-2 Repeat SP9.3-1 with $i_{as} = i_{bs} = i_{cs}$. [T_e is zero for all values of θ_{rm}.]

9.4 OPERATING CHARACTERISTICS OF MULTISTACK VARIABLE-RELUCTANCE STEPPER MOTORS

It is instructive to take a little closer look at the operating characteristics of a multistack variable-reluctance stepper motor from the standpoint of idealized, pseudo-steady-state conditions. For this purpose, let us consider the expression for torque given by (9.3-30) for a three-stack motor with opposite directions of rotation of the stator mmf and stepping. In particular,

$$T_e = -\frac{RT}{2}L_B\left\{i_{as}^2\sin\left(\frac{2\pi}{TP}\theta_{rm}\right) + i_{bs}^2\sin\left[\frac{2\pi}{TP}\left(\theta_{rm}+\frac{TP}{3}\right)\right]\right.$$
$$\left. + i_{cs}^2\sin\left[\frac{2\pi}{TP}\left(\theta_{rm}+\frac{2TP}{3}\right)\right]\right\} \qquad (9.4\text{-}1)$$

In Fig. 9.4-1, the three terms of (9.4-1) are plotted separately for equal, constant (steady-state) currents. Let us assume that there is no load torque, $T_L = 0$, and $i_{as} = I$, whereas i_{bs} and i_{cs} are zero. Only the first term of (9.4-1) is present; that is, only the steady-state torque due to i_{as} exists. The stable steady-state rotor position would be at $\theta_{rm} = 0$ denoted as point 1 on Fig. 9.4-1. Now, let us assume that i_{as} is instantaneously decreased from I to zero while i_{bs} is increased from zero to I. Hence, the steady-state torque plot due to i_{as} would instantaneously disappear from Fig. 9.4-1 and the torque due to i_{bs} would immediately appear. Now, we know that this cannot happen in practice since there would be electrical transients involved, but we are neglecting all transients in this discussion. Since the torque at point 2 is negative, the rotor will rotate in the clockwise direction. We will then proceed along the i_{bs} torque plot until we have reached point 3. Note that we have moved one step length in the clockwise direction. If, instead of energizing the *bs* winding after deenergizing the *as* winding, we energized the *cs* winding, then the torque at point 4 would appear. This is a positive T_e so the rotor will rotate in the counterclockwise direction and we will ride along the torque angle plot to point 5. Please realize that not only are we neglecting the electrical transients in this discussion but we are also neglecting the mechanical transients. Normally, there would be a damped oscillation about the new operating point, in this example, either point 3 or 5.

Half-step operation is depicted in Fig. 9.4-2. To explain this, let us again start at point 1, where $T_L = 0$ and only the *as* winding is energized ($i_{as} = I$). Instantaneously, the *bs* winding is energized and $i_{bs} = I$. Now, both i_{as} and i_{bs} are I and only the *as* + *bs* torque plot, shown in Fig. 9.4-2, exists. Immediately, the torque at point 2 appears and the rotor starts to rotate in the clockwise direction, coming to rest at point 3. The rotor has moved $SL/2$ clockwise.

Stepping action with a load torque is shown in Fig. 9.4-3. Assume that initial operation is at point 1 with $i_{as} = I$ and $i_{bs} = i_{cs} = 0$. Recall that T_e is positive in the counterclockwise direction, whereas T_L is positive in the clockwise direction, and stable operation occurs when $T_e = T_L$. Thus, at

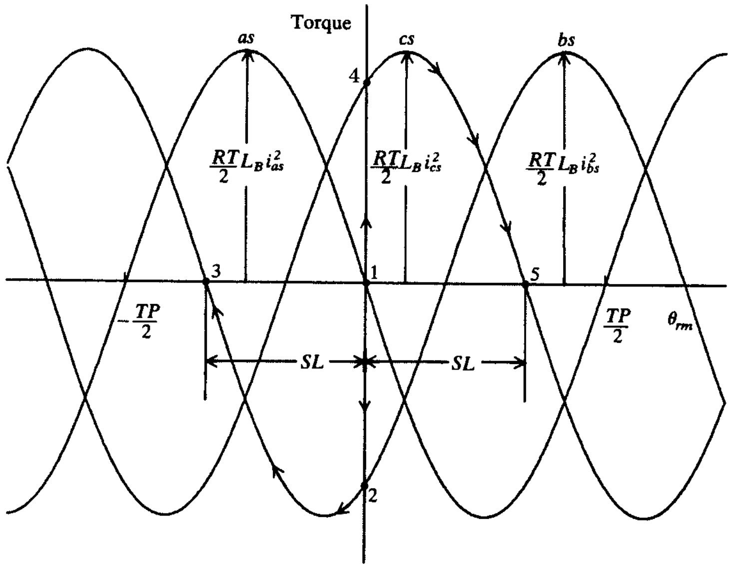

Figure 9.4-1: Stepping operation of a three-stack, variable-relucance stepper motor without load torque – steady-state torque-angle plots.

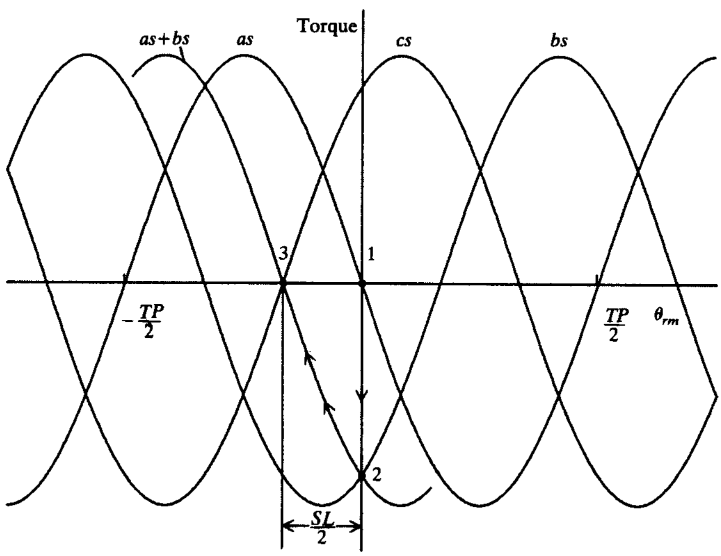

Figure 9.4-2: Half-step operation of a three-stack, variable-reluctance stepper motor – steady-state torque-angle plots.

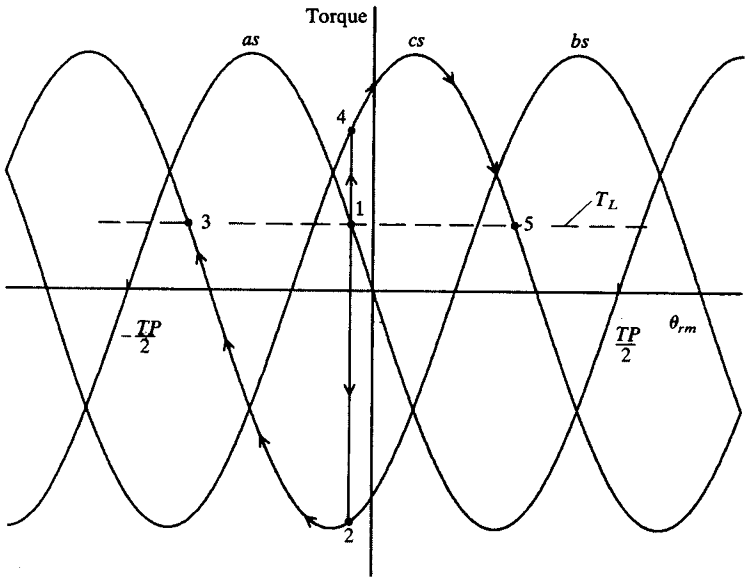

Figure 9.4-3: Stepping operation of a three-stack, variable-reluctance stepper motor with load torque – steady-state torque-angle plots.

point 1, $T_e = T_L$. The *as* winding is deenergized while the *bs* winding is energized. Immediately, the negative T_e at point 2 appears and the rotor will move clockwise to point 3. If the *cs* winding is energized rather than the *bs* winding, the torque at point 4 would appear and the rotor would move to point 5. Note that the step length is still the same in both directions. However, the rotor will move more rapidly in the clockwise direction than in the counterclockwise direction since the load torque is in the clockwise direction. In other words, there is a larger torque to accelerate the rotor in the clockwise direction than in the counterclockwise direction.

The plots of i_{as}, i_{bs}, i_{cs}, and θ_{rm} shown in Fig. 9.4-4 allow us to view stepping operation from another standpoint. Initially, there is no load torque and $i_{as} = I$. The current i_{as} is stepped off and i_{bs} is stepped on. The rotor rotates clockwise to $\theta_{rm} = -SL$. Here we have indicated the presence of a damped mechanical oscillation, which was not shown in the steady-state torque angle plots. Next, i_{bs} is switched off and i_{as} is switched back on. The rotor ends up back at $\theta_{rm} = 0$. Next, we see half-step operation; i_{as} remains at I while i_{bs} is switched to I. The rotor advances to $\frac{1}{2}SL$. When i_{as} is switched to zero, the rotor again advances by $\frac{1}{2}SL$ to $\theta_{rm} = SL$.

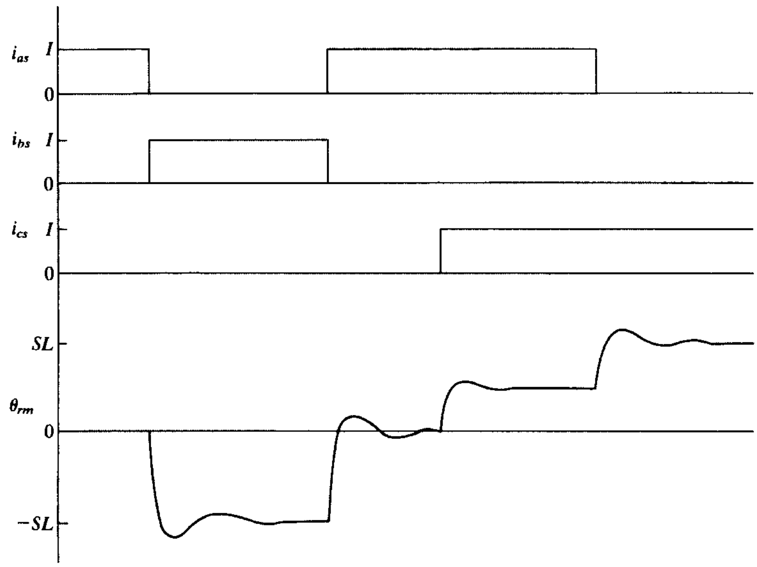

Figure 9.4-4: Stepping operation depicting θ_{rm} versus time – no load torque.

SP9.4-1 In Fig. 9.4-3, the load torque is such that the initial operating point with $i_{as} = I$ and $i_{bs} = i_{cs} = 0$ is at $\theta_{rm} = -TP/8$. The current in the *as* winding is switched to zero and the current in the *cs* winding is switched to I. Determine the final value of θ_{rm}. In which direction will the rotor rotate? [$\theta_{rm} = -TP/8 - 2SL$; cw]

SP9.4-2 It is desirable to step from $\theta_{rm} = 0$ to $\theta_{rm} = -SL/3$ for the device shown in Fig. 9.2-3. Assume that we have the facility to control the winding currents. Let $i_{as} = I$; determine i_{bs}. [i_{bs} =0.81I]

9.5 SINGLE-STACK VARIABLE-RELUCTANCE STEPPER MOTORS

As its name suggests, the single-stack, variable-reluctance stepper motor has only one stack and all stator phases are arranged on this single stack. A three-phase, single-stack, variable-reluctance stepper motor is shown in Fig. 9.5-1. Here, it appears that we have taken the three two-pole, single-phase

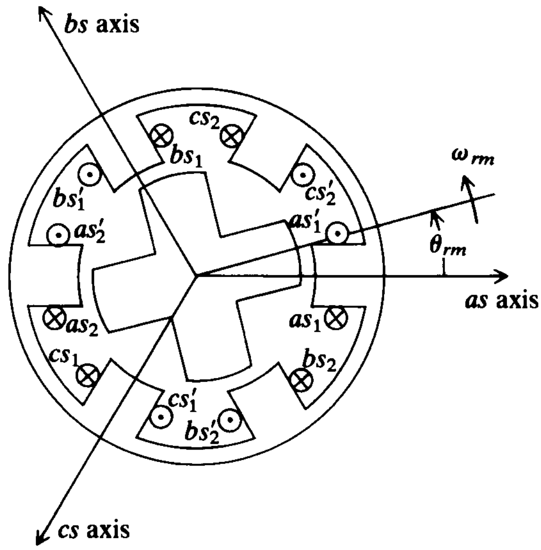

Figure 9.5-1: Two-pole, three-phase, single-stack, variable-reluctance stepper motor with six stator teeth and four rotor teeth.

stators shown in Fig. 9.2-2 and squeezed them into one stack. The magnetic axes of the stator windings are displaced 120° as in the case of the three-phase machines considered in earlier chapters; however, the stepper motor generally has stator teeth or poles that protrude rather than a circular inner stator surface.

Recall that in the case of the multistack variable-reluctance motor, the number of rotor and stator teeth per stack is the same. In the case of the single-stack stepper motor, the number of rotor teeth per stack, RT, is never equal to the number of stator teeth per stack, ST. If, for example, the rotor shown in Fig. 9.5-1 had the same number of teeth as the stator, then, when two diagonally opposite rotor teeth are aligned with two diagonally opposite stator teeth, all diagonally opposite rotor teeth would be aligned with diagonally opposite stator teeth and stepping action could not occur. The equations that we derived for the tooth pitch TP and step length SL for the multistack variable-reluctance stepper motor also apply for the single-stack stepper motor. For the two-pole, three-phase stepper motor shown in Fig. 9.5-1, $RT = 4$ and, thus, $TP = 2\pi/RT = 90°$ and $SL = TP/N = 30°$.

Note that the sequence *as, bs, cs, as,...* produces a counterclockwise stepping of the rotor.

Two other types of three-phase, single-stack, variable-reluctance stepper motors are shown in Figs. 9.5-2 and 9.5-3. The two-pole device shown in Fig. 9.5-2 has six stator teeth and eight rotor teeth. $TP = 45°$ and $SL = 15°$, and an *as, bs, cs, as,...* sequence produces a clockwise stepping of the rotor. For the four-pole, three-phase device shown in Fig. 9.5-3, $ST = 12$ and $RT = 8$. Thus, $TP = 45°$ and $SL = 15°$. The step length is the same as for the stator with six teeth (Fig. 9.5-2); however, counterclockwise stepping of the rotor occurs with the sequence *as, bs, cs, as,....* In Fig. 9.5-3, the labeling of the coil sides of the windings is omitted because of lack of space.

The expressions given for the self-inductances of the three-stack (phase) variable-reluctance stepper motor, (9.3-21) through (9.3-26), also apply to the three-phase, single-stack, variable-reluctance stepper motor. Therefore, it would appear that the operation of the single-stack and multistack variable-reluctance stepper motors may be described by the same set of equations. Although this perception is essentially valid from an idealized point of view, it is not valid in the practical world. We see from Figs. 9.5-1 through 9.5-3, that the stator windings share the same magnetic system. Hence, there is a possibility of mutual coupling between stator phases. For the purposes of discussion, let us consider Fig. 9.5-4, which is Fig. 9.5-1 with $\theta_{rm} = 0$. The dashed lines shown therein depict the flux linking the *bs* winding due to positive current flowing in the *as* winding. If we assume that the reluctance of the iron is small so that it can be neglected, the flux linkages cancel, whereupon mutual coupling would not exist between stator phases. From an idealized standpoint, this is a valid line of reasoning; from a practical standpoint it is not.

Stepper motors are generally designed to operate at current levels that saturate the iron of the machine. Hence, owing to the increased reluctance of the saturated iron, less flux will be circulating around the longer paths through iron than through the short paths. Hence, a net mutual flux would exist between stator phases. For the case depicted in Fig. 9.5-4, there would be a net flux in the direction of the positive *bs* axis as a result of the saturation of the iron. Albeit relatively small in amplitude, a mutual inductance does exist in the practical application of single-stack, variable-reluctance stepper motors. This complicates the analysis of these devices far beyond that which we care to deal with in this text. Instead, for our first look at stepper motors, we will consider it sufficient to neglect saturation and the mutual coupling

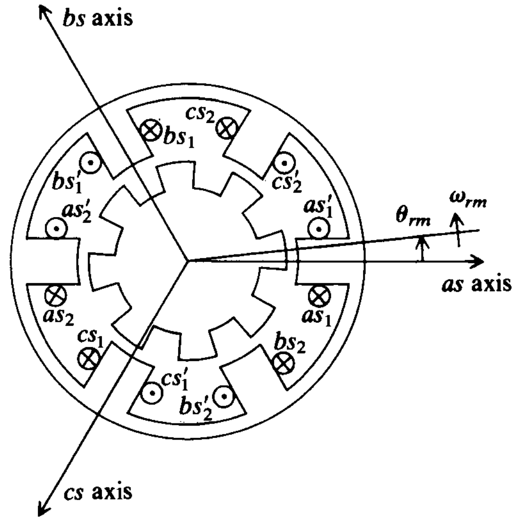

Figure 9.5-2: Two-pole, three-phase, single-stack, variable-reluctance stepper motor with six stator teeth and eight rotor teeth.

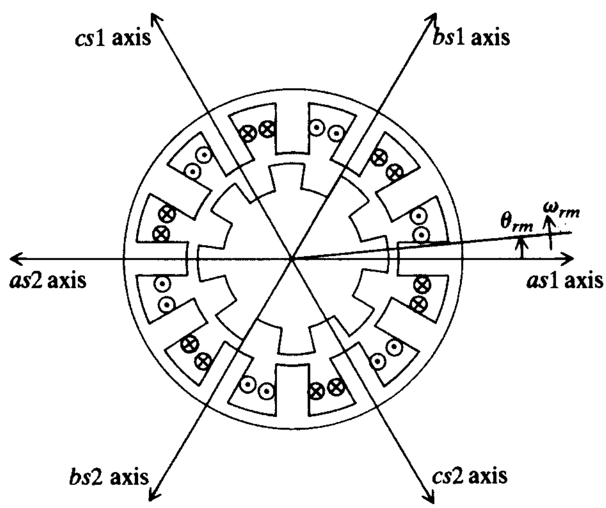

Figure 9.5-3: Four-pole, three-phase, single-stack, variable-reluctance stepper motor with twelve stator teeth and eight rotor teeth.

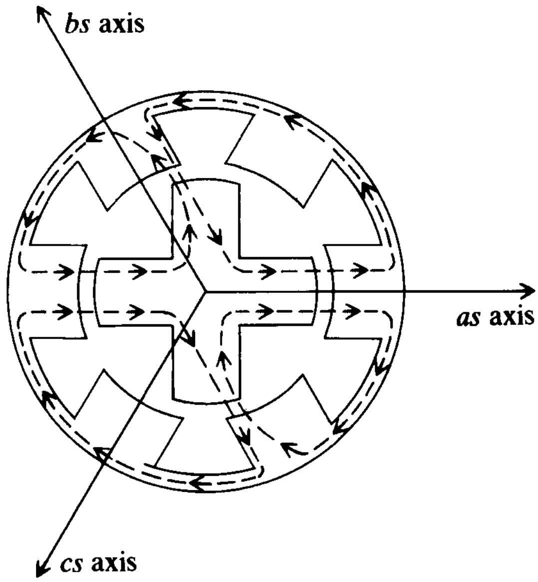

Figure 9.5-4: Two-pole, three-phase, single-stack, variable-reluctance stepper motor given in Fig. 9.5-1 with $\theta_{rm} = 0$.

it causes in single-stack, variable-reluctance stepper motors. A single-stack, variable-reluctance stepper motor is shown in Fig. 9.5-5. This device has a 15° step length and is equipped with an integral lead screw for translational motion.

SP9.5-1 Express the number of stator teeth possible for an N-phase, single-stack, variable-reluctance stepper motor. [$ST = n(2N)$, where $n = 1, 2, 3, ...$]

SP9.5-2 The rotor in Fig. 9.5-1 is replaced by the rotor from Fig. 9.5-3. Determine (a) TP, (b) SL, and (c) the direction of rotation with an *as, bs, cs, as,...* sequence. [(a) TP =45°; (b) SL =15°; (c) cw]

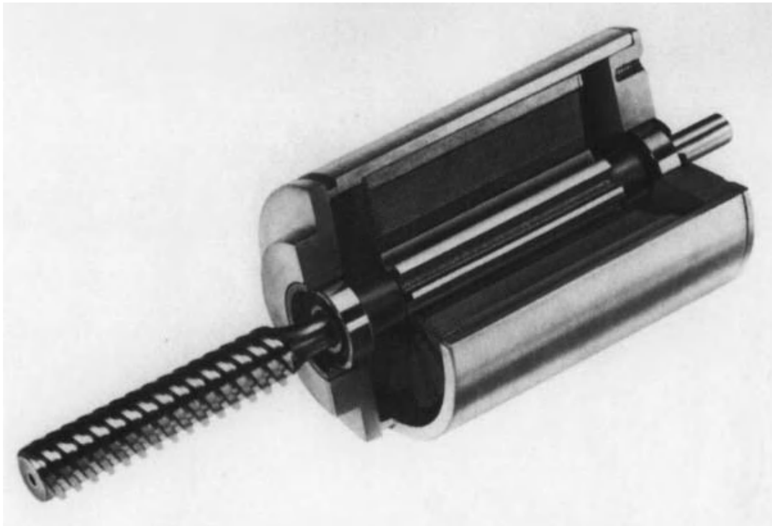

Figure 9.5-5: Single-stack, 15 °/step, variable-reluctance stepper motor. (*Courtesy of Warner Electric.*)

9.6 BASIC CONFIGURATION OF PERMANENT-MAGNET STEPPER MOTORS

The permanent-magnet stepper motor is quite common. Actually, it is a permanent-magnet ac machine and it may be operated either as a stepping motor or as a continuous-speed device. Here, we will concern ourselves only with its application as a stepping motor since continuous-speed operation is similar to the operation of a permanent-magnet ac machine.

A two-pole, two-phase, permanent-magnet stepper motor with five rotor teeth is shown in Fig. 9.6-1. Most permanent-magnet stepper motors have more than two poles and more than five rotor teeth; some may have as many as eight poles and as many as fifty rotor teeth. Nevertheless, the elementary device shown in Fig. 9.6-1 is sufficient to illustrate the principle of operation of the permanent-magnet stepper motor. The axial cross-sectional view shown in Fig. 9.6-1*b* illustrates the permanent magnet that is mounted on the rotor. The permanent magnet magnetizes the iron end caps that are also mounted on the rotor and are slotted to form the rotor teeth. The

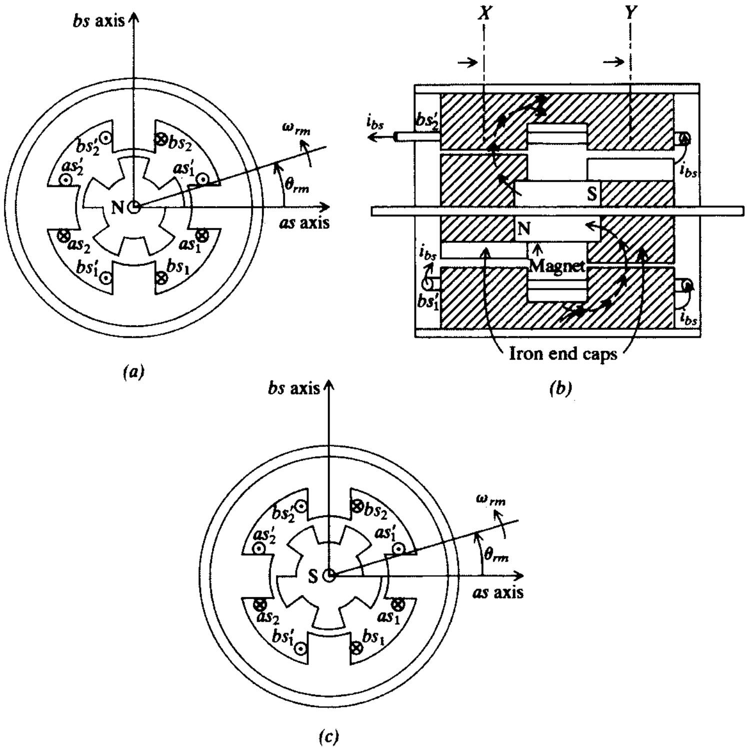

Figure 9.6-1: Two-pole, two-phase, permanent-magnet stepper motor: (a) Axial view at X; (b) side cross-sectional view; (c) axial view at Y.

view looking from left to right at X is shown in Fig. 9.6-1a. Figure 9.6-1c is the view from left to right at Y. The left end cap shown in Fig.9.6-1a is magnetized as a north pole; the right end cap shown in Fig. 9.6-1c is magnetized as a south pole. Note that the rotor teeth of the left end cap are displaced one-half a tooth pitch from the teeth on the right end cap. Also, note that the stator windings are wound over the full axial length of the device; a part of the bs winding is shown in Fig. 9.6-1b.

Let us trace the main path of flux linking the bs winding for the rotor position shown in Fig. 9.6-1. This path is depicted by dashed lines in Fig. 9.6-1b. However, it is necessary to visualize the drawing in three dimensions. Flux leaves the left end cap through the rotor tooth at the top of the rotor that is aligned with the stator tooth that has the bs_2 part of the bs winding.

The flux travels up through the stator tooth in the stator iron. The flux then splits and travels around the circumference of the stator and returns to the south pole of the rotor through the stator tooth positioned at the bottom in Fig. 9.6-1*c*, on which the bs_1 winding is wound. The main flux linking the *as* winding for the rotor position shown in Fig. 9.6-1 would enter the stator tooth on which the as_1 winding is wound from the rotor tooth on the right of Fig. 9.6-1*a*. The flux would travel around the circumference of the stator and return to the rotor through the stator pole upon which the as_2 winding is wound, Fig. 9.6-1*c*.

Stepping action can be explained by first assuming that the *bs* winding is open-circuited and a constant positive current is flowing in the *as* winding. As a result of this current, a south pole is established at the stator tooth on which the as_1 winding is wound, and a stator north pole is established at the stator tooth on which the as_2 winding is wound. The rotor would be positioned at $\theta_{rm} = 0$. Now let us simultaneously deenergize the *as* winding while energizing the *bs* winding with a positive current. The rotor will move one step length in the counterclockwise direction. To continue stepping in the counterclockwise direction, the *bs* winding is deenergized and the *as* winding is energized with a negative current. That is, counterclockwise stepping occurs with a current sequence of i_{as}, i_{bs}, $-i_{as}$, $-i_{bs}$, $i_{as}, \ldots$. Clockwise rotation is achieved by i_{as}, $-i_{bs}$, $-i_{as}$, $i_{bs} \ldots$.

The tooth pitch *TP* can be calculated from (9.2-1); however, the *SL* for a permanent-magnet stepper motor cannot be calculated from (9.2-3). As we have mentioned, counterclockwise rotation of the device shown in Fig. 9.6-1 is achieved by a sequence of i_{as}, i_{bs}, $-i_{as}$, $-i_{bs}$, $i_{as}, \ldots$. We see that it takes four switchings (steps) to advance the rotor one tooth pitch. Thus,

$$TP = 2N\,SL \tag{9.6-1}$$

where N is the number of phases. Substituting (9.2-1) into (9.6-1) and solving for SL yields

$$SL = \frac{\pi}{RT\,N} \tag{9.6-2}$$

For the device shown in Fig. 9.6-1, $RT = 5$ and $N = 2$. From (9.6-2), $SL = 18°$.

Recall that in the case of variable-reluctance stepper motors, it is unnecessary to reverse the direction of the current in the stator windings to achieve rotation; therefore, the stator voltage source need only be unidirectional. However, in the case of a permanent-magnet stepper motor, it is necessary for the phase currents to flow in both directions to achieve rotation. Generally, stepper motors are supplied from a dc voltage source; hence, the electronic interface between the phase windings and the dc source must be bidirectional; that is, it must have the capability of applying a positive and negative voltage to each phase winding. This requirement markedly increases the cost of the electronic interface and its associated controls relative to a unidirectional source. As an alternative, permanent-magnet stepper motors are often equipped with what is referred to as *bifilar windings*. Rather than only one winding on each stator tooth, there are two identical windings with one wound opposite to the other, each having separate independent external terminals. With this type of winding configuration, the direction of the magnetic field established by the stator windings is reversed, not by changing the direction of the current but by reversing the sense of the winding through which current is flowing. If, for example, the device shown in Fig. 9.6-1 is equipped with bifilar windings, there would be another *as* winding and another *bs* winding with separate, independent, external terminals wound opposite on the stator teeth to the windings shown. Although this increases the size and weight of the stepper motor, it eliminates the need for a bidirectional electronic interface. When this permanent-magnet stepper motor is equipped with bifilar windings as just described, it is (perhaps, inappropriately) called a four-phase device. Actually it has four windings, but it is still a two-phase device magnetically. Although we are not going to consider the bifilar-wound machine in detail, one should be aware of this somewhat ambiguous nomenclature. More specifically, care should be taken when using (9.6-2) to calculate the step length. The number of phases N in (9.6-2) is the number of phases magnetically rather than the number of windings. A cutaway view of a permanent-magnet stepper motor is shown in Fig. 9.6-2.

SP9.6-1 Consider the device shown in Fig. 9.6-1. The load torque is zero. Initially $i_{as} = I$ and $i_{bs} = 0$. From this condition, the following sequence occurs: $i_{as} = 0$ and $i_{bs} = I$, then $i_{as} = -I$ and $i_{bs} = I$. Determine the initial, intermediate, and final positions. [$\theta_{rm} = 0$, 18°, 27°]

SP9.6-2 A four-pole, two-phase, permanent-magnet stepper motor has 18 rotor teeth. Calculate TP and SL. [$TP = 20°$; $SL = 5°$]

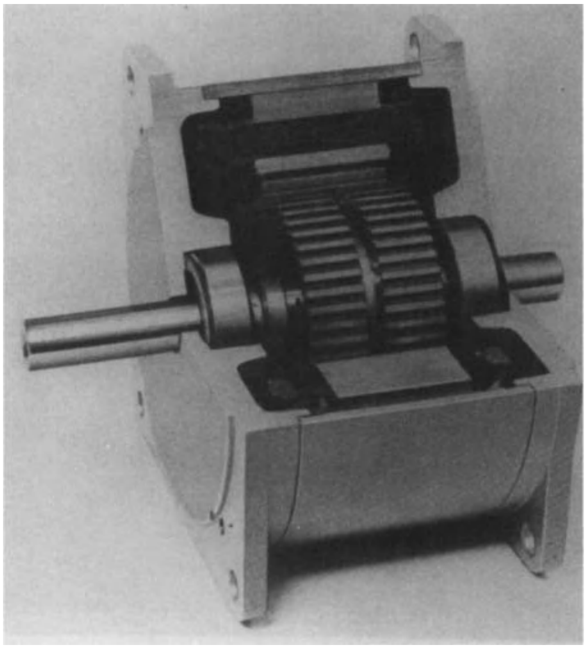

Figure 9.6-2: Cutaway view of a permanent-magnet stepper motor. (Courtesy of Sanyo Denki.)

9.7 EQUATIONS FOR PERMANENT-MAGNET STEPPER MOTORS

The voltage equations for a two-phase, permanent-magnet stepper motor may be written as

$$v_{as} = r_s i_{as} + \frac{d\lambda_{as}}{dt} \tag{9.7-1}$$

$$v_{bs} = r_s i_{bs} + \frac{d\lambda_{bs}}{dt} \tag{9.7-2}$$

In matrix form,

$$\mathbf{v}_{abs} = \mathbf{r}_s \mathbf{i}_{abs} + p\boldsymbol{\lambda}_{abs} \tag{9.7-3}$$

where p is the operator d/dt, and for voltages, currents, and flux linkages

$$(\mathbf{f}_{abs})^T = [f_{as} \quad f_{bs}] \tag{9.7-4}$$

with

$$\mathbf{r}_s = \begin{bmatrix} r_s & 0 \\ 0 & r_s \end{bmatrix} \tag{9.7-5}$$

The flux linkages may be expressed as

$$\lambda_{as} = L_{asas} i_{as} + L_{asbs} i_{bs} + \lambda_{asm} \tag{9.7-6}$$

$$\lambda_{bs} = L_{bsas} i_{as} + L_{bsbs} i_{bs} + \lambda_{bsm} \tag{9.7-7}$$

In matrix form,

$$\boldsymbol{\lambda}_{abs} = \mathbf{L}_s \mathbf{i}_{abs} + \boldsymbol{\lambda}'_m \tag{9.7-8}$$

where

$$\mathbf{L}_s = \begin{bmatrix} L_{asas} & L_{asbs} \\ L_{bsas} & L_{bsbs} \end{bmatrix} \tag{9.7-9}$$

$$\boldsymbol{\lambda}'_m = \begin{bmatrix} \lambda_{asm} \\ \lambda_{bsm} \end{bmatrix} \tag{9.7-10}$$

From Fig. 9.6-1, we can write, as a first approximation,

$$\boldsymbol{\lambda}'_m = \lambda'_m \begin{bmatrix} \cos(RT\,\theta_{rm}) \\ \sin(RT\,\theta_{rm}) \end{bmatrix} \tag{9.7-11}$$

where λ'_m is the amplitude of the flux linkages established by the permanent magnet as viewed from the stator phase windings. In other words, the magnitude of λ'_m is proportional to the magnitude of the open-circuit sinusoidal voltage induced in each stator phase winding. In (9.7-11),

$$\frac{d\theta_{rm}}{dt} = \omega_{rm} \tag{9.7-12}$$

Those who have read Chapter 8 on the permanent-magnet ac machine will recognize the similarity between (9.7-11) and (8.3-9). Also, the procedure for calculating λ'_m in the case of the stepper motor is identical to that illustrated in Example 8A.

From the idealized standpoint, the self-inductance of the stator phases of the device shown in Fig. 9.6-1 is constant, and the reluctance seen by the permanent magnet is also constant, independent of rotor position. However, in practice both the self-inductances and the reluctance vary with rotor position due to saturation of the stator iron and the differences from the idealized configuration that occur when shaping the poles. We shall disregard these departures from the idealized case and assume constant self-inductances and a constant reluctance seen by the permanent magnet independent of rotor position. When doing so, we are neglecting the reluctance torques caused by variation in self-inductances and the permanent magnet, both of which attempt to place the rotor in its minimum-reluctance position. The latter torque is often referred to as the *detent* or *retention torque,* since it exists whether or not the stator windings are excited, and, if the load torque is not too large, this detent torque will preserve the rotor position during a power failure. Nevertheless, the reluctance torques are small relative to the torque produced by the interaction of the permanent magnet and the stator currents and, although we are not looking at the complete picture when we neglect the reluctance torques, this approximation is certainly adequate for our first look at the permanent-magnet stepper motor.

With the assumption of constant self-inductances, we can write

$$L_{asas} = L_{ls} + L_{ms} = L_{ss} \tag{9.7-13}$$

$$L_{bsbs} = L_{ls} + L_{ms} = L_{ss} \tag{9.7-14}$$

Following a line of reasoning similar to that used in the case of the single-stack variable-relucance stepper motor, it can be shown that stator mutual inductances do not exist if saturation is neglected. Thus,

$$\mathbf{L}_s = \begin{bmatrix} L_{ss} & 0 \\ 0 & L_{ss} \end{bmatrix} \tag{9.7-15}$$

An expression for the electromagnetic torque may be obtained by taking the partial derivative of the coenergy with respect to θ_{rm}, as given in Table 2.5-1 and (9.3-27). Since the stator mutual inductances are zero, the coenergy may be expressed as

$$W_c = \tfrac{1}{2}L_{asas}i_{as}^2 + \tfrac{1}{2}L_{bsbs}i_{bs}^2 + \lambda_{asm}i_{as} + \lambda_{bsm}i_{bs} + W_{pm} \tag{9.7-16}$$

where L_{asas} and L_{bsbs} are given by (9.7-13) and (9.7-14), respectively, and λ_{asm} and λ_{bsm} are given by (9.7-11). The term W_{pm} is related to the energy associated with the permanent magnet. Since we are neglecting variations in the self-inductances and in W_{pm} taking the partial derivative of W_c with respect to θ_{rm} yields

$$T_e = -RT\,\lambda_m'\left[i_{as}\sin(RT\,\theta_{rm}) - i_{bs}\cos(RT\,\theta_{rm})\right] \tag{9.7-17}$$

The terms of (9.7-17) are plotted in Fig. 9.7-1, wherein it is assumed that constant currents are present in both phase windings. Each term of (9.7-17) is identified in Fig. 9.7-1. In particular, $\pm T_{eam}$ is the torque due to the interaction of the permanent magnet and $\pm i_{as}$, and $\pm T_{ebm}$ are due to the interaction of the permanent magnet and $\pm i_{bs}$.

The reluctance of the permanent magnet is large, approaching that of air. Since the flux established by the phase currents flows through the magnet, the reluctance of the flux path is relatively large. Hence, the variation in the reluctance due to rotation of the rotor is small and, consequently, the amplitudes of the reluctance torques are small relative to the torque produced by the interaction between the permanent magnet and the phase currents. For this reason, the reluctance torques are generally neglected, as we have done here, and the self-inductances are assumed to be constant. Therefore, the voltage equations for the permanent-magnet stepper motor become those of the permanent-magnet ac machine that we considered in Chapter 8, except for the use of θ_{rm} instead of θ_r and the difference in the referencing of θ_{rm} (to the minimum reluctance rather than the maximum reluctance). These equations are set forth in the following section.

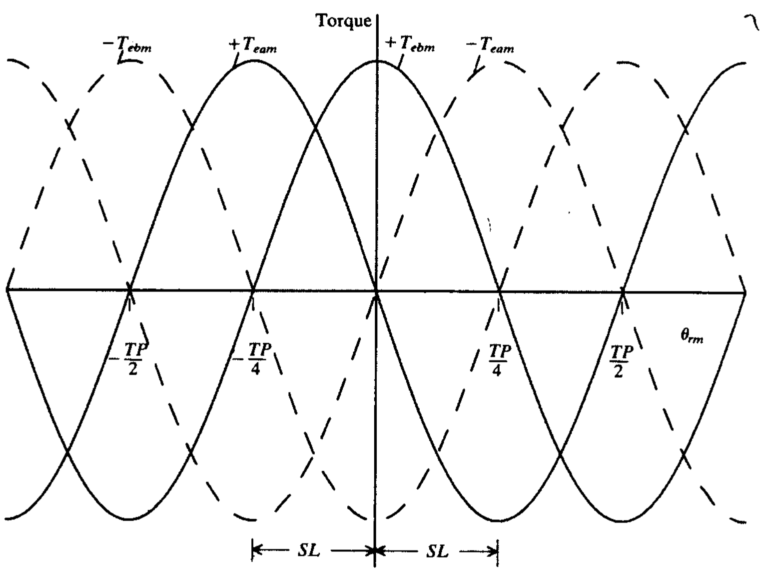

Figure 9.7-1: Plot of T_e versus θ_{rm} for a permanent-magnet stepper motor with constant phase currents.

Although a discussion of the stepping action of a permanent-magnet stepper motor using the steady-state torque-angle characteristics is appropriate, this explanation would be essentially a repeat of that given in Section 9.4 for the variable-reluctance devices. We will not do this. Instead, we will ask a few questions to help emphasize this similarity.

SP9.7-1 Express λ_{asm} in terms of SL rather than RT. Determine the number of step lengths in a period for the device shown in Fig. 9.6-1. $\{\lambda_{asm} = \lambda'_m \cos[\pi/(SL\ N)]\theta_{rm};\ 4\}$

SP9.7-2 Consider Fig. 9.7-l. The load torque is zero. Initially, $i_{as} = I$, then $i_{bs} = 0$ and $i_{bs} = -3I$, and, finally, $i_{as} = -\frac{1}{2}I$ and $i_{bs} = 0$. Determine the three positions. $[\theta_{rm} = 0,\ -TP/4,\ -TP/2]$

9.8 EQUATIONS OF PERMANENT-MAGNET STEPPER MOTORS IN ROTOR REFERENCE FRAME – RELUCTANCE TORQUES NEGLECTED

Stepper motors often operate for a time in a continuous rotational mode, especially when connected through a speed-reduction gear to the member being positioned. In some cases, the phase voltages may be stepped as fast as 500 to 1500 steps per second. When the permanent-magnet stepper motor is operated in this mode, it behaves very similar to either a permanent-magnet ac machine or a brushless dc machine, depending upon the type of control employed. It is, therefore, advantageous to set forth the voltage equations of the permanent-magnet stepper motor in the rotor reference frame. This transformation is of advantage only if the self-inductances are assumed constant and the detent torque is neglected.

A change of variables that, in effect, transforms the stator variables to the rotor reference frame is

$$\begin{bmatrix} f_{qs}^r \\ f_{ds}^r \end{bmatrix} = \begin{bmatrix} -\sin(RT\ \theta_{rm}) & \cos(RT\ \theta_{rm}) \\ \cos(RT\ \theta_{rm}) & \sin(RT\ \theta_{rm}) \end{bmatrix} \begin{bmatrix} f_{as} \\ f_{bs} \end{bmatrix} \tag{9.8-1}$$

or

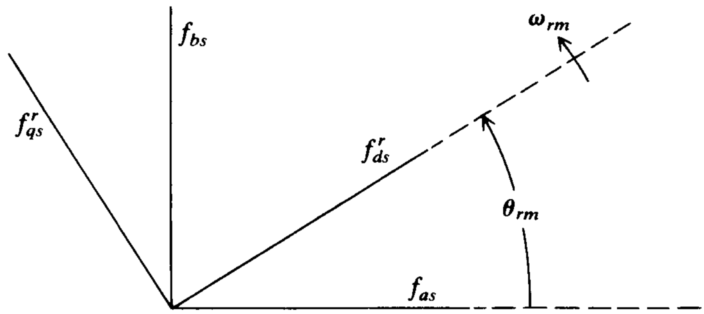

Figure 9.8-1: Trigonometric interpretation of change of stator variables.

$$\mathbf{f}_{qds}^r = \mathbf{K}_s^r \mathbf{f}_{abs} \tag{9.8-2}$$

where f can represent either voltage, current, or flux linkage and θ_{rm} is defined by (9.7-12). It follows that

$$\mathbf{f}_{abs} = (\mathbf{K}_s^r)^{-1} \mathbf{f}_{qds}^r \tag{9.8-3}$$

where $(\mathbf{K}_s^r)^{-1} = \mathbf{K}_s^r$. The s subscript denotes stator variables and the r superscript indicates that the transformation is to a reference frame rotating with the rotor.

If you have studied Chapters 7 and 8, you will recall that therein the stator variables of a synchronous machine (Chapter 7) and the stator variables of a permanent-magnet synchronous machine (Chapter 8) were transformed to the rotor reference frame by $\mathbf{K}_s^r$. However, the $\mathbf{K}_s^r$ used in Chaps. 7 and 8, (7.5-1) or (8.5-1), is different from that given by (9.8-1). Although both accomplish the same purpose of transforming the stator variables to the rotor reference frame, the expression for $\mathbf{K}_s^r$ used here for the permanent-magnet stepper is different from that used in Chapters 7 and 8. There are two reasons for this. The actual rotor displacement θ_{rm} is used here rather than θ_r, the electrical angular displacement of the rotor, and this angular displacement is referenced from the positive *as* axis to the minimum-reluctance path of the rotor rather than to the maximum-reluctance path as in Chapters 7 and 8. Hence, if we maintain the convention of the q axis positioned at the maximum-reluctance path of the rotor, then the transformation is that given by (9.8-1).

Substituting (9.8-3) into (9.7-3) yields

$$(\mathbf{K}_s^r)^{-1}\mathbf{v}_{qds}^r = \mathbf{r}_s(\mathbf{K}_s^r)^{-1}\mathbf{i}_{qds}^r + p[(\mathbf{K}_s^r)^{-1}\boldsymbol{\lambda}_{qds}^r] \tag{9.8-4}$$

Multiplying (9.8-4) by $\mathbf{K}_s^r$ and simplifying yields

$$\mathbf{v}_{qds}^r = \mathbf{r}_s\mathbf{i}_{qds}^r + RT\,\omega_{rm}\boldsymbol{\lambda}_{dqs}^r + p\boldsymbol{\lambda}_{qds}^r \tag{9.8-5}$$

where

$$(\boldsymbol{\lambda}_{dqs}^r)^T = [\boldsymbol{\lambda}_{ds}^r \quad -\boldsymbol{\lambda}_{qs}^r] \tag{9.8-6}$$

The last two terms of (9.8-5) are obtained from the last term of (9.8-4); in particular,

$$\mathbf{K}_s^r p[(\mathbf{K}_s^r)^{-1}\boldsymbol{\lambda}_{qds}^r] = \mathbf{K}_s^r[p(\mathbf{K}_s^r)^{-1}]\boldsymbol{\lambda}_{qds}^r + \mathbf{K}_s^r(\mathbf{K}_s^r)^{-1}p\boldsymbol{\lambda}_{qds}^r \tag{9.8-7}$$

It is left to the reader to show that the right-hand side of (9.8-7) reduces to the last two terms of (9.8-5).

The stator flux linkages are expressed as

$$\boldsymbol{\lambda}_{abs} = \mathbf{L}_s\mathbf{i}_{abs} + \boldsymbol{\lambda}_m' \tag{9.8-8}$$

where $\mathbf{L}_s$ is given by (9.7-15) and $\boldsymbol{\lambda}_m'$ is defined by (9.7-11). Substituting the change of variables into (9.8-8) yields

$$(\mathbf{K}_s^r)^{-1}\boldsymbol{\lambda}_{qds}^r = \mathbf{L}_s(\mathbf{K}_s^r)^{-1}\mathbf{i}_{qds}^r + \boldsymbol{\lambda}_m' \tag{9.8-9}$$

Premultiplying by $\mathbf{K}_s^r$ and substituting (9.7-15) for $\mathbf{L}_s$ and (9.7-11) for $\boldsymbol{\lambda}_m'$ yield

$$\boldsymbol{\lambda}_{qds}^r = \begin{bmatrix} L_{ss} & 0 \\ 0 & L_{ss} \end{bmatrix} \begin{bmatrix} i_{qs}^r \\ i_{ds}^r \end{bmatrix} + \lambda_m'^r \begin{bmatrix} 0 \\ 1 \end{bmatrix} \tag{9.8-10}$$

which is identical in form to (8.5-5). To be consistent with our previous notation, we have added the superscript r to λ_m'. We see from (9.8-10) that in our new system of variables, the flux linkage created by the permanent magnet appears constant. Hence, our fictitious circuits are fixed relative to the permanent magnet and, therefore, fixed in the rotor. We have accomplished the goal of eliminating flux linkages that vary with θ_{rm}.

In expanded form, the voltage equations are

$$v_{qs}^r = r_s i_{qs}^r + RT\,\omega_{rm}\lambda_{ds}^r + p\lambda_{qs}^r \tag{9.8-11}$$

$$v_{ds}^r = r_s i_{ds}^r - RT\,\omega_{rm}\lambda_{qs}^r + p\lambda_{ds}^r \tag{9.8-12}$$

where

$$\lambda_{qs}^r = L_{ss} i_{qs}^r \tag{9.8-13}$$

$$\lambda_{ds}^r = L_{ss} i_{ds}^r + \lambda_m'^r \tag{9.8-14}$$

Substituting (9.8-13) and (9.8-14) into (9.8-11) and (9.8-12), and since $\lambda_m'^r$ is constant, $p\lambda_m'^r = 0$.

$$v_{qs}^r = (r_s + pL_{ss}) i_{qs}^r + RT\,\omega_{rm} L_{ss} i_{ds}^r + RT\,\omega_{rm} \lambda_m'^r \tag{9.8-15}$$

$$v_{ds}^r = (r_s + pL_{ss}) i_{ds}^r - RT\,\omega_{rm} L_{ss} i_{qs}^r \tag{9.8-16}$$

The above equations may be written in matrix form as

$$\begin{bmatrix} v_{qs}^r \\ v_{ds}^r \end{bmatrix} = \begin{bmatrix} r_s + pL_{ss} & RT\,\omega_{rm} L_{ss} \\ -RT\,\omega_{rm} L_{ss} & r_s + pL_{ss} \end{bmatrix} \begin{bmatrix} i_{qs}^r \\ i_{ds}^r \end{bmatrix} + \begin{bmatrix} RT\,\omega_{rm} \lambda_m'^r \\ 0 \end{bmatrix} \tag{9.8-17}$$

The expression for the electromagnetic torque, with the reluctance torques neglected, is obtained by expressing i_{as} and i_{bs} in (9.7-17) in terms of i_{qs}^r and i_{ds}^r. In particular,

$$T_e = RT\,\lambda_m'^r i_{qs}^r \tag{9.8-18}$$

In Section 8.5, the *qs* and *ds* voltage equations are derived for a permanent-magnet ac machine, These equations are similar to those which we have derived in this section with the exception that ω_r is replaced by $RT\,\omega_{rm}$. Also, the expression for the electromagnetic torque given by (9.8-18) is identical in form to (8.5-17) if $P/2$ in (8.5-17) is replaced by the rotor teeth RT.

When operated in the continuous rotational mode, the fundamental component of the voltages applied to the stator windings of the permanent-magnet stepper motor can be expressed:

$$v_{as} = -\sqrt{2}\, v_s \sin\theta_{esv} \tag{9.8-19}$$

$$v_{bs} = \sqrt{2}\, v_s \cos\theta_{esv} \tag{9.8-20}$$

These equations form a balanced two-phase set, where the amplitude v_s may be a function of time. One may question the form of these voltages since in the past we have selected v_{as} as the $\cos\theta_{esv}$. Recall that, in the case of the stepper motor, we referenced θ_{rm} as being different from that of the synchronous machine. Consequently, the form of the change of variables, $\mathbf{K}_s^r$, is different. We have just pointed out that the equations given in Chapter

8 are identical to those for the permanent-magnet stepper motor with ω_r replaced with $RT\,\omega_{rm}$. To apply the material given in Chapter 8 to the permanent-magnet stepper motor, it is necessary to select the instantaneous values of v_{as} and v_{bs} so that v_{qs}^r and v_{ds}^r are the same as in Chapter 8. This is the case if v_{as} and v_{bs} are defined by (9.8-19) and (9.8-20) with

$$\frac{d\theta_{rm}}{dt} = \omega_{rm} \tag{9.8-21}$$

and $\theta_{esv}(0)$ is the time-zero position of the applied voltages.

Now then, when the permanent-magnet stepper motor is operated in the continuous rotational mode between target positions, it is operated either in the open-loop control mode or the closed-loop control mode. In the so-called open-loop control mode, stator voltages of a constant stepping rate are applied until the desired position is reached. In the case of the closed-loop control scheme, the rotor position of the permanent-magnet stepper motor is detected, and this information is supplied to the driving inverter that generates the voltages applied to the stator phases. In this case, the frequency of the stator voltages is made to correspond to the rotor speed and the stepper motor is operated as a permanent-magnet ac machine between target positions. Therefore, when the permanent-magnet stepper motor is operated in the closed-loop control mode, it is a permanent-magnet ac machine and ω_e is made equal to $RT\,\omega_{rm}$. It would appear that we need only to replace ω_r with $RT\,\omega_{rm}$ in all voltage equations given in Chapter 8 and they would apply to the permanent-magnet stepper motor with a closed-loop control. There is an exception, however. When converting between phasors and $qs^r$and ds^ras quantities, it is necessary to replace $\tilde{F}_{as}$ with $\tilde{F}_{bs}$. In particular, we see from (9.8-19) and (9.8-20) that, during steady-state closed-loop control operation, F_{as} and F_{bs} are expressed as

$$F_{as} = -\sqrt{2}\,F_s \sin[RT\,\omega_{rm}t + \theta_{esf}(0)] \tag{9.8-22}$$

$$F_{bs} = \sqrt{2}\,F_s \cos[RT\,\omega_{rm}t + \theta_{esf}(0)] \tag{9.8-23}$$

wherein ω_e has been set equal to $RT\,\omega_{rm}$. Substituting F_{as} and F_{bs} into the transformation equation, (9.8-1), yields

$$F_{qs}^r = \sqrt{2}\,F_s \cos[\theta_{esv}(0) - RT\,\theta_{rm}(0)] \tag{9.8-24}$$

$$F_{ds}^r = -\sqrt{2}\,F_s \sin[\theta_{esv}(0) - RT\,\theta_{rm}(0)] \tag{9.8-25}$$

Now, from (9.8-23),

$$\tilde{F}_{bs} = F_s e^{j\theta_{esf}(0)}$$
$$= F_s \cos\theta_{esf}(0) + jF_s \sin\theta_{esf}(0) \tag{9.8-26}$$

If we let $\theta_{rm}(0) = 0$, then (9.8-26) may be expressed in terms of (9.8-24) and (9.8-25) as

$$\sqrt{2}\,\tilde{F}_{bs} = F_{qs}^r - jF_{ds}^r \tag{9.8-27}$$

This is (8.8-13) with $\tilde{F}_{as}$ replaced by $\tilde{F}_{bs}$. Thus, for the permanent-magnet stepper motor during closed loop operation, (8.8-18) becomes

$$\tilde{V}_{bs} = (r_s + j\,RT\,\omega_{rm}L_{ss})\tilde{I}_{bs} + \tilde{E}_b \tag{9.8-28}$$

where $\tilde{E}_b$ is $\tilde{E}_a$ given by (8.8-17) with ω_r replaced by $RT\,\omega_{rm}$; in particular,

$$\tilde{E}_b = \frac{1}{\sqrt{2}}RT\,\omega_{rm}\lambda_m'^r e^{j0} \tag{9.8-29}$$

The stepper motor can be operated with or without phase shift, just as the permanent-magnet ac motor, and with $\theta_{rm}(0) = 0$ the phase shift for maximum torque is (8.8-24) with ω_r replaced with $RT\,\omega_{rm}$. In particular,

$$\phi_{vMT} = \tan^{-1}(\tau_s\,RT\,\omega_{rm}) \tag{9.8-30}$$

It follows that, with the appropriate substitutions of $RT\,\omega_{rm}$ for ω_r in the voltage equations and RT for $P/2$ in the torque equations, the time-domain block diagram given in Fig. 8.10-1 is valid for a permanent-magnet stepper motor operated with a closed-loop control scheme.

SP9.8-1 A permanent-magnet stepper motor with $RT = 7$ is operated at $\omega_{rm} = 100$ rad/s. $\tilde{V}_{bs} = (10/\sqrt{2})\underline{/0^\circ}$, $\tilde{I}_{bs} = (1/\sqrt{2})\underline{/-60.3^\circ}$, $\theta_{rm}(0) = 0$, $r_s = 4\,\Omega$, and L_{ss} =0.01 H. Calculate $\lambda_m'^r$. [$\lambda_m'^r$ =0.00277 V · s/rad]
SP9.8-2 The stepper motor given in SP9.8-1 is operated at ω_{rm} =100 rad/s with $\tilde{I}_{bs} = (1/\sqrt{2})\underline{/-20^\circ}$ and $\theta_{rm}(0) = 0$. Calculate ϕ_v. [ϕ_v= 32.8°]

9.9 RECAPPING

We have considered the two types of electromechanical stepping devices used most often: the variable-relucance and the permanent-magnet stepper motors. Although we have considered an important operating mode of the stepper motor, there are numerous aspects of stepper motor operation that we are unable to cover in an introductory text. For example, the types and control of the voltage source and stability problems that can occur during continuous rotation of the stepper motor are beyond the scope of this textbook. Nevertheless, the information presented in this chapter sets the stage for study of these more advanced topics.

9.10 REFERENCE

[1] P. P. Acarnley, *Stepping Motors: A Guide to Modern Theory and Practice*, Peter Pereginus Ltd. for the Institution of Electrical Engineers; Southgate House, Stevenage, Herts, SGl lHQ, England, 1984.

9.11 PROBLEMS

1. Sketch the configuration of a two-pole, four-stack, variable-reluctance stepper motor with two rotor teeth. Use *as, bs, cs,* and *ds* to denote the phase windings. Calculate *TP, SL,* and give the excitation sequence for ccw rotation.

2. For Prob. 1, express the self-inductances and the torque using *SL* in the arguments.

* 3. Those who have read Chapter 7 on synchronous and reluctance machines may wonder if Park's transformation can be used in the case of the variable-reluctance stepper motor to transform the stator circuits to fictitious circuits with constant inductances fixed in the rotor. The answer is no, and the reason is that mutual inductances must exist between stator phases as given by (7.9-6). To show this, take a two-pole, two-phase reluctance machine, assume $L_{asbs} = L_{bsas} = 0$, and evaluate $\mathbf{K}_s^r \mathbf{L}_s (\mathbf{K}_s^r)^{-1}$.

4. The four-pole, three-stack, variable-reluctance stepper motor shown in Fig. 9.2-3 is to be operated at a continuous speed of 30 rad/s. Neglect electrical transients and sketch the current i_{as}, indicating the time at which it is zero and nonzero.

5. A four-pole, five-stack, variable-reluctance stepper motor has eight rotor teeth, as shown in Fig. 9.2-4. Its magnetic axes are arranged *as, bs,* cs, *ds,* and *es,* in the counterclockwise direction. Express the self-inductances with the constant angular displacement in terms of step length.

6. Express the self-inductances for the single-stack, variable-reluctance stepper motor shown in Fig. 9.5-1 with the constant angular displacement in terms of step length.

7. A two-phase, permanent-magnet stepper motor has 50 rotor teeth. When the rotor is driven by an external mechanical source at ω_{rm} =100 rad/s, the measured open-circuit phase voltage is 25 V, peak to peak. Calculate λ_m and SL. If i_{as} =1 A, $i_{bs} = 0$, express T_e.

8. Consider the two-phase, permanent-magnet stepper motor of Fig. 9.6-1. Sketch i_{as} and i_{bs} versus time for the excitation sequence i_{as}, i_{bs}, $-i_{as}$,$-i_{bs}$, i_{as}... . Denote the time between steps as T_s and the stepping rate as $f_s = 1/T_s$. Establish a relationship between the fundamental frequency (ω_e) of i_{as} and i_{bs}, and the stepping rate f_s. Relate ω_{rm} to ω_e and to f_s.

9. A two-phase, permanent-magnet stepper motor has 50 rotor teeth. The parameters are $\lambda'_m = 0.00226$ V $\cdot$ s/rad, $r_s = 10\,\Omega$, and $L_{ss} = 1.1$ mH. The applied stator voltages form a balanced two-phase set with $V_s = 10$ V, $\omega_e = 314$ rad/s. Establish the steady-state rotor speed ω_{rm} and the maximum electromagnetic torque T_{eM} that can be developed at this speed.

* 10. Consider a permanent-magnet stepper motor. Neglect the reluctance torques and assume that the self-inductances are constant. Use the transformation to the rotor reference frame set forth in Chapter 8, (8.5-4), with θ_r replaced by $RT\ \theta_{rm}$ to express the voltage equations for v^r_{qs} and v^r_{ds} similar to (9.8-15) and (9.8-16).

* 11. The permanent-magnet stepper motor shown in Fig. 9.6-1 is equipped with bifilar windings. Assume that the *cs* winding (*ds* winding) is wound on the same stator pole as the *as* winding (*bs* winding) but opposite to it, and also assume that the windings are tightly coupled (no leakage inductances). Express $v_{as} - v_{cs}$ and $v_{bs} - v_{ds}$.

Chapter 10

UNBALANCED OPERATION AND SINGLE-PHASE INDUCTION MOTORS

10.1 INTRODUCTION

Although the voltage and torque equations derived in Chapter 6 for the induction machine are valid regardless of the mode of operation, we focused on balanced conditions. However, when the symmetrical two-phase induction motor is used as a single-phase motor, the stator phase voltages are normally unbalanced. Household power is generally single-phase and single-phase induction motors are used in washers, dryers, air conditioners, garbage disposals, and so on. Symmetrical two-phase induction motors are often used in these single-phase applications; however, in order to develop a starting torque, it is necessary to make the symmetrical two-phase induction motor think it is being supplied from a two-phase source or, at least, something that resembles a two-phase source. We will find that this can be accomplished by placing a capacitor in series with one of the stator phase windings until the rotor has accelerated to 60 to 80 percent of normal operating speed, whereupon the capacitor and the phase winding are disconnected from the source. The motor then operates with only one of its phases connected to the single-phase source. Hence, there are two common modes of unbalanced operation of a symmetrical two-phase induction motor when used as a single-phase device: first, during starting, the phase voltages are not a balanced two-phase set and the input impedance of one phase is different from the other owing to the series capacitor, and second, during normal operation one stator phase is open-circuited.

To analyze steady-state unbalanced operation of an induction machine, it is convenient to use the method of symmetrical components. This method is introduced in the following section and used to analyze unbalanced stator voltages, unequal stator impedances, and an open-circuited stator phase. All of these modes of operation occur either during operation as a symmetrical two-phase induction motor or as a single-phase induction motor.

In this chapter, steady-state and dynamic characteristics are illustrated for single-phase applications; however, only the symmetrical two-phase induction motor is considered in this chapter. Actually the unsymmetrical two-phase induction motor or the so called *split-phase* induction motor is often used rather than its symmetrical two-phase cousin. Although the last section of this chapter is devoted to a brief discussion of the split-phase machine, it is not analyzed. We have chosen to illustrate the salient operating features of single-phase induction machines by using the symmetrical device since it is far easier to analyze than the split-phase machine.

10.2 SYMMETRICAL COMPONENTS

We must deal with unbalanced conditions in the analysis of steady-state operation of the symmetrical two-phase induction motor when used in single-phase applications. This can be accomplished by using what is referred to as the method of symmetrical components. C. L. Fortescue [1] published the method of symmetrical components for the purpose of analyzing unbalanced multiphase systems. Since that time, this method has been extended, modified, and used widely, sometimes inappropriately. Nevertheless, it is a powerful analytical tool for steady-state unbalanced operation of symmetrical systems, even though the derivation and the procedure for applying this method often seemed to be without theoretical basis. It has been shown, however, that reference frame theory provides a rigorous derivation of the method of symmetrical components and sets clear guidelines for its application [2]. In this section, we will describe the concept of symmetrical components without derivation and establish the equations necessary to conduct the analysis of unbalanced operation. A theoretical justification of the concept of symmetrical components using reference frame theory is found in [2] and [3].

For convenience, Fig. 6.2-1 of the two-pole two-phase symmetrical induction machine is repeated in Fig. 10.2-1. The method of symmetrical components allows us to represent an unbalanced two-phase set as two balanced sets or an unbalanced three-phase set as two balanced sets and a single phasor. The balanced sets are referred to as the *positive-sequence* and *negative-sequence* components, and the single phasor is called the *zero-sequence* component. Here, we will deal only with a two-phase system. Also, the method of symmetrical components is valid only for steady-state conditions.

In general, an unbalanced two-phase set may be expressed as

$$F_{as} = \sqrt{2}\,F_a \cos[\omega_e t + \theta_{efa}(0)] \tag{10.2-1}$$

$$F_{bs} = \sqrt{2}\,F_b \sin[\omega_e t + \theta_{efb}(0)] \tag{10.2-2}$$

We realize that (10.2-1) and (10.2-2) form a balanced set if $F_a = F_b$ and $\theta_{efa}(0) = \theta_{efb}(0)$. It is convenient for us to work with qs^s and ds^s variables

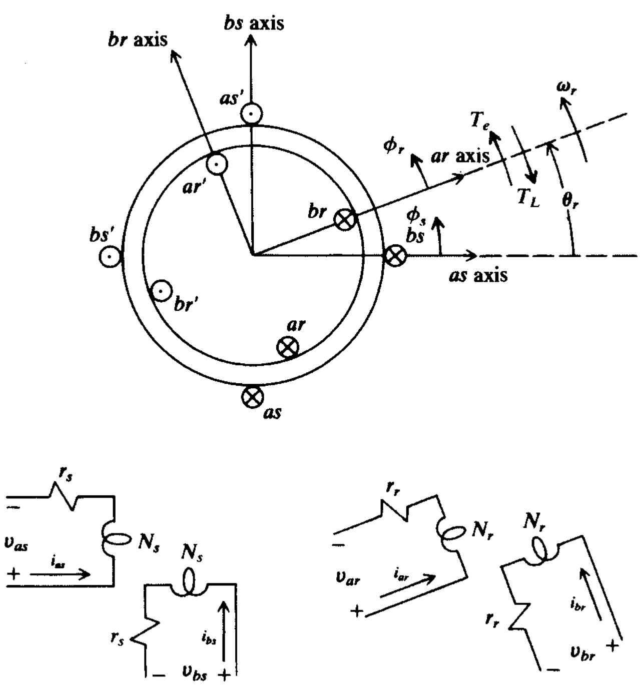

Figure 10.2-1: A two-pole, two-phase symmetrical induction machine.

rather than as and bs variables. Recall from Chapter 5 that with $\omega = \omega_e$ and $\theta(0) = 0$, $f_{as} = f_{qs}^s$ and $f_{bs} = -f_{ds}^s$ or $\tilde{F}_{as} = \tilde{F}_{qs}^s$ and $\tilde{F}_{bs} = -\tilde{F}_{ds}^s$ in the steady state.

It can be shown that an unbalanced two-phase set may be broken up into two balanced sets as

$$\tilde{F}_{qs}^s = \tilde{F}_{qs+}^s + \tilde{F}_{qs-}^s \tag{10.2-3}$$

$$\tilde{F}_{ds}^s = \tilde{F}_{ds+}^s + \tilde{F}_{ds-}^s \tag{10.2-4}$$

Here, we are departing somewhat from tradition. Rather than using $qs^s$and ds^s variables, it has been customary to use as and bs variables and, hence, (10.2-3) and (10.2-4) are written, respectively, as $\tilde{F}_{as} = \tilde{F}_{as+} + \tilde{F}_{as-}$ and $\tilde{F}_{bs} = \tilde{F}_{bs+} + \tilde{F}_{bs-}$. Later, we will substitute $\tilde{F}_{as}$ for $\tilde{F}_{qs}^s$ and $\tilde{F}_{bs}$ for $-\tilde{F}_{ds}^s$; however, for purposes of convenience, we will continue the break from tradition and use $\tilde{F}_{qs+}^s$, $\tilde{F}_{qs-}^s$, $\tilde{F}_{ds+}^s$, and $\tilde{F}_{ds-}^s$ rather than $\tilde{F}_{as+}$, $\tilde{F}_{as-}$, $-\tilde{F}_{bs+}$ and $-\tilde{F}_{bs-}$, respectively.

In (10.2-3) and (10.2-4), $\tilde{F}_{qs+}^s$ and $\tilde{F}_{ds+}^s$ form the balanced, positive-sequence set, where

$$\tilde{F}_{ds+}^s = j\tilde{F}_{qs+}^s \tag{10.2-5}$$

The negative-sequence set is $\tilde{F}_{qs-}^s$ and $\tilde{F}_{ds-}^s$ where

$$\tilde{F}_{ds-}^s = -j\tilde{F}_{qs-}^s \tag{10.2-6}$$

Both the positive- and negative-sequence sets are balanced, but in the case of the positive-sequence set $\tilde{F}_{ds+}^s$ leads $\tilde{F}_{qs+}^s(\tilde{F}_{bs+}$ lags $\tilde{F}_{as+})$ by 90°, whereas in the case of the negative-sequence set $\tilde{F}_{ds-}^s$ lags $\tilde{F}_{qs-}^s$ $(\tilde{F}_{bs-}$ leads $\tilde{F}_{as-})$. Why is one set called the positive sequence and the other the negative sequence? Well, probably the best explanation is to point out that positive-sequence currents flowing in the stator windings (Fig. 10.2-1) will produce an air-gap mmf that rotates counterclockwise, whereas negative-sequence currents will produce an air-gap mmf that rotates clockwise. (Do not forget that $\tilde{F}_{bs+} = -\tilde{F}_{ds+}$ and $\tilde{F}_{bs-} = -\tilde{F}_{ds}$.) It should be apparent that if $\tilde{F}_{as}$ and $\tilde{F}_{bs}$ are balanced with $\tilde{F}_{bs} = -j\tilde{F}_{as}$, then the negative-sequence variables ($\tilde{F}_{qs-}^s$ and $\tilde{F}_{ds-}^s$) would not exist.

Substituting (10.2-5) and (10.2-6) into (10.2-3) and (10.2-4) yields

$$\begin{bmatrix} \tilde{F}_{qs}^{s} \\ \tilde{F}_{ds}^{s} \end{bmatrix} = \begin{bmatrix} 1 & 1 \\ j & -j \end{bmatrix} \begin{bmatrix} \tilde{F}_{qs+}^{s} \\ \tilde{F}_{qs-}^{s} \end{bmatrix} \tag{10.2-7}$$

Now let us substitute $\tilde{F}_{as}$ for $\tilde{F}_{qs}^{s}$ and $\tilde{F}_{bs}$ for $-\tilde{F}_{ds}^{s}$, whereupon

$$\begin{bmatrix} \tilde{F}_{as} \\ \tilde{F}_{bs} \end{bmatrix} = \begin{bmatrix} 1 & 1 \\ -j & j \end{bmatrix} \begin{bmatrix} \tilde{F}_{qs+}^{s} \\ \tilde{F}_{qs-}^{s} \end{bmatrix} \tag{10.2-8}$$

Solving for $\tilde{F}_{qs+}^{s}$ and $\tilde{F}_{qs-}^{s}$ yields

$$\begin{bmatrix} \tilde{F}_{qs+}^{s} \\ \tilde{F}_{qs-}^{s} \end{bmatrix} = \tfrac{1}{2} \begin{bmatrix} 1 & j \\ 1 & -j \end{bmatrix} \begin{bmatrix} \tilde{F}_{as} \\ \tilde{F}_{bs} \end{bmatrix} \tag{10.2-9}$$

The symmetrical-component transformation matrix is defined from (10.2-9) as

$$\mathbf{S} = \frac{1}{2} \begin{bmatrix} 1 & j \\ 1 & -j \end{bmatrix} \tag{10.2-10}$$

and

$$(\mathbf{S})^{-1} = \begin{bmatrix} 1 & 1 \\ -j & j \end{bmatrix} \tag{10.2-11}$$

Example 10A. The steady-state variables of an unbalanced two-phase system are

$$\tilde{F}_{as} = 1\underline{/45^\circ} \tag{10A-1}$$

$$\tilde{F}_{bs} = \frac{1}{2}\underline{/-120^\circ} \tag{10A-2}$$

Calculate $\tilde{F}_{qs+}^{s}$ and $\tilde{F}_{qs-}^{s}$. Substituting into (10.2-9),

$$\begin{bmatrix} \tilde{F}_{qs+}^{s} \\ \tilde{F}_{qs-}^{s} \end{bmatrix} = \frac{1}{2} \begin{bmatrix} 1 & j \\ 1 & -j \end{bmatrix} \begin{bmatrix} 1\underline{/45^\circ} \\ \tfrac{1}{2}\underline{/-120^\circ} \end{bmatrix} \tag{10A-3}$$

From which

$$\begin{aligned} \tilde{F}_{qs+}^{s} &= \frac{1}{2}\left(1\underline{/45^\circ} + j\frac{1}{2}\underline{/-120^\circ}\right) \\ &= \tfrac{1}{2}\underline{/45^\circ} + \tfrac{1}{4}\underline{/-30^\circ} \\ &= 0.570 + j0.229 = 0.614\underline{/21.9^\circ} \end{aligned} \tag{10A-4}$$

$$\begin{aligned}\tilde{F}_{qs-}^{s} &= \tfrac{1}{2}\left(1\underline{/45^\circ} - j\tfrac{1}{2}\underline{/-120^\circ}\right)\\ &= \tfrac{1}{2}\underline{/45^\circ} - \tfrac{1}{4}\underline{/-30^\circ}\\ &= 0.137 + j0.479 = 0.498\underline{/74.0^\circ}\end{aligned} \tag{10A-5}$$

SP10.2-1 $\tilde{F}_{as} = \tilde{F}_{bs} = F_s\underline{/0^\circ}$, determine $\tilde{F}_{qs+}^{s}$ and $\tilde{F}_{qs-}^{s}$ where the asterisk denotes the conjugate. $[\tilde{F}_{qs-}^{s} = \tilde{F}_{qs+}^{s*} = (\sqrt{2}/2)F_s\ \underline{/45^\circ}\ ]$.

SP10.2-2 Express $\tilde{F}_{bs}$ in terms of $\tilde{F}_{as}$ so that the positive-sequence component is zero. $[\tilde{F}_{bs} = j\tilde{F}_{as}]$

SP10.2-3 $\tilde{F}_{ds+}^{s} = \tilde{F}_{ds-}^{s}$ determine $\tilde{F}_{as}$ and $\tilde{F}_{bs}$. $[\tilde{F}_{as} = 0,\ \tilde{F}_{bs} = -2j\tilde{F}_{qs+}^{s}]$

10.3 ANALYSIS OF UNBALANCED MODES OF OPERATION

The rotor windings of the two-phase induction machine are short-circuited (squirrel-cage windings). In this analysis, the rotor speed is assumed to be constant, whereupon, the equations that describe constant-speed operation are linear and the principle of superposition applies. Therefore, the substitute variables ($F_{qr}^{\prime s}$ and $F_{dr}^{\prime s}$) for the rotor variables may be broken up into positive- and negative-sequence quantities in the same manner as F_{qs}^{s} and F_{ds}^{s}. In particular, we can write

$$\tilde{F}_{qr}^{\prime s} = \tilde{F}_{qr+}^{\prime s} + \tilde{F}_{qr-}^{\prime s} \tag{10.3-1}$$

$$\tilde{F}_{dr}^{\prime s} = \tilde{F}_{dr+}^{\prime s} + \tilde{F}_{dr-}^{\prime s} \tag{10.3-2}$$

and

$$\tilde{F}_{dr+}^{\prime s} = j\tilde{F}_{qr+}^{\prime s} \tag{10.3-3}$$

$$\tilde{F}_{dr-}^{\prime s} = -j\tilde{F}_{qr-}^{\prime s} \tag{10.3-4}$$

Armed with this information, let us see what we can derive in the way of voltage equations. It is left to the reader to show that (6A-1) through (6A-4), which are the voltage equations for a two-phase induction machine in the stationary reference frame, become the following set of voltage equations for steady-state conditions:

$$\begin{bmatrix} \tilde{V}_{qs}^{s} \\ \tilde{V}_{ds}^{s} \\ \tilde{V}_{qr}^{\prime s} \\ \tilde{V}_{dr}^{\prime s} \end{bmatrix} = \begin{bmatrix} r_s + j\omega_e L_{ss} & 0 & j\omega_e L_{ms} & 0 \\ 0 & r_s + j\omega_e L_{ss} & 0 & j\omega_e L_{ms} \\ j\omega_e L_{ms} & -\omega_r L_{ms} & r_r' + j\omega_e L_{rr}' & -\omega_r L_{rr}' \\ \omega_r L_{ms} & j\omega_e L_{ms} & \omega_r L_{rr}' & r_r' + j\omega_e L_{rr}' \end{bmatrix} \begin{bmatrix} \tilde{I}_{qs}^{s} \\ \tilde{I}_{ds}^{s} \\ \tilde{I}_{qr}^{\prime s} \\ \tilde{I}_{dr}^{\prime s} \end{bmatrix} \tag{10.3-5}$$

Since for constant rotor speed ω_r the voltage equations are linear, superposition applies. Thus, we can express the four equations of (10.3-5) twice: once for the positive-sequence variables and once for the negative-sequence variables. This gives two sets of four equations each. One set relates the positive-sequence voltages and currents, the other relates the negative-sequence voltages and currents. However, since $\tilde{F}_{ds+}^{s} = j\tilde{F}_{qs+}^{s}$, $\tilde{F}_{dr+}^{\prime s} = j\tilde{F}_{qr+}^{\prime s}$, $\tilde{F}_{ds-}^{s} = -j\tilde{F}_{qs-}^{s}$, and $\tilde{F}_{dr-}^{\prime s} = -j\tilde{F}_{qr-}^{\prime s}$, the eight equations can be reduced back to four. If the d-variables are expressed in terms of the q-variables, the four equations are

$$\begin{bmatrix} \tilde{V}_{qs+}^{s} \\ \dfrac{\tilde{V}_{qr+}^{\prime s}}{s} \\ \tilde{V}_{qs-}^{s} \\ \dfrac{\tilde{V}_{qr-}^{\prime s}}{2-s} \end{bmatrix} = \begin{bmatrix} r_s + jX_{ss} & jX_{ms} & 0 & 0 \\ jX_{ms} & \dfrac{r_r'}{s} + jX_{rr}' & 0 & 0 \\ 0 & 0 & r_s + jX_{ss} & jX_{ms} \\ 0 & 0 & jX_{ms} & \dfrac{r_r'}{2-s} + jX_{rr}' \end{bmatrix} \begin{bmatrix} \tilde{I}_{qs+}^{s} \\ \tilde{I}_{qr+}^{\prime s} \\ \tilde{I}_{qs-}^{s} \\ \tilde{I}_{qr-}^{\prime s} \end{bmatrix} \tag{10.3-6}$$

where

$$X_{ss} = \omega_e(L_{ls} + L_{ms}) \tag{10.3-7}$$

$$X_{rr}' = \omega_e(L_{lr}' + L_{ms}) \tag{10.3-8}$$

$$X_{ms} = \omega_e L_{ms} \tag{10.3-9}$$

$$s = \frac{\omega_e - \omega_r}{\omega_e} \tag{10.3-10}$$

We realize that at any time we can change to the notation generally used by replacing $\tilde{F}_{qs+}^{s}$ with $\tilde{F}_{as+}$, $\tilde{F}_{qr+}^{\prime s}$ with $\tilde{F}_{ar+}'$, and so on.

When we look at (10.3-6), we see that the positive- and negative-sequence variables are decoupled. From this, we might be led to believe that the positive- and negative-sequence variables may be considered separately regardless of the mode of operation of the induction motor. Although the voltage equations given by (10.3-6) provide a starting point, system constraints may cause the positive- and negative-sequence variables to be coupled. In the modes of operation that we will consider, we shall find that the sequence variables are decoupled when unbalanced voltages are applied to a symmetrical two-phase induction motor but coupled when an impedance is placed in series with one of the stator phase windings or when one of the stator phase windings is open-circuited.

The expression for the steady-state electromagnetic torque may be obtained by expressing (6.7-1) in terms of steady-state, stationary reference frame currents:

$$T_e = \frac{P}{2} L_{ms}(I_{qs}^s I_{dr}^{\prime s} - I_{ds}^s I_{qr}^{\prime s}) \tag{10.3-11}$$

The instantaneous steady-state currents may each be expressed in terms of positive- and negative-sequence components. In particular, let

$$I_{qs}^s = \sqrt{2}\, I_{s+} \cos(\omega_e t + \phi_{s+}) + \sqrt{2}\, I_{s-} \cos(\omega_e t + \phi_{s-}) \tag{10.3-12}$$

$$I_{ds}^s = -\sqrt{2}\, I_{s+} \sin(\omega_e t + \phi_{s+}) + \sqrt{2}\, I_{s-} \sin(\omega_e t + \phi_{s-}) \tag{10.3-13}$$

$$I_{qr}^{\prime s} = \sqrt{2}\, I_{r+}^{\prime} \cos(\omega_e t + \phi_{r+}) + \sqrt{2}\, I_{r-}^{\prime} \cos(\omega_e t + \phi_{r-}) \tag{10.3-14}$$

$$I_{dr}^{\prime s} = -\sqrt{2}\, I_{r+}^{\prime} \sin(\omega_e t + \phi_{r+}) + \sqrt{2}\, I_{r-}^{\prime} \sin(\omega_e t + \phi_{r-}) \tag{10.3-15}$$

where the + and − subscripts denote positive- and negative-sequence quantities, respectively. If these expressions for the currents are substituted into (10.3-11) and with a few trigonometric identities, we can express the steady-state (constant-speed) torque as

$$\begin{aligned} T_e = 2\left(\frac{P}{2}\right) L_{ms}[&I_{s+}I_{r+}^{\prime} \sin(\phi_{s+} - \phi_{r+}) - I_{s-}I_{r-}^{\prime} \sin(\phi_{s-} - \phi_{r-}) \\ &+ I_{s+}I_{r-}^{\prime} \sin(2\omega_e t + \phi_{s+} + \phi_{r-}) - I_{s-}I_{r+}^{\prime} \sin(2\omega_e t + \phi_{s-} + \phi_{r+})] \end{aligned} \tag{10.3-16}$$

It is interesting that with the assumption of symmetrical rotor circuits, the electromagnetic torque during steady-state unbalanced operation is made up of a constant and a sinusoidal component that pulsates at twice the frequency of the stator variables. Recall that we have assumed that the steady-state stator variables contain only one frequency, ω_e. Multiple frequencies are treated in [2] and [3].

The above equation for torque may be expressed in terms of positive- and negative-sequence current phasors. After considerable work,

$$\begin{aligned} T_e = 2\frac{P}{2}L_{ms}\{&Re[j(\tilde{I}_{qs+}^{s*}\tilde{I}_{qr+}^{\prime s} - \tilde{I}_{qs-}^{s*}\tilde{I}_{qr-}^{\prime s})] \\ &+Re[j(-\tilde{I}_{qs+}^{s}\tilde{I}_{qr-}^{\prime s} + \tilde{I}_{qs-}^{s}\tilde{I}_{qr+}^{\prime s})]\cos 2\omega_e t \\ &+Re[\tilde{I}_{qs+}^{s}\tilde{I}_{qr-}^{\prime s} - \tilde{I}_{qs-}^{s}\tilde{I}_{qr+}^{\prime s}]\sin 2\omega_{et}\} \end{aligned} \tag{10.3-17}$$

where the asterisk denotes the conjugate. The constant term [first term on right-hand side of (10.3-17)] is made up of the positive-sequence torque and the negative-sequence torque. The last two terms, which represent the pulsating torque component, could be combined; however, separate terms are somewhat more convenient.

Unbalanced Stator Voltages

During the starting period of a single-phase induction motor, a capacitor is placed in series with one of the windings. This type of imbalance, wherein the stator circuits appear unsymmetrical to the source because of the series capacitor, must be analyzed differently than when the stator circuits are symmetrical. We will consider the case of unbalanced source voltages applied to a symmetrical machine first and leave the series capacitor case for later.

Let us return to the voltage equations given by (10.3-6). We can apply these equations directly to solve for the sequence currents with unbalanced source voltages applied to the stator windings of a symmetrical machine. We need only to determine $\tilde{V}_{qs+}^{s}$ and $\tilde{V}_{qs-}^{s}$ from $\tilde{V}_{as}$ and $\tilde{V}_{bs}$ by (10.2-9). We know that, since the rotor windings are short-circuited, $\tilde{V}_{qr+}^{\prime s}$ and $\tilde{V}_{qr-}^{\prime s}$ are zero.

Since this unbalanced mode of operation is described by positive- and negative-sequence quantities that are decoupled, it is instructive to portray the four voltage equations given by (10.3-6) in equivalent-circuit form as shown in Fig. 10.3-1. The positive-sequence equivalent circuit is identical in form to that given for balanced conditions in Fig. 6.8-1 with the rotor windings short-circuited. This was expected. The negative-sequence equivalent circuit differs only in that the slip s is replaced by $2 - s$. Recall that the

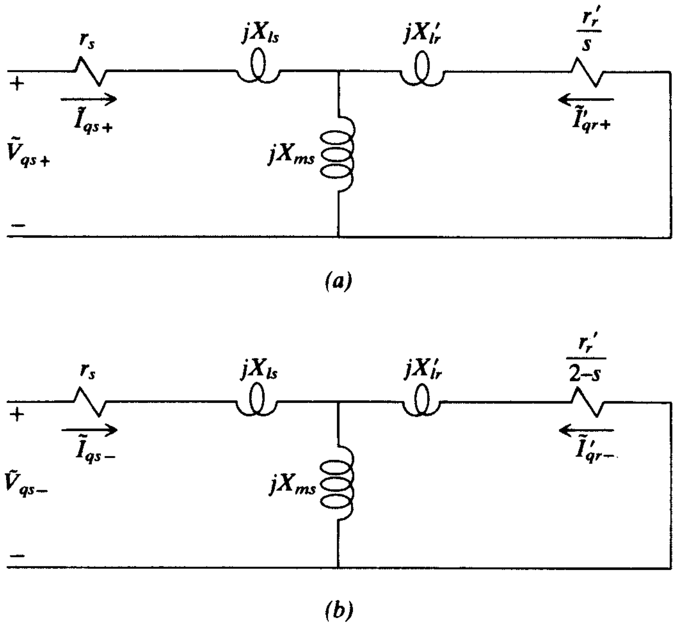

Figure 10.3-1: Equivalent-sequence circuits for unbalanced source voltages applied to a symmetrical two-phase induction motor. (a) Positive sequence; (b) negative sequence.

negative-sequence voltages cause negative-sequence currents which, in turn, cause a negatively rotating air-gap mmf. With respect to this negatively rotating air-gap mmf, the slip is $(\omega_e + \omega_r)/\omega_e$, which is $2 - (\omega_e - \omega_r)/\omega_e$ or $2 - s$. This line of reasoning is often used to obtain the negative-sequence equivalent circuit in place of a derivation.

Equation (10.3-6) or the equivalent circuits that come from (10.3-6) can be used to solve for the sequence currents. The steady-state electromagnetic torque can then be calculated by appropriate substitution of the sequence currents into (10.3-17). Since the positive- and negative-sequence circuits are decoupled, the positive- and negative-sequence torques may be expressed from (6.8-26). In particular, the positive-sequence torque, which is due to the product of the positive-sequence currents in the first term on the right-hand side of (10.3-17), may be expressed as

$$T_{e+} = \frac{2(P/2)(X_{ms}^2/\omega_e)r'_r s \left|\tilde{V}_{qs+}^s\right|^2}{[r_s r'_r + s(X_{ms}^2 - X_{ss}X'_{rr})]^2 + (r'_r X_{ss} + s r_s X'_{rr})^2} \tag{10.3-18}$$

The negative-sequence torque, which is due to the product of the negative-sequence currents in the first term on the right-hand side of (10.3-17), may be expressed as

$$T_{e-} = \frac{2(P/2)(X_{ms}^2/\omega_e)r_r'(2-s)\left|\tilde{V}_{qs-}^s\right|^2}{[r_s r_r' + (2-s)(X_{ms}^2 - X_{ss}X_{rr}')]^2 + [r_r' X_{ss} + (2-s)r_s X_{rr}']^2} \tag{10.3-19}$$

Equation (10.3-18) was obtained from (6.8-26) with $\tilde{V}_{as}$ replaced by $\tilde{V}_{qs+}^s$ and (10.3-19) was obtained from (6.8-26) with $\tilde{V}_{as}$ replaced by $\tilde{V}_{qs-}^s$ and s replaced by $(2-s)$. The average torque, $T_{e,\text{ave}}$, is the difference between the positive- and negative-sequence torques:

$$T_{e,\text{ave}} = T_{e+} - T_{e-} \tag{10.3-20}$$

Comparing the first two terms in (10.3-17) with (6.8-21), it is interesting to observe that, although torque, in general, is a nonlinear function of currents, we can use superposition to establish the total average torque by first calculating the positive- and negative-sequence currents from (10.3-6) or Fig. 10.3-1, then calculating individually the corresponding positive- and negative-sequence torques, and, finally, superimposing the results by using (10.3-20). However, it should be clear that, although superposition may be used to calculate the net average torque, the instantaneous torque (sum of average and pulsating components) cannot be calculated by using superposition since, from (10.3-17), the pulsating torque is related to the product of positive- and negative-sequence currents.

Although we could express the amplitude of the pulsating torque in terms of the sequence voltages, the algebraic manipulations necessary to do so are a bit prohibitive. It is sufficient, for our purposes, to take a little closer look at the phasor relationship $\tilde{I}_{qs+}^s \tilde{I}'^s_{qr-} - \tilde{I}_{qs-}^s \tilde{I}'^s_{qr+}$, which is common to the second and third terms of (10.3-17). With the rotor winding short-circuited, we can express

$$\tilde{I}'^s_{qr+} = -\frac{jX_{ms}}{r_r'/s + jX_{rr}'}\tilde{I}_{qs+}^s \tag{10.3-21}$$

$$\tilde{I}'^s_{qr-} = -\frac{jX_{ms}}{r_r'/(2-s) + jX_{rr}'}\tilde{I}_{qs-}^s \tag{10.3-22}$$

These equations are obtained from the equivalent circuits given in Fig. 10.3-1. Note the similarity between (10.3-21) and (6.8-22). Utilizing (10.3-21) and (10.3-22), we can write

$$\tilde{I}^s_{qs+}\tilde{I}'^s_{qr-} - \tilde{I}^s_{qs-}\tilde{I}'^s_{qr+} = -jX_{ms}\tilde{I}^s_{qs+}I^s_{qs-}\frac{2(1-s)/s(2-s)}{[r'_r/(2-s)+jX'_{rr}](r'_r/s+jX'_{rr})} \tag{10.3-23}$$

If we express the sequence currents in terms of the sequence voltages, we can write (10.3-23) as

$$\tilde{I}^s_{qs+}\tilde{I}'^s_{qr-} - \tilde{I}^s_{qs-}\tilde{I}'^s_{qr+} = -jX_{ms}\frac{\tilde{V}^s_{qs+}}{Z_+}\frac{\tilde{V}^s_{qs-}}{Z_-}\frac{2(1-s)/s(2-s)}{[r'_r/(2-s)+jX'_{rr}](r'_r/s+jX'_{rr})} \tag{10.3-24}$$

where Z_+ and Z_- are the input impedances of the positive- and negative-sequence equivalent circuits (Fig. 10.3-1), respectively.

The form of (10.3-24) allows a somewhat more direct means of calculating the amplitude of the pulsating torque. It is interesting, however, to evaluate (10.3-24) for the condition in which the rotor speed is zero. With $\omega_r = 0$, $s = 1$ and (10.3-24) is zero. Hence, a steady-state pulsating torque does not exist at stall. Actually, the amplitude of the pulsating torque is zero at $\omega_r = 0$ regardless of the stator conditions. That is, an impedance may be in series with one of the stator windings or one winding may be opened-circuited. Regardless of the value of the sequence currents, (10.3-23) is zero when $s = 1$. The only requirement is that the rotor windings must be symmetrical. This is an interesting observation.

Unbalanced Stator Impedances

When an impedance is placed in series with the *as* winding of the stator, we can write

$$e_{ga} = i_{as}z(p) + v_{as} \tag{10.3-25}$$

$$e_{gb} = v_{bs} \tag{10.3-26}$$

where v_{as} and v_{bs} are the voltages across the stator phase windings and e_{ga} and e_{gb} are the source voltages, which may be unbalanced. In (10.3-25), $z(p)$ is the operational notation of the impedance; for example, a series rL would be expressed $z(p) = r+pL$. The phasor equivalents of (10.3-25) and (10.3-26) are

$$\tilde{V}_{as} = \tilde{E}_{ga} - \tilde{I}_{as}Z \tag{10.3-27}$$

$$\tilde{V}_{bs} = \tilde{E}_{gb} \tag{10.3-28}$$

We can apply (10.2-9) to determine $\tilde{V}^s_{qs+}$ and $\tilde{V}^s_{qs-}$ as

$$\begin{bmatrix} \tilde{V}^s_{qs+} \\ \tilde{V}^s_{qs-} \end{bmatrix} = \frac{1}{2}\begin{bmatrix} 1 & j \\ 1 & -j \end{bmatrix}\begin{bmatrix} \tilde{E}_{ga} - \tilde{I}_{as}Z \\ \tilde{E}_{gb} \end{bmatrix} \tag{10.3-29}$$

which yields

$$\tilde{V}^s_{qs+} = \tfrac{1}{2}(\tilde{E}_{ga} + j\tilde{E}_{gb} - \tilde{I}_{as}Z) \tag{10.3-30}$$

$$\tilde{V}^s_{qs-} = \tfrac{1}{2}(\tilde{E}_{ga} - j\tilde{E}_{gb} - \tilde{I}_{as}Z) \tag{10.3-31}$$

Now,

$$\tilde{I}_{as} = \tilde{I}^s_{qs} = \tilde{I}^s_{qs+} + \tilde{I}^s_{qs-} \tag{10.3-32}$$

Substituting (10.3-32) into (10.3-30) and (10.3-31) for $\tilde{I}_{as}$ then substituting the result into (10.3-6), and assuming the rotor windings are short-circuited, we obtain

$$\begin{bmatrix} \tilde{E}_1 \\ 0 \\ \tilde{E}_2 \\ 0 \end{bmatrix} = \begin{bmatrix} \tfrac{1}{2}Z + r_s + jX_{ss} & jX_{ms} & \tfrac{1}{2}Z & 0 \\ jX_{ms} & \dfrac{r'_r}{s} + jX'_{rr} & 0 & 0 \\ \tfrac{1}{2}Z & 0 & \tfrac{1}{2}Z + r_s + jX_{ss} & jX_{ms} \\ 0 & 0 & jX_{ms} & \dfrac{r'_r}{2-s} + jX'_{rr} \end{bmatrix} \begin{bmatrix} \tilde{I}^s_{qs+} \\ \tilde{I}'^s_{qr+} \\ \tilde{I}^s_{qs-} \\ \tilde{I}'^s_{qr-} \end{bmatrix} \tag{10.3-33}$$

where

$$\tilde{E}_1 = \frac{1}{2}(\tilde{E}_{ga} + j\tilde{E}_{gb}) \tag{10.3-34}$$

$$\tilde{E}_2 = \frac{1}{2}(\tilde{E}_{ga} - j\tilde{E}_{gb}) \tag{10.3-35}$$

If the impedance is a series capacitor, then $Z = -j(1/\omega_e C)$. Also, note that the positive- and negative-sequence voltage equations are now coupled. Although we could derive an equivalent circuit to portray these equations, it is not worth the work. We can use (10.3-33) directly; however, a computer would be helpful. We will work more with this equation when we analyze the symmetrical two-phase induction motor used as a single-phase motor.

Open-Circuited Stator Phase

For the analysis of an open-circuited stator phase, let us assume that i_{as} (i_{qs}^s) is zero. Hence, from (6A-1),

$$v_{qs}^s = p\lambda_{qs}^s \tag{10.3-36}$$

Now since $i_{qs}^s = 0$, λ_{qs}^s may be expressed from (6.6-8) in stationary reference frame variables as

$$\lambda_{qs}^s = L_{ms} i_{qr}^{\prime s} \tag{10.3-37}$$

Since $v_{as} = v_{qs}^s$, we can write

$$v_{as} = L_{ms} p i_{qr}^{\prime s} \tag{10.3-38}$$

$$v_{bs} = e_{gb} \tag{10.3-39}$$

where e_{gb} is the source voltage. Now, in phasor form,

$$\tilde{V}_{as} = jX_{ms}\tilde{I}_{qr}^{\prime s} \tag{10.3-40}$$

$$\tilde{V}_{bs} = \tilde{E}_{gb} \tag{10.3-41}$$

Substituting (10.3-40) and (10.3-41) into (10.2-9), we obtain

$$\tilde{V}_{qs+}^s = \tfrac{1}{2}jX_{ms}\tilde{I}_{qr}^{\prime s} + \tfrac{1}{2}j\tilde{E}_{gb} \tag{10.3-42}$$

$$\tilde{V}_{qs-}^s = \tfrac{1}{2}jX_{ms}\tilde{I}_{qr}^{\prime s} - \tfrac{1}{2}j\tilde{E}_{gb} \tag{10.3-43}$$

From (10.3-1),

$$\tilde{I}_{qr}^{\prime s} = \tilde{I}_{qr+}^{\prime s} + \tilde{I}_{qr-}^{\prime s} \tag{10.3-44}$$

and, since $\tilde{I}_{qs}^s = 0$, (10.2-3) becomes

$$\tilde{I}_{qs-}^s = -\tilde{I}_{qs+}^s \tag{10.3-45}$$

Substituting (10.3-44) into (10.3-42) and (10.3-43), then substituting the result into (10.3-6) with (10.3-45) incorporated, we can write (rotor windings short-circuited)

$$\begin{bmatrix} \frac{1}{2}j\tilde{E}_{gb} \\ 0 \\ 0 \end{bmatrix} = \begin{bmatrix} r_s + jX_{ss} & j\frac{1}{2}X_{ms} & -j\frac{1}{2}X_{ms} \\ jX_{ms} & \frac{r'_r}{s} + jX'_{rr} & 0 \\ -jX_{ms} & 0 & \frac{r'_r}{2-s} + jX'_{rr} \end{bmatrix} \begin{bmatrix} \tilde{I}^s_{qs+} \\ \tilde{I}'^s_{qr+} \\ \tilde{I}'^s_{qr-} \end{bmatrix} \tag{10.3-46}$$

From (10.3-40), the open-circuit voltage of the *as* winding is

$$\tilde{V}_{as} = jX_{ms}(\tilde{I}'^s_{qr+} + \tilde{I}'^s_{qr-}) \tag{10.3-47}$$

where $\tilde{I}'^s_{qr+}$ and $\tilde{I}'^s_{qr-}$ are calculated from (10.3-46). If the open-circuit voltage is not of interest, then $\tilde{I}'^s_{qr+}$ and $\tilde{I}'^s_{qr-}$ may be eliminated from (10.3-46).

SP10.3-1 Determine the rotor speed at which the negative-sequence rotor currents $\tilde{I}'^s_{qr-}$ and $\tilde{I}'^s_{dr-}$ are zero for unbalanced applied stator voltages. $[\omega_r = -\omega_e]$
SP10.3-2 Assume that the steady-state T_e versus ω_r plot shown in Fig. 6.8-2 is for $\tilde{V}_{as} = j\tilde{V}_{bs} = 1\underline{/0^\circ}$. Plot the T_e versus ω_r for $\tilde{V}_{as} = -j\tilde{V}_{bs} = 1\underline{/0^\circ}$. [Inverted mirror image]
SP10.3-3 Determine the rotor speed at which $Z_+ = Z_-$ for a symmetrical induction motor. $[\omega_r = 0]$
SP10.3-4 Express Z_+ and Z_- for unbalanced stator voltages. [$Z_+ =$ (6.8-24), $Z_- =$ (6.8-24) with s replaced by $2 - s$]
SP10.3-5 Express v_{bs} when $i_{bs} = 0$. $[v_{bs} = -L_{ms}pi'^s_{dr}]$

10.4 SINGLE-PHASE INDUCTION MOTORS

In Chapter 4, we talked briefly about single-phase induction motors. Although we will find that we must provide some means of starting the device, the single-phase induction motor has only one stator winding energized during normal operation. With this in mind, let us calculate the steady-state torque-versus-speed characteristics with voltage applied to only one stator winding of a symmetrical two-phase induction motor with the other winding open-circuited. Recall that we have already derived the voltage equations necessary to make these calculations. In particular, (10.3-46) can be used to determine the sequence currents with the *as* winding open-circuited and a voltage source connected to the *bs* winding. Once these calculations are made, the sequence currents may be substituted into (10.3-17) to determine the average and pulsating components of the steady-state electromagnetic torque. The steady-state torque-versus-speed characteristics are shown in Fig. 10.4-1 for a symmetrical two-phase induction motor with rated voltage applied to one phase and the other phase open-circuited. The symmetrical two-phase induction machine is a four-pole, $\frac{1}{4}$-hp, 110-V, 60-Hz motor with the following parameters: $r_s = 2.02\,\Omega$, $X_{ls} = 2.79\,\Omega$, $X_{ms} = 66.8\,\Omega$, $r'_r = 4.12\,\Omega$, and $X'_{lr} = 2.12\,\Omega$. The total inertia is $J = 1.46 \times 10^{-2}\,\mathrm{kg \cdot m^2}$.

The average steady-state electromagnetic torque $T_{e,\mathrm{ave}} = T_{e+} - T_{e-}$ and the magnitude of the double-frequency component of the torque $|T_{e,\mathrm{pul}}|$ are plotted in Fig. 10.4-1. There are at least two features worth mentioning. First, the plot of the average torque $T_{e,\mathrm{ave}}$ for $\omega_{rm} < 0$ is the negative mirror image of that for $\omega_{rm} > 0$. Second, the plot of the pulsating torque $|T_{e,\mathrm{pul}}|$ is symmetrical about the zero-speed axis. Finally, we see verification of our earlier claim that the starting torque is zero; $T_e = 0$ at $\omega_{rm} = 0$.

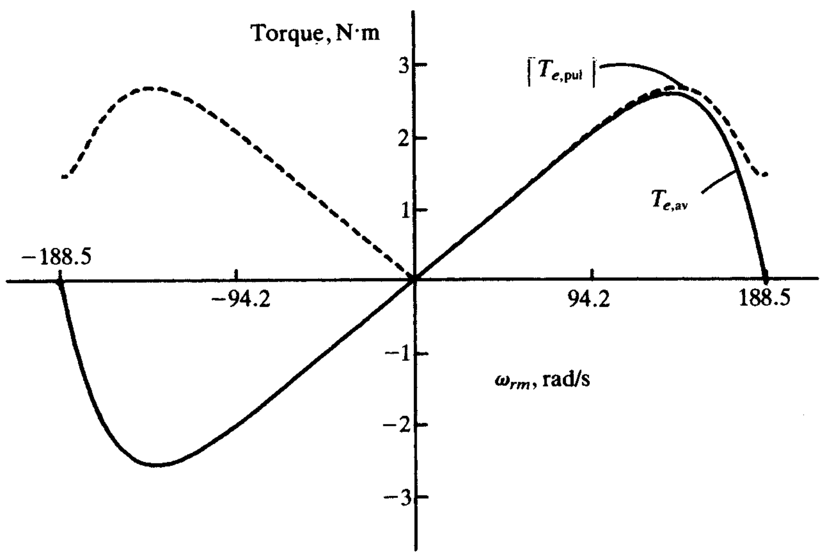

Figure 10.4-1: Steady-state torque-versus-speed characteristics for a single-phase induction motor.

SP10.4-1 Determine the frequency of the rotor currents when ω_{rm} is equal to synchronous speed in Fig. 10.4-1. [120 Hz]

SP10.4-2 For the torque-speed characteristics shown in Fig. 10.4-1, determine the approximate rotor speed at which the steady-state instantaneous torque first pulsates to a negative value. [$\omega_{rm} \cong 1000$ r/min]

10.5 CAPACITOR-START INDUCTION MOTOR

As we know, the single-phase induction motor will not develop a starting torque since two equal and oppositely rotating air-gap mmfs are generated by a sinusoidal winding current. If now we take a two-phase symmetrical induction motor and apply the same single-phase voltage to both phases, the net torque at stall will still be zero since the winding currents will be instantaneously equal and the air-gap mmf will pulsate along an axis midway between the *as* and *bs* axes. Consequently, two equal and oppositely rotating air-gap mmfs again result. If, however, we cause the current in one of the phases to be different instantaneously from that in the other phase, a starting torque can be developed since this would cause one of the rotating air-gap mmfs to be larger than the other. One way of doing this is to place a capacitor in series with one of the windings of a two-phase symmetrical induction motor. This will cause the current in the phase with the series capacitor to lead the current in the other winding when the same voltage is applied to both.

We have already derived the equations necessary to calculate the component currents with an impedance in series with the *as* winding. In particular, (10.3-33) can be used to calculate the component currents with a capacitor in series with the *as* winding. If we set $Z = -j1/\omega_e C$ and let $\tilde{E}_{ga} = \tilde{E}_{gb}$, the single-phase source voltage, counterclockwise rotation will occur since $\tilde{I}_{as}$ will lead $\tilde{I}_{bs}$. Recall that for the assumed positive direction of the magnetic axes and for a balanced two-phase set we have had $\tilde{I}_{as}$ leading $\tilde{I}_{bs}$ by 90° for counterclockwise rotation of the air-gap mmf.

Once the component currents are calculated, (10.3-17) can be used to determine the average steady-state electromagnetic torque $T_{e,\text{ave}}$ and the magnitude of the double-frequency component $|T_{e,\text{pul}}|$. These steady-state torque versus speed characteristics are shown in Fig. 10.5-1 for $C = 530.5\,\mu$F.

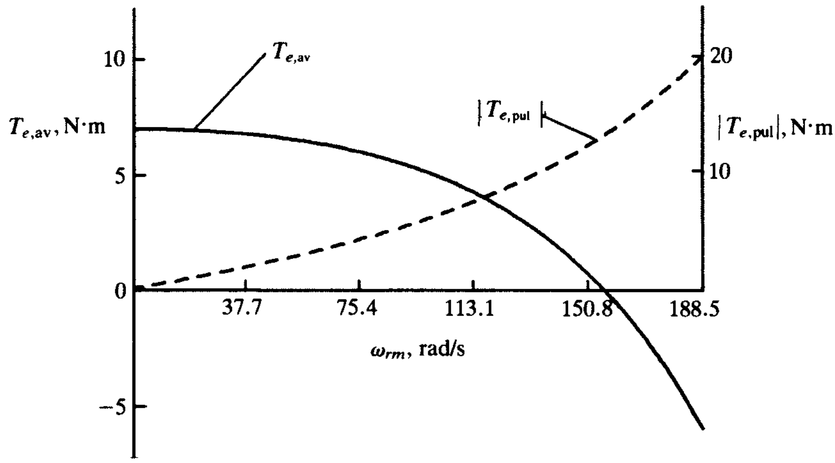

Figure 10.5-1: Steady-state torque-versus-speed characteristics with a capacitor in series with one winding of the two-phase induction machine.

In capacitor-start single-phase induction motors, the winding with the series capacitor is disconnected from the source after the rotor has reached 60 to 80 percent of synchronous speed. This is generally accomplished by using a centrifugal switching mechanism located inside the housing of the motor. Once the winding with the series capacitor is disconnected, the device then operates as a single-phase induction motor. In Fig. 10.5-2, the plot of average torque versus speed with a series capacitor in one phase (Fig. 10.5-1) is superimposed upon the plot of average torque versus speed with a single-phase winding (Fig. 10.4-1). The transition from capacitor-start to single-phase operation at 75 percent of synchronous speed is illustrated.

Although the capacitor-start single-phase induction motor is by far the most common type of single-phase induction motor, a capacitor-start capacitor-run induction motor is sometimes used. In this case, both phase windings are energized during normal operation. The value of the series capacitance is changed from the start value to the run value once the rotor reaches 60 to 80 percent of synchronous speed. This is accomplished by using two capacitors connected in parallel with provision to open-circuit one of the parallel paths. The purpose of the run capacitor is to establish a leading current during normal loads, thereby increasing the torque capability over that which is possible with only one stator winding energized. Since two capacitors are

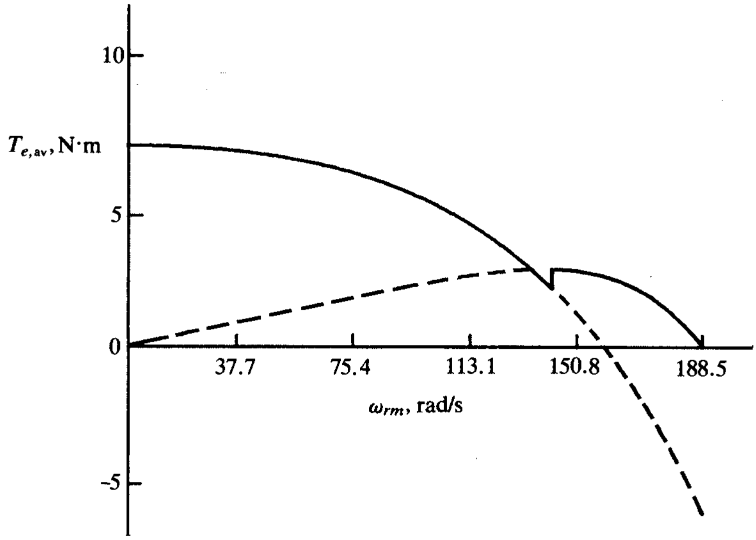

Figure 10.5-2: Average steady-state torque-versus-speed characteristics of a capacitor-start single-phase induction motor.

needed, this device is somewhat more expensive and often the application does not justify this added cost.

SP10.5-1 In Fig. 10.5-2, the device switches from capacitor-start to single-phase operation at a rotor speed of 75 percent of synchronous speed. Will the rotor accelerate faster or slower immediately following the switching? [Faster]

SP10.5-2 If the value of the capacitor were decreased, would you expect the starting torque to decrease or increase? Why? [Decrease, less-leading component of current]

10.6 DYNAMIC AND STEADY-STATE PERFORMANCE OF A CAPACITOR-START SINGLE-PHASE INDUCTION MOTOR

The free-acceleration characteristics of the example capacitor-start single-phase induction motor are shown in Fig. 10.6-1. The variables v_{as}, i_{as}, v_{bs}, i_{bs}, v_c, T_e, and ω_{rm} are plotted. The voltage v_c is the instantaneous voltage across the capacitor that is connected in series with the bs winding. The machine variables are shown with an expanded scale in Fig. 10.6-2 to illustrate the switching out of the bs winding, which is disconnected from the source at a normal current zero once the rotor reaches 75 percent of synchronous speed. The voltage across the capacitor is shown to remain constant at its value when the bs winding is disconnected from the source. In practice, this voltage would slowly decay owing to leakage currents within the capacitor, which are not considered in this analysis. The torque-versus-speed characteristics given in Fig. 10.6-3 are for the free acceleration shown in Fig. 10.6-1. The dynamic and steady-state characteristics following changes in load torque are illustrated in Fig. 10.6-4. Therein v_{as}, $i_{as,}$ v_{bs} (open-circuited), i'_{ar}, T_e, ω_{rm}, and T_L are plotted.

SP10.6-1 In Fig. 10.6-1, The capacitor is in series with the bs winding and the voltage applied to the as winding is $V_{as} = \sqrt{2}\,110\cos\omega_e t$. Calculate the steady-state stator currents I_{as} and I_{bs} at stall ($\omega_{rm} = 0$). Compare with the traces of i_{as} and i_{bs} in Fig 10.6-1. Neglect the magnetizing reactance X_{ms} in these calculations. [$I_{as} \cong 19.8\cos(377t-38.6°)$; $I_{bs} \cong -25.3\cos(377t-0.8°)$]
SP10.6-2 Determine the frequency of I'^s_{qr} and I'^s_{dr} for the loaded condition ($T_L = 1\,\mathrm{N\cdot m}$) in Fig. 10.6-4. [60Hz]

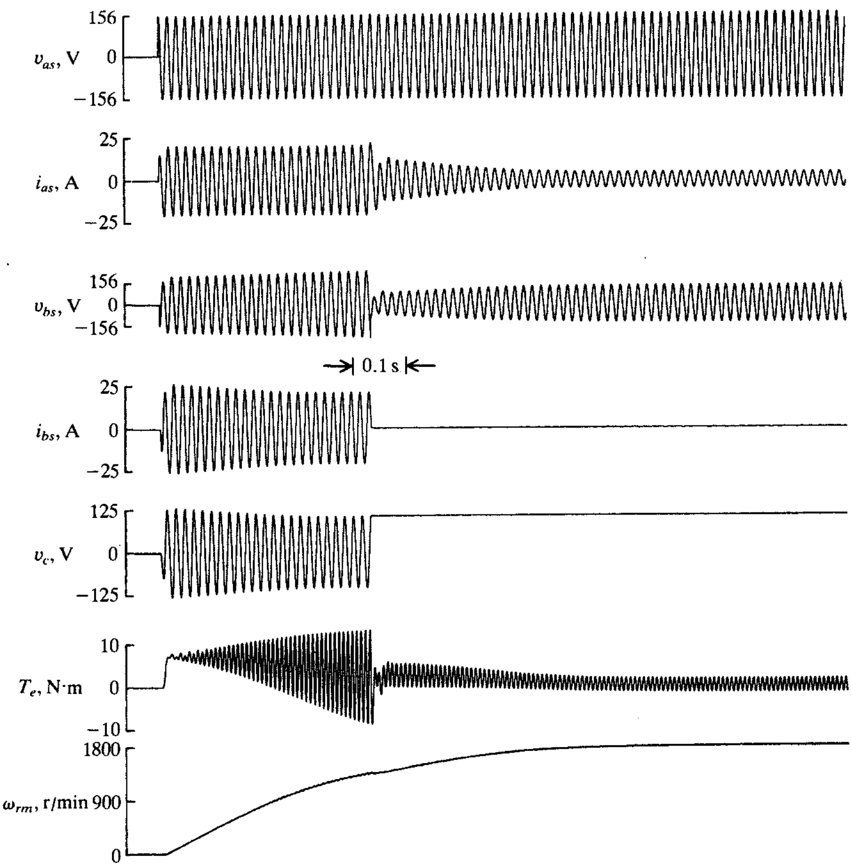

Figure 10.6-1: Free-acceleration characteristics of a capacitor-start, single-phase induction motor.

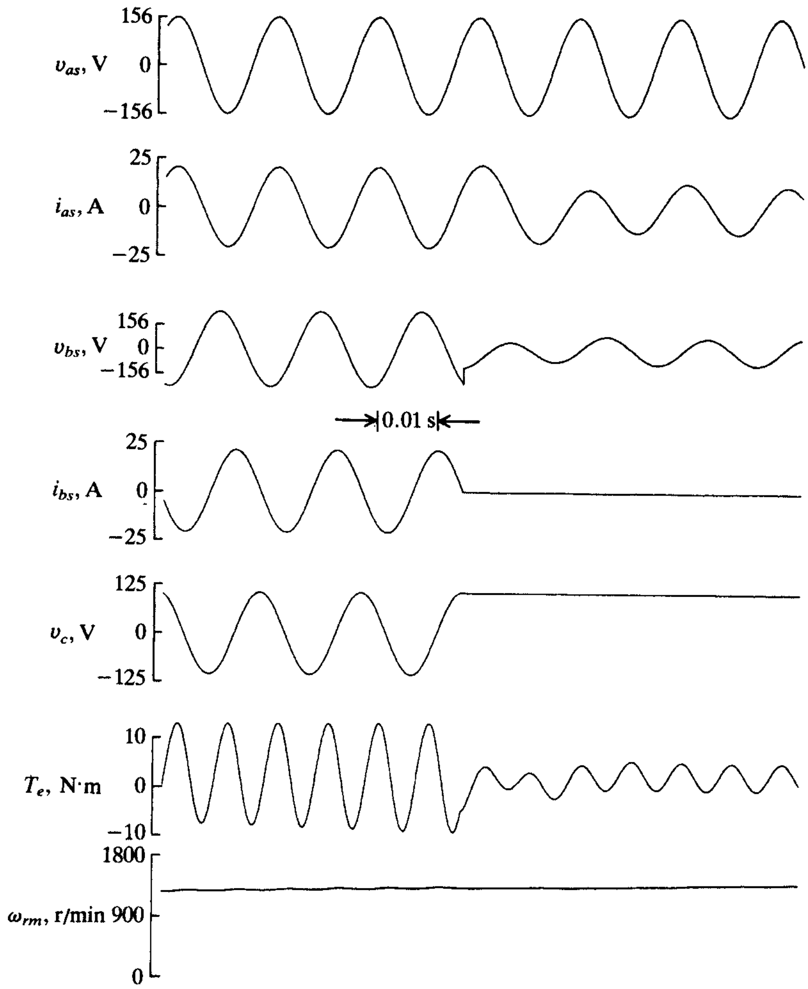

Figure 10.6-2: Expanded plot of Fig. 10.6-1 illustrating the disconnecting of the capacitor in the bs winding.

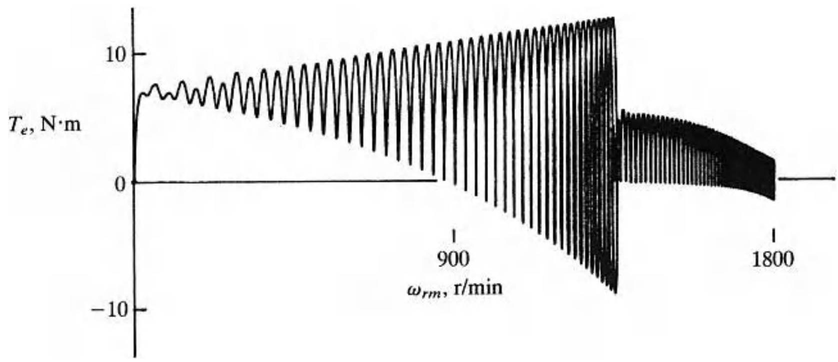

Figure 10.6-3: Torque-versus-speed characteristics for Fig. 10.6-1.

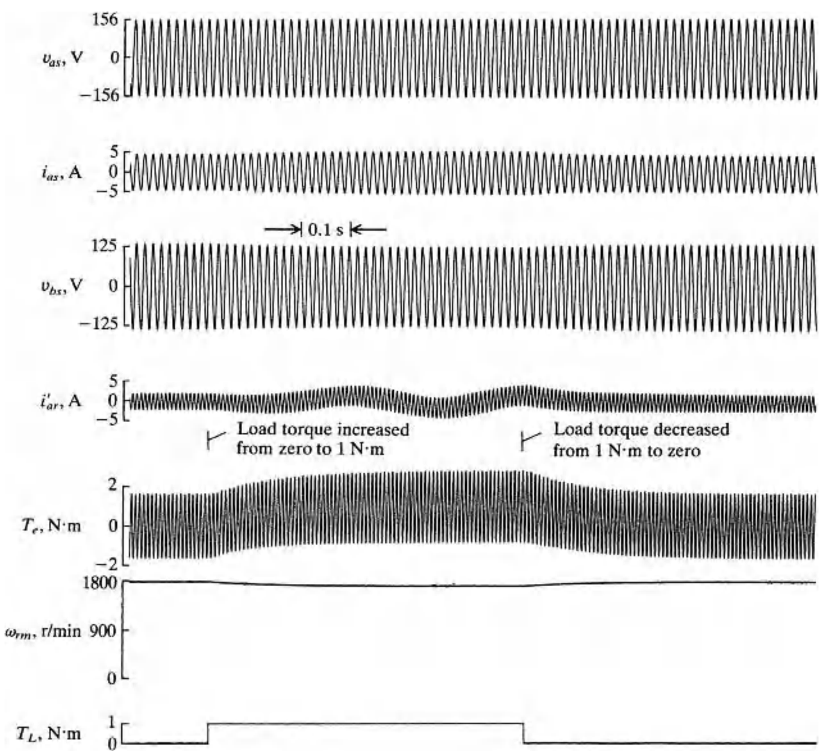

Figure 10.6-4: Step changes in load torque of single-phase induction motor.

10.7 SPLIT-PHASE INDUCTION MOTOR

Although we have considered only the symmetrical two-phase induction motor as a single-phase induction motor, the split-phase induction motor is often used. It is an asymmetrical two-phase induction machine; that is, the stator windings are different. The main or run winding remains energized during normal operation, whereas the start or auxiliary winding is switched out after the rotor reaches 60 to 80 percent of synchronous speed. The r-to-X ratio of the run winding would be much the same as that of the stator windings of a two-phase symmetrical machine; however, the start winding has a higher r-to-X ratio. Hence, with the same voltage applied to the start and run windings, the current flowing in the start winding would lead the current flowing in the run winding. We see the logic behind all of this. Rather than using only a capacitor to shift the phase of one of the winding currents in order to develop a starting torque, the machine is designed with different stator windings so that one current leads the other due to the difference in the winding impedances. Depending on the application and the design of the machine, a capacitor may or may not be used in series with the start winding.

We will not analyze the split-phase induction machine. The analysis is rather involved since the mutual inductances between the rotor windings and the run winding are different from those between the rotor windings and the start winding. Actually, we have established the main operating characteristics of single-phase induction motors with the least amount of effort by considering the symmetrical two-phase machine. If, however, one wishes to consider the split-phase device in more detail, this analysis is given in [3].

10.8 RECAPPING

Even though the analysis of unbalanced steady-state operation of a symmetrical two-phase induction machine is rather involved, it is the easiest of all electromechanical devices to analyze in the unbalanced mode of operation. We have taken advantage of this feature to provide a first look at the method of symmetrical components to analyze unbalanced modes of operation which not only occur in the operation of a single-phase machine but also in three-phase devices.

Although the split-phase induction motor was not analyzed, the application of the symmetrical two-phase induction motor as a single-phase device is sufficient coverage of the single-phase induction motor for our purposes. Even with this rather brief treatment of single-phase induction machines, we have been able to introduce the major operating features of most present-day single-phase induction motors.

10.9 REFERENCES

[1] C. L. Fortescue, "Method of Symmetrical Co-ordinates Applied to the Solution of Polyphase Networks," *AIEE Trans.*, vol. 37, 1918, pp. 1027-1115.

[2] P. C. Krause, "Method of Symmetrical Components Derived by Reference Frame Theory," *IEEE Trans., Power Apparatus and Systems,* vol. 104, June 1985, pp. 1492-1499.

[3] P. C. Krause, O. Wasynczuk, and S. D. Sudhoff, *Analysis of Electric Machinery*, IEEE Press 1^{st} Ed., 1986.

10.10 PROBLEMS

1. Calculate $\tilde{F}^s_{qs+}$ and $\tilde{F}^s_{qs-}$ for the following sets using (10.2-9). (a) $\tilde{F}_{as} = 10\underline{/30^\circ}$, $\tilde{F}_{bs} = 30\underline{/-60^o}$. (b) $\tilde{F}_{as} = 10\underline{/0^\circ}$, $\tilde{F}_{bs} = 0$. (c) $\tilde{F}_{as} = \cos(\omega_e t + 45^\circ)$, $\tilde{F}_{bs} = \cos(\omega_e t - 45^\circ)$.

2. Start with (10.3-5) and derive (10.3-6).

3. Derive (10.3-16).

* 4. Show that (10.3-16) and (10.3-17) are equivalent.

5. Express (10.3-46) with $\tilde{I}^s_{qr+}$ and $\tilde{I}^s_{qr-}$ eliminated.

* 6. The equivalent circuit for steady-state operation of an induction motor with only one stator winding is shown in Fig. 10.10-1. Show that this equivalent circuit is the same as that given by (10.3-46).

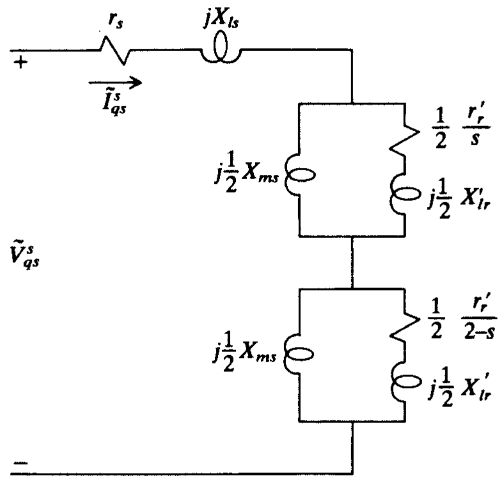

Figure 10.10-1: Equivalent circuit for single-phase stator winding.

Appendix A

ABBREVIATIONS, CONSTANTS, CONVERSIONS, AND IDENTITIES

Term	Abbreviation
alternating current	ac
ampere	A
ampere-turn	At
coulomb	C
direct current	dc
electromotive force	emf
foot	ft
gauss	G
gram	g
henry	H
hertz	Hz
horsepower	hp
inch	in
joule	J
kilogram	kg
kilovar	kvar
kilovolt	kV
kilovoltampere	kVA
kilowatt	kW
magnetomotive force	mmf
maxwell	Mx
megawatt	MW
meter	m
microfarad	μF
millihenry	mH
newton	N
newton meter	$\mathrm{N \cdot m}$
oersted	Oe
pound	lb
poundal	pdl
power factor	pf
pulse-width modulation	PWM
radian	rad
revolution per minute	r/min (rpm)
root mean square	rms
second	s
voltampere reactive	var
volt	V
voltampere	VA
watt	W
weber	Wb

Constants and Conversion Factors

permeability of free space	$\mu_0 = 4\pi \times 10^{-7}$ Wb/A · m
permittivity of free space	$\epsilon_0 = 8.854 \times 10^{-12}$ C^2/N · m^2
acceleration of gravity	$g = 9.807$ m/s^2
length	1 m = 3.218 ft = 39.37 in
mass	1 kg = 0.0685 slug = 2.205 lb (mass)
force	1 N = 0.225 lb = 3.6 oz
torque	1 N · m = 0.738 lb · ft
energy	1 J (W · s) = 0.738 lb · ft
power	1 W = 1.341×10^{-3} hp
moment of inertia	1 kg · m^2 = 0.738 slug · ft^2 = 23.7 lb · ft^2
magnetic flux	1 Wb = 10^8 Mx (lines)
magnetic flux density	1 Wb/m^2 = 10,000 G = 64.5 klines/in^2
magnetizing force	1 At/m = 0.0254 At/in = 0.0126 Oe

Trigonometric Identities

(I-1) $e^{j\alpha} = \cos\,\alpha + j\,\sin\,\alpha$

(I-2) $a\cos x + b\sin x = \sqrt{a^2+b^2}\,\cos(x+\phi) \qquad \phi = \tan^{-1}(-b/a)$

(I-3) $\cos^2 x + \sin^2 x = 1$

(I-4) $\sin 2x = 2\sin x\cos x$

(I-5) $\cos 2x = \cos^2 x - \sin^2 x = 2\,\cos^2 x - 1 = 1 - 2\,\sin^2 x$

(I-6) $\cos x\,\cos y = \frac{1}{2}\cos(x+y) + \frac{1}{2}\cos(x-y)$

(I-7) $\sin x\,\sin y = \frac{1}{2}\cos(x-y) - \frac{1}{2}\cos(x+y)$

(I-8) $\sin x\,\cos y = \frac{1}{2}\sin(x+y) + \frac{1}{2}\sin(x-y)$

(I-9) $\cos(x \pm y) = \cos x\,\cos y \mp \sin x\,\sin y$

(I-10) $\sin(x \pm y) = \sin x\,\cos y \pm \cos x\,\sin y$

(I-11) $\cos^2 x + \cos^2(x - \frac{2}{3}\pi) + \cos^2(x + \frac{2}{3}\pi) = \frac{3}{2}$

(I-12) $\sin^2 x + \sin^2(x - \frac{2}{3}\pi) + \sin^2(x + \frac{2}{3}\pi) = \frac{3}{2}$

(I-13) $\sin x \ \cos x + \sin(x - \frac{2}{3}\pi)\cos(x - \frac{2}{3}\pi) + \sin(x + \frac{2}{3}\pi)\cos(x + \frac{2}{3}) = 0$

(I-14) $\cos x + \cos(x - \frac{2}{3}\pi) + \cos(x + \frac{2}{3}\pi) = 0$

(I-15) $\sin \ x + \sin(x - \frac{2}{3}\pi) + \sin(x + \frac{2}{3}\pi) = 0$

(I-16) $\sin x \cos y + \sin(x - \frac{2}{3}\pi)\cos(y - \frac{2}{3}\pi) + \sin(x + \frac{2}{3}\pi)\cos(y + \frac{2}{3}\pi)$
$= \frac{3}{2}\sin(x - y)$

(I-17) $\sin x \sin y + \sin(x - \frac{2}{3}\pi)\sin(y - \frac{2}{3}\pi) + \sin(x + \frac{2}{3}\pi)\sin(y + \frac{2}{3}\pi)$
$= \frac{3}{2}\cos(x - y)$

(I-18) $\cos x \sin y + \cos(x - \frac{2}{3}\pi)\sin(y - \frac{2}{3}\pi) + \cos(x + \frac{2}{3}\pi)\sin(y + \frac{2}{3}\pi)$
$= -\frac{3}{2}\sin(x - y)$

(I-19) $\cos x \cos y + \cos(x - \frac{2}{3}\pi)\cos(y - \frac{2}{3}\pi) + \cos(x + \frac{2}{3}\pi)\cos(y + \frac{2}{3}\pi)$
$= \frac{3}{2}\cos(x - y)$

(I-20) $\sin x \cos y + \sin(x + \frac{2}{3}\pi)\cos(y - \frac{2}{3}\pi) + \sin(x - \frac{2}{3}\pi)\cos(y + \frac{2}{3}\pi)$
$= \frac{3}{2}\sin(x + y)$

(I-21) $\sin x \sin y + \sin(x + \frac{2}{3}\pi)\sin(y - \frac{2}{3}\pi) + \sin(x - \frac{2}{3}\pi)\sin(y + \frac{2}{3}\pi)$
$= -\frac{3}{2}\cos(x + y)$

(I-22) $\cos x \sin y + \cos(x + \frac{2}{3}\pi)\sin(y - \frac{2}{3}\pi) + \cos(x - \frac{2}{3}\pi)\sin(y + \frac{2}{3}\pi)$
$= \frac{3}{2}\sin(x + y)$

(I-23) $\cos x \ \cos y + \cos(x + \frac{2}{3}\pi)\cos(y - \frac{2}{3}\pi) + \cos(x - \frac{2}{3}\pi)\cos(y + \frac{2}{3}\pi)$
$= \frac{3}{2}\cos(x + y)$

Appendix B

MATRIX ALGEBRA

Basic Definitions

A rectangular array of numbers or functions

$$\mathbf{A} = \begin{bmatrix} a_{11} & a_{12} & \cdots & a_{1n} \\ a_{21} & a_{22} & \cdots & a_{2n} \\ \vdots & \vdots & \ddots & \vdots \\ a_{m1} & a_{m2} & \cdots & a_{mn} \end{bmatrix} \tag{B-1}$$

is known as a *matrix* and is denoted in the text by capital boldface letters. The numbers or functions a_{ij} are the elements of the matrix and the subscript i denotes the row and j the column. A matrix with m rows and n columns is of *order* (m, n) or an $m \times n$ (m by n) matrix. If $m = n$, the matrix is a *square matrix.*

If a matrix is an $m \times 1$ matrix, it is a *column vector.* If it is a $1 \times n$ matrix, it is a *row vector.* Generally, lower-case boldface letters are used to denote column or row vectors.

A square matrix in which all elements are zero except those on the main diagonal, a_{11}, a_{22},...,a_{nn}, is a *diagonal matrix.* If all elements of a diagonal matrix are unity, then the matrix is the *identity matrix* and is denoted as $\mathbf{I}$.

When $a_{ij} = a_{ji}$, the matrix is called a *symmetrical matrix.* A *null* or *zero matrix* is one in which all elements are zero.

Addition and Subtraction

Two matrices can be added or subtracted only if they are of the same order. Thus, if $\mathbf{A}$ has elements a_{ij} and $\mathbf{B}$ has elements b_{ij}, then, if

$$\mathbf{C} = \mathbf{A} + \mathbf{B} \tag{B-2}$$

$\mathbf{C}$ has elements c_{ij}, where

$$c_{ij} = a_{ij} + b_{ij} \tag{B-3}$$

or if

$$\mathbf{C} = \mathbf{A} - \mathbf{B} \tag{B-4}$$

then

$$c_{ij} = a_{ij} - b_{ij} \tag{B-5}$$

Also, addition is commutative,

$$\mathbf{A} + \mathbf{B} = \mathbf{B} + \mathbf{A} \tag{B-6}$$

and associative,

$$(\mathbf{A} + \mathbf{B}) + \mathbf{C} = \mathbf{A} + (\mathbf{B} + \mathbf{C}) \tag{B-7}$$

Obviously,

$$\mathbf{A} + \mathbf{O} = \mathbf{A} \tag{B-8}$$

where $\mathbf{O}$ is the zero matrix.

Multiplication

If the matrix $\mathbf{A}$ is multiplied by a scalar, every element of the matrix is multiplied by the scalar. For example, $k\mathbf{A}$ means all elements of $\mathbf{A}$ are multiplied by the constant k; $t\mathbf{A}$ means that all elements of $\mathbf{A}$ are multiplied by time t.

To multiply two matrices, say $\mathbf{AB}$, it is necessary that the number of columns of $\mathbf{A}$ equal the numbers of rows of $\mathbf{B}$. If $\mathbf{A}$ is of order $m \times n$ and $\mathbf{B}$ of order $n \times p$, then the order of $\mathbf{AB}$ is $m \times p$. The elements of

$$\mathbf{C} = \mathbf{AB} \tag{B-9}$$

are obtained by multiplying the elements by the ith row of $\mathbf{A}$ by the corresponding elements of the jth column of $\mathbf{B}$ and adding these products. In particular,

$$c_{ij} = a_{i1}b_{1j} + a_{i2}b_{2j} + \ldots + a_{in}b_{nj} \tag{B-10}$$

In (B-9), $\mathbf{A}$ is said to *premultiply* $\mathbf{B}$, whereas $\mathbf{B}$ is said to *postmultiply* $\mathbf{A}$. Let

$$\mathbf{A} = \begin{bmatrix} 1 & 2 & 3 \\ 4 & 5 & 6 \end{bmatrix} \tag{B-11}$$

and

$$\mathbf{B} = \begin{bmatrix} -7 & -8 \\ 9 & 10 \\ 0 & -11 \end{bmatrix} \tag{B-12}$$

Then

$$\mathbf{AB} = \begin{bmatrix} 11 & -21 \\ 17 & -48 \end{bmatrix} \tag{B-13}$$

However,

$$\mathbf{BA} = \begin{bmatrix} -39 & -54 & -69 \\ 49 & 68 & 87 \\ -44 & -55 & -66 \end{bmatrix} \tag{B-14}$$

We see that, in general, matrix multiplication is not commutative; thus,

$$\mathbf{AB} \neq \mathbf{BA} \tag{B-15}$$

Multiplying a matrix of $m\times n$ by a column vector of $n\times 1$ yields a column vector of $m\times 1$. Multiplication of a row vector of $1\times n$ and a column vector of $n\times 1$ yields a function (scalar) that is the sum of the product of specific elements of each vector.

Multiplying the identity matrix by **A** yields **A**, that is,

$$\mathbf{AI} = \mathbf{IA} = \mathbf{A} \tag{B-16}$$

We can show that

$$\mathbf{A(BC)} = \mathbf{(AB)C} \tag{B-17}$$

$$\mathbf{A(B + C)} = \mathbf{AB} + \mathbf{AC} \tag{B-18}$$

$$\mathbf{(B + C)A} = \mathbf{BA} + \mathbf{CA} \tag{B-19}$$

Finally, consider the simultaneous linear equations

$$5x + 3y - 2z = 14 \tag{B-20}$$

$$x + y - 4z = -7 \tag{B-21}$$

$$6x + 3z = 1 \tag{B-22}$$

Let us write the above equations in the form

$$\mathbf{Ax} = \mathbf{b} \tag{B-23}$$

Here

$$\mathbf{A} = \begin{bmatrix} 5 & 3 & -2 \\ 1 & 1 & -4 \\ 6 & 0 & 3 \end{bmatrix} \tag{B-24}$$

$$\mathbf{x} = \begin{bmatrix} x \\ y \\ z \end{bmatrix} \tag{B-25}$$

$$\mathbf{b} = \begin{bmatrix} 14 \\ -7 \\ 1 \end{bmatrix} \tag{B-26}$$

In this case, $\mathbf{A}$ is called the *coefficient matrix.* Care must be taken not to confuse the column vector $\mathbf{x}$ and the variable x.

Transpose

The *transpose* of a matrix $\mathbf{A}$ is denoted as $\mathbf{A}^T$. The transpose of $\mathbf{A}$ is obtained by interchanging the rows and columns of $\mathbf{A}$. Thus, if

$$\mathbf{A} = \begin{bmatrix} 1 & 2 & 3 & 4 \\ 5 & 6 & 7 & 8 \end{bmatrix} \tag{B-27}$$

$$\mathbf{A}^T = \begin{bmatrix} 1 & 5 \\ 2 & 6 \\ 3 & 7 \\ 4 & 8 \end{bmatrix} \tag{B-28}$$

The transpose possesses the following properties:

$$(\mathbf{A}^T)^T = \mathbf{A} \tag{B-29}$$

$$(\mathbf{A} + \mathbf{B} + \mathbf{C})^T = \mathbf{A}^T + \mathbf{B}^T + \mathbf{C}^T \tag{B-30}$$

$$(\mathbf{AB})^T = \mathbf{B}^T \mathbf{A}^T \tag{B-31}$$

$$(\mathbf{ABC})^T = \mathbf{C}^T\mathbf{B}^T\mathbf{A}^T \tag{B-32}$$

Partitioning

Partitioning of matrices is used throughout the text. It is helpful in matrix multiplication. For example, let **A** and **B** be partitioned as

$$\mathbf{A} = \begin{bmatrix} \mathbf{C} & \mathbf{D} \\ \mathbf{E} & \mathbf{F} \end{bmatrix} \tag{B-33}$$

$$\mathbf{B} = \begin{bmatrix} \mathbf{G} & \mathbf{H} \\ \mathbf{J} & \mathbf{K} \end{bmatrix} \tag{B-34}$$

where **C** through **K** are submatrices. The product of **AB** is

$$\mathbf{AB} = \begin{bmatrix} \mathbf{CG}+\mathbf{DJ} & \mathbf{CH}+\mathbf{DK} \\ \mathbf{EG}+\mathbf{FJ} & \mathbf{EH}+\mathbf{FK} \end{bmatrix} \tag{B-35}$$

Determinants

Every square matrix has a scalar associated with it called its *determinant.* In particular, if **A** is a square matrix, say,

$$\mathbf{A} = \begin{bmatrix} a_{11} & a_{12} & a_{13} \\ a_{21} & a_{22} & a_{23} \\ a_{31} & a_{32} & a_{33} \end{bmatrix} \tag{B-36}$$

then the determinant of **A** is denoted det **A** or $|\mathbf{A}|$:

$$\det \mathbf{A} = \begin{vmatrix} a_{11} & a_{12} & a_{13} \\ a_{21} & a_{22} & a_{23} \\ a_{31} & a_{32} & a_{33} \end{vmatrix} \tag{B-37}$$

It is important to note the difference between (B-36) and (B-37); (B-36) represents a matrix that is a square array of elements, whereas (B-37) represents a scalar associated with the matrix **A**.

The det **A** is determined by obtaining the *minors* and *cofactors.* Given a matrix **A**, a minor is the determinant of any square submatrix of **A**. The cofactor of the element a_{ij} is a scalar obtained by multiplying $(-1)^{i+j}$ times the minor obtained from **A** by removing the ith row and jth column. To find the determinant of the square matrix **A**:

1. Pick any one row or any one column of the matrix.

2. For each element in the row or column chosen, find its cofactor.

3. Multiply each element in the row or column chosen by its cofactor and sum the results.

The sum is the determinant of the matrix. For example, find det **A**, where

$$\mathbf{A} = \begin{bmatrix} 3 & 5 & 0 \\ -1 & 1 & 1 \\ 3 & -6 & 4 \end{bmatrix} \tag{B-38}$$

Expanding in the second column,

$$\begin{aligned} \det \mathbf{A} &= (5)(-1)^{1+2} \begin{vmatrix} -1 & 1 \\ 3 & 4 \end{vmatrix} + (1)(-1)^{2+2} \begin{vmatrix} 3 & 0 \\ 3 & 4 \end{vmatrix} + (-6)(-1)^{3+2} \begin{vmatrix} 3 & 0 \\ -1 & 1 \end{vmatrix} \\ &= (-5)(-7) + (1)(12) + (6)(3) = 65 \end{aligned} \tag{B-39}$$

Adjoint

The *adjoint matrix* of a square matrix **A**, denoted adjoint **A** or $\mathbf{A}^a$, is formed by replacing each element a_{ij} by the cofactor α_{ij} and transposing. Thus, the adjoint of (B-36) is

$$\begin{aligned} \text{adjoint } \mathbf{A} &= \begin{bmatrix} \alpha_{11} & \alpha_{12} & \alpha_{13} \\ \alpha_{21} & \alpha_{22} & \alpha_{23} \\ \alpha_{31} & \alpha_{32} & \alpha_{33} \end{bmatrix}^T \\ &= \begin{bmatrix} \alpha_{11} & \alpha_{21} & \alpha_{31} \\ \alpha_{12} & \alpha_{22} & \alpha_{32} \\ \alpha_{13} & \alpha_{23} & \alpha_{33} \end{bmatrix} \end{aligned} \tag{B-40}$$

Inverse

The *inverse* of a square matrix **A** is written as $\mathbf{A}^{-1}$ and is defined as

$$\mathbf{A}^{-1}\mathbf{A} = \mathbf{A}\mathbf{A}^{-1} = \mathbf{I} \tag{B-41}$$

In the text, parentheses are used to avoid confusion with superscripts, that is, the inverse is denoted $(\mathbf{A})^{-1}$. The inverse is defined only for square matrices. In particular,

$$\mathbf{A}^{-1} = \frac{\text{adjoint } \mathbf{A}}{\det\ \mathbf{A}} \tag{B-42}$$

If det $\mathbf{A}$ is zero, $\mathbf{A}$ does not possess an inverse and is said to be *singular*. Consider a 2×2 matrix:

$$\mathbf{A} = \begin{bmatrix} a_{11} & a_{12} \\ a_{21} & a_{22} \end{bmatrix} \tag{B-43}$$

$$\text{adjoint } \mathbf{A} = \begin{bmatrix} a_{22} & -a_{12} \\ -a_{21} & a_{11} \end{bmatrix} \tag{B-44}$$

$$\det \mathbf{A} = a_{11}a_{22} - a_{12}a_{21} \tag{B-45}$$

Find the inverse of (B-38). The cofactor of a_{11} is

$$\alpha_{11} = (3)(-1)^{1+1} \begin{vmatrix} 1 & 1 \\ -6 & 4 \end{vmatrix} = (3)(10) = 30 \tag{B-46}$$

Finding the cofactor of each element and transposing yields the adjoint of $\mathbf{A}$. Thus,

$$\text{adjoint } \mathbf{A} = \begin{bmatrix} 30 & 20 & 15 \\ 35 & 12 & 18 \\ 0 & 33 & 32 \end{bmatrix} \tag{B-47}$$

The det $\mathbf{A}$ is given by (B-39), hence,

$$\begin{aligned} \mathbf{A}^{-1} &= \frac{\text{adjoint } \mathbf{A}}{\det \mathbf{A}} \\ &= \frac{1}{65} \begin{bmatrix} 30 & 20 & 15 \\ 35 & 12 & 18 \\ 0 & 33 & 32 \end{bmatrix} \end{aligned} \tag{B-48}$$

Derivatives

The derivative of the matrix $\mathbf{A}$, denoted $(d/dt)\ \mathbf{A}$ or $p\mathbf{A}$, is the derivative of each element of the matrix. The derivative of $\mathbf{A}$, given by (B-1), is

$$p\mathbf{A} = \begin{bmatrix} pa_{11} & pa_{12} & \cdots & pa_{1n} \\ pa_{21} & pa_{22} & \cdots & pa_{2n} \\ \vdots & \vdots & \ddots & \vdots \\ pa_{n1} & pa_{n2} & \cdots & pa_{nn} \end{bmatrix} \tag{B-49}$$

where p is the operator d/dt.

Matrix Formulation

In the text, we deal with equations of the form

$$\mathbf{A}^{-1}\mathbf{y} = \mathbf{A}^{-1}r\mathbf{I}\mathbf{x} + p[\mathbf{A}^{-1}\mathbf{z}] \tag{B-50}$$

where $\mathbf{A}$ is a square, nonsingular matrix, the elements of which may be functions of time, and p is the operator d/dt. Solving (B-50) for $\mathbf{y}$ is achieved by premultiplying by $\mathbf{A}$. Thus,

$$\begin{aligned}\mathbf{A}\mathbf{A}^{-1}\mathbf{y} &= \mathbf{A}\mathbf{A}^{-1}r\mathbf{I}\mathbf{x} + \mathbf{A}p[\mathbf{A}^{-1}\mathbf{z}] \\ &= r\mathbf{A}\mathbf{A}^{-1}\mathbf{x} + \mathbf{A}[p\mathbf{A}^{-1}]\mathbf{z} + \mathbf{A}\mathbf{A}^{-1}[p\mathbf{z}] \end{aligned} \tag{B-51}$$

Since $\mathbf{A}\mathbf{A}^{-1} = \mathbf{I}$, (B-51) may be written as

$$\mathbf{y} = r\mathbf{I}\mathbf{x} + \mathbf{A}[p\mathbf{A}^{-1}]\mathbf{z} + p\mathbf{z} \tag{B-52}$$

Electromechanical Motion Devices, Second Edition
by Paul Krause, Oleg Wasynczuk and Steven Pekarek

Appendix C

THREE-PHASE SYSTEMS

In a three-phase system, there are two types of connections that are most often used: the *wye (Y) connection* and the *delta (Δ) connection*. Also, there are two phase sequences. In the *abc-sequence*, the a-phase variables lead the b-phase variables in time phase and the b-phase variables lead the c-phase variables. In the *acb-sequence*, the c-phase variables lead the b-phase variables.

Wye Connection

The wye (Y) connection is illustrated in Fig. C-1. Balanced three-phase currents are equal-amplitude sinusoidal currents displaced by 120°. The instantaneous sum of balanced currents is zero; hence, a fourth wire is not needed. In a Y connection, the assigned negative-potential sides of the windings are all connected to form what is called the *neutral point*, shown as n in Fig. C-1. The neutral may be grounded or left to float. As mentioned, if the currents are balanced, their instantaneous sum is zero. If the neutral is floating, it is clear that the sum of the currents must be zero regardless of their form.

The voltages across each phase are referred to as line-to-neutral voltages, whereas the voltages between two of the three phases are the line-to-line voltages. The phase currents are the line currents. We can relate the line-to-neutral and line-to-line voltages as

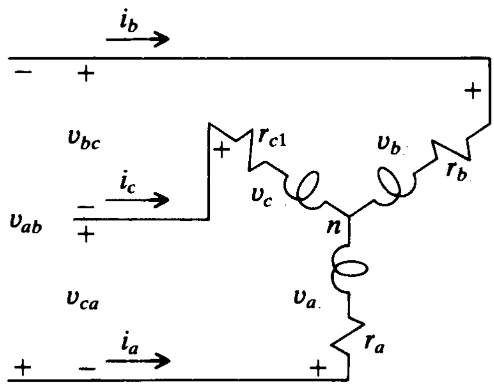

Figure C-1: Wye connection.

$$v_{ab} = v_a - v_b \tag{C-1}$$

$$v_{bc} = v_b - v_c \tag{C-2}$$

$$v_c = v_c - v_a \tag{C-3}$$

If the system is balanced, then we can express the steady-state phase voltages for an *abc* sequence as

$$V_a = \sqrt{2}\, V_s \cos \omega_e t \tag{C-4}$$

$$V_b = \sqrt{2}\, V_s \cos \left(\omega_e t - \tfrac{2}{3}\pi\right) \tag{C-5}$$

$$V_c = \sqrt{2}\, V_s \cos \left(\omega_e t + \tfrac{2}{3}\pi\right) \tag{C-6}$$

where the capital letters are used to denote steady-state conditions. For an *abc* sequence, the phase voltages may be written in phasor form as

$$\tilde{V}_a = V_s \underline{/0^\circ} \tag{C-7}$$

$$\tilde{V}_b = V_s \underline{/-120^\circ} \tag{C-8}$$

$$\tilde{V}_c = V_s \underline{/120^\circ} \tag{C-9}$$

The line-to-line voltages may be expressed as

$$\tilde{V}_{ab} = V_s\underline{/0^\circ} - V_s\underline{/-120}$$

$$= \sqrt{3}\,V_s\underline{/30^\circ} \qquad \text{(C-10)}$$

$$\tilde{V}_{bc} = V_s\underline{/-120^0} - V_s\underline{/120^\circ}$$

$$= \sqrt{3}\,V_s\underline{/-90^\circ} \qquad \text{(C-11)}$$

$$\tilde{V}_{ca} = V_s\underline{/120^\circ} - V_s\underline{/0^\circ}$$

$$= \sqrt{3}\,V_s\underline{/150^\circ} \qquad \text{(C-12)}$$

Hence, the line-to-line voltages form a balanced three-phase set that is $\sqrt{3}$ times the magnitude of the line-to-neutral voltages and shifted ahead in time phase by 30° for an *abc* sequence and shifted back by 30° for an *acb* sequence. For balanced steady-state conditions, we need to consider only one phase since once we have determined the variables associated with one of the phases we can express the other phase variables by shifting the phase ahead or back by 120°.

Delta Connection

The Δ connection is illustrated in Fig. C-2. In this type of connection, the line-to-line voltages are the voltages across the phases, that is, $v_a = v_{ab}$, $v_b = v_{bc}$, and so on. There is no neutral connection. The line currents are the sum of currents from two phases. For the connection shown in Fig. C-2,

$$i_{ac} = i_a - i_c \qquad \text{(C-13)}$$

$$i_{ba} = i_b - i_a \qquad \text{(C-14)}$$

$$i_{cb} = i_c - i_b \qquad \text{(C-15)}$$

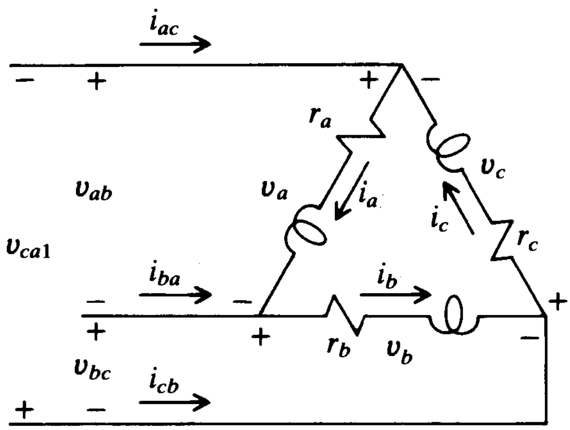

Figure C-2: Delta connection.

If, for example, the currents form a balanced *abc* sequence, then

$$\tilde{I}_a = I_s\underline{/0^\circ} \tag{C-16}$$

$$\tilde{I}_b = I_s\underline{/-120^\circ} \tag{C-17}$$

$$\tilde{I}_c = I_s\underline{/120^\circ} \tag{C-18}$$

The line currents become

$$\tilde{I}_{ac} = I_s\underline{/0^\circ} - I_s\underline{/120^\circ}$$

$$= \sqrt{3}\, I_s\underline{/-30^\circ} \tag{C-19}$$

Thus, for an *abc* sequence, $\tilde{I}_{ac}$ is $\sqrt{3}$ times the amplitude of $\tilde{I}_a$ and shifted 30° back in phase from it. Similarly, $\tilde{I}_{ba}$ is shifted back 30° from $\tilde{I}_b$ and $\tilde{I}_{cb}$ back 30° from $\tilde{I}_c$. In the case of the *acb* sequence, the line currents are shifted ahead of the phase currents.

Index

IEEE Press Series on Power Engineering

1. *Principles of Electric Machines with Power Electronic Applications, Second Edition*
M. E. El-Hawary

2. *Pulse Width Modulation for Power Converters: Principles and Practice*
D. Grahame Holmes and Thomas Lipo

3. *Analysis of Electric Machinery and Drive Systems, Second Edition*
Paul C. Krause, Oleg Wasynczuk, and Scott D. Sudhoff

4. *Risk Assessment of Power Systems: Models, Methods, and Applications*
Wenyuan Li

5. *Optimization Principles: Practical Applications to the Operations of Markets of the Electric Power Industry*
Narayan S. Rau

6. *Electric Economics: Regulation and Deregulation*
Geoffrey Rothwell and Tomas Gomez

7. *Electric Power Systems: Analysis and Control*
Fabio Saccomanno

8. *Electrical Insulation for Rotating Machines: Design, Evaluation, Aging, Testing, and Repair*
Greg Stone, Edward A. Boulter, Ian Culbert, and Hussein Dhirani

9. *Signal Processing of Power Quality Disturbances*
Math H. J. Bollen and Irene Y. H. Gu

10. *Instantaneous Power Theory and Applications to Power Conditioning*
Hirofumi Akagi, Edson H. Watanabe, and Mauricio Aredes

11. *Maintaining Mission Critical Systems in a 24/7 Environment, Second Edition*
Peter M. Curtis

12. *Elements of Tidal-Electric Engineering*
Robert H. Clark

13. *Handbook of Large Turbo-Generator Operation Maintenance, Second Edition*
Geoff Klempner and Isidor Kerszenbaum

14. *Introduction to Electrical Power Systems*
Mohamed E. El-Hawary

15. *Modeling and Control of Fuel Cells: Disturbed Generation Applications*
M. Hashem Nehrir and Caisheng Wang

16. *Power Distribution System Reliability: Practical Methods and Applications*
Ali A. Chowdhury and Don O. Koval

17. *Introduction to FACTS Controllers: Theory, Modeling, and Applications*
Kalyan K. Sen and Mey Ling Sen

18. *Economic Market Design and Planning for Electric Power Systems*
James Momoh and Lamine Mili

19. *Operation and Control of Electric Energy Processing Systems*
James Momoh and Lamine Mili

20. *Restructured Electric Power Systems: Analysis of Electricity Markets with Equilibrium Models*
Xiao-Ping Zhang

21. *An Introduction to Wavelet Modulated Inverters*
S.A. Saleh and M. Azizur Rahman

22. *Probabilistic Transmission System Planning*
Wenyuan Li

23. *Control of Electric Machine Drive Systems*
Seung-Ki Sul

24. *High Voltage and Electrical Insulation Engineering*
Ravindra Arora and Wolfgang Mosch

25. *Practical Lighting Design with LEDs*
Ron Lenk and Carol Lenk

26. *Electricity Power Generation: The Changing Dimensions*
Digambar M. Tagare

27. *Electric Distribution Systems*
Abdelhay A. Sallam and Om P. Malik

28. *Maintaining Mission Critical Systems in a 24/7 Environment, Second Edition*
Peter M. Curtis

29. *Power Conversion and Control of Wind Energy Systems*
Bin Wu, Yongqiang Lang, Navid Zargan, and Samir Kouro

30. *Integration of Distributed Generation in the Power System*
Math Bollen and Fainan Hassan

31. *High Voltage Protection for Telecommunications*
Steven W. Blume

32. *Doubly Fed Induction Machine: Modeling and Control for Wind Energy Generation*
Gonzalo Abad, Jesús Lopéz, Miguel Rodríguez, Luis Marroyo, and Grzegorz Iwanski

33. *Smart Grid: Fundamentals of Design and Analysis*
James Momoh

34. *Electromechanical Motion Devices, Second Edition*
Paul Krause, Oleg Wasynczuk, and Steven Pekarek